THESE de DOCTORAT DE L'UNIVERSITE DE LYON
opérée au sein de
l'Université Claude Bernard Lyon 1

Ecole Doctorale BMIC N° ED340
(Biologie Moléculaire, Intégrative et Cellulaire)

Spécialité de doctorat : Biologie

Monika Gjorgjieva

Identification des mécanismes moléculaires impliqués dans le développement des pathologies hépatiques et rénales dans des modèles murins de glycogénose de type Ia

Devant le jury composé de :

Foti Michelangelo	Professeur, Université de Genève, *Genève*	Rapporteur
Perret Christine	Directrice de recherche, HDR ; Institut Cochin, *Paris*	Rapporteur
Billaud Marc	Directeur de recherche, HDR CRCL, *Lyon*	Examinateur
Cochat Pierre	Professeur PU-PH ; Université Lyon 1, *Lyon*	Examinateur
Labrune Philippe	Professeur PU-PH ; APHP, *Paris*	Examinateur
Postic Catherine	Directrice de recherche, HDR ; Institut Cochin, *Paris*	Examinatrice
Rajas Fabienne	Directrice de recherche, HDR ; INSERM U1213, *Lyon*	Directrice de thèse

UNIVERSITE CLAUDE BERNARD - LYON 1

Président de l'Université	**M. le Professeur Frédéric FLEURY**
Président du Conseil Académique	M. le Professeur Hamda BEN HADID
Vice-président du Conseil d'Administration	M. le Professeur Didier REVEL
Vice-président du Conseil Formation et Vie Universitaire	M. le Professeur Philippe CHEVALIER
Vice-président de la Commission Recherche	M. Fabrice VALLÉE
Directrice Générale des Services	Mme Dominique MARCHAND

COMPOSANTES SANTE

Faculté de Médecine Lyon Est – Claude Bernard	Directeur : M. le Professeur G.RODE
Faculté de Médecine et de Maïeutique Lyon Sud – Charles Mérieux	Directeur : Mme la Professeure C. BURILLON
Faculté d'Odontologie	Directeur : M. le Professeur D. BOURGEOIS
Institut des Sciences Pharmaceutiques et Biologiques	Directeur : Mme la Professeure C. VINCIGUERRA
Institut des Sciences et Techniques de la Réadaptation	Directeur : M. X. PERROT
Département de formation et Centre de Recherche en Biologie Humaine	Directeur : Mme la Professeure A-M. SCHOTT

COMPOSANTES ET DEPARTEMENTS DE SCIENCES ET TECHNOLOGIE

Faculté des Sciences et Technologies	Directeur : M. F. DE MARCHI
Département Biologie	Directeur : M. le Professeur F. THEVENARD
Département Chimie Biochimie	Directeur : Mme C. FELIX
Département GEP	Directeur : M. Hassan HAMMOURI
Département Informatique	Directeur : M. le Professeur S. AKKOUCHE
Département Mathématiques	Directeur : M. le Professeur G. TOMANOV
Département Mécanique	Directeur : M. le Professeur H. BEN HADID
Département Physique	Directeur : M. le Professeur J-C PLENET
UFR Sciences et Techniques des Activités Physiques et Sportives	Directeur : M. Y.VANPOULLE
Observatoire des Sciences de l'Univers de Lyon	Directeur : M. B. GUIDERDONI
Polytech Lyon	Directeur : M. le Professeur E.PERRIN
Ecole Supérieure de Chimie Physique Electronique	Directeur : M. G. PIGNAULT
Institut Universitaire de Technologie de Lyon 1	Directeur : M. le Professeur C. VITON
Ecole Supérieure du Professorat et de l'Education	Directeur : M. le Professeur A. MOUGNIOTTE
Institut de Science Financière et d'Assurances	Directeur : M. N. LEBOISNE

I would like to thank the ***Ligue nationale contre le cancer*** for funding this PhD project.



Оваа докторантска теза ја посветувам на мојата мајка Марија Ѓорѓиева и мојот татко Доне Ѓорѓиев, за сите самопожртвувања, за сите непреспиени ноќи и за сите долги разговори на Скајп. Без нив немаше да бидам тоа што сум денес.

I dedicate this work to my mother Marija Gjorgjieva and my father Done Gjorgjiev, for all the sacrifices they have done for me, for all the sleepless nights and for all those long conversations on Skype. I wouldn't have been what I am today, if it weren't for them.

ACKNOLWEDGEMENTS

After hearing many, many stories about PhD trainings gone wrong due to mean bosses, incompetent colleagues and non-reproducible results, I can only be grateful that none of these things were a part of my PhD experience. I am immensely thankful to the whole INSERM U1213 «Nutrition, diabetes and the brain» team who made me feel like a part of a big family.

First, I have to thank Julie (alias Cindy) who taught me most of the techniques used in the lab, as well as handing me ”her baby” – her research project on GSDI. Her patience and her way of explaining things made me love the subject even more.

When it comes to techniques used in the lab, I can’t leave aside Adeline and Carine, which were always there with their advice, especially on mouse handling and staying safe in the lab. Not to mention that there is no item in the lab that cannot be found by them. Thank you for your help throughout these years! I would like to thank Anne S. as well, even though she started her well-deserved retirement this year, I will always remember her French grammar lessons and the way she frowned when I put music on, while analyzing the samples. Erwann, thank you for all the help around the lab, to me you will always be ”Mister Fridge manager from Bretagne”. Vincent, you’re one of the most efficient members of the lab. Thank you for putting up with all of my demands, hopefully those 1000 qPCRs will one day be published.

I would like to thank Amandine for all the scientific advice; to me she will always be the brilliant scientist to go to when something doesn’t go according to plan in the lab.

Maud, thank you for being the closest thing to a nutritional coach that I’ve had. Also, thank you for all those ”My baby did X, is that weird?” conversations, they were pretty reassuring. You can’t talk about Maud, without mentioning Justine and Margaux, of course. Justine, thank you for all the cakes, you know very well how I feel about them. Margaux, thank you for all the help with the mice, nobody knows how to perform submandibular bleeding quite like you!

Keizo, thank you for all the scientific debates! A doctor’s perspective is always welcome. Also, thank you for sharing your country’s culture and Japanese cuisine. While I wasn’t always sure what I was eating, it was very good!

Marie-Ange, thank you for all those laughs during lunch! I enjoyed how honest and direct you always are, and your great sense of humor. Also, I have to admit that you are one of the best pétanque players I’ve ever met.

Judith, while I didn't have the time to get to know you as much as the others, I've enjoyed all of those lunch-time conversation. Seeing your motivation that you invest in your thesis, I am confident that you will have great results and a successful thesis.

Laure and Marine, besides being my co-workers, I consider you as close friends. Thank you for being there for the important moments, thank you for visiting my country and discovering my culture with me. We've had countless great moments, and I can be only grateful that I've met you here in our lab. Marine, keep up the good work with the mice, I think that even the animals know when they're around an animal-lover. Laure, I wish you many, many great results and publications by the end of your thesis, and I am sure that one day you will become a great researcher. Gael and Amaury, our two part-time «hommes de ménage», thank you for bringing balance and showing that men can also handle a broom as good as any woman.

I would also like to thank immensely our personal Claude Bernard, Dr Gilles Mithieux, for the hundreds of hours of brain-storming on metabolism in GSDI and beyond. I was lucky to have you as my director. You always had an answer to everything (and many subsequent questions!).

Fabienne, you're every PhD student's dream for a thesis supervisor. Thank you for guiding me through every step, thank you for all the knowledge and comprehension and thank you for everything that you've done for me during these years, in the lab, as well as outside of it. I will never forget it. It's scientists like you that motivate students to pursue research.

As mentioned, I dedicate this thesis to my parents Marija and Done Gjorgjievi. Words are not enough to express my gratitude, because I can't imagine the strength it took to send their 18 year old daughter, alone, in a foreign country, to pursue her wish to do science. From the bottom of my heart, I thank you. Simon, thank you for being the coolest brother ever.

And last but not least, I would like to thank my newly formed family, my husband Olivier and my son Remi. Olivier, you were there through thick and thin, loving, caring and always understanding. Thank you for taking such good care of our son and thank you for always supporting me in achieving my goals, no matter what.

Remi, it might take a couple of years for you to read this. For me, you are the most important person in this world. I hope soon I'll be able to share with you this passion of mine that is science and that you too will be enchanted by the wonders that science has to offer.

ABBREVIATION LIST

AAV - adeno-associated virus
ACC - acetyl-CoA carboxylase
ACE - angiotensin converting enzyme
AFP - alpha-fetoprotein
ALT - alanine transaminase
AMPK - adenosine monophosphate-activated protein kinase
ARB - angiotensin receptor blockers
AST - aspartate transaminase
ATF4 - activating transcription factor 4
ATF6 - activating transcription factor 6
ATG - autophagy-related protein
ATP - adenosine triphosphate
cAMP - cyclic adenosine monophosphate
CDX - caudal-related transcription factor
C/EBP - CAAT / enhancer binding protein
CEA - carcinoembryogenic antigen
ChREBP - carbohydrate responsive element binding protein
CKD - chronic kidney disease
CNGDF - continuous nocturnal gastric drip-feeding
CPT-I - carnitine palmitoyltransferase I
CRISPR/Cas9 - clustered regularly interspaced short palindromic repeats-associated nuclease Cas9
CRP - C reactive protein
DAG - diacylglycerol
EGP - endogenous glucose production
eIF2a - eukaryotic translation initiation factor 2a
EMT - epithelial-mesenchymal transition
ER - endoplasmic reticulum
FAS - fatty acid synthase
FFA - free fatty acid
FIV - feline immunodeficiency virus
FNH - focal nodular hyperplasia
FOXO1 - forkhead box protein 1
G1P - glucose-1 phosphate
G6P - glucose-6 phosphate
G6Pase - glucose-6 phosphatase
G6PC - glucose-6 phosphatase catalytic subunit
G6PT - glucose-6 phosphatase transport subunit
GDE - glycogen debranching enzyme
GFR - glomerular filtration rate
GK - glucokinase
GLUL - glutamine synthetase
GLUT2 - glucose transporter 2
GNAS - guanine nucleotide binding protein
GNG - gluconeogenesis
GSDI - glycogen storage disease type I
GSDIII - glycogen storage disease type III
GSK3 - glycogen synthase kinase 3

HCA - hepatocellular adenoma
HCC - hepatocellular carcinoma
HGF - hepatocyte growth factor
HF/HS - high fat / high sucrose
HIV - human immunodeficiency virus
HNF1 - hepatic nuclear factor 1
IGF2R - Insulin-like growth factor 2 receptor
IGRP - islet-specific G6Pase related protein
IL6ST - interleukin-6 signal transducer
IRE1 - inositol-requiring enzyme 1
KAP - kidney androgen protein
LATS1 - large tumor suppressor kinase 1
LGR5 - leucine rich repeat containing G protein-coupled receptor 5
L-FABP1 - liver fatty acid binding protein 1
L-PK - liver pyruvate kinase
LXR - liver X receptor
MAPK - mitogen activated protein kinase
MODY- maturity-onset diabetes of the young
MPC1 - mitochondrial pyruvate carrier 1
mTOR - mammalian target of rapamycin
NAFLD - non-alcoholic fatty liver disease
NASH - non-alcoholic steatohepatitis
OAA - oxaloacetate
OXPHOS - oxidative phosphorylation
PDGF - platelet derived growth factor
PEP - phosphoenolpyruvate
PEPCK - phosphoenolpyruvate carboxykinase
PERK - PKR-like ER kinase
PI3K - phosphatidylinositol-3-kinase
PKB - protein kinase B
PKC - protein kinase C
PK-M2 - pyruvate kinase M2
PKD2- polycystic kidney disease 2
PKHD1 - polycystic kidney and hepatic disease 1
PP1 - protein phosphatase 1
PP2A - protein phosphatase 2A
PPARα - peroxisome proliferator-activated receptor α
PPP - pentose phosphate pathway
PTEN - phosphatase and tensin homolog
RAS - renin - angiotensin system
ROS – reactive oxygen species
SA - serum albumin
SAA - serum amyloid A
SIRT1 – sirtuin 1
SREBP1 - sterol regulatory element binding protein 1
TALEN - transcription activator-like effector nuclease
TG - triglyceride
TGF-β1 - transforming growth factor-β1
TNF-α - tumor necrosis factor-α

TSC1 - tuberous sclerosis complex 1
UCS - uncooked cornstarch
UDP-glucose - uridine diphosphate glucose
UGRP - ubiquitously expressed G6Pase catalytic subunit related protein
UGT2B7 - UDP Glucuronosyltransferase Family 2 Member B7
VEGF - vascular endothelial growth factor
VLDL - very low density lipoproteins
Vill - Villin
WT - wild type
XBP1 - X-box binding protein 1
XO - xanthine oxidase
ZFN - zinc finger nuclease

CONTENTS

ACKNOLWEDGEMENTS 5
ABBREVIATION LIST 7
FOREWORD 12
LITERATURE DATA 15
I) How does the body maintain normal glycaemia? 16
I.1) What happens right after a meal (post-prandial period)? 16
I.1.1) Glycogen synthesis is activated in the liver and muscles 17
I.1.2) *De novo* lipid synthesis in the liver is induced by excess of glucose 18
I.2) What happens during fasting periods? 19
I.2.1) Normal glycaemia is maintained *via* glycogenolysis in post-absorptive state 20
I.2.2) Normal glycaemia is maintained by gluconeogenesis during long-term fasting 22
II) Molecular basis of glycogen storage disease type I 23
II.1) Glucose-6 phosphatase complex & mutations 23
II.2) Metabolic consequences of glucose-6 phosphatase deficiency 26
II.2.1) Glycogen synthesis activation 26
II.2.2) Glycolysis activation 26
II.2.3) Krebs cycle alteration and amino acid imbalance 28
II.2.4) Down-regulation of mitochondrial oxidative phosphorylation 29
II.2.5) *De novo* lipogenesis activation and decrease in lipid oxidation lead to steatosis 30
II.2.6) Link between altered lipid metabolism and autophagy 31
II.2.7) Pentose phosphate pathway activation 32
III) GSDI symptoms, long-term complications and treatments 34
III.1) Clinical manifestations and diagnosis 34
III.2) Long-term hepatic complications 35
III.2.1) Hepatocellular adenoma 35
III.2.2) Hepatocellular carcinoma 38
III.3) Long-term renal complications 40
III.3.1) Chronic kidney disease 40
III.3.2) Molecular pathways involved in CKD development 41
III.4) Intestinal complications 42

IV) Treatment strategies for GSDI patients 44
IV.1) Nutritional treatment 44
IV.2) Pharmacological therapy 47
IV.3) Hepatic and / or renal transplantation in GSDI patients 48
V) Contribution of animal models of GSDI in the comprehension of the pathology and first gene therapy studies 50
V.1) Animal models of GSDI 50
V.2) Gene therapy 54
EXPERIMENTAL PROCEDURES AND RESULTS 61
Chapter I – Metabolic reprogramming leading to hepatic tumorigenesis in GSDI 64
Chapter II – Characterization of the long-term renal complications in a mouse model of GSDI nephropathy 67
Chapter III – The role of lipids in hepatic and renal complications in GSDI 69
DISCUSSION AND CONCLUSION 72
Hepatocellular carcinoma development – is fibrosis a must? 75
Metabolic reprograming in GSDI leads to deregulated cell defense mechanisms and tumor suppressors 77
Glycogen storage disease type III – similar name but different carcinogenic pathways? 80
Down-regulation of HNF1 in GSDI liver and kidneys: A common factor in the development of GSDI hepatic and renal complications? 82
Cyst development in end-stage kidneys in GSDI: a risk of renal neoplasia? 84
Treatment strategies for GSDI 86
PUBLICATIONS AND PRESENTATION OF DATA 90
Publications 91
Presentations and awards 92
Volunteer work 93
ANNEX I 94
ANNEX II 95
REFERENCES 96
RÉSUMÉ EN FRANÇAIS 117

FOREWORD

Maintaining normal glycaemia is a finely tuned, crucial physiological function. Indeed, most mammals, including humans, are incapable of tolerating hypoglycemia for more than a few minutes. Glucose obtained from the digestion of food is partially used right away in order to maintain glycaemia, and the rest is rapidly stored in the form of glycogen (in the liver and muscles) and lipids, in order to prevent abnormal glucose concentrations in the blood stream. Furthermore, during fasting periods, the organism maintains a plasmatic glycemic concentration of around 5 mM (=100 mg/dL) *via* the endogenous glucose production (EGP). EGP starts off by glucose production *via* glycogenolysis, by degrading hepatic glycogen stores. The second pathway of EGP is gluconeogenesis, which is generally activated in prolonged fasting periods, assuring the synthesis of glucose form non-carbohydrate substrates in the liver, kidneys and intestine (Mithieux et al., 2017).

The last common reaction for glycogenolysis and gluconeogenesis is the hydrolysis of glucose-6 phosphate (G6P) into free glucose and inorganic phosphate by glucose-6 phosphatase (G6Pase). The expression of G6Pase is restricted to the liver, kidneys and intestine, conferring to these organs the capacity to produce glucose. G6Pase is composed of two subunits, which are the G6Pase catalytic subunit (G6PC) and the G6Pase transport subunit (G6PT). Alterations affecting the activity of this enzyme are responsible for the development of different metabolic pathologies, such as type 2 diabetes, characterized by glucose overproduction leading to hyperglycemia, and glycogen storage disease type I (GSDI), characterized by the absence of EGP and hypoglycemia.

GSDI is a rare genetic disease (1/100,000 births), caused by G6Pase deficiency. There are two types of GSDI, which are GSDI type a, caused by mutations in *G6PC*, and GSDI type b, caused by mutations in *SLC37A* encoding G6PT. To date, there are 12 known glycogen storage diseases, all caused by mutations affecting different enzymes involved in glycogen synthesis or degradation (Özen, 2007). They are qualified as hepatic, muscular or both, depending on the tissue-specificity of the enzyme which is deficient. For example, GSDII (Pompe disease) is due to a deficiency in α-1,4-

glucosidase, GSDIII (Cori's disease) is due to a deficiency in glycogen debranching enzyme and GSDV (McArdle's disease) is due to a deficiency in glycogen phosphorylase. As hepatic glycogen is degraded into glucose to maintain blood glucose, hepatic GSDs are characterized by hypoglycemia during short fasting. On the other hand, as glycogen accumulated in the muscles is used to produce energy during a physical effort, muscular GSDs are classified as myopathies.

In GSDI, the loss of G6Pase activity leads to the absence of EGP and the accumulation of G6P that deeply modifies the hepatic, renal and intestinal metabolisms. GSDI is characterized by abnormal accumulation of glycogen in the liver and kidneys, resulting in hepatomegaly and nephromegaly, respectively (Kishnani et al., 2014; Rake et al., 2002a). In addition to severe hypoglycemic episodes, GSDI patients exhibit metabolic parameter alterations, such as hypercholesterolemia, hypertriglyceridemia, lactic acidosis and hyperuricemia. Unfortunately, GSDI is further characterized by hepatic and renal complications, which occur generally in adulthood. Most adult patients develop hepatocellular adenoma / carcinoma (HCA / HCC) and / or nephropathy, firstly characterized by microalbuminuria and leading to renal failure in some cases.

The only treatment available for GSDI so far is a controlled dietary regimen, consisting in regular consumption of raw cornstarch (every 3h-4h), which helps to maintain normal glycaemia and avoid lactatemia (Kishnani et al., 2014; Rake et al., 2002a, 2002b). This regimen, which was installed in the 1980s, is very effective and it significantly reduces mortality in GSDI patients. However, it does not allow the complete prevention of long-term pathology development.

Many aspects of the hepatic carcinogenesis, as well as chronic kidney disease (CKD) development remain unknown in the case of GSDI. Before the dietary regimen was recommended, the main complication that led to mortality in GSDI patients was hypoglycemia, and hepatic and renal pathologies were not followed appropriately. In order to understand the mechanisms behind these long-term complications, our laboratory developed mouse models in which G6Pase was deficient specifically in the liver or in the kidney. These mouse models were developed since total knock-out animal models present severe hypoglycemia and do not survive weaning periods in the

absence of frequent glucose injections. Interestingly, L.G6pc-/- mice, which present a deletion of *G6pc* in the liver, exhibit all of the hepatic hallmarks of GSDI, including hepatocellular tumor development (Mutel et al., 2011a). On the other hand, K.G6pc-/- mice, with a specific deletion of *G6pc* in the kidneys, develop progressive nephropathy over time, as observed in GSDI patients (Clar et al., 2014). In this work, these two models were used not only to understand the pathways leading to GSDI long-term complications, but also to test different approaches for a treatment strategy.

The first part of the literature data consists in the description of the EGP and the metabolic pathways altered by G6Pase deficiency. The following chapters highlight the hepatic and renal pathophysiology of GSDI. Finally, in the last chapter, the animal models developed to study GSDI are described, along with the gene therapy assays performed so far, aiming to develop a curative strategy for this rare disease.

LITERATURE DATA

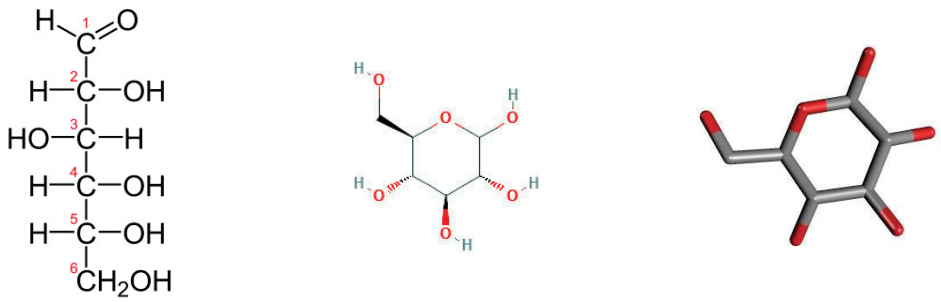

Fisher's projection 2D structure 3D structure

Figure 1: Different representations of glucose

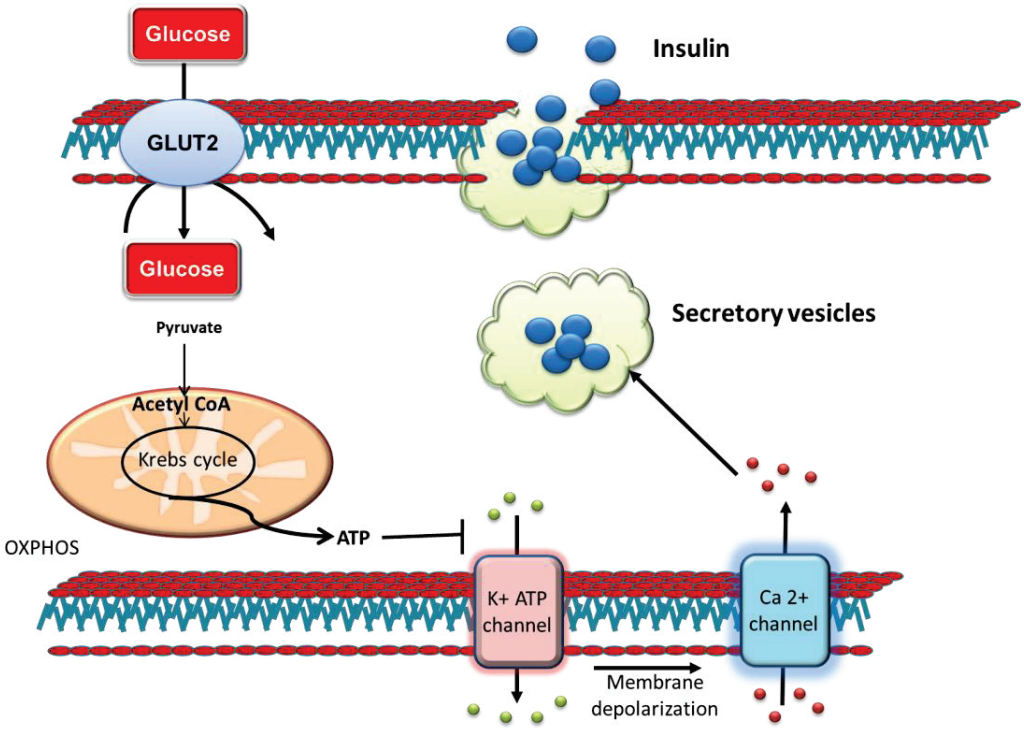

Figure 2: Insulin secretion induced by increased glucose concentrations during fed state

In order to detect ingested glucose, β cells in the pancreas express a specific glucose transporter (GLUT2), which transfers glucose into the cells proportionally to the plasmatic glucose concentrations. When blood glucose is high, the intake of glucose in β cells rises, increasing the ATP / ADP ratio in the cytoplasm. Increased ATP / ADP ratio signalizes an increase in energy levels, resulting in the inhibition of potassium channels sensitive to ATP, subsequent depolarization of the membrane of β cells, and an induction of the exocytosis of vesicles containing insulin.

I) How does the body maintain normal glycaemia?

Glucose is a simple carbohydrate, containing 6 carbon atoms (*Figure 1*). It is classified as a monosaccharide, a hexose, as well as an aldose. The term “glucose” derives from the Greek language, meaning “sweet”. Glucose is used as an energy source in almost all living organisms, from the lowest life-forms, such as bacteria, to the more complex ones, including humans. Plants synthetize this sugar by using carbon dioxide and sunlight *via* a well-known process called photosynthesis.

In mammals, glucose is maintained around 5 mM in the bloodstream at all times. While some organs can adapt and switch to other energy sources when glucose is scarce, such as ketone bodies, for others glucose represents more than half of the energy supplies used to function properly. Furthermore, «energy source» has always been the main function attributed to glucose, and while this may be true in some situations, the other essential roles of glucose in the cell, such as providing carbon skeletons on which all other specialized biochemical pathways ultimately depend, tend to be put aside (Soty et al., 2017). Interestingly, glucose can be a limiting factor in cell proliferation not only by its energetic role, but above all by providing carbons for nucleotide synthesis *via* the pentose shunt, required for DNA replication. Thus the many roles of glucose, including maintaining blood glucose levels in a very narrow range between 4 to 8 mM, are crucial for normal functioning of the organism. Glucose levels during fasting periods are assured first by the degradation of hepatic glycogen, and further on, when glycogen stores are depleted, by the gluconeogenesis (GNG) pathway, which is the synthesis of glucose from non-carbohydrate substrates.

I.1) What happens right after a meal (post-prandial period)?

After a meal, a portion of the glucose that has been ingested is immediately used in order to produce energy. Glucose is taken up from the blood into various organs *via* specific transporter systems, followed by a phosphorylation by hexokinases leading to glycolysis and pyruvate production. The inhibition of hexokinases activity in the muscle and adipose tissue by its product, i.e. G6P, ensures a controlled uptake of glucose in peripheral tissue.

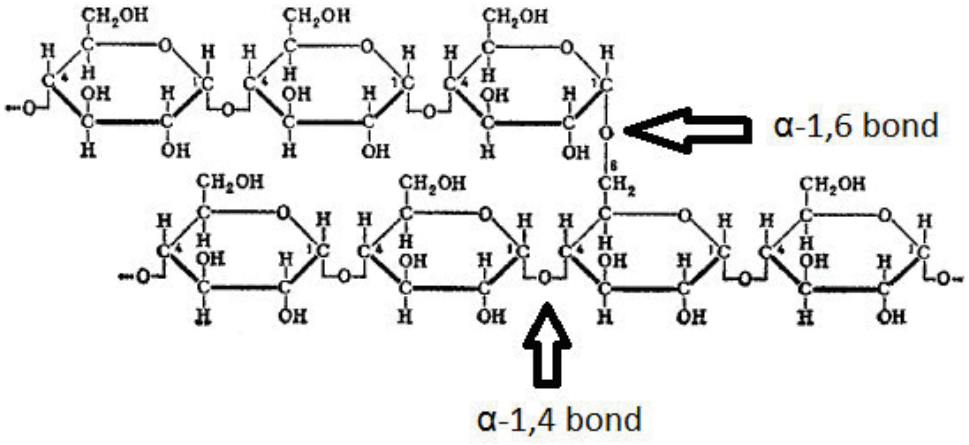

Figure 3: Glycogen structure

The linear chains of glucose in glycogen are linked with α(1,4) bonds, whereas the branches are linked with α(1,6) bonds.

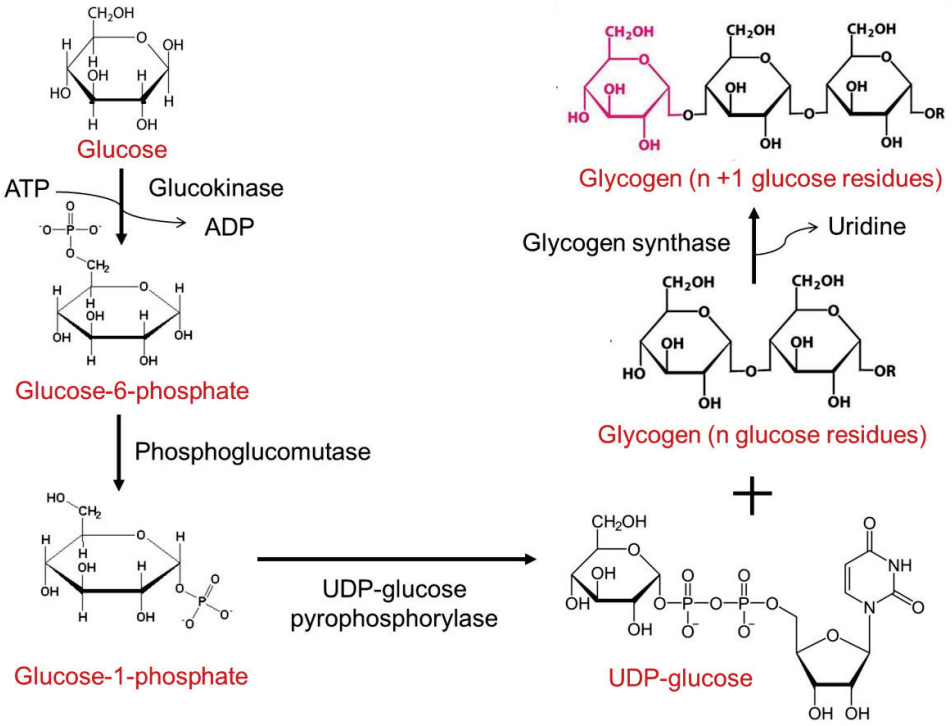

Figure 4: Glycogen synthesis pathway in the liver

Glucose is converted to G6P by glucokinase. G6P is further converted to G1P by phosphoglucomutase. An UDP residue is then transferred by the UDP - glucose pyrophosphorylase, leading to the formation of UDP-glucose. UDP-glucose is then attached to the glycogen polymer *via* the glycogen synthase, releasing uridine and thus elongating the linear chain of glycogen.

The rise of glucose levels in the blood stream stimulates the secretion of insulin, a hormone produced in the β cells of the pancreas (Henquin, 2000). The activation of insulin secretion by glucose is a complex process summarized in *Figure 2*. Once insulin is secreted, it targets the liver, muscle and adipose tissue, all of which express the insulin receptor (Van Obberghen et al., 2001). This increases the up-take of glucose in these organs and induces the storage of glucose in the form of glycogen and / or lipids, thus restoring normal blood glucose levels. The hypoglycemic effect of insulin is also mediated by inhibiting EGP during post-absorptive periods (Girard, 2006). Besides glycogen and lipids, glucose increase and the subsequent insulin release also lead to protein synthesis activation (Proud, 2006). Thus this hormone activates many anabolic pathways (i.e. glycogen, lipid and protein synthesis) in order to decrease blood glucose levels after a meal.

I.1.1) Glycogen synthesis is activated in the liver and muscles

As mentioned, right after a meal, the excess glucose which is not used right away is rapidly stored in the form of glycogen and lipids. Therefore, during postprandial periods, around 30% of alimentary glucose is stored in the form of glycogen.

Glycogen is a polymer of glucose, stored mainly in the liver and muscles (*Figure 3*). This polymer is composed of glucose molecules forming long linear chains linked by α(1-4) bonds, and fixed on main ramification chains by α(1-6) branching bonds (Roach et al., 2012). Hepatic glycogen represents around 5% of the weight of the liver in normal conditions.

The first stage of glycogen synthesis is the conversion of glucose to glucose-6 phosphate (G6P). In the liver, this conversion is done by the glucokinase (GK) enzyme. GK has a low affinity for glucose and it is therefore activated only when glucose is present in abundance (*Figure 4*). G6P is then converted to glucose-1 phosphate (G1P) and further to uridine diphosphate glucose (UDP-glucose), which is the substrate of glycogen synthase, the key enzyme responsible for glycogen synthesis (Adeva-Andany et al., 2016). Insulin stimulates the dephosphorylation of this enzyme by activating the protein phosphatase 1 (PP1) and by inhibiting glycogen synthase kinase 3 (GSK3).

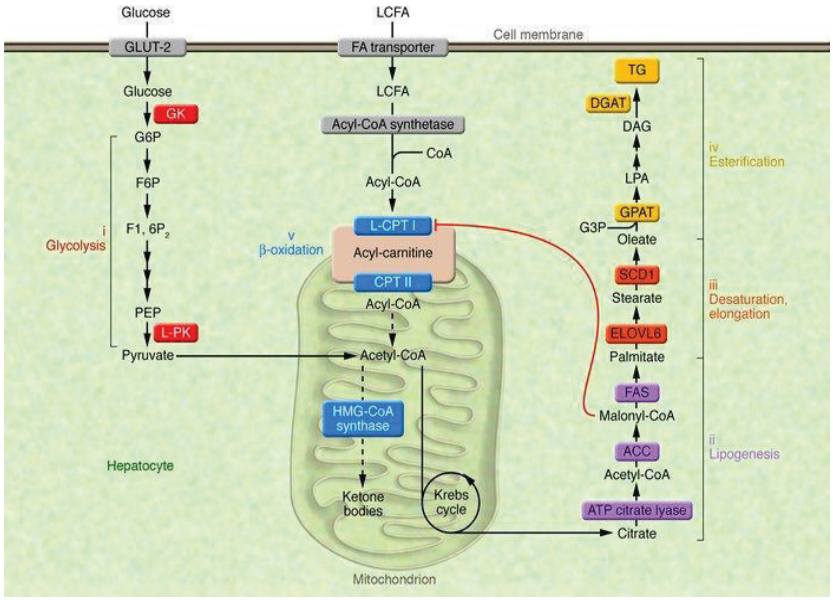

Figure 5: Metabolic pathways leading to the synthesis of triglycerides in the liver

Increased glucose levels induce (i) glucokinase (GK) and L-PK for glycolysis; (ii) ATP citrate lyase, ACC, and FAS for lipogenesis; (iii) ELOVL6 and SCD1 for fatty acid elongation and desaturation steps; and finally (iv) GPAT and DGAT for TG synthesis. Elevation in malonyl-CoA concentrations inhibits CPT I, the rate-limiting enzyme of β-oxidation (v), which regulates the transfer of long-chain acyl-CoAs from the cytosol into the mitochondria, thus resulting in a shift from an oxidative (production of ketone bodies) to an esterification pathway (TG synthesis). F6P, fructose 6-phosphate; F1, 6P2, fructose 1,6 diphosphate; G3P, glycerol 3-phosphate; G6P, glucose 6-phosphatase; PEP, phosphoenol pyruvate; LCFA, long-chain fatty acids; CPT II, carnitine palmitoyltransferase II. (Postic and Girard, J Clin Invest., 2008)

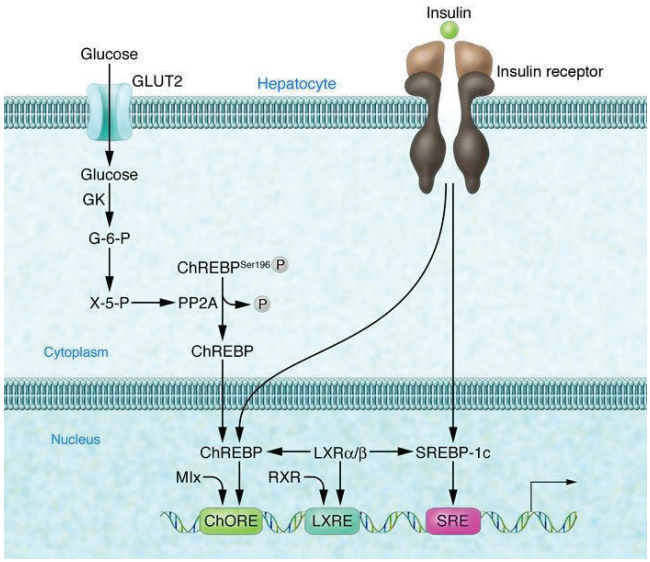

Figure 6: Lipogenesis mediated by ChREBP and SREBP1 in the liver

ChREBP is located in the cytoplasm under low plasma glucose concentration due to its phosphorylation on Ser196. As the plasma glucose level rises, glucose enters hepatocytes and is rapidly equilibrated due to the low-K_m glucose transporter GLUT2. Glucose phosphorylation is then initiated by GK, leading to the formation of xyulose-5-phosphate (X-5-P) by the hexose monophosphate shunt pathway. Increased xyulose-5-phosphate in turn appears to cause dephosphorylation of Ser196 on ChREBP (probably through activation of PP2A), thereby allowing ChREBP to enter the nucleus and affect gene expression. Insulin appears to affect hepatic lipogenesis principally by increasing transcription of both ChREBP and SREBP-1c genes. Furthermore, SREBP-1c function is also activated by insulin at the post-translational level. Activated SREBP-1c binds to SRE (Sterol Regulatory Element) sequences found on the promoters of its target genes. LXR is transcription factor that can also upregulate ChREBP and SREBP-1c gene expressions. In order to activate lipogenic gene transcription, LXR needs to dimerize with RXR. (Shiota et al., 2008)

Therefore, the dephosphorylated form of glycogen synthase is the active form. In parallel, PP1 and G6P stimulate the inhibition of glycogen degradation (Newgard et al., 2000). G6P is also a strong agonist of glycogen synthase. Indeed, this metabolite activates the enzyme allosterically and stimulates its dephosphorylation (Villar-Palasí and Guinovart, 1997).

I.1.2) *De novo* lipid synthesis in the liver is induced by excess of glucose

When the storage capacity of glucose in the form of glycogen in the liver is exceeded, glucose is stored under the form of lipids. Indeed, high glucose concentrations activate the glycolysis pathway, leading to the production of pyruvate (*Figure 5*). Pyruvate is then transported in the mitochondria, where it is converted into acetyl-CoA, a precursor for the synthesis of fatty acids and cholesterol. Fatty acid synthesis is initiated by the conversion of acetyl-CoA into malonyl-CoA *via* acetyl-CoA carboxylase (ACC). Furthermore, malonyl-CoA is transformed into palmitate *via* fatty acid synthase (FAS). Fatty acids can then be elongated, desaturated, esterified and used to synthesize triglycerides (TG). TG are stored in lipid vesicles, which can either stay in the cytosol or be transported to the adipose tissue *via* the export of very low density lipoproteins (VLDL) (Postic and Girard, 2008).

The key enzymes involved in TG synthesis i.e. ACC and FAS are activated by insulin (Girard et al., 1994). This activation is mediated *via* sterol regulatory element binding protein 1 (SREBP1). Indeed, when activated by insulin, SREBP1 binds to the promoters of *FASN*, *ACACA* and *GCK*, and therefore activates not only lipogenesis, but also glycolysis needed for the production of pyruvate (Foufelle and Ferré, 2002). SREBP1 is not the only actor involved in this broad regulation. During postprandial periods, carbohydrate responsive element binding protein α (ChREBP-α) is also activated by glucose metabolism (*Figure 6*). This transcription factor senses glucose levels in the cells and can also induce lipid synthesis, making it an important bridge between glucose and lipid metabolisms (Abdul-Wahed et al., 2017). Recently, a new glucose-insensitive isoform of ChREBP, called ChREBP-β has been identified. Interestingly, a feed-forward mechanism has been suggested placing ChREBP-β under the transcriptional control of ChREBP-α. In this scenario, ChREBP-α is first activated by

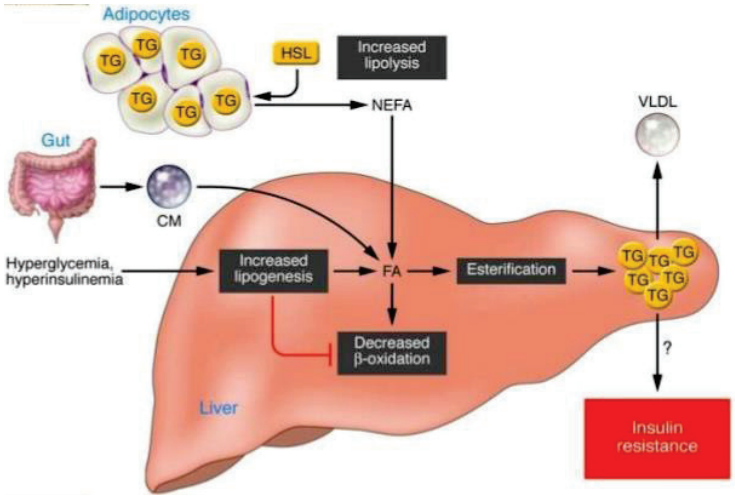

Figure 7: Representation of different sources of lipids leading to hepatic steatosis

Increased adipocyte lipolysis can lead to an increase in NEFA production, which can enter the liver and increase the pool of FA. Increased glucose levels and deregulated insulin signaling can subsequently activate lipogenesis, again increasing the pool of hepatic FA. Furthermore, by-products of the lipogenesis pathway can inhibit lipid oxidation which results in accumulation of lipids. Finally, a decrease in VLDL export from the liver can also contribute to hepatic steatosis. Hepatic steatosis is tightly associated to insulin resistance development.
TG – triglycerides, NEFA – non-esterified fatty acids, FA – fatty acids, VLDL – very low density lipoproteins

(Postic and Girard,. 2008)

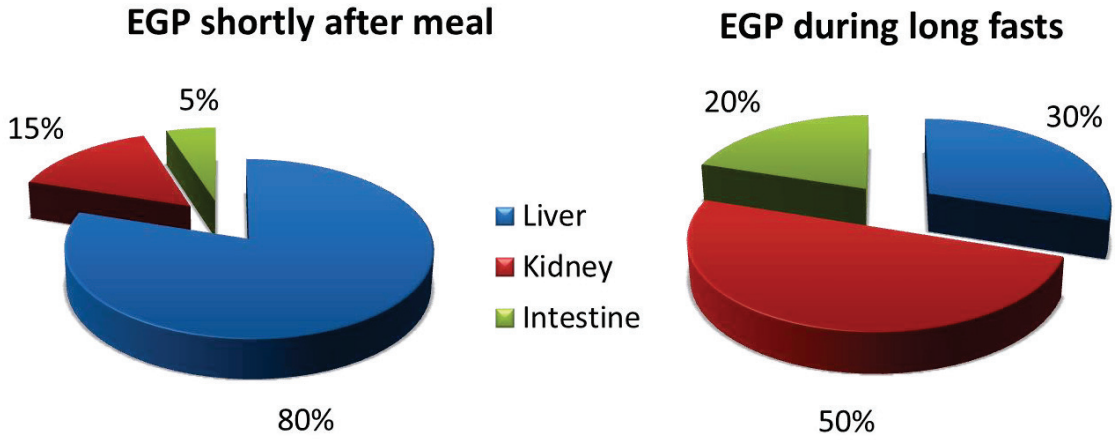

Figure 8: Relative contribution of the 3 organs capable of endogenous glucose production

These data were obtained in rats at 6h (left) of fasting and at 48h of fasting (right).

(Mithieux et al., 2017)

glucose metabolism and, in turn, stimulates Chrebp-β expression, amplifying the response to glucose (Abdul-Wahed et al., 2017). The main activator of ChREBP-α is xylulose-5-phosphate produced in the pentose phosphate pathway (PPP), which activates protein phosphatase 2A (PP2A), dephosphorylating ChREBP-α. ChREBP-α can then be translocated into the nucleus and induce the transcription of its target genes, such as *FASN*, *ACACA* and the liver pyruvate kinase (*L-PK*). Recent studies showed that G6P can also induce ChREBP-α's transcriptional activity (Dentin et al., 2012), rendering this transcription factor even more complex, joining glucose and lipid metabolisms.

While hepatic lipid synthesis is a normal physiological process, excessive storage of lipids in the liver represents a pathological state. Indeed, increased amount of lipid droplets in the liver leads to the development of steatosis. The degree of steatosis in the liver can vary greatly, according to the molecular origin of this event. Hepatic steatosis is the major hallmark of all of the non-alcoholic fatty liver diseases (NAFLD). Indeed, NAFLD are an array of metabolic diseases all characterized by hepatic lipid accumulation, which can be induced by viral, environmental or genetic factors. On a molecular level, lipid accumulation in NAFLD can be due to an excessive lipid synthesis or import of fatty acids, a decrease in lipid degradation or problems in the export of lipids out of the liver (*Figure 7*) (Postic and Girard, 2008). Histologically, NAFLD occurs as a spectrum from mild hepatic steatosis only, to non-alcoholic steatohepatitis (NASH), characterized by hepatocellular injury and inflammation, up to cirrhosis linked to marked fibrosis. The pathogenesis of NAFLD is frequently related to insulin resistance and, it is generally found in individuals who have central obesity or diabetes (Smith and Adams, 2011). Furthermore, NAFLD predisposes the liver to hepatic cancer development and a correlation between the two has been proven many times (Font-Burgada et al., 2016; Michelotti et al., 2013).

I.2) What happens during fasting periods?

During fasting periods, the decrease in blood glucose levels, due to the utilization of glucose as an energy source, is compensated by the induction of EGP. Glycogenolysis is the first pathway that is activated at the end of post-prandial periods,

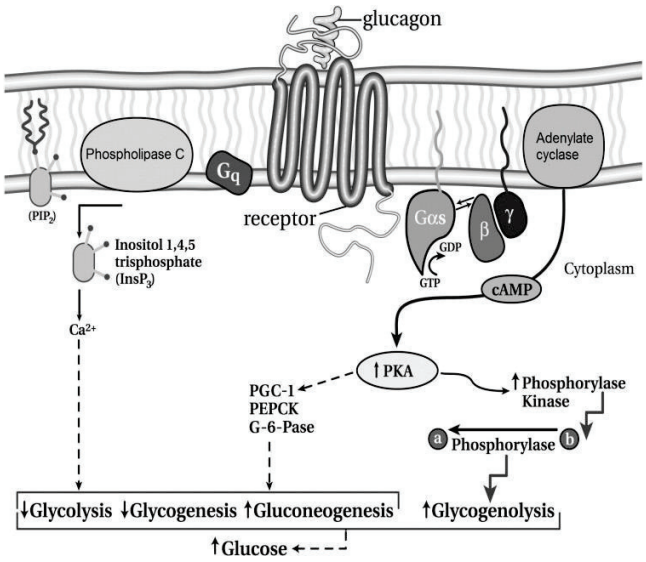

Figure 9: Molecular action of glucagon in glucose metabolism

Secreted glucagon binds to the glucagon receptor, leading to subsequent activation of the coupled G proteins. The G proteins lead to the activation of adenylate cyclase, increase in intracellular cAMP levels, and subsequent activation of protein kinase A (PKA). They also lead to the activation of phospholipase C, production of inositol 1,4,5-triphosphate, and subsequent release of intracellular calcium.
These molecular events translate in the modulation of glycogenolysis, glycogenesis, gluconeogenesis, and glycolysis, in order to enhance glucose production.

(Jiang and Zang, 2003)

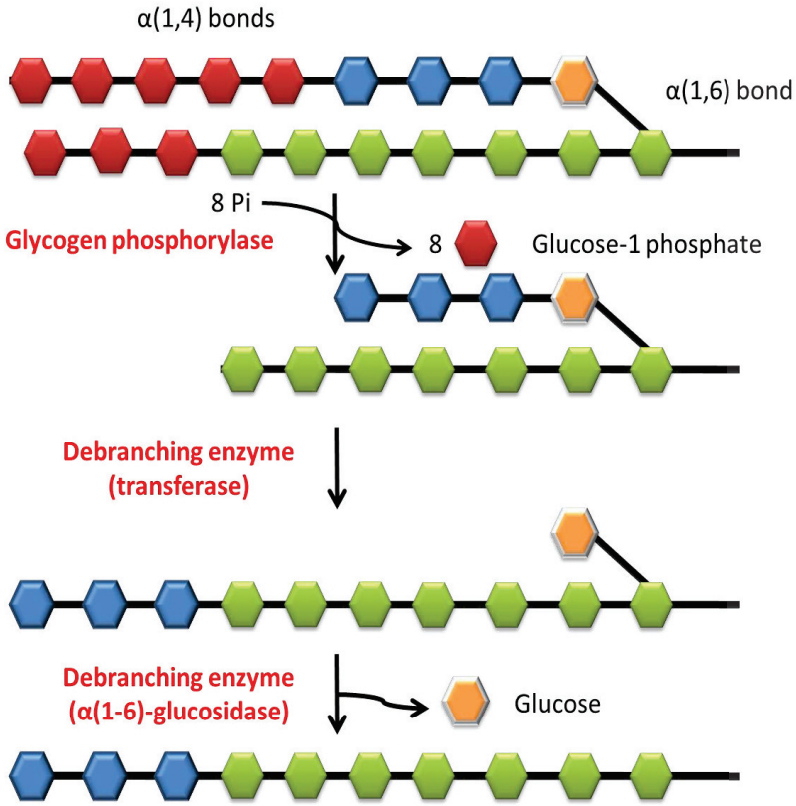

Figure 10: Glycogen degradation process

Degradation of glycogen is done by glycogen phosphorylase and glycogen debranching enzyme (GDE) to produce glucose-1 phosphate, which is immediately converted mainly into glucose-6 phosphate.

while gluconeogenesis (GNG) progressively takes place as fasting continues (Mithieux et al., 2017). Indeed, at the beginning of a post-absorptive period, a time where liver glycogen stores are still present and are being mobilized, the liver accounts for at least 80% of EGP (*Figure 8*). Renal GNG at this time accounts for about 15-20% and intestinal GNG is low, estimated between 5 and 10% of EGP (Croset et al., 2001; Mithieux et al., 2006). On the other hand, the repartition is different after 24h of fasting, a time at which glycogenolysis has ended in rodents because of glycogen store depletion. Indeed, renal and intestinal GNG are progressively activated at this time point. If the fast is further prolonged, in the next 48h-72h, renal and intestinal EGP can then contribute up to 50% and 20%, respectively (Croset et al., 2001; Mithieux et al., 2004a).

The decrease in blood glucose levels during fasting periods stimulates the secretion of glucagon by α cells of the pancreas, and thereby the ratio glucagon / insulin is increased. To increase blood glucose, glucagon acts rapidly and promotes hepatic glucose output by increasing glycogenolysis and GNG and by decreasing glycogen synthesis and glycolysis in a concerted fashion *via* multiple mechanisms summarized in *Figure 9* (Jiang and Zhang, 2003). While glucagon is mainly known to modulate hepatic EGP, it has recently been shown to modulate the transcription of *G6PC* in the kidneys and intestine, thus modulating renal and intestinal glucose production (Mutel et al., 2011b).

I.2.1) Normal glycaemia is maintained *via* glycogenolysis in post-absorptive state

Hepatic glycogen degradation is the first catabolic pathway activated as response to glucose decrease. One of the main enzymes involved in glycogen degradation is glycogen phosphorylase, which releases G1P units from the linear chains of glycogen, by breaking α(1-4) bonds (*Figure 10*). Once there are only 4 residues of glucose left in the linear chain, glycogen debranching enzyme (GDE) transfers 3 of the 4 residues left on another linear chain with its transferase subunit. Then the α(1-6)-glucosidase subunit of GDE hydrolyzes the α(1-6) bond of the last residue, thus releasing another glucose molecule and completing the degradation of the chain (*Figure 10*). Furthermore, G1P molecules previously released are isomerized into

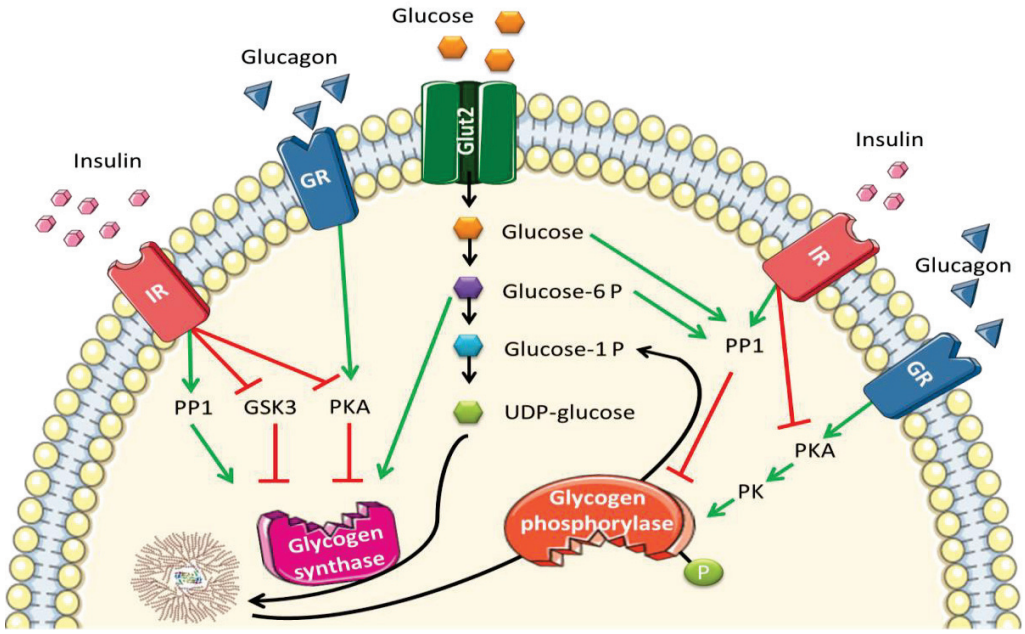

Figure 11: Schematic representation of the regulation of hepatic glycogen metabolism by insulin and glucagon

Insulin stimulates glycogen synthesis *via* the activating phosphorylation of PP1, which dephosphorylates both glycogen synthase (activation) and glycogen phosphorylase (inhibition). PP1 is also stimulated by glucose and glucose-6 P. Glucose-6 P also stimulates glycogen synthase allosterically. Furthermore, insulin inhibits the phosphorylation of the glycogen synthase, by inhibiting GSK3 and PKA. During fasting periods, glucagon inhibits the synthesis of glycogen and increases its degradation by increasing the phosphorylation of the glycogen synthase (inhibition) *via* PKA and glycogen phosphorylase (activation) *via* PK. (green arrows – activation; red – inhibition)
UDP glucose - uridine diphosphate glucose; GSK3 - glycogen synthase kinase 3; PP1 - protein phosphatase 1; PKA - protein kinase A; PK - phosphorylase kinase; IR – insulin receptor; GR – glucagon receptor.

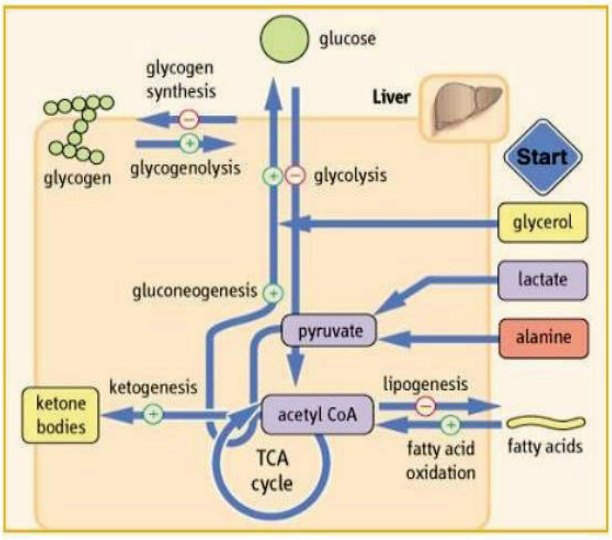

Figure 12: Entry of different metabolites in gluconeogenesis in the liver

Gluconeogenesis is not a linear process. Indeed, different metabolites (Acetyl-CoA, amino acids, glycerol etc.) issued from various metabolic pathways can contribute to this anabolic process. Pathways which are positively regulated by glucagon are marked in green, negatively regulated pathways are marked in red.

(Veerendra, 2014)

G6P via phosphoglucomutase. The last stage is the hydrolysis of G6P into glucose and inorganic phosphate, which is performed by glucose-6 phosphatase (G6Pase). This enzyme is expressed in the liver, kidneys and intestine, but not in the muscles. Therefore, G6P is not converted into glucose in the muscles nor it is released in the bloodstream for glucose maintenance, but it is used only in glycolysis, producing energy for muscle contraction.

Glycogen phosphorylase is a main switch responsible for the regulation of glycogenolysis. The inactive form b of this enzyme is activated by phosphorylation *via* phosphorylase kinase (PK), turning glycogen phosphorylase into its active form, called form a. Furthermore, glucose molecules can bind to the active site of the glycogen phosphorylase, inhibiting the enzyme by competing with its substrate and rendering it more sensitive to its inhibitor, the phosphorylase phosphatase (PP1) (Bollen et al., 1998). G6P is also involved in glycogenolysis inhibition, by inducing PP1 and by inhibiting PK (Aiston et al., 2003). Glycogen stores are considered to contribute to EGP for about 10-12 hours in rodents and 20h in human subjects (Mithieux et al., 2017; Mutel et al., 2011b).

To conclude, glycogen metabolism is a highly complex process, finely tuned by insulin and glucagon, in order to maintain normal blood glucose (*Figure 11*). Nevertheless, these hormones are not the only regulators of glycogen metabolism. The nervous system has been long-known to modulate glycogen metabolism independently. For example, stimulation of the splanchnic nerve system causes glycogenolysis in the liver by activation of glycogen phosphorylase, whereas stimulation of the vagus nerve system promotes glycogenesis in the liver by activation of glycogen synthase (Shimazu, 1981; Shimazu and Fujimoto, 1971). These stimuli are in dependence of the glucose levels detected by the brain *via* the glucose sensors, such as the portal vein. Thus the regulation of EGP in the liver is tightly regulated by the central nervous system (Yi et al., 2010).

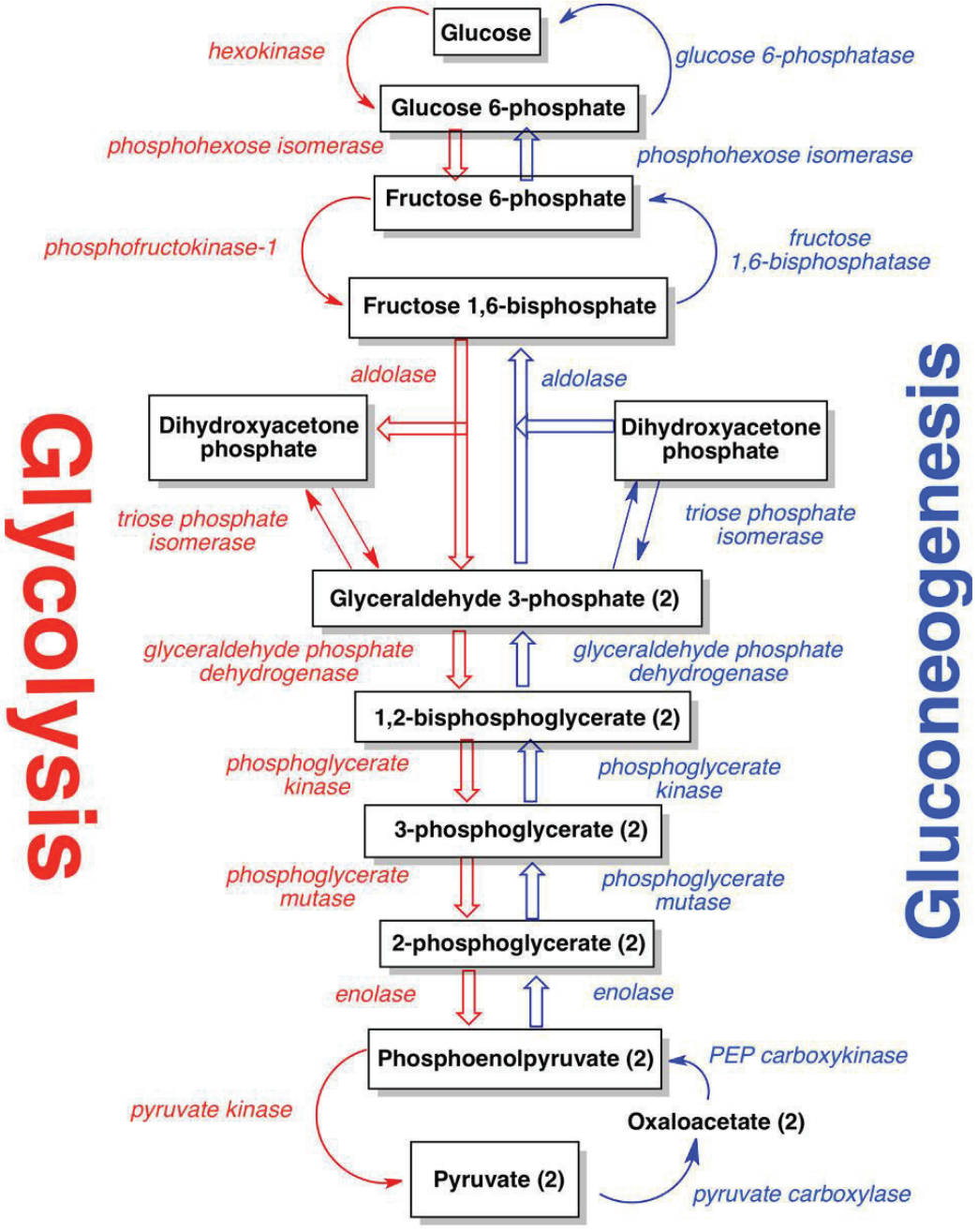

Figure 13: A representation of the gluconeogenesis pathway, in comparison to glycolysis

I.2.2) Normal glycaemia is maintained by gluconeogenesis during long-term fasting

GNG is the *de novo* synthesis of glucose from non-carbohydrate substrates. GNG consists of a maximum of 11 reactions (depending of the point of entry of the given metabolite), representing a crosstalk between the carbohydrate, lipid and protein metabolisms (*Figure 12*). Most of the reactions in GNG are the reverse steps of glycolysis (*Figure 13*). The only three reactions which are irreversible are: the transformation of pyruvate to phosphoenolpyruvate (PEP) *via* pyruvate carboxylase and phosphoenolpyruvate carboxykinase (PEPCK); the transformation of fructose-1,6 bisphosphate into fructose-6-phosphate by fructose-1,6-biphosphatase and the hydrolysis of G6P into glucose and inorganic phosphate by G6Pase. Thus the last reaction of the GNG pathway is common with glycogenolysis.

Pyruvate, lactate, amino acids and glycerol are the main substrates used in GNG (*Figure 12*). While alanine and lactate are mainly used in hepatic GNG, glutamine which is released by muscles during proteolysis, is mainly used in the kidneys and intestine to produce glucose (Mithieux et al., 2017). Glutamine cannot be used by the liver due to the kinetic properties of the liver glutaminase (Watford, 1993). Nevertheless, the degradation of glutamine in the gut leads to the production of alanine and pyruvate, captured by the liver and subsequently used for GNG, leading to the conclusion that intestinal GNG can also supply hepatic GNG (Croset et al., 2001). Interestingly, intestinal GNG can also use propionate produced by microbiota as substrate (De Vadder et al., 2014). Finally, adipose lipolysis can contribute by providing glycerol, a substrate used for GNG in all three gluconeogenic organs.

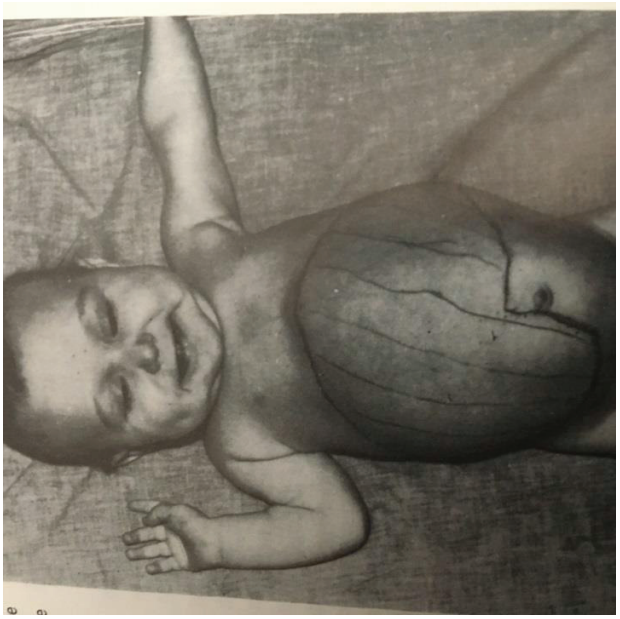

Figure 14: Hepatomegaly in a child with GSDI

The abdomen is enlarged due to the hepatomegaly induced by strong glycogen accumulation in the liver.

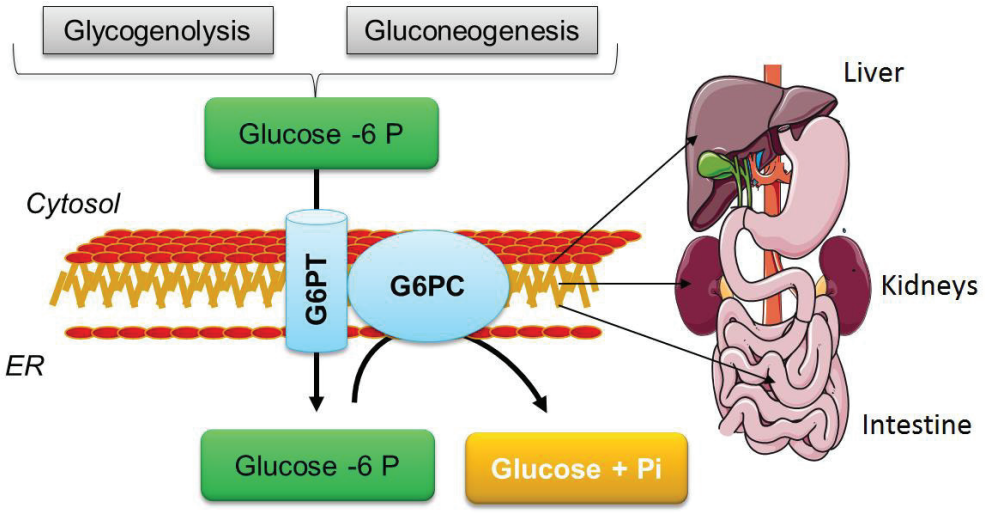

Figure 15: Glucose-6 phosphatase (G6Pase) complex

G6Pase is expressed in the liver, kidneys and intestine. Glucose-6-phosphate is transferred from the cytosol into the endoplasmic reticulum (ER) by the transport subunit (G6PT) of the enzyme, while the catalytic subunit (G6PC) converts glucose-6-phosphate into free glucose and inorganic phosphate.

II) Molecular basis of glycogen storage disease type I

Glycogen storage disease type I (GSDI) is a rare genetic autosomal recessive disease, with an incidence rate of 1/100,000 births, due to a deficiency of G6Pase. Consequently, patients with GSDI cannot produce glucose during short fasts and suffer from severe hypoglycemia.

GSDI is also known as the von Gierke's disease, named after Edgar von GIerke, who was a German pediatrician that first described the disease in 1929. Indeed, his autopsy reports described 2 children with large livers (hepatomegaly) containing excessive amount of glycogen (*Figure 14*). This hepatomegaly was due to the inability of the G6Pase-deficient hepatocytes to degrade glycogen. He also reported similar findings in the kidneys (nephromegaly). Later on, in 1952, Cori and Cori reported 6 similar patients (Cori and Cori, 1952). Interestingly, two of the patients had almost total deficiency of hepatic G6Pase activity, whereas the other 4 patients had normal enzyme activity determined in membrane-denatured conditions. These data were explained later, in the 1980s, when it was discovered that G6Pase was composed of two subunits (catalytic subunit G6PC and transport subunit G6PT) and that the loss of either one leads to the same pathological condition, which is GSDI (Narisawa et al., 1982). Thus the 4 patients analyzed by Cori and Cori, which had normal G6Pase activity in denatured conditions, actually had a loss of G6PT, and normal G6PC. This led to the conclusion that G6Pase activity assays need to be performed in non-denatured samples in order to detect a deficiency in G6PT. More importantly, this study highlighted the importance of the integrity of the membrane for the normal functioning of the G6Pase complex.

II.1) Glucose-6 phosphatase complex & mutations

G6Pase is an enzyme that has the important role to convert G6P into glucose and to assure the maintenance of normal blood glucose levels. Thus G6Pase completes the last reaction of both glycogenolysis and GNG (*Figure 15*). As mentioned, this enzyme is composed of a catalytic subunit G6PC, encoded by *G6PC* and a transport subunit G6PT, encoded by *SLC37A4*. In the genome, *G6PC* is located at 17q21.31, and

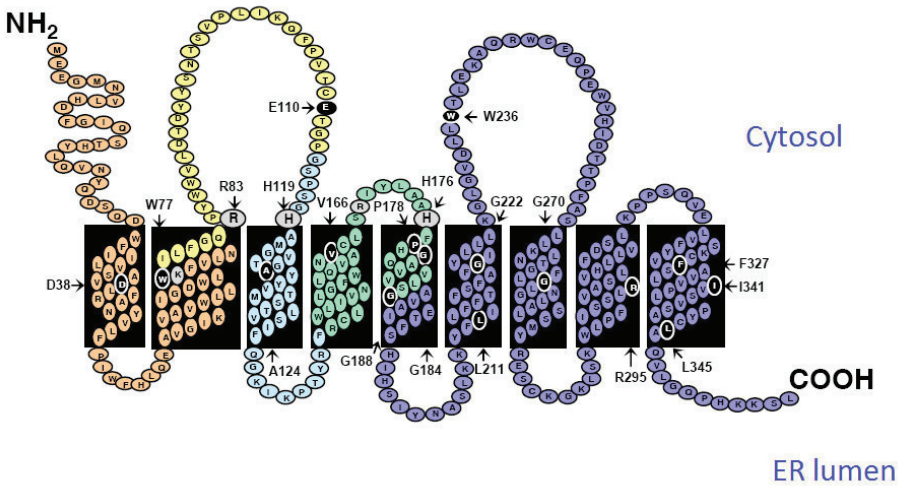

Figure 16: Representation of the structure of G6PC

The amino acids coded by each exon are represented in 5 different colors. Amino acids represented in black are the ones which were described as mutated in GSDI. Amino acids in grey are a part of the catalytic site.

(Adapted from Pan et al., 1998)

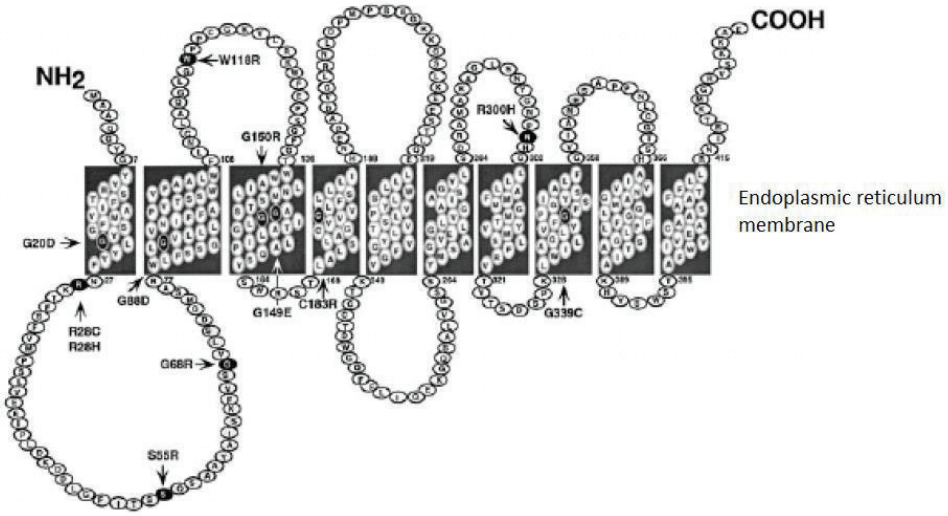

Figure 17: Representation of the structure of G6PT

Amino acids represented in black are the ones which were described as mutated in GSDI.

(Adapted from Pan et al., 1998)

SLC37A4 is located at 11q23.3. *G6pc / G6PC* was first isolated in mice and humans in 1993 (Lei et al., 1993; Shelly et al., 1993). It is composed of 5 exons, coding for a protein of 357 amino acids, with a molecular mass of 37 kDa (Lei et al., 1993, 1994; Mithieux et al., 1995) (*Figure 16*). Interestingly, G6PC is anchored at the membrane of the endoplasmic reticulum (ER) by 9 transmembrane domains and its catalytic site is located in the ER lumen, composed of 5 highly conserved amino acids (Ghosh et al., 2002). Other isoforms of G6PC have been identified, such as G6PC2 or IGRP (islet-specific G6Pase related protein) and G6PC3 or UGRP (ubiquitously expressed G6Pase catalytic subunit related protein). These isoforms have a moderate sequence homology with G6PC, but the catalytic structures are very similar (Hutton and O'Brien, 2009). G6PC2 is expressed in the pancreatic islets, yet several studies failed to report a G6Pase activity of this isoform (Arden et al., 1999; Martin et al., 2001). On the other hand, G6PC3 is expressed ubiquitously (Martin et al., 2002). This isoform does not seem to be involved in glucose metabolism regulation, since G6PC3 knock-out mice do not present hypoglycemia, but it rather translates to severe congenital neutropenia (Banka and Newman, 2013; Boztug et al., 2009).

SLC37A4 coding for G6PT was isolated in 1997 in humans (Gerin et al., 1997). This gene contains 9 exons and codes for a protein composed of 429 amino acids, with a molecular weight of 46 kDa, represented in *Figure 17* (Annabi et al., 1998; Gerin et al., 1997). G6PT is responsible for the import of G6P from the cytoplasm to the ER lumen, where it is hydrolyzed by G6PC (van Schaftingen and Gerin, 2002). G6PT is a transporter which is expressed ubiquitously, whereas G6PC is present only in the liver, kidneys and intestine (Minassian et al., 1996; Mithieux et al., 2004b; Rajas et al., 1999). To be more precise, the G6Pase complex was detected in hepatocytes, in proximal tubules of the kidney cortex and at the top of the villi of the small intestine, co-expressed with PEPCK-c, another key enzyme in GNG. The restriction of the expression of G6PC to these organs is mediated by transcription factors such as HNF1 (hepatic nuclear factor 1), C/EBP (CAAT / enhancer binding protein) and CDX (caudal-related transcription factor) (Gautier-Stein et al., 2005; Xu et al., 2007). Furthermore, intrahepatic bile ducts, collecting tubes of the nephron, urinary epithelium in the calices of the kidney, and the crypts of the small intestine also express G6Pase, while PEPCK

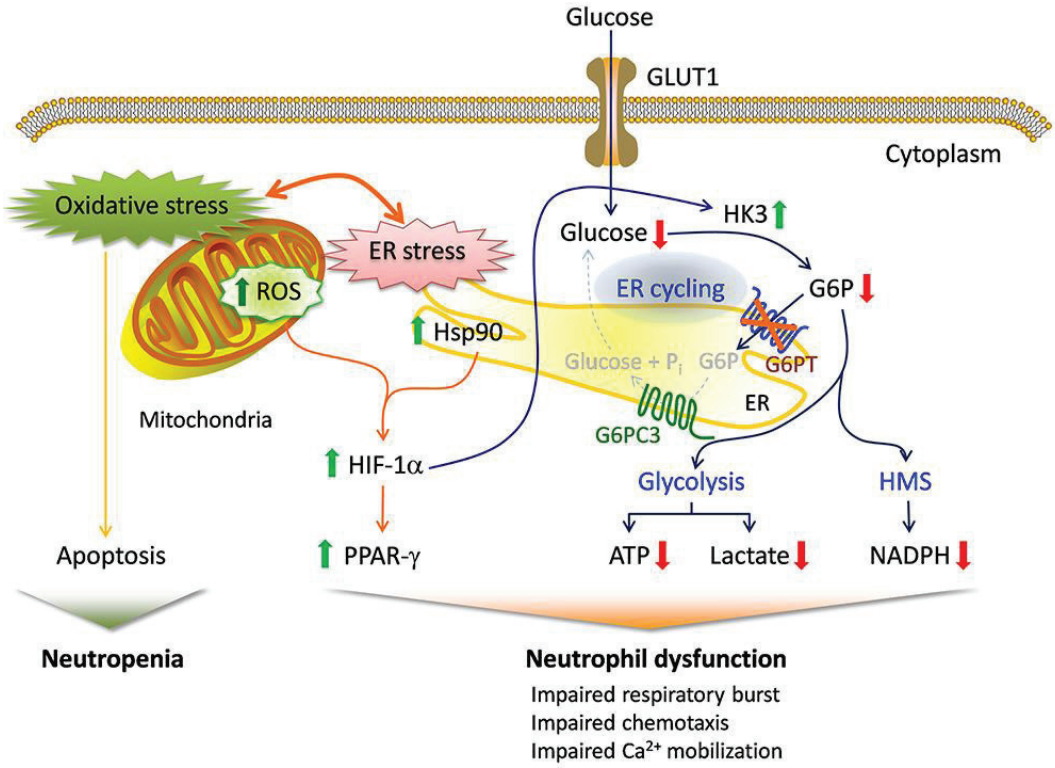

Figure 18: Proposed mechanisms underlying neutrophil dysfunction in G6PT-deficiency

Glucose transported into the cytoplasm *via* GLUT1 is metabolized by hexokinase (HK) to G6P, which participates in three major pathways: glycolysis, the hexose monophosphate shunt (HMS), and endoplasmic reticulum (ER) cycling. In cycling, G6P enters the ER *via* G6PT, where it can accumulate until it is hydrolyzed to glucose by G6Pase-β (G6PC3) and transported back into the cytoplasm. By limiting cytoplasmic glucose/G6P availability, cycling regulates the other two cytoplasmic pathways for G6P metabolism. Disruption of ER cycling in G6PT–deficient neutrophils results in reduced glucose uptake and impaired energy homeostasis and thus functionality. The underlying cause of neutropenia in G6PT-deficiency is enhanced neutrophil ER stress and oxidative stress. The increases in Hsp90 and reactive oxygen species (ROS) in G6PT–deficient neutrophils stabilize HIF-1α (hypoxia-inducible factor-1α), an upstream activator of PPAR-γ (peroxisome proliferators−activated receptor-γ).The increase in PPAR-γ downregulates neutrophil respiratory burst, chemotaxis, and calcium mobilization activities. Thick arrows indicate the changes caused by a defect in G6PT activity.

(Jun et al., 2014)

is not co-expressed here. Thus this expression was suggested to be related to the transepithelial transport of glucose characteristic of these tissues, rather than to the neoformation of glucose (Rajas et al., 2007).

As mentioned, G6PT protein is expressed ubiquitously. In addition to its role in G6Pase activity, G6PT plays a crucial role in neutrophils (Jun et al., 2014). Thus G6PT deficiency results in enhanced apoptosis of neutrophils and therefore causes neutropenia (*Figure 18*). As pointed out above, neutropenia is also observed in G6PC3-deficient mice and patients (Jun et al., 2012). Thus deficiency in either G6PT or G6PC3 was suggested to entail a loss of the G6PC3-G6PT complex, resulting in energy impairment and enhanced apoptosis in neutrophils (Jun et al., 2010, 2014).

Interestingly, a variant of G6PT (vG6PT) with additional 66 bp in exon 7 is expressed in the brain, heart and muscles, but not in the liver, kidneys and neutrophils (Lin et al., 2000). vG6PT has been shown to have a transport role as G6PT, yet its implication in pathological conditions remains unknown. Therefore this exon could have an important role in the transport function of G6PT and it could be involved in the substrate specificity of this transporter.

Depending on which subunit of the G6Pase is mutated, GSDI can be further classified as GSD type Ia (80% of GSDI cases) or type Ib (20% of GSDI cases). GSD type Ia is due to mutations in *G6PC* and GSDI type Ib is due to mutations in *SLC37A4*. There are at least 85 known mutations of the *G6PC* gene (Bruni et al., 1999; Chou and Mansfield, 2008), including missense, nonsense, insertion / deletion, and splicing mutations that can affect the catalytic site, transmembrane domains or the ER lumen domains (*Figure 16*). Nowadays, it is known that the degree to which this deficiency translates into a pathological state is in relation to the type of mutation leading to a partial or total loss of G6Pase activity (Chou and Mansfield, 2008; Matern et al., 2002; Peeks et al., 2017). Moreover, G6PT transport capacity can also be either completely absent or partially functional, depending on how the mutation affects the integrity of the G6PT protein (Chou and Mansfield, 2008).

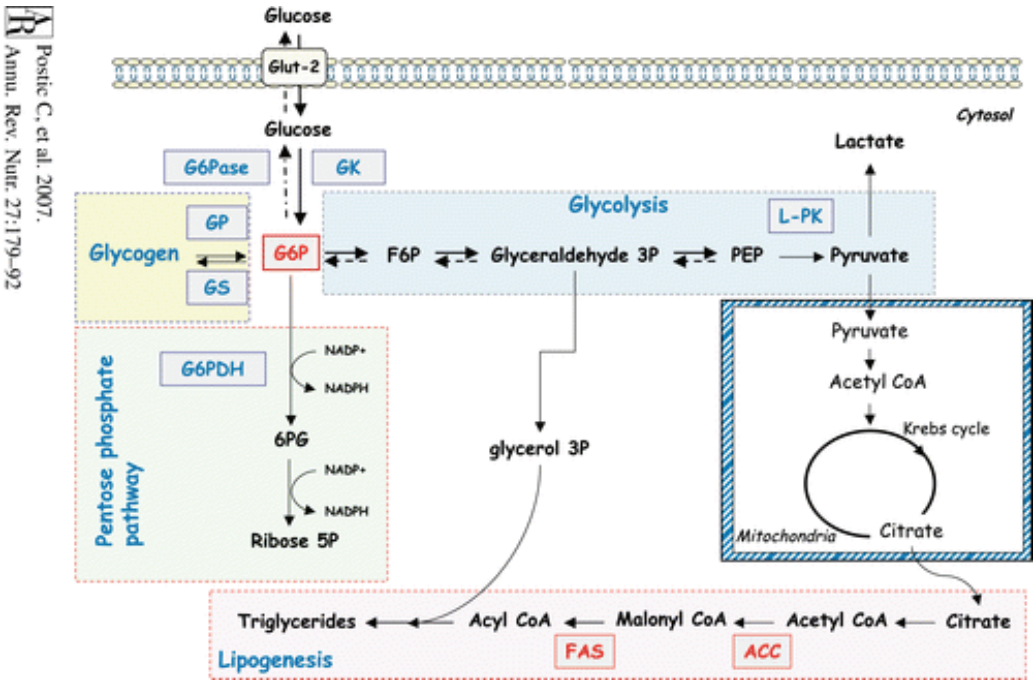

Figure 19: Metabolic pathways activated by glucose-6 phosphate

Increased levels of G6P activate the glycolysis pathway, glycogen synthesis, lipogenesis and the pentose phosphate pathway.

(Postic et al., 2007)

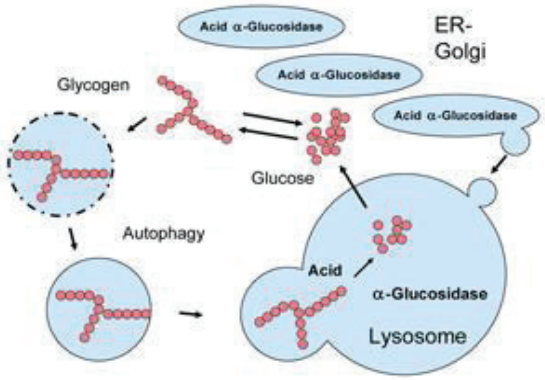

Figure 20: Degradation of glycogen in the lysosomes by acid α-glucosidase

In the cytoplasm, glucose is converted to glycogen as a way to store energy. When energy is needed, glycogen is again degraded to glucose. Some of the glycogen in the cytoplasm is captured in a membrane and transported to the lysosomes in a process called 'autophagy'. In the lysosomes, this glycogen is degraded by acid α-glucosidase, releasing free glucose.

(Pompe Center, 2007)

II.2) Metabolic consequences of glucose-6 phosphatase deficiency

In addition to the absence of glucose production, the loss of G6Pase activity translates to an increase of intracellular G6P in hepatocytes and renal tubular cells. G6P accumulation is responsible for the induction of glycogen synthesis, *de novo* lipogenesis, glycolysis and PPP (*Figure 19*).

II.2.1) Glycogen synthesis activation

As described earlier, glycogen synthesis is a process highly induced by G6P availability. Thus glycogen is stored in excessive amounts in the liver and kidneys in GSDI, resulting in hepatomegaly and nephromegaly. It is noteworthy that while the normal liver has the capacity to store glycogen, kidneys do not store glycogen in normal physiological conditions.

For a long time, it was an enigma how GSDI patients retain a limited capacity for EGP despite the loss of G6Pase activity. Thus scientists have been investigating alternative residual glucose production pathways that could ensure limited glucose production. Interestingly, it has recently been discovered by our team (in collaboration with Dr. M. Oosterveer, Netherlands) that the metabolic flux through glycogen phosphorylase is increased in L.G6pc-/- livers, coupled to the release of free glucose *via* GDE and lysosomal glycogen breakdown (*Figure 20*) (Hijmans et al., 2017). Thus an important turnover of glycogen synthesis and degradation was highlighted in the liver of these mice, which could explain the limited glucose production in GSDI. Finally, the same study indicated that GK activity is 95% reduced, due to a metabolic adaptation of GSDI hepatocytes, in order to reduce G6P production in the liver as much as possible.

II.2.2) Glycolysis activation

Glycolysis is a pathway which is not very efficient in energy production (2 ATP/ glucose), but it leads to the creation of 2 pyruvate molecules. Pyruvate is further used as a substrate for Krebs cycle and mitochondrial oxidative phosphorylation (OXPHOS) (import of pyruvate from the cytoplasm to the mitochondria and conversion to acetyl CoA), or diverted toward the production of lactate.

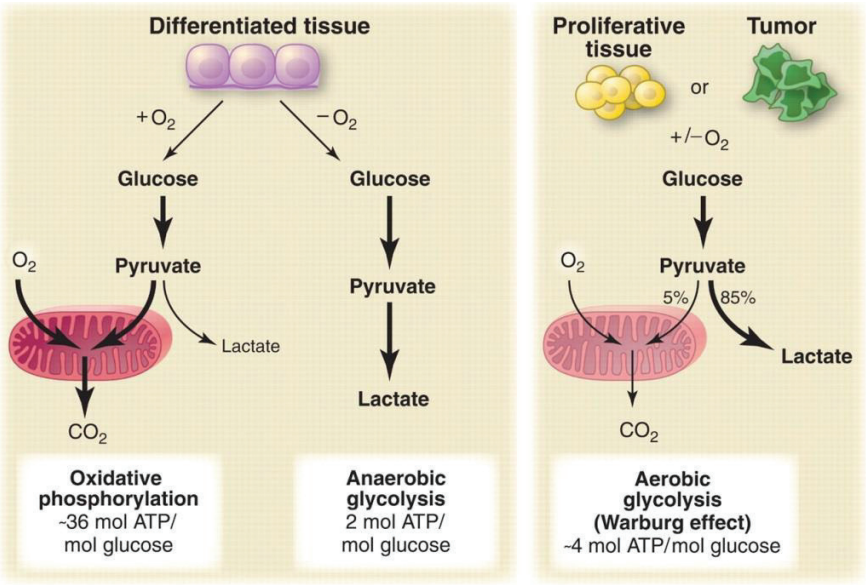

Figure 21: Schematic representation of the differences between oxidative phosphorylation, anaerobic glycolysis, and aerobic glycolysis (Warburg effect)

In the presence of oxygen, non-proliferating tissues first metabolize glucose to pyruvate *via* glycolysis and then completely oxidize most of that pyruvate in the mitochondria to CO_2 *via* oxidative phosphorylation (OXPHOS). Because oxygen is required as the final electron acceptor to completely oxidize the glucose, oxygen is essential for this process. When oxygen is limiting, cells can redirect the pyruvate generated by glycolysis away from OXPHOS by generating lactate (anaerobic glycolysis). This generation of lactate during anaerobic glycolysis allows glycolysis to continue (by cycling NADH back to NAD+), but results in minimal ATP production when compared with OXPHOS. Warburg observed that cancer cells tend to convert most glucose to lactate regardless of whether oxygen is present (aerobic glycolysis). This property is shared by normal proliferative tissues. Nevertheless, aerobic glycolysis is less efficient than OXPHOS for generating ATP. In proliferating cells, ~10% of the glucose is diverted into biosynthetic pathways upstream of pyruvate production. (Vander Heiden et al., 2009)

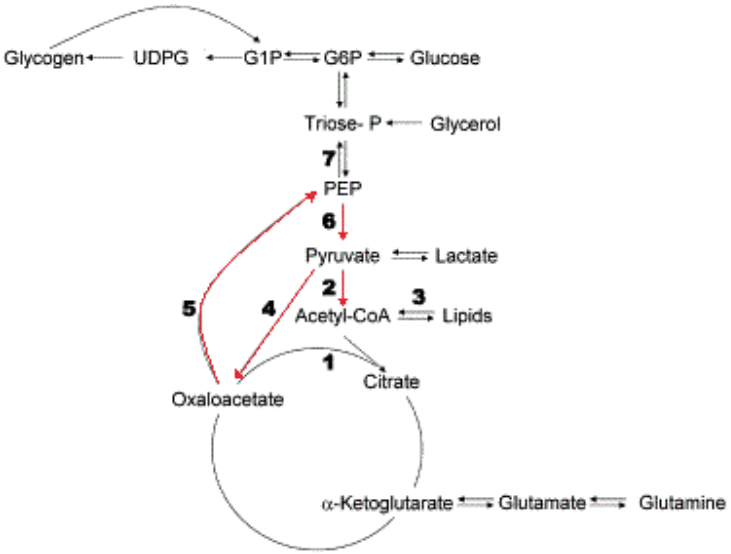

Figure 22: Increased pyruvate cycling in GSDI patients

Red arrows indicate significantly increased metabolic flows in GSDI patients, compared to normal subjects.

(Jones et al., 2009)

Increased G6P levels in GSDI induce hyper-activation of glycolysis (Hijmans et al., 2017; Sun et al., 2009). Interestingly, glycolysis is frequently up-regulated in cancer cells by preferential expression of transporters and enzyme isoforms that drive glucose flux forward, in order to adapt to the anabolic demands of cancer cells (Hay, 2016). This phenomenon of increased glycolysis, often accompanied by a decrease in OXPHOS, even in the presence of oxygen, is known as the Warburg effect (*Figure 21*). Therefore, a «Warburg-like» phenotype has been demonstrated in several studies in the hepatocytes of GSDI patients and animal models (Hijmans et al., 2017; Sun et al., 2009). This hyper-activation of glycolysis leads to the increase in pyruvate and a subsequent lactate production, confirmed by lactic acidosis (an increase in plasmatic lactate) in patients and animal models (Kishnani et al., 2014; Mutel et al., 2011a). As mentioned, down-regulation of GK has been confirmed in GSDI livers, an event frequently observed in glycolytic hepatocellular carcinomas (Guzman et al., 2015). The origin of GK downregulation in GSDI hepatocytes was assumed to be due to their attempt to limit glucose to G6P conversion (Hijmans et al., 2017). Nevertheless, G6P still remains elevated, since it cannot be converted back to glucose; it is blocked in the form of G6P and has to be metabolized through glycolysis. Therefore, G6P exerts a substrate pressure forcing the activation of this pathway, and the subsequent activation of lactate production.

Besides G6P production, another step which assures the commitment of glucose to glycolysis is the conversion of phosphoenolpyruvate into pyruvate by the liver pyruvate kinase (L-PK), resulting in the production of ATP. In GSDI, an increase in the expression of L-PK has been reported (Grefhorst et al., 2010; Jones et al., 2009). Interestingly, since GNG is blocked in GSDI, pyruvate recycling is significantly increased, as highlighted by the increase in pyruvate ➔ acetyl CoA, pyruvate ➔ oxaloacetate (OAA), OAA ➔ PEP and PEP ➔ pyruvate conversions (Jones et al., 2009) (*Figure 22*). This could further contribute to lactate production in GSDI patients, accounting for lactic acidosis in the plasma.

To summarize, even though different molecular mechanisms are involved in the reprogramming of cancer cells and GSDI hepatocytes, these cells reflect similar

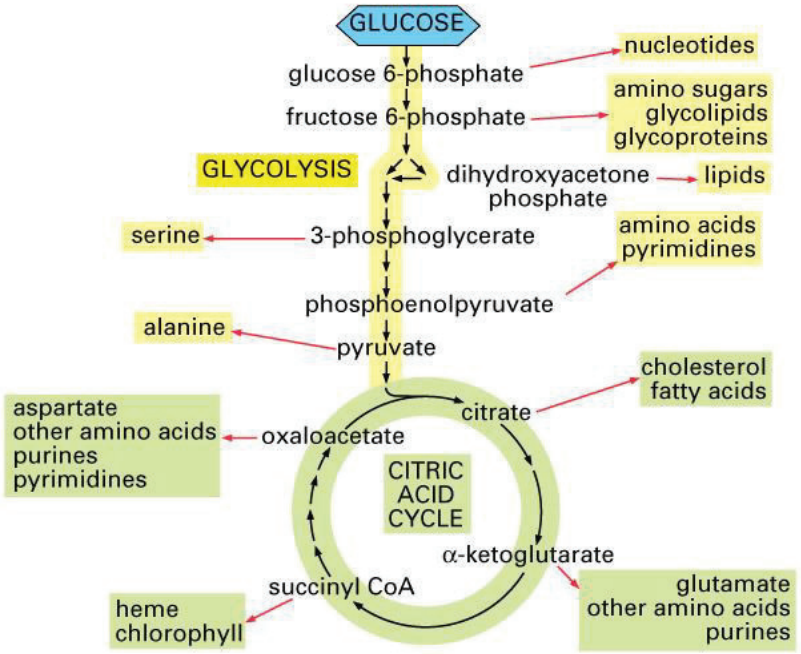

Figure 23: Glycolysis and the citric acid cycle (Krebs cycle)

Glycolysis (marked in yellow) and Krebs cycle (marked in green) provide the precursors needed to synthesize many important biological molecules, i.e. lipids, nucleotides, amino acids, sugars etc.

Each black arrow in this diagram denotes a single enzyme-catalyzed reaction; the red arrows generally represent pathways with many steps that are required to produce the indicated products.

(Essential cell biology, 2/e., 2004 Garland Science)

Figure 24: Glutamine metabolism in cancer cells

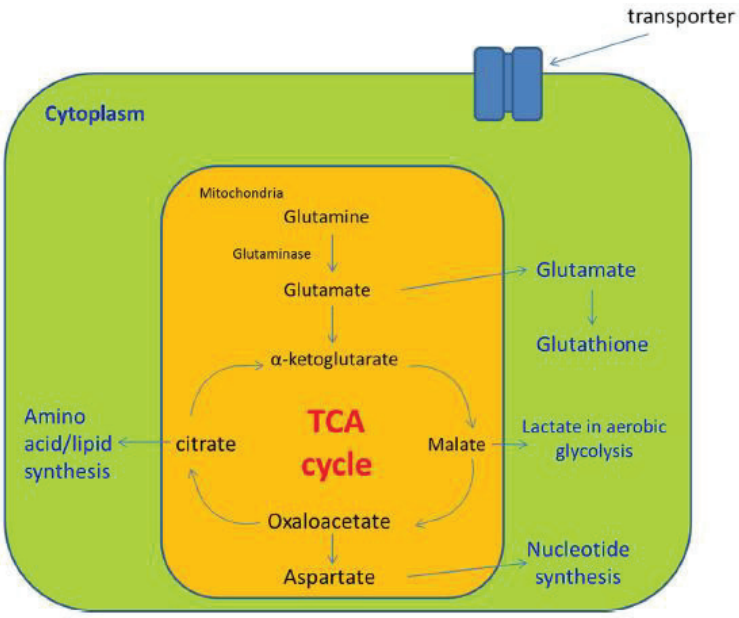

Glutamine enters the cells through glutamine transporter. After entering the mitochondria, glutamine is broken down into glutamate by glutaminase. Glutamate can be transported out to cytoplasm and be converted into glutathione, while in the mitochondria, glutamate is converted into α-ketoglutarate and enters the tricarboxylic acid cycle (TCA). Malate formed in TCA cycle is transported out to the cytoplasm and finally converted into lactate in aerobic glycolysis for energy release. Malate can also be converted into oxaloacetate in mitochondria, which in turn be converted into aspartate or citrate. Aspartate is transported out to the cytoplasm for nucleotide synthesis. Citrate formed from malate is transported out to the cytoplasm for amino acid and lipid synthesis.

(Fung and Chan et al., 2017)

metabolic phenotypes characterized by an increase in G6P, pyruvate and lactate levels, mediated by a hyper-activation of glycolysis, all contributing to a «Warburg-like» phenotype of GSDI hepatocytes.

II.2.3) Krebs cycle alteration and amino acid imbalance

The activation of glycolysis in GSDI was suspected to have a subsequent impact on Krebs cycle, since these pathways are tightly linked (*Figure 23*). In GSDIa mice (total knock-out of *G6pc*), an increase in citrate, lactate, and pyruvate was reported, with a concomitant decrease in the levels of succinate and α-ketoglutarate (Farah et al., 2017). Species beyond α-ketoglutarate in the cycle were present at similar levels as those found in wild-type mice, suggesting a partial blockage of the cycle in GSDI mice. Furthermore, the same study suggested that this blockade after citrate could be responsible for the alteration of amino acid metabolism, since the authors observed a relative increase in the levels of histidine, proline, and arginine in the livers of GSDI mice, with a relative decrease in glycine, phenylalanine, serine, tryptophan, and tyrosine levels. In another study glutamine was reported to be elevated in GSDI, along with alanine and proline (Slonim et al., 1979). These results on amino acid imbalance contribute to a cancerous-like metabolic reprogramming in GSDI hepatocytes. Indeed, with the increased metabolic rate and proliferation, cancer tissues have a much higher amino acid demand compared to normal tissues. As adaptation to fulfill the increased demand, these cells upregulate amino acid transporters, but also reprogram their metabolism in order to synthesize more amino acids (Fung and Chan, 2017). In particular, cancer cells are known to have enhanced glutaminolysis (conversion of glutamine into glutamate), (Fung and Chan, 2017) (*Figure 24*). As mentioned above, this amino acid is increased in GSDI along with alanine and proline, which can both be converted to glutamate and subsequently to glutamine (Phang et al., 2015). Thus amino acid imbalance in GSDI livers could be particularly favorable for increased cell proliferation rates.

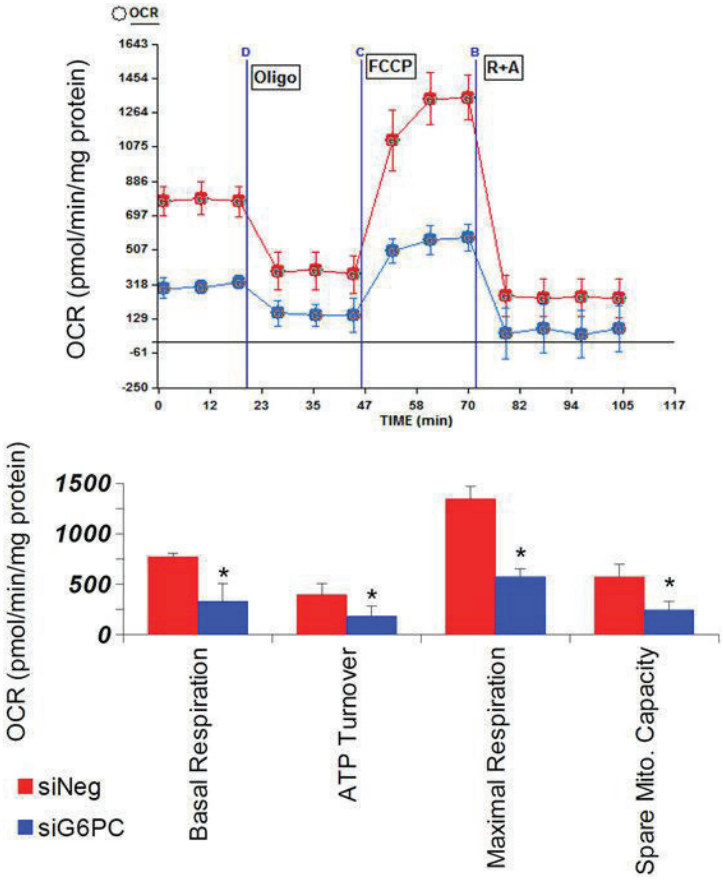

Figure 25: Mitochondrial respiration is impaired in G6PC Knock-Down versus control siRNA treated AML-12 cells

G6PC was knocked-down in AML-12 cells for 96 hours; then mitochondrial oximetry analysis was performed. Basal respiration, ATP turnover, maximal respiration, and spare mitochondrial capacity were determined. Oxygen consumption was normalized to total cellular protein content.

(Farah et al., 2017)

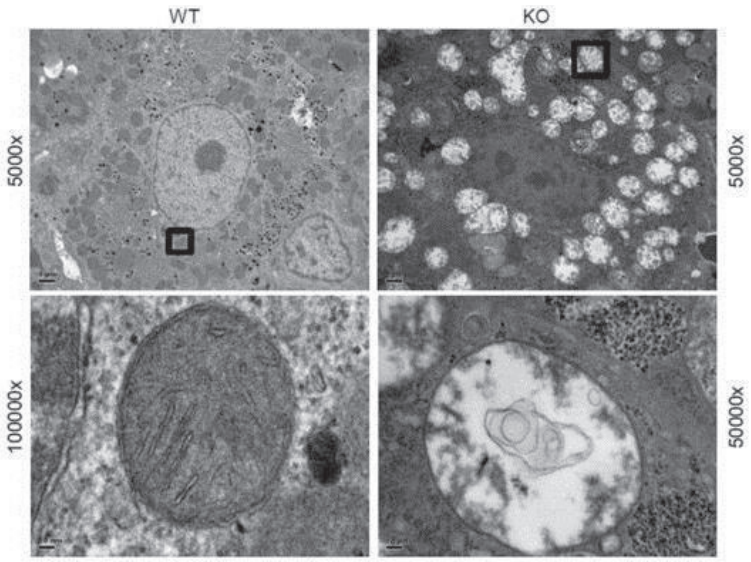

Figure 26: Abnormal mitochondrial morphology in the livers of total G6PC Knock-Out mice, compared to WT mice

Mitochondria were distended and swollen, with effacement of the cristae, disruption of the mitochondrial membranes, and influx of cytoplasmic contents into the mitochondria in G6pc-/- hepatocytes, compared to WT hepatocytes.

(Farah et al., 2017)

II.2.4) Down-regulation of mitochondrial oxidative phosphorylation

Metabolic alterations in GSDI livers, such as up-regulated glycolysis and unbalanced Krebs cycle can affect mitochondrial oxidative phosphorylation (OXPHOS) rates. This process was investigated in *G6pc-/-* hepatocytes (Farah et al., 2017). The team found a striking decrease in basal respiration, ATP turnover, maximal respiration, and spare mitochondrial capacity, implying a loss of mitochondrial function in GSDI (*Figure 25*). Furthermore, they observed distended and swollen mitochondria with outer membrane ruptures, effacement of the cristae, as well as an influx of cytoplasmic material into the mitochondria, further contributing to the down-regulation of OXPHOS (*Figure 26*). GSDI hepatocytes exhibited a decrease in mitochondrial number as well, possibly due to decreased mitochondrial biogenesis.

Furthermore, the abnormal morphology of the mitochondria might not be the only reason why OXPHOS is decreased in GSDI livers. Indeed, OXPHOS can be altered by impairment in β–oxidation of lipids, since this pathway contributes to OXPHOS by providing substrates for oxidation. One study by our laboratory indicated that lipid degradation in GSDI livers is down-regulated, since the main activator of this catabolic process, the peroxisome proliferator-activated receptor α (PPARα) and several PPARα–targeted genes, were found to be down-regulated in L.G6pc-/- mouse livers (Abdul-Wahed et al., 2014).

Interestingly, in other metabolic diseases affecting the liver, such as the ones characterized as NAFLD, OXPHOS down-regulation is often observed, usually resulting from the decrease in pyruvate import in the mitochondria (McCommis and Finck, 2015). Therefore, mitochondrial pyruvate transport should be analyzed in the case of GSDI. Finally, down-regulation of OXPHOS is frequently observed in glycolytic cancers. Indeed, this phenomenon is observed concomitantly to glycolysis elevation, as another component of the Warburg effect. Thus OXPHOS down-regulation in GSDI livers strongly confirms that these livers exhibit cancer-like metabolic behavior.

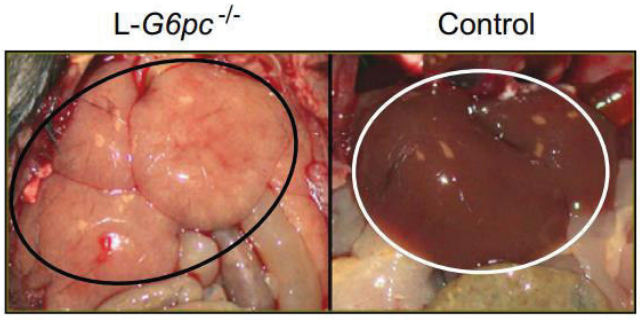

Figure 27: Liver-specific *G6pc* null mice develop liver hepatomegaly and steatosis

Livers of L-G6pc-/- mice were enlarged and pale and accounted for about 8% of total body mass, versus only 4% in control mice.

(Mutel et al., 2011)

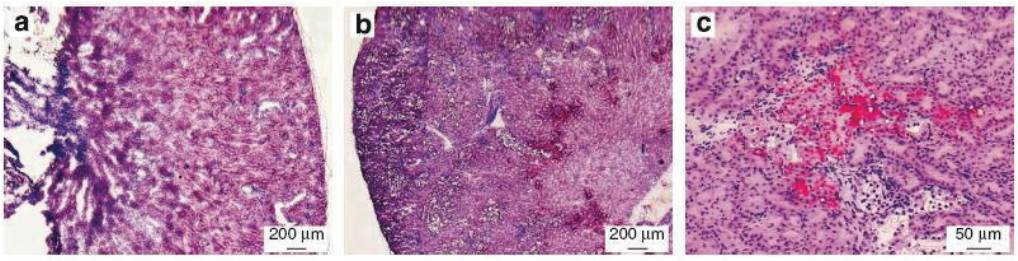

Figure 28: Renal lipid accumulation in kidney-specific G6Pase deficient mice

Histological analysis of Sudan red staining from WT (a) and K.G6pc-/- kidneys (b–c).

(Clar et al., 2014)

II.2.5) *De novo* lipogenesis activation and decrease in lipid oxidation lead to steatosis

Since in GSDI the capacity of G6P storage in the form of glycogen is chronically exceeded, G6P activates *de novo* lipogenesis and leads to hepatic steatosis (*Figure 27*). This was confirmed in GSDI mouse models and in GSDI patients (Bandsma et al., 2008, 2014; Mutel et al., 2011a). Indeed, in GSDI human livers, *de novo* lipogenesis and cholesterol synthesis were found to be increased 40-fold and 7-fold, respectively (Bandsma et al., 2008). Production of VLDL was unchanged compared to control values, but conversion of VLDL into intermediate density lipoproteins was relatively delayed in GSDI patients. Lipid vesicles are present in abundance in GSDI livers, mainly in the periportal zone, which corresponds to the location of the expression of G6Pase in the liver (Rajas et al., 2007). Associated to glycogen accumulation, lipids contribute further to the development of hepatomegaly.

In GSDI, lipid synthesis is activated *via* ChREBP, but independently of liver X receptor (LXR) and SREBP1c (Grefhorst et al., 2010). Besides lipogenesis, ChREBP is known to potentiate glycolysis and nucleotide biosynthesis, and it can have an inhibitory role on OXPHOS (Tong et al., 2009). Thus ChREBP could be a metabolic switch orchestrating the reprogramming in GSDI cells. Lack of SREBP1c activation could be due to low insulin signaling in GSDI (Rake et al., 2002a). As mentioned, this important increase in lipid synthesis translates to hepatic steatosis. In addition, it was suggested that accelerated glycolysis could supply acetyl-CoA molecules required for lipogenesis and thus potentiate this process.

Moreover, increased lipid synthesis was confirmed not only in GSDI livers, but also in GSDI kidneys. Thus lipid accumulation was reported in the proximal tubules of K.G6pc-/- kidneys, where G6Pase is normally expressed (Clar et al., 2014) (*Figure 28*). As observed in GSDI livers, *de novo* lipogenesis was suggested to be mediated by ChREBP (Clar et al., 2014).

Hepatic steatosis in GSDI is not only due to an increase in lipid synthesis, but also to a decrease in lipid β–oxidation. This catabolic pathway was shown to be down-

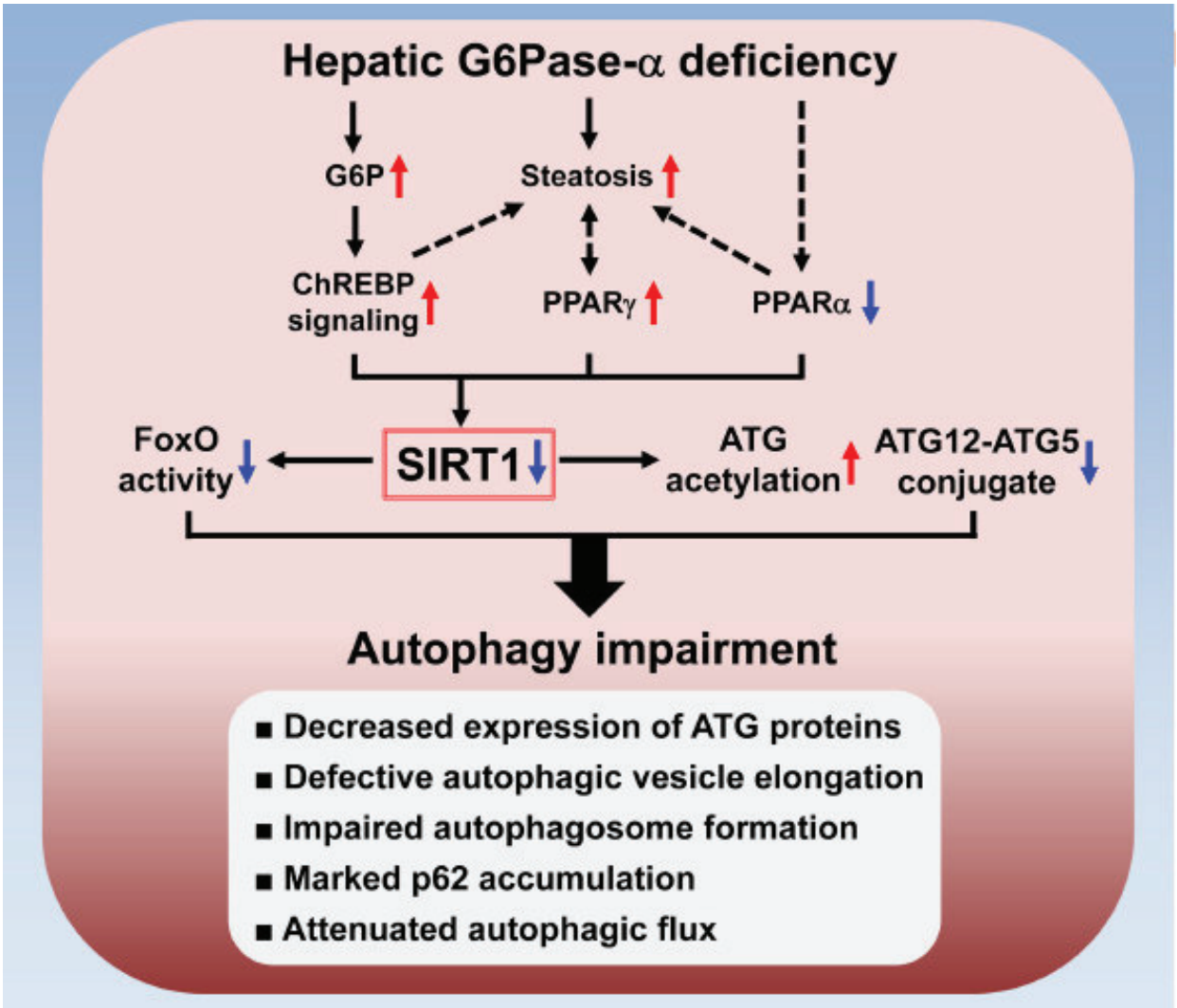

Figure 29: The mechanism underlying autophagy impairment in hepatic G6Pase deficiency

Hepatic G6Pase deficiency leads to metabolic alterations including G6P accumulation and suppressed expression of PPAR-α, a master regulator of fatty acid β-oxidation. The G6P-mediated activation of ChREBP signaling induces lipogenesis, leading to hepatic steatosis which increases the expression of PPAR-γ, another lipogenic factor. Moreover, aberrant PPAR-γ overexpression aggravates hepatic steatosis. The net outcome is down-regulation of hepatic SIRT1 signaling. Impaired SIRT1 signaling increases ATG acetylation and decreases ATG12-ATG5 conjugation along with downregulation of FoxO signaling that induces autophagy genes. Accordingly, hepatic G6Pase deficiency-mediated autophagy impairment is characterized by decreased expression of ATG proteins, defective autophagic vesicle elongation, impaired autophagosome formation, marked p62 accumulation and attenuated autophagic flux.

(Cho et al., 2017)

regulated in the liver of L.G6pc-/- mice (Abdul-Wahed et al., 2014), with a concomitant down-regulation of the main activator of β–oxidation, PPARα. It has been suggested that the production of malonyl CoA by ACC during lipogenesis could further contribute to the decrease in β–oxidation in GSDI livers (Derks and van Rijn, 2015). Finally, a decreased activity of AMP-activated protein kinase (AMPK) in GSDI hepatocytes might also contribute to impaired fatty acid oxidation and increased fatty acid and cholesterol synthesis (Farah et al., 2016; Viollet et al., 2006). AMPK regulates these processes by decreasing malonyl CoA production *via* ACC inhibition and by controlling SREBP1 and ChREBP activities (Kawaguchi et al., 2002; Zhou et al., 2001).

To conclude, lipid metabolism alterations have an important impact on the development of GSDI pathology. Increased lipid consumption is associated with a striking negative impact on GSDI liver (Rajas et al., 2015) and on GSDI kidneys (Gjorgjieva et al., 2015). Interestingly, this enhanced lipid synthesis is yet another hallmark of cancer cells observed in GSDI cells. Cancer cells are known to induce *de novo* lipogenesis in order to obtain an increased amount of lipids needed for rapid proliferation. They can also uptake free fatty acids (FFA) from the adjacent non-tumoral cells (Baenke et al., 2013). The importance of lipids and *de novo* lipogenesis activation needed for the progression of tumors has been proven in many studies from the specific inhibition of different enzymes involved in this pathway, such as FAS (Menendez and Lupu, 2007; Murata et al., 2010; Zaytseva et al., 2012).

II.2.6) Link between altered lipid metabolism and autophagy

Lipid metabolism is also connected to autophagy, a mechanism of self-degradation that is required for the removal of defective proteins and organelles, induced mainly under nutrient limitation. Lipids are components of the autophagic process and can alter it at different levels (Dall'Armi et al., 2013). Interestingly, the release of lipids from lipid droplets in response to nutrient deprivation requires components of the autophagic machinery, including ATG5, and inhibition of autophagy results in lipid droplet accumulation (Singh et al., 2009). A recent study demonstrated that a decrease in autophagy levels in GSDI hepatocytes resulted in an aberrant accumulation of lipid vesicles (Farah et al., 2016). Consequently, an induction of

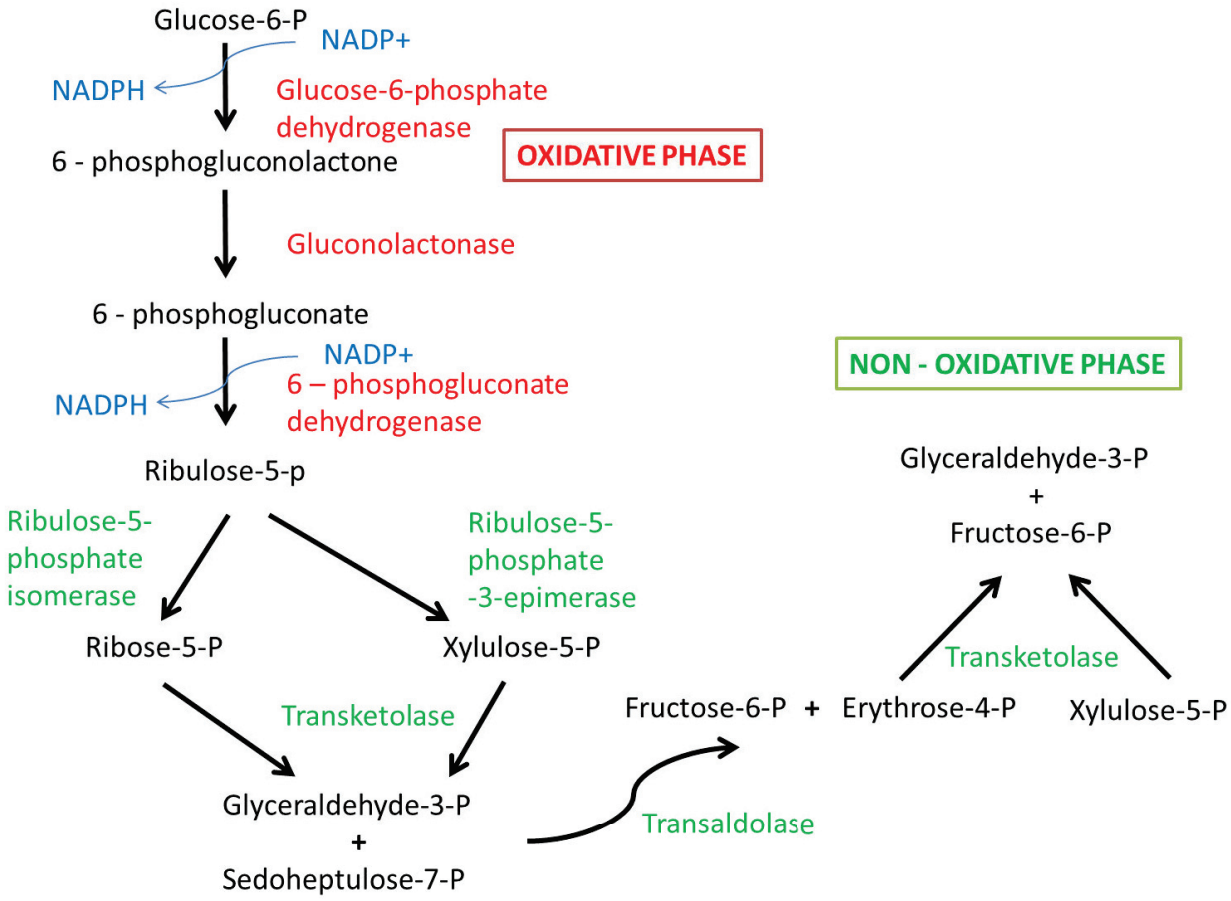

Figure 30: Pentose phosphate pathway

The pentose phosphate pathway generates NADPH (used for the biosynthesis of fatty acids, cholesterol and the production of reduced glutathione) and ribose 5-phosphate (precursor for the synthesis of nucleotides). There are two distinct phases in the pathway. The first is the oxidative phase (marked in red), in which NADPH is generated, and the second is the non-oxidative synthesis of 5-carbon sugars (marked in green).

autophagy in these cells resulted in an increase in lipid degradation, associated with an improved histology. While this study suggested that an activation of the mTOR pathway (generally considered as the canonical autophagy-regulation pathway) and down-regulation of AMPK were the main processes that were responsible for the inhibition of autophagy in GSDI, another study suggested that autophagy in GSDI is regulated *via* the SIRT / FOXO signaling axis (Cho et al., 2017) (*Figure 29*). Indeed, SIRT1 signaling is known to induce autophagy *via* deacetylation of autophagy-related (ATG) proteins and FoxO transcriptional factors, known to transactivate autophagy genes. Consistently, defective autophagy in GSDI liver is characterized by attenuated expressions of autophagy components, increased acetylation of ATG5 and ATG7, decreased conjugation of ATG5 and ATG12 and reduced autophagic flux, leading to p62 accumulation, but more importantly to lipid accumulation. Since SIRT1 is down-regulated during lipogenesis, this study highlighted a vicious circle between lipid accumulation and autophagy in GSDI. Indeed, SIRT1 is blocked due to lipid synthesis, which subsequently blocks autophagy and leads to further lipid accumulation (Cho et al., 2017).

II.2.7) Pentose phosphate pathway activation

Pentose phosphate pathway has been suggested to be activated in GSDI, due to the abundance of G6P, which is a precursor for this pathway, but this hypothesis has never been confirmed. Indeed, G6P can enter PPP, where it is oxidized by G6P-dehydrogenase and $NADPH^+$ H^+ is formed (*Figure 30*). NADPH is used for the biosynthesis of fatty acid, cholesterol and the production of reduced glutathione. PPP is also responsible for the production of ribose-5-phosphate, a precursor of nucleotide synthesis. Moreover, the final product of purine nucleotide degradation is uric acid (*Figure 31*).

Uric acid is accumulated in plasma of GSDI patients, as well as in mouse models of GSDI (Kishnani et al., 2014; Mutel et al., 2011a), translating into hyperuricemia. Indeed, the accumulation of metabolites implicated in glycolysis in the case of GSDI provokes a decrease in hepatic ATP concentration and inorganic phosphate, which stimulates the catabolism of purine nucleotides into uric acid (Cohen et al., 1985;

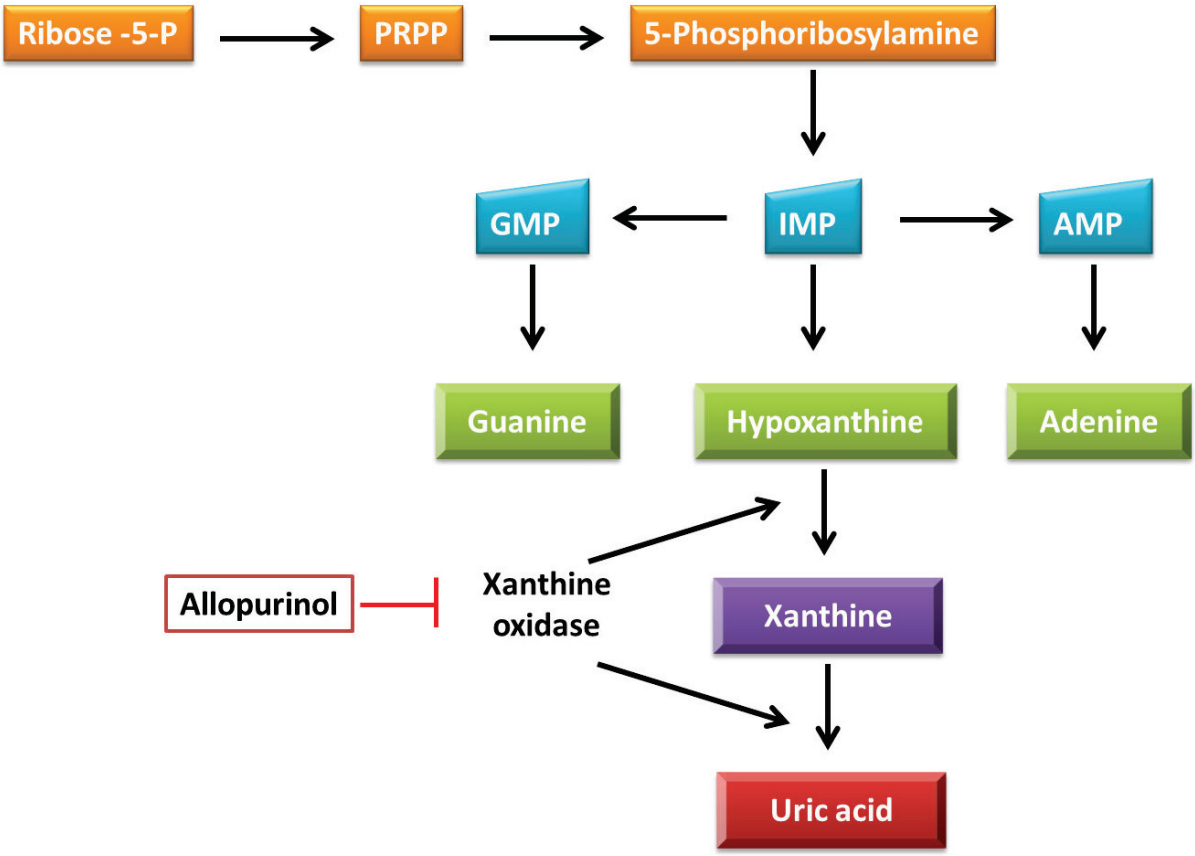

Figure 31: Purine synthesis and uric acid production

Shortened representation of the link between the pentose phosphate pathway, purine synthesis and uric acid production. Xanthine oxidase converts hypoxanthine to xanthine and xanthine to uric acid. In order to prevent hyperuricemia, patients are often treated with Allupurinol, an inhibitor of xanthine oxidase.

PRPP - phosphoribosyl pyrophosphate, GMP – guanosine monophosphate, IMP – inosine monophosphate, AMP – adenosine monophosphate.

(Adapted from Johnson and Patel, 1996)

Oberhaensli et al., 1988). Even though increase in nucleotide synthesis has never been clearly demonstrated in GSDI, several authors suggest that the increase in intracellular G6P could induce PPP and subsequently nucleotide synthesis and uric acid production (Schmitz et al., 1993). The production of NADPH by PPP could also be increased in order to compensate for the great usage of NADPH in lipid and cholesterol synthesis in GSDI.

In conclusion, G6Pase deficiency in GSDI reshapes the metabolic landscape in the liver and kidneys. Indeed, glycogen synthesis, glycolysis, lipogenesis and PPP are chronically increased, concomitantly with a decrease in OXPHOS and lipid oxidation. This particular metabolic reprogramming in GSDI presents striking similarities with glycolytic cancerous cells, conferring a «Warburg-like» phenotype, as well as a possible pre-neoplastic status to the cells in GSDI liver and kidneys.

III) GSDI symptoms, long-term complications and treatments

III.1) Clinical manifestations and diagnosis

Patients with GSDI are usually diagnosed very early, soon after birth. Indeed, some infants with GSDI exhibit hypoglycemic episodes and lactic acidosis during the neonatal period. This is due to the fact that breast milk and formula feeding are not administered often enough to avoid hypoglycemia in infants with GSDI. Nevertheless, these symptoms are more commonly present between 3 to 6 months of age, sometimes accompanied with seizures. Interestingly, some adult patients can tolerate low glucose levels by using lactate as an energy fuel for the brain (Froissart et al., 2011). Other clinical characteristics include doll-like facies, short stature, and an enlarged abdomen due to pronounced hepatomegaly (*Figure 14*) and nephromegaly. Hepatic steatosis confers a NAFLD-like aspect to GSDI, which is in accordance with the hyperlipidemia. Cognitive development is usually normal, unless the patient has cerebral damage from recurrent hypoglycemic episodes. Besides hypoglycemia, biochemical manifestations include hyperlipidemia, hypertriglyceridemia, hyperlactatemia, and hyperuricemia (Chou et al., 2010a; Froissart et al., 2011; Rake et al., 2002a). Furthermore, other occasional complications include anemia, osteoporosis, pulmonary hypertension, impaired platelet function, vitamin D deficiency, polycystic ovaries, atherosclerosis and acute pancreatitis (Kishnani et al., 2014; Rake et al., 2002a).

While all of these symptoms are common for both types of GSDI, patients with type Ib also exhibit neutropenia, impaired neutrophil function and enterocolitis, resulting in recurrent bacterial infections and oral and intestinal mucosa ulceration (Chou et al., 2010b; Rake et al., 2002a, 2002b). As described earlier (*Figure 18*), generation of mice lacking either G6PT or G6PC3 have shown that neutrophils express G6PT/G6PC3 complex capable of hydrolyzing G6P (Chou et al., 2010a; Jun et al., 2014; Shieh et al., 2003). Loss of G6PT activity leads to enhanced ER stress, oxidative stress, and apoptosis that underlie neutropenia and neutrophil dysfunction in GSDIb (Chou et al., 2010b). Neutrophil trafficking is also altered (Chen et al., 2003). These findings showed that G6PT is not just a G6P transport protein needed for G6Pase activity, but also an

important immunomodulatory protein, the activities of which need to be addressed in treating the complications in GSDIb patients.

Despite marked steatosis, moderate aspartate transaminase (AST) and alanine transaminase (ALT) are observed in plasma of GSDI patients, indicating hepatic injuries. Interestingly, when GSDI patients are metabolically controlled by an appropriate diet, these liver injury markers are usually normalized, as opposed to other GSD types, such as GSDIII, where these markers are never completely decreased (Kishnani et al., 2014). Furthermore, GSDI patients do not present an increase in ketone bodies in the blood, as opposed to GSD 0, III, VI and IX. These plasmatic differences are helpful during diagnosis in order to distinguish between GSDs.

Nevertheless, since the identification of *G6PC* and *SLC37A4,* sequencing analyses of these 2 genes are the most determining evidence in diagnosis of GSDI. More importantly, it avoids liver biopsy procedure, which can be risky and painful, since DNA is now purified from blood or saliva. In rare cases where no mutation is detected, yet the patient presents GSDI symptoms, the activity of G6Pase could be determined in order to diagnose the disease. Histology of the liver, requiring liver biopsy, can also distinguish GSDI from other GSDs. Indeed, even though all hepatic GSDs present glycogen accumulations in the hepatocytes, GSDI also presents lipid vesicle accumulation, that is far more important than in other GSDs.

III.2) Long-term hepatic complications

III.2.1) Hepatocellular adenoma

Hepatocellular adenomas (HCA) are rare monoclonal benign liver tumors of presumable epithelial origin that usually develop in healthy liver. It constitutes 2% of all liver neoplasms in the general population (Vijay et al., 2015). These tumors are usually solitary and can range from 1 – 30cm in diameter. Increased HCA incidence was detected in women who take oral contraception (Nault et al., 2017; Rooks et al., 1979; Zucman-Rossi et al., 2006). The role of estrogen in the development of these lesions has been established through multiple studies and withdrawal of this hormone was found to lead to tumor regression (Zucman-Rossi et al., 2006). Besides estrogen,

A

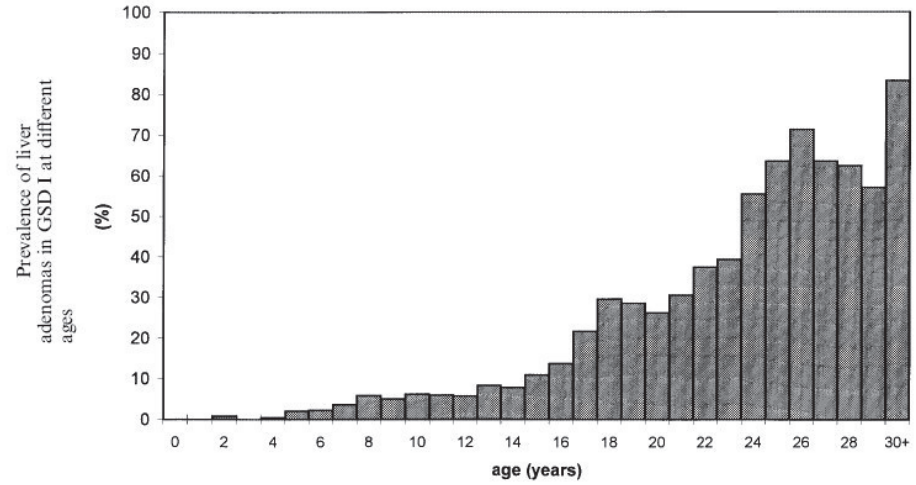

B

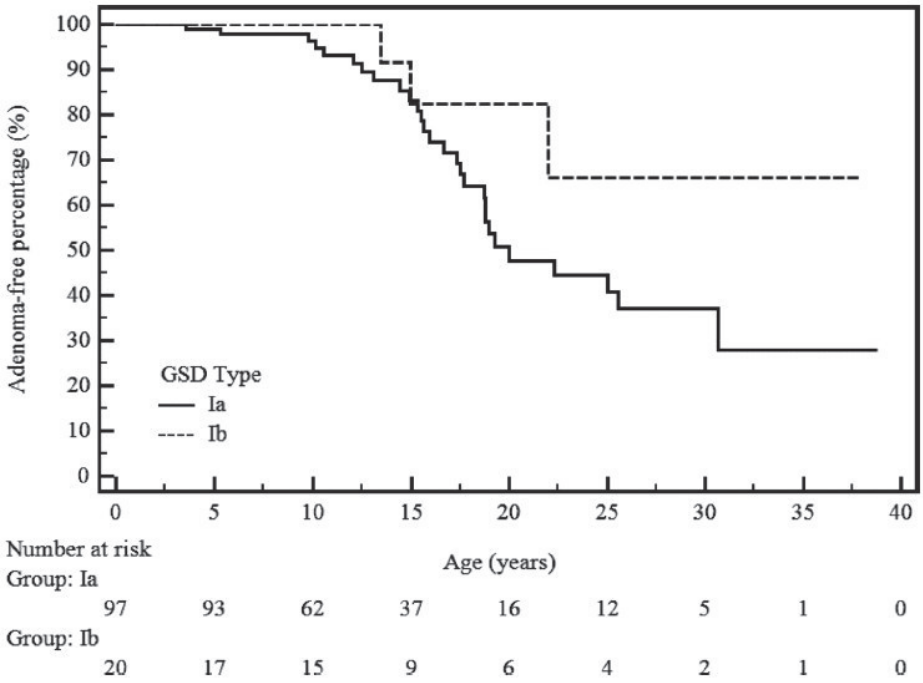

Figure 32: Hepatocellular adenoma incidence in GSDI patients

(A) Graphic representation of adenoma incidence in relation to the age of the patient, published in the European study of GSDI (Rake et al., 2002).

(B) Kaplan-Meier survival curve of adenoma-free progression in GSD types Ia and Ib; The number of patients analyzed at different ages is indicated below the graph (Wang et al., 2011).

anabolic steroids also lead to increased incidence of HCA. Furthermore, obesity, metabolic syndrome manifestations such as type 2 diabetes, insulin resistance, dyslipidemia and high blood pressure are increasingly postulated as risk factors for development and progression of HCA (Bioulac-Sage et al., 2012). Finally, GSDI and GSDIII are also characterized by HCA development (Calderaro et al., 2013; Kudo, 2001).

Incidence in GSDI

HCA is a major complication in GSDI (*Figure 32*) (Rake et al., 2002a, 2002b; Wang et al., 2011). Even though this disease was first described in 1929, the first tumors observed in GSDI were reported in 1955 (Mason and Andersen, 1955). This is mainly due to the fact that most patients at this time died very early (before 20 years of age) from hypoglycemia, which is too early to observe tumor development. Since the 1980's, blood lactate and glucose have been tightly controlled thanks to a strict diet (see below), allowing an improvement in life expectancy of GSDI patients. As a consequence, the number of hepatic tumors described in GSDI patients has subsequently increased these last ten years. The results of the European study on GSDI reported that, on average, HCA are detected for the first time at around 15 years of age (ranging 2 – 30 years), and at this point more than 60% of GSDI patients present multiple adenomas (Rake et al., 2002a) (*Figure 32*). The same study showed that 70-80% of patients above 25 years bare at least one HCA. Early studies suggested that there is a higher HCA incidence in male GSDI patients than in female patients (Bianchi, 1993), but the European study failed to confirm this observation.

Histology of HCA

HCA in GSDI livers resemble greatly to HCA developed in non-GSDI patients (Bianchi, 1993; Calderaro et al., 2013). They share many epidemiological features of estrogen-dependent tumors and yet do not necessarily behave in an estrogen-dependent manner (Lee, 2002). Nodules, ranging from 0.3 cm to several cm in size, are partially, and in some cases entirely surrounded by a fibrotic capsule (*Figure 33*). Hepatocytes in HCA present pale, swollen cytoplasm (*Figure 34-35*). HCA can be well

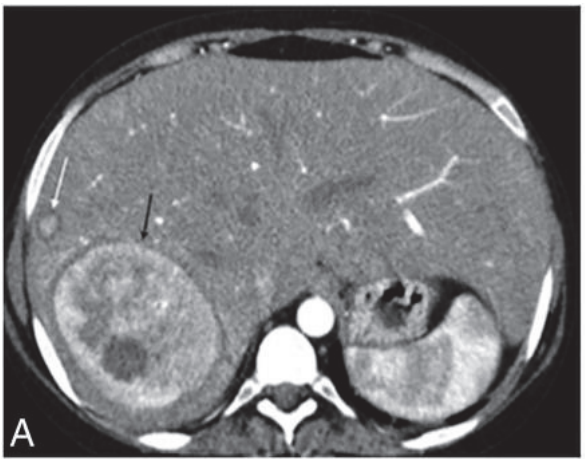

Figure 33: Imaging features of hepatocellular adenoma (HCA) in a 16 year old male with GSDI

Intensely enhancing lesions on arterial phase CT scan (black arrow). A smaller HCA with similar radiological features is also observed (white arrow).

(Husainy et al., 2017)

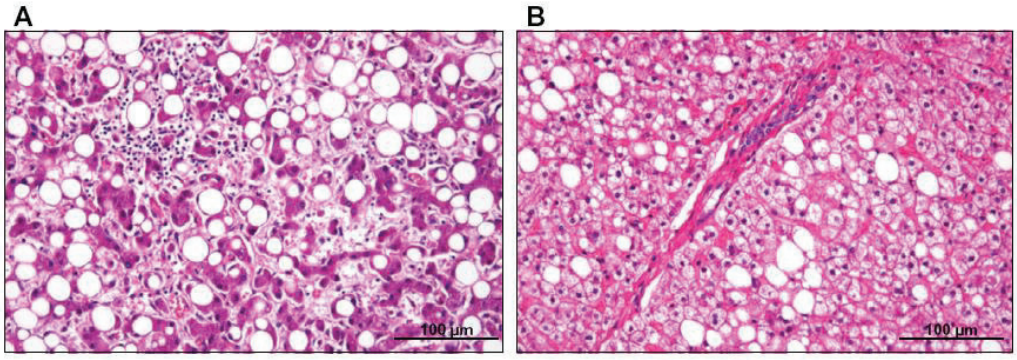

Figure 34: Histological features of hepatocellular adenoma and liver in a patient with GSDI

(A) Hepatocellular adenoma in GSDI with sinusoidal dilation, steatosis, and inflammatory infiltrates.

(B) GSDI non-tumor liver with hepatocyte clarification and steatosis.

(Calderaro et al., 2013)

developed, and in some cases of peliosis, bleeding and compression of HCA can occur. Kupffer cells can be observed inside HCA, yet their number varies greatly (Bianchi, 1993). One specific characteristics of GSDI HCA is the presence of Mallory bodies (damaged intermediate filaments) (Bianchi, 1993). This finding is important and needs to be studied further, since Mallory body presence is a trait generally characteristic for hepatocellular carcinoma (HCC), and not HCA. Thus Mallory body formation in HCA was speculated to be a risk factor for malignant transformation.

Molecular characterization of HCA

Several teams have analyzed the molecular background of HCA in GSDI. Analysis of 25 HCA samples from a French cohort of GSDI patients reported 3 different groups of classification based on the mutations present in HCA samples: inflammatory HCA (52%), β-catenin-mutated HCA (28%) and unclassified HCA (20%) (Calderaro et al., 2013). Most inflammatory HCA presented mutations in the gene coding for the interleukin-6 signal transducer (IL6ST), whereas one had a mutation in the gene coding for guanine nucleotide binding protein (GNAS). Consequently, all analyzed samples with either IL6ST or GNAS mutations had high C reactive protein (CRP) and/or serum amyloid A (SAA) expression, in accordance with the inflammatory phenotype. Interestingly, in β-catenin-mutated HCA, 4 mutations were classically located in β-catenin exon 3, whereas 3 were unusual and located in exon 7, as rarely described in HCC samples (associated with poor prognosis) (Guichard et al., 2012). Thus the elevated number of HCA that were β-catenin-mutated, as well as the type of mutations, suggest that these HCA have a strong predisposition to transform into HCC. In accordance, 6 out of the 7 β-catenin – mutated HCA showed high expression of leucine rich repeat containing G protein-coupled receptor 5 (LGR5) and/or glutamine synthetase (GLUL), two genes classically activated by β-catenin. This study confirmed that in GSDI there is a linear pattern of tumorigenesis, meaning that patients develop HCA, which can later be transformed in HCC, while HCC do not develop *de novo* in the liver (Calderaro et al., 2013). It is also noteworthy that HCAs issued from the same patient presented different mutations, indicating that when multiple adenomas are observed in

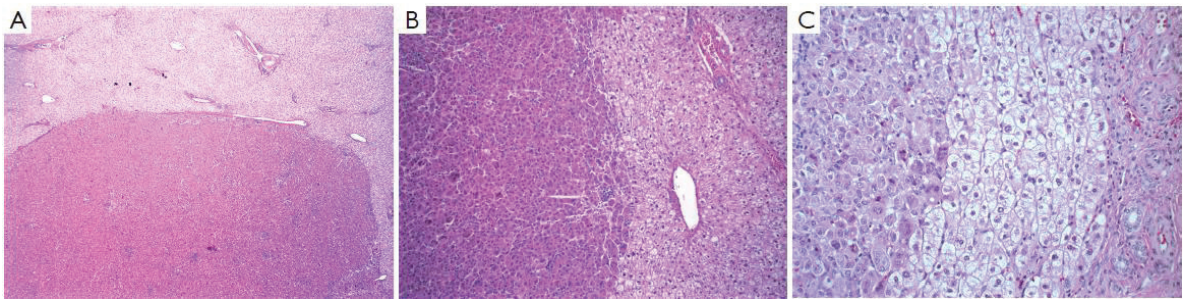

Figure 35: Hepatocellular adenoma in GSDI patients

Low-power (A) and higher magnification (B) and (C) images showing the interface between the adenoma and surrounding liver tissue. Note the glycogen in the pale swollen hepatocytes in the adjacent liver is sensitive to PAS-D, in contrast to the adenoma (C). Magnification, 40× in A, 100× in B, and 400× in C. PAS-D, periodic acid-schiff diastase.

(Schady et al., 2015)

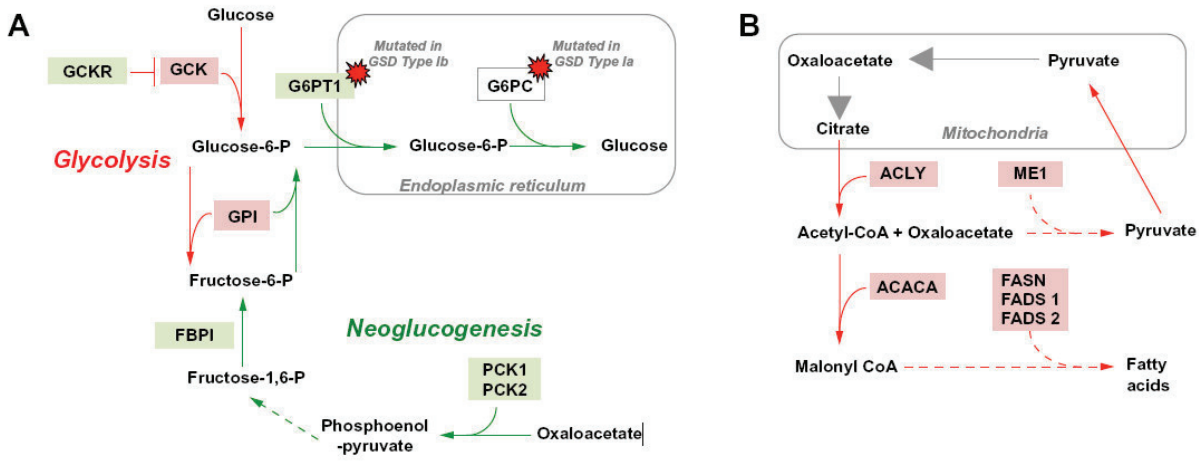

Figure 36: Common metabolic alterations in HNF1α - mutated HCA and GSDI liver

Schematic representation of (A) gluconeogenesis and glycolysis pathways, and (B) fatty acid synthesis pathway. Enzymes whose expression was found to be similarly deregulated in HNF1α - mutated HCA and GSD non-tumoral liver are in solid boxes (red = up-regulation; green = down-regulation).

(Calderaro et al., 2013)

a patient, they are not necessarily developed from the same clone (Calderaro et al., 2013).

This same classification system is used for non-GSDI HCA, and generally it includes an additional 4th group (HNF1α-mutated HCA). Interestingly, HNF1α mutation has never been reported in HCA in GSDI, but *HNF1a* mRNA expression has been reported to be decreased, not only in all GSDI HCA, but also in GSDI livers (Calderaro et al., 2013; Kishnani et al., 2009). Astonishingly, non-GSDI HCAs with a mutation in *HNF1α* have a metabolism resembling that of GSDI livers, characterized by a decrease in GNG and an increase in glycolysis (*Figure 36*) (Calderaro et al., 2013).

Furthermore, another study reported that HCA in GSDI present a recurrent chromosomal alteration on chromosome 6, with simultaneous gain of 6p and a loss of 6q (Kishnani et al., 2009). The size of HCA with these chromosome 6 alterations was significantly larger than HCA without these alterations. Interestingly, a gain of 6p and a loss of 6q is an event frequently observed in HCC in the general population of patients, but not in HCA. The expressions of Insulin-like growth factor 2 receptor (IGF2R) and large tumor suppressor kinase 1 (LATS1), tumor suppressor genes on chromosome 6, were reduced by 50%, which could potentially contribute to tumorigenesis. This phenomenon has been suggested to be a distinctive trigger of GSDI HCA, in accordance with their high potential of transformation into HCC.

III.2.2) Hepatocellular carcinoma

Incidence rates and detection

GSDI patients with HCA present about 10% rate of transformation of HCA in HCC (Calderaro et al., 2013; Franco et al., 2005; Kishnani et al., 2014; Lee, 2002). Interestingly, this HCA-to-HCC transformation seems to be characteristic for GSDI carcinogenesis. Furthermore, similar HCA-to-HCC formation has also been reported in obese patients (Bioulac-Sage et al., 2012; Bunchorntavakul et al., 2011). However, the incidence of transformation in GSDI is significantly higher than in non-GSDI HCA (Lee, 2002; Manzia et al., 2011). One study including 8 GSDI patients (6 male / 2 female) bearing HCC demonstrated that first detection of HCC ranged from 13-45 years (mean

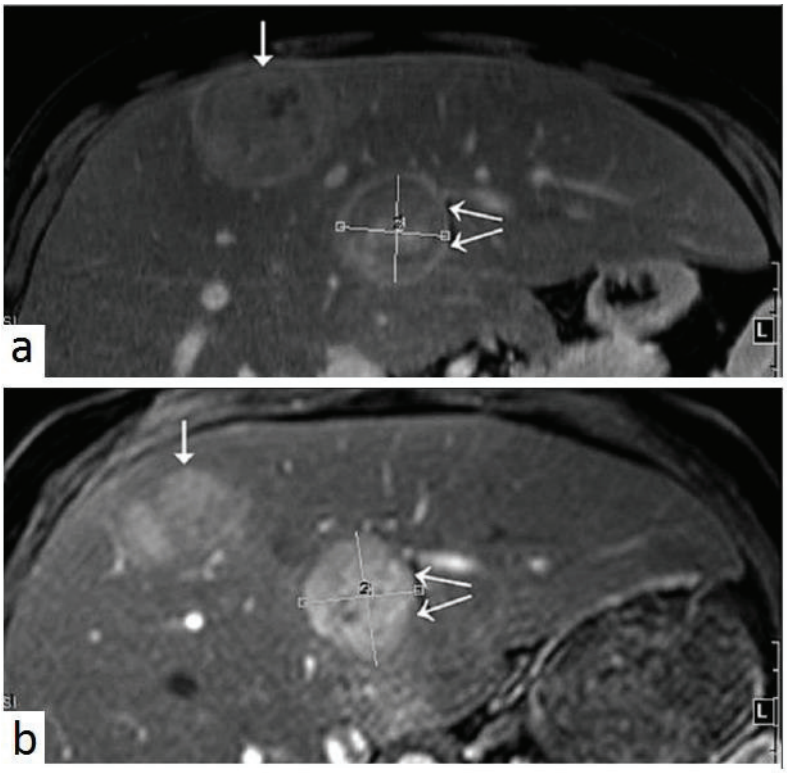

Figure 37: Abdominal MRI of a 31-year-old man with GSDIa

Index images of two hepatic lesions with an interval of 6 months. Fat-suppressed T1W fat post-contrast image acquired in May 2014 and in Nov 2014. The anterior lesion (single arrow) shows interval decrease in size on follow-up imaging, whereas the posterior lesion (double arrows) is slightly increased in size, later on diagnosed as HCC.

(Baheti et al., 2015)

Figure 38: Post - biopsy histopathology of a suspicious lesion detected by MRI in a 31-year-old man with GSDIa

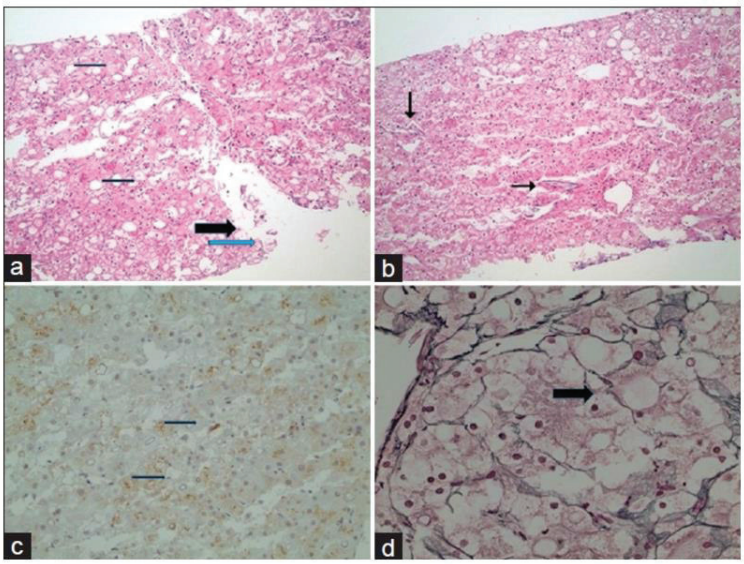

There is lack of portal tracts in all fragments.
(a) In low-power magnification (H&E stain), there is moderate steatosis (thin arrows) with many ballooned cells (thick arrow), some containing Mallory-Denk bodies (blue arrow).
(b) In low-power magnification (H&E stain), there are increased unpaired arteries (arrows).
(c) In low-power magnification, there is focal Glypican-3 staining of the tumor cells.
(d) In higher magnification, a reticulin stain shows focal loss of the reticulin framework (arrow).

(Baheti et al., 2015)

28 years) (Franco et al., 2005). Alpha-fetoprotein (AFP), which is considered as a plasmatic marker for HCC, was normal in 6 out of 8 patients. Carcinoembryogenic antigen (CEA), another HCC marker, was normal in 5 patients out of 8 patients, highlighting that HCC markers, which are used in general, are not adapted for HCC diagnosis in GSDI. Therefore, regular abdominal MRI or CT scan is a better solution to follow up tumor development in GSDI patients (*Figure 37*). Of course, the potential risks associated with excessive radiation exposure in patients receiving multiple CT scans need to be taken into consideration.

There are several challenges concerning the diagnosis of HCC in GSDI. Because of the abundance of HCA, biopsy is often not a good option. Not only is biopsy painful for patients, but it represents risks of tumor bleeding and dissemination of cancer cells. Indeed, in 9 cases of biopsy sampling in GSDI, cancer cells were disseminated along the biopsy tract (Kelly and Poon, 2001). One of the markers used to distinguish HCA from HCC at a histologic level is glypican 3 (*Figure 38*). Even though MRI and CT imaging are good tools for the detection of HCC, the distinction between HCC and well developed HCA is often difficult, especially if the tumor is in an intermediate stage of early malignancy. Thus high contrast imaging is recommended, in order to look for increase in lesion size, poorly defined / disrupted margins and / or spontaneous hemorrhage (Kishnani et al., 2014).

Characteristics of HCC in GSDI

Unfortunately, HCC in GSDI are not very well characterized at a molecular level. Most data arose from case study reports of GSDI patients with HCC. Patients usually presented several nodules in the liver that were stable and did not change until the onset of HCC. Lesions of HCC can have a fibrotic capsule delimitating tumor tissue, while in some cases they have been described as completely surrounded by HCA tissue, and the boundaries between normal hepatic tissue, HCA and HCC were not always clear (Kudo, 2001; Limmer et al., 1988). These complex cancerous structures can often lead to misdiagnosis. Unfortunately, several patients have been reported to present metastatic disease (Franco et al., 2005; Kelly and Poon, 2001). HCC metastases have been detected in the bone, lungs, spinal cord, portal vein and para-

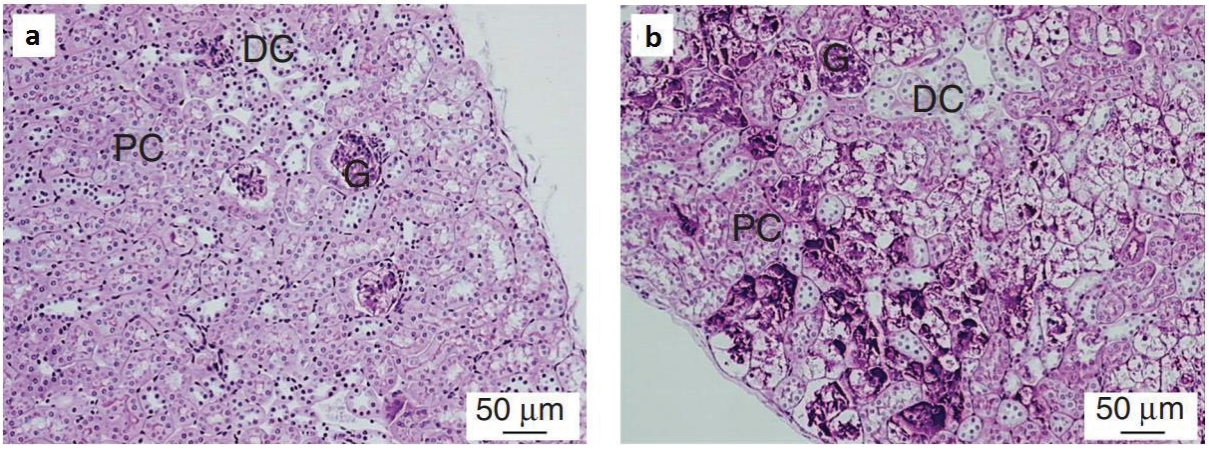

Figure 39: Histological analysis of PAS staining, highlighting glycogen accumulation in the kidney cortex in K.G6pc-/- mice

Kidneys of (a) WT mice and (b) mice with specific renal deletion of *G6pc* (K.G6pc -/-).

(Clar et al., 2014)

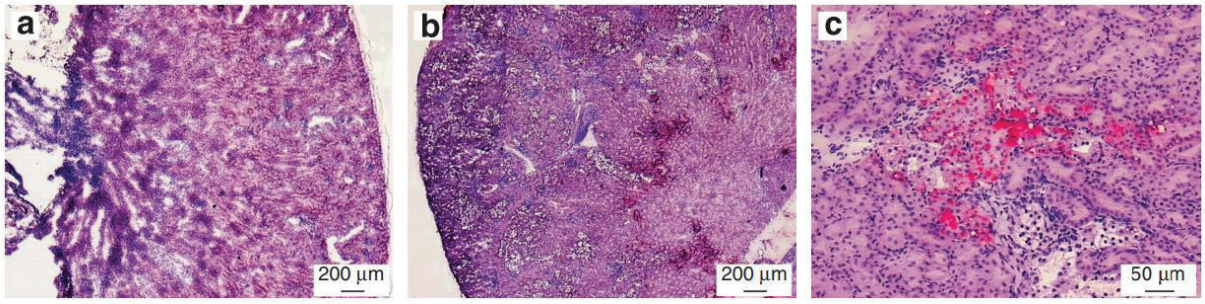

Figure 40: Histological analysis of Sudan red staining, marking lipid accumulation specifically in the kidney cortex in K.G6pc-/- mice

Kidneys of (a) WT mice and (b–c) mice with specific renal deletion of *G6pc* (K.G6pc -/-).

(Clar et al., 2014)

aortic lymph nodes in several patients. These findings are important in the case of GSDI, since the prognosis for HCC is poorly evaluated, due to the limited number of patients.

In the general human population, HCC occur in fibrotic / cirrhotic livers, sometimes associated with alcoholic liver disease or viral hepatitis infection. On the contrary, GSDI patients do not exhibit hepatic fibrosis / cirrhosis, and HCC are formed from preexisting HCA. This is a major difference between non-GSDI and GSDI associated HCC that needs to be taken into consideration when analyzing the potential triggers of carcinogenesis in GSDI livers.

HCA and HCC are not the only hepatic lesions observed in GSDI. Indeed, there have been reports of hepatoblastoma, focal fatty infiltration, focal fatty sparing, focal nodular hyperplasia and peliosis hepatitis (Lee, 2002). All of these render diagnostics in GSDI difficult, since often one complication can be mistaken for another.

III.3) Long-term renal complications

III.3.1) Chronic kidney disease

Chronic kidney disease (CKD) is a recent complication described in GSDI, since life expectancy has been increased after diet management introduction. As early as 1929, in the autopsy reports of two children with GSDI, Dr. von Gierke highlighted the presence of nephromegaly, due to strong glycogen accumulation in the kidneys. Nevertheless, hypoglycemia and metabolic perturbations were considered far more important than renal complications, due to their implication in mortality. CKD was acknowledged as a complication in GSDI later on in the 1980's, when renal histology of GSDI patients revealed glomerulosclerosis, interstitial fibrosis and tubular atrophy (Baker et al., 1989; Chen, 1991; Reitsma-Bierens et al., 1992).

G6Pase deficiency results in glycogen and lipid accumulation in renal proximal tubules of the kidney cortex (*Figures 39 and 40*). The first sign of CKD is progressive development of glomerular hyperperfusion and hyperfiltration (Chen, 1991). Glomerular filtration rates (GFR) are regularly measured in GSDI patients as an indicator of renal

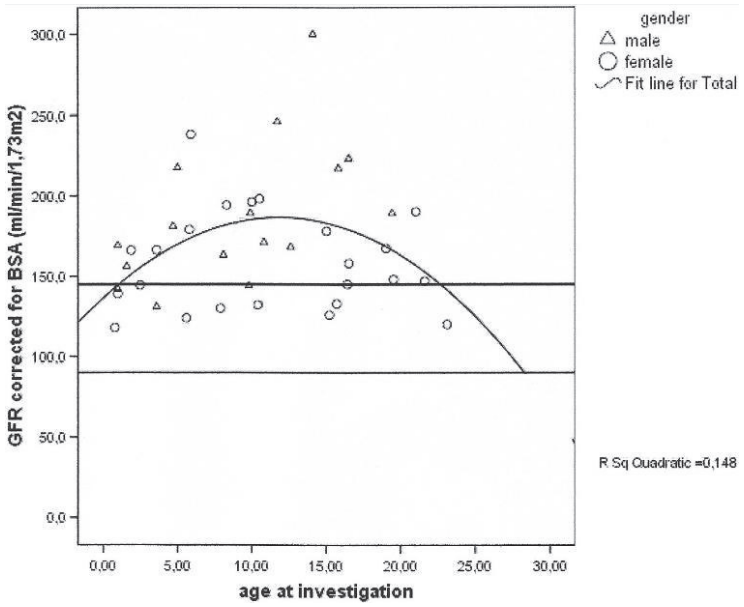

Figure 41: Natural course of glomerular filtration rate (GFR) in GSDI patients

(Martens et al., 2009)

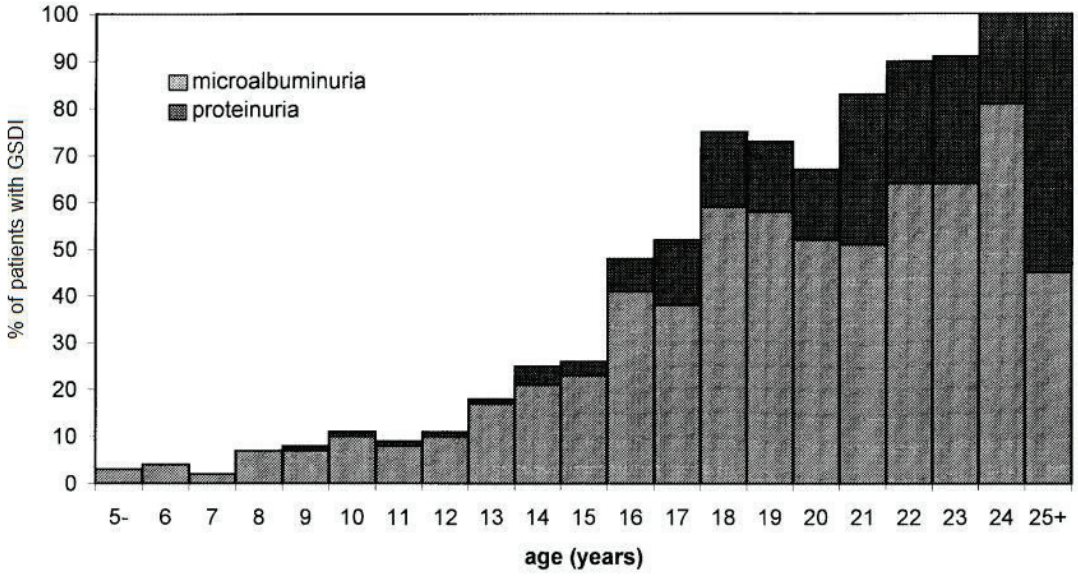

Figure 42: Microalbuminuria and proteinuria detection in GSDI patients, published in the European study of GSDI

(Rake et al., 2002)

function and a biphasic pattern in relation to age has been reported (*Figure 41*). This means that earlier in life, GSDI patients exhibit increased GFR, which reaches a peak on average at 15 years of age, and then starts declining, while albuminuria and proteinuria progress (Martens et al., 2009). Indeed, it has been reported that most adult GSDI patients over 25 years of age develop microalbuminuria and around 50% of them develop proteinuria (Kishnani et al., 2014; Rake et al., 2002b) (*Figure 42*). Another study reported similar results, stating that after 18 years, 67% of patients exhibit albuminuria and 42% present proteinuria (Martens et al., 2009). Many patients have nephrocalcinosis, due to hypercalciuria and hypocitraturia that enhance the likelihood of urine calcium precipitation. Because of hyperuricemia, uric acid nephrolithiasis and gout nephropathy can develop. Unfortunately, renal function loss, glomerulosclerosis and interstitial fibrosis can occur and these events can lead to renal failure at later stages.

III.3.2) Molecular pathways involved in CKD development

The molecular mechanism leading to CKD in GSDI patients has been proposed to be similar to the one observed in diabetic patients (Mundy and Lee, 2002; Rajas et al., 2013; Yiu et al., 2008a). Indeed, even though these two pathologies are highly different and even opposite in some aspects, the one point that they have in common is the increased metabolism of G6P. Also in line with this idea, the activation of Renin / Angiotensin system (RAS) is associated with both diabetic and GSDI CKD (Mundy and Lee, 2002; Yiu et al., 2008a).

High G6P levels in GSDI patients activate glycolysis and PPP, resulting in an increased pool of triose phosphate molecules, such as glycerol-3 phosphate and dihydroxyacetone phosphate (Yiu et al., 2008a, 2008b). These are precursors for the *de novo* synthesis of glycerolipids, including diacylglycerol (DAG). DAG is a potent activator of protein kinase C (PKC) and acts by binding to a specific domain on the regulatory subunit of the enzyme. This activation of PKC leads to the activation of the RAS (*Figure 43*). In RAS, angiotensinogen (Agt) is the precursor of the Ang II, which is produced from two sequential enzymatic reactions - the conversion of Agt to Ang I by renin and the conversion of Ang I to Ang II by the Ang converting enzyme (ACE). Ang II stimulates the proliferation of mesangial cells, glomerular endothelial cells, and

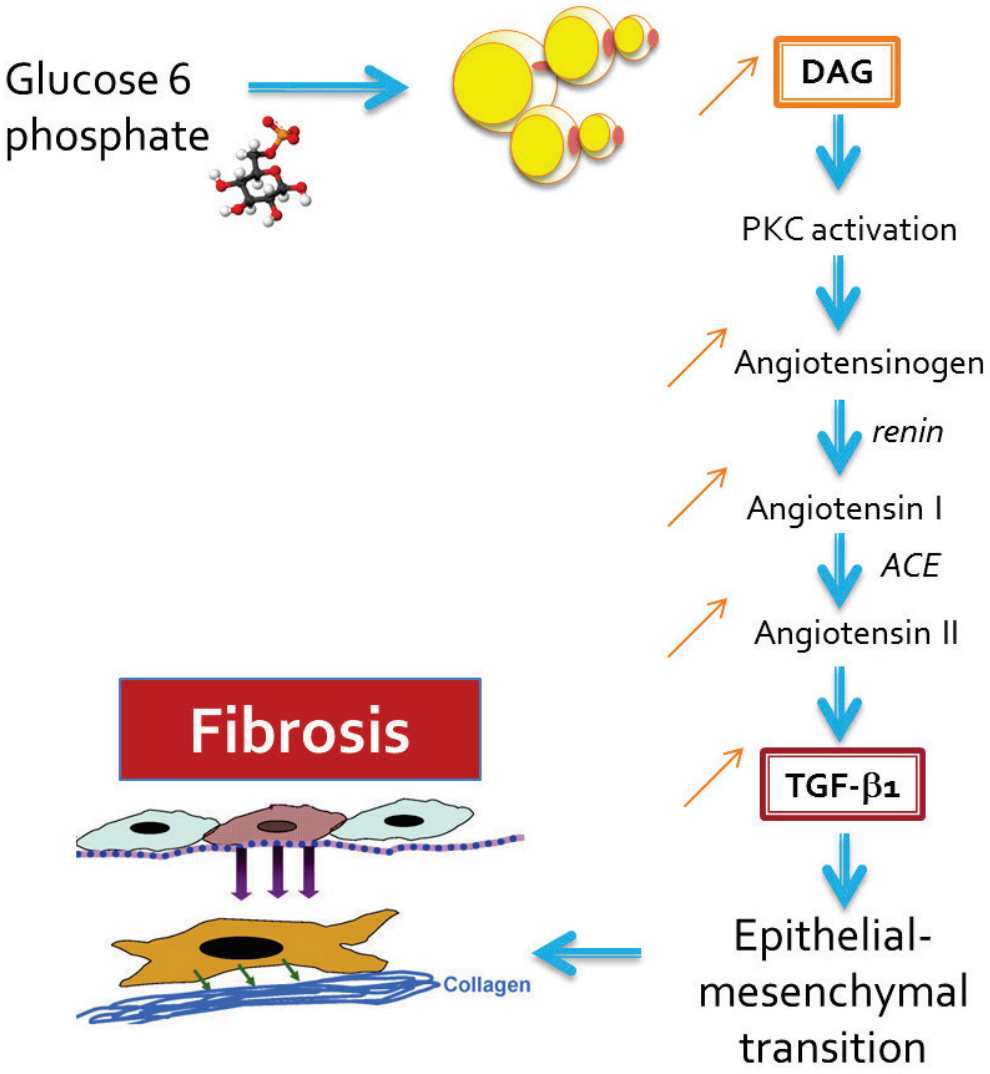

Figure 43: Schematic representation of the pathways responsible for the development of GSDI nephropathy

Glucose-6 phosphate accumulation in GSDI kidneys leads to an increase in DAG synthesis. Increased DAG levels activate PKC, which in turn leads to the activation of the RAS / TGF-β1 signalization axis. The RAS / TGF-β1 activation consists in the conversion of Angiotensinogen to Angiotensin I *via* renin, which is subsequently converted to Angiotensin II *via* ACE, finally leading to an increase in TGF-β1 levels. TGF-β1 is a profibrogenic factor capable of activating the epithelial – mesenchymal transition process, eventually leading to kidney fibrosis development.
DAG – diacylglycerol, PKC – protein kinase C, RAS – Renin Angiotensin system, TGF-β1 – transforming growth factor β1, ACE – Angiotensin converting enzyme.

fibroblasts, and acts as a profibrogenic factor. Many profibrotic effects of RAS are mediated by transforming growth factor-β1 (TGF-β1). Indeed, renal fibrosis development is induced by TGF-β1, which activates the expression of the extracellular matrix genes (Lan, 2011; Meng et al., 2015). In addition, TGF-β1 is a potent inducer of epithelial-to-mesenchymal transition (EMT) that characterizes the phenotype of renal interstitial fibrosis (Fragiadaki and Mason, 2011).

Even though several treatments inhibiting the RAS / TGF– β1 axis, such as ACE inhibitors, are being tested in GSDI patients, at the moment it is unclear whether they have an actual impact on the development of CKD. Indeed, while ACE inhibitors can decrease GFR and delay microalbuminuria, these drugs have no effect in patients with preexisting microalbuminuria / proteinuria (Martens et al., 2009).

III.4) Intestinal complications

In the 60's, a decrease in intestinal G6Pase activity associated with an intestinal accumulation of glycogen has been reported in two patients with GSDI (Field et al., 1965). Nevertheless, G6Pase expression was believed to be restricted to the liver and the kidneys at the time being. It was not until 1999 that the existence of intestinal G6Pase was confirmed by our laboratory in rat and human intestine (Rajas et al., 1999), more precisely in the mucosa of intestinal villi (Rajas et al., 2007).

The intestinal pathology of GSDI has not been studied as much as the hepatic and renal pathologies. Since it is considered that this complication is not involved in morbidity and mortality of GSDI patients, not many studies have been conducted in order to understand the molecular basis and its impact. It has been reported several times that patients with GSDIa as well as patients with GSDIb suffer from intermittent diarrhea, which seems to worsen with age (Visser et al., 2002). No common cause for diarrhea in GSDIa was found, while in GSDIb a loss of mucosal barrier function due to inflammation, documented by increased faecal α1-antitrypsin excretion and inflammation in the colonic biopsies, seems to be the main cause (Visser et al., 2002). The inflammation is most likely related to disturbed neutrophil function, which is often found in GSDIb. Indeed, in the European study of GSDI, it has been reported that up to

55% of GSDIb patients suffer from diarrhea (Rake et al., 2002b). This intestinal pathology is highly similar to Crohn's disease. Furthermore, the diet of GSDI patients, consisting mainly of slow-release carbohydrates, could contribute to these intestinal manifestations.

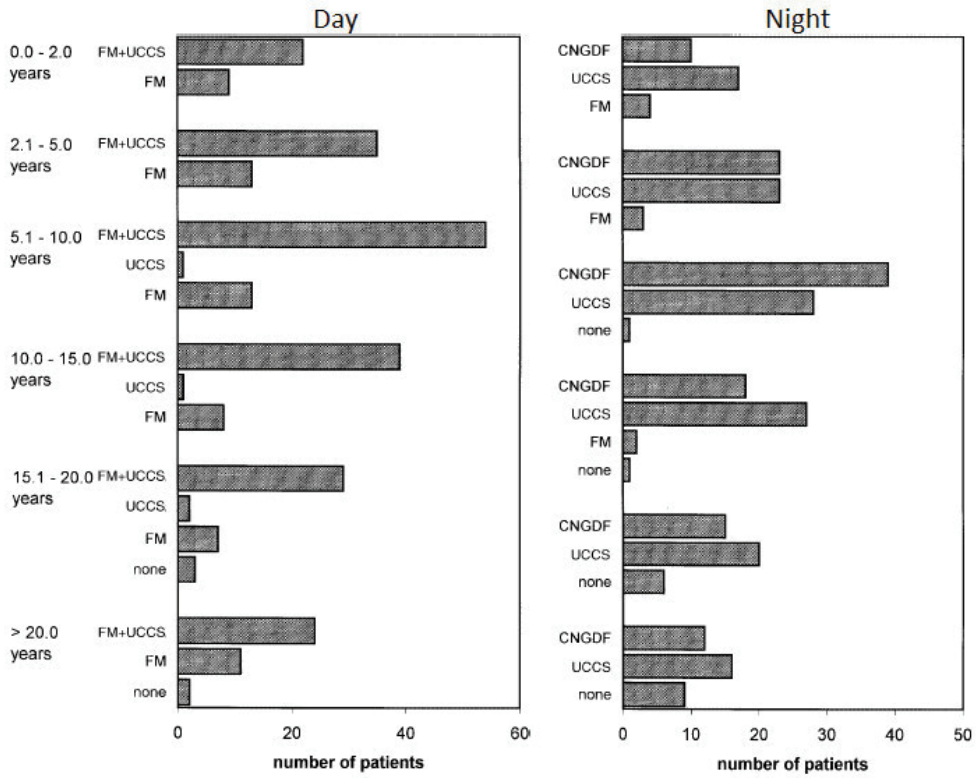

Figure 44: Dietary treatment during the day and during the night in GSDI patients

FM – frequent meals; UCCS – uncooked corn starch; CNGDF – continuous nocturnal gastric drip feeding.

European study of GSDI (Adapted by Rake et al., 2002)

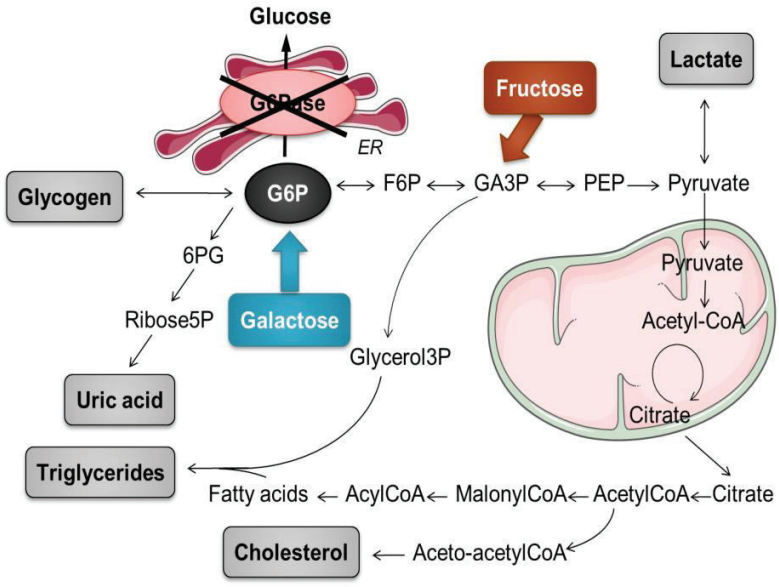

Figure 45: Potential entry points of fructose and galactose in GSDI metabolism

Schematic representation of the empiric predictions of the entry points of fructose and galactose in GSDI hepatic metabolism and the subsequent activation of metabolic pathways.

(Rake et al.,2002; Heller et al., 2008; Bhattaacharya, 2011)

IV) Treatment strategies for GSDI patients

IV.1) Nutritional treatment

Currently, a curative treatment is still not available for GSDI patients. Nevertheless, nutritional management guidelines have been proposed in the early 1980s. This nutritional treatment for GSDI patients was designed in order to avoid hypoglycemia and suppress increased lactate production, but also to limit excessive accumulation of glycogen and lipids in the liver and kidneys. A breakthrough in the treatment was the introduction of continuous nocturnal gastric drip-feeding (CNGDF), providing a continuous dietary supply of glucose. This treatment allowed a substantial increase in life expectancy in GSDI patients.

The dietary guidelines depend on the age of the patient (*Figure 44*). In infants, the primary source of concern is the management of hypoglycemic episodes. Nevertheless, children are not only in need of constant glucose levels, but also sufficient protein intake, as well as balanced vitamin and mineral intake, in order to grow and develop normally. To prevent hypoglycemia in infancy, soy-based, sugar-free formula, or formula free of sucrose, lactose and fructose is given on demand every 2-3h. Fructose, lactose and sucrose are avoided, since they are considered as «fast sugars» which can easily be converted into G6P and thus further stimulate lipid and glycogen accumulation (*Figure 45*). However, there has never been a study confirming these statements in GSDI, and therefore the avoidance of « fast sugars » is purely based on empirical conclusions from metabolic pathway knowledge (Froissart et al., 2011; Rake et al., 2002a, 2002b).

Once the child sleeps more than 3-4h, it has to be either woken up to eat, or CNGDF needs to be employed. Continuous glucose infusion is performed either by intragastric feeding by inserting a nasogastric tube, or by a total parenteral nutrition, requiring a surgically inserted G-tube, through which a specially designed formula drips (*Figure 46*). Although gastric feeding seems as a good way to prevent hypoglycemia, it comes with risks, such as failure to deliver the formula due to occlusions or spilling, as well as recurrent infections due to the G-tube, especially in GSDIb patients. Thus the

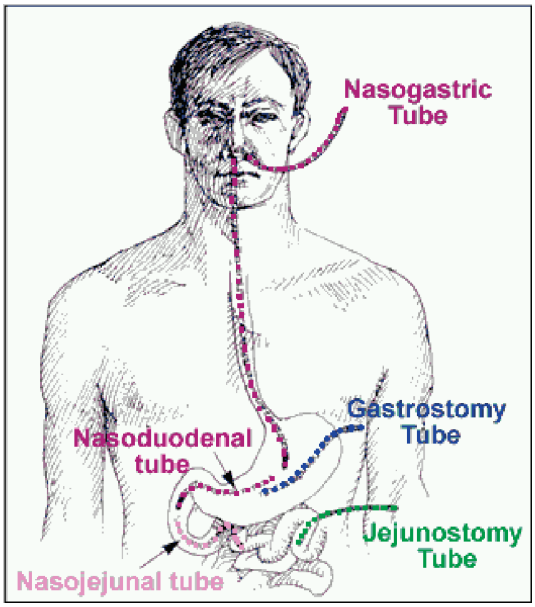

Figure 46: Different ways of providing tube feeding, depending on the individual's medical condition

For temporary access, tubes can be placed through the nose and mouth. For permanent tubes, several options in the stomach and intestine are available.

pros and cons of using this option need to be evaluated regarding the patient concerned.

Solid food is introduced at around 4-6 months. Blood glucose is maintained by frequent meals and uncooked cornstarch (UCS), which is introduced between 6 months and 1 year. UCS is digested slowly, providing a steady release of glucose, which allows more stable glucose levels over a long period of time, as compared with other sources of carbohydrates. In addition, sweet products, fruit and dairy product consumption is restricted or avoided, since these contain galactose and fructose. This results in a decrease in vitamin and mineral intake, which need to be given as supplements. As the child grows, small frequent meals rich in UCS supplemented with fibers are usually recommended.

Most adult GSDI patients maintain their glycaemia by consuming UCS at a dose of 1.7-2.5g UCS/kg, every 4h-5h (sometimes 6h). Some adults may eventually require only one dose of UCS at bedtime (Rake et al., 2002a, 2002b). Less than 2 years ago, a modified UCS, Glycosade (Vitaflo), became available in Europe and the United States, allowing an increase in fasting periods, compared with Maizena in France.

Many beneficial effects of this dietary approach have been observed in GSDI patients. Mortality rates were decreased with this nutritional management, as reported in the European study of GSDI, mainly due to a decrease in fatal hypoglycemia incidence (Chen et al., 1993; Rake et al., 2002a; Wolfsdorf et al., 1990). Plasmatic parameters are improved, but not entirely corrected with the dietary therapy, since some patients respond better than others (Rake et al., 2002a). Severe hypercholesterolemia has been observed in 12% of treated GSDIa patients and in 5% of the treated GSDIb patients. Furthermore, severe hypertriglyceridemia was observed in 73% of GSDIa and 46% of GSDIb treated patients. Thus hyperlipidemia was found to be more present and more severe in GSDIa patients, even under dietary regimen (Greene et al., 1991; Levy et al., 1988; Rake et al., 2002a). Therapeutic agents such as clofibrate, lovastatin, and niacin, intended to decrease lipids and cholesterol, have been used in these patients (Geberhiwot et al., 2007; Greene et al., 1991), to counterbalance the dietary treatment.

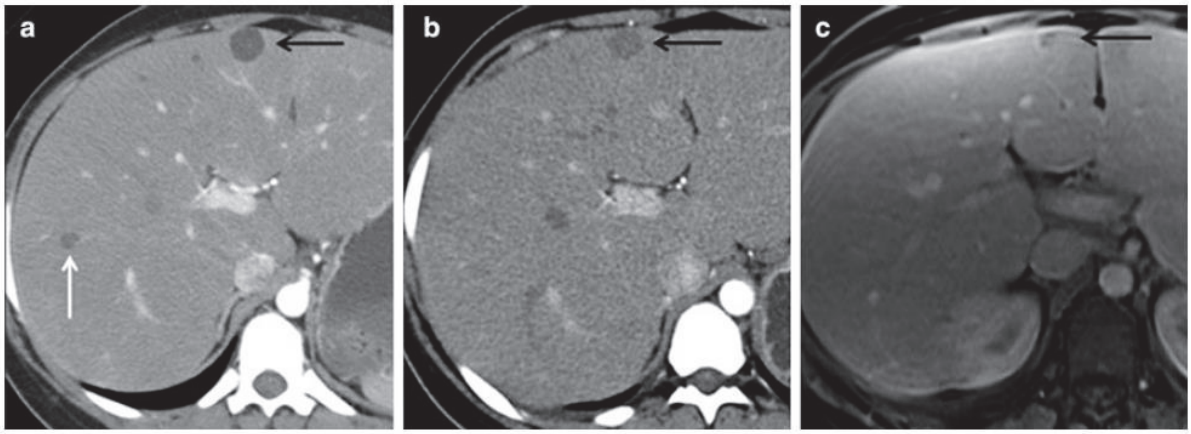

Figure 47: Regression of hepatic tumor detected via CT scan and MRI of a patient with GSDI

(a) CT image of the liver demonstrates two lesions in the liver representing HCAs (black and white arrows). (b) CT image of the same patient 18 months later demonstrates decrease in size of the HCA (black arrow). The lesion in the right hepatic lobe, white arrow in (a), has completely resolved. (c) MR image of the liver in the same patient 8 years later demonstrates continued decrease in size of the HCA (black arrow). Patients analyzed in this study followed strictly the guidelines for GSDI nutritional therapy and had optimal metabolic control.

(Beegle et al., 2014)

Finally, it has been reported that growth was improved in GSDI patients who received standard nutritional therapy, in comparison with that in a control group who did not receive this dietary therapy (Mundy et al., 2003).

Even though this diet has extremely improved life expectancy in GSDI patients, it is unable to prevent entirely all of the symptoms and long-term complications of GSDI, including HCA and HCC development. Increased life expectancy leaves more time for hepatocellular tumors to develop. On the other hand, regression of HCA right after the implementation of the dietary regimen has been observed as early as 1981 (Parker et al., 1981). This study including 3 treated and 2 non-treated patients reported that 2 of the patients who started dietary intervention presented a disappearance of the hepatic lesions, and a marked reduction in size of the adenoma occurred in the third patient. The hepatic lesions remained present in the 2 untreated patients. The same results were confirmed recently (Beegle et al., 2014), and it was concluded that when HCAs are documented in a patient with suboptimal metabolic control, intensive medical therapy may be an alternative to surgical intervention in some individuals (*Figure 47*). Optimal metabolic control in this study was defined as: triglycerides less than 2 g/L, lactate less than 2.2 mmol/L, and serum glucose greater than 75 mg/dL.

Diet improved not only hepatic parameters, but it also had a positive effect on the renal tubular dysfunction in GSDI patients (Chen et al., 1990). Indeed, even though the histological aspects of the kidneys were not analyzed in this study, the tubular function in patients with GSDI was assessed by measuring urinary excretion of amino acids, phosphate, and β2-microglobulin (a sensitive indicator of tubulo-interstitial lesions). These parameters of kidney injury were different in patients that followed or not the recommended dietary therapy, highlighting once again the importance of this regimen and its beneficial effects. Similar results were observed in another study, demonstrating that in patients with optimal metabolic control due to strict diet, microalbuminuria and proteinuria incidence was decreased (Martens et al., 2009).

In conclusion, even though dietary therapy is not 100% effective in the prevention of GSDI complications, it has a striking effect on life expectancy, metabolic control,

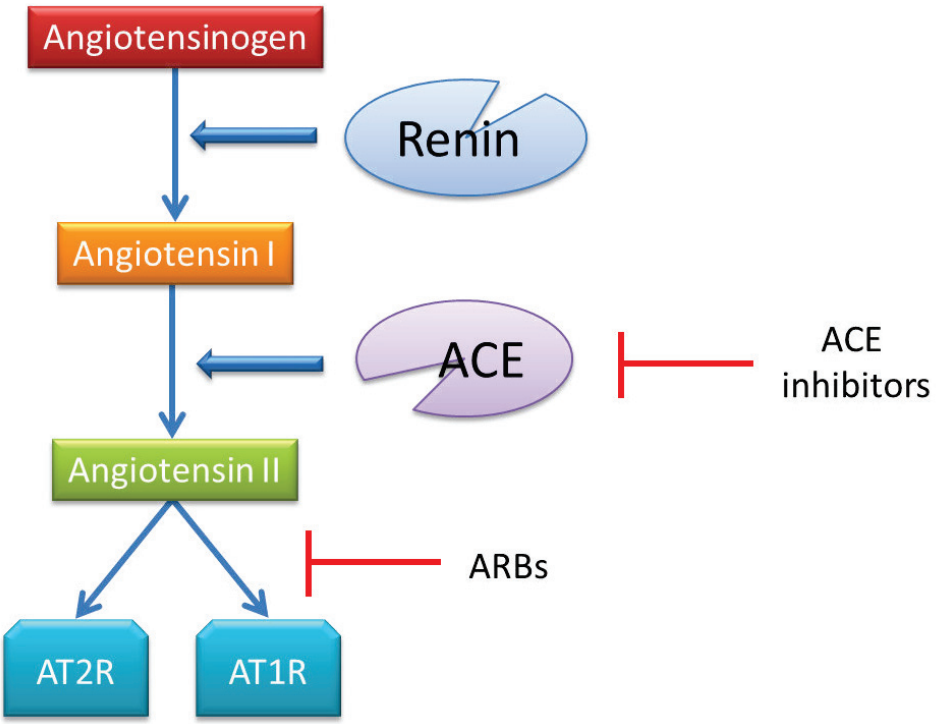

Figure 48: Representation of the mechanistic actions of Angiotensin converting enzyme (ACE) inhibitors and Angiotensin II receptor blockers (ARBs) often used to prevent chronic kidney disease

AT1R and AT2R – Angiotensin II receptors

glycaemia maintenance and even long-term complications. Thus it is imperative that the patients follow the nutritional guidelines.

IV.2) Pharmacological therapy

Angiotensin converting enzyme (ACE) inhibitors, such as benazepril or enalapril, have been used for many years in GSDI patients exhibiting kidney dysfunction, in order to block the RAS / TGF-β1 signaling axis and subsequently inhibit kidney fibrosis development (*Figure 48*). This strategy has been developed mainly for diabetic patients, since they present the same molecular mechanisms leading to nephropathy. Several studies have reported that this therapeutic strategy can normalize GFR for a limited time span and can improve glomerular hyperfiltration in GSDI patients (Martens et al., 2009; Melis et al., 2005). Angiotensin receptor blockers (ARBs), which are angiotensin II receptor antagonists, such as losartan or irbesartan (*Figure 48*), are also used by GSDI patients, sometimes combined with ACE inhibitors (Gjorgjieva et al., 2016a; Kishnani et al., 2014).

Allopurinol, a xanthine oxidase (XO) inhibitor, is used by many patients in order to prevent hyperuricemia (*Figure 31*). In a cohort of 32 patients followed by Prof. Philippe Labrune in Paris, 84% of the patients declared using this treatment (Gjorgjieva et al., 2016a), whereas the European study of GSDI has reported only 57% (Rake et al., 2002a). Nevertheless, in 29% of the patients using Allopurinol or other XO inhibitors, serum uric acid levels were still elevated, raising the question of the efficiency of this treatment in GSDI patients.

Lipid lowering strategies are also commonly used in GSDI patients with hyperlipidemia and hypercholesterolemia. Fibrates and other lipid lowering drugs are administered, generally in extreme hyperlipidemic conditions, when patients present more than 10 g/L of triglycerides in blood plasma. For example, 34% of the patients followed by Prof. Philippe Labrune in Paris reported the use of lipid-lowering treatments (Gjorgjieva et al., 2016a).

IV.3) Hepatic and / or renal transplantation in GSDI patients

Dietary treatment has an important beneficial effect on GSDI long-term outcome, but it is not entirely effective in the inhibition of tumor development and the progression of CKD. These complications can still occur in GSDI patients and the last resort when the pathologies are highly advanced is hepatic and / or renal transplantation.

Liver replacement is the ultimate therapy for hepatic metabolic disease. It is recommended in GSDI patients with multifocal, growing lesions that do not regress with improved dietary regimens, with bleeding tumors and tumors that do not have evidence of distant metastatic disease (Kishnani et al., 2014; Rake et al., 2002b). The first liver transplantation in a GSDI patient was performed in 1983, and after that, hundreds of patients have undergone this procedure (Kishnani et al., 2014; Malatack et al., 1983). After liver transplantation, all GSDI patients achieve resolution of their metabolic derangement, including correction of hypoglycemia, lactic acidosis, hyperuricemia, and hyperlipidemia (O'Leary et al., 2008). Nevertheless, hepatic transplantation comes with important risk factors, such as transplant rejection and kidney failure, which were observed frequently in GSDI patients (Boers et al., 2014). Indeed, liver transplantation does not improve renal complications, which suggested that the hepatic and renal pathologies in GSDI are completely independent (Rake et al., 2002a). This finding was further confirmed by the development of two mouse models with organ-specific deletion of *G6pc* in the liver or kidneys, which developed the hepatic or renal GSDI pathology, respectively (Clar et al., 2014; Mutel et al., 2011a). Therefore, mice which present normal expression of *G6pc* in the kidneys and *G6pc* deletion in the liver still develop the hepatic GSDI pathology and inversely, mice *with* G6pc deletion in the kidneys develop GSDI nephropathy, even with normal *G6pc* expression in the liver. Finally, liver transplantations are associated to mortality rates that need to be taken into consideration (Reddy et al., 2009). Indeed, GSDI patients that had undergone liver transplantation in North America exhibited a 1-, 5-, and 10-year survival rate of 82%, 76%, and 64%, respectively (Maheshwari et al., 2012).

Renal transplantation has also been performed in GSDI patients when patients exhibit renal failure (Rake et al., 2002a). Nevertheless, kidney transplants do not allow a

normalization of glycaemia (Labrune, 2002). Several studies indicate the beneficial effects of combined liver-kidney transplantation in the case of GSDI even in the absence of serious liver lesions, with the aim of improving the quality of life of these patients (Belingheri et al., 2007; Labrune, 2002; Panaro et al., 2004).

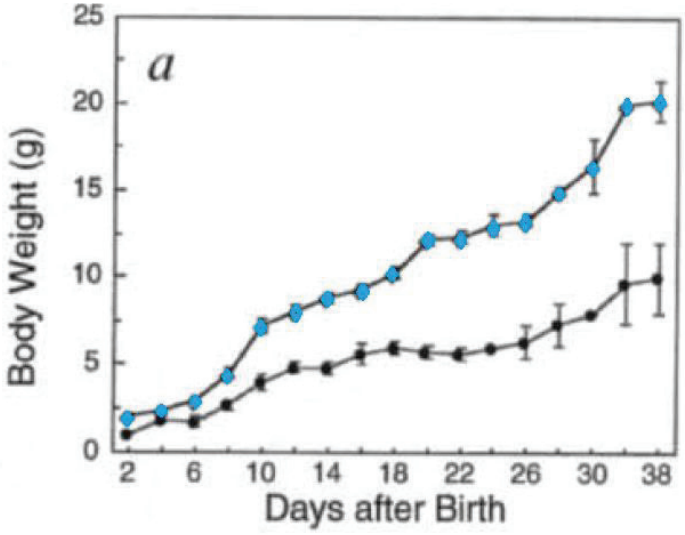

Figure 49: Growth retardation in G6pc-/- mice

Weight gain of G6pc+/+ and G6pc+/- mice (blue), compared to G6pc-/- mice (black), during the first 38 days after birth.

(Lei et al., 1996)

V) Contribution of animal models of GSDI in the comprehension of the pathology and first gene therapy studies

Many aspects of GSDI are still unclear at a molecular level. A better understanding of the molecular pathways involved in long-term pathologies associated with GSDI will allow us to find new pharmacological targets. One of the reasons why so many questions are left unanswered is the limited number of patients, but also the evident risk of testing potential treatment strategies in patients, especially since a major part of these patients are children. This is why the need of animal models of GSDI is essential in order to decipher the mechanisms of this disease.

V.1) Animal models of GSDI

Total Knock-out G6pc mouse model

The first mouse model of GSDIa was developed in 1996, by the team of Janice Chou. These mice exhibit a total knock-out of *G6pc* obtained by transgenesis by the deletion of *G6pc* exon 3 (G6pc-/- mice) (Lei et al., 1996). G6pc-/- mice present low birth weight, growth retardation (*Figure 49*), severe hypoglycemia and significant increase in serum cholesterol and triglyceride levels. Moreover, only 60% of mice treated with glucose injections, glucose-fortified water and food supplementation survive through weaning and have a life expectancy of about 6 months (Lei et al., 1996). As observed in GSDI patients, G6pc-/- mice exhibit hepatomegaly and nephromegaly. Interestingly, the size, agility, serum lipids and glycemic control were shown improve dramatically in adult G6pc-/- mice that have survived the frail weaning period, reaching levels approaching their wild-type (WT) littermates (Salganik et al., 2009). In addition, adult G6pc-/- mice were shown to be able to mate and produce viable offspring. However, liver histology and glycogen accumulation do not improve with age (Salganik et al., 2009). Hepatic tumorigenesis was not described in this study. Furthermore, these mice exhibit the renal complications associated with GSDI.

While total knock-out mice represent a great tool to investigate deregulated metabolism pathways in GSDIa, long-term complications such as HCA / HCC could not be observed in these mice because they do not survive long enough to develop them.

	Total G6pc$^{-/-}$ mice	Liver G6pc$^{-/-}$ mice	Kidney G6pc$^{-/-}$ mice	Intestinal G6pc$^{-/-}$ mice
Glycaemia	≈40–50mg/dL in the fed state	Normal in the fed state (≈150–200 mg/dL) 50–60 mg/dL at 6h of fasting	Normal in the fed state Normal at 6h of fasting (≈140 mg/dL)	Normal
Plasmatic parameters	Hypertriglyceridemia (≈1.8–2.0 g/L)	Hypertriglyceridemia (≈1.2 mg/L)	Normal TG	Normal
	Hypercholesterolemia (≈1.8 g/L)	Hypercholesterolemia (≈1.2 g/L)	Normal cholesterol	
	Hyperuricemia (≈25 mg/L)	Hyperuricemia (≈25 mg/L)	Hyperuricemia (≈11 mg/L)	
	No or slight lactic acidemia	Lactic acidemia	Normal lactic acid	
Liver	Hepatomegaly (liver weight 10% BW) Steatosis	Hepatomegaly (liver weight: 8% of BW) Steatosis Late development of HCA*	Normal	Normal
Kidney	Nephromegaly (kidney weight: ≈3.5% BW)	Normal	Nephromegaly (kidney weight: ≈1.8% BW) Renal lipid accumulation Microalbumineria Partial electrolyte imbalance	Normal
Intestine	Not determined	Normal	Normal	To be analyzed
Life expectancy	Need intensive glucose therapy or gene therapy to survive weaning	Normal	Over 12 months	Normal

Figure 50: Characterization of the total and organ-specific *G6pc*-deleted mice

The characteristics of total G6pc−/− mice were described by Kim et al. 2008; Lei et al. 1996. The data of liver G6pc−/− mice were described in Mutel et al. 2011. The data of kidney G6pc−/− mice were described in Clar et al. 2014. BW: body weight.

(Rajas et al., 2015)

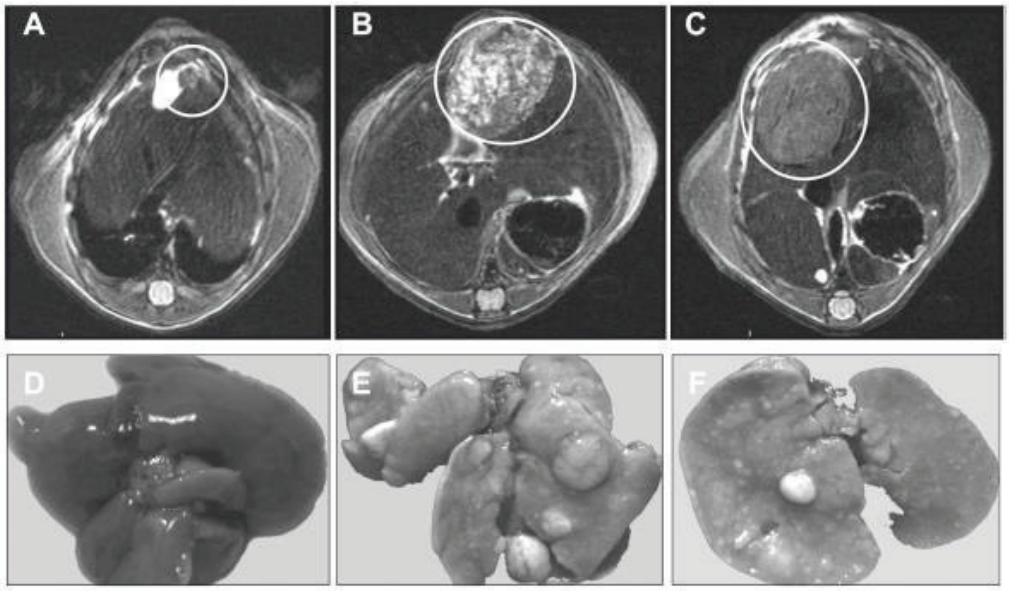

Figure 51: Development of liver nodules in L.G6pc-/- mice after one year of gene deletion

MR images showing the evolution of liver lesions at 12 months (A) and 18 months (B and C) after *G6pc* deletion. Liver resection after 18 months in control mice (D) or in L.G6pc-/- mice (E and F) with multiple tumour nodules.

(Mutel et al., 2011)

These mice exhibit hypoglycemic episodes, which are severe and need constant treatment with glucose. This generates difficulties in the manipulation of the mice and in the organization of the study protocols.

To gain further insights into the long-term mechanisms of the disease and to evaluate potential treatment strategies, an animal model with sufficient life expectancy was required. By disrupting G6Pase activity specifically in the liver (L.G6pc-/- mice), kidneys (K.G6pc-/- mice) or intestine (I.G6pc-/- mice), using a tamoxifen-inducible Cre^{ERT2}-lox system (conditional), our laboratory obtained viable mouse models of GSDIa (*Figure 50*) (Rajas et al., 2015).

Liver-specific G6pc knock-out mouse model (L.G6pc-/- mice)

To obtain a liver-specific invalidation of *G6pc*, the exon 3 of *G6pc* was deleted in the liver of L.G6pc-/- mice by crossing B6.G6pc$^{ex3lox/ex3lox}$ mice with B6.SA$^{CreERT2/+}$ mice (SA= serum albumin) (Mutel et al., 2011a). Thus L.G6pc-/- mice exhibit normal glycemia during fed state and have normal life expectancy. Glucose production is still assured by the kidneys and intestine in these mice, and they develop only moderate hypoglycemia (40-60 mg/dL) in post-absorptive periods (6h-fast), since they cannot mobilize their glycogen storages. During long fasting periods, the induction of renal and intestinal glucose production allows L.G6pc-/- mice to maintain blood glucose in a range similar to wild-type mice, around 90 mg/dL (Mutel et al., 2011a, 2011b). Furthermore, hepatic G6Pase deficiency translated to hepatic glycogen and G6P accumulation, as well as steatosis. Hypertriglyceridemia, hypercholesterolemia, hyperuricemia and lactic acidosis are observed in L.G6pc-/- mice as early as 10 days after *G6pc* deletion, but interestingly, these parameters have a tendency to normalize with age, with the exception of cholesterol (Mutel et al., 2011a).

L.G6pc-/- mice develop hepatocellular tumors, similar to those observed in GSDI patients (*Figure 51*). In around 15% of L.G6pc-/- livers, small lesions can be detected as early as 9 months of *G6pc* deletion. At 18 months, all L.G6pc-/- mice have liver nodules between 1 and 10 mm in diameter, histologically classified mainly as HCA. However, at this stage, 5-10% of the mice develop HCC, as observed in GSDI patients.

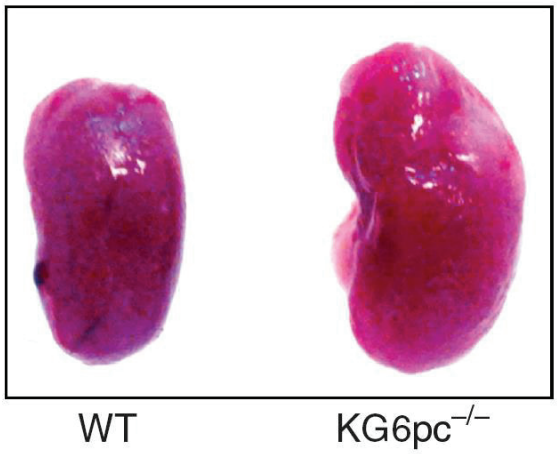

Figure 52: Nephromegaly in K.G6pc-/- mice

Increase in kidney size in K.G6pc-/- mice (right) compared to WT mice (left) at 6 months of *G6pc* deletion.

(Clar et al., 2014)

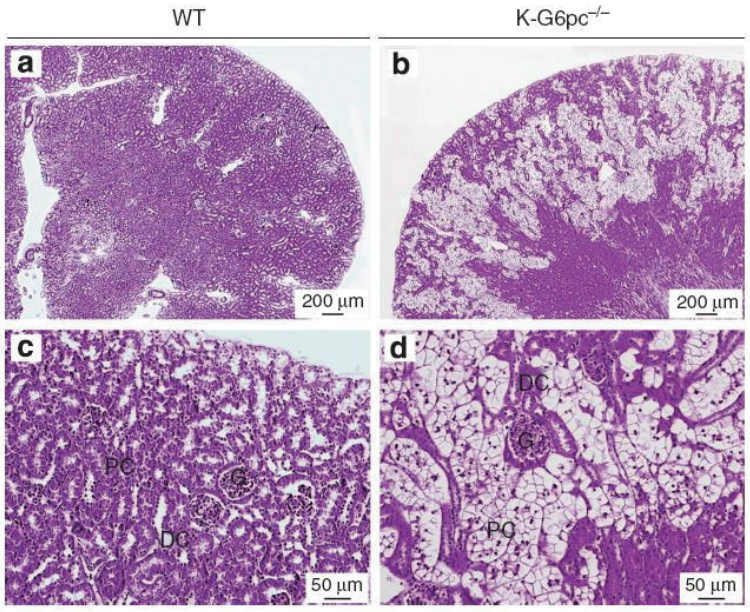

Figure 53: Morphological alterations in K.G6pc-/- kidneys at 6 months of *G6pc* deletion

Histological analyses of hematoxylin-eosin staining from WT (a, c) and K.G6pc-/- kidneys (b, d).
(c, d) correspond to a higher magnification of the kidney cortex observed in a and b, respectively. These analyses clearly show tubular dilatation and clarification in K.G6pc-/- kidneys.

(Clar et al., 2014)

This mouse model allowed the confirmation of the importance of the dietary regimen given to GSDI patients. Indeed, tumor incidence and the transformation rates of HCA to HCC were increased in L.G6pc-/- mice fed a high fat / high sucrose (HF/HS) diet (Rajas et al., 2015). Finally, this mouse model could allow an evaluation of the effects of various diets, such as galactose-enriched or fructose-enriched diet, in order to see whether these sugars actually have a negative impact on the long-term complications in GSDI. Furthermore, it can also be used to test pharmaceutical therapies, such as lipid-lowering drugs (see results), in order to analyze their effect on GSDI livers.

Kidney-specific G6pc knock-out mouse model (K.G6pc-/- mice)

K.G6pc-/- mice present a targeted deletion of *G6pc* specifically in the kidneys; they were obtained by crossing B6.G6pc$^{ex3lox/ex3lox}$ mice with B6.Kap$^{CreERT2/+}$ mice (Kap= kidney androgen protein) (Clar et al., 2014; Rajas et al., 2015). Even though *G6pc* deletion is only partial (50% decrease in G6Pase activity), these mice present all of the hallmarks of GSDI nephropathy, yet have normal life expectancy. Indeed, they exhibit glycogen and lipid accumulation in the kidney cortex, resulting in nephromegaly (*Figure 52*). Blood glucose levels are normal in K.G6pc-/- mice, compared to WT mice, since they produce glucose by the liver and intestine, and partially by the kidneys (Clar et al., 2014). On a histology level, as early as 6 months after *G6pc* deletion, tubular clarification and dilatation can be observed in the kidneys (*Figure 53*), but at this stage, it is not associated to interstitial fibrosis (Clar et al., 2014). Renal lipid accumulation is due to an activation of *de novo* lipogenesis and is responsible for the activation of the profibrotic pathway RAS and subsequently TGF-β1 and EMT (Clar et al., 2014; Rajas et al., 2015).

As L.G6pc-/- mice, K.G6pc-/- mice could be used to evaluate the effect of diet on the development of CKD, thus improving the dietary guidelines for the patients. Furthermore, the effects of renoprotective drugs used to treat diabetic CKD could be analyzed by treating K.G6pc-/- mice with ACE inhibitors and ARB inhibitors, in order to understand better if these drugs should be prescribed in human patients.

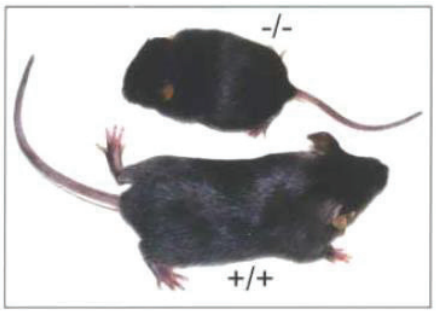

Figure 54: Size comparison of G6pt-/- mice and G6pt+/+ mice at 3 weeks of age, showing growth retardation of the G6pt-/- mice

(Chen et al., 2003)

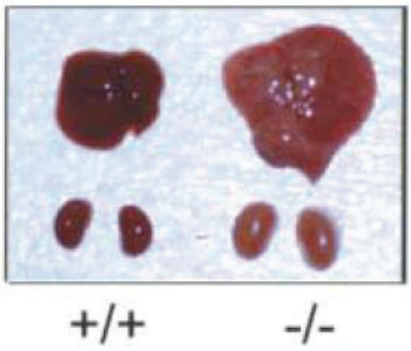

Figure 55: Marked hepatomegaly and nephromegaly in G6pt-/- mice, compared to G6pt+/+ mice at 21 days of age

(Chen et al., 2003)

Intestine-specific G6pc knock out mouse model (I.G6pc-/- mice)

I.G6pc-/- mice present a targeted deletion of *G6pc* specifically in the intestine; they were obtained by crossing B6.G6pc$^{ex3lox/ex3lox}$ mice with B6.Vill$^{CreERT2/+}$ mice (Vill= villin) (Penhoat et al., 2011). Indeed, these mice present a deficiency in G6Pase in the intestine, making them incapable to produce glucose in this organ. During the first year after *G6pc* gene deletion, I.G6pc−/− mice exhibit a growth rate similar to that of WT mice. Meanwhile, no diarrhea or abnormal consistency of the stools has been observed in I.G6pc−/− mice, while these symptoms are often experienced in GSDI patients. However, the quality of diet could influence intestine metabolism in the patients. Furthermore, histology analysis of I.G6pc−/− intestine did not show glycogen or lipid accumulation, nor inflammation. Thus I.G6pc-/- mice need to be thoroughly analyzed and characterized in order to see if they can actually be used as a model of intestinal GSDI pathology.

Total G6PT knock-out mouse model of GSDIb

A total knock-out of the glucose transporter G6PT was created by the deletion of the exon 1 of *Slc37a4* (Chen et al., 2003). These G6pt-/- mice exhibit growth retardation (*Figure 54*) and the same metabolic derangements as GSDIb patients, including neutrophil alterations. Indeed, increased circulating cholesterol, triglycerides, lactate and uric acid are observed in these mice, while blood glucose levels are decreased, leading to hypoglycemia. As expected, G6pt-/- mice present hepatomegaly and nephromegaly (*Figure 55*). Differential peripheral blood leukocyte counts reveal lower neutrophils and lymphocytes in the G6pt-/- mice, compared with age-matched controls, as well as altered hematopoiesis in the bone marrow and spleen.

G6pt-/- mice are a good model of GSDIb, due to the fact that not only do they present the metabolic GSDI alterations, but also exhibit neutropenia. However, G6pt-/- mice exhibit strong hypoglycemia in the absence of treatment, similarly to G6pc-/- mice and therefore long-term studies are challenging. Nevertheless, different pharmacological treatments could be tested in these mice in order to see if we can improve the complications specific for GSDIb.

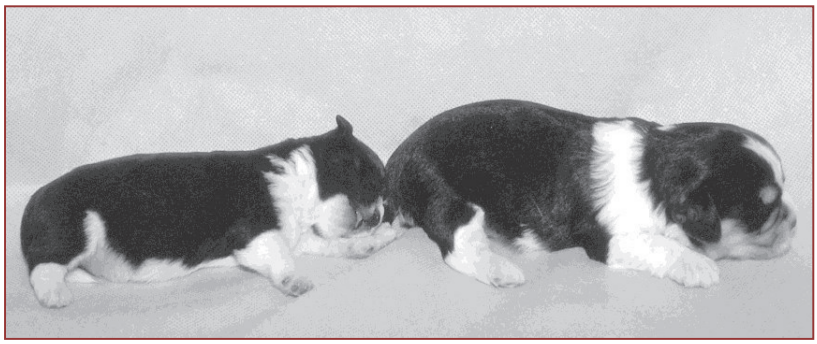

Figure 56: GSDI puppy compared with normal littermate

An affected GSDIa puppy (left), weighted 380 g, is compared with a normal littermate (right), weighted 660 g, at 14 days of age. Notice the abdominal distention in the affected puppy.

(Kishnani et al., 2001)

Naturally obtained G6Pase-deficient dogs

Two Maltese puppies presenting massive hepatomegaly, growth retardation and failure to thrive were diagnosed with GSDIa, since they exhibited G6Pase deficiency in the liver and kidneys (Kishnani et al., 1997). Indeed, a single mutation in the nucleotide position 450 was found in *G6pc*, leading to a guanine to cytosine (G to C) conversion, resulting in substitution of a methionine by isoleucine at codon 121. Later on, in order to maintain the colony of these dogs and increase their life expectancy, a cross breed between Maltese and Beagle breeds was obtained (Kishnani et al., 2001). Affected puppies exhibited tremors, weakness, and neurologic signs when hypoglycemic. They had postnatal growth retardation and progressive hepatomegaly (*Figure 56*). Biochemical abnormalities included fasting hypoglycemia, hyperlactacidemia, hypercholesterolemia, hypertriglyceridemia, and hyperuricemia. Microscopic examination of livers from affected puppies showed diffuse, marked hepatocellular vacuolation, with distended clear hepatocytes and central to marginally located rounded nuclei. Furthermore, segmental glomerular sclerosis and vacuolation of proximal convoluted tubular epithelium was detected in the kidneys.

Since canine G6PC sequence shares 90% similarities with human G6PC, G6pc-/- dogs represent a larger animal model than G6pc-/-mice for testing curative therapies applicable to human patients, such as gene therapy.

V.2) Gene therapy

Even though dietary and pharmacological treatments have many beneficial effects in GSDI patients, these strategies are treating the symptoms of the disease but are not curative. The only therapeutic strategy that could have a curative effect in GSDI patients is gene therapy. Indeed, replacing the mutated gene (G6PC or SLC37A4) with a new copy expressing the protein that was initially deficient would be ideal. Nevertheless, developing a vector that delivers this gene precisely in the target cells, and by doing so, not inducing inflammatory reactions or additional mutations along the ways, is extremely complicated. Assays of gene therapy strategies have started in the 2000s', thanks to mouse and canine models, using various defective virus vectors. First

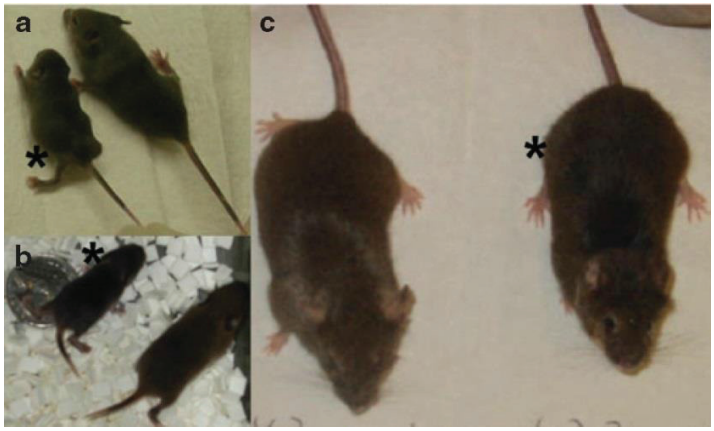

Figure 57: Restoration of normalcy of body habitus following helper-dependent adenovirus vector administration

Affected mice indicated (*), shown in comparison to unaffected age-matched mice. (a) G6pc-/- mice were 2 weeks old (w.o.). (b) G6pc-/- mice were 2 w.o. with coin (U.S. quarter) for comparison of sizes. (c) One-year-old G6pc-/- mice following HDAd vector administration.

(Koeberl et al., 2007)

viruses used were adenovirus (Koeberl et al., 2007; Zingone et al., 2000) (*Figure 57*). While the normalization of glucose and other plasmatic parameters has been generally observed in treated animals, the efficiency of cell transduction was very low. Interestingly, adenovirus-treated mice survived, even though only a small percentage of the hepatocytes were transduced. Thus targeting 100% of the hepatocytes and proximal tubules, as well as expressing the vector in long-term protocols remain big challenges. Fortunately, new viral vectors, less inflammatory than adenovirus, were developed these last years.

Recombinant adeno-associated virus vectors

Recombinant adeno-associated virus (rAAV) gene therapy has progressed rapidly over the past decade, especially due to novel capsid serotype development, organ-specific promoters, and an increased understanding of the immune response to AAVs. In particular, liver-directed therapy has made remarkable advancements, with a number of clinical trials currently planned and ongoing in hemophilia A and B, as well as other liver disorders (Ahmed et al., 2013; Kattenhorn et al., 2016). Thus it is not surprising that this strategy was considered for GSDI gene therapy strategy.

In 2002, a sustained hepatic and renal G6Pase expression was reported in G6pc-/- mice, using a rAAV vector (AAV2-G6PC), expressing *G6pc* under the chicken β-actin promoter/CMV enhancer, in combination with an adenovirus vector previously used (Ad-mG6PC) (Sun et al., 2002). AAV2 vectors ensure a more stable long-term expression than adenovirus, even though these vectors are not integrative and stay in an episomal form in the cell. The strategy prevented premature deaths and corrected metabolic abnormalities in G6pc-/- mice for full 12 months. Unfortunately, injection of AAV2-G6PC alone did not have this effect. While this dual vector injection presented great results in mice, considering it as a strategy in humans could entail many risk factors.

Targeting both the liver and kidneys is an important criterion for GSDI gene therapy. Since kidney transduction is optimal with an AAV serotype 2, while liver transduction requires AAV type 8 or 9, combining the ITR sequences of AAV2 and the

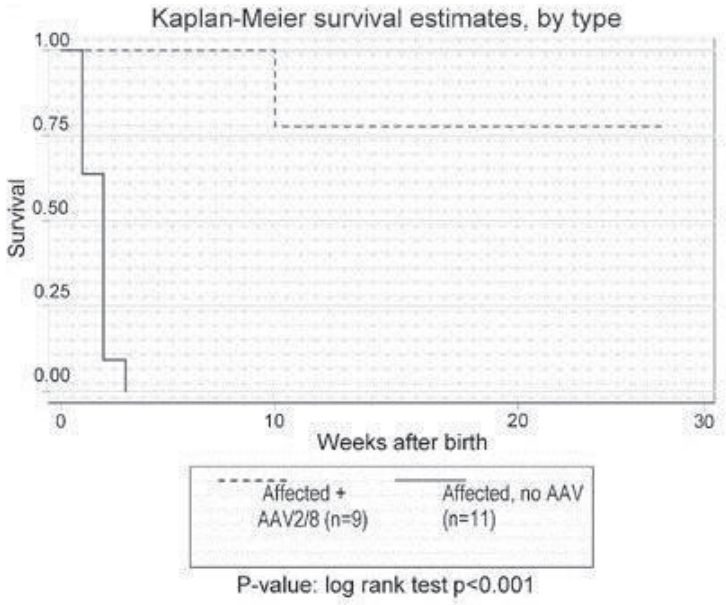

Figure 58: Survival and growth of G6pc-/- mice treated by gene therapy

Kaplan–Meier analysis for treated, affected mice (affected + AAV), in comparison to untreated, affected mice (affected).

(Koeberl et al., 2006)

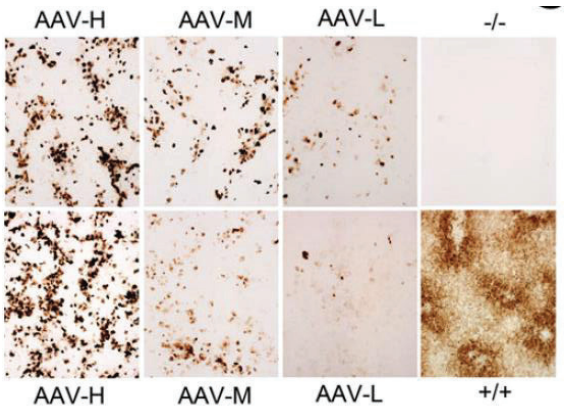

Figure 59: Histochemical analysis of hepatic G6Pase-a activity in 70-90 week old WT and G6pc-/- mice

Freshly sectioned liver specimens were analyzed for G6Pase activity using the method of lead trapping of phosphate generated by G6P hydrolysis. Each image represents an individual mouse. Treatments are indicated by the following notation: -/- untreated G6pc-/- mice; +/+ WT mice; AAV panels are mice infused with various dosages of AAV-GPE. AAV-L (n = 6), AAV-M (n= 9), and AAV-H (n = 5) representing AAV-GPE–treated G6pc-/- mice expressing 3%-9%, 22%-63%, and 81%-128% normal hepatic G6Pase-a activity, respectively.

(Lee et al., 2012)

capsid proteins of AAV8 and AAV9, resulting in AAV2/8 and AAV2/9 serotypes, is an interesting strategy to target both organs in GSDI (Wu et al., 2006). Interestingly, the use of AAV2/9 was able to restore 40-50% of hepatic and renal G6Pase expression, successfully decreasing glycogen stores in both the liver and kidneys. Aside from resolving hypoglycemia, AAA2/9 gene therapy impeded nephropathy development in G6pc-/- mice for 12 months (Luo et al., 2011). Moreover, AAV2/8 vectors carrying *G6pc* under the G6Pase promoter have been tested in G6pc-/- mice, resulting in a significant increase in survival rates (*Figure 58*) (Koeberl et al., 2006). Unfortunately, important hepatic vector loss was detected, along with an inefficiency of kidney targeting by the vector. Later on, to improve kidney targeting, another strategy using AAV2/1 and AAV2/8 serotypes expressing *G6pc* under the chicken β-actin promoter/CMV enhancer was tested (Ghosh et al., 2006). Interestingly, only AAV2/1 achieved significant increase in G6Pase expression in the liver and the kidneys. More importantly, this study reflected the need of re-injection when using AAVs, due to the gradual loss of the vector overtime. Indeed, during the neonatal period hepatocytes divide intensively resulting in a dilution of the vector, since AAVs are not integrated in the genome. More recent long-term studies using AAV2/8 with *G6pc* under the human promoter of G6PC corrected glycaemia, glycogen and TG accumulation, normalized G6Pase activity in the liver (*Figure 59*) and prevented tumor development in G6pc-/- mice, even in the presence of light hepatomegaly (Lee et al., 2012b, 2013). Nevertheless, renal expression of *G6pc* was not reported.

Gene therapy with AAV2/8 carrying *G6pt* expressed under the chicken β-actin promoter/CMV enhancer was also tested in the GSDIb mouse model (Yiu et al., 2009). While this vector allowed the stabilization of plasmatic parameters in G6pt-/- mice, tumor development was still detected. To improve the strategy, a more recent study used a new AAV2/8, expressing *G6pt* under the human G6PC promoter/enhancer (GPE). Similar results were observed, since the transduced G6pt-/- mice lived almost a year, but all of them expressed only low levels of hepatic G6PT and several developed multiple HCAs undergoing malignant transformation (Kwon et al., 2016).

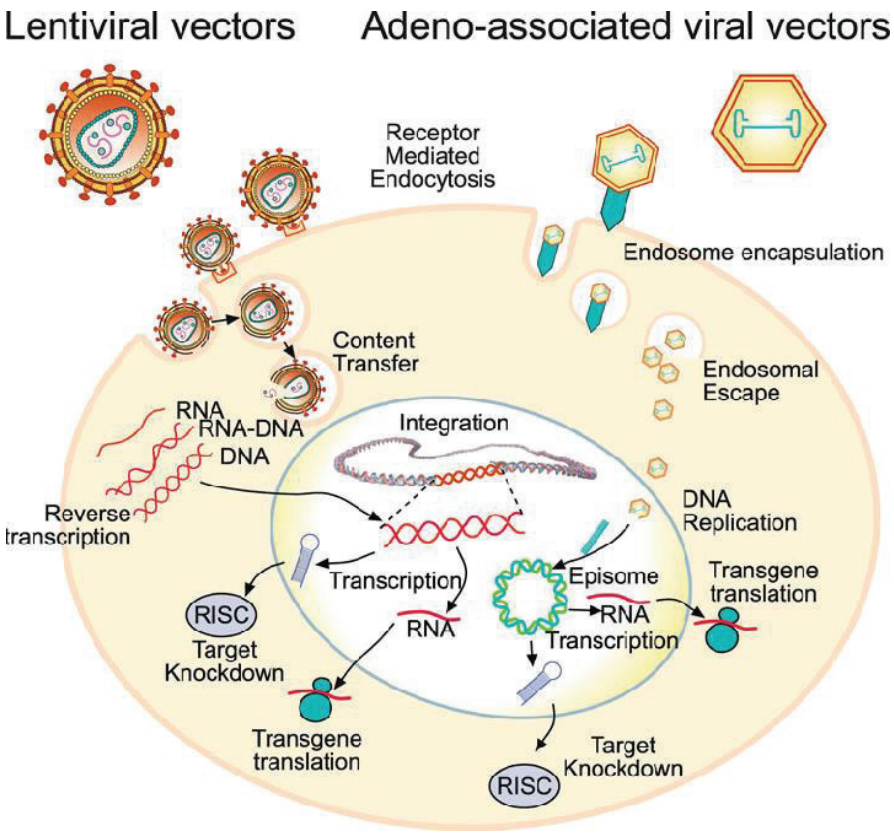

Figure 60: Diagram comparing lentiviral and AAV vector infection and distinctive methods of expression of transgene products

Both vector systems are capable of transgene expression and endogenous gene knockdown using siRNA technology. Genetic material from Lentivirus is translocated to the nucleus, where it can be integrated in the host's genome and transcribed. The resulting RNA serves either for protein coding, or as a siRNA silencing matrix. AAV vectors release the genetic material in an episomal form in the nucleus (rarely integrated) and this DNA is used, as for Lentiviral vectors, for the synthesis of the target RNA.

(Dissen et al., 2012)

In the canine model of GSDIa, recent studies reported normoglycemia achievement, glycogen accumulation decrease and growth retardation improvement with AAV2/8 and AAV2/9 vectors (Brooks et al., 2013; Koeberl et al., 2008). Nevertheless, a dilution of the vector overtime is still observed. Finally, a study in 2012 clearly showed that re-administration of a new type of AAV is needed nearly every 9 months (in this study the first administered vector was AAV2/9, then AAV2/7, and finally AAV2/8) to sustain normoglycemia in GSDIa dogs (Demaster et al., 2012). Unfortunately, no long-term studies in GSDI dogs report an actual effect on tumor development, representing one of the major concerns in the development of a gene strategy for human patients.

Lentivirus vectors

Lentiviruses can integrate in the host's genome, even in cells that are actively dividing (Ferry et al., 2011; Zahler et al., 2000) and are not associated with insertional mutagenesis in the liver (Ferry et al., 2011; Rittelmeyer et al., 2013; Themis et al., 2005) thus assuring a long-term expression of the transgene (*Figure 60*). The efficiency of lentiviral-mediated therapy has been validated in several animal models of inherited liver diseases, such as Crigler-Najjar type 1, Wilson disease and haemophilia ((Brown et al., 2007; Merle et al., 2006; Schmitt et al., 2010).

In order to stably transduce hepatocytes, a feline immunodeficiency virus (FIV)-based lentiviral approach has been considered in G6pc-/- mice (Grinshpun et al., 2010). This therapy led to normalized blood glucose levels, extended survival, improved body weight, and decreased accumulation of liver glycogen. Nevertheless, targeting of the liver and especially the kidneys was suboptimal, resulting in the persistence of nephromegaly and hepatomegaly. More recently, our laboratory has also started a lentiviral gene therapy assay (human immunodeficiency virus (HIV)-based) in L.G6pc-/- mice (Clar et al., 2015). This strategy restored G6Pase activity levels sufficient to prevent fasting hypoglycemia for more than 8 months after *G6pc* deletion (*Figure 61*). Lentivirus-treated L.G6pc-/- mice presented a large decrease in hepatic glycogen and triglyceride content and were protected against the development of HCA after 9 months of gene therapy (*Figure 62*). The major advantage of this strategy is the insertion of the

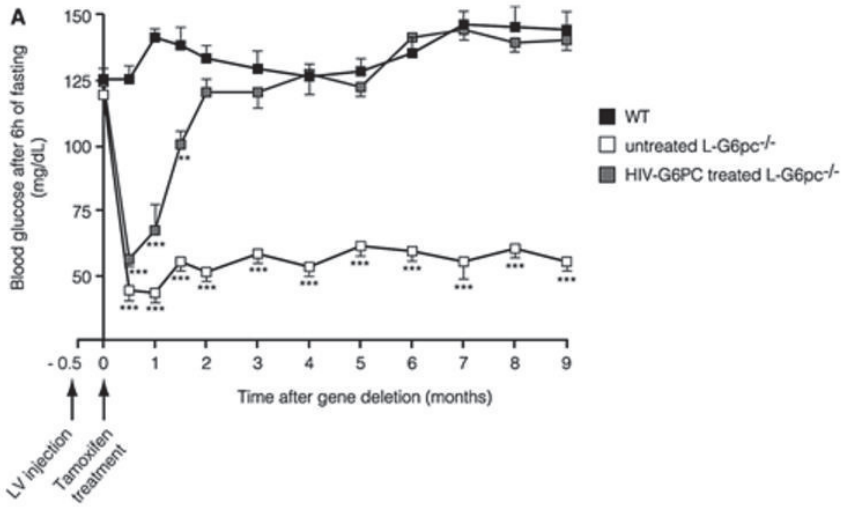

Figure 61: Glycaemia restoration in L.G6pc-/- mice with a lentiviral vector

Blood glucose after 6 h of fasting following during 9 months after gene deletion in WT (black squares), untreated L.G6pc−/− (white squares) and HIV-G6PC treated L.G6pc−/− mice (dark grey squares).

(Clar et al., 2015)

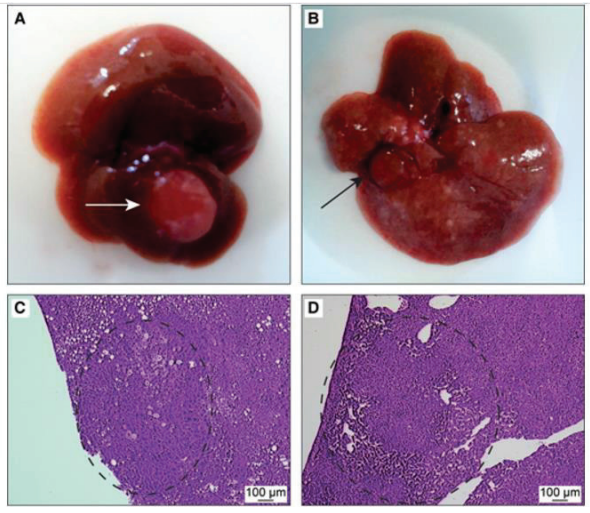

Figure 62: Tumor development in L.G6pc−/− mice

(A and B) Liver resection after 9 months of hepatic *G6pc* deletion. Arrows point nodules of about 3–4 mm of diameter. (C–D) Histological analysis by H&E staining of an HCA (C) and HCC (D) developed in untreated L.G6pc−/− mice.

(Clar et al., 2015)

vector in the host's genome, and thus during cellular division, a copy of the vector is kept in both daughter cells, preventing the dilution of the virus. While this lentiviral approach is attractive since it seems to allow a long-term expression of the transgene, the use in humans is much more complex. Genotoxicity risk associated with the preferential intragenic integration events represents the most obvious concern. Fortunately, the substantial flexibility of the lentiviral vector genome offers opportunities for redesigning sequences of the backbone as well as the therapeutic cargo to further reduce this risk.

In conclusion, developing an optimal gene strategy for GSDI is a very complex task. It is noteworthy that restoring normoglycemia was achieved in numerous gene therapy assays, proving that only a small amount of cells need to be targeted (about 5 - 10%) to normalize this parameter. However, stabilizing glycaemia levels does not prevent hepatomegaly, hepatic tumor or CKD development. Thus in contrast to other monogenic diseases, such as Crigler-Najjar disease or coagulation defects that require the expression of only low levels of the related hepatic protein in the blood stream to treat the systemic illness manifestations, gene therapy approach for GSDI has to correct a maximum of hepatocytes and proximal tubules. Indeed, the rest of the hepatocytes which did not receive the vector still accumulate glycogen and lipids, and can still lead to the development of HCA / HCC. However, it has been suggested that a limited transfer of G6P might be possible between cells that could allow alleviation of metabolic burden of the neighboring cells, but this hypothesis has never been proven. Furthermore, finding a vector for gene therapy in GSDI patients requires a meticulous selection, since this vector is not supposed to induce immune reactions, and should be able to integrate safely in the genome of the patient, in order to assure a long-term expression of the transgene. Finally, hepatocytes and proximal tubules have different tropisms, which render this task difficult to achieve with one vector.

Finally, advances in the development of genome editing technologies based on programmable nucleases have significantly improved our ability to make precise changes in the genome. Nowadays, there are new tools that can be used for gene therapy, such as zinc finger nucleases (ZFNs), transcription activator like effector

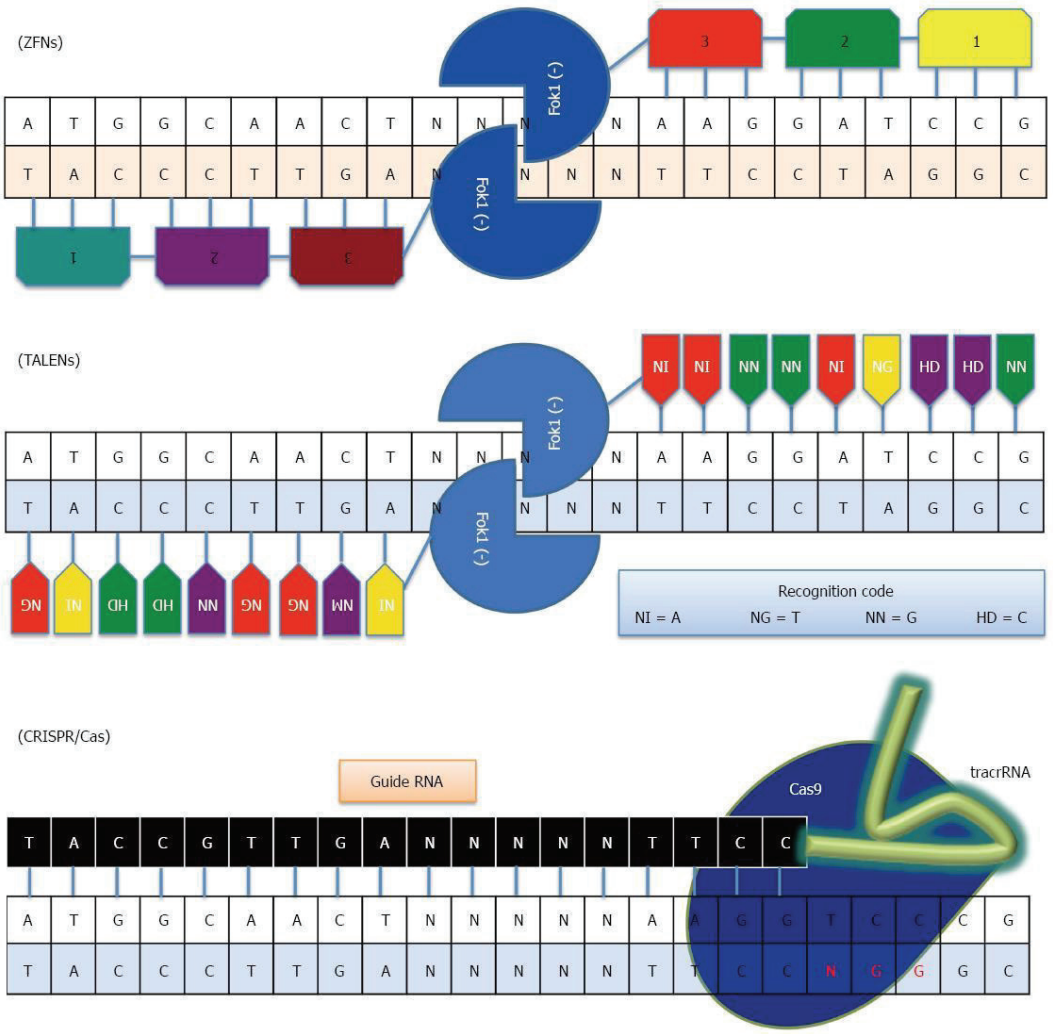

Figure 63: Schematic representation of programmable engineered nucleases of ZFNs, TALENs and CRISPR/Cas

Zinc finger nucleases (ZFN) have domains that recognize groups of 3bp, transcription activator-like effector nucleases (TALEN) have domains that recognize 2bp (NI=A, NG=T, NN=G, HD=C) and (CRISPR/Cas9) recognize each bp, thus present high specificity.

(Lu et al., 2015)

nucleases (TALENs) and Clustered Regularly Interspaced Short Palindromic Repeats (CRISPR)-associated nuclease Cas9 (Chou et al., 2012; Cox et al., 2015; Engelholm et al., 2017; Gaj et al., 2013). These strategies allow site-specific genome editing and thus in GSDI they can be used to insert a novel copy of G6PC or SLC37A4 in order to replace the mutated gene.

A ZFN is composed of a site-specific DNA-binding domain and a Fok1 restriction enzyme endonuclease domain (*Figures 63 and 64*). The zinc finger protein recognizes a 3-bp sequence of DNA, with its tandem repeats potentially attaching to a stretch of nucleotides between 9 and 18 bp. To perform site-specific cleavage of DNA, one monomer recognizes the binding site on the forward strand, while the other recognizes it on the reverse, so that the pair of Fok1 nuclease domains can cleave the DNA generating a DSB (Urnov et al., 2010).

TALENs are similar to ZFN (*Figures 63 and 64*) and contain a DNA-binding domain and a Fok1 catalytic domain (Joung and Sander, 2013). A DNA-binding domain is constructed with an N-terminal segment, a central repeat domain, and a half repeat. The central repeat domain is comprised of several monomers that are called transcription activator-like effectors (TALEs). TALEs are tandem repeats, containing repeat-variable di-residue (RVD) domains, used to determine the specificity of the TALEs. There are four RVD domains, NN, NI, HD, and NG, for the recognition of guanine, adenine, cytosine, and thymidine, respectively. Fok1 is located in the C-terminal segment and generates a DSB.

Finally, the CRISPR-Cas9 technology became wildly popular in the gene editing field. The CRISPR-associated protein Cas9, an endonuclease, uses a guide sequence within an RNA duplex, tracrRNA/crRNA, to form base pairs with DNA target sequences, enabling Cas9 to introduce a site-specific double-strand break in the DNA (Doudna and Charpentier, 2014) (*Figures 63 and 64*). The dual tracrRNA/crRNA was engineered as a single guide RNA (sgRNA) that retains two critical features: a sequence at the 5′ side that determines the DNA target site and a duplex RNA structure at the 3′ side that binds to Cas9. This finding created a simple system in which changes in the guide sequence of the sgRNA program Cas9 to target any DNA sequence of interest.

Nucleases	ZFN	TALEN	CRISPR/Cas
DNA binding domain	Multiple zinc finger peptides	Transcription-activator like effectors	CRISPR-derived RNA/Single-guide RNA
Endonuclease	Fok1	Fok1	Cas9
Binding specificity of each repeat	3 bp	2 bp	1 bp
Target site length	18 to 36 bp	30 to 40 bp	23 bp
Off-target	High probability	Low probability	Variable
Libraries generation	No	Feasible, depend on technology	Yes, cloning 20 bp, oligos targeting each gene into a plasmid

Figure 64: Summary of the different characteristics of ZFN, TALEN, and CRISPR/Cas gene editing tools

(Lu et al., 2015)

ZFN, TALENS and CRISPR-Cas9 nucleases have been demonstrated to achieve efficient genome editing in a wide range of model organisms and mammalian cells and efforts are made in order to develop these tools as therapeutics (Cox et al., 2015).

EXPERIMENTAL PROCEDURES AND RESULTS

Dietary therapy was proven to have highly beneficial effects in the stabilization of plasmatic parameters in GSDI patients. Indeed, hypoglycemic episodes seem to occur far less in patients with optimal metabolic control. Nevertheless, this treatment strategy does not impede completely the long-term pathologies that characterize GSDI. Since dietary therapy has allowed a substantial extension of the life span of GSDI patients, these complications are observed more often than in the past. Thus the focus invested in glycaemia maintenance is nowadays diverted to the understanding of molecular phenomena involved in the long-term complications.

In this work, our goal was to decipher the underlying mechanisms behind hepatocarcinogenesis and CKD development in GSDI. To achieve this, we used the L.G6pc-/- and K.G6pc-/- mice, which are unique GSDIa viable mouse models that develop all hepatic and renal long-term complications of GSDIa.

The **first chapter** consists in the results related to hepatocarcinogenesis, obtained in L.G6pc-/- mice. Indeed, this project consisted in the analysis of the hepatic metabolism in these mice and how «Warburg-like» metabolic reprograming observed in GSDI livers could promote tumor formation, progression and transformation in this organ. Furthermore, taking into account many studies which reported involvement of autophagy, ER stress and altered oxidative state in tumorigenesis, all of these pathways were characterized in the liver and tumors of L.G6pc-/- mice. Since tumorigenesis in GSDI is a very characteristic process which occurs in the absence of liver fibrosis / cirrhosis, different from what is observed in the general population, EMT, a known profibrotic pathway, was assessed in the livers and tumors of L.G6pc-/- mice. Last, since bibliography reported a loss of the hepatic tumor suppressor HNF1α in GSDI, we analyzed other tumor suppressor candidates that could also be involved in GSDI tumorigenesis.

In the same chapter, we have added a review describing the «Warburg-like» metabolic reprograming already reported in the literature. This review summarized the similarities between GSDI hepatocytes and cancer cells.

The **second chapter** consists in the description of the long-term renal complications in GSDI, since this process remains relatively unclear. Furthermore, many renal injury markers used to detect nephropathy symptoms in GSDI patients are not sensitive enough to report early stages of the disease. Thus nephropathy is usually detected at a later stage in GSDI, when the damages caused in the kidneys are irreversible. Therefore, there is a crucial need for a more sensitive biomarker indicating kidney injury in GSDI. In this work, kidneys of K.G6pc-/- mice were analyzed at different stages of the disease by characterizing histological damages, metabolism, molecular RAS/TGF-β1 pathway and renal function. Furthermore, a new urinary marker, i.e. lipocalin 2, was proposed in order to earlier detect nephropathy. In addition, CKD progression was studied in human patients, by analyzing biological data and kidney images obtained by MRI from a 32 GSDI patient cohort. This data highlighted the development of renal cysts in K.G6pc-/- mice and GSDI patients at a late stage of CKD, just before the occurrence of renal failure.

The **third chapter** of the results summarizes a mechanistic study aiming to pinpoint the exact role of lipids in the hepatic and renal GSDI pathologies. Indeed, while hepatic and renal glycogen accumulation represents a major hallmark of GSDI, these organs also present ectopic and excessive lipid accumulation, possibly inducing additional damage, independently from glycogen. In the general population, hepatic lipid accumulation is associated to NAFLD / NASH, translated to various metabolic complications. In the kidneys, lipids have been shown to induce irreversible damages such as kidney fibrosis, especially in obese / diabetic patients. Thus the role of lipids needed to be defined in the case of GSDI. Therefore, by exacerbating lipid accumulation in the liver and the kidneys of L.G6pc-/- and K.G6pc-/- mice, respectively, thanks to a HF/HS diet, we examined the effect of lipids and their influence on the progression of the disease, by assessing liver and kidney injury markers, histology and metabolism. On the other hand, the same analyses were performed after strongly decreasing lipid content in both mouse models, using a lipid-lowering drug in order to see whether the hepatic and renal GSDI pathologies will be delayed / prevented.

Chapter I – Metabolic reprogramming leading to hepatic tumorigenesis in GSDI

While one might say that it is obvious that metabolic reprogramming due to G6Pase deficiency is the key initiator of tumorigenesis in GSDI, the actual mechanisms involved remain unknown. In **the review published in the Journal of Inherited Errors of Metabolism and Screening (JIEMS) in 2016** (Gjorgjieva et al., 2016b), we have summarized all of the metabolic perturbations in GSDI livers that were already reported in the literature, highlighting the presence of a Warburg-like phenotype. These findings were compared to what is usually observed in glycolytic cancers. Furthermore, the involvement of oxidative stress, autophagy and apoptosis during GSDI tumorigenesis was described, highlighting the modulations of these functions induced by the altered metabolism. Finally, the last part of the review points out the similarities already reported between the metabolism of non-GSDI HCA and GSDI livers. Thus this review summarizes the potential mechanisms favorable for tumor formation and progression in GSDI livers.

In the next paper, in order to shed light on hepatic tumor development, we characterized the metabolism and cellular defense mechanisms in GSDIa livers and tumors at different stages. The livers of L.G6pc-/- mice were analyzed after 4 months of HF/HS diet, entitled “pretumoral stage”, and after 9 months, entitled “tumoral stage”, where 90% of the mice bore hepatic tumors. Compared to previous reports by our laboratory showing only 20% of L.G6pc-/- developed tumors at this age with a standard diet (Mutel et al., 2011a), these data highlighted the importance of dietary treatment in GSDI. Furthermore, HCA developed in L.G6pc-/- mice fed a HF/HS diet had a tendency to increase Glypican3, a marker known to be specific to HCC, pointing out the major capacity of these HCA to transform into HCC. Furthermore, HCC had increased β–catenin and Glypican3, often observed in HCC in the general population.

As in GSDI patients, L.G6pc-/- mice developed HCA and HCC in the **absence of fibrosis and cirrhosis** in the liver. Lack of EMT activation was suggested to be the answer to the absence of fibrosis. Indeed, we observed epithelial marker up-regulation, concordantly with a normal level of mesenchymal markers in L.G6pc-/- livers, indicating an absence of EMT. The incidence of HCC in GSDI in the absence of fibrosis / cirrhosis could be explained by the fact that HCC does not occur *de novo* in GSDI livers, but it

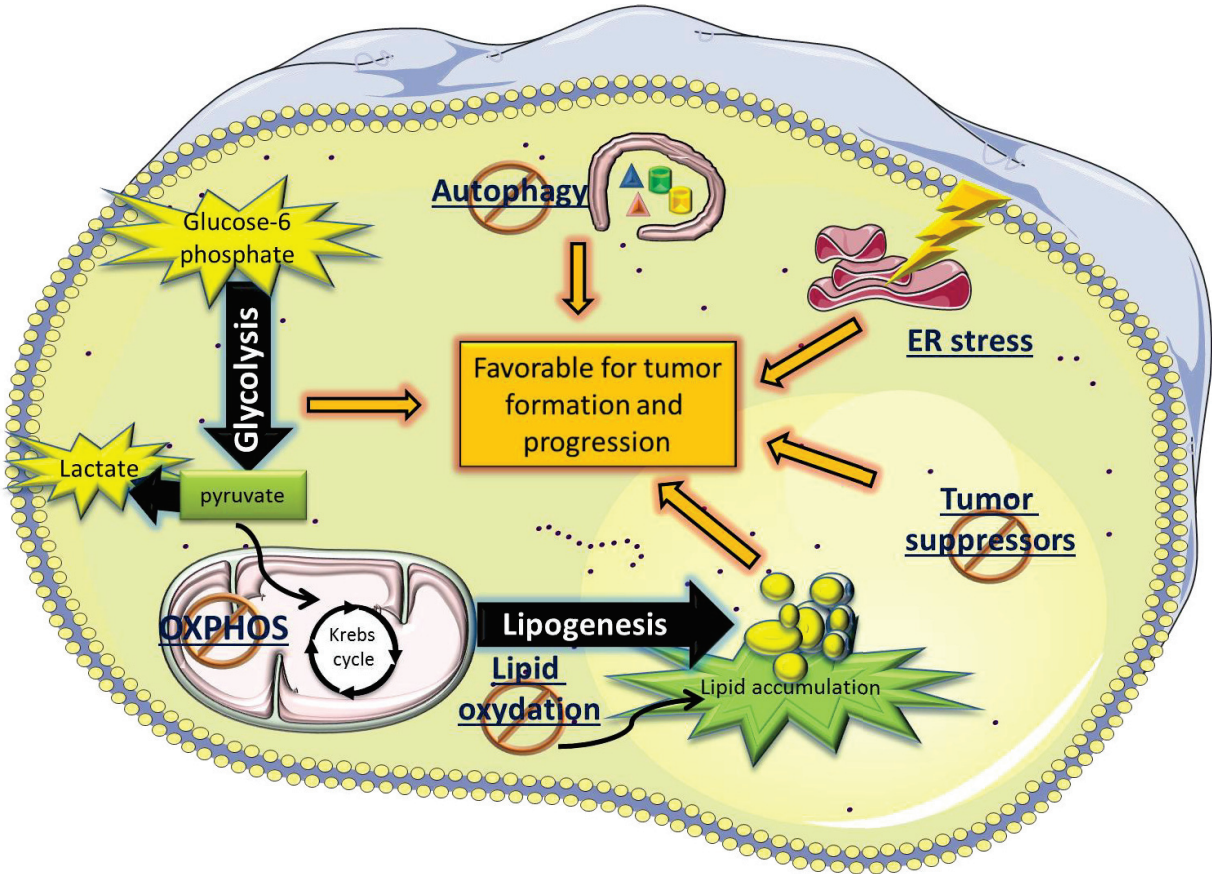

Figure 65: Schematic representation of the consequences of G6Pase deficiency on GSDI metabolism and cell defense mechanisms

In GSDI hepatocytes, glucose-6 phosphatase (G6Pase) deficiency leads to a marked increase in glucose-6 phosphate (G6P). G6P then activates glycolysis and leads to a subsequent increased production of lactate, responsible for lactic acidosis in GSDI patients and animal models. Furthermore, oxidative phosphorylation (OXPHOS) in the mitochondria is decreased, contributing to a Warburg-like phenotype in these cells. Lipid synthesis is also increased, leading to lipid accumulation (hepatic steatosis), further accentuated by the inhibition of lipid oxidation. Hyper-glycolysis and lipogenesis are known to be favorable for cancer formation and progression. Moreover, autophagy is inhibited, resulting in further accumulation of glycogen, lipids and non-functional organelles, contributing to genotoxicity and thus tumorigenesis. The endoplasmic reticulum (ER) stress pathways are chronically activated. Finally, tumor suppressor (HNF1a, PTEN, p53) expression / activity is decreased, potentiating tumorigenesis in GSDI livers.

(Gjorgjieva et al., submitted)

was suggested to always arise from HCA. Furthermore, tumor suppressors, such as PTEN (phosphatase and tensin homolog), HNF1α and p53 were down-regulated, not only in tumor samples, but also in the liver, rendering it favorable for tumorigenesis.

As expected, we have observed a strong activation of glycolysis and *de novo* lipogenesis in the livers and tumors, with a concomitant decrease in mitochondrial OXPHOS, confirming a **Warburg-like effect** in the liver, as observed in cancer cells in general, suggesting these livers exhibit a neoplastic status.

Finally, we observed a decrease in autophagosome number and a decrease in ATG proteins in L.G6pc-/- livers (at 4 and 9 months), indicating a **decrease in autophagy**. Surprisingly, autophagy was reactivated in all HCA / HCC samples. Moreover, antioxidant enzyme expression was decreased at both pretumoral and tumoral stages. Finally, BiP (ER stress pathway regulator) expression was markedly decreased at pretumoral and tumoral stages, facilitating the activation of ER stress pathways, indicating **chronic ER stress activation in GSDI**. Autophagy down-regulation in GSDI livers could contribute to genetic instability, and its increase in tumors could facilitate tumor progression, by providing recycled metabolites as building blocks and energy sources for growth and proliferation. Oxidative damage can further promote tumorigenesis by favoring DNA mutations. Finally, the activation of the ER stress pathway could make the tumor-adjacent environment hospitable for tumor survival and tumor expansion.

To conclude, we suggest that glycolytic cancer cells and GSDI hepatocytes present a similar metabolic reprograming, facilitating the formation and progression of tumors in the liver. Furthermore, the metabolic alterations induced by G6Pase deficiency have a strong effect on the cellular defense pathways and the expression of tumor suppressors, which are then unable to fulfill their duty and protect the liver from tumorigenesis (*Figure 65*).

Review

Journal of Inborn Errors of Metabolism & Screening
2016, Volume 4: 1–10
© The Author(s) 2016
DOI: 10.1177/2326409816679429
iem.sagepub.com
SAGE

Mechanisms by Which Metabolic Reprogramming in GSD1 Liver Generates a Favorable Tumorigenic Environment

Monika Gjorgjieva, PhD Student[1,2,3], Maaike H. Oosterveer, PhD[4], Gilles Mithieux, PhD[1,2,3], and Fabienne Rajas, PhD[1,2,3]

Abstract

Glycogen storage disease type 1 (GSD1) is an inherited disorder caused by impaired glucose 6-phosphatase activity. This impairment translates into the inhibition of endogenous glucose production and the subsequent accumulation of cellular glucose 6-phosphate. Excess glucose 6-phosphate enhances glycolysis, increases the production of fatty acids, uric acid, and lactate, causes hepatomegaly due to glycogen and lipid accumulation, and finally results in liver tumor development. Although the exact mechanisms of tumorigenesis in patients with GSD1 remain unclear, GSD1 hepatocytes undergo a Warburg-like metabolic switch. The consequent hyperactivation of specific metabolic pathways renders GSD1 hepatocytes susceptible to tumor development, presumably by providing the building blocks and energy required for cell proliferation. In addition to this, enhanced apoptosis in GSD1 may promote mitotic activity and hence result in DNA replication errors, thereby contributing to tumorigenesis. Increased carbohydrate responsive element-binding protein (ChREBP) and mammalian target of rapamycin (mTOR) activity and impaired AMP-activated protein kinase (AMPK) function likely play key roles in these pro-oncogenic processes.

Keywords

glycogen storage disease type 1, steatosis, hepatocellular adenomas and carcinomas, carcinogenesis, glucose and lipid metabolism, autophagy, liver

Introduction

Glycogen storage disease type 1 (GSD1) is a rare genetic disease, due to an impairment in glucose 6-phosphatase (G6Pase)[1,2] activity. Glucose 6-phosphatase is a key enzyme for energy and metabolite production that catalyzes the conversion of glucose 6-phosphate (G6P) to free glucose, the final step in both glycogenolysis and gluconeogenesis.[3,4] Therefore, it is a crucial enzyme in the maintenance of blood glucose levels in the postabsorptive phase and upon fasting. The G6Pase complex is composed of 2 subunits, that is, a catalytic domain (G6PC) and a transport protein (G6PT). G6PT is expressed ubiquitously, whereas G6PC is exclusively expressed in the 3 gluconeogenic organs: the liver, kidneys and intestine.[3,4] *G6PC* mutations lead to GSD type 1a (GSD1a),[5-7] whereas GSD type 1b (GSD1b) is caused by mutations in *SLC37A4*, the gene encoding G6PT.[2] Both GSD1a and GSD1b are characterized by hepatic, renal, and intestinal pathologies and exhibit largely the same metabolic symptoms.[8,9] Because G6Pase activity is impaired in patients with GSD1, blood glucose levels are low upon fasting, resulting in hypoglycemic episodes. On the other hand, cellular G6P storage and utilization are strongly increased, thereby activating specific metabolic pathways, including glycolysis, as well as uric acid, lactate, fatty acid, and cholesterol synthesis. Besides fasting hypoglycemia, the metabolic symptoms of GSD1 therefore involve hyperuricemia, lactic acidosis, hypertriglyceridemia,

[1] Institut National de la Santé et de la Recherche Médicale, U1213 "Nutrition, Diabetes and the Brain", Lyon, France
[2] Université de Lyon, Lyon, France
[3] Université Lyon 1, Villeurbanne, France
[4] Department of Pediatrics, Center for Liver, Digestive, and Metabolic Diseases, University Medical Center Groningen, University of Groningen, Groningen, the Netherlands

Received March 31, 2016, and in revised form July 15, 2016. Accepted for publication August 24, 2016.

Corresponding Author:
Fabienne Rajas, Inserm U1213, Université Lyon 1 Laennec, 7 rue Guillaume Paradin, 69372 Lyon Cedex 08, Lyon, France.
Email: fabienne.rajas@univ-lyon1.fr

This article is distributed under the terms of the Creative Commons Attribution 3.0 License (http://www.creativecommons.org/licenses/by/3.0/) which permits any use, reproduction and distribution of the work without further permission provided the original work is attributed as specified on the SAGE and Open Access pages (https://us.sagepub.com/en-us/nam/open-access-at-sage).

and hypercholesterolemia. Glucose 6-phosphatase-deficient hepatocytes are chronically stressed due to abnormal glycogen and lipid accumulation, which induce hepatomegaly and liver steatosis.[8,9] Similarly, patients with GSD1 and animal models exhibit nephromegaly,[8-10] leading to tubular injury, glomerulosclerosis, and a progressive loss of renal function, characterized by albuminuria, proteinuria, and at the last stage, by renal failure.[11,12] Strikingly, almost all patients with GSD1 develop hepatocellular adenoma (HCA) during adulthood, with a 10% incidence of transformation to hepatocellular carcinoma (HCC).[13,14] Liver tumor formation in GSD1 induces significant morbidity and impairment of quality of life, and these patients frequently require partial hepatectomy or liver transplantation.[15,16] The European Study on GSD1 showed that HCA can be observed from 15 years of age on, and up to 75% of patients bear at least 1 HCA at the age of 25.[14] The molecular mechanisms of tumor development in GSD1 are unclear. It has been hypothesized that the early switch to a Warburg-like metabolism in nontumoral G6Pase-deficient hepatocytes promotes oncogenesis by providing substrates for cell proliferation, such as lipids and nucleotides. It has been proposed that tumor development in GSD1 may be a rectilinear process, characterized by the initial appearance of HCAs, which may subsequently transform into HCC.[17] To our knowledge, development of HCC in the absence of preexisting/coexisting HCA has not yet been reported for GSD1.

Because the primary consequence of GSD1 is a metabolic derangement, it is of interest to understand *via* what mechanisms perturbed intrahepatic metabolism may initiate and/or drive tumor formation. In this review, we discuss the metabolic reprogramming, stress-inducing, and cellular death pathways in G6Pase-deficient hepatocytes that may initiate and/or facilitate HCA and HCC development.

Tumor Metabolism

Tumor initiation and progression may be considered as a rather anarchical process; however, several metabolic pathways are very frequently hyperactivated in tumors. These pathways provide tumor cells with energy (ATP), carbon skeletons, lipids, amino acids, nucleotides, and other metabolites required for biomass gain, growth, and progression.[18,19]

The Warburg Effect

In normal quiescent cells, ATP is derived mostly from glycolysis, subsequent Krebs cycle activity, and mitochondrial oxidative phosphorylation (OXPHOS).[20] This oxygen-dependent metabolic profile ensures an efficient ATP production.

On the contrary, in cancer cells or rapidly proliferating cells, metabolism is orientated toward increased glucose uptake and aerobic glycolysis, resulting in a high lactate production, independent of cellular oxygen availability. This metabolic shift is known as the Warburg effect. Initially, the Warburg effect was considered as the driving force for cancer development.[21] Nowadays, it is generally believed that this effect is rather the result of metabolic reprogramming induced by oncogenic mutations. Otto Warburg's research and other studies suggest that cancer cells shut down their mitochondrial activity, hence decreasing OXPHOS, and concluded that a hypoxic tumor environment selects cells that are dependent on anaerobic metabolism. However, it has been confirmed that most cancers exhibit normal mitochondrial activity and normal rates of OXPHOS, suggesting that other mechanisms drive metabolic reprogramming of cancer cells toward aerobic glycolysis.[18] Several regulatory proteins, including hypoxia-induced factor 1α (HIF1α),[22-24] avian myelocytomatosis viral oncogene homolog (MYC[24,25]), and tumor protein p53 (P53[25,26]), are known to promote this metabolic switch. Most tumors are not very well vascularized during initial growth and oxygen supply is therefore not optimal. However, the Warburg effect has also been observed in lung tumors[27] that have sufficient oxygen supply, indicating that the Warburg effect is not necessarily related to impaired oxygen availability. Moreover, in aerobic tissues, HIF1α is stabilized by high presence of lactate,[22] indicating that this pro-oncogenic protein also operates when oxygen supply is not limiting. The energy yield of the glucose catabolism by aerobic glycolysis is much lower (2 ATP/glucose) compared to mitochondrial OXPHOS (38 ATP/glucose), yet it can generate ATPs at a higher rate. However, high ATP synthesis rate associated with aerobic glycolysis may be of minor relevance to tumor growth, since energy alone is not enough for proliferation. More importantly, in order to increase their biomass and growth rate, proliferating cells need carbon skeletons, amino acids, lipids, and cholesterol to synthesize biomembranes and nucleotides. This accelerated metabolism results in increased reactive oxygen species (ROS) production. Even though ROS can be highly oncogenic and therefore promote tumor development, they can also render tumor cells vulnerable to oxidative and energetic stress.[28] In order to combat ROS, but also to increase anabolic activity, cancer cells increase nicotinamide adenine dinucleotide phosphate (NADPH) production via the pentose phosphate pathway (PPP), as well as other reducing equivalents. This allows not only the detoxification of cancer cells but also the synthesis of macromolecules required for proliferation.[29,30] Altogether, metabolic reprogramming allows the cells to maintain sufficient energy levels, but it also provides them with substrates for growth. One of the main players providing cancer cells with these substrates is pyruvate kinase (PK), the enzyme responsible for the conversion of phosphoenolpyruvate (PEP) to pyruvate and ATP, the final step of glycolysis. This enzyme exists under different isoforms (M1, M2, L, and R) and can form dimers or tetramers, which makes it the key switch between OXPHOS and aerobic glycolysis. Because the M2 dimer isoform has a low affinity for PEP, glycolytic metabolites upstream of PEP accumulate when this isoform is predominant in the cell, and metabolism is redirected to nucleotide, lipid, and amino acid synthesis.[31] This phenomenon is observed in almost every cancer type.[32,33] Many important signaling pathways, such as MYC,[34] HIF1α,[33,35,36] STAT3 (for Signal Transducer and Activator of Transcription),[36] and Epidermal Growth Factor Receptor (EGFR),[37] are responsible for the upregulation

of pyruvate kinase isoform M2 (PKM2) in cancer cells. Interestingly, recent studies indicate that PKM2 is not only involved in the regulation of glucose metabolism but also plays a role in cancer metastasis in HCC.[38,39]

Pro-Oncogenic Changes in Lipid Metabolism

Nonalcoholic fatty liver disease (NAFLD)[40] is commonly used to describe liver pathologies characterized by abnormally high lipid content in the liver, in the absence of alcohol consumption. It is mostly observed in developed countries and frequently associates with obesity, diabetes, and metabolic syndrome. Multiple studies have established a link between NAFLD and increased risk of HCC.[41,42] Multiple factors, such as increased lipogenesis, oxidative stress, cytokine-induced signaling pathways, and environmental and genetic components, have been proposed to contribute to liver tumor formation in patients with steatosis.[43,44] Increased *de novo* lipogenesis (DNL) requires high concentrations of NADPH, rendering NADPH a limiting factor in tumor growth. Nevertheless, as mentioned earlier, an increase in PPP activity is frequently observed in tumors, thereby facilitating NADPH production.[29] The activity of malic enzyme also generates NADPH synthesis, and the repression of its expression has been shown to inhibit tumor progression.[45,46] Furthermore, increased DNL promotes malonyl-CoA production, which in turn inhibits carnitine palmitoyltransferase 1 (CPT1) activity, thereby reducing intramitochondrial fatty acid availability for β-oxidation. Thus, under conditions of increased DNL, the degradation of fatty acids is reduced, which further enhances steatosis.[43] High lipid concentrations induce the production of ROS in hepatocytes. Reactive oxygen species subsequently lead to lipid peroxidation, inflammatory cytokine (interleukin [IL] 6,[47] tumor necrosis factor α[48]) release, and DNA and protein damage. For example, the trans-4-hydroxy-2-nonenal, a product of lipid peroxidation, causes mutations in the tumor suppressor P53 in HCC.[49,50] In addition to this, ROS-induced DNA damage can also result in oncogene activation and/or tumor suppressor inactivation, thereby driving carcinogenesis.[28] Once neoplastic lesions are formed, accumulated lipids are highly favorable for tumor growth, as they are crucial for the assembly of biomembranes for new tumor cells. A wide range of DNL-inhibiting drugs are currently being developed to decrease hepatic stress and even halt tumor development. Most of these drugs target the fatty acid synthase (FASN), a key enzyme in DNL.[51,52] As this enzyme is frequently overexpressed in cancer cells, its inhibition has been proven successful to attenuate cancer progression and metastasis.[51,52]

Nucleotide Provisions

Besides synthesizing biomembranes, tumor cells need to produce nucleotides for DNA replication during cell division. In order to increase nucleotide synthesis, the high glycolytic flux associated with the Warburg effect is directed toward PPP.[53] PKM2 is mainly responsible for the redirection.[32] The PPP produces ribose 5-phosphate, which serves as a substrate for de novo nucleotide synthesis.[54] Interestingly, yet not surprisingly, HIF1α[55] and C-MYC[56] also promote nucleotide production by increasing the PPP activity, thereby likely potentiating tumor development and growth.

Metabolic Reprogramming in GSD1 Hepatocytes

Hepatocytes have different physiological roles and converge many metabolic pathways. They are involved in protein, glucose, and lipid metabolism, and their functioning has systemic effects. Glycogen storage disease type 1 hepatocytes display an abnormal metabolic phenotype, primarily caused by G6P accumulation. Metabolic pathways that use G6P as a substrate, such as glycolysis, DNL, glycogen synthesis, and degradation, are hyperactivated in GSD1 livers.[57,58]

Hyperactive Glycolysis and Warburg-Like Metabolism

It has been established that excess G6P forces metabolism toward glycolysis[57-59] in G6Pase-deficient nontumoral hepatocytes. Increased glycolysis leads to increased pyruvate levels and subsequent lactate production. Lactate production due to enhanced glycolysis explains the lactic acidosis observed in both GSD1 animal models and in patients with GSD1.[60,61] This metabolic phenotype resembles the Warburg effect in cancer cells (Figure 1). In normal hepatocytes, lactate can be converted back to glucose in the liver *via* the Cori cycle, thereby preventing lactic acidosis. On the contrary, it has been hypothesized that G6Pase-deficient hepatocytes cannot convert lactate back to glucose, since they cannot dephosphorylate G6P, the final step of the Cori cycle. An impaired Cori cycle in GSD1 may therefore lead to a further increase in circulating lactate concentrations. Although the expression of the liver isoform of PK (*PKLR*) is markedly increased in GSD1,[62,63] an induction of PKM2 has not yet been reported in G6Pase-deficient hepatocytes. However, from a therapeutic perspective, it would be interesting to assess its enzymatic activity in GSD1, as many PKM2-inhibiting drugs are currently being developed. In case PKM2 is activated in GSD1, such drugs may be effective to reduce nucleotide, lipid, and amino acid synthesis,[31] and hence perhaps impair tumor development in GSD1.[64,65]

Increased Hepatic Lipid Synthesis Contributing to Liver Steatosis

In GSD1, increased pyruvate production *via* glycolysis due to excess G6P results in increased production of acetyl-CoA, which subsequently enters the Krebs cycle. Besides generating energy *via* OXPHOS, citrate produced in the Krebs cycle can be transported to the cytosol, converted back to acetyl-CoA, and serve as a substrate for the synthesis of fatty acids and cholesterol. Bandsma et al observed a 40-fold increase in *de novo* synthesized palmitate in very low density lipoprotein (VLDL) from patients with GSD1 (Figure 1), in parallel to a

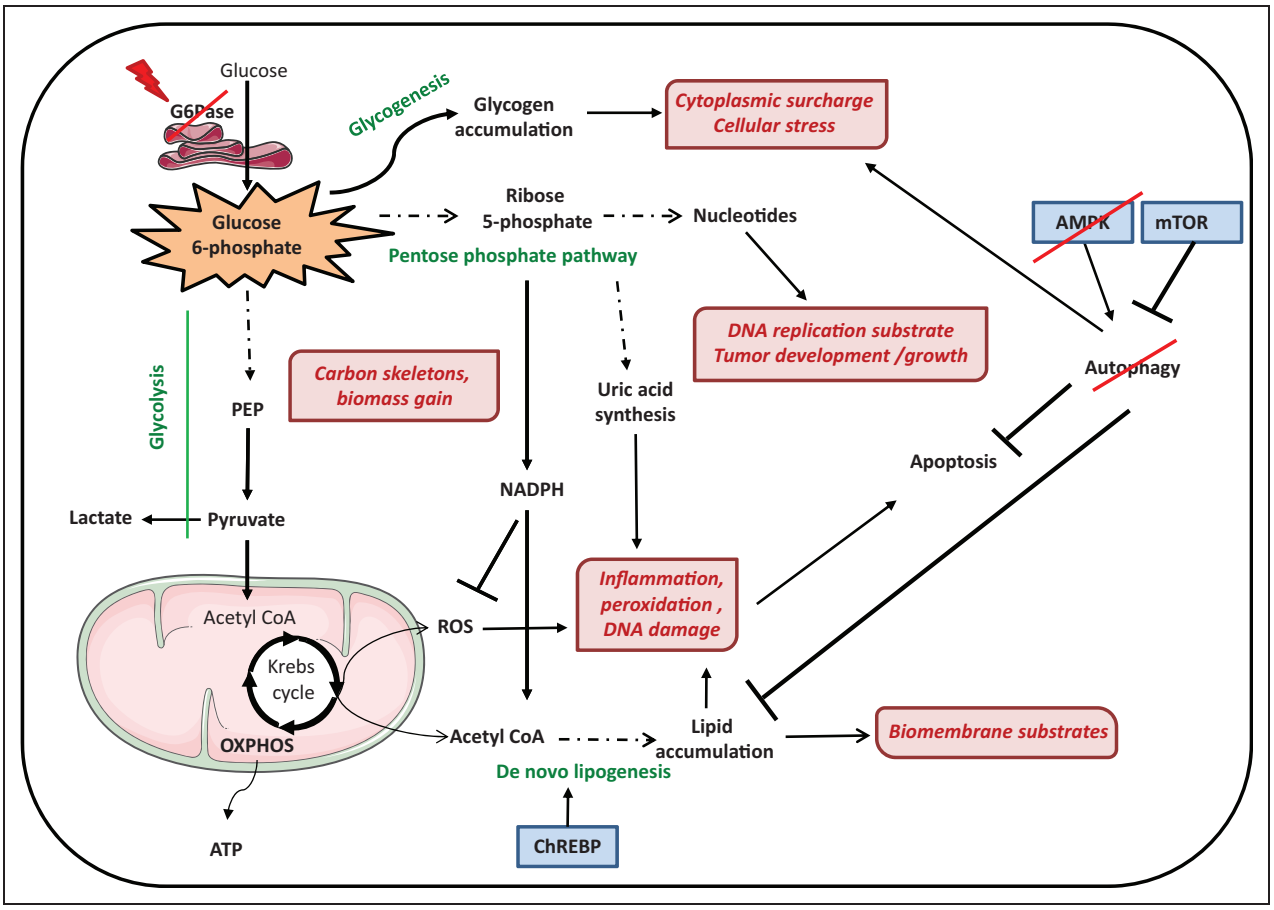

Figure 1. Metabolic deregulation and pro-tumorigenic pathways in the GSD1 liver. Images were drawn by Sevier Medical Art.

7-fold increase in cholesterol synthesis and a slower conversion of VLDL to low density lipoprotein (LDL).[66] An increased expression of genes involved in mitochondrial citrate export and DNL, such as ATP citrate lyase (ACLY), acetyl CoA carboxylase (ACACA), FASN, sterol CoA desaturase (SCD1), and fatty acid desaturase 1 and 2 (FADS1 and 2), has already been confirmed in GSD1 livers.[58,59] These enzymes are physiologically induced in the fed state by elevated insulin and glucose levels. Insulin and glucose act *via* 2 transcription factors, that is, sterol regulatory element binding protein 1c (SREBP1c) and carbohydrate responsive element binding protein (ChREBP).[67] In a mouse model of GSD1b, the induction of glycolytic and lipogenic genes in the liver was found to be mediated by ChREBP.[62] Increased DNL likely represents an important pathophysiological process in GSD1 hepatocytes, as it contributes to the accumulation of lipids and potentially lipotoxicity in the liver, causing NAFLD-like complications in both patients with GSD1 and GSD1 animal models.[60,68] Several studies suggested that dietary treatment can partially reduce lipid levels in plasma and liver, although hepatic lipid accumulation cannot be completely alleviated.[68,69] The β-oxidation pathway, responsible for fatty acid degradation, is likely reduced in GSD1, as it was shown that the expression of peroxisome proliferator-activated receptor α is significantly decreased in hepatocyte-specific *G6PC* null mice.[70] As mentioned earlier, excessive malonyl-CoA production caused by DNL induction may result in the inhibition of CPT1 and a consequent reduction in fatty acid β-oxidation. Finally, a decreased activity of AMP-activated protein kinase (AMPK) in GSD1 non-tumoral hepatocytes[71] may contribute to impaired fatty acid oxidation and increased fatty acid and cholesterol synthesis[72] (Figure 1). AMP-activated protein kinase regulates these processes by decreasing malonyl-CoA production *via* ACC inhibition and by controlling SREBP1[73] and ChREBP[74] activities.

As mentioned earlier, ChREBP is the key transcription factor responsible for the elevated hepatic lipogenic gene expression in GSD1a and GSD1b mouse models.[62,71] Increased levels of ChREBP have already been shown to promote tumorigenesis.[75,76] This transcription factor not only promotes lipogenesis but also increases glucose uptake and glycolysis, cell proliferation, and glucose-dependent *de novo* nucleotide synthesis in hepatocytes.[77] Carbohydrate responsive element binding protein–deficient cells exhibit increased OXPHOS, suggesting that ChREBP is yet another potential metabolic switch in GSD1, deviating the metabolism from OXPHOS toward aerobic glycolysis. In the same study, ChREBP deficiency was shown to activate P53-dependent cell cycle arrest, indicating that this transcription factor interferes with tumor suppression.

Altogether, as a result of metabolic reprogramming and deregulated intracellular signaling, GSD1 livers present the full spectrum of NAFLD, including increased lipid synthesis, hepatic steatosis, and lipotoxicity, which are associated with tumorigenesis.

Enhanced Nucleotide Metabolism

Because G6P serves as a substrate for the PPP, it can be assumed that its accumulation in GSD1 promotes *de novo* nucleotide synthesis. Although an actual increase in PPP activity in GSD1 has not yet been reported, an increased flux through this pathway potentially provides the nucleotides required for neoplastic cellular proliferation and reducing equivalents for DNL. On the other hand, when inorganic phosphate is depleted, for example, due to the increased retention of phosphate in G6P, cells start to degrade nucleotides, resulting in uric acid production.[78] Hyperuricemia is a very well-documented feature of GSD1 animal models and patients with GSD1.[14,60] Uric acid has pro-inflammatory properties contributing to tumor development and growth.[79] Nevertheless, patients with GSD1 are frequently treated with drugs to lower circulating uric acid concentrations, hence protecting against uric acid–induced inflammation. Because these treatments do not prevent tumor development in patients with GSD1, it seems unlikely that hyperuricemia is the sole oncogenic factor in GSD1.

Cellular Defense and Death Mechanisms in GSD1 Livers

Oxidative Stress

Mitochondrial and peroxisome activities generate ROS that are degraded by cellular antioxidant enzymes such as catalase, superoxide dismutase, and glutathione peroxidase. Failure to neutralize excess ROS results in disturbed redox levels, causing serious tissue injury. Hepatic steatosis renders the liver more susceptible to ROS.[41] Reactive oxygen species not only damage intracellular molecules but also alter the activities of cellular signaling pathways. It has been reported that markers of oxidative stress and antioxidant defense systems are both increased in the plasma of patients with GSD1,[80] while no data are currently available on ROS levels in G6Pase-deficient livers. Accumulated ROS in G6Pase-deficient hepatocytes can react with the nucleic acids, proteins, lipids, and other metabolites, thereby impairing organelle functions and inducing membrane damage as well as chromosomal instability and mutations. All of these processes are favorable to tumor development[28] (Figure 1).

Autophagy

Reactive oxygen species–induced cellular stress is frequently accompanied by mitochondrial dysfunction, because these organelles are not only the generator but also a target of ROS.[81] Mitochondrial turnover *via* autophagy, also referred to as mitophagy, is tightly linked to oxidative stress.[82] Autophagy enables the elimination of nonfunctional proteins, organelles, and metabolites, providing the cell with energy and recycled metabolites for reuse. The autophagic substrates can be, in part, a consequence of increased ROS concentrations. The autophagy-related (ATG) proteins initiate the formation of and serve as building blocks for autophagic vesicles. This initiation and progression is regulated by an orchestrated network that includes the AMPK and the AKT/mTOR (for Serine/Threonine Kinase 1/mammalian target of rapamycin) pathways, which are both key proteins involved in energy and nutrient sensing.[83] Although AMPK activation promotes autophagy, mTOR is known to suppress it.

Recently, it was reported that autophagy is decreased in G6Pase-deficient livers.[71] This study showed that AMPK activity was impaired, while mTOR was activated, translating in decreased autophagy (Figure 1). Furthermore, it was shown that mTOR inhibition by rapamycin restored autophagy and reduced hepatic lipid and glycogen content in GSD1 livers. Autophagy depletion in the early stages of cancer development is a frequently observed phenomenon that generates a tumorigenic environment, as free radical accumulation, nonfunctional proteins, and organelle persistence increase chromosome instability.[84,85] For example, a mouse model of impaired autophagy induced by ATG5 ablation developed HCA, suggesting a tumor suppressive role for autophagy. The HCAs from these animals showed damaged mitochondria, oxidative stress, and genomic damage responses.[86] Almost the same phenotype, including liver tumors, was observed in ATG7-deficient mice.[86] Thus, autophagy appears to have an important anti-oncogenic role in the liver, and its impairment in a pretumor stage may facilitate oncogenesis in GSD1 livers as well.

Metformin is a drug that is commonly used to treat diabetes.[87] This hypoglycemic agent reduces circulating glucose and lipid levels and induces autophagy by activating AMPK.[73] Aside from its antidiabetic properties, metformin was shown to exert anticancerous actions as well.[88] Although it is tempting to evaluate whether metformin treatment activates autophagy and subsequently impedes tumorigenesis in the GSD1 liver, a putative decrease in blood glucose levels upon metformin treatment in these patients poses a potential risk. However, metformin acts mainly on the liver and reduces hyperglycemia by inhibiting hepatic glucose production.[89] Given that G6Pase-dependent glucose production is absent in GSD1, the risk for metformin-induced hypoglycemia in these patients may be negligible, making this treatment appealing for the prevention/treatment of HCA in patients with GSD1.

Apoptosis

Once autophagy fails to improve the metabolic and energy state of the cell, molecular mechanisms induce a switch from autophagy to apoptotic or even necrotic cell death.[90] G6Pase–deficient mice display increased apoptosis in the liver[57] (Figure 1). Caspase3/7 protein levels were significantly increased in the livers of these mice, implying a Fas-mediated apoptosis.

The authors considered that apoptosis in GSD1a mice was activated through glyceraldehyde 3-phosphate dehydrogenase (GAPDH) and further promoted by steatosis-derived inflammation.[57] The expression of GAPDH, an enzyme that is primarily involved in activated glycolysis, was elevated as well. Interestingly, GAPDH has recently been associated with increased apoptosis.[91,92] Increased apoptosis in G6Pase-deficient cells results in low viability of isolated primary hepatocytes (A. Gautier-Stein, PhD, unpublished data 2012). Although apoptosis is commonly regarded as an anti-oncogenic mechanism, it has been shown that high apoptotic rates can also promote tumorigenesis.[93] To retain proper functioning of the liver, apoptotic hepatocytes must be replaced rapidly. Thus, an increase in apoptosis in the G6Pase-deficient liver may trigger hepatocyte proliferation to compensate for hepatocytes loss. Rapid and constant cell division and growth of mitotic G6Pase-deficient hepatocytes may consequently induce DNA replication errors and tumor formation.

Necrosis

Hepatocellular necrosis has also been observed in G6Pase-deficient livers.[94] Necrotic foci, neutrophil infiltration, and elevated expression of chemokines were documented, indicative of liver injury in mice and patients bearing HCA but also in liver material in a pretumor stage. Glycogen[95] and lipid accumulation[96] are known to induce inflammation. Taken together, the origin of this inflammatory response needs to be investigated, as it may significantly contribute to the tumor development in GSD1.

GSD1 Metabolism Drives Adenoma Formation: Similarities With *HNF1A*-Mutated Tumors

Genome sequencing and subsequent classification of HCAs from non-GSD1 patients has identified 3 main groups of mutations associated with HCA.[97] In HCAs from the first group, hepatic nuclear factor 1α (HNF1α), a transcription factor involved in glucose and lipid metabolism, is mutated. Hepatic nuclear factor 1α is considered as a tumor suppressor and a key factor that maintains hepatocytes in a differentiated state.[98,99] In *HNF1A*-mutated HCAs, the expression of the fatty acid–binding protein 1 (*FABP1*) gene, a direct target of HNF1α, is downregulated, leading to steatosis and lipotoxicity.[100] Tumors bearing a *HNF1A* mutation have an increased proliferation rate due to the subsequent activation of the Phosphoinositide 3-kinase/AKT pathway.[101,102] The second group represents inflammatory HCAs. These HCAs are characterized by mutations that activate the IL-6 and JAK (Janus kinase)/STAT pathways and are the most prevalent HCAs, representing 50% of all HCAs.[103] The third group is β-catenin (*CTNNB1*)-mutated HCAs. Hepatocellular adenomas with an activating mutation of β-catenin represent around 10% to 15% of all HCAs[103] and are associated with poor prognosis, since they represent a great risk of malignant transformation.[104]

In order to investigate the origin of tumorigenesis in GSD1, HCAs from patients with GSD1 were subjected to gene expression and DNA sequencing analysis. This analysis showed that 52% of the HCAs bared inflammatory mutations, 28% were *CTNNB1* mutated, and 20% were unclassified.[59] Intriguingly, none of the GSD1 HCAs were *HNF1A* mutated, whereas all of the GSD1 HCAs, even the ones in the inflammatory and β-catenin groups, had a decreased expression of *FABP1*. Since HNF1α is the main regulator of *FABP1* expression, one could infer that HNF1α could be decreased in all of the GSD1 HCAs. As HNF1α regulates G6PC and G6PT[105-107] expression, HNF1α and G6Pase-mutated hepatocytes may display a similar phenotype. Consequently, comparison of GSD1 nontumoral liver tissue and *HNF1A*-inactivated HCAs revealed similarities with regard to the expression of glycolytic, gluconeogenic, and lipogenic enzymes. In both GSD1 nontumoral tissue and *HNF1A*-invalidated HCAs, gluconeogenesis was repressed, and glycolysis and lipogenesis were induced.[100] Decreased *Hnf1a* messenger RNA expression was observed in the liver-specific *G6pc* knockout mice as compared to their wild-type littermates (M. Gjorgjieva, PhD student, and F. Rajas, PhD, unpublished data 2015). To summarize, GSD1 nontumoral liver displays striking phenotypic similarities with *HNF1A*-inactivated HCAs, indicating that even in the pretumor stage, GSD1 livers exhibit a tumor-like metabolism.

Conclusion

Glycogen storage disease type 1 is a complex metabolic disease that exhibits all the hallmarks of NAFLD. Liver steatosis and hepatic glycogen accumulation are already present during infancy, resulting in hepatomegaly. The hepatic accumulation of lipids and glycogen induces severe stress and causes chronic inflammation and ROS production, which potentially contributes to the development of liver tumors. The abnormal intrahepatic G6P content activates metabolic pathways that support tumor growth, such as aerobic glycolysis, lipid synthesis, uric acid and lactate production, glycogen storage, and nucleotide synthesis. Moreover, autophagy is impaired, which may further promote accumulation of nonfunctional proteins and organelles, and possibly translates into cellular stress and DNA and protein damage. ChREBP and mTOR activation and AMPK inhibition likely represent key molecular events that orchestrate metabolic reprogramming in GSD1. The rates of apoptotic cell death in advanced GSD1 are elevated, probably due to a switch from autophagy to apoptosis, as well as increased GAPDH concentrations. Increased levels of ROS and inflammatory cytokines may also contribute to the increase in apoptosis. As increased hepatocellular apoptosis may trigger cell division to repopulate the liver, continuous mitosis in G6Pase-deficient hepatocytes may lead to DNA replication errors, hence inducing HCA development. In addition, hepatocyte necrosis represents another mechanism activated that likely contributes to inflammation and cell death in GSD1 livers. Finally, by comparing HNF1α-deficient HCAs and G6Pase-deficient nontumoral tissue, many similarities were

found, despite a lack of *HNF1A* mutations. It was suggested that both groups exhibited HNF1α deficiency, accompanied by lipotoxicity, due to the reduced *FABP1* expression. HNF1α is considered as a tumor suppressor, and therefore, its impairment in G6Pase-deficient hepatocytes could lead to dedifferentiation and further susceptibility to tumor development.[101,108]

These data accentuate the need for strict metabolic control of patients with GSD1 in order to slow down the tumorigenesis process. The consumption of ''fast sugars'' such as fructose and galactose represents an important source of the substrate for the activation of glycolysis, glycogen synthesis, and DNL, therefore potentiating tumor formation. Even though a strict dietary regimen does not appear to fully prevent HCA/HCC formation, the European study of GSD1 has clearly shown an increase in life expectancy in patients who followed the nutritional guidelines.[14]

Altogether, different metabolic and cellular adaptations render GSD1 hepatocytes prone to tumor formation and growth. Although the exact contribution of these different features needs to be mechanically elucidated, nontumoral G6Pase-deficient hepatocytes may be considered as preneoplastic cells that develop to GSD1 HCA, which in some cases even progress to HCC.

Acknowledgments

The authors would like to thank the ''Ligue Nationale Contre le Cancer'' and the ''Ligue Régionale contre le cancer'' for the financial support attributed to the project for analyzing the mechanisms involved in GSD1 hepatic tumor development.

Declaration of Conflicting Interests

The author(s) declared no potential conflicts of interest with respect to the research, authorship, and/or publication of this article.

Funding

The author(s) disclosed receipt of the following financial support for the research, authorship, and/or publication of this article: Maaike H. Oosterveer holds a Rosalind Franklin Fellowship from the University of Groningen. The research is financially supported by the ''Ligue Nationale Contre le Cancer,'' ''Ligue Régionale contre le cancer,'' and ''Stichting Metakids.''

References

1. Chou JY. The molecular basis of type 1 glycogen storage diseases. *Curr Mol Med*. 2001;1(1):25-44.
2. Janecke AR, Mayatepek E, Utermann G. Molecular genetics of type 1 glycogen storage disease. *Mol Genet Metab*. 2001;73(2): 117-125.
3. Mithieux G. New knowledge regarding glucose-6 phosphatase gene and protein and their roles in the regulation of glucose metabolism. *Eur J Endocrinol*. 1997;136(2):137-145.
4. van Schaftingen E, Gerin I. The glucose-6-phosphatase system. *Biochem J*. 2002;362(pt 3):513-532.
5. Lei KJ, Chen YT, Chen H, et al. Genetic basis of glycogen storage disease type 1a: prevalent mutations at the glucose-6-phosphatase locus. *Am J Hum Genet*. 1995;57(4):766-771.
6. Chevalier-Porst F, Bozon D, Bonardot AM, et al. Mutation analysis in 24 French patients with glycogen storage disease type 1a. *J Med Genet*. 1996;33(5):358-360.
7. Bruni N, Rajas F, Montano S, Chevalier-Porst F, Maire I, Mithieux G. Enzymatic characterization of four new mutations in the glucose-6 phosphatase (G6PC) gene which cause glycogen storage disease type 1a. *Ann Hum Genet*. 1999;63(pt 2): 141-146.
8. Froissart R, Piraud M, Boudjemline AM, et al. Glucose-6-phosphatase deficiency. *Orphanet J Rare Dis*. 2011;6(1):27.
9. Kishnani PS, Austin SL, Abdenur JE, et al; American College of Medical Genetics and Genomics. Diagnosis and management of glycogen storage disease type I: a practice guideline of the American College of Medical Genetics and Genomics. *Genet Med*. 2014;16(11):e1.
10. Clar J, Gri B, Calderaro J, et al. Targeted deletion of kidney glucose-6 phosphatase leads to nephropathy. *Kidney Int*. 2014; 86(4):747-756.
11. Martens DHJ, Rake JP, Navis G, Fidler V, van Dael CML, Smit GPA. Renal function in glycogen storage disease type I, natural course, and renopreservative effects of ACE inhibition. *Clin J Am Soc Nephrol*. 2009;4(11):1741-1746.
12. Reitsma-Bierens WCC, Smit GPA, Troelstra JA. Renal function and kidney size in glycogen storage disease type I. *Pediatr Nephrol*. 1992;6(3):236-238.
13. Limmer J, Fleig WE, Leupold D, Bittner R, Ditschuneit H, Berger HG. Hepatocellular carcinoma in type I glycogen storage disease. *Hepatology*. 1988;8(3):531-537.
14. Rake JP, Visser G, Labrune P, Leonard JV, Ullrich K, Smit GPA. Glycogen storage disease type I: diagnosis, management, clinical course and outcome. Results of the European Study on Glycogen Storage Disease Type I (ESGSD I). *Eur J Pediatr*. 2002; 161(suppl 1):S20-S34.
15. Belingheri M, Ghio L, Sala A, et al. Combined liver-kidney transplantation in glycogen storage disease Ia: a case beyond the guidelines. *Liver Transpl*. 2007;13(5):762-764.
16. Boers SJ, Visser G, Smit PG, Fuchs SA. Liver transplantation in glycogen storage disease type I. *Orphanet J Rare Dis*. 2014; 9:47.
17. Kudo M. Hepatocellular adenoma in type Ia glycogen storage disease. *J Gastroenterol*. 2001;36(1):65-66.
18. Wu W, Zhao S. Metabolic changes in cancer: beyond the Warburg effect. *Acta Biochim Biophys Sin (Shanghai)*. 2013;45(1):18-26.
19. Dang CV. Links between metabolism and cancer. *Genes Dev*. 2012;26(9):877-890.
20. Cooper GM. *The Cell: A Molecular Approach: The Mechanism of Oxidative Phosphorylation*. 2nd ed. Sunderland, MA: Sinauer Associates; 2000.
21. Koppenol WH, Bounds PL, Dang CV. Otto Warburg's contributions to current concepts of cancer metabolism. *Nat Rev Cancer*. 2011;11(5):325-337.
22. Lu H, Forbes RA, Verma A. Hypoxia-inducible factor 1 activation by aerobic glycolysis implicates the Warburg effect in carcinogenesis. *J Biol Chem*. 2002;277(26):23111-23115.
23. Semenza GL. HIF-1 mediates the Warburg effect in clear cell renal carcinoma. *J Bioenerg Biomembr*. 2007;39(3):231-234.

24. Zwaans BMM, Lombard DB. Interplay between sirtuins, MYC and hypoxia-inducible factor in cancer-associated metabolic reprogramming. *Dis Model Mech*. 2014;7(9):1023-1032.
25. Vander Heiden MG, Cantley LC, Thompson CB. Understanding the Warburg effect: the metabolic requirements of cell proliferation. *Science*. 2009;324(5930):1029-1033.
26. Bensaad K, Tsuruta A, Selak MA, et al. TIGAR, a p53-inducible regulator of glycolysis and apoptosis. *Cell*. 2006;126(1): 107-120.
27. Nolop KB, Rhodes CG, Brudin LH, et al. Glucose utilization in vivo by human pulmonary neoplasms. *Cancer*. 1987;60(11): 2682-2689.
28. Liou GY, Storz P. Reactive oxygen species in cancer. *Free Radic Res*. 2010;44(5):479-496.
29. Patra KC, Hay N. The pentose phosphate pathway and cancer. *Trends Biochem Sci*. 2014;39(8):347-354.
30. Gorrini C, Harris IS, Mak TW. Modulation of oxidative stress as an anticancer strategy. *Nat Rev Drug Discov*. 2013;12(12): 931-947.
31. Wong N, Ojo D, Yan J, Tang D. PKM2 contributes to cancer metabolism. *Cancer Lett*. 2015;356(2, pt A):184-191.
32. Christofk HR, Vander Heiden MG, Harris MH, et al. The M2 splice isoform of pyruvate kinase is important for cancer metabolism and tumour growth. *Nature*. 2008;452(7184):230-233.
33. Mazurek S, Boschek CB, Hugo F, Eigenbrodt E. Pyruvate kinase type M2 and its role in tumor growth and spreading. *Semin Cancer Biol*. 2005;15(4):300-308.
34. Luan W, Wang Y, Chen X, et al. PKM2 promotes glucose metabolism and cell growth in gliomas through a mechanism involving a let-7a/c-Myc/hnRNPA1 feedback loop. *Oncotarget*. 2015; 6(15):13006-13018.
35. Dong T, Yan Y, Chai H, et al. Pyruvate kinase M2 affects liver cancer cell behavior through up-regulation of HIF-1α and Bcl-xL in culture. *Biomed Pharmacother*. 2015;69:277-284.
36. Demaria M, Poli V. PKM2, STAT3 and HIF-1α: the Warburg's vicious circle. *JAKSTAT*. 2012;1(3):194-196.
37. Yang W, Xia Y, Ji H, et al. Nuclear PKM2 regulates β-catenin transactivation upon EGFR activation. *Nature*. 2011;480(7375): 118-122.
38. Chen YL, Song JJ, Chen XC, et al. Mechanisms of pyruvate kinase M2 isoform inhibits cell motility in hepatocellular carcinoma cells. *World J Gastroenterol*. 2015;21(30):9093-9102.
39. Liu WR, Tian MX, Yang LX, et al. PKM2 promotes metastasis by recruiting myeloid-derived suppressor cells and indicates poor prognosis for hepatocellular carcinoma. *Oncotarget*. 2015;6(2): 846-861.
40. Lomonaco R, Sunny NE, Bril F, Cusi K. Nonalcoholic fatty liver disease: current issues and novel treatment approaches. *Drugs*. 2013;73(1):1-14.
41. Streba LAM, Vere CC, Rogoveanu I, Streba CT. Nonalcoholic fatty liver disease, metabolic risk factors, and hepatocellular carcinoma: an open question. *World J Gastroenterol*. 2015;21(14): 4103-4110.
42. Fujii M, Shibazaki Y, Wakamatsu K, et al. A murine model for non-alcoholic steatohepatitis showing evidence of association between diabetes and hepatocellular carcinoma. *Med Mol Morphol*. 2013;46(3):141-152.
43. Streba LAM, Cârstea D, Mitruţ P, Vere CC, Dragomir N, Streba CT. Nonalcoholic fatty liver disease and metabolic syndrome: a concise review. *Rom J Morphol Embryol*. 2008;49(1):13-20.
44. Kneeman JM, Misdraji J, Corey KE. Secondary causes of nonalcoholic fatty liver disease. *Therap Adv Gastroenterol*. 2012; 5(3):199-207.
45. Jiang P, Du W, Mancuso A, Wellen KE, Yang X. Reciprocal regulation of p53 and malic enzymes modulates metabolism and senescence. *Nature*. 2013;493(7434):689-693.
46. Zheng FJ, Ye HB, Wu MS, Lian YF, Qian CN, Zeng YX. Repressing malic enzyme 1 redirects glucose metabolism, unbalances the redox state, and attenuates migratory and invasive abilities in nasopharyngeal carcinoma cell lines. *Chin J Cancer*. 2012; 31(11):519-531.
47. Wieckowska A, Papouchado BG, Li Z, Lopez R, Zein NN, Feldstein AE. Increased hepatic and circulating interleukin-6 levels in human nonalcoholic steatohepatitis. *Am J Gastroenterol*. 2008; 103(6):1372-1379.
48. Das SK, Balakrishnan V. Role of cytokines in the pathogenesis of non-alcoholic fatty liver disease. *Indian J Clin Biochem*. 2011; 26(2):202-209.
49. Hu W, Feng Z, Eveleigh J, et al. The major lipid peroxidation product, trans-4-hydroxy-2-nonenal, preferentially forms DNA adducts at codon 249 of human p53 gene, a unique mutational hotspot in hepatocellular carcinoma. *Carcinogenesis*. 2002; 23(11):1781-1789.
50. Feng Z, Hu W, Tang MS. Trans-4-hydroxy-2-nonenal inhibits nucleotide excision repair in human cells: a possible mechanism for lipid peroxidation-induced carcinogenesis. *Proc Natl Acad Sci U S A*. 2004;101(23):8598-8602.
51. Zaytseva YY, Rychahou PG, Gulhati P, et al. Inhibition of fatty acid synthase attenuates CD44-associated signaling and reduces metastasis in colorectal cancer. *Cancer Res*. 2012;72(6): 1504-1517.
52. Murata S, Yanagisawa K, Fukunaga K, et al. Fatty acid synthase inhibitor cerulenin suppresses liver metastasis of colon cancer in mice. *Cancer Sci*. 2010;101(8):1861-1865.
53. Jiang P, Du W, Wu M. Regulation of the pentose phosphate pathway in cancer. *Protein Cell*. 2014;5(8):592-602.
54. Deberardinis RJ, Sayed N, Ditsworth D, Thompson CB. Brick by brick: metabolism and tumor cell growth. *Curr Opin Genet Dev*. 2008;18(1):54-61.
55. Tuttle SW, Maity A, Oprysko PR, et al. Detection of reactive oxygen species via endogenous oxidative pentose phosphate cycle activity in response to oxygen concentration: implications for the mechanism of HIF-1alpha stabilization under moderate hypoxia. *J Biol Chem*. 2007;282(51):36790-36796.
56. Mannava S, Grachtchouk V, Wheeler LJ, et al. Direct role of nucleotide metabolism in C-MYC-dependent proliferation of melanoma cells. *Cell Cycle*. 2008;7(15):2392-2400.
57. Sun B, Li S, Yang L, et al. Activation of glycolysis and apoptosis in glycogen storage disease type Ia. *Mol Genet Metab*. 2009; 97(4):267-271.

58. Carvalho PMS, Silva NJMM, Dias PGD, Porto JFC, Santos LC, Costa JMN. Glycogen storage disease type 1a—a secondary cause for hyperlipidemia: report of five cases. *J Diabetes Metab Disord*. 2013;12(1):25.
59. Calderaro J, Labrune P, Morcrette G, et al. Molecular characterization of hepatocellular adenomas developed in patients with glycogen storage disease type I. *J Hepatol*. 2013;58(2):350-357.
60. Mutel E, Abdul-Wahed A, Ramamonjisoa N, et al. Targeted deletion of liver glucose-6 phosphatase mimics glycogen storage disease type 1a including development of multiple adenomas. *J Hepatol*. 2011;54(3):529-537.
61. Sever S, Weinstein DA, Wolfsdorf JI, Gedik R, Schaefer EJ. Glycogen storage disease type Ia: linkage of glucose, glycogen, lactic acid, triglyceride, and uric acid metabolism. *J Clin Lipidol*. 2012;6(6):596-600.
62. Grefhorst A, Schreurs M, Oosterveer MH, et al. Carbohydrate-response-element-binding protein (ChREBP) and not the liver X receptor α (LXRα) mediates elevated hepatic lipogenic gene expression in a mouse model of glycogen storage disease type 1. *Biochem J*. 2010;432(2):249-254.
63. Jones JG, Garcia P, Barosa C, Delgado TC, Diogo L. Hepatic anaplerotic outflow fluxes are redirected from gluconeogenesis to lactate synthesis in patients with type 1a glycogen storage disease. *Metab Eng*. 2009;11(3):155-162.
64. Vander Heiden MG, Christofk HR, Schuman E, et al. Identification of small molecule inhibitors of pyruvate kinase M2. *Biochem Pharmacol*. 2010;79(8):1118-1124.
65. Li W, Liu J, Zhao Y. PKM2 inhibitor shikonin suppresses TPA-induced mitochondrial malfunction and proliferation of skin epidermal JB6 cells. *Mol Carcinog*. 2014;53(5):403-412.
66. Bandsma RHJ, Prinsen BH, de Sain-van der Velden M, et al. Increased de novo lipogenesis and delayed conversion of large VLDL into intermediate density lipoprotein particles contribute to hyperlipidemia in glycogen storage disease type 1a. *Pediatr Res*. 2008;63(6):702-707.
67. Benhamed F, Filhoulaud G, Caron S, Lefebvre P, Staels B, Postic C. O-GlcNAcylation links ChREBP and FXR to glucose-sensing. *Front Endocrinol (Lausanne)*. 2015;5:230.
68. Bandsma RHJ, Smit GPA, Kuipers F. Disturbed lipid metabolism in glycogen storage disease type 1. *Eur J Pediatr*. 2014;161(1): S65-S69.
69. Fernandes J, Alaupovic P, Wit JM. Gastric drip feeding in patients with glycogen storage disease type I: its effects on growth and plasma lipids and apolipoproteins. *Pediatr Res*. 1989;25(4): 327-331.
70. Abdul-Wahed A, Gautier-Stein A, Casteras S, et al. A link between hepatic glucose production and peripheral energy metabolism via hepatokines. *Mol Metab*. 2014;3(5):531-543.
71. Farah BL, Landau DJ, Sinha RA, et al. Induction of autophagy improves hepatic lipid metabolism in glucose-6-phosphatase deficiency. *J Hepatol*. 2016;64(2):370-379.
72. Viollet B, Foretz M, Guigas B, et al. Activation of AMP-activated protein kinase in the liver: a new strategy for the management of metabolic hepatic disorders. *J Physiol*. 2006; 574(pt 1):41-53.
73. Zhou G, Myers R, Li Y, et al. Role of AMP-activated protein kinase in mechanism of metformin action. *J Clin Invest*. 2001; 108(8):1167-1174.
74. Kawaguchi T, Osatomi K, Yamashita H, Kabashima T, Uyeda K. Mechanism for fatty acid ''sparing'' effect on glucose-induced transcription: regulation of carbohydrate-responsive element-binding protein by AMP-activated protein kinase. *J Biol Chem*. 2002;277(6):3829-3835.
75. Airley RE, McHugh P, Evans AR, et al. Role of carbohydrate response element-binding protein (ChREBP) in generating an aerobic metabolic phenotype and in breast cancer progression. *Br J Cancer*. 2014;110(3):715-723.
76. Wang XL, Wen XF, Li RB, et al. Chrebp regulates the transcriptional activity of androgen receptor in prostate cancer. *Tumour Biol*. 2014;35(8):8143-8148.
77. Tong X, Zhao F, Mancuso A, Gruber JJ, Thompson CB. The glucose-responsive transcription factor ChREBP contributes to glucose-dependent anabolic synthesis and cell proliferation. *Proc Natl Acad Sci U S A*. 2009;106(51):21660-21665.
78. Barankiewicz J, Cohen A. Purine nucleotide metabolism in resident and activated rat macrophages in vitro. *Eur J Immunol*. 1985; 15(6):627-631.
79. Fini MA, Elias A, Johnson RJ, Wright RM. Contribution of uric acid to cancer risk, recurrence, and mortality. *Clin Transl Med*. 2012;1(1):16.
80. Wittenstein B, Klein M, Finckh B, Ullrich K, Kohlschütter A. Plasma antioxidants in pediatric patients with glycogen storage disease, diabetes mellitus, and hypercholesterolemia. *Free Radic Biol Med*. 2002;33(1):103-110.
81. Murphy MP. How mitochondria produce reactive oxygen species. *Biochem J*. 2009;417(1):1-13.
82. Lee J, Giordano S, Zhang J. Autophagy, mitochondria and oxidative stress: cross-talk and redox signalling. *Biochem J*. 2012; 441(pt 2):523-540.
83. Glick D, Barth S, Macleod KF. Autophagy: cellular and molecular mechanisms. *J Pathol*. 2010;221(1):3-12.
84. Yang S, Kimmelman AC. A critical role for autophagy in pancreatic cancer. *Autophagy*. 2011;7(8):912-913.
85. Apel A, Zentgraf H, Büchler MW, Herr I. Autophagy-A double-edged sword in oncology. *Int J Cancer*. 2009;125(5): 991-995.
86. Takamura A, Komatsu M, Hara T, et al. Autophagy-deficient mice develop multiple liver tumors. *Genes Dev*. 2011;25(8): 795-800.
87. Bosi E. Metformin—the gold standard in type 2 diabetes: what does the evidence tell us? *Diabetes Obes Metab*. 2009;11(suppl 2):3-8.
88. Kasznicki J, Sliwinska A, Drzewoski J. Metformin in cancer prevention and therapy. *Ann Transl Med*. 2014;2(6):57.
89. Hundal RS, Krssak M, Dufour S, et al. Mechanism by which metformin reduces glucose production in type 2 diabetes. *Diabetes*. 2000;49(12):2063-2069.
90. Maiuri MC, Zalckvar E, Kimchi A, Kroemer G. Self-eating and self-killing: crosstalk between autophagy and apoptosis. *Nat Rev Mol Cell Biol*. 2007;8(9):741-752.

91. Sirover MA. New nuclear functions of the glycolytic protein, glyceraldehyde-3-phosphate dehydrogenase, in mammalian cells. *J Cell Biochem*. 2005;95(1):45-52.
92. Shashidharan P, Chalmers-Redman RM, Carlile GW, et al. Nuclear translocation of GAPDH-GFP fusion protein during apoptosis. *Neuroreport*. 1999;10(5):1149-1153.
93. Guicciardi ME, Gores GJ. Apoptosis: a mechanism of acute and chronic liver injury. *Gut*. 2005;54(7):1024-1033.
94. Kim SY, Weinstein DA, Starost MF, Mansfield BC, Chou JY. Necrotic foci, elevated chemokines and infiltrating neutrophils in the liver of glycogen storage disease type Ia. *J Hepatol*. 2008; 48(3):479-485.
95. Yamashita T, Ishibashi Y, Nagaoka I, et al. Studies of glycogen-induced inflammation of mice. Dynamics of inflammatory responses and influence of antiinflammatory drugs and protease inhibitors. *Inflammation*. 1982;6(1):87-101.
96. McCullough AJ. Pathophysiology of nonalcoholic steatohepatitis. *J Clin Gastroenterol*. 2006;40(suppl 1):S17-S29.
97. Nault JC, Zucman Rossi J. Molecular classification of hepatocellular adenomas. *Int J Hepatol*. 2013;2013:e315947.
98. Marchetti A, Bisceglia F, Cozzolino AM, Tripodi M. New tools for molecular therapy of hepatocellular carcinoma. *Diseases*. 2015;3(4):325-340.
99. Cereghini S, Yaniv M, Cortese R. Hepatocyte dedifferentiation and extinction is accompanied by a block in the synthesis of mRNA coding for the transcription factor HNF1/LFB1. *EMBO J*. 1990;9(7):2257-2263.
100. Rebouissou S, Imbeaud S, Balabaud C, et al. HNF1alpha inactivation promotes lipogenesis in human hepatocellular adenoma independently of SREBP-1 and carbohydrate-response element-binding protein (ChREBP) activation. *J Biol Chem*. 2007; 282(19):14437-14446.
101. Pelletier L, Rebouissou S, Paris A, et al. Loss of hepatocyte nuclear factor 1alpha function in human hepatocellular adenomas leads to aberrant activation of signaling pathways involved in tumorigenesis. *Hepatology*. 2010;51(2):557-566.
102. Farrelly AM, Kilbride SM, Bonner C, Prehn JHM, Byrne MM. Rapamycin protects against dominant negative-HNF1A-induced apoptosis in INS-1 cells. *Apoptosis*. 2011;16(11): 1128-1137.
103. Nault JC, Bioulac-Sage P, Zucman-Rossi J. Hepatocellular benign tumors-from molecular classification to personalized clinical care. *Gastroenterology*. 2013;144(5):888-902.
104. Zucman-Rossi J, Jeannot E, Nhieu JTV, et al. Genotype-phenotype correlation in hepatocellular adenoma: new classification and relationship with HCC. *Hepatology*. 2006;43(3): 515-524.
105. Gautier-Stein A, Zitoun C, Lalli E, Mithieux G, Rajas F. Transcriptional regulation of the glucose-6-phosphatase gene by cAMP/vasoactive intestinal peptide in the intestine. Role of HNF4α, CREM, HNF1α, and C/EBPα. *J Biol Chem*. 2006; 281(42):31268-31278.
106. Streeper RS, Svitek CA, Goldman JK, O'Brien RM. Differential role of hepatocyte nuclear factor-1 in the regulation of glucose-6-phosphatase catalytic subunit gene transcription by cAMP in liver- and kidney-derived cell lines. *J Biol Chem*. 2000;275(16): 12108-12118.
107. Hiraiwa H, Pan C-J, Lin B, Akiyama TE, Gonzalez FJ, Chou JY. A molecular link between the common phenotypes of type 1 glycogen storage disease and HNF1α-null mice. *J Biol Chem*. 2001;276(11):7963-7967.
108. Luo Z, Li Y, Wang H, et al. Hepatocyte nuclear factor 1A (HNF1A) as a possible tumor suppressor in pancreatic cancer. *PLoS One*. 2015;10(3):e0121082.

*Manuscript
Click here to view linked References

Metabolic stress associated with hepatic carcinogenesis in the absence of fibrosis in Glycogen storage disease type Ia

Monika Gjorgjieva[1-3], Julien Calderaro[4-5], Laure Monteillet[1-3], Marine Silva[1-3], Margaux Raffin[1-3], Marie Brevet[2-3,6], Caroline Romestaing[2-3,7], Damien Roussel[2-3,7], Jessica Zucman-Rossi[4-5,8], Gilles Mithieux[1-3] & Fabienne Rajas[1-3]

[1]Institut National de la Santé et de la Recherche Médicale, U1213, Lyon, F-69008, France

[2]Université de Lyon, Lyon, F-69008 France

[3]Université Lyon I, Villeurbanne, F-69622 France

[4]Inserm UMR-1162, Université Paris Descartes, Université Paris Diderot, Université Paris 13, Labex Immuno-Oncology, Paris, France

[5]APHP, Assistance-Publique Hôpitaux-de-Paris, Département de Pathologie, Hôpital Henri Mondor, Créteil, F-94010, France

[6] Service de Pathologie Lyon Est, Centre hospitalier universitaire de Lyon, Lyon, F-69437, France

[7]Centre National de la Recherche Scientifique, UMR 5023, Villeurbanne, F-69622 France

[8]Hôpital Européen Georges Pompidou, AP-HP, Assistance Publique-Hôpitaux de Paris, Paris, F-75015, France

Running title: Tumorigenesis in GSDIa liver.

Corresponding author: Dr. Fabienne Rajas, Ph.D.

Inserm U1213, Université Lyon 1 Laennec

7 rue Guillaume Paradin, 69372 Lyon cedex 08 France

Tel: 33 478 77 10 28/Fax: 33 478 77 87 62

E-mail: fabienne.rajas@univ-lyon1.fr

Keywords: Non-alcoholic fatty liver disease; hepatocellular adenoma and carcinoma; cellular defenses; tumor suppressor; epithelial-mesenchymal transition.

Electronic word count: 6667 words

Number of figures and tables: 7 figures and 1 table

Conflict of interest statement: The authors who have taken part in this study declare that they do not have anything to disclose regarding funding or there is no conflict of interest with respect to this manuscript.

Financial support: This work was supported by research grants from the Agence Nationale de la Recherche (ANR11-BSV1-009-01), the Association Francophone des Glycogénoses (AFG) and the Ligue régionale contre le cancer. MG is a recipient of the Ligue nationale contre le cancer funding. JZR team is « équipe Labellisée par la Ligue Nationale Contre le Cancer », LNCC, and funded by INSERM with the « Cancer et Environnement » (plan Cancer) and HETCOLI projects (Tumor Heterogeneity and Ecosystem program). The group is supported by the Ligue Nationale contre le Cancer (Equipe Labellisée), Labex

OncoImmunology (investissement d'avenir), Coup d'Elan de la Fondation Bettencourt-Shueller, the SIRIC CARPEM and Fondation Mérieux.

Author contributions: M.G. designed, conducted experiments, analyzed the data and wrote the paper. J.C. designed, conducted experiments and analyzed the data. M.S. and M.R. were in charge of mouse breeding and animal experiments. L.M., C.R. and D.R conducted experiments. J.C. and M. B. are anatomopathologists and classified hepatic tumors. J.C., L.M., D.R., J.Z-R., and G.M. critically edited the manuscript. FR supervised the studies and wrote the paper.

ABSTRACT

Background & aims: Glycogen storage disease type Ia (GSDIa) is a rare genetic disease associated with glycogen accumulation in hepatocytes and steatosis. With age, most adult GSDIa patients develop hepatocellular adenomas (HCA), which can progress to hepatocellular carcinomas (HCC). In this study, we characterized metabolism reprogramming and cellular defense alterations during tumorigenesis in the liver of hepatocyte-specific *G6pc* deficient (L.G6pc-/-) mice, which develop all hepatic hallmarks of GSDIa.

Methods: Liver metabolism and cellular defenses were assessed at pretumoral (4 months) and tumoral (9 months) stages in L.G6pc-/- mice fed a high fat/high sucrose (HF/HS) diet.

Results: In response to HF/HS diet, hepatocarcinogenesis was highly accelerated since 90% of L.G6pc-/- mice developed multiple hepatic tumors after 9 months, classified for 72% as HCA and 28% as HCC. Tumor development was associated with high expression of malignancy markers of HCC, i.e α-fetoprotein, glypican3 and β-catenin. In addition, L.G6pc-/- livers exhibited loss of tumor suppressors. Interestingly, L.G6pc-/- steatosis exhibited a low-inflammatory state and was less pronounced than in WT livers. This was associated with an absence of epithelial-mesenchymal transition (EMT) and fibrosis, while HCA/HCC showed a partial EMT in the absence of TGF-β1 increase. In HCA/HCC, glycolysis was characterized by a marked expression of PK-M2, decreased mitochondrial OXPHOS and a decrease of pyruvate entry in the mitochondria, confirming a "Warburg-like" phenotype. These metabolic alterations led to a decrease in antioxidant defenses and autophagy and chronic ER-stress in L.G6pc-/- livers and tumors. Interestingly, autophagy was reactivated in HCA/HCC.

Conclusion: The metabolic remodeling in L.G6pc -/- liver generates a preneoplastic status and leads to a loss of cellular defenses and tumor suppressors that facilitates tumor development in GSDI.

LAY SUMMARY

Glycogen storage disease type Ia is a rare metabolic disease characterized by hypoglycemia, steatosis, excessive glycogen accumulation and tumor development in the liver. In this study, we have observed that GSDIa livers reprogram their metabolism similarly to a cancer cell, which facilitates tumor formation and progression, in the absence of hepatic fibrosis. Moreover, hepatic burden due to overload of glycogen and lipids in the cells leads to a decrease in cellular defenses, such as antioxidant enzymes and autophagy, which could further promote tumorigenesis in the case of GSDI.

INTRODUCTION

Hepatocellular carcinoma (HCC) is one of the most common primary malignancies of the liver[1]. Many studies have demonstrated a strong link between hepatic tumorigenesis and non-alcoholic fatty liver diseases (NAFLDs), including obesity, diabetes and other genetic metabolic liver diseases, such as Glycogen storage disease type I (GSDI)[2,3,4]. NAFLD can go from simple steatosis characterized by hepatic fat accumulation, to the more aggressive form called non-alcoholic steatohepatitis (NASH), associated with inflammation and fibrosis. While it is considered that NASH/NAFLD can lead to liver cirrhosis, predisposing the liver to HCC, studies have reported that HCC can also develop in the absence of cirrhosis. Moreover, hepatocellular adenomas (HCA), which are rare benign tumors, can later transform into HCC in the absence of cirrhosis[5,6].

GSDI is due to a deficiency in glucose-6 phosphatase (G6Pase) activity[7,8]. The mutations in *G6PC*, encoding the catalytic subunit of G6Pase[9,10], are responsible for GSD type Ia (GSDIa), while mutations in *SLC37A4* encoding the transport subunit of the G6Pase, are responsible for GSD type Ib (GSDIb). G6Pase is an enzyme expressed only in the liver, kidneys and intestine, converting glucose-6 phosphate (G6P) into glucose, ensuring normal glycaemia[11,12]. G6Pase deficiency results in hypoglycemia, associated with hypercholesterolemia, hypertriglyceridemia, lactic acidosis and hyperuricemia in GSDI patients and animal models [7,8,13]. Furthermore, increased accumulation and intracellular flow through G6P lead to glycogen and lipid accumulation in the hepatocytes, resulting in hepatomegaly and hepatic steatosis[7,8,13]. As mentioned above, most adult GSDI patients develop HCA, which can transform in HCC, with about 10% incidence of transformation, in the absence of liver fibrosis and cirrhosis[14,15]. In a French cohort of GSDI patients, about 50% of HCA were diagnosed as inflammatory, nearly 30% of HCA showed β-catenin mutations and 20% of HCA were unclassified[14].

While the molecular mechanisms involved in GSDI tumorigenesis remain unclear, there are several pathways suspected to be involved in this process[16]. Since GSDI can be considered as a NAFLD-like condition, lipid-related risks could lead to tumorigenesis. Glycogen and lipid storages in massive quantities can induce inflammation, apoptosis and even necrosis[17,18,19]. Impaired metabolism can induce abnormal responses in the hepatocytes, such as autophagy dysregulation and activation of endoplasmic reticulum (ER) stress pathways. Indeed, recent studies showed a decrease in autophagic flux in GSDI livers[20,21]. All these mechanisms could promote tumorigenesis in the case of GSDI.

In order to investigate the pathways involved in tumorigenesis, our laboratory has developed a GSDIa mouse model, in which *G6pc* is deleted specifically in the liver. These L.G6pc-/- mice exhibit the same hepatic and plasmatic complications observed in GSDIa patients, including HCA and HCC development[13,22].

In this study, we analyzed cellular and metabolic stress in L.G6pc-/- livers at a pretumoral and at a tumoral stage that leads to the loss of tumor suppressors, such as PTEN and p53. Indeed, G6Pase deficiency in the liver translates in a metabolic reprogramming in the hepatocytes, characterized as a «Warburg-like» effect that alters many aspects of cell homeostasis, thus triggering tumorigenesis.

MATERIALS AND METHODS

Generation of liver-specific G6pc knock-out mice (L.G6pc-/-)

L.G6pc -/- mice were obtained by tamoxifen treatment of B6.G6pc$^{lox/lox}$.SA^{CreERT2} mice at the age of 8 weeks as previously described[13]. C57Bl6/J mice (Charles Rivers, L'Arbresle, France) were used as control (referred to as wild-type [WT] mice). After tamoxifen treatment, male and female L.G6pc-/- and control mice were fed a high fat / high sucrose

(HF/HS) diet (35% fat, 20% proteins, 35% carbohydrates including starch and sucrose) during 4 months or 9 months. Animals were housed in groups of 4-6 mice, with "Lignocel" bedding (JRS, Rosenberg, Germany) in an enriched environment at 21°C, with a light/darkness cycle 12h/12h and free access to water and food. All the procedures were performed in accordance with the principles and guidelines established by the European Convention for the Protection of Laboratory Animals. The regional animal care committee (C2EA-55, Université Lyon 1, Lyon) approved all the experiments.

Histological and immunohistological analysis

Hematoxylin and eosin (H&E) staining of liver and tumors was done as previously described[13]. Liver sections were stained using PCNA or p53 antibodies (Supplem. Table 1), as described in the Cell signaling technology immunohistochemistry protocol. For transmission electron microscopy (TEM), ultrathin sections were obtained and observed as previously described[23]. Four to five tissue samples were prepared from each group of mice. Ten liver or tumor sections from each mouse were documented and the number of autophagic vesicles per field was assessed.

Metabolic studies

Blood was withdrawn by submandibular bleeding 6h after food removal. Plasmatic and hepatic metabolites were determined as previously described[13,23]. Alpha- fetoprotein (AFP) (R&D Systems Inc, Lille, France) and C reactive protein (CRP) (Abcam, Cambridge, UK) levels were determined by ELISA. AST/ALT activities were determined with colorimetric activity assays (Abcam, Cambridge, UK).

Gene and protein expression analysis

Antibodies for western blot analyses are cited in Supplemental CTAT Table. The visualization and quantification of the proteins were performed using the BioRad ChemiDoc™ Touch Imaging System (Marnes La Coquette, France).

Total RNAs were isolated according to the Trizol protocol (Invitrogen Life Technologies, Thermofisher, France). RT-qPCR were performed as previously described, expressed in 2-DDCT value with WT normal liver as normalizator[13,23]. The mouse ribosomal protein mL19 (*Rpl19*) was used as reference. Primer sequences are indicated in Supplemental CTAT Table.

Statistics

The results are reported as the mean ± s.e.m. At the pretumoral stage, WT and L.G6pc-/- groups were compared with a Student's t-test. At the tumoral stage, tissue samples were compared with one-way ANOVA. Differences were considered to be statistically significant at P-value < 0.05.

RESULTS

High fat/high sucrose diet accelerates hepatic carcinogenesis in L.G6pc-/- mice

Wild-type (WT) and L.G6pc-/- mice were fed a HF/HS diet for 4 months or for 9 months. As shown previously[24], L.G6pc-/- mice fed a HF/HS diet were resistant to obesity compared to WT mice, which became obese (Supplem. Fig.1). No tumors were observed in L.G6pc-/- and WT livers at 4 months of HF/HS diet; this stage will be referred to as the pretumoral stage. Nevertheless, L.G6pc-/- mice exhibited hepatomegaly associated with hepatic glycogen and G6P, which were significantly increased (Table 1). However, triglycerides were decreased in comparison to WT mice (Table 1). At plasmatic level, a significant increase in cholesterol, triglycerides and lactate was observed in L.G6pc-/- mice, whereas plasmatic and hepatic

glucose levels were decreased (Table 1). Plasmatic uric acid and non-esterified fatty acids (NEFA) were unchanged. Strikingly, 90% of L.G6pc-/- mice had hepatic nodules after 9 months on HF/HS diet (Fig.1A). This stage will be referred to as the tumoral stage. Among all L.G6pc-/- tumors (n=26), 72% were histologically diagnosed as HCA and 28% were HCC (Fig.1B panels c and d, respectively). Mice developed multiple millimetric nodules, associated with one or several macroscopic tumors. None of the WT mice developed hepatic nodules. At this stage, all plasmatic and hepatic parameters were similar to L.G6pc-/- mice at the pretumoral stage, with the exception of hepatic triglycerides, which were further decreased, compared to pretumoral L.G6pc-/- livers (Table 1). Liver weight increased slightly, compared to the pretumoral stage, due to the weight of the tumors. HCAs were mainly steatotic (Fig.1B panel c). In general, HCC cells were smaller than L.G6pc-/- hepatocytes, with a denser cytoplasm (Fig.1B panel d). At the pretumoral and tumoral stages no difference in proliferating cell nuclear antigen (PCNA) staining was observed between WT and L.G6pc-/- livers (Fig.1C, panels a-d). As expected, an increased number of PCNA-positive cells were observed in HCA and HCC samples (Fig.1C panels e and f), indicating an increase in cell proliferation in GSDI tumors. At the tumoral stage, no differences in circulating CRP, aspartate transaminase (AST) and alanine transaminase (ALT) levels were observed between WT and L.G6pc-/- mice (Fig.1D), probably due to the low grade inflammation in WT mice fed a HF/HS diet, since these mice also developed steatosis[25]. Interestingly, the expression of malignancy markers of HCC were increased in L.G6pc-/- mice bearing tumors[26,27]. Indeed, the plasmatic concentration of AFP was significantly increased in L.G6pc-/- mice bearing HCA/HCC (Fig.1D). Furthermore, glypican3 (*Gpc3*) had a strong tendency to increase in HCC, but also in some low atypia histologically classified as HCA (Fig.1E). Glypican3 expression in some HCA samples could be due to a more advanced

stage and a tendency to transform into HCC, implying early acquirement of malignant traits in HCA.

L.G6pc-/- mice exhibit hepatic loss of tumor suppressors

In order to analyze further potential actors involved in tumorigenesis, the expression of several tumor suppressors i.e. hepatic nuclear factor 1 α (HNF1α), phosphatase and tensin homolog (PTEN) and p53[28,29,30] was assessed in L.G6pc-/- livers and tumors. Interestingly, we observed no change in *Hnf1a* mRNA expression at the pretumoral stage (Fig.2A). Nevertheless, *Hnf1a* mRNA was significantly decreased in L.G6pc-/- livers and tumors at the tumoral stage, compared to WT livers, as previously reported in human GSDI livers and tumors[14,28] (Fig.2B). *Pten* expression was decreased in L.G6pc-/- livers at both pretumoral and tumoral stage and in tumors (Fig.2A-B). Interestingly, p53 acetylation at Lys379, which activates the accumulation of p53 as a stress response following DNA damage[31], was increased in L.G6pc-/- livers at the pretumoral stage (Fig.2C). On the contrary, acetylated p53 was decreased in L.G6pc-/- livers and in HCA/HCC at the tumoral stage (Fig.2D), thus indicating a switch in p53 signaling between the stages. Furthermore, phosphorylation of p53 at Ser392[32], which influences the growth suppressor function, DNA binding, and transcriptional activation of p53, was increased in L.G6pc-/- livers at both stages and in HCA/HCC. It is noteworthy that immunohistochemistry analysis revealed that p53 was translocated in the nuclei of WT and L.G6pc-/- hepatocytes, after 4 and 9 months of HF/HS diet (Fig.2E), while we observed the presence of p53-negative nuclei in HCA samples (Fig.2E panel e). In HCC samples, most nuclei were p53-negative, while p53 preferentially accumulated in the cytoplasm of hepatocytes (Fig.2E panel f).

Lack of EMT is responsible for the absence of liver fibrosis in L.G6pc-/- livers

In the general population, hepatic fibrosis / cirrhosis generally precede the development of HCC. As already observed in GSDI patients[8], L.G6pc-/- livers did not show signs of fibrosis (Fig.1), yet HCC occurred. In order to investigate the lack of fibrosis in L.G6pc-/- livers, epithelial-mesenchymal transition (EMT), which is known to lead to hepatic fibrosis[33], was analyzed. At the tumoral stage, the epithelial marker E-cadherin was up-regulated in L.G6pc-/- livers compared to WT, while none of the mesenchymal markers , i.e. vimentin (*Vim*), α-smooth muscle actin (*Acta*) and plasminogen activator inhibitor-1 (*Pai1*), were increased (Fig.3A-B). Furthermore, transforming growth factor beta 1 (*Tgfβ1*), which can activate EMT in the liver[34], was unchanged, confirming the absence of EMT and fibrosis induction (Fig.3B). Surprisingly, E-cadherin remained increased in hepatic tumors (Fig.3A). In addition, an increase in the epithelial marker β-catenin was observed only in HCC, as already observed in GSDI patients[14] (Fig.3A). Concomitantly, the mesenchymal markers were all increased in hepatic tumors (tendency for *Pai-1*), more substantially in HCC than in HCA (Fig.3B). Surprisingly, *Tgfβ1* expression was decreased in HCA and HCC (Fig.3B). These results indicate a concomitant up-regulation of epithelial and mesenchymal markers in HCA/HCC which was mediated in a TGF-β1 –independent manner.

Finally, we analyzed the expression of the β-catenin target genes, i.e. glutamine synthetase (*Glul*) and leucine-rich repeat-containing G-protein coupled receptor 5 (*Lgr5*). Surprisingly, the expressions of *Glul* and *Lgr5* were decreased in L.G6pc-/- livers, and further decreased in HCA and HCC (Fig.3C), indicating that the β-catenin pathway was not activated during tumorigenesis.

Metabolic reprogramming of L.G6pc-/- hepatocytes makes them favorable to tumorigenesis

Hyperactivation of the glycolysis pathway has already been confirmed in GSDI livers[35]. Interestingly, mRNA expressions of the glucokinase (*Gck*) and the glucose transporter Glut1 (*Slc2a1*), usually increased in glycolytic conditions, were dramatically decreased in L.G6pc-/- livers at both stages, as well as in HCA and HCC (Fig.4A-B), probably to limit G6P accumulation. Concomitantly, a significant increase in plasmatic lactate concentrations was observed at both stages (Table 1), confirming increased glycolysis. However, lactate dehydrogenase A (LDHA), which catalyzes the conversion of pyruvate to lactate, was unchanged in L.G6pc-/- livers (Fig.4C-D). The expression of the M2 isoform of pyruvate kinase (PK-M2), which is an alternatively spliced variant expressed in cancer cells[36], was unchanged in L.G6pc-/- livers at both stages (Fig.4C-D). Interestingly, PK-M2 was significantly increased in tumors, conferring a strong glycolytic profile on HCA and HCC (Fig.4D).

OXPHOS analyses revealed a decrease in mitochondrial respiration in L.G6pc-/- livers compared to WT livers at both stages, characterized by a decrease in pyruvate oxidation (Supplem. Fig.2). The global respiration values were low, consistent with the hepatic steatosis observed in both L.G6pc-/- and WT mice, due to the HF/HS diet[37]. Pyruvate dehydrogenase (PDH), a key factor in pyruvate oxidation, was similar in WT and L.G6pc-/- livers and tumors (Fig.4C-D). In addition, pyruvate dehydrogenase kinase 4 (PDK4), an inhibitor of PDH, was downregulated in L.G6pc-/- livers at both stages. Interestingly, the mitochondrial pyruvate carrier 1 (MPC1) was slightly decreased in L.G6pc-/- livers at the pretumoral stage (Fig.4C), further decreased at the tumoral stage, and even more in HCA and HCC (Fig.4D). Thus a decrease in pyruvate transport in the mitochondria could explain, at least in part, the decreased pyruvate oxidation.

Analysis of the main actors in lipid metabolism at the pretumoral stage revealed an increase in *de novo* lipogenesis in L.G6pc-/- livers, concomitantly with a decrease in fatty acid oxidation (FAO) (Fig.5A), as previously reported[13,24]. This was linked to an increase in carbohydrate-responsive element binding protein (*Chrebp*), especially *Chrebp* β–isoform mRNA expression at this stage. On the contrary, the expression of sterol regulatory element-binding protein 1 (*Srebp1*) was unchanged in L.G6pc-/- livers, compared with WT livers, while *Srebp2* expression was decreased (Fig.5A). At the tumoral stage, a similar increase in lipogenesis gene expression was observed in L.G6pc-/- livers, while this increase was less pronounced in HCA and HCC (Fig.5B). In addition, *Srebp1* and *Pparg* expressions were significantly decreased in L.G6pc-/- livers and tumors at this stage. Concomitantly, the expression of genes involved in FAO was more decreased in tumors than in L.G6pc-/- livers. Interestingly, total *Chrebp* expression decreased in L.G6pc-/- livers and tumors at this stage (Fig.5B), contrarily to the pretumoral stage. Nevertheless, *Chrebp*-β isoform expression remained increased in L.G6pc-/- livers and tumors. During malignant transformation, increased formation of small lipid droplets is often detected and perilipin is an important factor in this process[38]. Interestingly, perilipin was detected only in HCC samples (Fig.5C). As expected, L.G6pc-/- mice exhibited an increase in hepatic lipid synthesis and a decrease in FAO in pretumoral and tumoral stage livers. In tumors, FAO was considerably decreased, concomitantly with a decrease in lipogenesis. This switch in lipid metabolism is possibly related to an intriguing switch in ChREBP expression that could be a potential trigger of tumorigenesis.

Impairment in cellular defenses in L.G6pc-/- livers

Altered metabolism and steatosis can lead to an increased production of reactive oxygen species (ROS) and cause oxidative stress. In order to maintain homeostasis, hepatocytes activate antioxidant enzyme production against ROS-induced damage. However, the expression of catalase (*Cat*) and glutathione peroxidase (*Gpx1*) was decreased at the pretumoral and the tumoral stages (Fig.6A-B). These results indicate an oxidative stress in L.G6pc-/- livers and tumors that was confirmed by the presence of donut-shaped mitochondria in L.G6pc-/- livers and in HCA/HCC (Fig.6C). In order to analyze the importance of antioxidant loss in L.G6pc-/- livers, mice were treated with Tempol, an antioxidant agonist for 9 months. Although we observed a significant increase in *Cat* and *Gpx1* expressions in L.G6pc-/- mice treated with Tempol (Fig.6D), 9 out of 12 treated L.G6pc-/- mice developed hepatic tumors with the same characteristics as non-treated L.G6pc-/- mice, proving that an increase in antioxidant defenses is not capable of impeding HCA/HCC development.

Recent studies showed a decreased autophagic flux in GSDI livers[20,21] that was confirmed in L.G6pc-/- livers at both stages (Supplem. Fig.3). However, HCA and HCC showed a reactivation of autophagy since we observed a decrease in p62 accumulation (Supplem. Fig.3). This was confirmed by the quantification of autophagic vesicles *via* TEM. Thus a 5-fold decrease in autophagic vesicle number in L.G6pc-/- livers was observed at the pretumoral and tumoral stages, while the number of autophagic vesicles was only decreased by 2-fold in tumors, compared to WT livers (Fig.6E).

Endoplasmic reticulum stress - another contributor to tumorigenesis in GSDI livers?

Disrupted cellular homeostasis can lead to ER stress and thus to malignancy[39] and/or altered lipid metabolism[40]. Interestingly, a marked decrease in BiP protein expression (chaperone protein that attenuates hepatic steatosis[41]) was observed in L.G6pc-/- livers at the pretumoral and the tumoral stage, and furthermore in HCA/HCC (Fig.7A). BiP downregulation can lead to the activation of the three main axes of ER stress (IRE1α /XBP1, PERK/ATF4 and ATF6). IRE1α was increased in L.G6pc-/- livers and tumors at both stages, while the active form of its target XBP1-S was decreased at the pretumoral stage and increased at the tumoral stage (Fig.7A-B). Analysis of the PERK/ATF4 pathway revealed no change in the phosphorylation of eIF2α (target of PERK) (Fig.7A-B) and *Atf4* mRNA expression (data not shown) in L.G6pc-/- livers at both stages. Nevertheless, this pathway was markedly inhibited in HCA/HCC, as illustrated by the decrease in eIF2 phosphorylation (Fig.7B). ATF6 was increased in pretumoral and tumoral stage L.G6pc-/- livers, and varied in tumors (Fig.7A-B). Finally, a decrease in CHOP and cleaved caspase 3 was observed in L.G6pc-/- livers at the pretumoral stage, indicating a decrease in ER stress-activated apoptosis (Fig.7A). Contrarily to the pretumoral stage, at the tumoral stage CHOP was increased in L.G6pc-/- livers, with a concomitant increase in cleaved caspase 3, indicating an increase in ER stress-activated apoptosis (Fig.7B). As expected, a strong inhibition of caspase 3 was observed in the HCA/HCC (Fig.7B), confirming the blockade of apoptosis in tumors.

In conclusion, ER stress activation was observed in L.G6pc-/- livers. It was mainly mediated *via* the IRE1/XBP1 and ATF6 pathways, but not through PERK/ATF4. Surprisingly, at the pretumoral stage, this activation led to decreased apoptosis, whereas at the tumoral level, apoptosis levels were restored.

CONCLUSION

In GSDIa, the loss of G6Pase activity is characterized by G6P accumulation in hepatocytes, leading to metabolic reprogramming that promotes tumorigenesis[14,16]. In this work, we investigated how G6Pase deficiency affects the cellular defense mechanisms and triggers tumorigenesis in a mouse model of GSDIa. We definitely showed that GSDIa hepatocytes exhibited the main characteristics of cancer cell metabolism, i.e. a preferential high rate of glycolysis, rather than mitochondrial pyruvate oxidation, leading to an increase in lactate production. In addition, the accumulation of hepatic lipids was exacerbated by a concomitant increase in *de novo* lipogenesis and a decrease in FAO. This offers advantages to proliferating cells, since increased fatty acids provide substrates for cellular membrane biogenesis. Altogether, these metabolic perturbations were associated with the loss of several cellular defenses, i.e. autophagy, oxidative stress response, dysregulation of ER stress responses and apoptosis, which were characterized in this study at a pretumoral and at a tumoral stage in livers of L.G6pc-/- mice. In addition, L.G6pc-/- livers did not exhibit EMT at the tumoral stage and were characterized by a low-grade inflammatory response and the absence of fibrosis, concomitantly with the development of HCA/HCC.

L.G6pc-/- mice represent a unique viable model of GSDIa that reproduces all hepatic hallmarks of GSDIa pathology. As shown in our previous study[13], about 30-40% of L.G6pc-/- mice developed millimetric hepatic lesions after 9 months of *G6pc* deletion, while all L.G6pc-/- mice developed hepatic nodules after 18 months. Most of these tumors were histologically classified as HCA. Recently, we estimated a 5-10% incidence of transformation to HCC at this age (unpublished data). Interestingly, tumor development was highly accelerated in L.G6pc-/- mice fed a HF/HS diet, since nearly all mice developed large hepatic nodules after 9 months. Some HCA already presented increased expression of

glypican 3, a characteristic marker of HCC, highlighting HCA potential to transform into HCC. Furthermore, the transformation ratio of HCA to HCC was increased, since almost 30% of tumors were diagnosed as HCC in L.G6pc-/- mice fed a HF/HS diet. As already published, L.G6pc-/- mice fed a HF/HS diet, unlike WT mice, resist obesity development[24]. In addition, the hepatic accumulation of triglycerides was less pronounced in L.G6pc-/- than in WT livers, probably due to a decrease in *Pparg* expression. Lipotoxicity in NAFLD is considered to be primarily due to the harmful effect of free fatty acids and free cholesterol rather than triglycerides, which are considered relatively inoffensive, and even possibly protective. Since GSDI shares common metabolic dysregulations with NASH/NAFLD, many of the complications that lead to HCC in this set of metabolic diseases could be accountable for HCC development in GSDI[16]. NAFLD-associated complications include inflammation, necrosis, lipotoxicity, adipokine imbalance and liver injury and remodeling. In spite of hepatic tumor development, we showed that these metabolic dysregulations did not lead to liver injury in GSDI. Thus ASL/ALT and CRP were slightly above healthy control values[25], but were similar in L.G6pc-/- mice bearing or not bearing tumors. Thus as in obesity, GSDIa is characterized by a low-grade chronic inflammatory response that is associated with increased tumor development and L.G6pc-/- mice are a very good model to study this pathology. Contrarily to the majority of HCC, which arise in fibrotic/cirrhotic livers, HCC in L.G6pc-/- livers develop in non-fibrotic conditions. This lack of fibrosis could be explained, at least in part, by the absence of inflammation and low levels of the profibrotic factor TGF-β1[42]. It is noteworthy that unlike HCC in the general population, HCC in GSDI are developed from HCA transformation, while *de novo* formation of HCC has never been reported[14]. Furthermore, while EMT is known to occur during the progression of HCC[34] to facilitate tumor dissemination, we observed a paradoxical concomitant up-regulation of epithelial and mesenchymal markers in HCA/HCC, in the absence of TGF-β1 increase. E-cadherin and

vimentin co-expression was already observed in breast cancer, associated with poor prognosis[43]. While the co-expression of epithelial and mesenchymal markers might indicate only an intermediate stage of EMT or a reverse mesenchymal to epithelial transition (MET) in these tumors[44], this can still favor metastasis formation, which has already been reported in GSDI patients[45]. Therefore it is important to pinpoint the exact role of EMT in GSDI tumorigenesis. Last, increased inflammation and EMT have been reported to occur in GSDI kidneys and contrarily to the liver, here this process leads to renal fibrosis and cyst development[23], but not cancer. Thus the difference in inflammation status in the liver and the kidneys in GSDI leads to different outcomes in these organs, and warrants to be further studied.

In L.G6pc-/- mice, HCA and HCC were characterized by a downregulation of tumor suppressors such as HNF1α, p53 and PTEN. The loss of tumor suppressors was also observed in L.G6pc-/- liver, conferring important neoplastic characteristics on the non-transformed GSDI hepatocytes. Furthermore, p53 was recently characterized as an important factor in lipid metabolism, independently of its role as a tumor suppressor[46]. Thus its deregulation could imply additional lipid metabolism alterations. In addition, AMPK and SIRT1, also qualified as tumor suppressors, were already found to be downregulated in GSDI livers[21,24]. Interestingly, the development of HCA to HCC was linked to a significant increase in plasma AFP and the overexpression of β-catenin and glypican 3. The presence of glypican 3 in some HCA samples, as well as the increase of AFP in mice that bore HCA accentuated the strong malignant transformation potential of HCA to HCC.

Contrarily to cancer cells, glucose phosphorylation is significantly decreased in L.G6pc-/- hepatocytes and HCA/HCC, limiting the accumulation of G6P. However, as observed in cancer cells, L.G6pc-/- hepatocytes preferentially metabolize glucose into lactate, conferring a “Warburg-like” phenotype to GSDIa hepatocytes. Interestingly, PK-M2 isoform was

overexpressed only in HCA/HCC. As many strategies are being developed to target this protein in order to block tumorigenesis[47], it is important to confirm this result in human patients, to consider PK-M2 inhibition as an anti-tumoral strategy for GSDIa. "Warburg-like" metabolism could also be promoted by the impairment of mitochondrial pyruvate transport, illustrated by a decrease of MPC1 expression in L.G6pc-/- livers and tumors. This deficient pyruvate transport may concur to lactic acidosis observed in GSDIa patients, as observed in patients with MPC1 deficiency[48]. A decreased import of pyruvate into mitochondria is in accordance with the observed downregulation of mitochondrial OXPHOS activity in L.G6pc-/- livers. In this work, we did not observe an increase in ROS production (data not shown), despite the presence of NAFLD. Interestingly, FAO was strongly decreased as well, especially in tumoral samples. Indeed, the liver-specific deletion of *G6pc* results in suppressed expression of PPARα, a master regulator of FAO. However, lipid oxidation is generally increased in cancer cells[49]. In conclusion, increased glycolysis along with the downregulation of mitochondrial respiration represents a marked reprogramming of hepatic metabolism favoring tumor development in GSDIa liver.

As previously mentioned, these metabolic perturbations lead to the impairment of cellular defenses, i.e. autophagy, ER stress and antioxidant defenses in L.G6pc-/- livers. First, we confirmed the suppression of autophagy previously reported in L.G6pc-/- livers[20,21]. Indeed, it was shown that the downregulation of autophagy in GSDI was mediated *via* SIRT1 and FoxO, and was independent of the canonical autophagy regulator mTOR[21]. Nevertheless, in HCA/HCC we observed a reactivation of autophagy, which could be favorable for tumor progression, since it provides building blocks and substrate for tumor proliferation and biomass gain. Secondly, we showed a specific ER stress response, induced by a significant decrease in BiP, accentuated in HCA/HCC. Variations in ER stress responses led to a decrease in apoptosis at the pretumoral and an increase in apoptosis at the tumoral stage.

Oxidative stress and autophagy can also induce apoptosis in cases where the cell cannot adapt to the overbearing cell damage[50]. Increased apoptosis rates in hepatocytes have been reported in both GSDIa patients and animal models, yet the actual cause of apoptosis induction is still to be deciphered[35]. Autophagy, oxidative stress responses and ER stress responses are finely tuned mechanisms that can interact at many levels and the result of these interactions conditions cell fate. Failure to activate these responses probably leads to tumorigenesis.

In conclusion, the various metabolic alterations in L.G6pc-/- livers, along with the decrease in several tumor suppressors, as well as cell defense deregulations, predispose GSDI livers to HCA/HCC development. Therefore, G6Pase deficiency in the liver initiates a complex metabolic reprogramming that affects many aspects of cell homeostasis, thus favoring tumorigenesis. The precise description here of the various mechanistic changes initiated by *G6pc* deficiency offers as many possible targets and rationales to envision future interventions aimed at moderating the severity (or treat) the disease.

ACKNOWLEDGEMENTS

We would like to thank the members of "Animalerie Lyon Est Conventionnelle et SPF (Université Lyon I, SFR Santé Lyon Est)" for the animal care, the members of the CIQLE platform (Université Lyon I) for the TEM analyses, the members of the "Centre d'histopathologie du petit animal Anipath" for the histological experiments (Université Lyon I) and Dr. Fabienne Foufelle (Centre de Recherche des Cordeliers, Paris) for the first analyses of ER-stress.

REFERENCES

1. Waghray A, Murali AR, Menon KN. Hepatocellular carcinoma: From diagnosis to treatment. *World J Hepatol*. 2015;7(8):1020-1029.

2. Margini C, Dufour JF. The story of HCC in NAFLD: from epidemiology, across pathogenesis, to prevention and treatment. *Liver Int Off J Int Assoc Study Liver*. 2016;36(3):317-324.

3. Marengo A, Rosso C, Bugianesi E. Liver Cancer: Connections with Obesity, Fatty Liver, and Cirrhosis. *Annu Rev Med*. 2016;67:103-117.

4. Bianchi L. Glycogen storage disease I and hepatocellular tumours. *Eur J Pediatr*. 1993;152 Suppl 1:S63-70.

5. Stoot JH, Coelen RJ, de Jong MC, Dejong CH. Malignant transformation of hepatocellular adenomas into hepatocellular carcinomas: a systematic review including more than 1600 adenoma cases. *HPB*. 2010;12(8):509-522.

6. Nault J-C, Couchy G, Balabaud C, et al. Molecular Classification of Hepatocellular Adenoma Associates With Risk Factors, Bleeding, and Malignant Transformation. *Gastroenterology*. 2017;152(4):880-894.e6.

7. Froissart R, Piraud M, Boudjemline AM, et al. Glucose-6-phosphatase deficiency. *Orphanet J Rare Dis*. 2011;6(1):27.

8. Kishnani PS, Austin SL, Abdenur JE, et al. Diagnosis and management of glycogen storage disease type I: a practice guideline of the American College of Medical Genetics and Genomics. *Genet Med Off J Am Coll Med Genet*. 2014;16(11):e1.

9. Chou JY, Mansfield BC. Mutations in the glucose-6-phosphatase-alpha (G6PC) gene that cause type Ia glycogen storage disease. *Hum Mutat*. 2008;29(7):921-930.

10. Bruni N, Rajas F, Montano S, Chevalier-Porst F, Maire I, Mithieux G. Enzymatic characterization of four new mutations in the glucose-6 phosphatase (G6PC) gene which cause glycogen storage disease type 1a. *Ann Hum Genet*. 1999;63(Pt 2):141-146.

11. Soty M, Gautier-Stein A, Rajas F, Mithieux G. Gut-Brain Glucose Signaling in Energy Homeostasis. *Cell Metab*. 2017;25(6):1231-1242.

12. Rajas F, Jourdan-Pineau H, Stefanutti A, Mrad EA, Iynedjian PB, Mithieux G. Immunocytochemical localization of glucose 6-phosphatase and cytosolic phosphoenolpyruvate carboxykinase in gluconeogenic tissues reveals unsuspected metabolic zonation. *Histochem Cell Biol*. 2007;127(5):555-565.

13. Mutel E, Abdul-Wahed A, Ramamonjisoa N, et al. Targeted deletion of liver glucose-6 phosphatase mimics glycogen storage disease type 1a including development of multiple adenomas. *J Hepatol*. 2011;54(3):529-537.

14. Calderaro J, Labrune P, Morcrette G, et al. Molecular characterization of hepatocellular adenomas developed in patients with glycogen storage disease type I. *J Hepatol*. 2013;58(2):350-357.

15. Labrune P, Trioche P, Duvaltier I, Chevalier P, Odièvre M. Hepatocellular adenomas in glycogen storage disease type I and III: a series of 43 patients and review of the literature. *J Pediatr Gastroenterol Nutr*. 1997;24(3):276-279.

16. Gjorgjieva M, Oosterveer MH, Mithieux G, Rajas F. Mechanisms by Which Metabolic Reprogramming in GSD1 Liver Generates a Favorable Tumorigenic Environment. *J Inborn Errors Metab Screen*. 2016;4:2326409816679429.

17. Yamashita T, Ishibashi Y, Nagaoka I, et al. Studies of glycogen-induced inflammation of mice. Dynamics of inflammatory responses and influence of antiinflammatory drugs and protease inhibitors. *Inflammation*. 1982;6(1):87-101.

18. Jung UJ, Choi M-S. Obesity and Its Metabolic Complications: The Role of Adipokines and the Relationship between Obesity, Inflammation, Insulin Resistance, Dyslipidemia and Nonalcoholic Fatty Liver Disease. *Int J Mol Sci*. 2014;15(4):6184-6223.

19. Feldstein AE, Canbay A, Angulo P, et al. Hepatocyte apoptosis and fas expression are prominent features of human nonalcoholic steatohepatitis. *Gastroenterology*. 2003;125(2):437-443.

20. Farah BL, Landau DJ, Sinha RA, et al. Induction of autophagy improves hepatic lipid metabolism in glucose-6-phosphatase deficiency. *J Hepatol*. 2016;64(2):370-379.

21. Cho J-H, Kim G-Y, Pan C-J, et al. Downregulation of SIRT1 signaling underlies hepatic autophagy impairment in glycogen storage disease type Ia. *PLOS Genet*. 2017;13(5):e1006819.

22. Rajas F, Clar J, Gautier-Stein A, Mithieux G. Lessons from new mouse models of glycogen storage disease type 1a in relation to the time course and organ specificity of the disease. *J Inherit Metab Dis*. 2015;38(3):521-527.

23. Gjorgjieva M, Raffin M, Duchampt A, et al. Progressive development of renal cysts in glycogen storage disease type I. *Hum Mol Genet*. 2016;25(17):3784-3797.

24. Abdul-Wahed A, Gautier-Stein A, Casteras S, et al. A link between hepatic glucose production and peripheral energy metabolism via hepatokines. *Mol Metab*. 2014;3(5):531-543.

25. Fernández I, Peña A, Del Teso N, Pérez V, Rodríguez-Cuesta J. Clinical biochemistry parameters in C57BL/6J mice after blood collection from the submandibular vein and retroorbital plexus. *J Am Assoc Lab Anim Sci JAALAS*. 2010;49(2):202-206.

26. Arrieta O, Cacho B, Morales-Espinosa D, Ruelas-Villavicencio A, Flores-Estrada D, Hernández-Pedro N. The progressive elevation of alpha fetoprotein for the diagnosis of hepatocellular carcinoma in patients with liver cirrhosis. *BMC Cancer*. 2007;7:28.

27. Shafizadeh N, Ferrell LD, Kakar S. Utility and limitations of glypican-3 expression for the diagnosis of hepatocellular carcinoma at both ends of the differentiation spectrum. *Mod Pathol Off J U S Can Acad Pathol Inc*. 2008;21(8):1011-1018.

28. Pelletier L, Rebouissou S, Paris A, et al. Loss of hepatocyte nuclear factor 1alpha function in human hepatocellular adenomas leads to aberrant activation of signaling pathways involved in tumorigenesis. *Hepatol Baltim Md*. 2010;51(2):557-566.

29. Song MS, Salmena L, Pandolfi PP. The functions and regulation of the PTEN tumour suppressor. *Nat Rev Mol Cell Biol*. 2012;13(5):283-296.

30. Kruiswijk F, Labuschagne CF, Vousden KH. p53 in survival, death and metabolic health: a lifeguard with a licence to kill. *Nat Rev Mol Cell Biol*. 2015;16(7):393-405.

31. Ito A, Lai CH, Zhao X, et al. p300/CBP-mediated p53 acetylation is commonly induced by p53-activating agents and inhibited by MDM2. *EMBO J*. 2001;20(6):1331-1340.

32. Lu H, Fisher RP, Bailey P, Levine AJ. The CDK7-cycH-p36 complex of transcription factor IIH phosphorylates p53, enhancing its sequence-specific DNA binding activity in vitro. *Mol Cell Biol*. 1997;17(10):5923-5934.

33. ZHAO Y-L, ZHU R-T, SUN Y-L. Epithelial-mesenchymal transition in liver fibrosis. *Biomed Rep*. 2016;4(3):269-274.

34. Mikulits W. Epithelial to mesenchymal transition in hepatocellular carcinoma. *Future Oncol Lond Engl*. 2009;5(8):1169-1179. doi:10.2217/fon.09.91.

35. Sun B, Li S, Yang L, et al. Activation of glycolysis and apoptosis in glycogen storage disease type Ia. *Mol Genet Metab*. 2009;97(4):267-271.

36. Christofk HR, Vander Heiden MG, Harris MH, et al. The M2 splice isoform of pyruvate kinase is important for cancer metabolism and tumour growth. *Nature*. 2008;452(7184):230-233.

37. Nassir F, Ibdah JA. Role of Mitochondria in Nonalcoholic Fatty Liver Disease. *Int J Mol Sci*. 2014;15(5):8713-8742.

38. Tirinato L, Pagliari F, Limongi T, et al. An Overview of Lipid Droplets in Cancer and Cancer Stem Cells. Stem Cells International. /1656053/ 2017.

39. Yadav RK, Chae S-W, Kim H-R, Chae HJ. Endoplasmic Reticulum Stress and Cancer. *J Cancer Prev*. 2014;19(2):75-88.

40. Han J, Kaufman RJ. The role of ER stress in lipid metabolism and lipotoxicity. *J Lipid Res*. 2016;57(8):1329-1338.

41. Kammoun HL, Chabanon H, Hainault I, et al. GRP78 expression inhibits insulin and ER stress–induced SREBP-1c activation and reduces hepatic steatosis in mice. *J Clin Invest*. 2009;119(5):1201-1215.

42. Fransvea E, Angelotti U, Antonaci S, Giannelli G. Blocking transforming growth factor-beta up-regulates E-cadherin and reduces migration and invasion of hepatocellular carcinoma cells. *Hepatol Baltim Md*. 2008;47(5):1557-1566.

43. Chao YL, Shepard CR, Wells A. Breast carcinoma cells re-express E-cadherin during mesenchymal to epithelial reverting transition. *Mol Cancer*. 2010;9:179.

44. Kalluri R, Weinberg RA. The basics of epithelial-mesenchymal transition. *J Clin Invest*. 2009;119(6):1420-1428.

45. Franco LM, Krishnamurthy V, Bali D, et al. Hepatocellular carcinoma in glycogen storage disease type Ia: a case series. *J Inherit Metab Dis*. 2005;28(2):153-162.

46. Goldstein I, Ezra O, Rivlin N, et al. p53, a novel regulator of lipid metabolism pathways. *J Hepatol*. 2012;56(3):656-662.

47. Baas T. What to do with PKM2. *SciBX Sci-Bus Exch*. 2013;6(2).

48. Vanderperre B, Herzig S, Krznar P, et al. Embryonic Lethality of Mitochondrial Pyruvate Carrier 1 Deficient Mouse Can Be Rescued by a Ketogenic Diet. *PLoS Genet*. 2016;12(5):e1006056.

49. Beloribi-Djefaflia S, Vasseur S, Guillaumond F. Lipid metabolic reprogramming in cancer cells. *Oncogenesis*. 2016;5(1):e189.

50. Navarro-Yepes J, Burns M, Anandhan A, et al. Oxidative Stress, Redox Signaling, and Autophagy: Cell Death Versus Survival. *Antioxid Redox Signal*. 2014;21(1):66-85.

Table 1: Plasmatic and hepatic parameters of L.G6pc-/- mice.

Parameters	Pretumoral stage		Tumoral stage	
	WT (n=6)	L.G6pc-/- (n=11)	WT (n=10)	L.G6pc-/- (n=27)
Glucose (mg/dL)	181.1 ±3.1	84.7 ±3.6***	151.3 ±5.4	89.3 ±3.2***
Cholesterol (g/L)	1.7 ±0.1	2.1 ±0.1**	1.5 ±0.1	2.5 ±0.2***
Triglycerides (g/L)	0.61 ±0.01	0.79 ±0.05*	0.69 ±0.04	0.85 ±0.03*
NEFA (g/L)	24.4 ±1.0	27.4 ±1.5	22.3 ±0.9	30.3 ±1.3**
Uric acid (mg/L)	9.0 ±0.7	12.9 ±2.4	9.1 ±0.3	12.5 ±0.8
Lactate (mM)	5.6 ±0.4	7.4 ±1.0*	4.2 ±0.2	5.2 ±0.5*
Liver weight (g)	2.67 ±0.10	3.53 ±0.20*	2.46 ±0.09	4.53 ±0.25***$$
Liver weight (% of total body weight)	5.4 ±0.2	9.4 ±0.3***	4.5 ±0.2	14.5 ±0.7*** $$$
Hepatic glycogen (mg/g)	38.3 ±1.7	52.1 ±0.8***	27.0 ±3.0	52.8 ±1.4***
Hepatic G6P (µmol/g)	0.19 ±0.02	2.30 ±0.24***	0.40 ±0.03	3.08 ±0.25*** $
Hepatic glucose (µmol/g)	19.9 ±0.8	5.0 ±1.1***	22.7 ±1.0	6.1 ±0.6***
Hepatic triglycerides (mg/g)	184.0 ±11.7	83.7 ±12.4***	112.6 ±6.9	65.0 ±3.4*** $

Data were obtained from WT and L.G6pc-/- mice at 4 months (pretumoral stage) or 9 months (tumoral stage) of HF/HS diet, after 6h of fasting. Data are expressed as the mean ± s.e.m. Significant differences between WT and L.G6pc-/- are indicated as * $p<0.05$; ** $p<0.01$; *** $p<0.001$ and differences between pretumoral and tumoral stage L.G6pc-/- mice are indicated as $ $p<0.05$; $$ $p<0.01$; $$$ $p<0.001$.

FIGURE LEGENDS

Fig.1. Hepatic tumor development in L.G6pc-/- mice.

(A) WT and L.G6pc-/- livers after 9 months of HF/HS diet. **(B)** Histological analyses by H&E staining of **a)** WT liver, **b)** L.G6pc-/- liver, **c)** HCA and **d)** HCC. HCC was characterized by a trabecular pattern with thickened cords of cells. **(C)** Immunohistochemical staining of PCNA in **a)** WT and **b)** L.G6pc-/- liver at 4 months of HF/HS diet; **c)** WT and **d)** L.G6pc-/- liver at 9 months of HF/HS diet; **e)** HCA and **f)** HCC. **(D)** Plasmatic CRP and AFP levels and AST and ALT activities from WT, non-tumor bearing and tumor-bearing L.G6pc-/- mice after 9 months of HF/HS diet. **(E)** Quantitative analysis of *Gpc3* gene expression by RT-qPCR in WT livers (n=7), L.G6pc-/- livers (n=8), HCA (n=15) and HCC (n=9) at 9 months of HF/HS diet. The results are expressed as the mean ± s.e.m. * $p<0.05$; ** $p<0.01$; *** $p<0.001$.

Fig.2. Downregulation of tumor suppressors in L.G6pc-/- livers and tumors.

Quantitative analyses of *Hnf1a* and *Pten* expression by RT-qPCR in **(A**) WT (n=9) and L.G6pc-/- (n=14) livers at 4 months of HF/HS diet and in **(B)** WT livers (n=7), L.G6pc-/- livers (n=8), HCA (n=15) and HCC (n=9) at 9 months of HF/HS diet. Quantitative analyses of phospho-Ser392 p53, acetyl-Lys379 p53 and total p53 by Western Blot after 4 months **(C**) or 9 months **(D)** of HF/HS diet. The results are expressed as the mean ± s.e.m. * $p<0.05$; ** $p<0.01$; *** $p<0.001$. **(E)** Immunohistochemical staining of p53 in **a)** WT and **b)** L.G6pc-/- liver at 4 months of HF/HS diet; **c)** WT and **d)** L.G6pc-/- liver at 9 months of HF/HS diet; **e)** HCA and **f)** HCC. Arrows indicate p53-negative nuclei.

Fig.3. Epithelial-mesenchymal transition in L.G6pc-/- livers and tumors.

(A) Western blot analyses of β-catenin, E-cadherin and vimentin and quantitative analyses of **(B)** *Acta*, *Pai1*, *Vim* and *TGFβ1* and **(C)** *Glul* and *Lgr5* expression by RT-qPCR in WT livers (n=7), L.G6pc-/- livers (n=8), HCA (n=15) and HCC (n=9) at 9 months of HF/HS diet. The results are expressed as the mean ± s.e.m. * p<0.05; ** p<0.01; *** p<0.001.

Fig.4. Remodeling of glucose metabolism in L.G6pc-/- livers and tumors.

Quantitative analyses of *Gck* and *Slc2a1* expression by RT-qPCR in **(A)** WT (n=9) and L.G6pc-/- livers (n=14) at 4 months of HF/HS diet and in **(B)** in WT livers (n=7), L.G6pc-/- livers (n=8), HCA (n=15) and HCC (n=9) at 9 months of HF/HS diet. Quantitative analyses of LDHA, PK-M2, phospho-Ser293 PDH, PDK4 and MPC1 by Western Blot after at 4 months **(C)** or 9 months **(D)** of HF/HS diet. The results are expressed as the mean ± s.e.m. * p<0.05; ** p<0.01; *** p<0.001.

Fig.5. Lipid metabolism alterations in L.G6pc-/- livers and tumors.

Quantitative analyses of lipid metabolism gene expression by RT-qPCR in **(A**) WT (n=9) and L.G6pc-/- livers (n=14) at 4 months of HF/HS diet and in **(B)** WT livers (n=7), L.G6pc-/- livers (n=8), HCA (n=15) and HCC (n=9) at 9 months of HF/HS diet. **(C)** Quantitative analyses of PPARα and perilipin by Western Blot at 9 months of HF/HS diet. The results are expressed as the mean ± s.e.m. * p<0.05; ** p<0.01; *** p<0.001.

Fig.6. Alterations of antioxidant defenses and autophagy in L.G6pc-/- livers and tumors.

Quantitative analyses of *Cat* and *Gpx1* expression by RT-qPCR and western blots in **(A)** WT (n=9) and L.G6pc-/- (n=14) livers at 4 months of HF/HS diet and **(B)** in WT livers (n=7), L.G6pc-/- livers (n=8), HCA (n=15) and HCC (n=9) at 9 months of HF/HS diet. **(C)** TEM

images of **a)** WT liver, **b)** L.G6pc-/- liver and **c)** HCC at 9 months of HF/HS diet. Arrows in panels **b-c** indicate donut-shaped mitochondria. Bar represents 0.5 µm. **(D)** Quantitative analyses of *Cat* and *Gpx1* expression by RT-qPCR in L.G6pc-/- livers treated or not with Tempol (0.2% in drinking water) for 9 months. **(E)** TEM images and quantification of autophagic vesicles in **a)** WT liver, **b)** L.G6pc-/- liver and **c)** HCC sample. Arrows indicate autophagic vesicles. The results are expressed as the mean ± s.e.m. * $p<0.05$; ** $p<0.01$; *** $p<0.001$.

Fig.7. ER stress activation and apoptosis in L.G6pc-/- livers and tumors.

Quantitative analyses of ER stress and apoptosis pathways by Western Blot after 4 months **(A)** or 9 months **(B)** of HF/HS diet. The results are expressed as the mean ± s.e.m. * $p<0.05$; ** $p<0.01$; *** $p<0.001$.

Figure 1

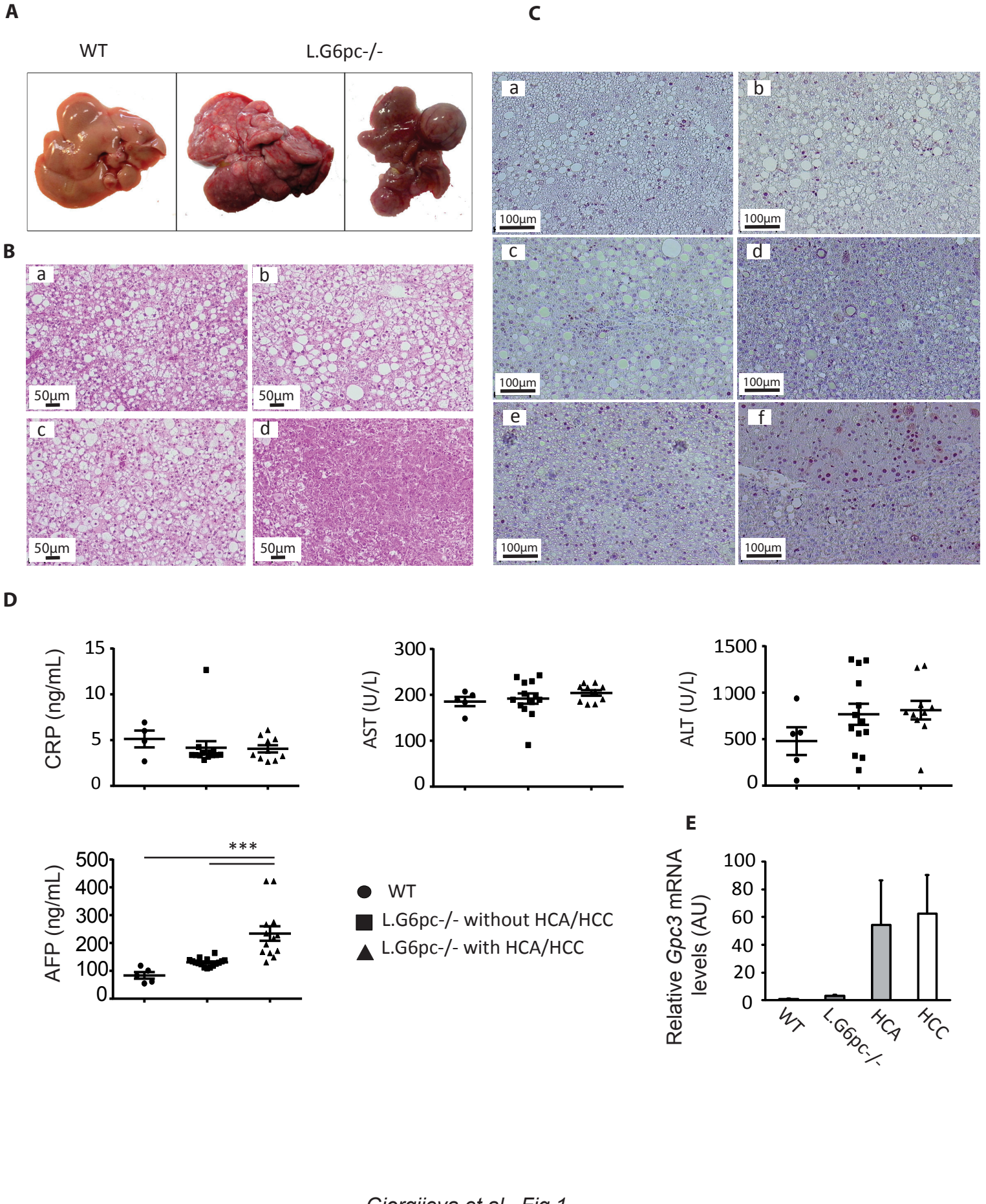

Gjorgjieva et al., Fig.1

Figure 2

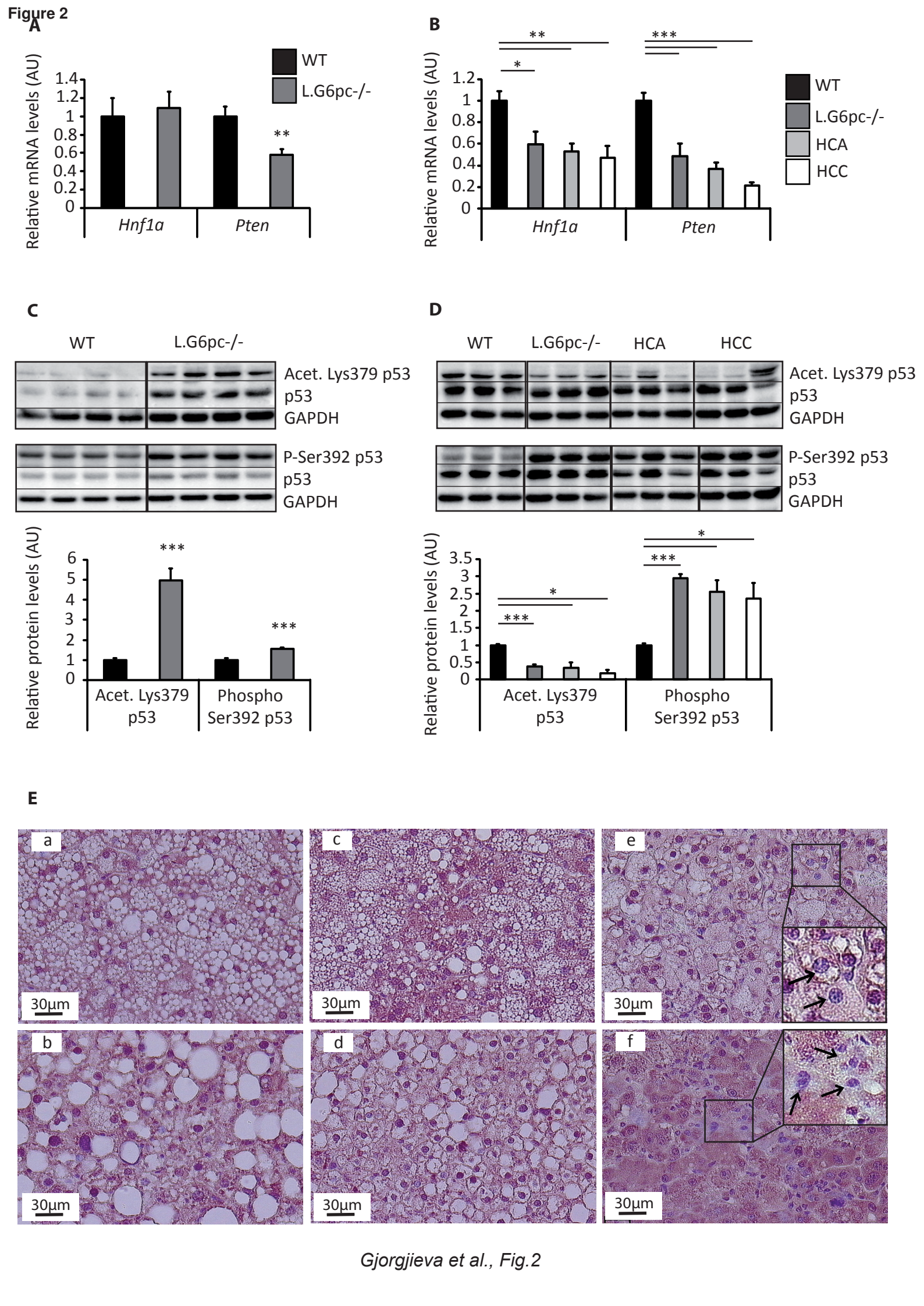

Gjorgjieva et al., Fig.2

Figure 3

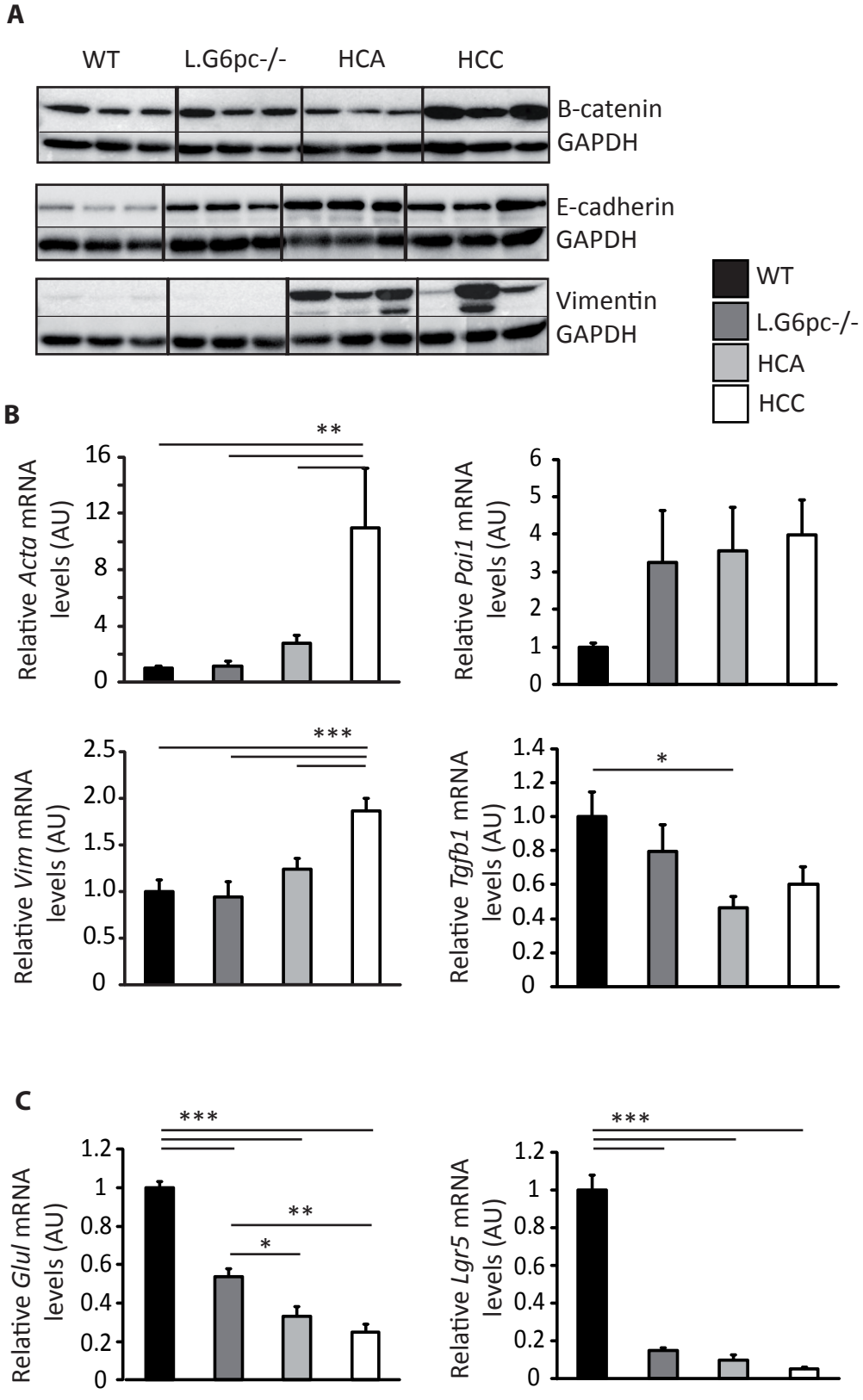

Gjorgjieva et al., Fig.3

Figure 4

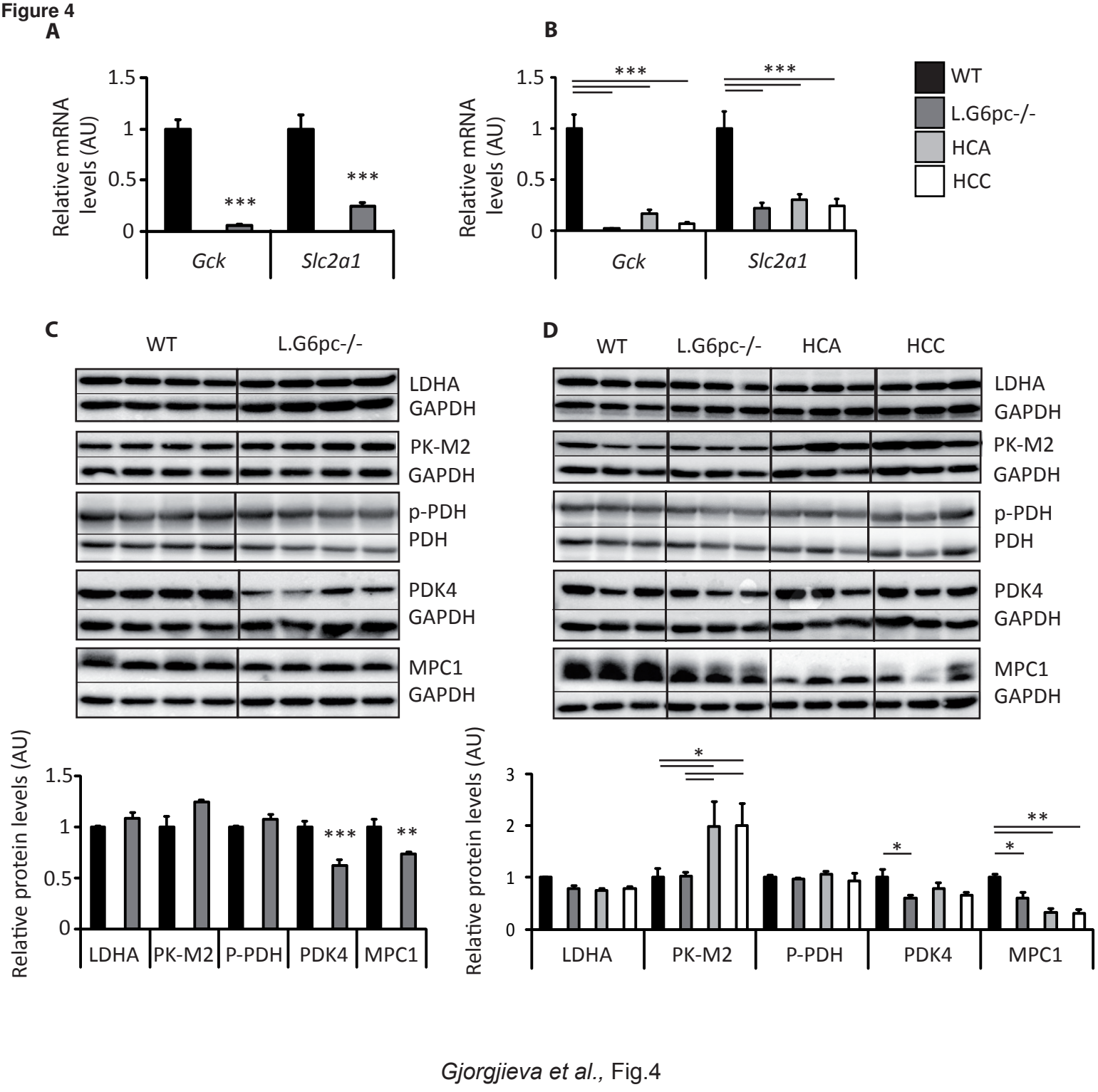

Gjorgjieva et al., Fig.4

Figure 5 A

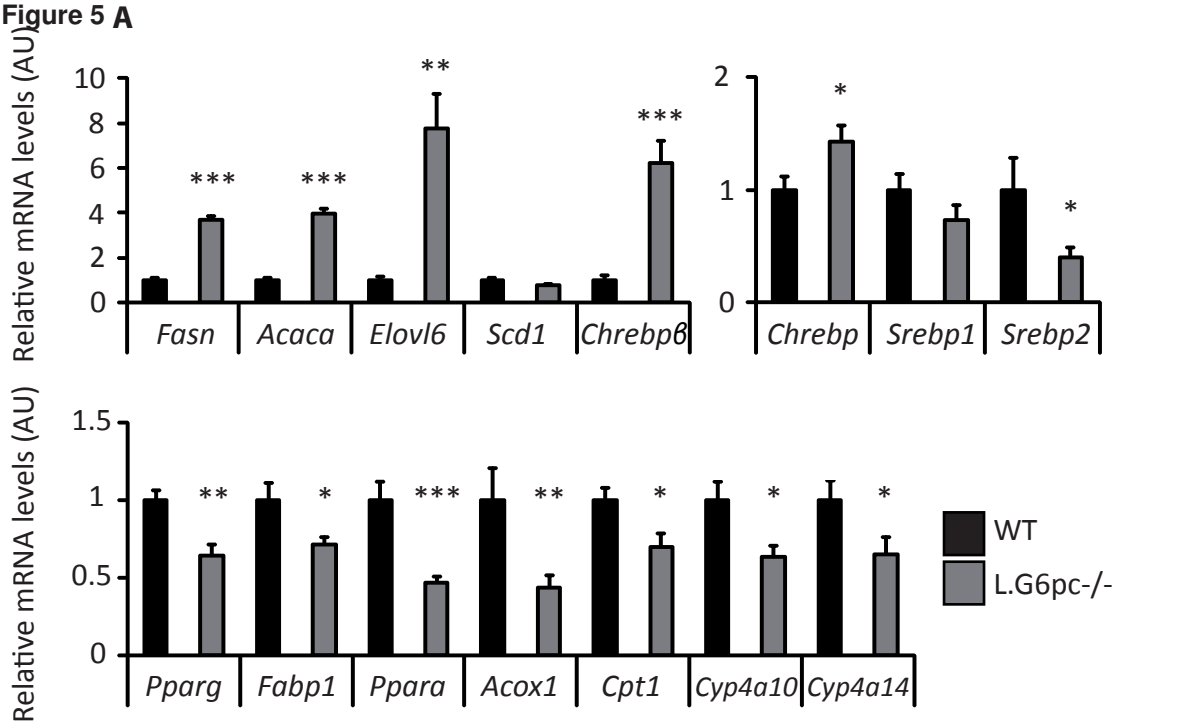

B

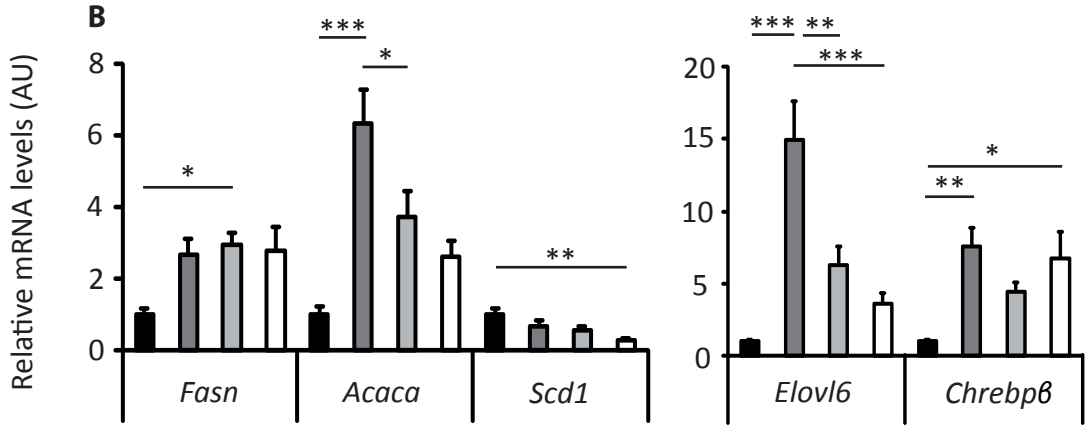

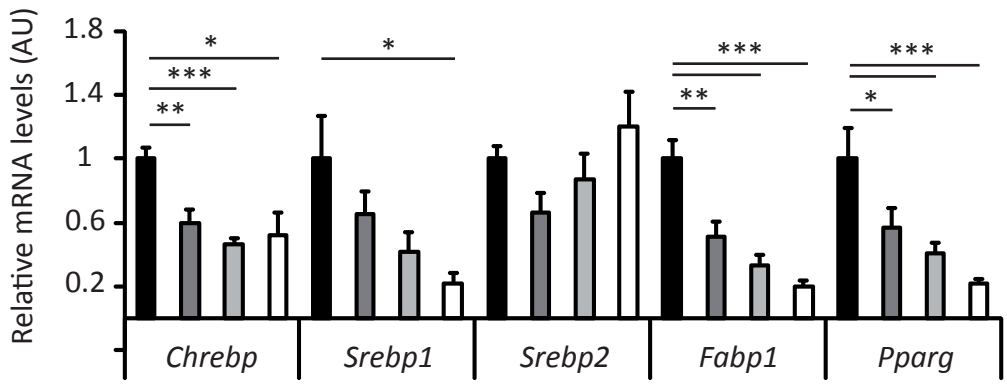

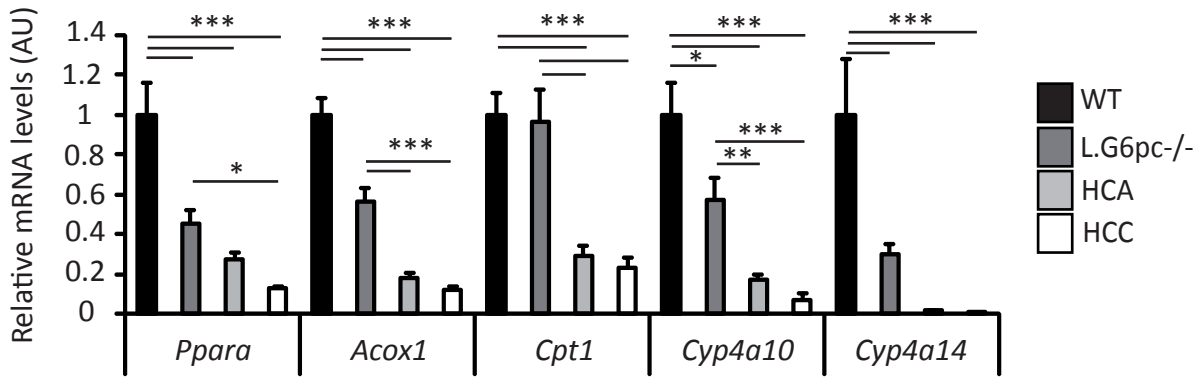

C

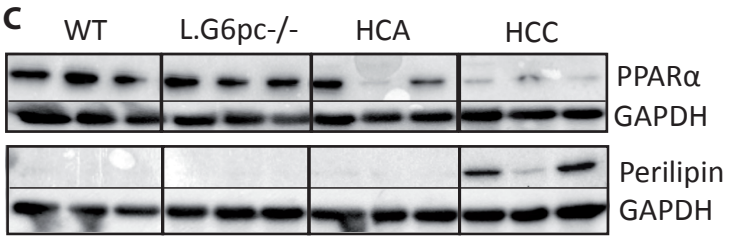

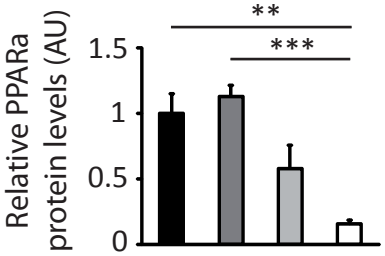

Gjorgjieva et al., Fig.5

Figure 6

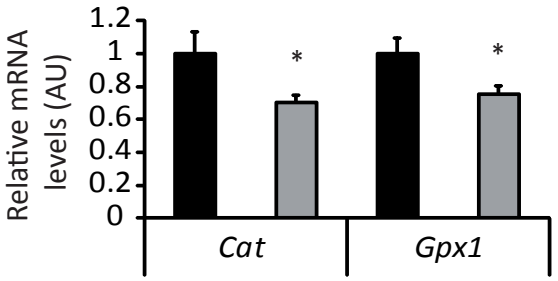

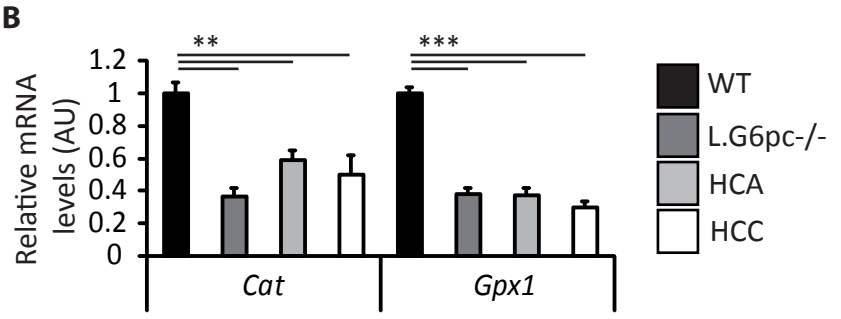

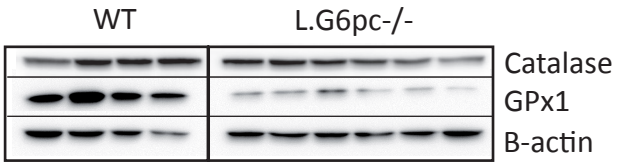

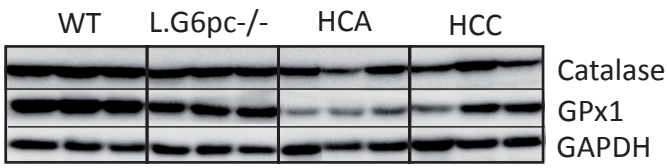

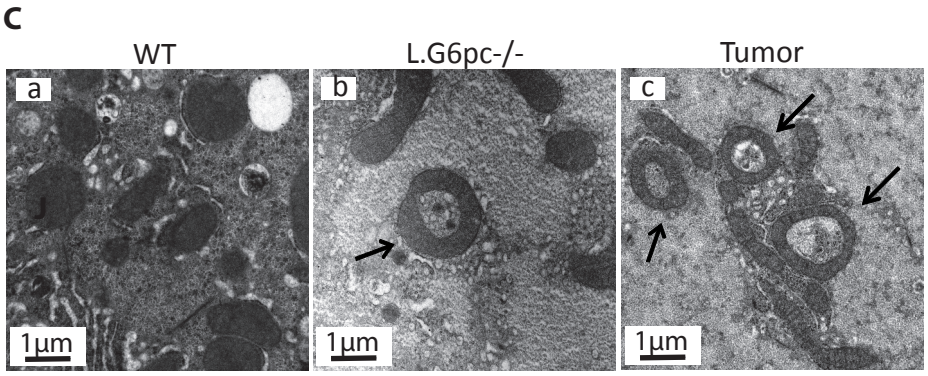

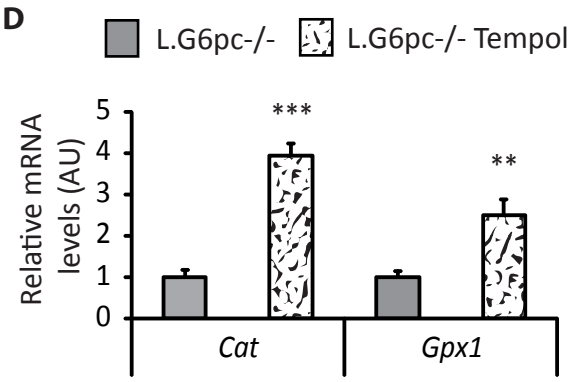

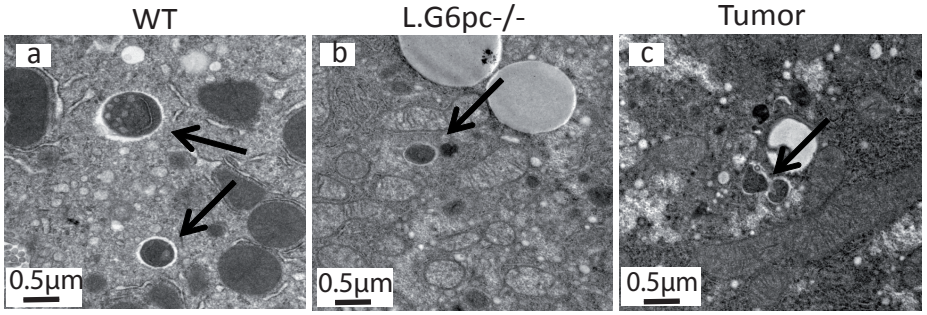

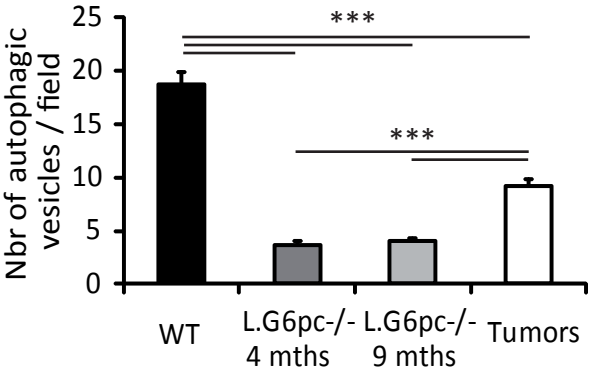

Gjorgjieva et al., Fig.6

Figure 7

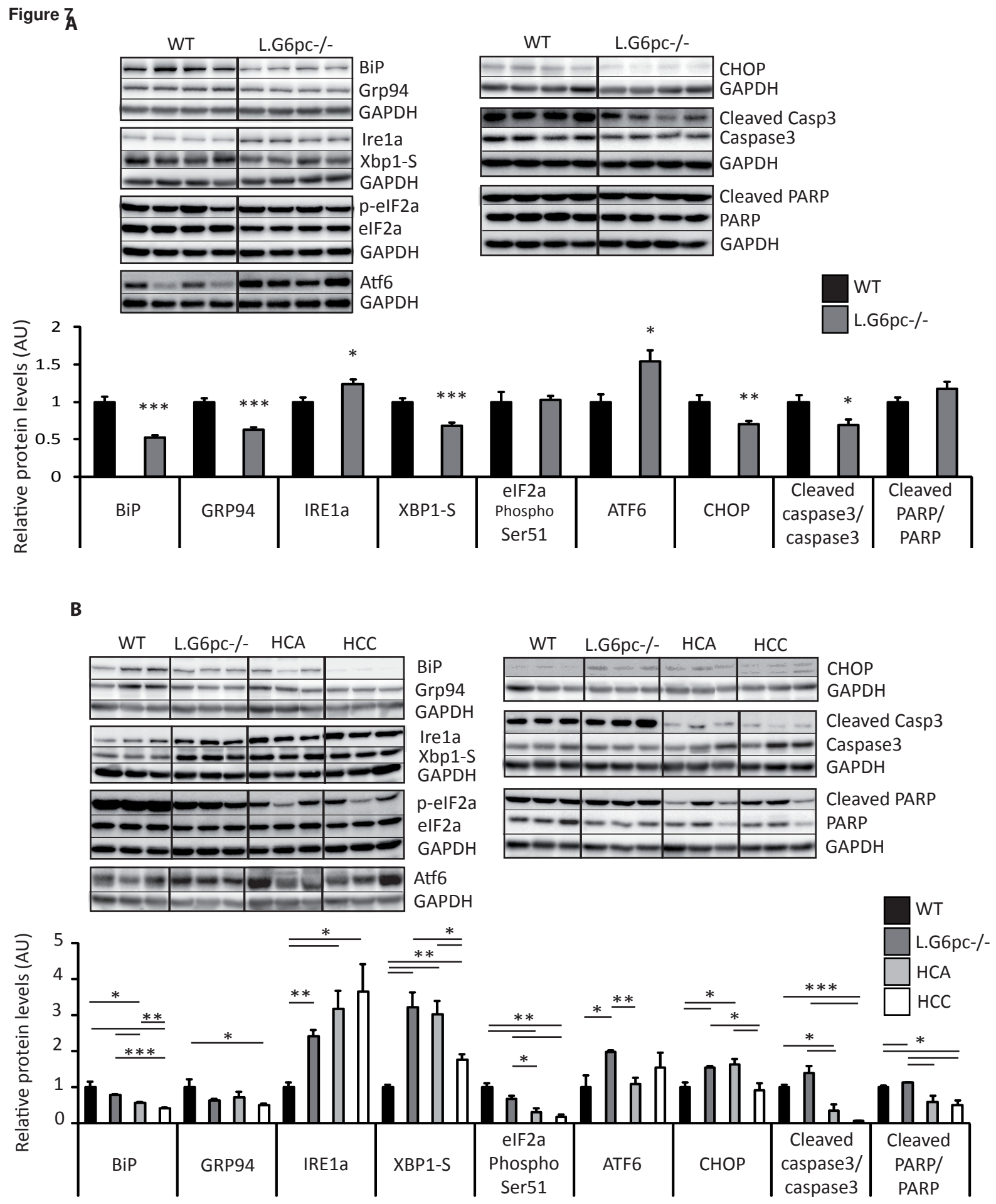

Gjorgjieva et al., Fig.7

EASL JOURNAL OF HEPATOLOGY

Journal of Hepatology

CTAT methods

Tables for a "Complete, Transparent, Accurate and Timely account" (CTAT) are now mandatory for all revised submissions. The aim is to enhance the reproducibility of methods.

- Only include the parts relevant to your study
- Refer to the CTAT in the main text as 'Supplementary CTAT Table'
- Do not add subheadings
- Add as many rows as needed to include all information
- Only include one item per row

If the CTAT form is not relevant to your study, please outline the reasons why:

1.1 Antibodies

Name	Citation	Supplier	Cat no.	Clone no.
B-catenin	Szlachcic et al., Front. Mol. Neurosc., 2017	Cell signaling	8480	D10A8
E-cadherin	Liang et al., Nature Com, 2017	Cell signaling	3195	24E10
Vimentin	Li et al., Nature Com, 2017	Cell signaling	5741	D21H3
PK-M2	Li et al., Oncology Letters, 2017	Cell signaling	4053	D78A4
LDHA	Shankar et al., Sci. Reports, 2017	Cell signaling	2012	Polyclonal
MPC1	N/A	Cell signaling	14462	D2L9I
PPARα	Kodo et al, PLoS One, 2017	Abcam	ab8934	Polyclonal
Perilipin	Boutant et al., EMBO, 2017	Cell signaling	9349	D1D8
Cleaved Caspase 3	Kim et al., Front. Mol. Neurosc., 2017	Cell signaling	9664	5A1E
Caspase 3	Kim et al., Front. Mol. Neurosc., 2017	Cell signaling	9665	8G10
Cleaved Caspase 9	Lee et al., Oncology Letters, 2017	Cell signaling	7237	D2D4
Cleaved PARP	Burger et al., J. Cell Biol., 2017	Cell signaling	5625	D64E10
PARP	Zeng et al., Exp. Therap. Med., 2017	Cell signaling	9542	Polyclonal
ATG3	Kaufman et al., Mol.Biol.Cell, 2017	Cell signaling	3415	Polyclonal
ATG5	Jeong et al., Oncotarget, 2017	Cell signaling	8540	D1G9
LC3B	Dembitz et al., Cell Death Discovery, 2017	Cell signaling	3868	D11
PDK4	N/A	Abcam	ab214938	EPR19727-245
p62	Madill et al., Mol Brain, 2017	Abcam	ab56416	N/A
Catalase	Kaczor et al., Mol Genet Metab Rep, 2017	Abcam	ab16731	polyclonal
GPx1	Magierowski et al., J	Abcam	ab22604	polyclonal

	Gastroenterol, 2017			
PDH Phospho Ser293	Ward et al., PLoS One, 2017	Abcam	ab92696	Polyclonal
PDH	Moretton et al., PLoS One, 2017	Abcam	ab110334	8D10E6
p53	Pajk et al., Biogerontology, 2017	Abcam	ab131442	Polyclonal
p53 Acetyl Lys379	Shao et al., Antioxidants & Redox Signaling, 2017	Cell signaling	2570	Polyclonal
p53 Phospho Ser392	Ashraf et al., Sci. reports, 2017	Cell signaling	9281	Polyclonal
BiP	Bedau, T., Schumacher, N., et al., Oncotarget, 2017	Cell signaling	3177	C50B12
GRP94	Bedau et al., Oncotarget, 2017	Cell signaling	2104	Polyclonal
IRE1α	Zhang et al., Theranostics, 2017	Cell signaling	3294	14C10
eIF2α Phospho Ser51	Wu et al., Oncotarget, 2017	Cell signaling	9721	Polyclonal
eIF2α	Wu et al., Oncotarget, 2017	Cell signaling	9722	Polyclonal
CHOP	Asano et al., Sci.Reports, 2017	Cell signaling	2895	L63F7
ATF6	Pereira et al., Life Sci, 2015	Novus	NBP1-40256	70B1413.1
XBP1	Aivazidis et al., PLoS One, 2017	Abcam	ab37152	Polyclonal
GAPDH	N/A	Millipore	ABS16	Polyclonal
B-actin	Park et al., Int. J. Mol. Sci., 2017	Cell signaling	4970	13E5
PCNA	Wei et al., Oncotarget, 2017	Cell signaling	13110	D3H8P
Goat Anti-Rabbit Antibody Conjugated to HRP	N/A	BioRad	170-5046	

1.2 Cell lines

Name	Citation	Supplier	Cat no.	Passage no.	Authentication test method
NO					

1.3 Organisms

Name	Citation	Supplier	Strain	Sex	Age	Overall n number
WT	Mutel et al., 2011	Charles River Laboratory	C57BL6/J	Male and female	6 and 11 months	36
L.G6PC-/-	Mutel et al., 2011	Animalerie Lyon Est Conventionnelle	B6.G6pc$^{lox/lox}$.SA^{CreERT2}	Male and female	6 and 11 months	86

		et SPF				

1.4 Sequence based reagents

Name	Sequence	Supplier
Ribosomal protein mL19 (Rpl19) forward	GGTGACCTGGATGAGAAGGA	Eurogentec, USA
Ribosomal protein mL19 (Rpl19) reverse	TTCAGCTTGTGGATGTGCTC	Eurogentec, USA
Hepatic nuclear factor 1a (HNF1a) forward	GAGGACACTGTGGGACTGGT	Eurogentec, USA
Hepatic nuclear factor 1a (HNF1a) reverse	TCACAGACACCAACCTCAGC	Eurogentec, USA
Phosphatase and tensin homolog (Pten) forward	TGGGTTGGGAATGGAGGGAATGC T	Eurogentec, USA
Phosphatase and tensin homolog (Pten) reverse	GGACAGCAGCCAATCTCTCGGA	Eurogentec, USA
α 2 -Smooth muscle actin (Acta2) forward	GTCCCAGACATCAGGGAGTAA	Eurogentec, USA
α 2 -Smooth muscle actin (Acta2) reverse	TCGGATACTTCAGCGTCAGGA	Eurogentec, USA
Plasminogen activator inhibitor (Pai1) forward	TTCAGCCCTTGCTTGCCTC	Eurogentec, USA
Plasminogen activator inhibitor (Pai1) reverse	ACACTTTTACTCCGAAGTCGGT	Eurogentec, USA
Vimentin (Vim) forward	CGGCTGCGAGAGAAATTGC	Eurogentec, USA
Vimentin (Vim) reverse	CCACTTTCCGTTCAAGGTCAAG	Eurogentec, USA
Transforming growth factor b1 (Tgfb1) forward	CAACAATTCCTGGCGTTACCTTGG	Eurogentec, USA
Transforming growth factor b1 (Tgfb1) reverse	GAAAGCCCTGTATTCCGTCTCCTT	Eurogentec, USA
Glucokinase(Gck) forward	CCCTGAGTGGCTTACAGTTC	Eurogentec, USA
Glucokinase(Gck) reverse	ACGGATGTGAGTGTTGAAGC	Eurogentec, USA
Glucose transporter1, Glut1 (Slc2a1) forward	GCTGTGCTTATGGGCTTCTC	Eurogentec, USA
Glucose transporter1, Glut1 (Slc2a1) reverse	CACATACATGGGCACAAAGC	Eurogentec, USA
Glucose transporter2, Glut2 (Slc2a2) forward	TGTACGCAAAACCCGAAGTCT	Eurogentec, USA
Glucose transporter2, Glut2 (Slc2a2) reverse	CACATTCAAACTGACTTTCTGTTAC C	Eurogentec, USA
Cytochrome C oxidase subunit 4 (Cox4) forward	CAAATCAGAACGAGCGCAG	Eurogentec, USA
Cytochrome C oxidase subunit 4 (Cox4) reverse	CCGACTGGAGCAGCCTTTC	Eurogentec, USA
Sterol regularory element binding protein 1c, SREBP1C (Srebp1c) forward	GCAGCCACCATCTAGCCTG	Eurogentec, USA
Sterol regularory element binding protein 1c, SREBP1C (Srebp1c) reverse	CAGCAGTGAGTCTGCCTTGAT	Eurogentec, USA
Sterol regularory element binding protein 2, SREBP2 (Srebp2) forward	GCAGCAACGGGACCATTCT	Eurogentec, USA
Sterol regularory element binding protein 2, SREBP2 (Srebp2) reverse	CCCCATGACTAAGTCCTTCAACT	Eurogentec, USA
Carbohydrate-responsive element-binding protein, CHREBP (Chrebp), total forward	GAAGCCACCCTATAGCTCCC	Eurogentec, USA
Carbohydrate-responsive element-binding protein, CHREBP (Chrebp), total reverse	CTGGGGACCTAAACAGGAGC	Eurogentec, USA
Carbohydrate-responsive element-binding protein - isoform β, (Chrebpb) forward	TCTGCAGATCGCGTGGAG	Eurogentec, USA
Carbohydrate-responsive element-binding protein - isoform β, (Chrebpb) reverse	CTTGTCCCGGCATAGCAAC	Eurogentec, USA
Fatty acid synthase, FAS (Fasn) forward	TTCCAAGACGAAAATGATGC	Eurogentec, USA
Fatty acid synthase, FAS (Fasn) reverse	AATTGTGGGATCAGGAGAGC	Eurogentec, USA
Acetyl-CoA carboxylase1, ACC (Acaca) forward	TGGCAGACCACTATGTTCCA	Eurogentec, USA
Acetyl-CoA carboxylase1, ACC (Acaca) reverse	GAGCAGTTCTGGGAGTTTCG	Eurogentec, USA
Fatty acid elongase 6 (Elovl6) forward	ACAATGGACCTGTCAGCAAA	Eurogentec, USA
Fatty acid elongase 6 (Elovl6) reverse	GTACCAGTGCAGGAAGATCAGT	Eurogentec, USA
Stearoyl-CoA desaturase 1 (Scd1) forward	TGGGTTGGCTGCTTGTG	Eurogentec, USA

Stearoyl-CoA desaturase 1 (Scd1) reverse	GCGTGGGCAGGATGAAG	Eurogentec, USA
Peroxisome proliferator-activated receptor gamma PPARγ (Pparg) forward	AGTCTGCTGATCTGCGAGCC	Eurogentec, USA
Peroxisome proliferator-activated receptor gamma PPARγ (Pparg) reverse	CTTTCCTGTCAAGATCGCCC	Eurogentec, USA
Fatty acid binding protein (Fabp1) forward	GTCTCCAGTTCGCACTCCTC	Eurogentec, USA
Fatty acid binding protein (Fabp1) reverse	GCAGAGCCAGGAGAACTTTG	Eurogentec, USA
Peroxisome proliferator-activated receptor alpha PPARα (Ppara) forward	AGTTCACGCATGTGAAGGCTG	Eurogentec, USA
Peroxisome proliferator-activated receptor alpha PPARα (Ppara) reverse	TTCCGGTTCTTCTTCTGAATC	Eurogentec, USA
Acyl-CoA Oxidase 1 (Acox1) forward	TGCCAAATTCCCTCATCTTC	Eurogentec, USA
Acyl-CoA Oxidase 1 (Acox1) reverse	CTTGGATGGTAGTCCGGAGA	Eurogentec, USA
Carnitine palmitoyltransferase1 (Cpt1a) forward	ACCTCCATGGCTCAGACAG	Eurogentec, USA
Carnitine palmitoyltransferase1 (Cpt1a) reverse	AGCAGAGGCTCAAGCTGTTCA	Eurogentec, USA
Cytochrome P450 (Cyp4a10) forward	TCCAGCAGTTCCCATCACCT	Eurogentec, USA
Cytochrome P450 (Cyp4a10) reverse	TTGCTTCCCCAGAACCATCT	Eurogentec, USA
Cytochrome P450 (Cyp4a14) forward	TCAGTCTATTTCTGCTGTTC	Eurogentec, USA
Cytochrome P450 (Cyp4a14) reverse	GAGCTCCTTGTCCTTCAGATGGT	Eurogentec, USA
X-box binding protein 1 Unspliced (Xbp1-U) forward	CAGCACTCAGACTATGTGCA	Eurogentec, USA
X-box binding protein 1 Unspliced (Xbp1-U) reverse	GTCCATGGGAAGATGTTCTGG	Eurogentec, USA
X-box binding protein 1 Spliced (Xbp1-S) forward	CTGAGTCCGAATCAGGTGCAG	Eurogentec, USA
X-box binding protein 1 Spliced (Xbp1-S) reverse	GTCCATGGGAAGATGTTCTGG	Eurogentec, USA
Catalase (Cat) forward	AACGCTGGATGGATTCTCCC	Eurogentec, USA
Catalase (Cat) reverse	GCCCTAACCTTTCATTTCCCTTCAG	Eurogentec, USA
Glutathione peroxidase 1 (Gpx1) forward	TTGGCTTGGTGATTACTGGC	Eurogentec, USA
Glutathione peroxidase 1 (Gpx1) reverse	CATTAGGTGGAAAGGCATCG	Eurogentec, USA

1.5 Biological samples

Description	Source	Identifier

1.6 Deposited data

Name of repository	Identifier	Link
Raw and analysed data		This paper

1.7 Software

Software name	Manufacturer	Version
ChemiDoc Software	Biorad	Version 1.2.0.12
Image Lab	Biorad	Version 5.2.1 ; RRID: SCR_014210
GraphPad Prism 5	http://www.graphpad.com/	Version 5.04 ; RRID: SCR_002798

1.8 Other (e.g. drugs, proteins, vectors etc.)

NO		

1.9 Please provide the details of the corresponding methods author for the manuscript:

2.0 Please confirm for randomised controlled trials all versions of the clinical protocol are included in the submission. These will be published online as supplementary information.

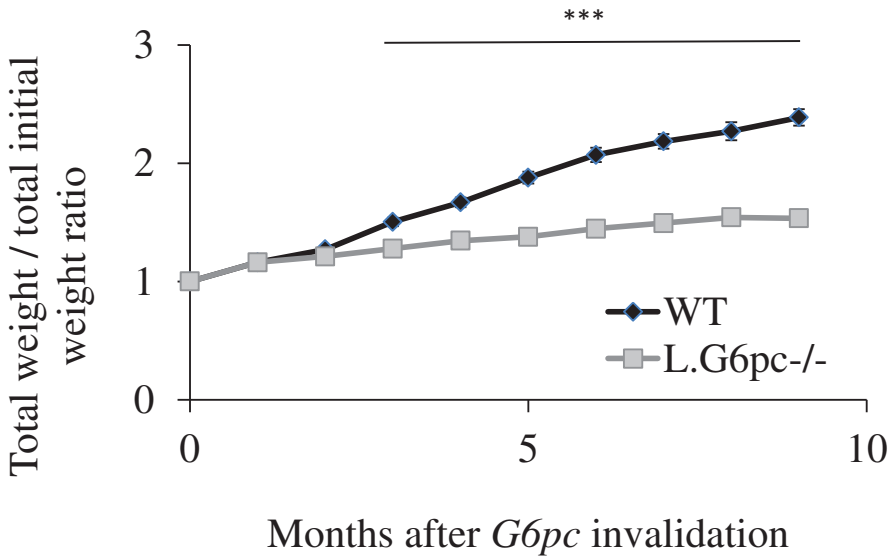

Supplementary Figure 1: Growth rates of WT and L.G6pc-/- mice.

The weight of WT (n=32; black symbols) and L.G6pc-/- mice (n=74; gray symbols) fed HF/HS diet was followed once a month, during 9 months. The values are expressed as the ratio current weight / initial weight.

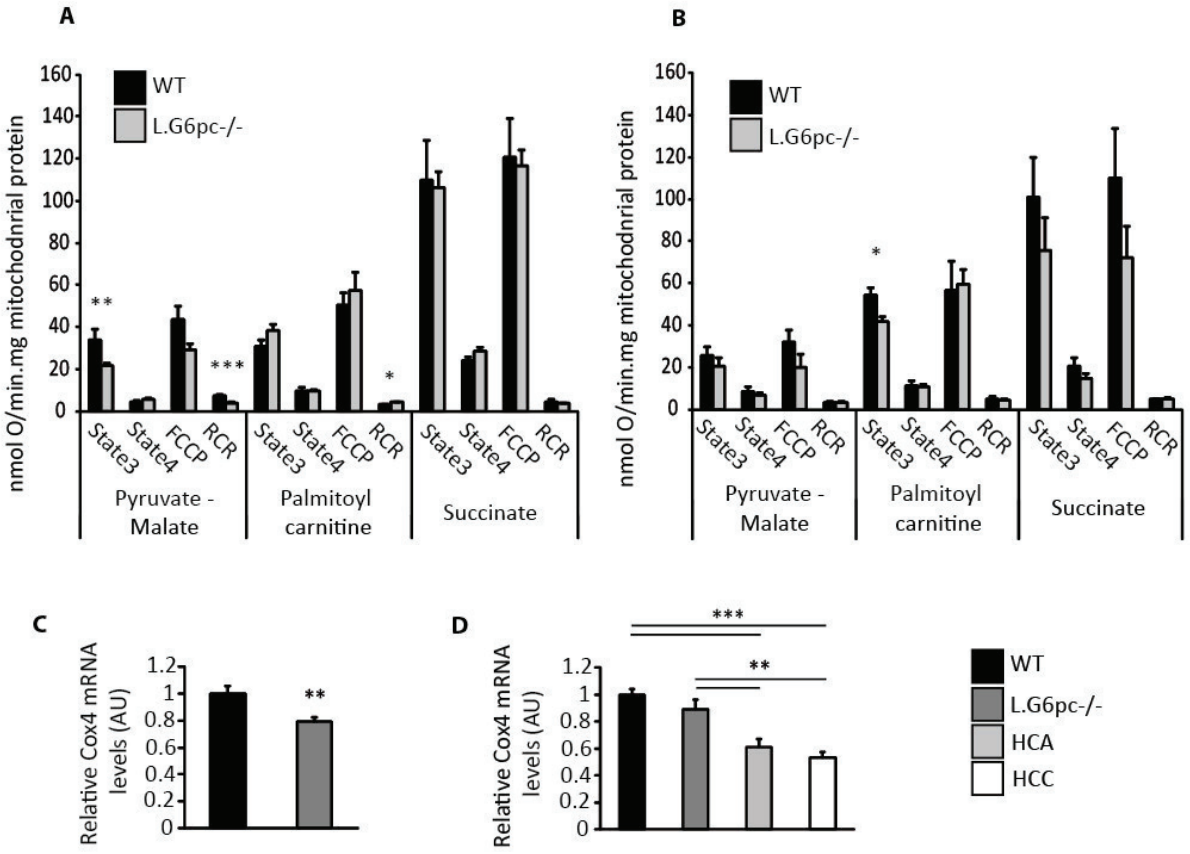

Supplementary Figure 2: Mitochondrial oxidative phosphorylation activity in L.G6pc-/- livers.

Oxidative phosphorylation rates in mitochondria isolated form **(A)** WT (n=5) and L.G6pc-/- livers (n=8) at 4 months of HF/HS diet and from **(B)** WT (n=5) and L.G6pc-/- livers (n=5) at 9 months of HF/HS diet were analyzed *via* mitochondrial oximetry analysis. Mitochondrial oxidative phosphorylation activity was measured at 37°C in a thermostatic cell glass using a Clark electrode (Rank Brothers Ltd, UK), as previously described (Abdul-Wahed et al., 2014). Isolated liver mitochondria were incubated in a respiratory buffer (120 mM KCl, 5 mM KH_2PO_4, 1 mM EGTA, 2 mM $MgCl_2$, 3 mM Hepes, 0.3% bovine serum albumin, pH 7.4) with 5 mM pyruvate and 2.5 mM malate, 5 mM succinate in the presence of 5 µM rotenone, or 40 µM pamitoyl-carnitine and 2.5 mM malate as respiratory substrates. The phosphorylating respiration (state 3) was initiated with 1 mM ADP. The basal non-phosphorylating respiration (state 4) was obtained by the addition of 2 µg/ml oligomycin (an inhibitor of ATP synthase), and maximal respiration was obtained with 2 µM carbonyl-cyanide p-trifluoromethoxyphenylhydrazone

(FCCP, a mitochondrial uncoupler). The respiratory control ratio (RCR) refers to the ratio of ADP-stimulated oxygen consumption (state 3) to that consumed in the presence of oligomycin (state 4).

Quantitative analyses of *Cox4* expression by RT-qPCR in **(C)** WT (n=9) and L.G6pc-/- (n=14) livers at 4 months of HF/HS diet and in **(D)** WT livers (n=7), L.G6pc-/- livers (n=8), HCA (n=15) and HCC (n=9) at 9 months of HF/HS diet. The results are expressed as the mean ± SEM. * $p<0.05$; ** $p<0.01$; *** $p<0.001$.

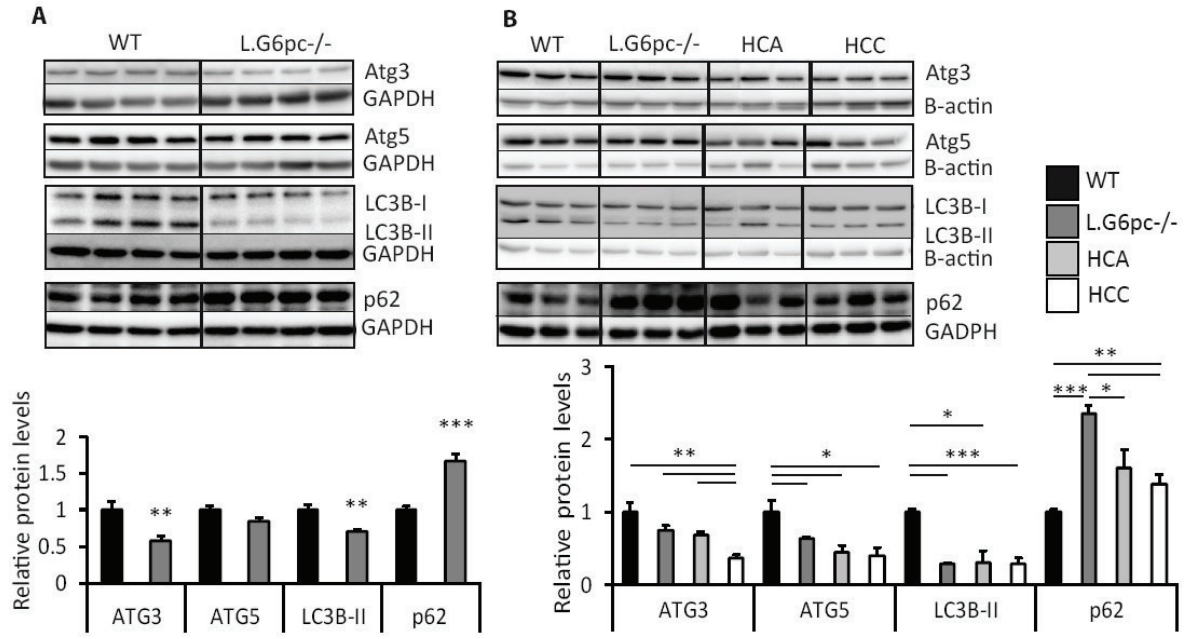

Supplementary Figure 3: Autophagy in L.G6pc-/- livers and tumors.

Quantitative analyses of ATG3, ATG5, LC3B and p62 by Western Blot in **(A)** WT and L.G6pc-/- mice at 4 months of HF/HS diet and **(B)** in WT livers, L.G6pc-/- livers, HCA and HCC at 9 months of HF/HS diet. The results are expressed as the mean ± SEM. * $p<0.05$; ** $p<0.01$; *** $p<0.001$.

Chapter II – Characterization of the long-term renal complications in a mouse model of GSDI nephropathy

Although renal disease was mentioned in von Gierke's original pathological description, CKD in GSDI was recognized much later as a major complication. Renal failure is one of the main causes of morbidity in patients with aging (Martens et al., 2009). While it was reported that it is the lipid-induced RAS signalization pathway that is responsible for fibrosis in GSDI kidneys (Yiu et al., 2008b), further characterization of this process was required.

In this study, we have characterized the long-term development of the nephropathy, between 9 and 18 months in K.G6pc-/- mice. We have thus reported a progressive installation of fibrosis during this period. Overtime, glomerulosclerosis and pedicel effacement was detected, concomitantly with a more pronounced EMT. This led to the development of fibrosis in accordance with an increase of TGF-β1 expression, concomitantly with the development of renal cysts. Thus, at 18 months of *G6pc* deletion, several mice developed macroscopic renal cysts, which were never reported in GSDI. Thanks to a collaboration with Prof. Philippe Labrune (referent pediatrician for GSDI patients in Paris), we have found that renal cysts are frequently observed in GSDI patients, yet this occurrence was not considered as a major complication. Interestingly, we have established that in the cohort of 32 patients followed by Prof. Labrune, 7 patients presented macroscopic renal cysts, which appeared independently from the type of GSDI, the sex and the age of the patient. Nevertheless, a correlation between aggravated parameters of renal function and cyst development has been established, situating cyst occurrence in the later stages of GSDI nephropathy.

It is noteworthy that, in this study, we have reported that the biomarker of kidney injury, Lipocalin-2, was increased in the urine of K.G6pc-/- mice, in the early stages of the nephropathy. Thus we propose that the utility of this biomarker should be evaluated in GSDI patients at different stages of the nephropathy.

To conclude, while many efforts are made to prevent hypoglycemia in children, renal complications should also be closely monitored from the youngest age. Indeed, kidney imaging as well as an evaluation of the renal function should be done once a year, in young and in older patients, in order to avoid renal cyst development and failure.

Human Molecular Genetics, 2016, Vol. 25, No. 17 3784–3797

doi: 10.1093/hmg/ddw224
Advance Access Publication Date: 19 July 2016
Original Article

ORIGINAL ARTICLE

Progressive development of renal cysts in glycogen storage disease type I

Monika Gjorgjieva[1,2,3], Margaux Raffin[1,2,3], Adeline Duchampt[1,2,3], Ariane Perry[4], Anne Stefanutti[1,2,3], Marie Brevet[2,5], Antonin Tortereau[2,6], Laurence Dubourg[2,3,7,8], Aurélie Hubert-Buron[4], Mylène Mabille[9,10], Coralie Pelissou[9,10], Louis Lassalle[9,10], Philippe Labrune[4,10], Gilles Mithieux[1,2,3] and Fabienne Rajas[1,2,3,*]

[1]Institut National de la Santé et de la Recherche Médicale, U1213, Lyon, France, [2]Université de Lyon, Lyon, France, [3]Université Lyon1, Villeurbanne, France, [4]APHP, Hôpitaux Universitaires Paris Sud, Hôpital Antoine Béclère, Centre de référence des maladies héréditaires du métabolisme hépatique, Clamart, France, [5]Service de pathologie et de neuropathologie Est, Institut de Cancérologie des Hospices Civils de Lyon, Lyon, France, [6]VetAgro Sup, UPSP 2011-03-101, ICE, Marcy L'Etoile, France, [7]UMR 5305 CNRS/Université Claude-Bernard, Biologie tissulaire et Ingénierie thérapeutique, Lyon, France, [8]Exploration Fonctionnelle Rénale, Groupement Hospitalier Edouard Herriot, Hospices civils de Lyon, Lyon, France, [9]APHP, Hôpitaux Universitaires Paris Sud, Hôpital Antoine Béclère, Service de radiologie, Clamart, France and [10]Université Paris Sud, Orsay, France

*To whom correspondence should be addressed at: Fabienne Rajas, Inserm U1213, Université Lyon 1 Laennec, 7 rue Guillaume Paradin, 69372 Lyon cedex 08 France. Tel: +33-478-77 10 28; Fax: +33 478-77-87-62; Email: fabienne.rajas@univ-lyon1.fr

Abstract

Glycogen storage disease type I (GSDI) is a rare metabolic disease due to glucose-6 phosphatase deficiency, characterized by fasting hypoglycemia. Patients also develop chronic kidney disease whose mechanisms are poorly understood. To decipher the process, we generated mice with a kidney-specific knockout of glucose-6 phosphatase (K.G6pc$^{-/-}$ mice) that exhibited the first signs of GSDI nephropathy after 6 months of *G6pc* deletion. We studied the natural course of renal deterioration in K.G6pc$^{-/-}$ mice for 18 months and observed the progressive deterioration of renal functions characterized by early tubular dysfunction and a later destruction of the glomerular filtration barrier. After 15 months, K.G6pc$^{-/-}$ mice developed tubular-glomerular fibrosis and podocyte injury, leading to the development of cysts and renal failure. On the basis of these findings, we were able to detect the development of cysts in 7 out of 32 GSDI patients, who developed advanced renal impairment. Of these 7 patients, 3 developed renal failure. In addition, no renal cysts were detected in six patients who showed early renal impairment. In conclusion, renal pathology in GSDI is characterized by progressive tubular dysfunction and the development of polycystic kidneys that probably leads to the development of irreversible renal failure in the late stages. Systematic observations of cyst development by kidney imaging should improve the evaluation of the disease's progression, independently of biochemical markers.

Received: April 17, 2016. **Revised:** June 15, 2016. **Accepted:** June 15, 2016

© The Author 2016. Published by Oxford University Press.
All rights reserved. For Permissions, please email: journals.permissions@oup.com

Downloaded from https://academic.oup.com/hmg/article-abstract/25/17/3784/2525836/Progressive-development-of-renal-cysts-in-glycogen
by guest
on 18 September 2017

Introduction

Chronic kidney disease (CKD) is a frequent complication in glycogen storage disease type I (GSDI) and can progress to renal failure. GSDI is a rare metabolic disease caused by deficient glucose-6 phosphatase (G6Pase) activity, resulting in the decrease in endogenous glucose production (1,2). G6Pase catalytic subunit (G6PC) deficiency results in GSD type Ia and glucose-6 phosphate translocase deficiency results in GSD type Ib (3–5). Patients with GSDIa or GSDIb present a wide spectrum of clinical manifestations, including fasting hypoglycemia, hypertriglyceridemia, hypercholesterolemia, hyperuricemia and lactic acidosis. Excessive accumulation of glycogen and fat in the liver and kidneys leads to chronic hepatic and renal complications (6–8). Patients with GSDIb also suffer from neutropenia associated with recurrent bacterial infections (6,7). The view on renal complications in GSDI is merely based on the collaborative European Study on GSDI (ESGSDI) cohort, which retrospectively included 231 GSDIa and 57 GSDIb patients. Thus, renal manifestations of GSDI appear in early childhood (8,9). Almost 70% of young adult patients exhibit hyperfiltration and microalbuminuria, and 40% develop proteinuria (8,9). Many patients also have nephrocalcinosis, due to hypercalciuria and hypocitraturia that enhance the likelihood of urinary calcium precipitation. As with diabetic nephropathy, this dysfunction remains clinically silent for a long time (6,10,11). Unfortunately, few data are available on the evolution of this CKD over time, because of the small number of patients and a lack of longitudinal clinical data.

To characterize the evolution of kidney dysfunctions in GSDIa, we generated a viable mouse model in which G6PC deletion was restricted to the kidneys (K.G6pc$^{-/-}$ mice). Interestingly, K.G6pc$^{-/-}$ mice developed early-onset nephropathy, including nephromegaly and microalbuminuria after 6 months of *G6pc* deletion (12). However, long-term renal complications, such as interstitial fibrosis and focal segmental glomerulosclerosis observed in GSDI patients (6), were not observed in mice at this stage (12). In this study, we show that the development of renal interstitial fibrosis and glomerular sclerosis induced by long-term *G6pc* deletion results in the later development of polycystic kidneys, and then to the development of renal failure in the final stage of the disease. On the basis of our findings in mice, we were able to detect the development of cysts in 22% of GSDI patients (6 patients with GSDIa and 1 patient with GSDIb) in a cohort of 32 individuals. Strikingly, renal cysts were never reported in individuals with GSDI.

Results

Deterioration in tubule function in K.G6pc$^{-/-}$ mice

To characterize the development of nephropathy in GSDIa, we studied the natural course of deterioration of the renal function in K.G6pc$^{-/-}$ mice for 18 months. In contrast to total *G6pc* knockout mice (3), K.G6pc$^{-/-}$ mice showed no growth retardation and had similar weight gain and glycaemia to control (WT) mice. However, K.G6pc$^{-/-}$ mice exhibited gradual weight loss after 14 months of *G6pc* deletion (Supplementary Material, Fig. S1). As previously observed, K.G6pc$^{-/-}$ mice exhibited enlarged and paler kidneys compared to WT kidneys (Figure 1) . Kidney enlargement increased with age (Figure 1A and B) and the kidney weight of K.G6pc$^{-/-}$ mice was about 2.5-fold higher than that of WT mice at 18 months (Figure 1C). As expected, we observed an accumulation of excessive glycogen in the proximal tubule cells in K.G6pc$^{-/-}$ kidneys (Figure 2A). As we had previously observed deposits of lipids in the K.G6pc$^{-/-}$ kidneys (12), we quantified the renal lipid content. The content in triglycerides reached 9.0 ± 1.2 mg/g of tissue compared to 3.5 ± 0.7 mg/g of tissue in WT mice after 9 months of *G6pc* deletion. However, no further increase in triglyceride accumulation was observed between 9 and 18 months (Figure 2B). Histological observations revealed large lipid droplets in the tubule cells in K.G6pc$^{-/-}$ kidneys at 9 months (Figure 2C). Thus, both the accumulation of lipids and excessive glycogen in the proximal tubules led to the clarification and enlargement of tubular cells (Figure 3A). Renal tubules play an important role in urine formation, and fluid electrolyte and acid-base homeostasis. Consequently, tubular damage appeared early since K.G6pc$^{-/-}$ mice presented polyuria, urinary acidification and electrolyte imbalance at this stage (12). However, polyuria gradually worsened with age (Table 1), concomitantly with polydipsia (Supplementary Material, Fig. S2), confirming an inability to concentrate urine. Thus, urine production was about 4-fold higher that of WT mice at 18 months (Table 1). As previously observed at 6 months, the urinary pH of K.G6pc$^{-/-}$ mice was also more acidic than that of WT mice at each stage (Table 1). In addition, the excretion of urea and uric acid increased with age (Table 1). In parallel, biochemical analyses also revealed normal plasma uric acid, cholesterol and triglyceride levels, indicating normal liver metabolism in K.G6pc$^{-/-}$ mice (Table 2).

Contrary to most GSDIa patients, no nephrolithiasis was observed in K.G6pc$^{-/-}$ mice despite hypercalciuria. This can be explained by the fact that hypocitraturia was not observed concomitantly with a hypercalciuria. On the contrary, K.G6pc$^{-/-}$ mice developed hypercitraturia and hypercalciuria (Supplementary Material, Table S1). We previously suggested that this could protect mice from calcium stone development (12). In addition, K^+ concentration was increased in the urine of K.G6pc$^{-/-}$ mice (Supplementary Material, Table S1). No modification in chloride, magnesium, phosphate, sodium and oxalate excretion was observed in K.G6pc$^{-/-}$mice (Supplementary Material, Table S1).

In conclusion, these data show that tubular damage is an early hallmark of K.G6pc$^{-/-}$ kidneys, and suggest that these defects are probably secondary to the accumulation of glycogen and lipids.

Development of filtration barrier damage and renal failure in K.G6pc$^{-/-}$ mice with age

Our previous study showed that the first signs of impairment of the filtration barrier (i.e. microalbuminuria) occurred after 6 months of *G6pc* deletion (12). However, electron microscopy images and histological analyses of K.G6pc$^{-/-}$ kidneys showed intact glomerular structures and no fibrosis at this age (12). Comparable alterations in biochemical urine and plasma parameters were observed at 9 months (Tables 1 and 2). Nevertheless, albuminuria increased considerably in K.G6pc$^{-/-}$ mice at 15 and 18 months, reaching 776 ± 264 mg/24h in K.G6pc$^{-/-}$ mice compared to 97 ± 18 mg/24h in WT mice at 18 months (Table 1). Interestingly, the accumulation of blood urea nitrogen (BUN) was observed after only 15 months of *G6pc* deletion (but not after 12 months, data not shown) (Table 2). These results suggest the onset of renal failure, potentially responsible for the weight loss observed at this age (Supplementary Material, Fig. S1). Interestingly, the level of Lipocalin 2 (LCN2), recently considered as a promising biomarker of CKD

Downloaded from https://academic.oup.com/hmg/article-abstract/25/17/3784/2525836/Progressive-development-of-renal-cysts-in-glycogen
by guest
on 18 September 2017

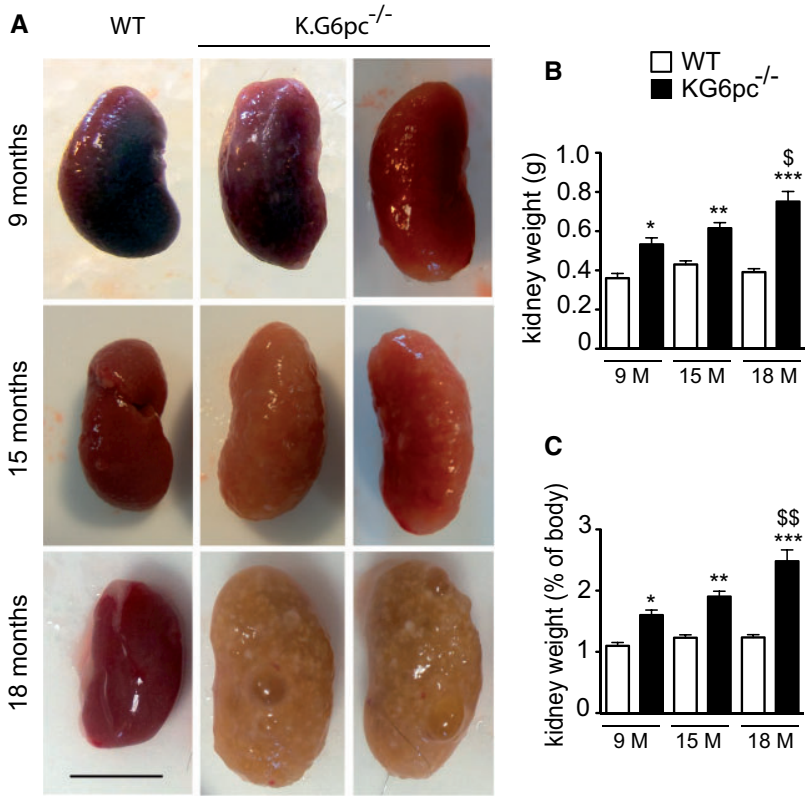

Figure 1. Kidney phenotype of K.G6pc$^{-/-}$ mice. **(A)** Representative images of WT and K.G6pc$^{-/-}$ kidneys at 9, 15 and 18 months after tamoxifen treatment. Scale bar = 0.5 cm. **(B)** Additional weight of the two kidneys and **(C)** relative weight of the kidneys compared with body mass in WT (white bars) and K.G6pc$^{-/-}$ (black bars) mice. Data are expressed as the mean ± s.e.m. Significant differences between WT mice and K.G6pc$^{-/-}$ mice are indicated as *, $P < 0.05$; **, $P < 0.01$; *** $P < 0.001$, respectively. Significant differences between 9 month- and 18 month-K.G6pc$^{-/-}$ mice are indicated as $, $P < 0.05$ and $$, $P < 0.01$.

progression (13,14), progressively increased in urine in K.G6pc$^{-/-}$ mice (Table 1) and was significantly higher in the plasma in the renal failure stage (Table 2). This was associated with a marked increase in *Lcn2* mRNA expression in K.G6pc$^{-/-}$ kidneys observed after only 9 months of *G6pc* deletion (Supplementary Material, Fig. S3), confirming that the kidney is the major source of urinary LCN2 (13,15).

These results suggest a gradual degradation of the filtration barrier with aging in K.G6pc$^{-/-}$mice, leading to a late-onset of renal failure after 15 months of *G6pc* deletion.

Progressive tubular and glomerular fibrosis and development of renal cysts in K.G6pc$^{-/-}$ mice with age

As the process of excessive fibrosis is a major cause of CKDs, we analyzed the progression of fibrosis in K.G6pc$^{-/-}$ kidneys. It is noteworthy that the kidneys were macroscopically sclerotic after 15 months of *G6pc* deletion and cystic after 18 months (Figure 1A). As observed after 6 months, neither renal fibrosis nor glomerular injury were observed after 9 months of *G6pc* deletion (Figures 3 and 4, Supplementary Material, Fig. S4). After 15 months, early cell degeneration and necrosis were observed in tubules with condensed nuclei. In addition, inflammatory (lymphoid and plasma cells) areas and fibrosis were observed in the interstitium of the cortex (Figure 3A and B). At 18 months, tubular dilation, inflammation and fibrosis were more significant and numerous microscopic and macroscopic cysts up to 3–4 mm were observed (Figure 3). This was consistent with the progressive increase in mRNA expression of the proinflammatory cytokine TNF-α (Figure 3C). In addition to large areas of interstitial fibrosis, glomerular scarring was observed (Figure 3B). As observed in diabetes, the glomeruli showed mesangial hypertrophy and expansion at 15 and 18 months, leading to an increase of glomerular size (Supplementary Material, Fig. S4). No tubular dysplasia or preneoplastic lesion was observed in K.G6pc$^{-/-}$kidneys. In agreement with histological observations, the thickness of the glomerular basement membrane was more prominent in K.G6pc$^{-/-}$ mice after 15 and 18 months compared to WT mice (Figure 4A and B). In addition, foot process effacement was observed at both ages (Figure 4A) and confirmed the substantial podocyte injury. Furthermore, Western Blot analyses showed that the amount of structural proteins of the filtration barrier (podocin and nephrin) had already slightly decreased at 9 months and was markedly reduced at 18 months (Figure 4C).

Thus, these results show that the development of interstitial and glomerular fibrosis results in the later development of polycystic kidneys in GSDIa mice. This is associated with a marked destruction of the filtration barrier that finally leads to renal failure.

Molecular mechanisms involved in renal fibrosis in K.G6pc$^{-/-}$ mice

One widely recognized pro-fibrotic factor orchestrating renal fibrosis is the TGF-β1 cytokine (16,17), which was already

Downloaded from https://academic.oup.com/hmg/article-abstract/25/17/3784/2525836/Progressive-development-of-renal-cysts-in-glycogen
by guest
on 18 September 2017

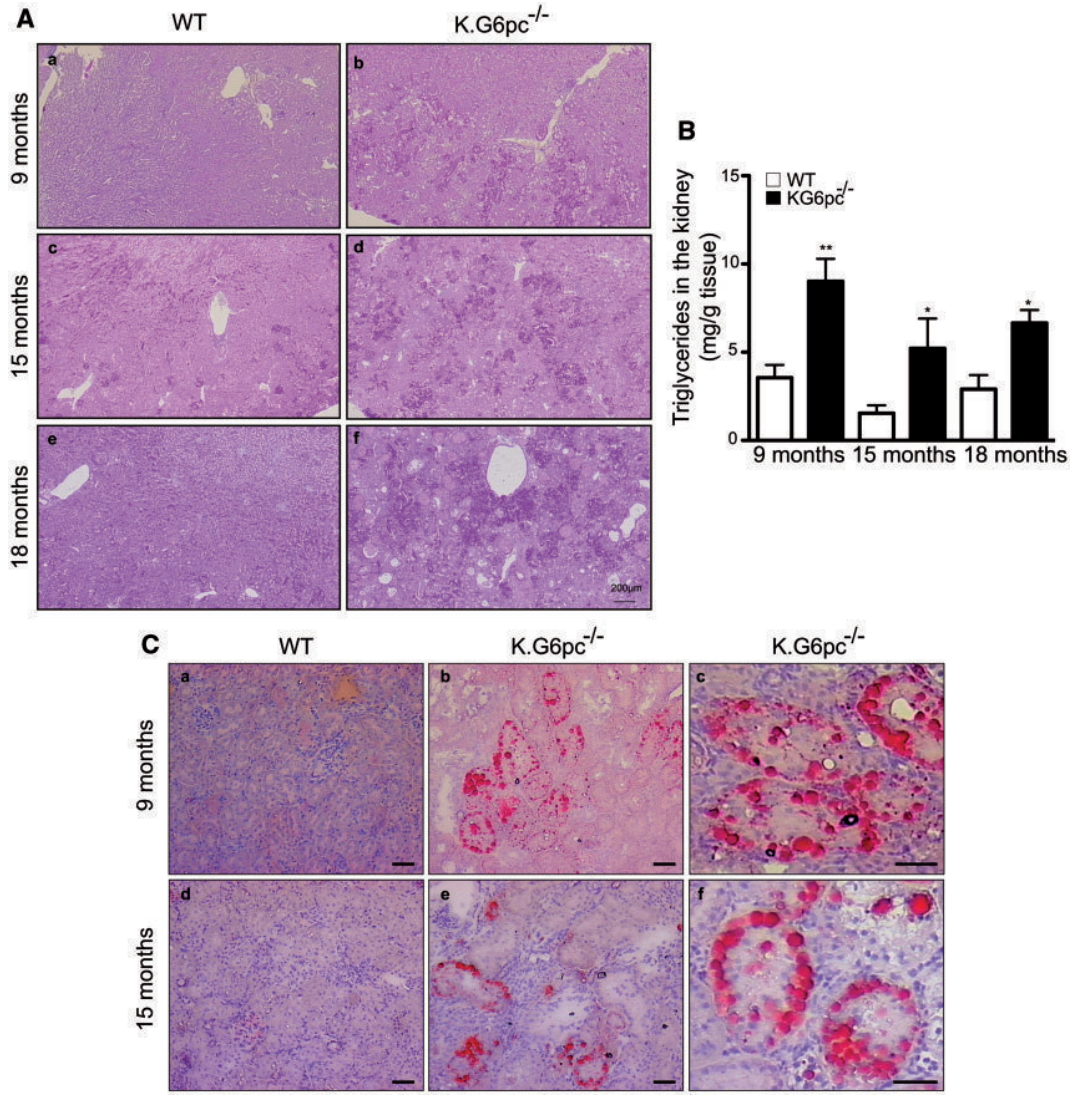

Figure 2. Glycogen and lipid accumulation in K.G6pc$^{-/-}$ kidneys. **(A)** PAS-stained kidneys from WT (a, c, e) and K.G6pc$^{-/-}$ mice (b, d, f) at 9, 15 and 18 months after tamoxifen treatment. The same magnification was used for each panel. Scale bar = 200 µm. **(B)** Triglyceride content of kidneys from WT (white bars) and K.G6pc$^{-/-}$ mice (black bars) after 9, 15 and 18 months of tamoxifen treatment. Data are expressed as the mean ± s.e.m. Significant differences between WT mice and K.G6pc$^{-/-}$ mice are indicated as *, $P < 0.05$; **, $P < 0.01$, respectively. **(C)** Histological analysis of Sudan red staining from WT (a, d) and K.G6pc$^{-/-}$ mice (b–c, e–f). Scale bars = 50 µm.

overexpressed in K.G6pc$^{-/-}$ kidneys at 6 months. In line with the development of fibrosis, the expression of *Tgfb1* mRNA progressively increased with age in K.G6pc$^{-/-}$ kidneys (Figure 5B). As previously shown, the activation of the RAS (illustrated here by the increase in renal angiotensinogen expression) could account for the increase in TGF-β1 expression (Figure 5A). Concomitantly with the increase in TGF-β1, epithelial-to-mesenchymal transition (EMT) and/or endothelial-to-mesenchymal transition (EndoMT) were progressively observed in K.G6pc$^{-/-}$ kidneys over time. The progression of CKD was associated with a 2-fold decrease in the expression of epithelial markers, such as E-Cadherin (*Cdh1*) and β-catenin (*Ctnnb1*) (Figure 5C). Concomitantly, we observed a progressive increase in the expression of mesenchymal markers, such as vimentin (*Vim*), fibronectin (*Fn1*), and collagen type I (*Col1a1*) (Figure 5D). After 18 months, a 10-fold induction of plasminogen activator inhibitor-1 (*Pai1*) expression was observed in K.G6pc$^{-/-}$ mice compared to WT mice and was significantly higher than after 9 and 15 months of *G6pc* deletion (Figure 5D). In addition to the changes in the EMT markers, we observed a decrease in the amount of two main antioxidant enzymes, catalase and glutathione peroxidase (GPX) after 18 months (Supplementary Material, Fig. S5), probably leading to an increase in reactive oxygen species (ROS) accumulation and oxidative stress (18).

Cystic renal disease and kidney failure in GSD1a patients

Renal status was studied in 32 patients with GSDI (27 with type Ia and 5 with type Ib), in order to detect renal cysts and/or kidney dysfunction (Tables 3 and 4). Renal failure was defined on the basis of the estimated glomerular filtration rate (eGFR) <60ml/min/1.73 m^2 for more than 3 months. Patients in the cohort were born between 1962 and 2014. The median age of the cohort when the data was collected was 26 years (ranging

Downloaded from https://academic.oup.com/hmg/article-abstract/25/17/3784/2525836/Progressive-development-of-renal-cysts-in-glycogen
by guest
on 18 September 2017

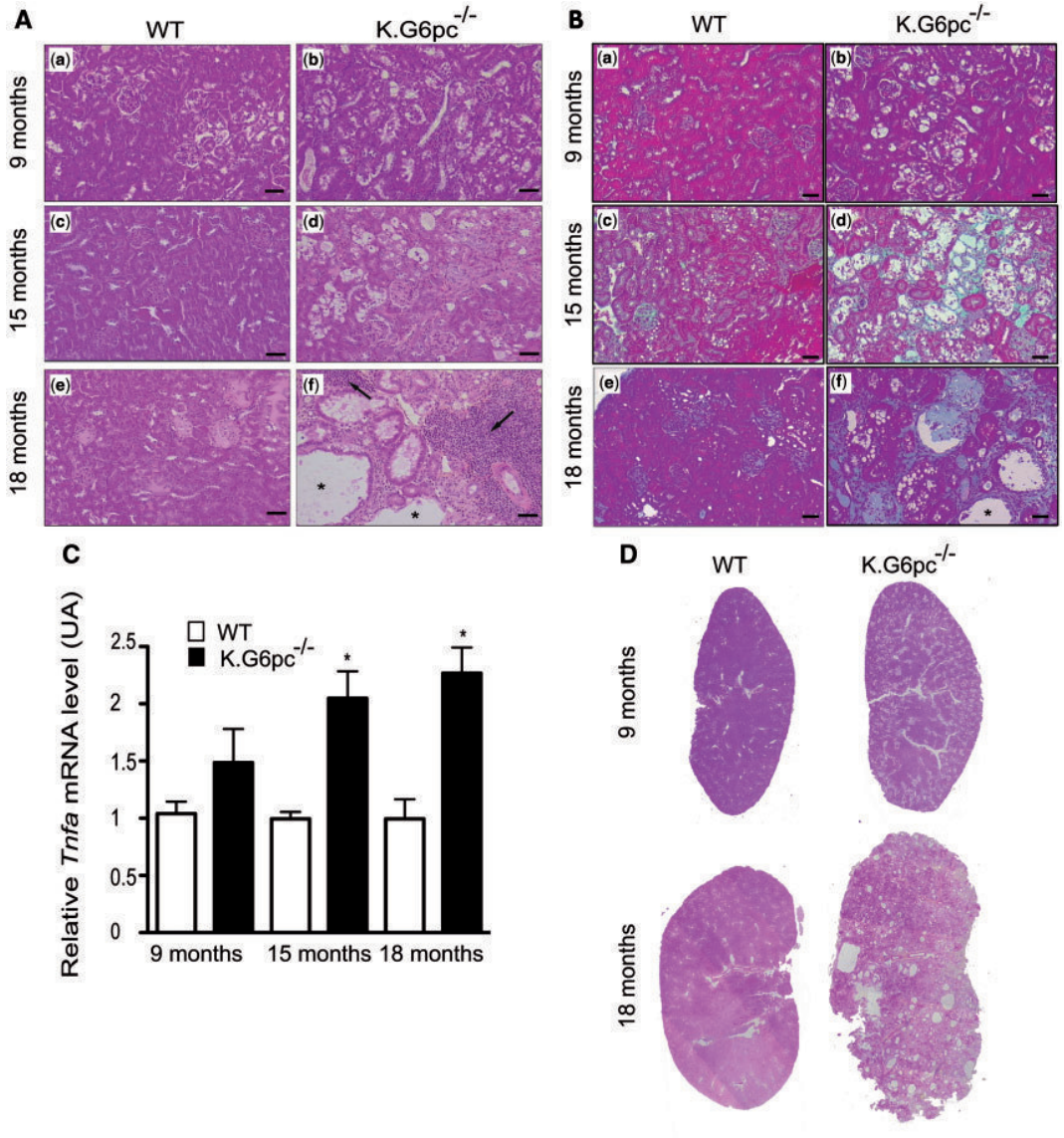

Figure 3. Histological alterations in K.G6pc$^{-/-}$ kidneys. **(A)** Hematoxylin-eosin staining of WT (a, c, e,) and K.G6pc$^{-/-}$ mice (b, d, f) at 9, 15 and 18 months after tamoxifen treatment. Scale bars = 50 μm **(B)** Masson's trichrome staining of WT (a, c, e) and K.G6pc$^{-/-}$ mice (b, d, f). Scale bars = 50 μm. Arrows show inflammation areas. Asterisks localize cysts. **(C)** Relative *Tnfa* mRNA expression. Significant differences between WT mice and K.G6pc$^{-/-}$ mice are indicated as *$P < 0.05$. **(D)** Scans of the kidney slides observed on panel A.

from 1 to 53 years). The median age of GSDI patients with renal dysfunction was higher than in patients without renal dysfunction (33 and 34 years for groups 2 and 3, respectively versus 22 years for group 1; Table 3). Our data suggest that early renal impairment was detected in the young adult GSDI patients (20–30 year-old) (Supplementary Material, Fig. S6). The overall prevalence of patients with urinary albumin/creatinine ratio > 20 or of patients treated with renoprotective drugs was 37.5% (13 patients) but only three patients developed renal failure (about 10% of GSDI patients) (Tables 3 and 4). Out of the three patients with renal failure, Patient 1 was waiting for renal transplantation and Patient 2 underwent kidney transplantation in 2014. Seven patients (6 with GSDIa and 1 with GSDIb) presented renal cysts, representing 22% of GSDI patients in this cohort (Table 5) and 54% of GSDI patients with renal dysfunction. Interestingly, cysts appeared in GSDI patients at later stages of CKD, characterized by a high albumin/creatinine ratio and a significant decrease of eGFR (Group 3, Table 3). Furthermore, all three patients with renal failure (Patients 1 to 3) have developed cysts (Table 4; Figure 6). Among these 7 patients, one or multiple cysts were detected in both kidneys, mainly in the cortical area (Table 5). The size and number of cysts increased over a 6–8-year follow-up period (Table 5 and Figure 6). Most of them were small (size <10mm) but some were supracentimetric (Table 5). One cyst in Patient 5 was classified as Bosniak II. These results suggest that the development of renal cysts probably appears before kidney failure in patients with GSDI. Despite intensive dietary treatment, hyperlipidaemia was observed in all patients with GSDI, even when patients were treated with lipid-lowering drugs. Indeed, mild and severe (TG > 10g/l) hypertriglyceridemia were observed in GSDI patients with cysts while hypertriglyceridemia was more moderated in GSDI patients without cysts

Downloaded from https://academic.oup.com/hmg/article-abstract/25/17/3784/2525836/Progressive-development-of-renal-cysts-in-glycogen
by guest
on 18 September 2017

Table 1. Urinary parameters of wild-type and K-G6pc-/- mice after 9, 15 and 18 months of *G6pc* deletion.

	9 months		15 months		18 months	
	WT	K.G6pc-/-	WT	K.G6pc-/-	WT	K.G6pc-/-
pH	6.4±0.4	6.0±0.1*	6.2±0.1	5.8±0.1**	ND	ND
volume (ml/24h)	1.1±0.1	2.1±0.2*	0.9±0.1	2.8±0.4**	0.9±0.1	3.8±0.9**
creatinine (µmol/24h)	23.4±2.3	26.2±2.1	18.1±1.5	20.7±0.9	9.5±1.0	11.5±1.6
albumin (µg/24h)	36±4	64±4*	72±15	255±40***,$	97±18	776±264***,$$
uric acid (mg/24h)	0.11±0.01	0.18±0.04	0.28±0.01	0.59±0.07**	0.25±0.03	0.68±0.15**
urea (mmol/24h)	1.5±0.2	2.6±0.1	2.3±0.4	3.1±0.4*	1.7±0.2	3.7±0.5**
lipocalin 2 (ng/24h)	27.2±4.2	148.5±33.8*	30.4±9.4	247.±41.5**	58.1±23.4	319.8±68.9**

Data were obtained from mouse urine samples collected during 24h using a metabolic cage and are expressed as the mean ± s.e.m ($n = 7$–8 mice in each group). Significant differences between WT and K-G6pc-/- mice are indicated as *$P < 0.05$; **$P < 0.01$ and ***$P < 0.001$. Significant differences between K-G6pc-/- mice over age are indicated as $$P < 0.05$ and $$$P < 0.01$. ND: not determined.

Table 2. Plasmatic parameters of wild-type and K-G6pc$^{-/-}$ mice.

	9 months		15 months		18 months	
	WT	K.G6pc-/-	WT	K.G6pc-/-	WT	K.G6pc-/-
uric acid (mg/l)	6.2±1.3	8.8±0.6	6.2±0.7	8.3±1.1	7.9±0.9	7.5±1.6
cholesterol (g/l)	0.95±0.02	0.91±0.04	1.07±0.02	1.28±0.06*	0.99±0.03	1.12±0.03
triglycerides (g/l)	0.54±0.02	0.53±0.02	0.51±0.04	0.50±0.03	0.52±0.03	0.47±0.04
BUN (mg/dl)	23.8±0.9	21.7±0.7	31.9±0.6	44.1±5.2**	27.1±3.6	53.9±3.6**
lipocalin 2 (mg/dl)	127.7±30.3	138.7±17.5	103.4±3.5	187.7±34.3	135.8±43.7	305.7±68.2*

Data were obtained from mice after 6 h of fasting and are expressed as the mean ± s.e.m. Significant differences between WT and K-G6pc$^{-/-}$ mice are indicated (*$P < 0.05$*, **$P < 0.01$, ***$P < 0.001$); $n = 7$–8 mice in each group.

(Table 3). Uric acid levels were similar in all GSDI patients but a majority of them, if not all, were treated with xanthine oxidase inhibitors (Table 3). However, metabolic parameters could not be associated with the compliance with dietary treatment in this cohort.

Discussion

Until recently, liver damage in GSDI was considered of greater concern than nephropathy. To date, owing to improved nutritional and medical management, GSDI patients have a considerably longer life expectancy and develop renal complications that were not frequently observed before. In this study, a longitudinal study of the progression of CKD in mice with kidney-specific knockout of G6Pase (K.G6pc$^{-/-}$ mice) allowed us to detect renal cysts before the development of renal failure. Retrospective analyses of the renal status of 32 patients with GSDI showed that renal cysts were detected in seven patients who developed advanced kidney dysfunction.

First, we analyzed the progression of CKD in K.G6pc$^{-/-}$ mice that reproduce early-onset GSDIa nephropathy observed in humans (19). In a previous study, we showed that K.G6pc$^{-/-}$ mice accumulated glycogen in proximal tubules leading to tubular clarification and nephromegaly as well as microalbuminuria after 6 months of *G6pc* deletion (12). At this early stage, the first signs of EMT were observed but no fibrosis was detected in the kidneys (12). Interestingly, we observed almost the same symptoms at 9 months, with increased in albuminuria and polyuria. This indicated the worsening of the nephropathy stage, with considerable tubular dysfunction since the kidneys could no longer concentrate urine successfully. Nevertheless, the glomerular filtration barrier was not damaged at this stage. Between 9 and 18 months, albuminuria increased progressively and the first signs of kidney failure were observed after 15 months of disease. Interestingly, this age corresponded to significant destruction of the glomerular filtration barrier, podocyte depletion, mesangial expansion, tubular fibrosis and inflammation, glomerular sclerosis and to the early development of microscopic cysts. The symptoms worsened at 18 months, with the development of macroscopic cysts. These results suggest that tubular dysfunction leads to the destruction of glomeruli and the filtration barrier, as previously suggested by Lee *et al.* (20).

The extent to which EMT contributes to renal fibrosis *in vivo* remains a matter of intense debate (21,22). In the context of GSDIa, we observed progressive but partial EMT leading to the development of fibrosis. At the early stages of the nephropathy, we observed a decrease in the expression of epithelial markers. Mesenchymal markers appeared progressively, after 15 months of *G6pc* deletion. This intermediate stage corresponds with the initiation of chronic inflammation. In addition, glomerular podocytes also undergo transformation after injury, which can lead to podocyte depletion and to defective glomerular filtration and glomerulosclerosis (23,24). This process is often accompanied with the fusion of the remaining pedicels in order to decrease filtration damage. In K.G6pc$^{-/-}$ kidneys, podocyte injury and the thickening of the glomerular basement membrane were observed after 15 months, corresponding to kidney failure. Finally, elevated expression of PAI-1 was observed after 15 months, leading to high accumulation of collagen and the development of severe interstitial and glomerular fibrosis (25). The major driving factors behind EMT during the fibrogenic phase of renal

Downloaded from https://academic.oup.com/hmg/article-abstract/25/17/3784/2525836/Progressive-development-of-renal-cysts-in-glycogen
by guest
on 18 September 2017

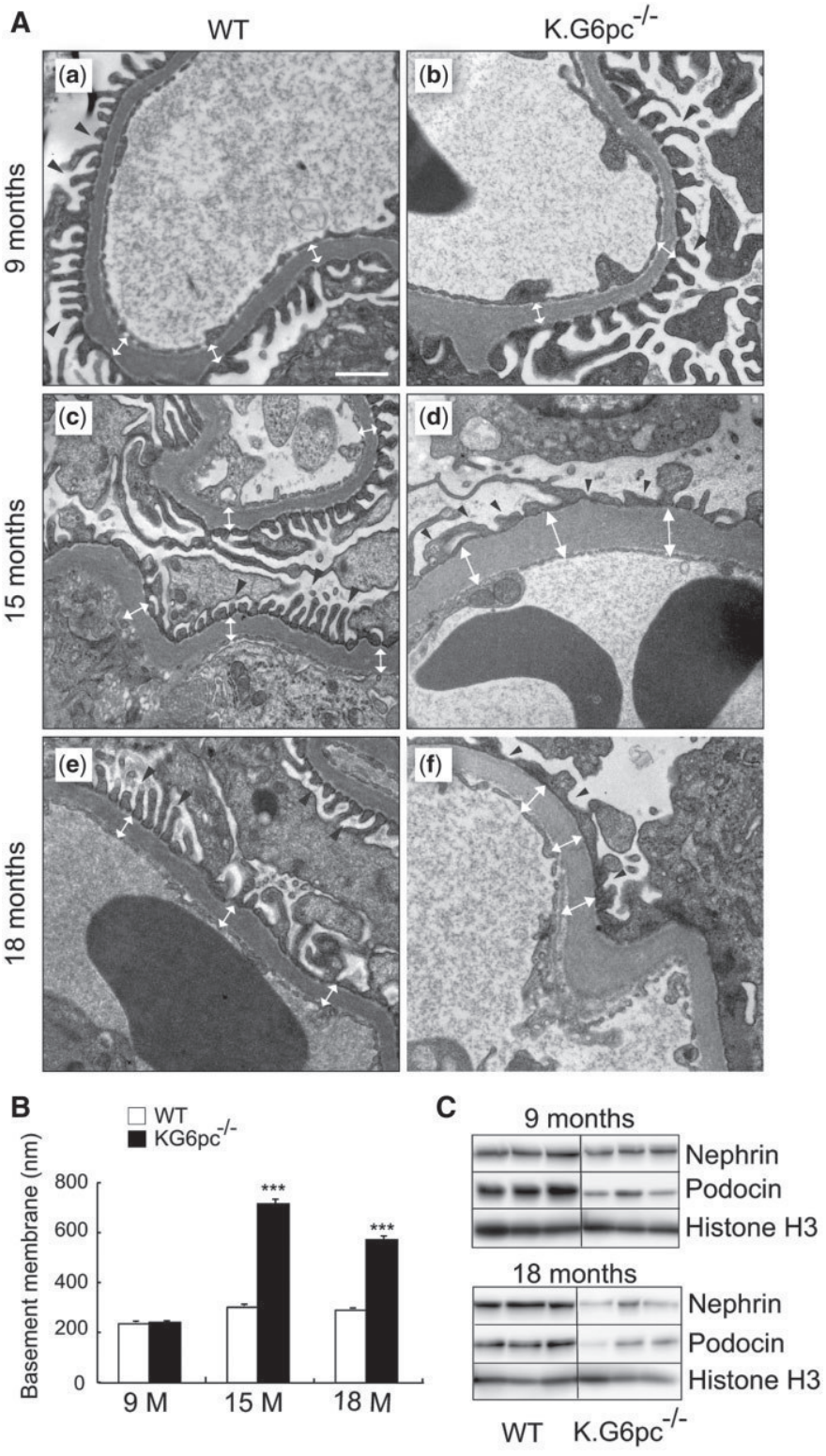

Figure 4. Glomerular alterations in K.G6pc$^{-/-}$ kidneys. **(A)** Electron microscopy analyses of glomeruli of WT (a, c, e) and K.G6pc$^{-/-}$ mice (b, d, f) at 9, 15 and 18 months after tamoxifen treatment. Double white arrows delimit the basement membrane. Black arrowheads show pedicels. Scale bar = 500 nm **(B)** Thickness of the basement membrane of WT (white bars) and K.G6pc$^{-/-}$ glomeruli (black bars). Significant differences between WT mice and K.G6pc$^{-/-}$ mice are indicated as $^{***}P < 0.001$. **(C)** Representative Western Blot of Nephrin, Podocin and Histone H3 (control) proteins in the kidneys of WT and K.G6pc$^{-/-}$ mice. At 9 months, quantification analyses performed by densitometry (student's *t* test) showed a 1.4-fold (ns, $n = 4$) decrease in the quantity of Nephrin and Podocin in K.G6pc$^{-/-}$ compared to WT mice. After 18 months of *G6pc* deletion, the quantity of Nephrin decreased 1.9-fold ($P = 0.03$, $n = 4$) and the quantity of Podocin decreased 2.3-fold ($P = 0.003$, $n = 4$).

Downloaded from https://academic.oup.com/hmg/article-abstract/25/17/3784/2525836/Progressive-development-of-renal-cysts-in-glycogen
by guest
on 18 September 2017

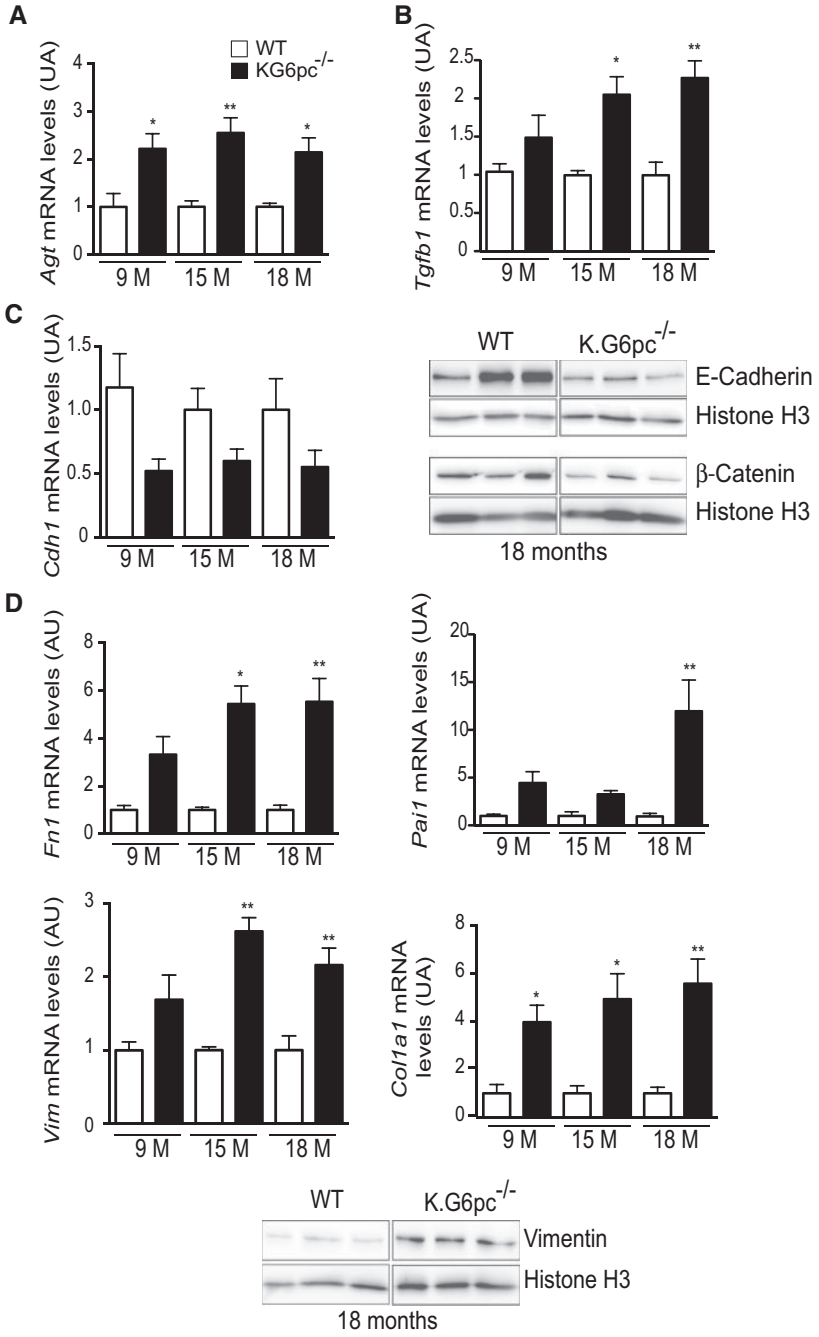

Figure 5. Progressive development of epithelial-to-mesenchymal transition during chronic kidney disease in K.G6pc$^{-/-}$ mice. Quantitative analyses of *Agt* **(A)**, *TGF-β1* **(B)**, epithelial- **(C)** and mesenchymal- **(D)** markers by RT-qPCR or Western Blot. The expression of target mRNA in K.G6pc$^{-/-}$ kidneys was expressed relative to WT kidneys at 9, 15 and 18 months. Significant differences between WT mice and K.G6pc$^{-/-}$ mice are indicated as $^{*}P < 0.05$ and $^{**}P < 0.01$. Representative Western Blots were shown after 18 months of *G6pc* deletion. Statistical analyses (student's T test) of Western Blot densitometry analyses showed a 2-fold decrease of E-Cadherin ($P = 0.02$, $n = 4$) and *β*-Catenin ($P = 0.001$, $n = 4$) quantity in K.G6pc$^{-/-}$ compared to WT mice. The quantity of Vimentin increased by 2.5-fold ($P = 0.01$, $n = 4$) in K.G6pc$^{-/-}$ compared to WT mice.

fibrosis appear to be various profibrotic growth factors, especially TGF-β1 (17). The latter was progressively increased during CKD development in K.G6pc$^{-/-}$ mice. We previously suggested that the persistent activation of the RAS is mainly responsible for the induction of TGF-β1 (12). Nevertheless, there are other mechanisms that might contribute to this profibrotic stimulus, such as activation of the endoplasmic reticulum stress (ER stress) and the subsequent Unfolded Protein Response (UPR), which were shown to activate TGF-β1 and promote fibrosis in the kidney (26,27). ER stress can be easily triggered by glucose concentration imbalance, as well as metabolite accumulation, both of which being observed in GSD1. Furthermore, apoptosis induced by ER stress alone is sufficient to induce fibrosis. In addition, inflammatory cells

Downloaded from https://academic.oup.com/hmg/article-abstract/25/17/3784/2525836/Progressive-development-of-renal-cysts-in-glycogen
by guest
on 18 September 2017

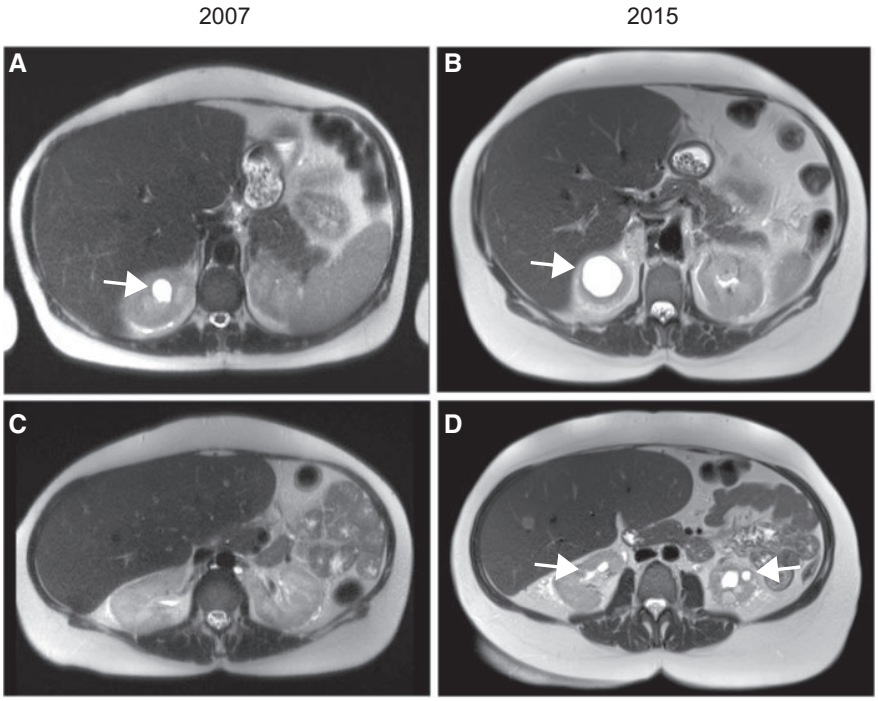

Figure 6. Axial T_2-weighted MRI images from patient 3 with GSDIa. Two different sections are shown in 2007 (panels **A–C**) and in 2015 (panels **B–D**). Arrows indicate renal cysts.

Table 3. Clinical and biochemical parameters of the 32 GSDI patients.

Characteristics	Group 1 No cysts - No renal impairment	Group 2 No cysts - Early renal impairment	Group 3 Cysts and renal impairment	All GSDI patients
number of patients	19	6	7	32
GSDIa/GSDIb	16/3	5/1	6/1	27/5
Male/Female	7/12	5/1	4/3	16/16
Median Age	22 years	34 years	33 years	26 years
(range)	(1–44)	(26–48)	(23–53)	(1–53)
Creat (μmol/l)	49.3±2.4	66.0±6.7	125.9±26.2***	69.2±7.9
(range)	(27–64)	(52–88)	(69–228)	(27-228)
Alb/Creat (mg/mmol)	0.7±0.3	15.7±5.7	150.8±60.8***	28.3±14.0
(range)	(0–4.8)	(0–37.9)	(26.5–375)	(0-375)
eGFR (min/min/1.73m2)	126.0±7.6	117.5±10.1	75.7±15.4	113.4±6.8
(range)	(63–200)	(95–152)	(23–119)	(23-200)
TG (g/l)	3.8±0.5	5.9±1.9	7.7±1.8*	5.1±0.6
(range)	(1.5–11.5)	(2.1–14.7)	(2–16.8)	(1.7-16.8)
Uric acid (μmol/l)	379.8±24.4	401.8±74.8	383.0±30.4	384.6±20.3
(range)	(179–577)	(177–705)	(258–486)	(177-705)
Lipid lowering therapies (% of patients)	15.8%	50%	71.4%	34.4%
Treatments for hyperuricemia (% of patients)	73.7%	100%	100%	84.3%
Renoprotective treatments (% of patients)	0%	83.3%	100%	37.5%

Group 1 corresponds to GSDI patients without renal dysfunction and cysts. Group 2 corresponds to GSDI patients without cyst but with microalbuminuria and/or treated with ACE inhibitors. Group 3 corresponds to GSDI patients with advanced renal impairment and renal cysts. All data were collected in 2015. Creat: creatinine; Alb: albumin, a: data available from only 4 GSDI patients. Data are expressed as mean ± s.e.m. Significant differences with Group 1 are indicated as *$P < 0.05$; ***$P < 0.001$.

and cytokines certainly play a vital role in the process of fibroblast activation, as has been demonstrated for diabetic nephropathy (28). Taken together, these results suggest that EMT and/or EndoMT occur in GSDIa kidneys and play a vital role in the progression of CKD. Finally, the decrease in antioxidant defenses, which is also observed in diabetic kidneys (29), could participate to the progression of nephropathy in GSDI (30). Indeed, the production of ROS and oxidative stress are interlinked with TGF-β1 production and thus are key factors in fibrosis (31).

Downloaded from https://academic.oup.com/hmg/article-abstract/25/17/3784/2525836/Progressive-development-of-renal-cysts-in-glycogen
by guest
on 18 September 2017

Table 4. Clinical and biochemical parameters of GSDI patients who developed renal cysts.

Patients	Gender	Age (years)	GSDI Type	G6PC mutations	Creat (μmol/l)	Alb/creat (mg/mmol)	Prot/creat (g/mmol)	eGFR (ml/min per 1.73m^2)	TG (g/l)	Uric acid (μmol/L)	Renoprotective treatment
1	M	24	Ia	c.1039C>T	215	375	0.55	36	6.6	304	Ibersatan (since 2008) Waiting for a transplant
2	F	37	Ia	c.328G>A c.1039C>T	228	nd	0.34	23	6.8	258	Ramipril/ Hydrochlorothiazide (since 2003) Transplanted in 2014
3	F	44	Ib	c.82C>T c.1015G>T	137	160	0.17	40	2	402	Ibersatan/Ramipril (since 2004)
4	F	23	Ia	c.247C>T c.734_735insG	71	nd	0.06	103	16.8	486	Enalapril (since 2006)
5	M	25	Ia	c.209G>A c.323C>T	86	nd	<0.01	107	4.5	450	Ramipril (since 2005)
6	M	27	Ia	c.809G>T	75	26.5	0.15	119	>10	363	Ramipril/ Hydrochlorothiazide (since 2006)
7	M	43	Ia	c.793DelC c.1039C>T	69	41.8	0.06	102	7.6	417	Enalapril (since 2005)

Data were collected in 2015. Creat: creatinine; Alb: albumin; Prot: Protein. Nd: not determined. The date of the beginning of treatment is indicated in brackets.

Table 5. Cyst development in GSDI patients.

	Renal MRI at T1			Renal MRI at T2		
Patients	Date	cysts<10mm	cysts > 10mm	Date	cysts<10mm	cysts > 10mm
1	2007	1/1 cortical	0	2015	0/2 cortical 2/1 medullar	0
2	2007	2/2cortical 0/2 medullar	1/0 cortical	2013	4/2 cortical 0/1 medullar	1/1 cortical (10 to 19mm)
3	2007	3/4 cortical 1/1 medullar	1/0 cortical (16mm)	2015	9/6 cortical 3/2 medullar	3/1 cortical (10 to 33 mm) 0/3 medullar (11 to 16 mm)
4	2008	0/2cortical 2/10 medullar	2/1 cortical (12 to 16 mm) 2/4 medullar (10 to 18 mm)	2014	6/3 cortical 3/8 medullar	2/2 cortical (10 to 13 mm) 1/2 medullar (11 to 13 mm)
5	2008	2/3 cortical 2/1 medullar	1/1 cortical (10 to12mm)	2013	4/3 cortical 4/0 medullar	3/4 cortical (11 to 21 mm)
6	2008	1/3 cortical 1/0 medullar	1/0 cortical (12mm)	2015	3/7 cortical 5/4 medullar	0
7	2007	23/27 cortical	3/4 cortical (11 to 19 mm) 1/0 medullar (17 mm)	2015	25/30 cortical	4/11 cortical (10 to 17 mm) 1/0 medullar (18 mm)

The number, size and localization of cysts were analyzed by MRI by two radiologists. A first set of data was obtained at T1 (in 2007–2008) and a second set was obtained 6 to 8 years later at T2 (in 2013–2015). Number of cysts on the right kidney/number of cysts on the left kidney observed in the cortical or medulla area are indicated. The size of supracentimetric cysts was indicated in brackets.

In clinical practice, the most commonly used markers of the progression of renal disease are urinary albumin/creatinine excretion, measurement of serum electrolytes, blood urea and serum creatinine with calculation of eGFR. Unfortunately, not all of them are sufficiently sensitive to detect the early stages of the disease. Urinary LCN2 was recently considered as a promising biomarker of CKD progression, mainly reflecting early defective tubular function (13–15). This protein is released from the kidneys in the case of acute kidney injury, long before a decrease in the glomerular rate can be detected (32). Elevated levels of urinary LCN2 and their inverse correlation with eGFR have also been shown in CKD patients with autosomal dominant polycystic kidney disease (PKD) (33). In the context of diabetes, conflicting results have failed to confirm urinary LCN2 as a reliable biomarker of CKD progression (32). Here, the progressive increase in urinary LCN2 levels during the development of kidney disease in K.G6pc$^{-/-}$ mice probably reflects the deterioration of tubular function. Thus LCN2 could be proposed as a specific biomarker of CKD progression in GSDIa patients. It is noteworthy that recent work has suggested that LCN2 might participate in the pathogenesis of cysts and CKD, by inducing EGFR (Epithelial Growth Factor Receptor) signalling (13). Interestingly, it might also activate cell proliferation of renal tubules and cysts in other pathological contexts (34). Consequently, the overexpression of LCN2 in K.G6pc$^{-/-}$ kidneys could be involved in the progression of the CKD in GSDIa.

Finally, GSDIa nephropathy is associated with the activation of a variety of pathways, in particular glycolysis, *de novo* lipogenesis, and the RAS that leads to the progression of kidney disease (Figure 7). The accumulation of glycogen and lipids in the kidneys probably leads to the activation of cell defenses involved in the maintenance of cell homeostasis. Impaired autophagic activity, ER stress and ROS production are involved in the development of CKD (35). In GSDI, oxidative stress was already shown to mediate nephropathy (30). Interestingly, recent publications have proposed

Downloaded from https://academic.oup.com/hmg/article-abstract/25/17/3784/2525836/Progressive-development-of-renal-cysts-in-glycogen
by guest
on 18 September 2017

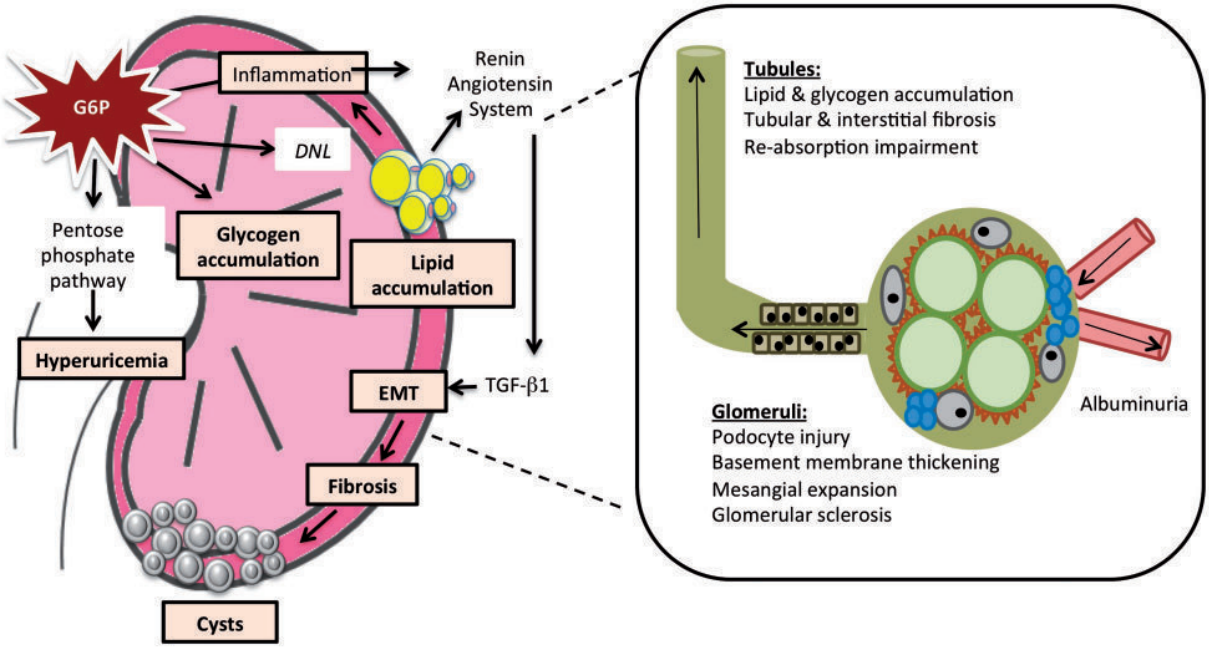

Figure 7. Proposed model for the progression of CKD in GSDI. The accumulation of G6P in tubules induces the activation of metabolic pathways, such as glycogen synthesis, *de novo* lipogenesis (DNL), and the pentose phosphate pathway. These dysregulations lead to the accumulation of glycogen and lipids and to inflammation. This is associated with the activation of the renin-angiotensin system, which could account for the increased expression of the pro-fibrotic factor TGF-β1. Ultimately, the progression of tubular and interstitial fibrosis and glomerular sclerosis leads to the development of polycystic kidneys. Blue cells around glomeruli represent the mesangial expansion.

pharmacological modulation of ER stress for preserving renal function and morphology (15,36). In addition, better control of metabolism could be crucial for preventing the progression of renal damage. As suggested for diabetic nephropathy, fat accumulation in K.G6pc$^{-/-}$ kidneys probably causes renal damage due to lipotoxicity and oxidative stress (37,38). Moreover, the progression of renal damage has been recently associated with dyslipidemia (39). In this cohort, hyperlipidaemia tended to be higher in the groups of patients with renal dysfunction (Table 3, Groups 2 and 3), while more than 50% of these patients were treated with lipid-lowering drugs. The synergistic effects of lipid-lowering drugs and blockers of the RAS system in renal protection have been documented in diabetic patients (40). In addition, the overproduction of uric acid by GSDIa kidneys (due to PPP activation) possibly contributes to the development of CKD. Indeed, uric acid exerts a deleterious effect on renal tubular cells by inducing EMT (41). The treatment of hyperuricemia with allopurinol was reported to preserve kidney function (7). Thus, a combined therapy including allopurinol, ACE-inhibitors and lipid-lowering drugs has been proposed to slow down CKD in patients with cysts. Despite this combined treatment, three GSDI patients developed renal failure. As CKD appears in young GSDI adults or earlier (8,9), a combined therapy from the youngest age could be more efficient, in order to obtain preventive effects rather than curative results. This suggests that care management of GSDI patients should be coordinated by a paediatrician and a nephrologist from the youngest age. It is noteworthy that the ACE-inhibitors significantly delayed the progression of renal damage only in the cases where the therapy was given right when glomerular hyperfiltration was detected (39,42). Nephrology recommendations were reported in the clinical practice guidelines of the American College of Medical Genetics and Genomics (6). In addition to these recommendations, systematic observations of cyst development by kidney imaging should provide a better estimation of the progression of the disease, independently of biochemical markers. Indeed, until recently, abdominal real-time ultrasonography was performed occasionally in order to estimate the enlargement of the kidneys and detect nephrolithiasis or nephrocalcinosis. The quality of the images was not sufficient to precisely detect cysts. More recently, the detection of renal cysts has been facilitated by improved abdominal imaging techniques (higher resolution), such as MRI. Interestingly, imaging of the kidneys has been systematically proposed once a year in patients with GSDI. This allowed us to detect cysts in patients with advanced stage of CKD, before the development of renal failure. Thus renal imaging by MRI should be performed once a year to increase the likelihood of detecting renal cysts in GSDI patients. It is noteworthy that cysts were detected in young adult GSDI patients, as well as in older patients, who all developed severe impairment of kidney function. No cysts were observed in patients with early kidney impairment. Thus, our results suggest that the appearance of cysts is strongly linked to the progression of CKD in GSDI.

In conclusion, the renal pathology of GSDI is characterized by the progressive development of polycystic kidneys, leading to the development of irreversible renal failure in a late stage of the disease. Interestingly, K.G6pc$^{-/-}$mice developed all of the hallmarks of the nephropathy observed in GSDIa patients. Thus they can be a useful tool in future studies relating to the pharmacological treatment of CKD.

Materials and Methods

Patients

A cohort of 32 patients with GSDI was reviewed retrospectively. All cases of GSDI with mutations were identified at Antoine

Downloaded from https://academic.oup.com/hmg/article-abstract/25/17/3784/2525836/Progressive-development-of-renal-cysts-in-glycogen
by guest
on 18 September 2017

Beclere Hospital (Clamart), which is the reference centre for rare diseases of hepatic metabolism. Seven patients of this cohort (i.e. 22%) developed renal cysts, which were detected by abdominal real-time ultrasonography and MRI. These examinations are systematically proposed once a year. For this study, the images were retrospectively reviewed on the Picture Archiving and Communication System (PACS), the radiology software, since 2007–2008. To count the number of cysts, two radiologists recorded any cyst detected by axial T2-weighted images (Table 5). The clinical and biochemical parameters of these patients, shown in Tables 3 and 4, were collected in 2015. Urine was collected over 24h. Urinary albumin and protein excretion are expressed as a ratio to creatinine to account for differences in urinary dilution. The eGFR was calculated using the CKI-EPI formula (43).

Generation of kidney-specific G6pc knock-out mice

Deficiency in renal G6Pase was obtained by specific deletion of *G6pc* exon 3 in the kidney as previously described (12). Adult male (6–8 weeks old) B6.G6pc$^{lox/lox}$.Kap$^{creERT2/w}$ and C57Bl/6J mice (Charles Rivers Laboratories, L'Arbresle, France) were intraperitoneally injected daily with 1mg of tamoxifen on five consecutive days to obtain K-G6pc$^{-/-}$ and wild-type (WT) mice, respectively (12). Mice were housed in the animal facility of Lyon 1 University under temperature controlled (22 °C) conditions and with a 12h/12 h light/dark cycle. Mice had free access to water and standard chow (A04 Safe, Augy, France). They were studied from 9 to 18 months after tamoxifen treatment. After 6 h of fasting (with continuous access to water), mice were killed by cervical dislocation. A piece of fresh kidney was fixed in formaldehyde (for histology) or glutaraldehyde (for transmission electron microscopy - TEM). The rest of the kidney was frozen by freeze-clamping in liquid nitrogen, and then stored at −80 °C. All the procedures were performed in accordance with the principles and guidelines established by the European Convention for the Protection of Laboratory Animals. The regional animal care committee (C2EA-55, Université Lyon 1, Lyon) approved all the experiments.

Histological analysis

Formalin-fixed and paraffin-embedded kidneys were cut in 4 μm thick sections and stained with hematoxylin and eosin (H&E), or periodic acid Schiff (PAS) staining, or Masson's trichrome staining. Cross-sections (10 μm thick) were obtained from frozen, OCT-embedded tissues and stained with Sudan red. The slides were examined under a Coolscope microscope (Nikon). Section preparations and staining were performed by the "Centre d'histopathologie du petit animal" (Anipath) - University Lyon 1 Laennec, Lyon.

Transmission electron microscopy

A piece of kidney cortex was cut into smaller pieces (1 mm^3) and fixed in 2% glutaraldehyde at 4 °C. Ultrathin sections (approximately 70 nm thick) were cut on a Reichert ultracut E (Leica) ultramicrotome, mounted on 200 mesh copper grids coated with 1:1,000 polylysine, stabilized for 1 day at room temperature (RT) and contrasted with uranyl acetate and lead citrate by the CIQLE platform (Lyon, Laennec). Sections were examined with a Jeol 1400JEM (Tokyo, Japan) transmission electron microscope equipped with an Orius 1000 camera and Digital Micrograph. Four kidney samples were prepared from each group of mice. Ten glomerular sections from each mouse were documented and the thickness of the basal membrane was measured and noted at 5 random spots.

Plasma parameters

Blood was withdrawn by submandibular bleeding using a lancet after 6h of fasting and collected in EDTA (0.5M, pH8.0). Plasma triglyceride, cholesterol and uric acid concentrations were determined with Biomérieux colorimetric kits (Marcy l'Etoile, France). Blood urea nitrogen concentration was measured using a BioAssay Systems colorimetric kit (Hayward, CA, USA).

Urine parameters

Mice were housed in individual metabolic cages (UgoBasile, Comerio, Italy) for 24 h for acclimation before the experiment. Urine was collected for 24 h. Urine urea, creatinine and electrolytes were measured in an automatic analyzer (Konelab, Thermo, France). Albuminuria was assessed using a mouse albumin Elisa kit (Neobiotech) and the uric acid concentration was determined using a colorimetric kit (Biomérieux, Marcy l'Etoile, France). LCN2 levels were assessed using a mouse Lipocalin-2/NGAL Elisa kit (R&D Systems, Abingdon, UK). Urine pH was determined using strips with $\Delta pH = 0.2$. Oxalate was measured using gas chromatography mass spectrometry with stable isotope dilution. Citrates were assessed by an enzymatic method using a commercial set (R-Biopharm AG, Darmstadt, Germany).

Gene expression analysis

Western blot analyses were carried out using rabbit polyclonal antibodies against Podocin (Abcam, 1:5,000), Nephrin (Abcam, 1:5,000), E-cadherin (Cell Signalling, 1:1,000), β-catenin (Cell Signalling, 1:1,000), Vimentin (Cell Signalling, 1:1,000), GPX (Abcam, 1:1,000), Catalase (Abcam, 1:2,000), and Histone H3 (Cell Signalling, 1:2,000). Total RNA was isolated according to the Trizol protocol (Invitrogen Life Technologies, Saint Aubin, France). Reverse transcription was done using the Qiagen Quantitec Reverse Transcription kit. Real-time PCRs were performed using sequence-specific primers with SsoAdvanced™ Universal SYBR® Green Supermix in a CFX Connect™ Real-Time System (Bio-Rad). The mouse ribosomal protein ml 19 transcript (Rpl19) was used as reference. Primer sequences are indicated in Supplementary Material, Table S2.

Statistics

The results are reported as the mean ± s.e.m. Groups were compared using two-way ANOVA followed by Tukey's *post hoc* test (against all groups), except for the quantification analyses by Western Blot. An unpaired two-tailed a Student's *t* test was performed for Western Blot analyses. Differences were considered to be statistically significant at P-value < 0.05.

Study approval

The regional animal care committee (C2EA-55, Université Lyon 1, Lyon) approved all the experiments. Written informed consent was obtained from participants prior to inclusion in the study.

Supplementary Material

Supplementary Material is available at *HMG* Online.

Downloaded from https://academic.oup.com/hmg/article-abstract/25/17/3784/2525836/Progressive-development-of-renal-cysts-in-glycogen
by guest
on 18 September 2017

Acknowledgements

We thank Dr. Fabiola Terzi for helpful suggestions and critically reading the manuscript. We would like to thank the members of Animalerie Lyon Est Conventionnelle et SPF (Université Lyon 1-Laennec, SFR Santé Lyon Est) for the animal care, the members of the CIQLE platform (Université Lyon 1, Laennec) and the members of the Anipath platform for the histological experiments (Université Lyon 1- Laennec). We also thank Dr. Gaëlle Brideau and the members of the Plateforme d'exploration fonctionnelle rénale des Cordeliers (Paris), Dr. Annie Varennes and Dr. Cécile Acquaviva (Hospices Civils de Lyon, 69500 Bron, France; Université de Lyon) for urine analyses.

Conflict of Interest statement. None declared.

Funding

This work was supported by research grants from the Agence Nationale de la Recherche [ANR11-BSV1-009-01]; and the Association Francophone des Glycogénoses. Monika Gjorgjieva holds a fellowship from "La ligue Nationale contre le Cancer" (2014-2017).

References

1. Chou, J.Y., Matern, D., Mansfield, B.C. and Chen, Y.T. (2002) Type I glycogen storage diseases: disorders of the glucose-6-phosphatase complex. *Curr. Mol. Med.*, **2**, 121–143.
2. Cori, G.T. and Cori, C.F. (1952) Glucose-6-phosphatase of the liver in glycogen storage disease. *J. Biol. Chem.*, **199**, 661–667.
3. Lei, K.J., Shelly, L.L., Pan, C.J., Sidbury, J.B. and Chou, J.Y. (1993) Mutations in the glucose-6-phosphatase gene that cause glycogen storage disease type 1a. *Science*, **262**, 580–583.
4. Bruni, N., Rajas, F., Montano, S., Chevalier-Porst, F., Maire, I. and Mithieux, G. (1999) Enzymatic characterization of four new mutations in the glucose-6 phosphatase (G6PC) gene which cause glycogen storage disease type 1a. *Ann. Hum. Genet*, **63**, 141–146.
5. Chevalier-Porst, F., Bozon, D., Bonardot, A.M., Bruni, N., Mithieux, G., Mathieu, M. and Maire, I. (1996) Mutation analysis in 24 French patients with glycogen storage disease type 1a. *J. Med. Genet.*, **33**, 358–360.
6. Kishnani, P.S., Austin, S.L., Abdenur, J.E., Arn, P., Bali, D.S., Boney, A., Chung, W.K., Dagli, A.I., Dale, D., Koeberl, D., *et al.* (2014) Diagnosis and management of glycogen storage disease type I: a practice guideline of the American College of Medical Genetics and Genomics. *Genet. Med. Off. J. Am. Coll. Med. Genet*, **16**, e1.
7. Froissart, R., Piraud, M., Boudjemline, A.M., Vianey-Saban, C., Petit, F., Hubert-Buron, A., Eberschweiler, P.T., Gajdos, V. and Labrune, P. (2011) Glucose-6-phosphatase deficiency. *Orphanet. J. Rare Dis.*, **6**, 27.
8. Rake, J.P., Visser, G., Labrune, P., Leonard, J.V., Ullrich, K. and Smit, G.P.A. (2002) Glycogen storage disease type I: diagnosis, management, clinical course and outcome. Results of the European Study on Glycogen Storage Disease Type I (ESGSD I). *Eur. J. Pediatr.*, **161 Suppl 1**, S20–S34.
9. Martens, D.H.J., Rake, J.P., Navis, G., Fidler, V., van Dael, C.M.L. and Smit, G.P.A. (2009) Renal function in glycogen storage disease type I, natural course, and renopreservative effects of ACE inhibition. *Clin. J. Am. Soc. Nephrol. CJASN*, **4**, 1741–1746.
10. Rajas, F., Labrune, P. and Mithieux, G. (2013) Glycogen storage disease type 1 and diabetes: learning by comparing and contrasting the two disorders. *Diabetes Metab.*, **39**, 377–387.
11. Mundy, H.R. and Lee, P.J. (2002) Glycogenosis type I and diabetes mellitus: a common mechanism for renal dysfunction? *Med. Hypotheses*, **59**, 110–114.
12. Clar, J., Gri, B., Calderaro, J., Birling, M.C., Hérault, Y., Smit, G.P.A., Mithieux, G. and Rajas, F. (2014) Targeted deletion of kidney glucose-6 phosphatase leads to nephropathy. *Kidney Int.*, **86**, 747–756.
13. Viau, A., El Karoui, K., Laouari, D., Burtin, M., Nguyen, C., Mori, K., Pillebout, E., Berger, T., Mak, T.W., Knebelmann, B., *et al.* (2010) Lipocalin 2 is essential for chronic kidney disease progression in mice and humans. *J. Clin. Invest.*, **120**, 4065–4076.
14. Liu, K.D., Yang, W., Anderson, A.H., Feldman, H.I., Demirjian, S., Hamano, T., He, J., Lash, J., Lustigova, E., Rosas, S.E., *et al.* (2013) Urine neutrophil gelatinase-associated lipocalin levels do not improve risk prediction of progressive chronic kidney disease. *Kidney Int.*, **83**, 909–914.
15. El Karoui, K., Viau, A., Dellis, O., Bagattin, A., Nguyen, C., Baron, W., Burtin, M., Broueilh, M., Heidet, L., Mollet, G., *et al.* (2016) Endoplasmic reticulum stress drives proteinuria-induced kidney lesions via Lipocalin 2. *Nat. Commun.*, **7**, 10330.
16. López-Hernández, F.J. and López-Novoa, J.M. (2012) Role of TGF-β in chronic kidney disease: an integration of tubular, glomerular and vascular effects. *Cell Tissue Res.*, **347**, 141–154.
17. Loeffler, I. and Wolf, G. (2014) Transforming growth factor-β and the progression of renal disease. *Nephrol. Dial. Transplant. Off. Publ. Eur. Dial. Transpl. Assoc. - Eur. Ren. Assoc.*, **29 Suppl 1**, i37–i45.
18. Noh, H. and Ha, H. (2011) Reactive oxygen species and oxidative stress. *Contrib. Nephrol.*, **170**, 102–112.
19. Rajas, F., Clar, J., Gautier-Stein, A. and Mithieux, G. (2015) Lessons from new mouse models of glycogen storage disease type 1a in relation to the time course and organ specificity of the disease. *J. Inherit. Metab. Dis.*, **38**, 521–527.
20. Lee, P.J., Dalton, R.N., Shah, V., Hindmarsh, P.C. and Leonard, J.V. (1995) Glomerular and tubular function in glycogen storage disease. *Pediatr. Nephrol. Berl. Ger.*, **9**, 705–710.
21. Kriz, W., Kaissling, B. and Le Hir, M. (2011) Epithelial-mesenchymal transition (EMT) in kidney fibrosis: fact or fantasy? *J. Clin. Invest.*, **121**, 468–474.
22. Loeffler, I. and Wolf, G. (2015) Epithelial-to-Mesenchymal Transition in Diabetic Nephropathy: Fact or Fiction? *Cells*, **4**, 631–652.
23. Kalluri, R. and Weinberg, R.A. (2009) The basics of epithelial-mesenchymal transition. *J. Clin. Invest.*, **119**, 1420–1428.
24. Liu, Y. (2010) New insights into epithelial-mesenchymal transition in kidney fibrosis. *J. Am. Soc. Nephrol.*, **21**, 212–222.
25. Ghosh, A.K. and Vaughan, D.E. (2012) PAI-1 in tissue fibrosis. *J. Cell. Physiol.*, **227**, 493–507.
26. Lenna, S. and Trojanowska, M. (2012) The role of endoplasmic reticulum stress and the unfolded protein response in fibrosis. *Curr. Opin. Rheumatol.*, **24**, 663–668.
27. Tanjore, H., Lawson, W.E. and Blackwell, T.S. (2013) Endoplasmic reticulum stress as a pro-fibrotic stimulus. *Biochim. Biophys. Acta*, **1832**, 940–947.
28. Kanasaki, K., Taduri, G. and Koya, D. (2013) Diabetic nephropathy: the role of inflammation in fibroblast activation and kidney fibrosis. *Front. Endocrinol.*, **4**, 7.
29. Jha, J.C., Gray, S.P., Barit, D., Okabe, J., El-Osta, A., Namikoshi, T., Thallas-Bonke, V., Wingler, K., Szyndralewiez, C., Heitz, F., *et al.* (2014) Genetic targeting or pharmacologic inhibition of NADPH oxidase nox4 provides renoprotection in long-term diabetic nephropathy. *J. Am. Soc. Nephrol.*, **25**, 1237–1254.

Downloaded from https://academic.oup.com/hmg/article-abstract/25/17/3784/2525836/Progressive-development-of-renal-cysts-in-glycogen
by guest
on 18 September 2017

30. Yiu, W.H., Mead, P.A., Jun, H.S., Mansfield, B.C. and Chou, J.Y. (2010) Oxidative stress mediates nephropathy in type Ia glycogen storage disease. *Lab. Investig. J. Tech. Methods Pathol.*, **90**, 620–629.
31. Richter, K., Konzack, A., Pihlajaniemi, T., Heljasvaara, R. and Kietzmann, T. (2015) Redox-fibrosis: Impact of TGFβ1 on ROS generators, mediators and functional consequences. *Redox Biol.*, **6**, 344–352.
32. Hojs, R., Ekart, R., Bevc, S. and Hojs, N. (2015) Biomarkers of Renal Disease and Progression in Patients with Diabetes. *J. Clin. Med.*, **4**, 1010–1024.
33. Bolignano, D., Coppolino, G., Campo, S., Aloisi, C., Nicocia, G., Frisina, N. and Buemi, M. (2007) Neutrophil gelatinase-associated lipocalin in patients with autosomal-dominant polycystic kidney disease. *Am. J. Nephrol.*, **27**, 373–378.
34. Paragas, N., Nickolas, T.L., Wyatt, C., Forster, C.S., Sise, M., Morgello, S., Jagla, B., Buchen, C., Stella, P., Sanna-Cherchi, S., *et al.* (2009) Urinary NGAL marks cystic disease in HIV-associated nephropathy. *J. Am. Soc. Nephrol.*, **20**, 1687–1692.
35. Yuan, Y., Xu, X., Zhao, C., Zhao, M., Wang, H., Zhang, B., Wang, N., Mao, H., Zhang, A. and Xing, C. (2015) The roles of oxidative stress, endoplasmic reticulum stress, and autophagy in aldosterone/mineralocorticoid receptor-induced podocyte injury. *Lab. Investig. J. Tech. Methods Pathol.*, **95**, 1374–1386.
36. Wang, T.N., Chen, X., Li, R., Gao, B., Mohammed-Ali, Z., Lu, C., Yum, V., Dickhout, J.G. and Krepinsky, J.C. (2015) SREBP-1 Mediates Angiotensin II-Induced TGF-β1 Upregulation and Glomerular Fibrosis. *J. Am. Soc. Nephrol.*, **161**, 99–107.
37. Bobulescu, I.A. (2010) Renal lipid metabolism and lipotoxicity. *Curr. Opin. Nephrol. Hypertens.*, **19**, 393–402.
38. Murea, M., Freedman, B.I., Parks, J.S., Antinozzi, P.A., Elbein, S.C. and Ma, L. (2010) Lipotoxicity in diabetic nephropathy: the potential role of fatty acid oxidation. *Clin. J. Am. Soc. Nephrol.*, **5**, 2373–2379.
39. Melis, D., Cozzolino, M., Minopoli, G., Balivo, F., Parini, R., Rigoldi, M., Paci, S., Dionisi-Vici, C., Burlina, A., Andria, G., *et al.* (2015) Progression of renal damage in glycogen storage disease type I is associated to hyperlipidemia: a multicenter prospective Italian study. *J. Pediatr.*, **166**, 1079–1082.
40. Toyama, T., Shimizu, M., Furuichi, K., Kaneko, S. and Wada, T. (2014) Treatment and impact of dyslipidemia in diabetic nephropathy. *Clin. Exp. Nephrol.*, **18**, 201–205.
41. Ryu, E.S., Kim, M.J., Shin, H.S., Jang, Y.H., Choi, H.S., Jo, I., Johnson, R.J. and Kang, D.H. (2013) Uric acid-induced phenotypic transition of renal tubular cells as a novel mechanism of chronic kidney disease. *Am. J. Physiol. Renal Physiol.*, **304**, F471–F480.
42. Melis, D., Parenti, G., Gatti, R., Casa, R.D., Parini, R., Riva, E., Burlina, A.B., Vici, C.D., Di Rocco, M., Furlan, F., *et al.* (2005) Efficacy of ACE-inhibitor therapy on renal disease in glycogen storage disease type 1: a multicentre retrospective study. *Clin. Endocrinol. (Oxf.)*, **63**, 19–25.
43. Levey, A.S., Stevens, L.A., Schmid, C.H., Zhang, Y.L., Castro, A.F., Feldman, H.I., Kusek, J.W., Eggers, P., Van Lente, F., Greene, T., *et al.* (2009) A new equation to estimate glomerular filtration rate. *Ann. Intern. Med*, **150**, 604–612.

Downloaded from https://academic.oup.com/hmg/article-abstract/25/17/3784/2525836/Progressive-development-of-renal-cysts-in-glycogen
by guest
on 18 September 2017

Supplemental Figure 1:

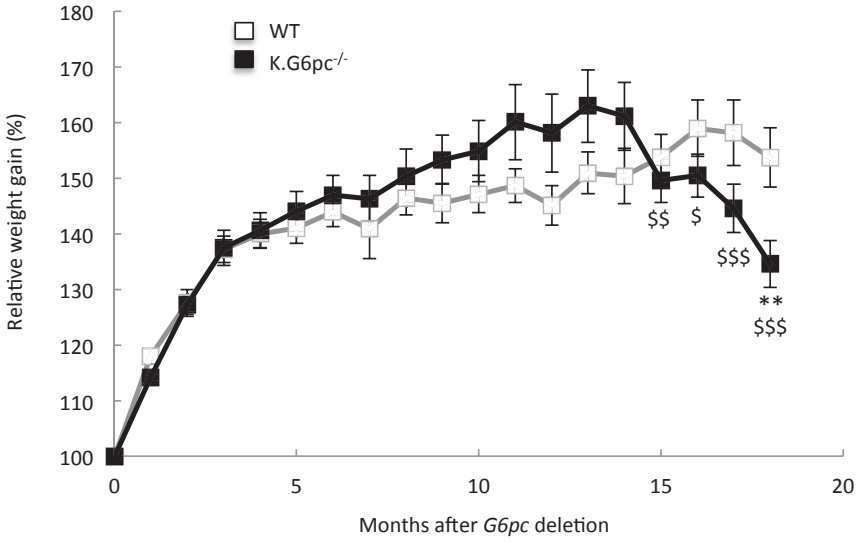

Figure S1: Relative weight gain of wild-type mice (white square) and K.G6pc$^{-/-}$ mice (black square) after the tamoxifen treatment (T=0). Data are expressed as the mean ± s.e.m. Significant differences between WT and K.G6pc$^{-/-}$ mice are indicated as **, $p<0.01$. Significant differences between the weight of 14 month-aged K.G6pc$^{-/-}$ mice and older K.G6pc$^{-/-}$ mice are indicated as $$, $p<0.01$ and $$$, $p<0.001$.

Supplemental Figure 2:

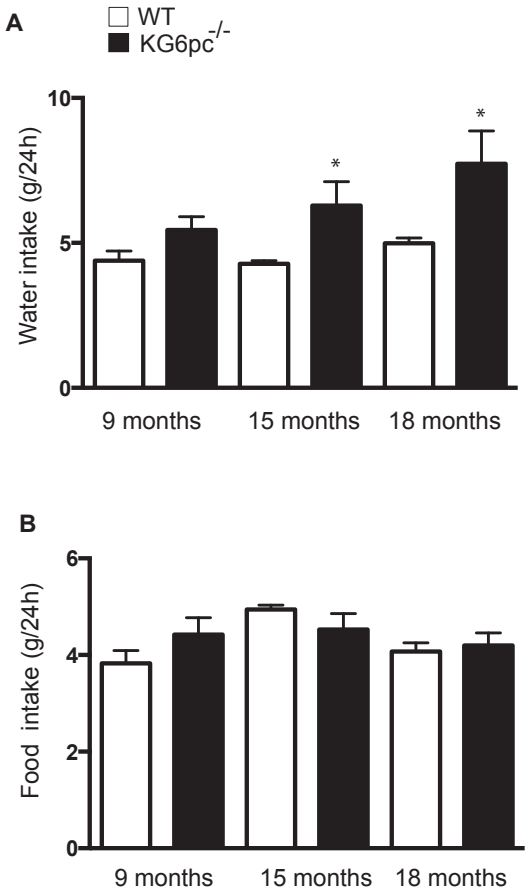

Figure S2: Water intake (A) and food intake (B) of WT (white bars) and K.G6pc$^{-/-}$ (black bars) mice at 9, 15 and 18 months after tamoxifen treatment. Parameters were measured on individual mice during 24h. n=5-7 mice. Significant differences between WT and K.G6pc$^{-/-}$ mice are indicated as *, $p<0.05$. Groups were compared using two-way ANOVA followed by Tukey's *post hoc* test.

Supplemental Figure 3:

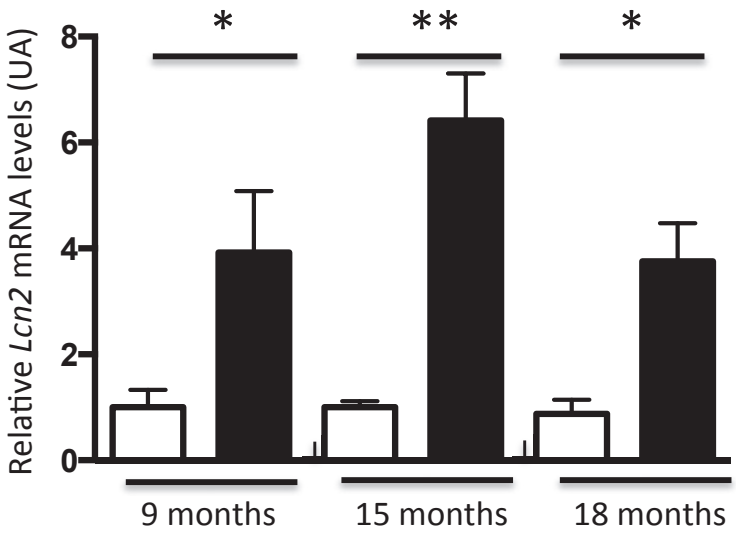

Figure S3: Lipocalin 2 expression in the kidneys of WT (black circle) and K.G6pc$^{-/-}$ (white circle) mice at 9, 15 and 18 months after tamoxifen treatment. The expression of Lcn 2 mRNA in K.G6pc$^{-/-}$ mice was expressed relatively to WT mice. N=5-8. Data are expressed as the mean ± s.e.m. Significant differences between WT and K.G6pc$^{-/-}$ mice are indicated as *, $p<0.05$ and **, $p<0.01$. Groups were compared using two-way ANOVA followed by Tukey's *post hoc* test.

Supplemental Figure 4:

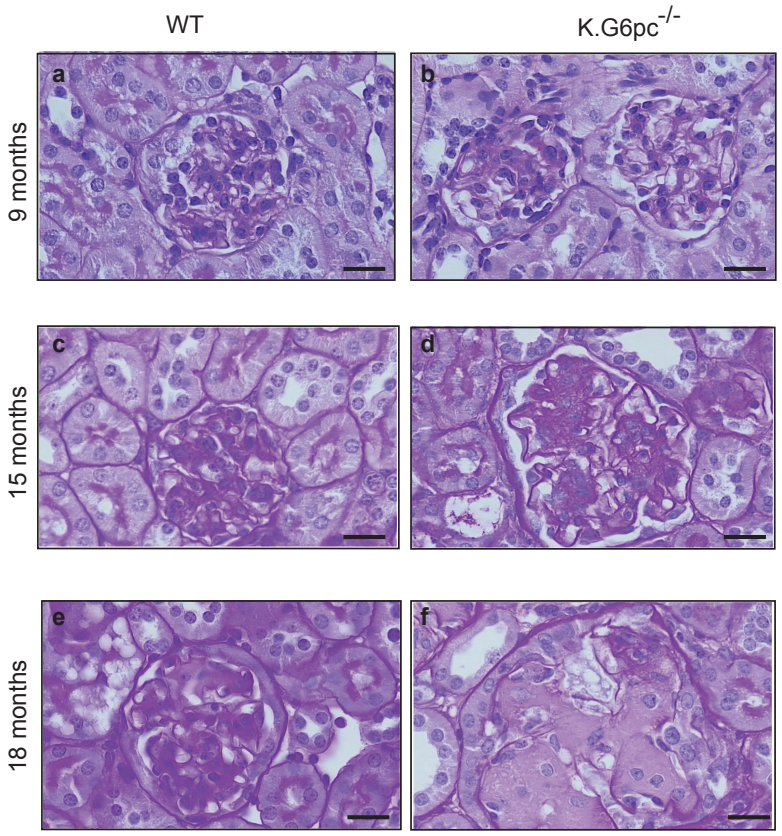

Figure S4: Structure of glomeruli of WT and K.G6pc$^{-/-}$ kidneys. PAS-stained kidneys from WT (a, c, e) and K.G6pc$^{-/-}$ (b, d, f) mice at 9, 15 and 18 months after tamoxifen treatment. Scale bars = 20 µm.

Supplemental Figure 5:

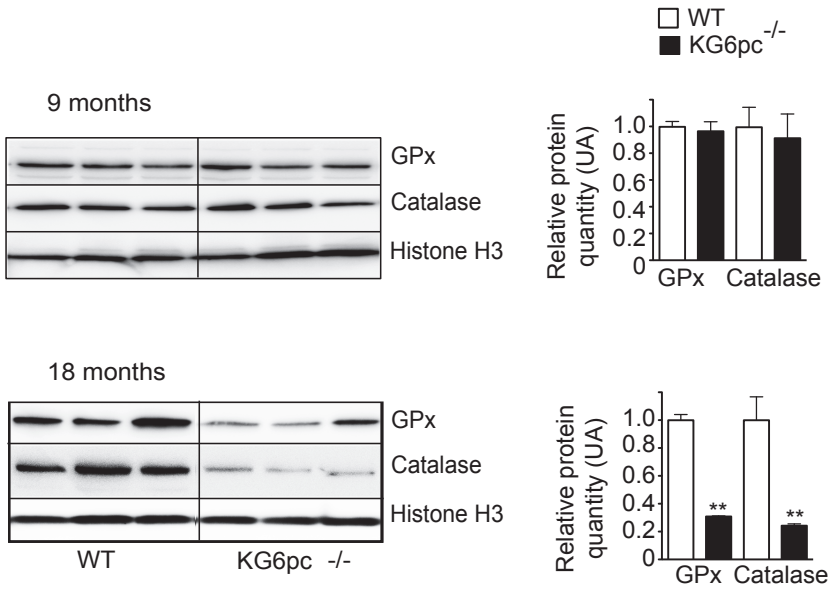

Figure S5: Decrease in the quantity of antioxidant enzymes in the kidneys of WT and K.G6pc$^{-/-}$ mice at 9, 15 and 18 months after tamoxifen treatment. Representative western blot of GPx, Catalase and Histone H3 (referent protein) were shown on the left. Quantification analyses of western blot, shown on the right, were performed by densitometry (t-student test). Data are expressed as the mean ± s.e.m. Significant differences between WT mice and K.G6pc$^{-/-}$ mice are indicated as **, $p<0.01$.

Supplemental Figure 6:

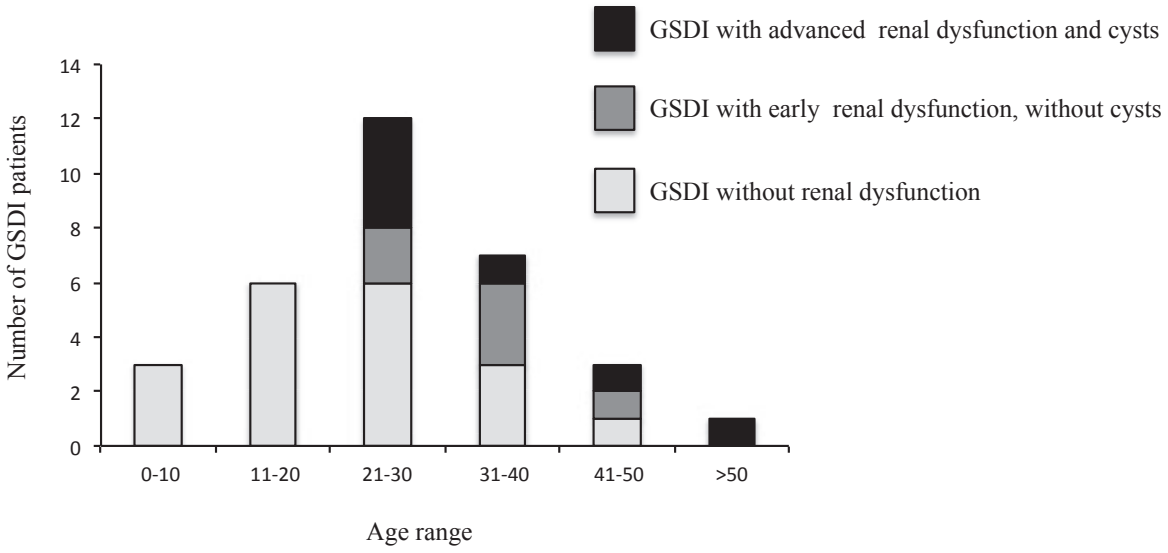

Figure S6: Prevalence of renal dysfunction and cyst development in GSDI patients at different ages.

Supplemental Table 1: Urinary parameters of wild-type and K-G6pc$^{-/-}$ mice after 9, 15 and 18 months of *G6pc* deletion.

	9 months		15 months		18 months	
	WT	K.G6pc-/-	WT	K.G6pc-/-	WT	K.G6pc-/-
Ca (µmol/24h)	2.1±0.2	3.0±0.2	1.1±0.1	3.8±0.6*	1.3±0.1	6.5±2.0**
Cl (µmol/24h)	493±21	664±107	259±27	380±26	242±26	333±37
Mg (µmol/24h)	35.5±4.1	57.6±4.0	34.6±4.9	50.3±3.0	41.8±4.8	53.9±6.7
P (µmol/24h)	86±12	96±9	75±10	108±5	60±9	101±15
K (µmol/24h)	387±22	564±39**	331±35	502±32**	360±29	526±30***
Na (µmol/24h)	285±32	388±25	199±22	334±25	181.4±2	288±402
citrate (µmol/24h)	47±5	74±14*	33±4	76±11**	ND	ND
oxalate (µmol/24h)	1.9±0.1	1.6±0.1	1.4±0.1	1.6±0.1	ND	ND

Data were obtained from mouse urine samples collected during 24h using a metabolic cage and are expressed as the mean ± SEM (n = 7-8 mice in each group). Significant differences between WT and K-G6pc$^{-/-}$ mice are indicated ($p<0.05$*, $p < 0.01$**, $p<0.001$***). ND: not determined. Groups were compared using two-way ANOVA followed by Tukey's *post hoc* test.

Supplemental Table 2: Oligodeoxyribonucleotide primer sequences for qPCR.

Name of gene	Forward sequence	Reverse sequence
Agt	TTCACTGCTCCAGGCTTTCGTCTA	TTCTCAGTGGCAAGAACTGGGTCA
Col1a1	GCTCCTCTTAGGGGCCACT	CCACGTCTCACCATTGGGG
Cdh1	CTCCAGTCATAGGGAGCTGTC	TCTTCTGAGACCTGGGTACAC
Fn1	TGGCTGCCTTCAACTTCTCCT	TGTTTGATCTGGACTGGCAGTTT
mL19	GGTGACCTGGATGAGAAGGA	TTCAGCTTGTGGATGTGCTC
Pai1	TTCAGCCCTTGCTTGCCTC	ACACTTTTACTCCGAAGTCGGT
Tgfb1	CAACAATTCCTGGCGTTACCTTGG	GAAAGCCCTGTATTCCGTCTCCTT
Tnfa	AGGCTGCCCCGACTACGT	GACTTTCTCCTGGTATGAGATAGCAAA
Vim	CGGCTGCGAGAGAAATTGC	CCACTTTCCGTTCAAGGTCAAG

Chapter III – The role of lipids in hepatic and renal complications in GSDI

GSDI is a disease whose most characteristic feature is excessive glycogen accumulation. Nevertheless, it is also characterized by hepatic steatosis, due to strong activation of lipid synthesis and a decrease in lipid oxidation (Bandsma et al., 2008, 2014; Derks and van Rijn, 2015; Mutel et al., 2011a). Strong lipid accumulation is known to induce hepatic injury and even tumor development, as observed in diabetic and obese patients (Alkhouri et al., 2009; Baffy, 2013; Baffy et al., 2012; El-Serag et al., 2006). Similarly, GSDI kidneys present strong lipid accumulation also due to increased lipid synthesis and decreased lipid oxidation (Clar et al., 2014; Rajas et al., 2015). Thus lipids were suggested to play an important role in GSDI hepatic and renal pathologies, yet this role was never fully dissociated from the negative effects of excessive glycogen.

To highlight the role of lipids in GSDI hepatic and renal complications, L.G6pc-/- and K.G6pc-/- mice were submitted to a HF/HS diet, in order to exacerbate lipid accumulation in the liver and the kidneys, respectively. Interestingly, increased lipid content led to further injury in both organs, even though glycogen levels remained unchanged in the liver and even decreased in the kidneys.

On the other hand, we studied liver and kidney injury in L.G6pc-/- and K.G6pc-/- mice treated with a lipid-lowering drug, fenofibrate. Fenofibrate is a pharmacological agonist of PPARα which is the main activator of lipid oxidation (Balfour et al., 1990; Montagner et al., 2016). As expected, we observed an increase in lipid oxidation in L.G6pc-/- livers and K.G6pc-/- kidneys, illustrated by the marked increase in PPARα and its target genes. Furthermore, PPARα activation by fenofibrate led to an increase in lipid synthesis. This indicated an increase in lipid turnover in both the liver and the kidneys, resulting in normalization of hepatic and renal lipid content. Interestingly, since lipid turnover was increased, G6P accumulated in the cell was diverted from glycogen metabolism to the lipid metabolism, resulting in a decrease in glycogen synthesis. Therefore, glycogen levels were normalized in L.G6pc-/- livers of mice treated with fenofibrate, and were drastically decreased in the kidneys of K.G6pc-/- mice treated with fenofibrate.

Finally, a decrease in lipids accumulated in the liver of L.G6pc-/- mice led to the decrease of hepatic injury markers, normalization of the histology of the liver and a

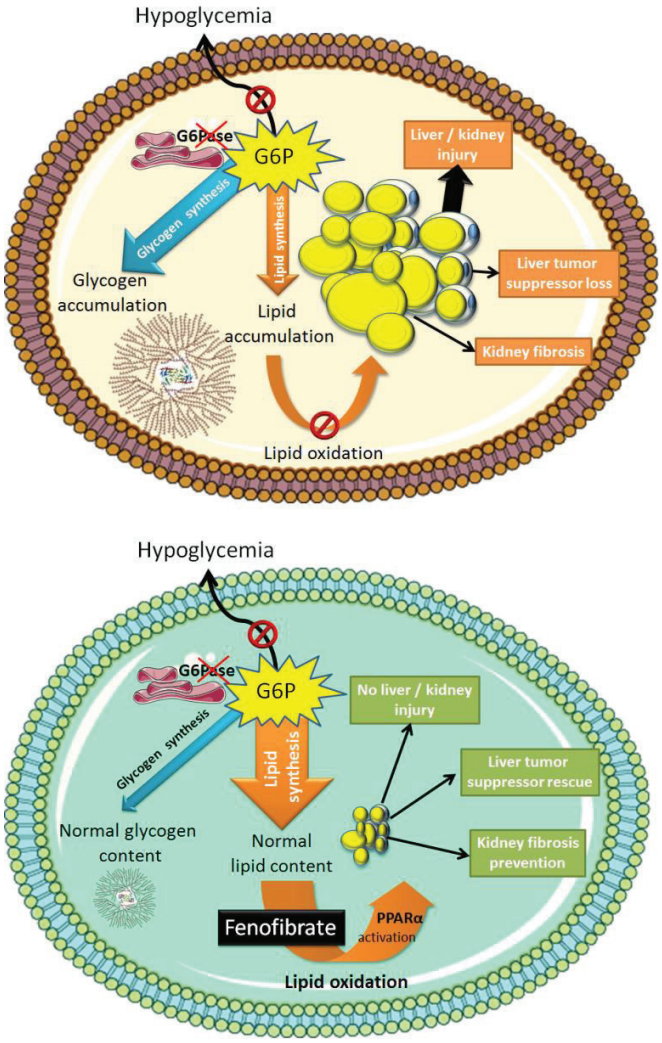

Figure 66: Schematic representation of GSDI metabolism with or without fenofibrate-mediated PPARα activation

In non-treated GSDI hepatocytes and renal tubular cells the loss of glucose-6 phosphatase (G6Pase) stimulates glucose-6 phosphate (G6P) accumulation leading to a subsequent activation of glycogen and lipid synthesis. These result in strong glycogen and lipid accumulation, respectively, and lipid accumulation is further promoted by lipid oxidation inhibition. Thus lipid accumulation results in liver / kidney injury, liver tumor suppressor loss and kidney fibrosis. Fenofibrate-induced lipid oxidation increases the turnover of lipids in the cell and results in decreased lipid accumulation, as well as subsequent decrease in liver and kidney injury. Furthermore, excessive G6P is diverted from glycogen synthesis toward lipid metabolism, resulting in a decrease of glycogen synthesis and accumulation.

(Monteillet*, Gjorgjieva* et al., submitted; *co-authors)

restoration of tumor suppressor gene expression. Moreover, decreased renal lipid content led to a normalization of renal function parameters, an inhibition of the pro-fibrotic RAS / TGF-β1 pathway and a subsequent prevention of fibrosis development in K.G6pc-/- mice.

In conclusion, while we cannot exclude glycogen and other hepatic and renal alterations as potential triggers in organ injury, lipids seem to have a key role in the development of these pathologies. Thus maintaining quasi-normal lipid levels in GSDI through dietary therapy management and / or with lipid-lowering drugs is a crucial strategy to avoid premature development of GSDI long-term complications (*Figure 66*).

Lipid burden alleviation – a common target to prevent hepatic and renal complications in Glycogen Storage Disease type Ia

Laure Monteillet[1-3,5], Monika Gjorgjieva[1-3,5], Marine Silva[1-3], Vincent Verzieux[1-3], Linda Imikirene[1-3], Adeline Duchampt[1-3], Hervé Guillou[4], Gilles Mithieux[1-3], Fabienne Rajas*[1-3]

[1]Institut National de la Santé et de la Recherche Médicale, U1213, Lyon, F-69008, France

[2]Université de Lyon, Lyon, F-69008 France

[3]Université Lyon1, Villeurbanne, F-69622 France

[4] Toxalim, Université de Toulouse, INRA, ENVT, INP-Purpan, UPS, Toulouse 31027, France.

[5]These authors contributed equally

Address for correspondence: *Dr. Gilles Mithieux

Inserm U1213, Université Lyon 1 Laennec

7 rue Guillaume Paradin, 69372 Lyon cedex 08 France

Tel: +33 478 77 10 28 / Fax: +33 478 77 87 62

E-mail: fabienne.rajas@univ-lyon1.fr

Running title: Fenofibrate effects in GSDI pathology.

Word count of the abstract: 148

Word count of the text: 7600

SUMMARY

Glycogen storage disease type I (GSDI) is a genetic disease, characterized by excessive glycogen and lipid accumulation in the liver and kidneys. These metabolic perturbations lead to long-term complications, i.e. non-alcoholic fatty liver disease (NAFLD) and chronic kidney disease (CKD). Here, we show the central role of ectopic lipids in the development of liver injury and CKD. Exacerbated lipid accumulation upon high-calorie diet strongly accelerated hepatic and renal pathologies in mouse models of GSDI, while glycogen contents remained unchanged in the liver or even decreased in the kidneys. Interestingly, the activation of lipid oxidation by a PPARα-agonist led to decreased lipid accumulation and prevented the development of NAFLD and CKD. In addition, inducing lipid turnover redirected glucose metabolism, resulting in decreased glycogen synthesis. To conclude, our study highlights the crucial role that lipids play in hepatic and renal GSDI pathologies, demonstrating the importance of lipid-lowering treatments in GSDI.

Key words: metabolic disease, steatosis, non-alcoholic fatty liver disease, chronic kidney disease, glycogen, glucose and lipid metabolism, fenofibrate, PPARα, fibrosis.

INTRODUCTION

Lipid accumulation in non-adipose tissues can induce organ damage and dysfunction (Schaffer, 2003). Abnormal lipid content observed in many metabolic diseases, such as non-alcoholic fatty liver disease (NAFLD), diabetes and obesity, is responsible for cell injury, inflammation, necrosis and activation of pathological pathways, due to lipotoxicity (Asrih and Jornayvaz, 2013; Park et al., 2010; Streba et al., 2015).

The ectopic accumulation of lipid droplets in the liver and kidneys is an important feature of a rare disease named Glycogen Storage Disease type I (GSDI) (Gjorgjieva et al., 2016a; Mutel et al., 2011). GSDI is due to glucose-6 phosphatase (G6Pase) deficiency, leading to severe hypoglycemia during short fasts (Chou, 2001; Froissart et al., 2011; Kishnani et al., 2014). G6Pase operates the hydrolysis of glucose-6 phosphate (G6P) in glucose, and it allows the liver and kidneys, the main organs responsible for endogenous glucose production, to release glucose in the blood and regulate plasma glucose concentration (Soty et al., 2017), Mutations in the gene encoding the catalytic subunit of G6Pase (G6PC) are responsible for GSD type Ia and mutations in *SLC37A4,* encoding the glucose-6 phosphate translocase (G6PT), result in GSD type Ib (Bruni et al., 1999; Lei et al., 1995). The lack of G6Pase induces G6P accumulation in the liver and kidneys, leading to metabolic reprogramming in these organs (Gjorgjieva et al., 2016b). The first consequence of G6P increase is abnormal accumulation of glycogen in both organs (Clar et al., 2014; Kishnani et al., 2014; Mutel et al., 2011; Rake et al., 2002), which gives its name to the disease. However, the hepatic and renal lipid metabolism is also altered, characterized by an increase in *de novo* lipogenesis and fatty acid chain elongation, associated with a decrease in fatty

acid oxidation (Bandsma et al., 2008; Clar et al., 2014; Gjorgjieva et al., 2016a; Mutel et al., 2011; Rajas et al., 2013). Furthermore, a delay in the export of very low density lipoproteins (VLDL) has been reported in GSDI patients (Bandsma et al., 2008).

All of these phenomena lead to hepatic steatosis, characterized by a low-inflammatory state but no fibrosis in patients (Bandsma et al., 2014; Derks and van Rijn, 2015), as well as excessive lipid deposition in the kidney cortex (Clar et al., 2014). Interestingly, even in the absence of liver fibrosis, most adult patients with GSDI develop hepatocellular adenomas (HCA), which can later transform in hepatocellular carcinomas (HCC) (Calderaro et al., 2013; Labrune et al., 1997). Moreover, lipid deposition in the kidneys could play a major role in the development of a chronic kidney disease (CKD) in GSDI, as observed in diabetic CKD (Clar et al., 2014). Indeed, in both diabetes and GSDI, lipids are responsible for the induction of pro-fibrotic pathways, entailing renal fibrosis and in some cases renal failure (Gjorgjieva et al., 2016a; Rajas et al., 2013; Yiu et al., 2008). Thus almost 70% of young adult GSDI patients show first signs of CKD, i.e. microalbuminuria and glomerular hyperfiltration, which can progress to kidney failure with age (Froissart et al., 2011; Gjorgjieva et al., 2016a; Kishnani et al., 2014). Importantly, the extent to which glycogen and lipid accumulations are involved in the long-term GSDI complications remains unclear. Thereby, modulating the lipid content in both the liver and kidneys could reveal the degree of implication of lipids in the development of the hepatic and renal GSDI pathologies. Fenofibrate is a lipid-lowering drug, acting as an agonist of the Peroxisome Proliferator Activated Receptor α (PPARα), clinically used to treat dyslipidemia (Duval et al., 2007). PPARα regulates lipid catabolism by stimulating fatty acid transport, as well as lipid oxidation (Kersten, 2014;

Montagner et al., 2016; Pawlak et al., 2015). In mouse models of NAFLD, fenofibrate reduces hepatic steatosis and inflammation (Kostapanos et al., 2013a; Pawlak et al., 2015; van der Veen et al., 2017). Human data from large clinical trials on NAFLD are lacking. However, several studies reported that fenofibrate treatment leads to weight loss and improves vascular circulation in obese and/or diabetic patients (Kostapanos et al., 2013a; Najib, 2002). Interestingly, some studies in obese and/or diabetic patients have suggested renoprotective effects of fenofibrate, as illustrated by the prevention of nephropathy (Kostapanos et al., 2013b). Renal benefits of fenofibrate have also been suggested in *db/db* mice (Hong et al., 2014; Park et al., 2006) and high-fat diet induced obese mice (Sohn et al., 2017; Tanaka et al., 2011). Therefore, lowering ectopically accumulated lipids could be beneficial in a variety of metabolic diseases.

In order to elucidate the role of lipids in the development of hepatic and renal complications in GSDIa, we first investigated whether an exacerbation of lipid accumulation could accelerate liver and kidney injury in mouse models of GSDIa. Secondly, in the same mouse models, we examined whether lipid-lowering *via* fenofibrate could prevent or delay NAFLD and CKD. Previously, we developed two mouse models of GSDIa. L.G6pc-/- mice, in which *G6pc* was deleted specifically in the liver, develop all hallmarks of GSDIa hepatic NAFLD-like complications (Mutel et al., 2011). K.G6pc-/-mice, in which *G6pc* was deleted specifically in the kidneys, developed first signs of CKD after 6 months of *G6pc* deletion (Clar et al., 2014). Thus these two mouse models are ideally suited for unraveling the molecular mechanisms underlying hepatic and renal complications in GSDIa.

RESULTS

High fat / high sucrose diet aggravates ectopic lipid accumulation and exacerbates hepatic and renal complications in GSDIa mice

To elucidate the role of lipids in GSDIa hepatic and renal pathologies, we decided to exacerbate lipid accumulation in both the liver and kidneys of L.G6pc-/- and K.G6pc-/- mice with a high fat / high sucrose (HF/HS) diet. The progression of the hepatic and renal pathologies with the HF/HS diet was compared with L.G6pc-/- and K.G6pc-/- mice fed a standard diet. As previously observed, L.G6pc-/- mice fed a standard diet developed marked steatosis as indicated by elevated triglyceride (TG) content in the liver, while K.G6pc-/- mice exhibited a discrete TG accumulation in the kidneys (Fig.1A). As expected, hepatic and renal lipid accumulation was increased when L.G6pc-/- and K.G6pc-/- mice were fed a HF/HS diet, as illustrated by the significant increase in hepatic and renal TG contents (Fig.1A). Strikingly, HF/HS diet exacerbated liver injury and CKD that were characteristic of L.G6pc-/- and K.G6pc-/- mice, respectively (Fig.1B-D). Accordingly, assessment of liver injury markers showed a significant increase in plasmatic aspartate transaminase (AST) and alanine transaminase (ALT) activities in L.G6pc-/- mice fed a HF/HS diet, compared to a standard diet (Fig.1B). Nephropathy was also worsened by the HF/HS diet, since urinary excretion of albumin and lipocalin 2, two markers of renal injury, was higher than that observed in K.G6pc-/- fed a standard diet (Fig.1C). In accordance with the loss of renal function, marked fibrosis was observed in the kidneys of HF/HS-fed K.G6pc-/- mice, while fibrosis was more discrete in the kidneys of standard-fed K.G6pc-/- mice (Fig.1D). Interestingly, the worsening of hepatic injury and CKD was independent of glycogen content. Indeed, the hepatic glycogen content in L.G6pc-/-mice fed a HF/HS diet, although high compared to

WT mice, was similar to that observed in L.G6pc-/- mice fed a standard diet (Fig.1E). Moreover, renal glycogen content was drastically decreased in K.G6pc-/- mice fed a HF/HS diet, compared to K.G6pc-/- mice fed a standard diet (Fig.1E). These results suggest a critical role of ectopic lipid accumulation in the development of hepatic and renal pathologies in GSDIa, independently of glycogen storage.

Fenofibrate exerts a blood lipid-lowering effect in both L.G6pc-/- and K.G6pc-/- mice.

To further assess the role of lipids, L.G6pc-/- and K.G6pc-/- mice fed a standard diet were treated with a lipid-lowering drug fenofibrate. This treatment was initiated at 6 months after *G6pc* deletion, the starting point of the first signs of long-term hepatic (i.e. NAFLD) and renal (i.e. microalbuminuria) pathologies (Clar et al., 2014; Mutel et al., 2011), and was continued during 3 months.

The lipid-lowering effect of fenofibrate was confirmed by the assessment of several plasmatic parameters in L.G6pc-/- and K.G6pc-/- mice, compared to WT mice fed a standard diet. While hypertriglyceridemia was observed right after *G6pc* deletion in L.G6pc-/- mice (Mutel et al., 2011), plasmatic TG levels in L.G6pc-/- mice and K.G6pc-/- mice were similar to those in WT mice after 9 months of *G6pc* deletion (Table 1), as previously shown (Gjorgjieva et al., 2016a; Mutel et al., 2011). Nevertheless, the levels of plasmatic TG and non-esterified fatty acids (NEFA) were strongly reduced by fenofibrate (Table 1). Moreover, L.G6pc-/- and K.G6pc-/- mice showed a 20% decrease in body weight during fenofibrate treatment, compared to untreated mice (Table 1).

Taken together, these results confirmed the lipid-lowering effect of fenofibrate. Interestingly, cholesterol level in L.G6pc-/- mice was slightly increased under fenofibrate; this could be explained by the fact that fenofibrate is known to increase the synthesis of the HDL cholesterol (van der Hoogt et al., 2007). Furthermore, as expected, L.G6pc-/- mice exhibited hypoglycemia in the post-prandial state (6h-food deprivation), since they are unable to mobilize their glycogen stores (Mutel et al., 2011), and fenofibrate was not capable of normalizing this parameter (Table 1). K.G6pc-/- mice showed similar blood glucose as WT mice in the absence or presence of fenofibrate. Concomitantly, L.G6pc-/- and K.G6pc-/- mice had increased plasma ketone body concentration, which was further increased with fenofibrate. Finally, plasmatic uric acid concentration, which was slightly increased in K.G6pc-/- mice compared to WT, was further increased with fenofibrate and had a tendency to increase in fenofibrate-treated L.G6pc-/- mice (Table 1).

Fenofibrate normalizes hepatic and renal triglycerides in L.G6pc-/- and K.G6pc-/- mice

Next, lipid metabolism in GSDIa liver and GSDIa kidneys was analyzed to characterize the lipid-lowering effect of fenofibrate in these organs. As expected, lipid catabolism was strongly induced in both L.G6pc-/- livers and K.G6pc-/- kidneys after the treatment with fenofibrate, compared to untreated L.G6pc-/- and K.G6pc-/- mice, respectively. Indeed, we observed a marked PPARα increase in the liver of L.G6pc-/- mice treated with fenofibrate (Fig.2A), associated with a restoration of *Ppara* gene expression (Fig.2B). Concomitantly, a strong increase in the expression of several

genes implicated in lipid catabolism, such as carnitine palmitoyltransferase 1a (*Cpt1a*), fatty acid binding protein 1 (*Fabp1*), acyl-CoA oxidase 1 (*Acox1*), acyl-CoA dehydrogenase long-chain (*Acadl*), cytochrome P450 4A10 (*Cyp4a10*) and cytochrome P450 4A14 (*Cyp4a14*) was observed in the fenofibrate-treated L.G6pc-/- livers (Fig.2B). In addition, the expression of *Fgf21*, a well-known hepatokine up-regulated by PPARα (Badman et al., 2007), was highly increased by fenofibrate, confirming, once again, the efficiency of the treatment. Furthermore, in the kidneys of K.G6pc-/- mice treated with fenofibrate, we observed a normalization of PPARα protein levels, the latter being decreased in untreated K.G6pc-/- mice (Fig.2C). Thereby, PPARα increase was accompanied with a rise in the expression of *Fabp1*, *Cyp4a10* and *Cyp4a14* (Fig.2D), resulting in a marked activation of renal lipid catabolism.

Since pharmacological activation of PPARα has also been shown to promote the expression of lipogenic genes (Montagner et al., 2016; Oosterveer et al., 2009), we analyzed the expression of the key enzymes of *de novo* lipogenesis. In the liver of L.G6pc-/- mice and in the kidneys of K.G6pc-/- mice treated with fenofibrate, we observed a high increase in fatty acid synthase (*Fasn*) and fatty acid elongase 6 (*Elovl6*), while both enzymes were already up-regulated in untreated KO-mice, compared to WT mice (Fig.3A and B). The expression of stearoyl-CoA desaturase-1 (*Scd1*) was also increased after fenofibrate treatment (Fig.3A and B). Concomitantly, an increase in the expression of 3-Hydroxy-3-Methylglutaryl-CoA Synthase 2 (*Hmgcs2*), a key enzyme in ketogenesis, was observed with the fenofibrate treatment in both L.G6pc-/- and K.G6pc-/- mice (Fig.3A and B), in accordance with the increased plasmatic ketone body levels (Table 1). The rise in the expression of genes involved in

de novo fatty acid synthesis in L.G6pc-/- fenofibrate-treated livers might be mediated *via* the Carbohydrate-responsive element-binding protein (ChREBP). Indeed, the expression of its total and β isoform mRNA was increased in L.G6pc-/- livers treated with fenofibrate, compared to untreated L.G6pc-/- liver, while sterol regulatory element-binding protein 1c (*Srebp1c*) and *Srebp2* expression remained unchanged (Fig.2A). On the other hand, lipid synthesis in K.G6pc-/- fenofibrate-treated kidneys might be mediated *via* SREBP1c, since fenofibrate significantly decreased the expression of the total *Chrebp* and *Chrebpb* mRNA in K.G6pc-/- kidneys, whereas it slightly increased *Srebp1* expression, and normalized *Srebp2* expression (Fig.3B).

Interestingly, this increase in lipid anabolism did not induce further hepatic and renal lipid accumulation. Indeed, we observed a normalization of TG content in the liver of L.G6pc-/- mice treated with fenofibrate, compared to untreated L.G6pc-/- mice, which exhibited severe hepatic steatosis (Fig.3C). In the kidneys, TG content had a tendency to decrease in K.G6pc-/- fenofibrate-treated mice and was similar to that of WT mice (Fig.3D).

In conclusion, these data suggest a stimulation of lipid turnover by fenofibrate, resulting in a normalization of lipid content in both the liver and kidneys of GSDIa mice.

Fenofibrate decreases glycogen synthesis and prevents hepatic and renal glycogen accumulation

As the modifications of lipid metabolism could have an impact on the whole cell energy homeostasis, we next assessed glycogen metabolism in GSDIa liver and kidneys. Interestingly, L.G6pc-/- mice presented excessive glycogen accumulation in the liver, while fenofibrate-treated L.G6pc-/- mice exhibited normalized hepatic glycogen content (Fig.4A). In accordance, L.G6pc-/- mice treated with fenofibrate showed a decrease in serine 9 phosphorylation of glycogen synthase kinase 3β (GSK3β), which is known to decrease glycogen synthase activity, thereby decreasing glycogen synthesis (Fig.4B). In addition, glycogen debranching enzyme (AGL), which was increased in untreated L.G6pc-/- mice, was normalized with fenofibrate, suggesting a decrease in glycogen degradation (Fig.4B). These results indicated that the decrease in glycogen content in fenofibrate-treated L.G6pc-/- livers was probably due to a decrease in glycogen synthesis, rather than an increase in degradation. Moreover, hepatic glucose content, which was already decreased in L.G6pc-/- mice compared to WT, was further decreased in fenofibrate-treated L.G6pc-/- mice (Fig.4C). Glucose transporter 1 (*Slc2a1*) expression was decreased in L.G6pc-/- mice treated with fenofibrate, compared to untreated L.G6pc-/- mice, while glucose transporter 2 (*Slc2a2*) expression remained unchanged (Fig.4D). As previously observed, glucokinase (*Gck*) expression was decreased in L.G6pc-/- mice (Hijmans et al., 2017). Interestingly, *Gck* expression was further decreased with fenofibrate (Fig.4D). Thus these results suggest a decrease in hepatic glucose uptake and phosphorylation, in accordance with the decrease in hepatic glucose levels and in glycogen synthesis. Finally, hepatomegaly, which was

observed in L.G6pc-/- mice, was further aggravated with fenofibrate (Fig.4E), probably due to the proliferation of peroxisomes (observed by transmission electronic microscopy in Fig.6B, panel c) induced by PPARα activation in rodents (Balfour et al., 1990; Oosterveer et al., 2009) (Fig.3E).

As observed in L.G6pc-/- livers, K.G6pc-/- kidneys presented excessive glycogen content, which was drastically decreased after fenofibrate treatment (Fig.4F). This was associated with a decrease in both glycogen synthesis and degradation, as illustrated by the decrease in phospho-GSK3β at Ser9 and AGL levels (Fig.4G). Renal glucose content was lower in K.G6pc-/- mice than in WT mice and was further decreased after fenofibrate treatment (Fig.4H). This was consistent with concomitant decrease in glucose uptake and phosphorylation, highlighted *via* the decreased expression in glucose transporters Slc2a1 and Slc2a2a and in hexokinase enzyme (HK) (Fig.4I). As observed in the liver, these data suggest that the decrease in uptake and phosphorylation of glucose results in a decrease in glycogen synthesis. Interestingly, the decrease in glycogen accumulation in the fenofibrate-treated kidneys was associated with a decrease in nephromegaly, which is a hallmark of GSDIa (Fig.4J).

Fenofibrate treatment prevents nephropathy development in K.G6pc-/- mice

In order to investigate whether the decrease in renal lipid content had an effect on the nephropathy development, renal structure and function were assessed. As mentioned before, K.G6pc-/- mice developed first signs of CKD, i.e. microalbuminuria, associated with an increase in urine excretion and renal expression of lipocalin 2 (Fig.5A and B). In addition, urea and uric acid excretions were slightly increased in

K.G6pc-/- mice. Interestingly, renal function was normalized after fenofibrate treatment in K.G6pc-/- mice, since we observed a concomitant decrease in albumin, lipocalin 2, urea and uric acid excretion (Fig.5A and B). This was in accordance with histological observations of the kidneys. Indeed, H&E staining of K.G6pc-/- kidneys showed a strong tubular clarification due to lipid and glycogen accumulation in the proximal tubules (Fig.5C panel b). Furthermore, strong collagen accumulation was observed owing to Trichrome Masson's staining, confirming the development of fibrosis (Fig.5C panel e). On the contrary, histology features of fenofibrate-treated K.G6pc-/- kidneys (Fig.5C panel c) were similar to those in WT mice (Fig.5C panel a). In addition, fibrosis was significantly decreased and even nearly absent in the presence of fenofibrate (Fig.5C, panel f).

As CKD was prevented in K.G6pc-/- mice treated with fenofibrate, we analyzed molecular mechanisms behind GSDIa nephropathy, which were characterized in previous studies (Clar et al., 2014; Gjorgjieva et al., 2016a). In K.G6pc-/- mice, the Renin-Angiotensin system (RAS) was induced, which in turn increased *Tgf-β1* expression, responsible for the activation of the epithelial-mesenchymal transition (EMT) and subsequent fibrosis development. Here, renal angiotensinogen (*Agt*) expression was significantly decreased in fenofibrate-treated K.G6pc-/- mice, compared to untreated K.G6pc-/- mice (Fig.5D). Consequently, *Tgf-β1* expression was normalized with fenofibrate, indicating a decrease in RAS/TGF-β1 signaling. This result was confirmed with the decrease in EMT. Indeed, the expression of the epithelial markers E-cadherin and β–catenin, which was decreased in untreated K.G6pc-/- kidneys, was restored with fenofibrate (Fig.5D). Furthermore, the expression of the mesenchymal

markers vimentin (*Vim*), fibronectin (*Fn1*), α-smooth muscle actin 2 (*Acta2*) and plasminogen activator inhibitor 1 (*Pai1*), which was increased in K.G6pc-/- kidneys, was significantly reduced with the fenofibrate treatment (Fig.5D).

In conclusion, these results strongly suggest that fenofibrate down-regulated the RAS/TGF-β1 pathway of signalization, subsequently inhibiting the EMT process. This inhibition markedly prevents renal fibrosis and thereby maintains the integrity of renal function.

Liver injury is prevented by fenofibrate in L.G6pc-/- mice

As hepatic steatosis was markedly decreased by fenofibrate in L.G6pc-/- livers, liver structure and function were further characterized. Histological analyses confirmed a marked accumulation of lipid droplets and glycogen in L.G6pc-/- livers (Fig.6A and B; panels b and e), which was strongly reduced with the fenofibrate treatment (Fig.6A and B; panels c and f). Furthermore, TEM revealed a large reduction in the size of the lipid vesicles in the livers of fenofibrate-treated L.G6pc-/- mice (Fig.6B panel c), compared to untreated L.G6pc-/- mice (Fig.6B panel b). This observation was in accordance with the increase in Perilipin 2 (*Plin2*), an important factor in small lipid droplet formation, in the livers of L.G6pc-/- mice treated with fenofibrate (Fig.6C). Interestingly, we observed donut-shaped mitochondria (indicator of cellular stress) in the livers of L.G6pc-/- mice (Fig.6B panel e) that were observed neither in WT (Fig. 6B panel d), nor in fenofibrate-treated L.G6pc-/- livers (Fig. 6B panel f).

Finally, fenofibrate treatment allowed the normalization of liver injury markers, i.e. AST and ALT activities, compared to untreated L.G6pc-/- mice (Fig. 6D). Furthermore,

previous studies showed that the metabolic reprogramming occurring in GSDIa livers, as a consequence of the excessive G6P levels, promotes hepatic tumorigenesis (Calderaro et al., 2013; Gjorgjieva et al., 2016b). Recent data have shown a decrease in tumor suppressors in L.G6pc-/- livers (unpublished data), in accordance with the pre-neoplastic status of G6pc-/- hepatocytes (Gjorgjieva et al., 2016b). Interestingly, several tumor suppressors, such as AMP-activated protein kinase (AMPK) and phosphatase and tensin homolog (PTEN) were down-regulated in L.G6pc-/- livers, while fenofibrate restored the their expression to the level observed in WT mice (Fig.6E).

To conclude, these data suggest that the normalization in hepatic lipid content in L.G6pc-/- mice results in the restoration of liver function and rescue of tumor suppressor expression.

DISCUSSION

GSDI is a pathology characterized by abnormal lipid and glycogen accumulation, specifically in the liver and kidneys, leading to hepatic tumor development and CKD with age. The deficiency in G6Pase and the subsequent G6P accumulation in hepatocytes and renal proximal tubules is at the origin of an important metabolic remodeling (Calderaro et al., 2013; Gjorgjieva et al., 2016b; Rajas et al., 2007). Indeed, the accumulation of G6P, a common substrate for both lipid and glycogen synthesis, markedly induces these anabolic pathways in GSDI. Interestingly, in GSDIa mouse models and patients, excessive lipid accumulation is caused by an increase in *de novo* lipogenesis and an impairment of fatty acid oxidation, which is characterized by a significant decrease in PPARα in both the liver and kidneys (Abdul-Wahed et al., 2014;

Bandsma et al., 2008; Clar et al., 2014; Mutel et al., 2011). Until now, the degree of contribution of lipids in GSDIa pathology was a subject of speculation. In this study, we demonstrate that excessive ectopic lipid accumulation in the liver and kidneys is a major contributor in the development of long-term complications, i.e. NAFLD and CKD, independently of glycogen content. Furthermore, our results indicate an important induction in lipid turnover by chronic activation of PPARα *via* fenofibrate. This leads to a normalization of glycogen stores by remodeling the carbohydrate metabolism through the availability of the intermediary substrate G6P. Thus increasing lipid oxidation and consequently lipid turnover appears to be an original option to prevent both the hepatic and renal GSDIa complications.

Submitting L.G6pc-/- mice and K.G6pc-/- mice to a HF/HS diet exacerbated the hepatic and renal lipid accumulations, whereas glycogen content was not increased in the liver and even decreased in the kidneys. Nevertheless, both chronic hepatic and renal pathologies were strongly aggravated, suggesting an important role of lipids in the induction of GSDIa long-term complications, independently of glycogen content.

The central role of lipids was confirmed by decreasing ectopic lipid accumulation using fenofibrate. Indeed, enhanced PPARα activity strongly stimulated the expression of genes involved in lipid catabolism in L.G6pc-/- livers and K.G6pc-/- kidneys, that entailed a decrease in hepatic and renal TG content and prevention of NAFLD and CKD. In the K.G6pc-/- kidneys, this beneficial effect of lipid-lowering was associated with the inhibition of RAS and TGF-β1 pathways, preventing EMT and thereby, tubulointerstitial fibrosis and glomerulosclerosis. These results are in accordance with

previous data reporting that fenofibrate prevented the induction of RAS/TGF-β1 pathway and fibrosis in diabetic and/or obese mice by decreasing lipids (Cheng et al., 2016; Hong et al., 2014; Li et al., 2010; Park et al., 2006; Tanaka et al., 2011). At the molecular level, it was proposed that lipid derivates, such as diacylglycerol and ceramides, are potent activators of protein kinase C, leading to the activation of *Agt* expression in the kidneys (Bobulescu, 2010; Koya and King, 1998). In the L.G6pc-/- liver, the decrease in steatosis by fenofibrate treatment lowered the risks associated with NAFLD, since L.G6pc-/- mice exhibited a decrease in liver injury markers, concomitantly with a rescue of hepatocyte histology features. Even though fenofibrate seems to prevent the loss of tumor suppressors in L.G6pc-/- livers, a limitation of this study is that we did not examine the effect of fenofibrate on the long-term development of hepatic tumors. Indeed, fenofibrate has been suggested to play a role in hepatic tumorigenesis in rodents (Nesfield et al., 2005; Nishimura et al., 2007), which was fortunately not observed in humans (Bonovas et al., 2012; Pawlak et al., 2015). Thus, as many studies have demonstrated a strong link between hepatic tumorigenesis and NAFLD, like in the case of obesity / diabetes (Baffy, 2013; Streba et al., 2015), we could expect to limit HCA /HCC incidence by decreasing lipid accumulation in GSDIa. The adverse effects of lipids have also been confirmed in a previous study, since HF/HS diet accelerated hepatocarcinogenesis in L.G6pc-/- mice (Rajas et al., 2015). Taking into account our results obtained with the HF/HS diet and fenofibrate, these data highlight that lipid accumulation is the main contributor to liver injury and CKD in GSDIa, independently of excessive glycogen content. Therefore, lipid lowering is a novel unconventional strategy that should be particularly considered in GSDIa to prevent, not

only hypertriglyceridemia, but also hepatic and renal long-term complications. Currently, fenofibrate treatment was only recommended in GSDIa patients who present severe hypertriglyceridemia (generally over 10 g/L), in order to lower plasmatic TGs (Froissart et al., 2011). Unfortunately, there is no data addressing effects of fibrates on the onset of CKD, as well as on hepatic complications in patients with GSDIa. Indeed, most patients presenting the first signs of CKD are also generally treated with an inhibitor of ACE or an angiotensin receptor analogue (Gjorgjieva et al., 2016a). Therefore, the use and the effects of fenofibrate alone in GSDIa patients should be further examined, independently of other treatments.

This study also provides evidence that fenofibrate treatment induced lipid turnover since the expression of several genes involved in *de novo* lipogenesis was enhanced concomitantly with increased lipid catabolism in L.G6pc-/- and K.G6pc-/- mice. This may protect the liver and kidneys against the putative toxic effects of excess intracellular NEFA and their oxidation products (Oosterveer et al., 2009). Moreover, lipid turnover induction, by a PPARα agonist, radically changed glycogen metabolism in GSDIa. It is noteworthy that an additional and unexpected benefit of fenofibrate is that the treatment markedly decreased hepatic and renal glycogen accumulation observed in L.G6pc-/- and K.G6pc-/- mice, respectively. This decrease was not due to an increase in glycogen degradation but rather to an inhibition of glycogen synthesis. Thereby, we suggest that the glycogen metabolism remodeling by fenofibrate derives from the diversion of G6P from glycogen synthesis towards lipid anabolism and thus results in a decrease in glycogen synthesis. The decrease in glucose uptake by glucose transporters and glucose phosphorylation should also participate to the decrease in

G6P availability for glycogen synthesis. These processes may play a key role in the correction of nephromegaly observed after treatment.

In conclusion, this study shows for the first time that the mechanisms involved in the development of hepatic and renal long-term complications of GSDIa are mainly induced by lipid accumulation, independently of excessive glycogen contents in these organs. Moreover, it provides evidence that pharmacological activation of PPARα could be a therapeutically suitable strategy to prevent the development of GSDIa hepatic and renal complications. Therefore, lipid-lowering is a novel unconventional strategy that should be particularly considered in GSDIa treatment and that could considerably improve life quality and expectancy of GSDIa patients. In addition, a recent overview of PPARα agonist action in human highlighted the potential efficacy of these drugs to treat NAFLD (Kersten and Stienstra, 2017). Finally, our results suggest that promoting lipid turnover *via* PPARα agonists may represent a potential therapeutic target to prevent NAFLD and CKD development in GSDIa and other metabolic diseases, such as obesity and diabetes.

AUTHOR CONTRIBUTIONS: L.M. and M.G. designed, conducted experiments, analyzed the data and wrote the paper. M.S. and V.V. were in charge of mouse breeding and animal experiments. L.I. and A.D conducted experiments. H.G. and G.M. critically edited the manuscript. FR supervised the studies and wrote the paper.

ACKNOWLEDMENTS

We would like to thank the members of Animalerie Lyon Est Conventionnelle et SPF (ALECS, Université Lyon 1, SFR Santé Lyon Est) for the animal care, the members of the CIQLE platform (Université Lyon 1, SFR Santé Lyon Est) for the TEM observations and the members of the Anipath platform for the histological experiments (Université Lyon 1).

This work was supported by research grants from the Agence Nationale de la Recherche (ANR-15-CE14-0026-03 and ANR16-CE14-0022-02), the Association Francophone des Glycogénoses, and the Ligue régionale contre le cancer. LM and MG are recipients of funding of the Fondation pour la Recherche Médicale and the Ligue nationale contre le cancer, respectively.

REFERENCES

Abdul-Wahed, A., Gautier-Stein, A., Casteras, S., Soty, M., Roussel, D., Romestaing, C., Guillou, H., Tourette, J.-A., Pleche, N., Zitoun, C., et al. (2014). A link between hepatic glucose production and peripheral energy metabolism via hepatokines. Mol. Metab. *3*, 531–543.

Asrih, M., and Jornayvaz, F.R. (2013). Inflammation as a potential link between nonalcoholic fatty liver disease and insulin resistance. J. Endocrinol. *218*, R25-36.

Badman, M.K., Pissios, P., Kennedy, A.R., Koukos, G., Flier, J.S., and Maratos-Flier, E. (2007). Hepatic fibroblast growth factor 21 is regulated by PPARalpha and is a key mediator of hepatic lipid metabolism in ketotic states. Cell Metab. *5*, 426–437.

Baffy, G. (2013). Hepatocellular Carcinoma in Non-alcoholic Fatty Liver Disease: Epidemiology, Pathogenesis, and Prevention. J. Clin. Transl. Hepatol. *1*, 131–137.

Balfour, J.A., McTavish, D., and Heel, R.C. (1990). Fenofibrate. A review of its pharmacodynamic and pharmacokinetic properties and therapeutic use in dyslipidaemia. Drugs *40*, 260–290.

Bandsma, R.H.J., Prinsen, B.H., de Sain-van der Velden, M., Rake, J.-P., Boer, T., Smit, G.P.A., Reijngoud, D.-J., and Kuipers, F. (2008). Increased de novo Lipogenesis and Delayed Conversion of Large VLDL into Intermediate Density Lipoprotein Particles Contribute to Hyperlipidemia in Glycogen Storage Disease Type 1a. Pediatr. Res. *63*, 702–707.

Bandsma, R.H.J., Smit, G.P.A., and Kuipers, F. (2014). Disturbed lipid metabolism in glycogen storage disease type 1. Eur. J. Pediatr. *161*, S65–S69.

Bobulescu, I.A. (2010). Renal lipid metabolism and lipotoxicity. Curr. Opin. Nephrol. Hypertens. *19*, 393–402.

Bonovas, S., Nikolopoulos, G.K., and Bagos, P.G. (2012). Use of Fibrates and Cancer Risk: A Systematic Review and Meta-Analysis of 17 Long-Term Randomized Placebo-Controlled Trials. PLOS ONE *7*, e45259.

Bruni, N., Rajas, F., Montano, S., Chevalier-Porst, F., Maire, I., and Mithieux, G. (1999). Enzymatic characterization of four new mutations in the glucose-6 phosphatase (G6PC) gene which cause glycogen storage disease type 1a. Ann. Hum. Genet. *63*, 141–146.

Calderaro, J., Labrune, P., Morcrette, G., Rebouissou, S., Franco, D., Prévot, S., Quaglia, A., Bedossa, P., Libbrecht, L., Terracciano, L., et al. (2013). Molecular characterization of hepatocellular adenomas developed in patients with glycogen storage disease type I. J. Hepatol. *58*, 350–357.

Cheng, R., Ding, L., He, X., Takahashi, Y., and Ma, J.-X. (2016). Interaction of PPARα With the Canonic Wnt Pathway in the Regulation of Renal Fibrosis. Diabetes *65*, 3730–3743.

Chou, J.Y. (2001). The molecular basis of type 1 glycogen storage diseases. Curr. Mol. Med. *1*, 25–44.

Clar, J., Gri, B., Calderaro, J., Birling, M.-C., Hérault, Y., Smit, G.P.A., Mithieux, G., and Rajas, F. (2014). Targeted deletion of kidney glucose-6 phosphatase leads to nephropathy. Kidney Int. 2014; 86(4):747-56

Derks, T.G.J., and van Rijn, M. (2015). Lipids in hepatic glycogen storage diseases: pathophysiology, monitoring of dietary management and future directions. J. Inherit. Metab. Dis. *38*, 537–543.

Duval, C., Müller, M., and Kersten, S. (2007). PPARalpha and dyslipidemia. Biochim. Biophys. Acta *1771*, 961–971.

Froissart, R., Piraud, M., Boudjemline, A.M., Vianey-Saban, C., Petit, F., Hubert-Buron, A., Eberschweiler, P.T., Gajdos, V., and Labrune, P. (2011). Glucose-6-phosphatase deficiency. Orphanet J. Rare Dis. *6*, 27.

Gjorgjieva, M., Raffin, M., Duchampt, A., Perry, A., Stefanutti, A., Brevet, M., Tortereau, A., Dubourg, L., Hubert-Buron, A., Mabille, M., et al. (2016a). Progressive development of renal cysts in glycogen storage disease type I. Hum. Mol. Genet. *25*, 3784–3797.

Gjorgjieva, M., Oosterveer, M.H., Mithieux, G., and Rajas, F. (2016b). Mechanisms by Which Metabolic Reprogramming in GSD1 Liver Generates a Favorable Tumorigenic Environment. J. Inborn Errors Metab. Screen. *4*, 2326409816679429.

Hijmans, B.S., Boss, A., van Dijk, T.H., Soty, M., Wolters, H., Mutel, E., Groen, A.K., Derks, T.G.J., Mithieux, G., Heerschap, A., et al. (2017). Hepatocytes contribute to residual glucose production in a mouse model for glycogen storage disease type Ia. Hepatol. Baltim. Md.

Hong, Y.A., Lim, J.H., Kim, M.Y., Kim, T.W., Kim, Y., Yang, K.S., Park, H.S., Choi, S.R., Chung, S., Kim, H.W., et al. (2014). Fenofibrate Improves Renal Lipotoxicity through Activation of AMPK-PGC-1α in db/db Mice. PLOS ONE *9*, e96147.

Kersten, S. (2014). Integrated physiology and systems biology of PPARα. Mol. Metab. *3*, 354–371.

Kersten, S., and Stienstra, R. (2017). The role and regulation of the peroxisome proliferator activated receptor alpha in human liver. Biochimie *136*, 75–84.

Kishnani, P.S., Austin, S.L., Abdenur, J.E., Arn, P., Bali, D.S., Boney, A., Chung, W.K., Dagli, A.I., Dale, D., Koeberl, D., et al. (2014). Diagnosis and management of glycogen storage disease type I: a practice guideline of the American College of Medical Genetics and Genomics. Genet. Med. Off. J. Am. Coll. Med. Genet. *16*, e1.

Kostapanos, M.S., Kei, A., and Elisaf, M.S. (2013a). Current role of fenofibrate in the prevention and management of non-alcoholic fatty liver disease. World J. Hepatol. *5*, 470–478.

Kostapanos, M.S., Florentin, M., and Elisaf, M.S. (2013b). Fenofibrate and the kidney: an overview. Eur. J. Clin. Invest. *43*, 522–531.

Koya, D., and King, G.L. (1998). Protein kinase C activation and the development of diabetic complications. Diabetes *47*, 859–866.

Labrune, P., Trioche, P., Duvaltier, I., Chevalier, P., and Odièvre, M. (1997). Hepatocellular adenomas in glycogen storage disease type I and III: a series of 43 patients and review of the literature. J. Pediatr. Gastroenterol. Nutr. *24*, 276–279.

Lei, K.J., Chen, Y.T., Chen, H., Wong, L.J., Liu, J.L., McConkie-Rosell, A., Van Hove, J.L., Ou, H.C., Yeh, N.J., and Pan, L.Y. (1995). Genetic basis of glycogen storage disease type 1a: prevalent mutations at the glucose-6-phosphatase locus. Am. J. Hum. Genet. *57*, 766–771.

Li, L., Emmett, N., Mann, D., and Zhao, X. (2010). Fenofibrate attenuates tubulointerstitial fibrosis and inflammation through suppression of nuclear factor-κB and transforming growth factor-β1/Smad3 in diabetic nephropathy. Exp. Biol. Med. Maywood NJ *235*, 383–391.

Mithieux, G., Guignot, L., Bordet, J.-C., and Wiernsperger, N. (2002). Intrahepatic mechanisms underlying the effect of metformin in decreasing basal glucose production in rats fed a high-fat diet. Diabetes *51*, 139–143.

Montagner, A., Polizzi, A., Fouché, E., Ducheix, S., Lippi, Y., Lasserre, F., Barquissau, V., Régnier, M., Lukowicz, C., Benhamed, F., et al. (2016). Liver PPARα is crucial for whole-body fatty acid homeostasis and is protective against NAFLD. Gut gutjnl-2015-310798.

Mutel, E., Abdul-Wahed, A., Ramamonjisoa, N., Stefanutti, A., Houberdon, I., Cavassila, S., Pilleul, F., Beuf, O., Gautier-Stein, A., Penhoat, A., et al. (2011). Targeted deletion of liver glucose-6 phosphatase

mimics glycogen storage disease type 1a including development of multiple adenomas. J. Hepatol. *54*, 529–537.

Najib, J. (2002). Fenofibrate in the treatment of dyslipidemia: a review of the data as they relate to the new suprabioavailable tablet formulation. Clin. Ther. *24*, 2022–2050.

Nesfield, S.R., Clarke, C.J., Hoivik, D.J., Miller, R.T., Allen, J.S., Selinger, K., and Santostefano, M.J. (2005). Evaluation of the carcinogenic potential of clofibrate in the rasH2 mouse. Int. J. Toxicol. *24*, 301–311.

Nishimura, J., Dewa, Y., Muguruma, M., Kuroiwa, Y., Yasuno, H., Shima, T., Jin, M., Takahashi, M., Umemura, T., and Mitsumori, K. (2007). Effect of fenofibrate on oxidative DNA damage and on gene expression related to cell proliferation and apoptosis in rats. Toxicol. Sci. Off. J. Soc. Toxicol. *97*, 44–54.

Oosterveer, M.H., Grefhorst, A., van Dijk, T.H., Havinga, R., Staels, B., Kuipers, F., Groen, A.K., and Reijngoud, D.-J. (2009). Fenofibrate Simultaneously Induces Hepatic Fatty Acid Oxidation, Synthesis, and Elongation in Mice. J. Biol. Chem. *284*, 34036–34044.

Park, C.W., Zhang, Y., Zhang, X., Wu, J., Chen, L., Cha, D.R., Su, D., Hwang, M.-T., Fan, X., Davis, L., et al. (2006). PPARalpha agonist fenofibrate improves diabetic nephropathy in db/db mice. Kidney Int. *69*, 1511–1517.

Park, E.J., Lee, J.H., Yu, G.-Y., He, G., Ali, S.R., Holzer, R.G., Osterreicher, C.H., Takahashi, H., and Karin, M. (2010). Dietary and genetic obesity promote liver inflammation and tumorigenesis by enhancing IL-6 and TNF expression. Cell *140*, 197–208.

Pawlak, M., Lefebvre, P., and Staels, B. (2015). Molecular mechanism of PPARα action and its impact on lipid metabolism, inflammation and fibrosis in non-alcoholic fatty liver disease. J. Hepatol. *62*, 720–733.

Postic, C., and Girard, J. (2008). Contribution of de novo fatty acid synthesis to hepatic steatosis and insulin resistance: lessons from genetically engineered mice. J. Clin. Invest. *118*, 829–838.

Rajas, F., Jourdan-Pineau, H., Stefanutti, A., Mrad, E.A., Iynedjian, P.B., and Mithieux, G. (2007). Immunocytochemical localization of glucose 6-phosphatase and cytosolic phosphoenolpyruvate carboxykinase in gluconeogenic tissues reveals unsuspected metabolic zonation. Histochem. Cell Biol. *127*, 555–565.

Rajas, F., Labrune, P., and Mithieux, G. (2013). Glycogen storage disease type 1 and diabetes: learning by comparing and contrasting the two disorders. Diabetes Metab. *39*, 377–387.

Rajas, F., Clar, J., Gautier-Stein, A., and Mithieux, G. (2015). Lessons from new mouse models of glycogen storage disease type 1a in relation to the time course and organ specificity of the disease. J. Inherit. Metab. Dis. *38*, 521–527.

Rake, J.P., Visser, G., Labrune, P., Leonard, J.V., Ullrich, K., and Smit, G.P.A. (2002). Glycogen storage disease type I: diagnosis, management, clinical course and outcome. Results of the European Study on Glycogen Storage Disease Type I (ESGSD I). Eur. J. Pediatr. *161 Suppl 1*, S20-34.

Schaffer, J.E. (2003). Lipotoxicity: when tissues overeat. Curr. Opin. Lipidol. *14*, 281–287.

Sohn, M., Kim, K., Uddin, M.J., Lee, G., Hwang, I., Kang, H., Kim, H., Lee, J.H., and Ha, H. (2017). Delayed treatment with fenofibrate protects against high-fat diet-induced kidney injury in mice: the possible role of AMPK autophagy. Am. J. Physiol. Renal Physiol. *312*, F323–F334.

Soty, M., Gautier-Stein, A., Rajas, F., and Mithieux, G. (2017). Gut-Brain Glucose Signaling in Energy Homeostasis. Cell Metab. *25*, 1231–1242.

Streba, L.A.M., Vere, C.C., Rogoveanu, I., and Streba, C.T. (2015). Nonalcoholic fatty liver disease, metabolic risk factors, and hepatocellular carcinoma: An open question. World J. Gastroenterol. WJG *21*, 4103–4110.

Tanaka, Y., Kume, S., Araki, S., Isshiki, K., Chin-Kanasaki, M., Sakaguchi, M., Sugimoto, T., Koya, D., Haneda, M., Kashiwagi, A., et al. (2011). Fenofibrate, a PPARα agonist, has renoprotective effects in mice by enhancing renal lipolysis. Kidney Int. *79*, 871–882.

van der Veen, J.N., Lingrell, S., Gao, X., Takawale, A., Kassiri, Z., Vance, D.E., and Jacobs, R.L. (2017). Fenofibrate, but not ezetimibe, prevents fatty liver disease in mice lacking phosphatidylethanolamine N-methyltransferase. J. Lipid Res. *58*, 656–667.

Yiu, W.H., Pan, C.-J., Ruef, R.A., Peng, W.-T., Starost, M.F., Mansfield, B.C., and Chou, J.Y. (2008). The angiotensin system mediates renal fibrosis in glycogen storage disease type Ia nephropathy. Kidney Int. *73*, 716–723.

FIGURE LEGENDS

Figure 1: High fat/high sucrose diet exacerbates hepatic and renal complications in GSDIa mice.

(A) TG content in the livers and kidneys, **(B)** Plasmatic AST and ALT activities **(C)** Urinary parameters obtained from mouse urine samples collected during 24h (n=5-11 mice/group). Data were obtained from WT mice fed a standard (STD) diet, and L.G6pc-/- or K.G6pc-/- mice fed a STD or high fat / high sucrose (HF/HS) diet (n=5-10 mice/group). **(D)** Histological analyses of Masson's Trichrome staining of the kidneys from WT and K.G6pc-/- mice fed a STD diet, and K.G6pc-/- mice fed a HF/HS diet **(E)** Glycogen content of livers and kidneys of WT mice fed a STD diet, and L.G6pc-/- or

K.G6pc-/- mice fed a STD or HF/HS diet (n=5-8 mice/group). ND= not detected. Data are expressed as the mean ± sem. Significant differences are indicated as * p<0.05; ** p<0.01; *** p<0.001.

Figure 2: Fenofibrate induces strong lipid catabolism in L.G6pc-/- and K.G6pc-/- mice.

(A,C) Quantitative analyses of hepatic (A) and renal (C) PPARα by western Blot (n=4-5 mice/group). **(B,D)** Quantitative analyses of hepatic (B) and renal (D) lipid catabolism by RT-qPCR. The expression of target mRNA of L.G6pc-/- (B) or K.G6pc-/- (D) mice treated or not with fenofibrate is expressed relatively to the WT mice (n=7-8 mice/group). Data are expressed as the mean ± sem. Significant differences are indicated as * p<0.05; ** p<0.01; *** p<0.001.

Figure 3: Fenofibrate entails an induction of lipid anabolism in L.G6pc-/- and K.G6pc-/- mice.

(A-B) Quantitative analyses of hepatic lipid (A) and renal (B) anabolism by RT-qPCR. The expression of target mRNA of L.G6pc-/- (A) or K.G6pc-/- (B) mice treated or not with fenofibrate is expressed relatively to the WT mice (n=7-8 mice/group). **(C-D)** Triglycerides (TG) content in the livers (C) and kidneys (D) from WT and L.G6pc-/- (C) or K.G6pc-/- (D) mice treated or not with fenofibrate (n=5-7 mice/group). Data are expressed as the mean ± sem. Significant differences are indicated as * p<0.05; ** p<0.01; *** p<0.001.

Figure 4: Fenofibrate decreases glycogen synthesis and prevents hepatic and renal glycogen accumulation.

(A,F) Glycogen content of L.G6pc-/- livers (A) and K.G6pc-/- kidneys (F) treated or not with fenofibrate, compared to WT liver / kidney (n=5-7 mice/group). **(B-G)** Quantitative analyses of hepatic (B) and renal (G) GSK3β phosphorylation and AGL by Western Blot (n=4-5 mice/group). **(C,H)** Glucose content of L.G6pc-/- livers (C) and K.G6pc-/- kidneys (H) treated or not with fenofibrate, compared to WT liver / kidney. (n=5-7 mice/group). **(D,I)** Quantitative analyses of hepatic (D) and renal (I) glucose utilization by RT-qPCR. The expression of target mRNA in the L.G6pc-/- livers (D) and K.G6pc-/- kidneys treated or not with fenofibrate is expressed relatively to WT liver / kidney (n=7-8 mice/group). **(E,J)** Weight of L.G6pc-/- liver (E) and K.G6pc-/- kidney (J) treated or not with fenofibrate, compared to WT liver / kidney (n=7-8 mice/group). Data are expressed as the mean ± sem. Significant differences are indicated as * $p<0.05$; ** $p<0.01$; *** $p<0.001$.

Figure 5: Prevention of nephropathy development by fenofibrate treatment in K.G6pc-/- mice.

(A) Urinary parameters of WT mice and K.G6pc-/- mice treated or not with fenofibrate. Data were obtained from mouse urine samples collected during 24h (n=5-11 mice/group). **(B)** Relative lipocalin-2 gene expression in the kidneys of K.G6pc-/- mice treated or not with fenofibrate, expressed relatively to WT mice. **(C)** Histological analyses of H&E-staining (panels a-c) and Masson's Trichrome staining (panels d-f) of the kidneys from **(a,d)** WT, **(b,e)** K.G6pc-/- and **(c,f)** fenofibrate-treated K.G6pc-/- mice.

(D) Quantitative analyses of renal pro-fibrotic pathways by RT-qPCR (n=7-8 mice/group) and western Blot (n=4-5 mice/group). The expression of target mRNA of K.G6pc-/- mice treated or not with fenofibrate is expressed relative to the WT mice. Data are expressed as the mean ± sem. Significant differences are indicated as * p<0.05; ** p<0.01; *** p<0.001.

Figure 6: Liver injury is prevented by fenofibrate in L.G6pc-/- mice.

(A) Histological analysis of H&E-staining of the livers and **(B)** Transmission electron microscopy analysis of hepatocytes from WT **(a,d)**, L.G6pc-/- **(b,e)** and fenofibrate-treated L.G6pc-/- **(c,f)** mice. Arrows show donut-shaped mitochondria. **(C)** Quantitative analysis of *Plin2* gene expression by RT-qPCR; **(D)** Plasmatic AST and ALT activities; **(E)** Quantitative analysis of AMPK phosphorylation (Thr172) by western Blot (n=4-5 mice/group) and **(F)** Quantitative analyses of *Pten* gene expression by RT-qPCR from WT and L.G6pc-/- treated or not with fenofibrate. The expression of target mRNA in the livers is expressed relative to WT livers (n=7-8 mice/group). Data are expressed as the mean ± sem. Significant differences are indicated as * p<0.05; ** p<0.01; *** p<0.001.

Table 1: Body weight and plasmatic parameters of WT, L.G6pc$^{-/-}$ and K.G6pc$^{-/-}$ mice treated or not with fenofibrate.

	WT	L.G6pc$^{-/-}$	L.G6pc$^{-/-}$ + fenofibrate	WT	K.G6pc$^{-/-}$	K.G6pc$^{-/-}$ + fenofibrate
TG (g/L)	0.77 ± 0.05	0.75 ± 0.08	0.36 ± 0.05 *** ##	0.86 ± 0.03	0.86 ± 0.02	0.68 ± 0.01 *** #
NEFA (mg/dL)	26.2 ± 1.8	28.2 ± 1.9	18.4 ± 1.5 * ##	27.6 ± 1	29.1 ± 0.9	21.1 ± 0.9 *** ###
Cholesterol (g/L)	1.7 ± 0.2	1.5 ± 0.3	2.4 ± 0.2 ##	1.4 ± 0.1	1.2 ± 0.1	1.4 ± 0.1
Glucose (mg/dL)	121 ± 9	57 ± 7 ***	64 ± 4 ***	149 ± 5	138 ± 7	133 ± 8
Ketone bodies (nmol/L)	0.19 ± 0.03	0.72 ± 0.15 *	1.21 ± 0.25 **	0.65 ± 0.05	1.02 ± 0.06 **	1.49 ± 0.05 *** ##
Uric acid (mg/L)	7.8 ± 1.6	7.9 ± 0.7	10.7 ± 1.6	8.3 ± 0.2	10.4 ± 0.6 *	14.1 ± 0.6 *** ###
Body weight (g)	38.7 ± 1.1	36.1 ± 0.9	29.1 ± 0.4 *** ###	37.6 ± 1.2	33.5 ± 0.6	27.6 ± 0.6 *** ###

Data were obtained from mice after 6h of fasting and are expressed as the mean ± S.E.M. (n=5-14). Significant differences between WT and L.G6pc-/- and between WT and K.G6pc-/- are indicated as * $p<0.05$; ** $p<0.01$; *** $p<0.001$. Significant differences between L.G6pc-/- and fenofibrate-treated L.G6pc-/- and between K.G6pc-/- and fenofibrate-treated K.G6pc-/- are indicated as $^{\#}$ $p<0.05$; $^{\#\#}$ $p<0.01$; $^{\#\#\#}$ $p<0.001$.

Highlights

- Exacerbating lipid accumulation aggravated liver / kidney injury in GSDI.
- Fenofibrate-mediated PPARα activation induced hepatic and renal lipid turnover.
- Increased lipid turnover inhibited glycogen synthesis and accumulation.
- PPARα–mediated metabolic reprograming prevented hepatic and renal GSDI complications.

eTOC Blurb

In this article, the authors showed a clear aggravation of renal and hepatic GSDI pathologies by lipid accumulation exacerbation. On the contrary, a decrease in lipids, mediated via a PPARα-agonist fenofibrate, prevented these complications, highlighting the crucial role of lipids in GSDI, independently from glycogen.

STAR METHODS

Experimental model and subject details

L.G6pc$^{-/-}$ mice and K.G6pc$^{-/-}$ mice were obtained by specific deletion of exon 3 of the *G6pc* in the livers or kidneys, respectively, thanks to an inducible CRE-lox strategy, as previously described (Clar et al., 2014; Mutel et al., 2011). Briefly, B6.G6pc$^{ex3lox/lox}$ mice were crossed with transgenic mice expressing the inducible CRE^{ERT2} recombinase under the control of the serum albumin promoter (B6.SA$^{creERT2/w}$) or under the control of the kidney androgen-regulated protein promoter (B6.Kap$^{creERT2/w}$) to generate L.G6pc-/- and K.G6pc-/- mice, respectively. CRE^{ERT2} recombinase was activated by daily intraperitoneal injections of tamoxifen on five consecutive days in 6-8 weeks old male B6.G6pc$^{lox/lox}$.SA$^{creERT2/w}$ and B6.G6pc$^{lox/lox}$.Kap$^{creERT2/w}$ mice, in order to obtain L.G6pc$^{-/-}$ and K.G6pc$^{-/-}$ mice, respectively. Male C57Bl/6J mice (Charles Rivers Laboratories) were also treated with tamoxifen (here referred to as WT mice). Female mice were not used because Kap promoter is under androgenic control.

Mice were housed in the animal facility of Lyon 1 University (ALECS) under temperature controlled (22°C) conditions and with a 12/12h light/dark cycle, in enriched environment in groups of 4 to 6 mice. All mouse linage was C57Bl/6J backcrossed (two generations per year). Mice were fed a standard (STD) chow diet (A04 diet, Safe, Augy, France). After tamoxifen treatment, mice were fed either a STD diet or a HF/HS diet (consisting of 36.1% fat, 35% carbohydrates composed by maltodextrine (50%, wt/wt) and sucrose (50%, wt/wt), 19.8% proteins, produced at the “Unité de Préparation des Aliments Expérimentaux”; UE0300 INRA, Jouy-en-Josas, France) for 9 months. Fenofibrate-treated mice were first fed a STD chow diet for 6 months and then a STD diet

supplemented with 0.2% fenofibrate (Sigma, wt/wt) (Safe, Augy, France) for additional 3 months. All mice were killed 9 months after tamoxifen treatment by cervical dislocation at 6 h of fasting (with continuous access to water). Tissue was frozen by freeze-clamping in liquid nitrogen, and then stored at -80°C. All the procedures were performed in accordance with the principles and guidelines established by the European Convention for the Protection of Laboratory Animals. The regional animal care committee (C2EA-55, Université Lyon 1, Lyon) approved all the experiments.

Method details

Histological analysis

A piece of fresh liver and kidney was fixed in formaldehyde and embedded in paraffin. The 4 µm-thick sections were stained with hematoxylin and eosin (H&E) or Masson's Trichrome staining. The slides were examined under a Coolscope microscope (Nikon).

Transmission electron microscopy

Small pieces of the liver (1mm^3) were immediately fixed in 2% glutaraldehyde at 4°C. The sample was dehydrated in a grade series of ethanol and embedded in an epoxy resin. Tissue was surveyed with a series of 70 nm sections and observed with a Jeol 1400JEM (Tokyo, Japan) transmission electron microscope equipped with a Orius 100 camera and digital micrograph.

Urine parameters

K.G6pc$^{-/-}$ mice were housed in individual metabolic cages (Ugo Basile) for a 24h-acclimation period before urine collection. Urine production and food intake were measured for another 24h period. Urine was collected and stored at -20°C. Urea

concentration was assessed using a BioAssay Systems colorimetric kit (Hayward, CA, USA). Uric acid concentration was measured with a colorimetric kit (DiaSys, Holzheim, Germany). Albuminuria and lipocalin 2 levels were assessed using a mouse albumin ELISA kit (Neobiotech, Clinisciences, Nanterre, France) and a mouse Lipocalin-2/NGAL ELISA kit (R&D Systems, Lille, France), respectively.

Plasma parameters

Blood was withdrawn by submandibular bleeding using a lancet after 6h of fasting and collected into EDTA (0.5M, pH8.0). Blood glucose was measured with an Accu-Check Go glucometer (Roche Diagnostic, Meylan, France). Plasma TG, cholesterol, NEFAs, and uric acid concentrations were determined with colorimetric kits (DiaSys, Holzheim, Germany). B-hydroxybutyrate concentration, AST and ALT activities were assessed with colorimetric kits (Abcam, Cambridge, UK).

Glycogen assay

A piece of 100 mg of frozen tissue was added to 8 volumes of perchloric acid 6% and crushed with the Fast Prep® system (MP Biomedicals). After a centrifugation at 10,000g for 15 min at 4°C, the supernatant was neutralized with 3.2 mM K_2CO_3 and pH was adjusted between 6.5 and 8.5. The solution was then centrifuged at 10,000g for 5 min at 4°C and glycogen quantity was then indirectly determined on the supernatant, by using the Keppler and Decker method as previously described (Mithieux et al., 2002) Glycogen was partially hydrolyzed with by boiling for 20min in NaOH 0.15M and then digested into glucose by α-amyloglucosidase for 1h at 45°C. Glucose released was measured after the addition of 0.7U of hexokinase and glucose-6-phosphate deshydrogenase in the presence of $NADP^+$. NADPH production was detected at 340nm.

Triglyceride assay

Hepatic and renal TG were extracted by the “Folch” procedure. Briefly, a piece of 100 mg of frozen tissue was added to chloroform/methanol 2/1 solution (1.7mL for 100mg of tissue) and crushed with the Fast Prep® system. The solution was centrifuged twice at 2,000g for 10 min at 4°C. By adding 2mL of NaCl 0.73% to the supernatant, two phases were created. The inferior organic phase, which contains TG, was kept. After chloroform evaporation, TG were diluted in 100µL of propanol and measured with a colorimetric kit (DiaSys, Holzheim, Germany).

Western blots

Western blot analysis were carried out using the whole cell extracts from 50mg of tissues lysed in lysis buffer (50 mM Tris pH 7.5, 5 mM MgCl2, 100 mM KCl, 1 mM EDTA, 10% glycerol, 1 mM DTT, 1% NP40, protease and phosphatase inhibitors) and homogenized thanks to the FastPrep® system, at 4 °C. Proteins were dosed in triplicate with Pierce™ BCA Protein Assay Kit. Aliquots of 30 µg proteins, denatured in Laemmli buffer (containing β-mercaptoethanol and SDS), were separated by 9 or 12%-SDS polyacrylamide gel electrophoresis and transferred to PVDF Immobilon membranes (Millipore). After 1h-saturation in TBS/0.2% Tween/5% BSA at room temperature, the membranes were probed (overnight at 4°C) with rabbit polyclonal antibodies (see Table-template 1) diluted in TBS/0.2% Tween/5% BSA. After washing with TBST/Tween 0.2%, membranes were incubated (1h at room temperature) with goat anti-rabbit IgG antibody linked to peroxidase diluted in TBS/Tween 0,2%/BSA 5%. Membranes were rinsed again and exposed to ClarityTM Western ECL Substrate. The visualization and

quantification of proteins were performed using the BioRad ChemiDoc™ Touch Imaging system (Marnes La Coquette, France).

Gene expression analyses

A piece of 50 mg of frozen tissue was homogenised thanks to Fast Prep® system and total RNAs were isolated according to the Trizol protocol (Invitrogen Life Technologies, Saint Aubin, France). Reverse transcription was done on 1µg of mRNA using the Qiagen QuantiTect Reverse Transcription kit. Real-time qPCRs were performed using sequence-specific primers with SsoAdvanced™ Universal SYBR® Green Supermix in a CFX Connect™ Real-Time System (Bio-Rad, Marnes La Coquette, France). Primer sequences are indicated in Table-template 1.

Quantification and statistical analyses

Western blot quantification

The spots intensity was determined by densitometry with ChemiDoc Software (Biorad) and analysed using the Image Lab™ software (Biorad).

RT-qPCR quantification

The expression of mRNA was normalized to the mouse ribosomal protein mL19 transcript (*Rpl19*) expression thanks to the 2-ΔΔCt method. The expression of target mRNA in the L.G6pc-/- livers and K.G6pc-/- kidneys was expressed relatively to WT liver / kidney.

Statistical analysis

The results are reported as the mean ± s.e.m (standard error of the mean). Groups were compared using one-way ANOVA followed by Tukey's *post hoc* test (against all groups), except for western Blot analyses. An unpaired two-tailed Student's T test was performed for western Blot analyses. Differences were considered to be statistically significant at P-value < 0.05.

Study approval

The regional animal care committee (C2EA-55, Université Lyon 1, Lyon) approved all the experiments performed on lived mice.

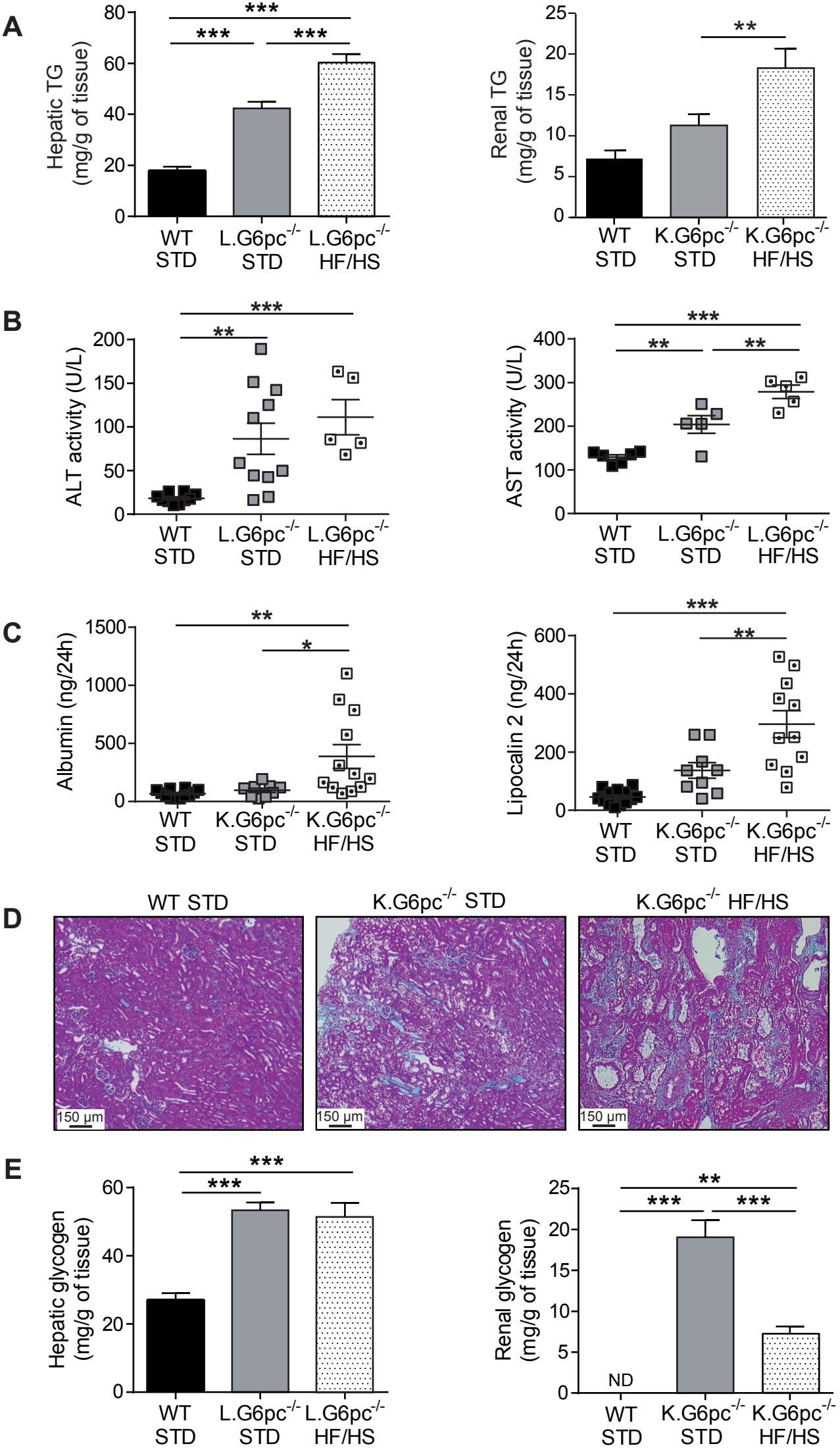

Monteillet, Gjorgjieva *et al.*, 2017 Fig.1

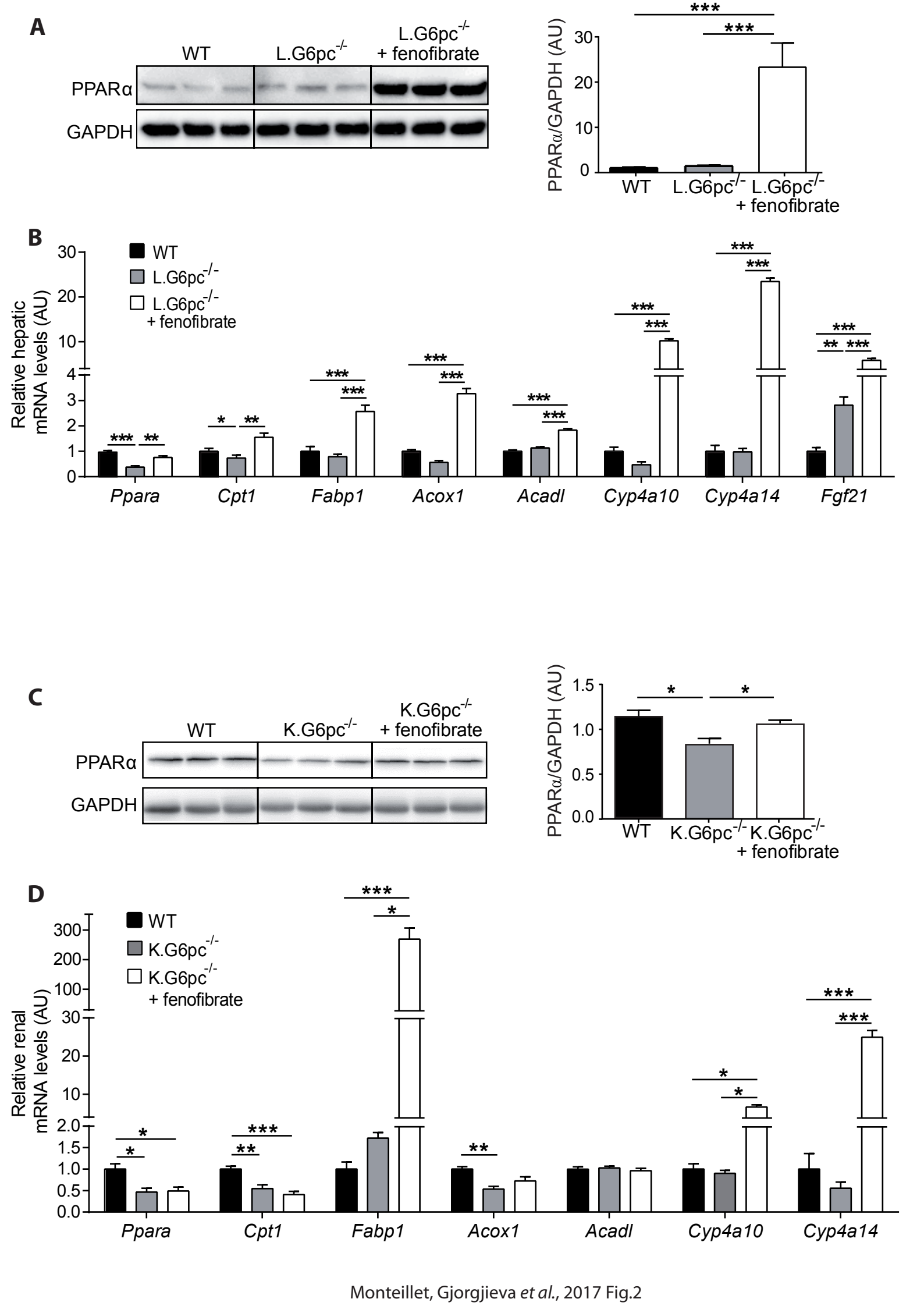

Monteillet, Gjorgjieva *et al.*, 2017 Fig.2

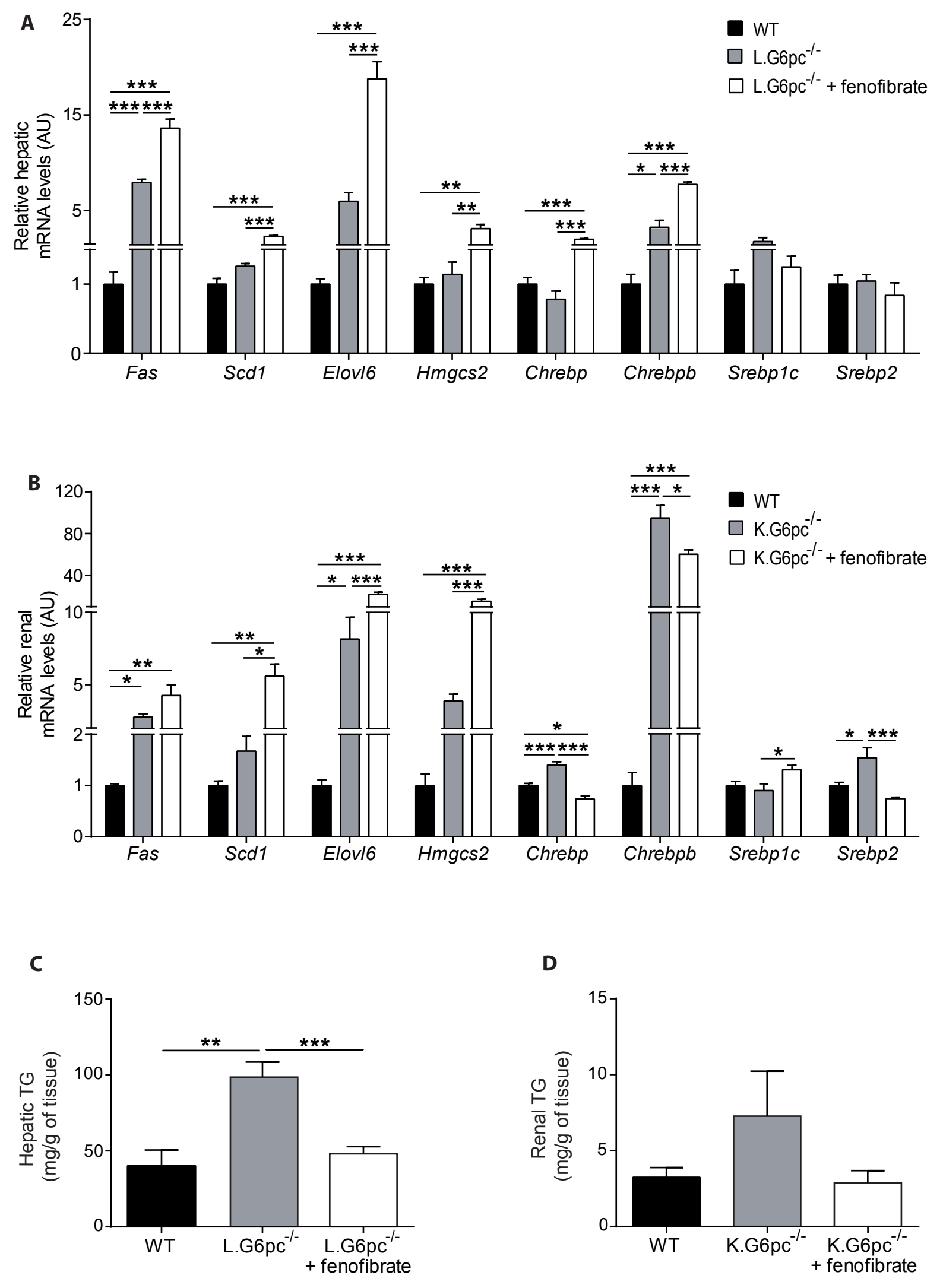

Monteillet, Gjorgjieva *et al.*, 2017 Fig.3

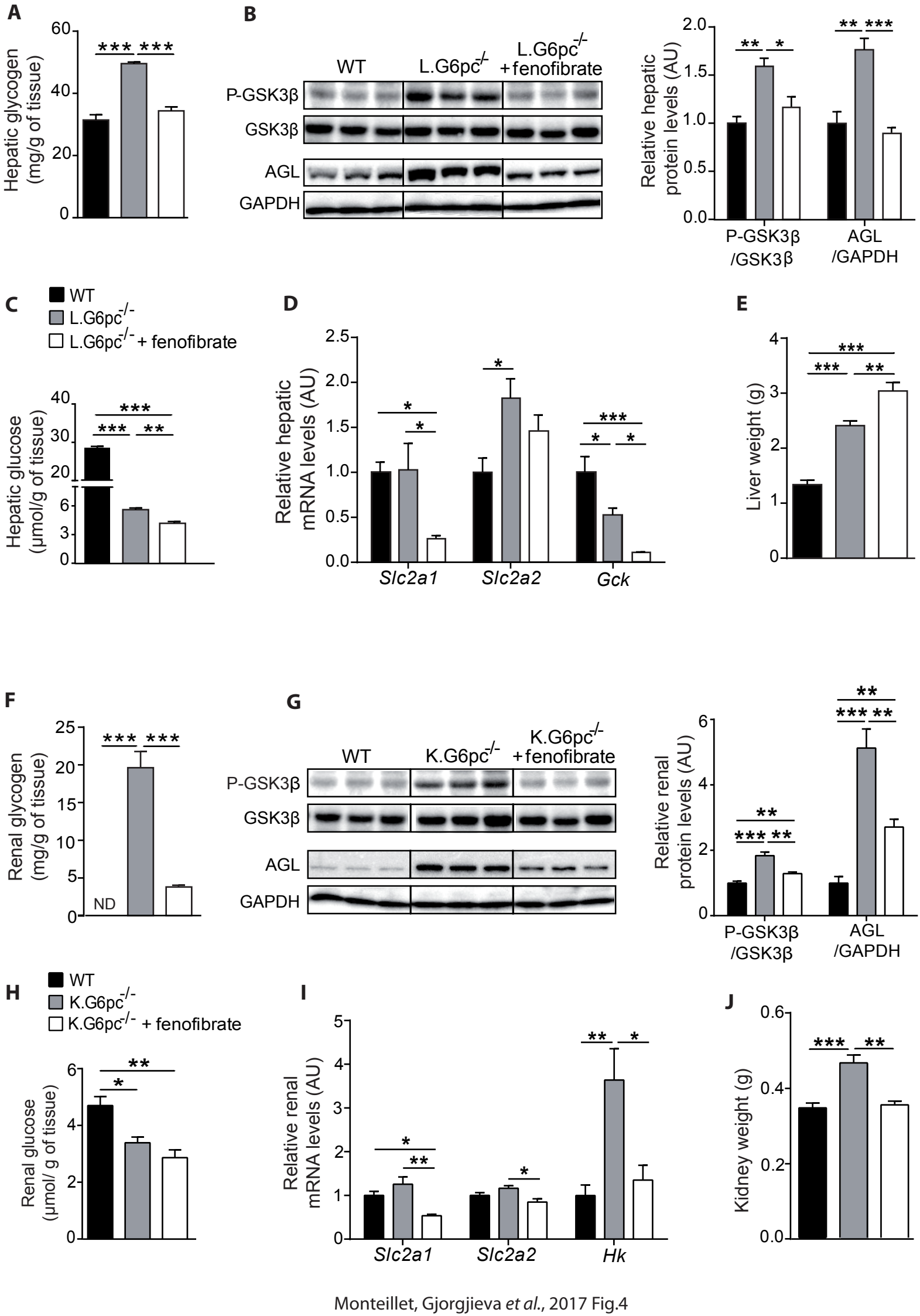

Monteillet, Gjorgjieva *et al.*, 2017 Fig.4

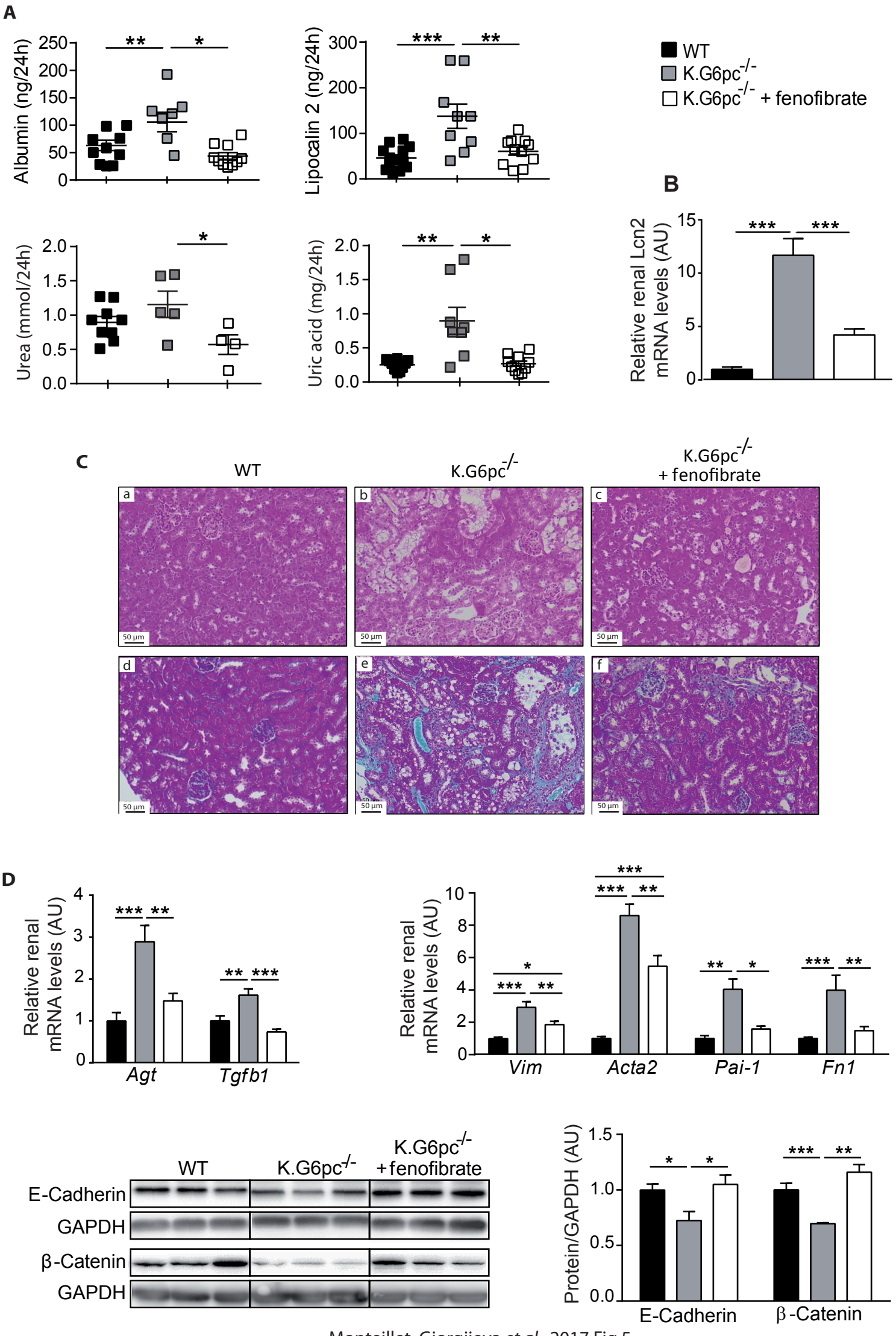

Monteillet, Gjorgjieva *et al.*, 2017 Fig.5

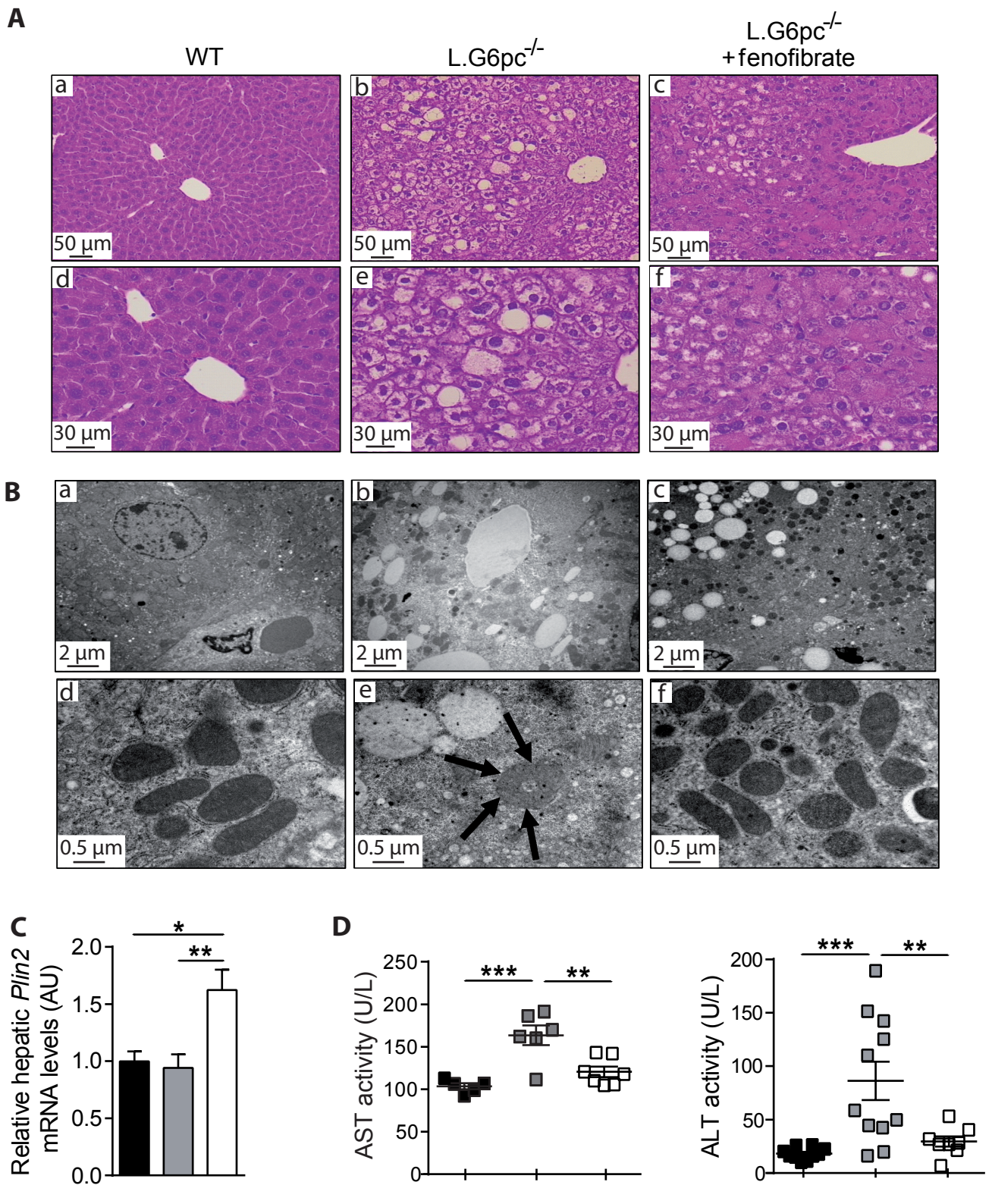

Monteillet, Gjorgjieva *et al.*, 2017 Fig.6

KEY RESOURCES TABLE

REAGENT or RESOURCE	SOURCE	IDENTIFIER
Antibodies		
Rabbit monoclonal anti-phospho AMPKα (Thr172) (40H9)	Cell Signaling technology	Cat n° : #2535
Rabbit monoclonal anti- AMPKα (23A3)	Cell Signaling technology	Cat n° : #2603
Rabbit monoclonal anti-PPARα	Abcam	Cat n°: Ab8934 **RRID:AB_306869**
Rabbit monoclonal anti-AGL	Abcam	Cat n°: Ab133720
Rabbit monoclonal anti-phospho-GSK3β (Ser9) (D3A4)	Cell Signaling technology	Cat n°: #9322
Rabbit monoclonal anti-GSK3β (27C10)	Cell Signaling technology	Cat n°: #9315
Rabbit monoclonal anti-E-cadherin (24E10)	Cell Signaling technology	Cat n°: #3195
Rabbit monoclonal anti-β-catenin (D10A8)	Cell Signaling technology	Cat n°: #8480
Rabbit monoclonal anti-GAPDH (D16H11)	Cell Signaling technology	Cat n°: #5174
Goat secondary anti-rabbit IgG linked to peroxidase	Biorad	Cat n°: 170-5046
Mouse Lipocalin-2/NGA ELISA kit	R&D Systems	Cat n°: MLCN20
Mouse Albumin ELISA kit	NeoBiotech	Cat n°: NB-06-0062
Bacterial and Virus Strains		
Biological Samples		
Chemicals, Peptides, and Recombinant Proteins		

Critical Commercial Assays		
Pierce™ BCA Protein Assay Kit	Thermo Scientifique	Cat n°: 23225
Clarity™ Western ECL Substrate	Biorad	Cat n°: 170-5061
Trizol	Life technologies	Cat n°: 15596018
QuantiTect® Reverse Transcription	Quiagen	Cat n°: 205314
NEFA FS*	DiaSys	Cat n°: 1 5781 99 10 930
Uric acid FS*	DiaSys	Cat n°: 1 3001 99 10 021
Cholesterol FS*	DiaSys	Cat n°: 1 1300 99 10 021
Triglycerides FS*	DiaSys	Cat n°: 1 5710 99 10 026
QuantiChrom™Urea Assay Kit (DIUR-500)	BioAssay Systems	Cat n°: DIUR-500
Alanine Transaminase Activity Assay Kit (Colorimetric/ Fluorometric)	Abcam	Cat n°: Ab105134
Aspartate Aminotransferase Activity Assay Kit	Abcam	Cat n°: Ab105135
Beta Hydroxybutyrate (betaHB) Assay Kit (Colorimetric)	Abcam	Cat n°: Ab83390
Deposited Data		
Experimental Models: Cell Lines		
Experimental Models: Organisms/Strains		
Mouse : L.G6pc -/-		
Mouse : K.G6pc-/-		
Mouse : WT : C57BL6/J	Charles River Laboratory	JAX : 000664
Oligonucleotides		
α 2 -Smooth muscle actin (Acta2)	Fw : GTCCCAGACATCAGGGAGTAA Rev : TCGGATACTTCAGCGTCAGGA	Eurogentech

3-hydro-3-methylglutaryl-CoenzymeA synthase 2	Fw : AGCTTTGTGCGTTCCATCAG Rev : CCGTATGGGCTTCTGTTCAG	Eurogentech	
Acyl-CoenzymeA deshydrogenase long chain (Acadl)	Fw : AGAAGTTCATCCCCCAGATGAC Rev : GGCGTTCGTTCTTACTCCTTGT	Eurogentech	
Acyl-CoA Oxidase 1 (Acox1)	Fw : TGCCAAATTCCCTCATCTTC Rev : CTTGGATGGTAGTCCGGAGA	Eurogentech	
Angiotensinogen (Agt)	Fw : TTCACTGCTCCAGGCTTTCGTCTA Rev : TTCTCAGTGGCAAGAACTGGGTCA	Eurogentech	
Carbohydrate-responsive element-binding protein - isoform β, (Chrebp - β)	Fw : TCTGCAGATCGCGTGGAG Rev : CTTGTCCCGGCATAGCAAC	Eurogentech	
Carbohydrate-responsive element-binding protein, CHREBP (Chrebp), total	Fw : GAAGCCACCCTATAGCTCCC Rev : CTGGGGACCTAAACAGGAGC	Eurogentech	
Carnitine palmitoyltransferase1 (Cpt1a)	Fw : ACCTCCATGGCTCAGACAG Rev : AGCAGAGGCTCAAGCTGTTCA	Eurogentech	
Cytochrome P450 (Cyp4a10)	Fw : TCCAGCAGTTCCCATCACCT Rev : TTGCTTCCCCAGAACCATCT	Eurogentech	
Cytochrome P450 (Cyp4a14)	Fw : TCAGTCTATTTCTGCTGTTC Rev : GAGCTCCTTGTCCTTCAGATGGT	Eurogentech	
Fatty acid binding protein (Fabp1)	Fw : GTCTCCAGTTCGCACTCCTC Rev : GCAGAGCCAGGAGAACTTTG	Eurogentech	
Fatty acid elongase 6 (Elovl6)	Fw : ACAATGGACCTGTCAGCAAA Rev : GTACCAGTGCAGGAAGATCAGT	Eurogentech	
Fatty acid synthase, FAS (Fasn)	Fw : TTCCAAGACGAAAATGATGC Rev : AATTGTGGGATCAGGAGAGC	Eurogentech	
Fibronectin (Fn1)	Fw : TGGCTGCCTTCAACTTCTCCT Rev : TGTTTGATCTGGACTGGCAGTTT	Eurogentech	
Glucokinase(Gck)	Fw : CCCTGAGTGGCTTACAGTTC Rev : :ACGGATGTGAGTGTTGAAGC	Eurogentech	
Glucose transporter1, Glut1 (Slc2a1)	Fw : GCTGTGCTTATGGGCTTCTC Rev : CACATACATGGGCACAAAGC	Eurogentech	

Glucose transporter2, Glut2 (Slc2a2)	Fw : TGTACGCAAAACCCGAAGTCT Rev : CACATTCAAACTGACTTTCTGTTACC	Eurogentech	
Hepatic nuclear factor 1α (HNF1α)	Fw : GAGGACACTGTGGGACTGGT Rev : TCACAGACACCAACCTCAGC	Eurogentech	
Perilipin 2 (Plin2)	Fw : GACCTTGTGTCCTCCGCTTAT Rev : CAACCGCAATTTGTGGCTC	Eurogentech	
Peroxisome proliferator-activated receptor alpha PPARα (Ppara)	Fw : AGTTCACGCATGTGAAGGCTG Rev : TTCCGGTTCTTCTTCTGAATC	Eurogentech	
Phosphatase and tensin homolog (Pten)	Fw : TGGGTTGGGAATGGAGGGAATGCT Rev : GGACAGCAGCCAATCTCTCGGA	Eurogentech	
Plasminogen activator inhibitor (Pai1)	Fw : TTCAGCCCTTGCTTGCCTC Rev : ACACTTTTACTCCGAAGTCGGT	Eurogentech	
Ribosomal protein mL19 (Rpl19)	Fw :GGTGACCTGGATGAGAAGGA Rev: TTCAGCTTGTGGATGTGCTC	Eurogentech	
Stearoyl-CoA desaturase 1 (Scd1)	Fw : TGGGTTGGCTGCTTGTG Rev : GCGTGGGCAGGATGAAG	Eurogentech	
Sterol regularory element binding protein 1c, SREBP1C (Srebp1c)	Fw : GCAGCCACCATCTAGCCTG Rev : CAGCAGTGAGTCTGCCTTGAT	Eurogentech	
Sterol regularory element binding protein 2, SREBP2 (Srebp2)	Fw : GCAGCAACGGGACCATTCT Rev : CCCCATGACTAAGTCCTTCAACT	Eurogentech	
Transforming growth factor β1 (Tgfβ1)	Fw : CAACAATTCCTGGCGTTACCTTGG Rev : GAAAGCCCTGTATTCCGTCTCCTT	Eurogentech	
Vimentin (Vim)	Fw : CGGCTGCGAGAGAAATTGC Rev : CCACTTTCCGTTCAAGGTCAAG	Eurogentech	
Recombinant DNA			
Software and Algorithms			
ChemiDoc Software		Biorad	Version 1.2.0.12

Image Lab	Biorad	Version 5.2.1 ; RRID: SCR_014210
ImageJ	http://imagej.nih.gov/ij	Version 1.47 ; RRID: SCR_003070
GraphPad Prism 5	http://www.graphpad.com/	Version 5.04 ; RRID: SCR_002798
Other		
Standard diet	SAFE Laboratory	A04
Fenofibrate-enriched diet	INRA	N/A
High-Fat/High Sucrose diet	INRA	N/A

DISCUSSION AND CONCLUSION

Over the last decades, several advancements in the knowledge and management of GSDI have been achieved. Indeed, dietary treatment has greatly improved life expectancy of GSDI patients. Hypoglycemic episodes are rarer with this treatment and an effect on the long-term complications has also been reported (Kishnani et al., 2014; Okechuku et al., 2017; Rake et al., 2002a, 2002b). Nevertheless, while some patients respond very well, this regimen is not completely effective in abolishing all of the complications of GSDI. Furthermore, by expanding the life span of GSDI patients, hepatic complications become more frequent and new types of complications arise, such as renal cysts, which were not observed previously. Thus in order to treat GSDI and to propose a curative strategy, we need to unravel all of the underlying molecular mechanisms leading to hepatic and renal complications. Since GSDI is a rare disease, the number of patients is restrained and does not allow us to study important cohort studies. Furthermore, tissue biopsy needed for research purposes is not largely available due to these reasons, but also due to the risks associated with the sampling. Thus animal models of GSDI represent a valuable tool to study this pathology and to test different treatment strategies.

Total *G6pc* knock-out mice exhibit the hepatic and renal complications observed in GSDI patients, but do not allow long-term studies on hepatic tumor development or CKD, due to severe hypoglycemia in the absence of treatments. This is why our laboratory has developed organ-specific *G6pc* knock-out mouse models. Indeed, L.G6pc-/- mice, which have a liver-specific deletion of *G6pc*, have previously allowed us to understand the hepatic, but also the peripheral metabolism alterations induced by the absence of hepatic G6Pase activity (Abdul-Wahed et al., 2014; Mutel et al., 2011a, 2011b). This mouse model has also enabled our laboratory to test a lentiviral approach for GSDI gene therapy (Clar et al., 2015). In this work, L.G6pc-/- mice were used to decipher the altered molecular pathways and cellular defenses of the liver in two different conditions (at a pretumoral and tumoral stage) as well as in the tumors, in order to understand the possible mechanisms triggering tumorigenesis. Interestingly, this study revealed a metabolic **«Warburg-like» reprogramming favoring tumorigenesis, associated with a decrease in tumor suppressors and down-**

regulated cellular defenses in GSDI livers (Gjorgjieva et al., 2016a, Gjorgjieva et al. submitted). A decrease in mitochondrial respiration and activation of *de novo* lipogenesis was also confirmed, contributing to the «Warburg-like» phenotype. This reprogramming is favorable for tumor formation and progression. Furthermore, this study showed that while glycolysis is elevated in both GSDI liver and tumors, PK-M2 is overexpressed only in tumor samples. It would be interesting to confirm this result in tumor samples from GSDI patients, in order to possibly propose this enzyme as a target for a treatment strategy. In parallel, L.G6pc-/- mice were used to test the effect of lipid-lowering drugs, in order to understand the impact that lipids have on the progression of GSDI hepatic complications. We demonstrated that a **decrease in hepatic lipid accumulation led to a net blunting in liver injury and a restoration of tumor suppressors** in GSDI livers (Monteillet*, Gjorgjieva* et al., submitted; *co-authors). Interestingly, this treatment led to a decrease in glycogen levels, possibly by diverting G6P flux from glycogen synthesis to lipogenesis, thus preventing glycogen accumulation.

Another mouse model with a kidney-specific *G6pc* deletion (K.G6pc-/- mice) was developed in our laboratory. This mouse model was previously described as an excellent model of GSDI nephropathy (Clar et al., 2014) yet the long-term development of the nephropathy was not characterized. In this work, we have described the development of CKD in K.G6pc-/- mice and in a collaboration with Prof. Philippe Labrune (General pediatrics, Hospital Antoine-Béclère, Paris) we have reported for the first time the **development of renal cysts** in both K.G6pc-/- mice and in GSDI patients at a late stage of the nephropathy (Gjorgjieva et al., 2016a). Thus the development of renal cysts needs to be taken seriously into account during the annual medical follow-up of the patients. K.G6pc-/- mice, like L.G6pc-/- mice, were also used to test the effect of lipid-lowering on the development of GSDI nephropathy. Interestingly, similarly to hepatic complications, **CKD was strongly delayed in fenofibrate-treated K.G6pc-/- mice, thanks to the prevention of lipid accumulation,** highlighting the important role of lipids in GSDI long-term complications.

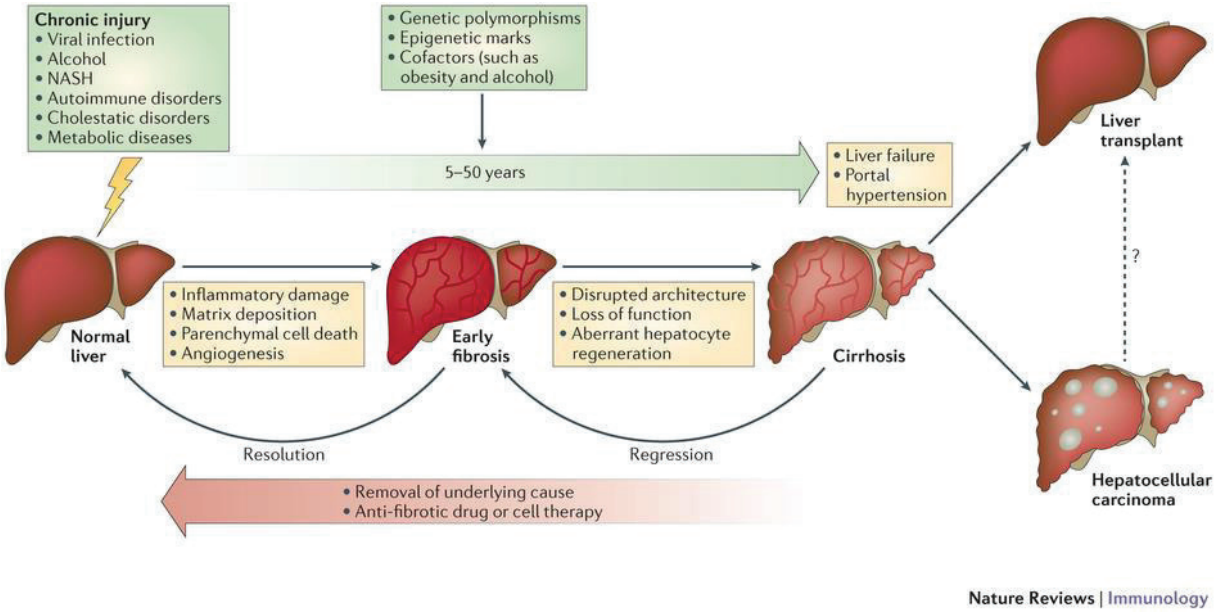

Figure 67: Chronic liver injury and fibrosis / cirrhosis development

Hepatic fibrosis is the wound-healing response of the liver to many causes of chronic injury, of which viral infection, alcohol and non-alcoholic steatohepatitis (NASH) are the most common. Regardless of the underlying cause, injury causes inflammatory damage, matrix deposition, parenchymal cell death and angiogenesis leading to progressive fibrosis. The scar matrix typically accumulates very slowly, but once cirrhosis is established the potential for reversing this process is decreased and complications develop. Genetic polymorphisms, epigenetic marks and cofactors (such as obesity and alcohol) can modulate the risk of fibrosis progression. If the cause of fibrosis is eliminated, resolution (that is, complete reversal to near-normal liver architecture) of early hepatic fibrosis can occur. In cirrhosis, although resolution is not possible, regression of fibrosis improves clinical outcomes. Anti-fibrotic therapies are emerging that can slow, halt or reverse fibrosis progression. Currently, liver transplantation is the only available treatment for liver failure or for some cases of primary liver cancer. Hepatocellular carcinoma is rising in incidence worldwide and is a major cause of liver-related death in patients with cirrhosis.

(Pellicoro et al., 2014)

Hepatocellular carcinoma development – is fibrosis a must?

While many aspects of GSDI are being deciphered, the tumorigenesis process observed is not completely understood. In the general population, the major triggers of hepatic carcinogenesis include hepatic viral infection, alcohol overconsumption and metabolic syndrome (Cha and DeMatteo, 2005; Ingle et al., 2016). In most cases, these chronic liver injury factors induce chronic inflammation, tissue damage, regeneration and remodeling, leading to a multistage process including fibrosis, cirrhosis and finally carcinogenesis (*Figure 67*). While fibrogenesis is a process meant to repair liver injury and prevent further damage, chronic exposure to hepatic stress results in an imbalance between the production and dissolution of the extracellular matrix, thus leading to fibrosis development (Elpek, 2014; Pellicoro et al., 2014) (*Figure 67*). Induction of fibrosis is mainly mediated by inflammation. Many pathways were reported to contribute to this process, such as NF-κB, TGF-β1, TNF-1α, JAK/STAT, IL-1β etc (Elpek, 2014; Seki and Schwabe, 2015). If left untreated, fibrosis can progress to liver cirrhosis, ultimately leading to organ failure and death. Cirrhosis is the histological development of regenerative nodules surrounded by fibrous bands in response to chronic liver injury, that leads to portal hypertension and end stage liver disease (Schuppan and Afdhal, 2008). Finally, this condition leads to HCC development.

Interestingly, hepatic carcinogenesis is very different in GSDI. Indeed, *de novo* HCC development has never been reported in patients and animal models. Instead, in GSDI livers, which resemble a NAFLD condition, HCA formation is firstly observed, and these benign tumors can later undergo malignant transformation in HCC. This malignant transformation is observed in about 10% of the cases, which is an incidence of transformation significantly higher than in non-GSDI HCA transformation cases (4.2%) (Kishnani et al., 2014; Stoot et al., 2010). Furthermore, carcinogenesis occurs in the absence of fibrosis and cirrhosis in GSDI. This absence of fibrosis could be due to the low-grade inflammation in GSDI livers. Indeed, in our work, we did neither observe TGF-β1 overexpression, nor a subsequent EMT needed for the activation of profibrotic pathways in the livers (Gjorgjieva et al., submitted). Besides TGF-β1, platelet derived growth factor (PDGF), hepatocyte growth factor (HGF), connective tissue growth factor

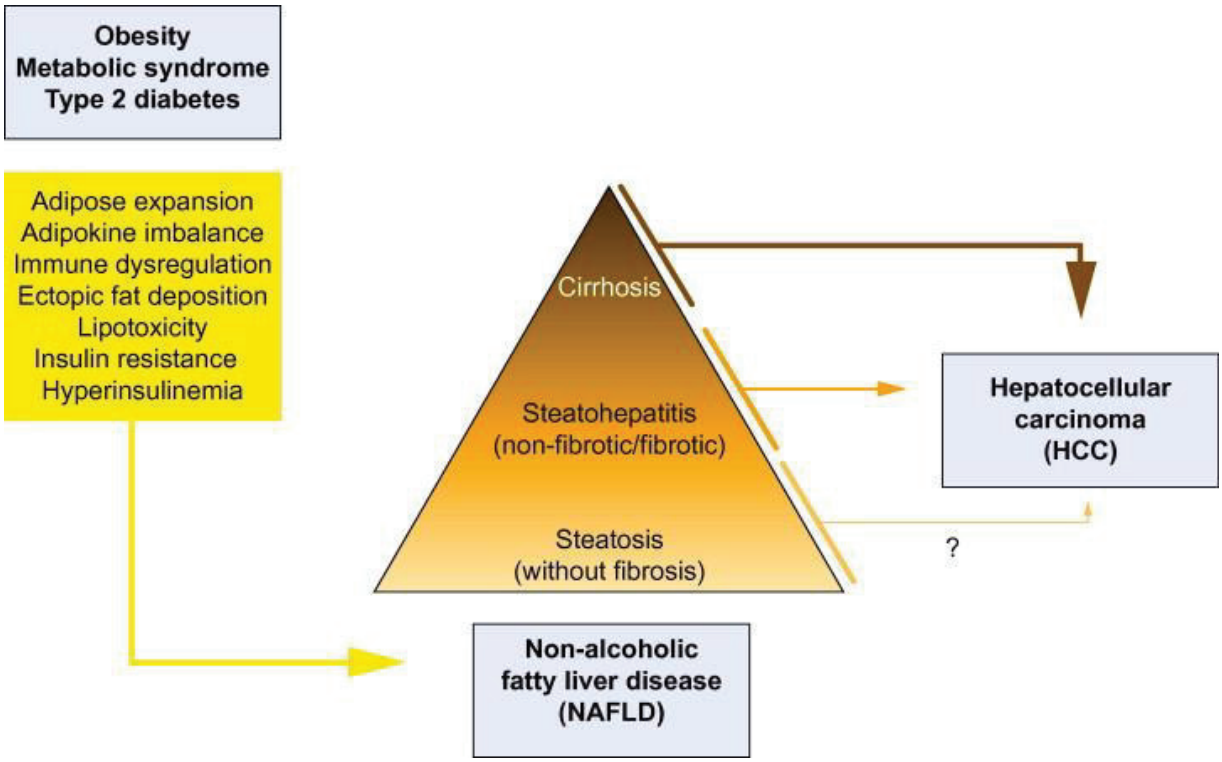

Figure 68: Development of hepatocellular carcinoma in non-alcoholic fatty liver disease

NAFLD is closely linked to obesity and related adverse health effects such as the metabolic syndrome and type 2 diabetes. NAFLD manifests primarily as steatosis and can further progress into steatohepatitis associated to fibrosis or cirrhosis due to obesity-associated metabolic derangements. HCC may complicate any stage of NAFLD, yet the mechanisms leading to HCC in non – fibrotic conditions are still relatively unknown.
Arrows illustrate relative probabilities of disease transitions based on current evidence.

(Baffy et al., 2012)

(CTGF), tumor necrosis factor-α (TNF-α) and vascular endothelial growth factor (VEGF) can also induce fibrosis (Elpek, 2014). While the activation of these pathways was not previously assessed in GSDI literature, VEGF and TNF-α were also found to be unchanged in L.G6pc-/- livers (Gjorgjieva, unpublished data). Furthermore, liver injury markers such as AST/ ALT are relatively normal in GSDI patients, especially with dietary treatment. All these data highlight that the canonical pathways involved in fibrosis / cirrhosis development are inactive in GSDI.

Hepatocarcinogenesis is also observed in non-fibrotic, non-cirrhotic NAFLD livers, but this event remains relatively rare (Baffy, 2013; Baffy et al., 2012; Calzadilla Bertot and Adams, 2016; Inayat et al.). An uncertain fraction of tumors in non-fibrotic livers likely arise through transformation of HCA, just like in GSDI, yet the etiology of these tumors is hard to pinpoint (Baffy et al., 2012; Stoot et al., 2010) (*Figure 68*). In the last decades, metabolic syndrome has become more and more prevalent, and has been associated with HCC development (Paradis et al., 2009). The definition of metabolic syndrome is based on the presence of several clinical and biological parameters reflecting dyslipidemia, insulin resistance, hypertension, and obesity (Eckel et al., 2005). Interestingly, HCC development in metabolic syndrome was shown to occur mainly in the absence of liver fibrosis and cirrhosis, but in the presence of hepatic steatosis. This incidence of HCC in non-fibrotic / cirrhotic livers is statistically different from what is observed in the general population in HCC induced by viral infections, alcoholic liver diseases etc. (Paradis et al., 2009). Paradis and coll. reported that HCA-to-HCC transformation was observed only in metabolic syndrome livers in the absence of fibrosis and this transformation sequence was not observed in HCC developed in fibrotic livers. These HCC were described as well-differentiated and larger than tumors which are developed in fibrotic/cirrhotic livers, which is not surprising, since it has been reported that liver fibrosis limits tumor growth (Osada et al., 2008). Interestingly, metabolic syndrome and GSDI are both characterized by a rare carcinogenesis process, in which the striking reprograming of the metabolism probably leads to benign lesion formations that have the capacity to acquire malignant traits. Thus the L.G6pc-/- mouse model can be exploited to study this specific tumorigenesis process in order to understand not only GSDI, but also other metabolism-related tumorigenic events. Since

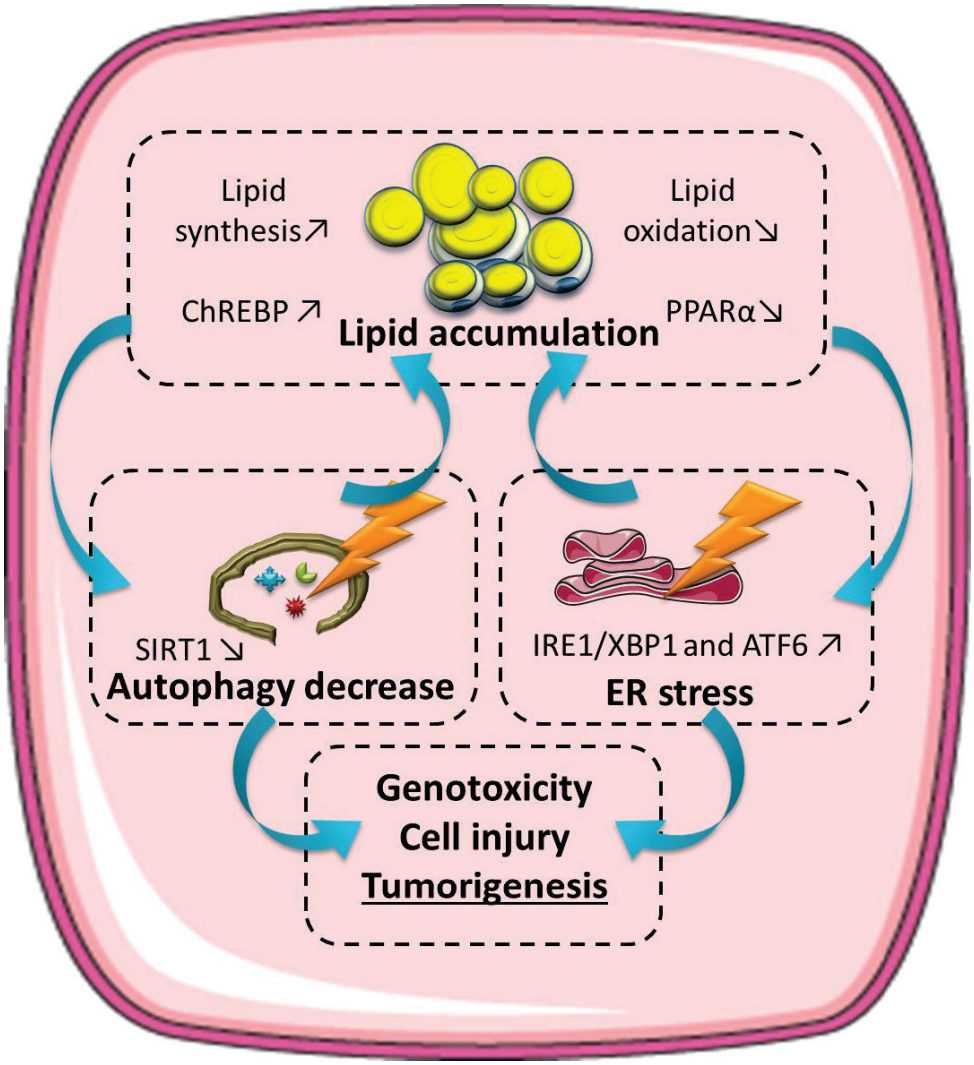

Figure 69: Representation of the interplay of lipid accumulation, autophagy decrease and ER stress activation in GSDI

Excessive G6P in GSDI activates lipid synthesis *via* ChREBP. Lipid synthesis leads to lipid accumulation, further promoted by a decrease in lipid oxidation, characterized by PPARα down-regulation. SIRT1, a target of PPARα, is therefore down-regulated, entailing a decrease in autophagy levels. This leads to further metabolite, cell debris and lipid accumulations, which can lead to DNA damage, cell injury and finally, it can potentiate tumorigenesis. Furthermore, lipids activate ER stress pathways such as IRE1/XBP1 and ATF6, which can then activate lipogenesis on their own. Moreovere, ER stress can contribute to genotoxicity, cell injury and eventually tumorigenesis.

ER – endoplasmic reticulum; ChREBP - carbohydrate responsive element binding protein; SIRT1- sirtuin 1; IRE1 - inositol-requiring enzyme 1; XBP1 - X-box binding protein 1; ATF6 - activating transcription factor 6; PPARα - peroxisome proliferator-activated receptor α.

the lowering of lipid accumulation in GSDI produced promising results, we might be soon able to propose a comparable strategy of prevention in NAFLD patients.

Metabolic reprograming in GSDI leads to deregulated cell defense mechanisms and tumor suppressors

The comparison of the HCC occurrence in NAFLD and GSDI livers, in addition to the beneficial effect of fenofibrate, argue for a dominant role of metabolic reprogramming in the molecular induction of tumor development. We indeed showed that hepatic metabolism reprograming leads to a decrease in cellular defenses, as a consequence of the accumulation of glycogen and lipids in L.G6pc-/- livers. Interestingly, as observed in GSDI, a decrease in autophagy levels has also been reported in other NAFLD (Koga et al., 2010; Mao et al., 2016; Yang et al., 2010). Long-term lipid load changes membrane lipid composition and reduces autophagosome / lysosome fusion both *in vitro* and *in vivo*, which partly explains why excessive lipid content reduces autophagy and accelerates lipid accumulation (Koga et al., 2010). Furthermore, lipid accumulation and defective autophagy induce ER stress in NAFLD conditions (Yang et al., 2010). Interestingly, chronic ER stress is also a potential contributor to hepatic steatosis, since the main actors of the unfolded protein response pathway (UPR) could activate *de novo* lipogenesis and decrease FAO by decreasing C/EBPα (Basseri and Austin, 2011; Han and Kaufman, 2016). Thus chronic ER stress induced by steatosis could further contribute to lipid accumulation (*Figure 69*). As in NAFLD, chronic ER stress activation was observed in the liver of L.G6pc-/- mice (Gjorgjieva et al., submitted). Moreover, a recent study demonstrated that activating autophagy pathways in GSDI mice reduces lipid content (Farah et al., 2016), suggesting that inhibition of autophagy by lipids in NAFLD and GSDI livers closes a vicious circle that promotes steatosis.

The canonical autophagy-regulation pathway involves the mammalian target of rapamycin (mTOR), but SIRT1 can also regulate this degradation process, in relation to the nutrient status of the cell. SIRT1 is known to induce autophagy *via* deacetylation of ATG proteins and FoxO family of transcriptional factors, which transactivate autophagy genes. Moreover, SIRT1 is regulated by AMPK and *vice versa*, enclosing a positive

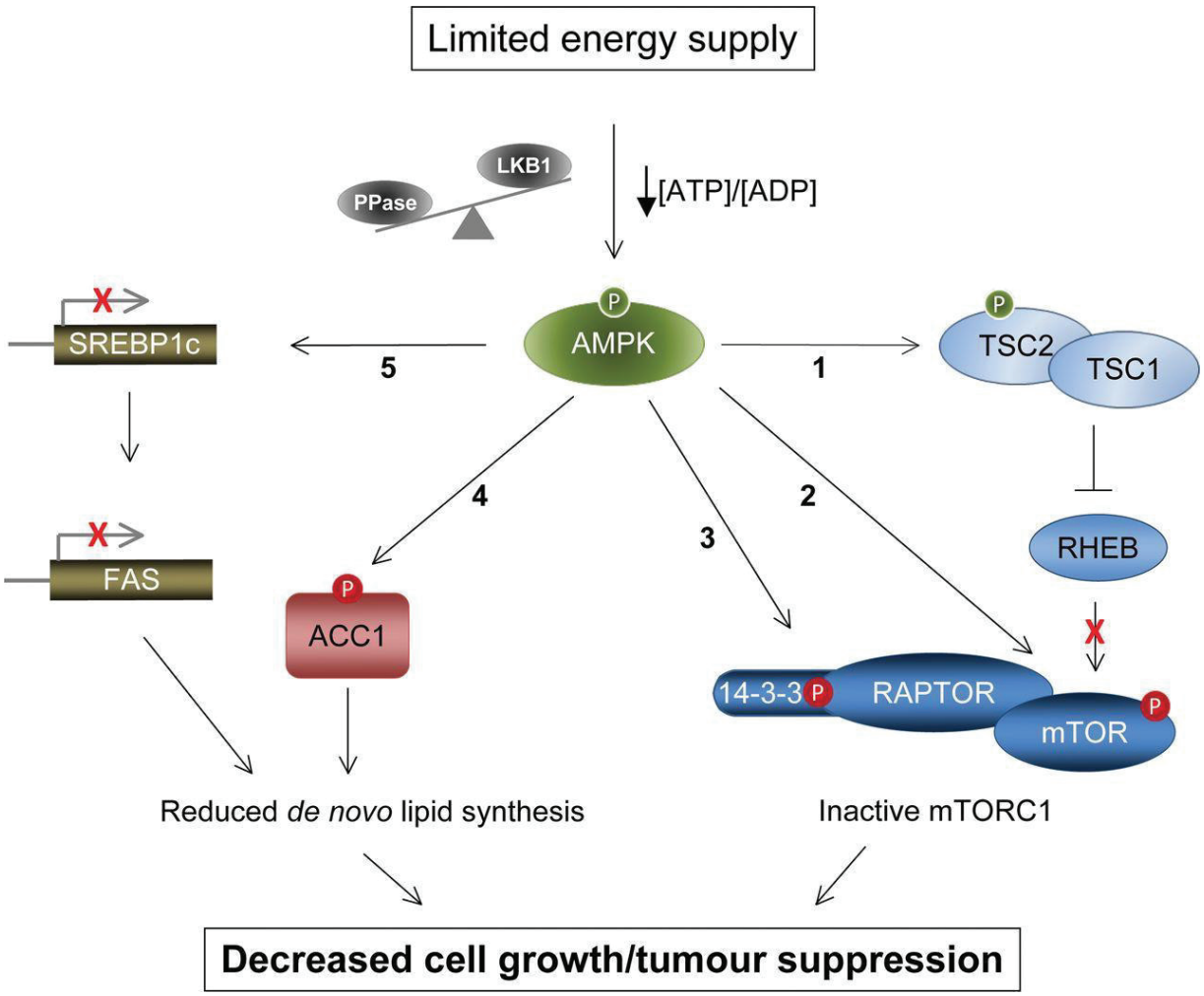

Figure 70: AMPK-mediated cell growth / tumor suppression activity

Under conditions of limited energy supply the ratio of ATP/ADP drops, switching the balance towards phosphorylation (p) and activation of AMPK, predominantly catalysed by LKB1, and away from dephosphorylation and inactivation by protein phosphatases (PPase). Activation of AMPK can lead to a reduction in cell growth through a number of different pathways: 1) phosphorylation and activation of TSC2 prevents activation of mTORC1 by inhibiting the GTPase activity of RHEB; 2) direct phosphorylation of mTOR by AMPK antagonizes phosphorylation and activation by Akt; 3) phosphorylation of RAPTOR increases 14-3-3 binding causing inhibition of mTORC1 activity; 4) phosphorylation of ACC1 decrease *de novo* fatty-acid synthesis; 5) suppression of SREBP1c expression leads to down-regulation of FAS gene expression resulting in a reduction in fatty acid synthesis. Activatory phosphorylation sites are depicted in green and inhibitory phosphorylation sites are shown in red.

(Carling et al., 2012)

feedback loop (Ruderman et al., 2010). Interestingly, autophagy is regulated by SIRT1 in GSDI livers (*Figures 69 and 29*), rather than mTOR. Concordantly, SIRT1 restoration resulted in reactivation of autophagy (Cho et al., 2017). Indeed, liver-specific knockout of *G6pc* leads to the downregulation of *Sirt1* and AMPK (Cho et al., 2017, Monteillet, Gjorgjieva et al., submitted) in accordance with the decreased autophagy levels. Since glucose production is virtually absent and G6P is accumulated in GSDI, it is not surprising that AMPK is inhibited, as a consequence of elevated energy stores (increased G6P). Interestingly, besides their role in autophagy regulation, SIRT1 and AMPK have many other roles in the cell. Both SIRT1 and AMPK were shown to have properties of a tumor suppressor or tumor promoter, depending on the context, their targets in specific signaling pathways or in specific cancers (Lin and Fang, 2013; Luo et al., 2010; Zadra et al., 2015).

This ambiguity relating to SIRT1 is due to its connection to many crucial pathways, such as its interaction with p53, NF-kB, TGF-β1, etc (Lin and Fang, 2013). For example, SIRT1-mediated deacetylation suppresses the function of p53, a well-known tumor suppressor, suggesting a pro-oncogenic role of SIRT1 (Herbert et al., 2014; Lee and Gu, 2013; Lin and Fang, 2013). In contrast, SIRT1 may have a suppressive activity in tumor cell growth by suppressing NF-κB, a transcription factor playing a central role in carcinogenesis and malignancy (Kauppinen et al., 2013; Yeung et al., 2004). Therefore, besides its role on autophagy in GSDI, SIRT1 down-regulation could be highly involved in tumorigenesis.

On the other hand, AMPK is known to regulate many pathways involved in energy homeostasis, including the increase in FAO and inhibition of hepatic glucose production (Luo et al., 2010; Zadra et al., 2015), but also cell cycle arrest, cell polarity, senescence, autophagy and apoptosis (Jansen et al., 2009; Shackelford and Shaw, 2009). All these findings lead to the conclusion that AMPK is a tumor suppressor (Luo et al., 2010). Interestingly, AMPK is a downstream effector of LKB1 (a recognized tumor suppressor) and carries out many of the key functions of LKB1, such as mTOR inhibition (Faubert et al., 2015; Gwinn et al., 2008; Inoki et al., 2003) (*Figure 70*). However, these two can act independently as well. Indeed, recent studies have

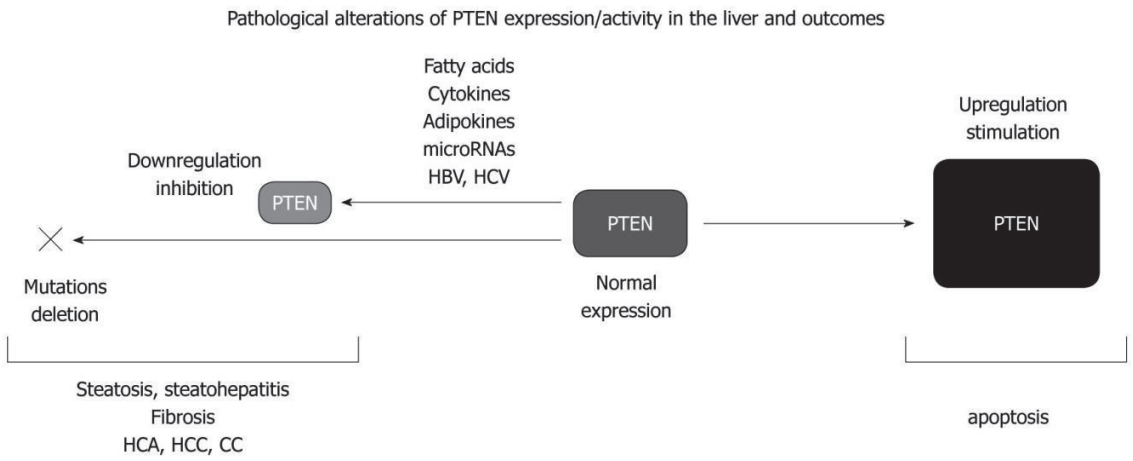

Figure 71: Alterations of PTEN expression/activity in the liver by various etiological factors and associated liver disorders

Down-regulation of PTEN, mediated by fatty acids, cytokines, adipokines, miRNAs and hepatic viral infections as well as mutations / deletions, lead to steatosis and fibrosis development. Furthermore, these events can potentiate HCA, CC and HCC development, due to the loss of the tumor suppressor functions of PTEN. On the other hand, upregulated expression of PTEN results in increased apoptosis levels.

HBV: Hepatitis B virus; HCV: Hepatitis C virus; HCA: Hepatocellular adenomas; CC: Cholangiocellular carcinomas; HCC: Hepatocellular carcinomas; HCA: hepatocellular carcinoma; PTEN: Phosphatase and tensin homolog.

(Adapted from Peyrou et al., 2010)

identified ROS as an upstream activator of AMPK, and this appears to be LKB1-independent (Emerling et al., 2009). Loss of LKB1 due to somatic mutations, leading to failure of AMPK activation is frequently observed in cancer and was estimated to occur in approximately 30% of non-small cell lung cancers, 20% of cervical cancers, and 10% of cutaneous melanomas (Liu et al., 2012; Sanchez-Cespedes et al., 2002; Wingo et al., 2009). More importantly, under-expression of AMPK is frequently observed in HCC, and inactivation of AMPK was shown to promote hepatocarcinogenesis by destabilizing p53 in a SIRT1-dependent manner (Lee et al., 2012a). Thus the down-regulation of AMPK observed in GSDI livers, accompanied with a decrease of SIRT1, could play a major role in GSDI hepatic tumorigenesis.

In our study, other tumor suppressors were reported to be down-regulated, not only in tumor samples, but also in the liver of L.G6pc-/- mice. These include PTEN, HNF1α and p53. PTEN is one of the most commonly lost tumor suppressors in human cancer, and its loss is also observed in NAFLD livers (*Figure 71*) (Leslie and Downes, 2004; Peyrou et al., 2010; Sanchez-Pareja et al., 2016). Moreover, even a haplo-insufficiency of PTEN and a subsequent reduction in protein levels was observed to be responsible for some human inherited conditions and cancer development (Cook and McCaw, 2000; Kwabi-Addo et al., 2001; Leslie and Foti, 2011; Peyrou et al., 2010). Interestingly, PTEN could also contribute to liver steatosis in GSDI, since *de novo* fatty acids synthesis was shown to be enhanced in liver-specific Pten-/- mice (Horie et al., 2004). Indeed, L.Pten-/- mice revealed ballooning hepatocytes, lobular inflammatory cell infiltration, and fibrosis that are characteristic of NASH (Watanabe et al., 2005). Furthermore, at a later stage L.Pten-/- mice presented HCA and HCC development, confirming the tumor suppressor role of this phosphatase in the liver. The tumor suppressor activities of PTEN include maintenance of genomic integrity (Puc et al., 2005), inhibition of cell migration (Liliental et al., 2000) and cellular senescence and interactions with p53 (Chen et al., 2005; Stambolic et al., 2001).

For the first time, we have shown a deregulation of another well-known tumor suppressor in L.G6pc-/- livers, which is p53. While we did not observe a complete loss of p53, the “guardian of the genome” presented an increase in Lys379 acetylation at the

pretumoral stage in L.G6pc-/- livers and a decrease in livers and tumors at the tumoral stage. This acetylation is observed following DNA damage to enhance p53-DNA binding and promote the expression of p53 target genes (Sakaguchi et al., 1998). The switch observed between the two stages might indicate a lesser response to DNA damage, facilitating tumor development and progression in L.G6pc-/- mice. Furthermore, we observed an increase in phosphorylation of p53 at Ser392 not only in L.G6pc-/- livers at both pretumoral and tumoral stages, but also in tumors (Cox and Meek, 2010; Lu et al., 1997). This phosphorylation was reported to be increased in human tumors (Ullrich et al., 1993). Confirming this result in GSDI patients is an urgent matter, seen as p53 is the most commonly lost tumor suppressor in human cancers (Kruiswijk et al., 2015; Rivlin et al., 2011).

Taken together, G6Pase deficiency leads to a profound reprogramming of the metabolism, but also of the cellular defense mechanisms and tumor suppressors. The exact contribution to tumorigenesis by each of these processes remains unclear, but for now we can only speculate if restoring one of these mechanisms or tumor suppressors could impede GSDI pathology. Thus further studies need to be conducted in order to evaluate if one of these pathways represents a suitable therapy target for GSDI patients.

Glycogen storage disease type III – similar name but different carcinogenic pathways?

Interestingly, GSDI is not the only glycogen storage disease characterized with HCC development. Indeed, HCC development has also been reported in GSDIII, GSDIV and GSDVI, whereas the underlying mechanisms were found to be very different. For example, GSDIII is characterized by hepatic fibrosis development, followed by cirrhosis, eventually leading to HCC formation (Demo et al., 2007; Haagsma et al., 1997; Kishnani et al., 2010). During adulthood, around 15% of patients with GSDIII present cirrhosis and are at risk of developing HCC. Interestingly, GSDIII hepatocytes exhibit excessive glycogen accumulation, but unlike GSDI, glycogen presents a modified structure, due to the lack of GDE activity (Kishnani et al., 2010). Indeed, the degradation of glycogen in GSDIII is only partial, leading to the

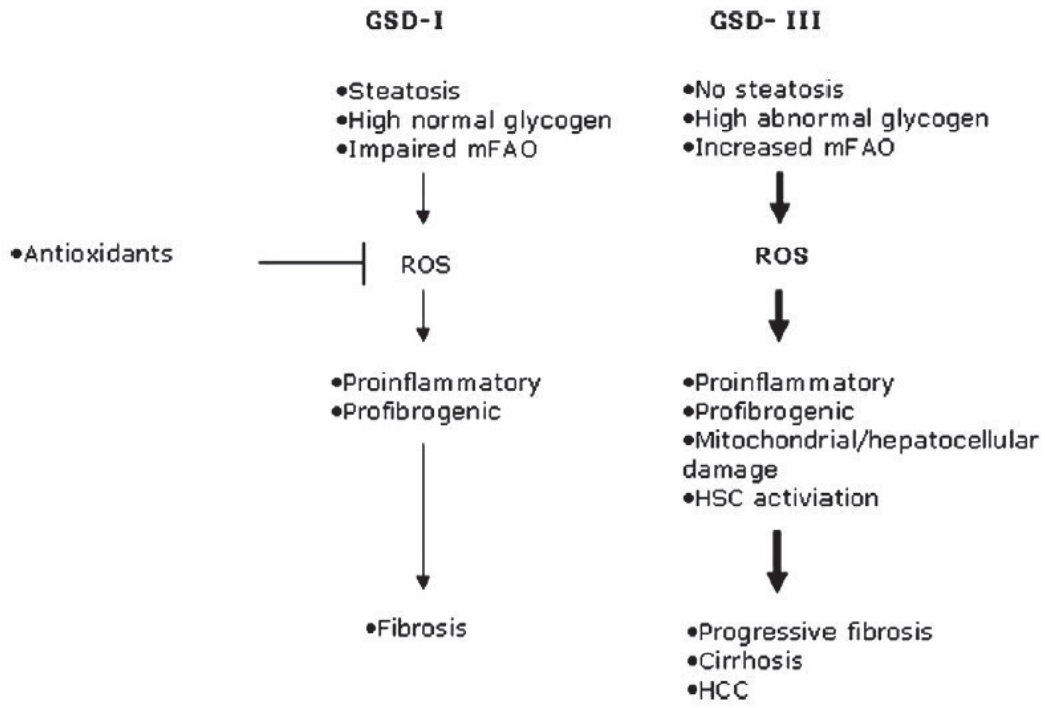

Figure 72: Events contributing to differential development of fibrosis and cirrhosis in GSD-I and GSD-III

In GSDI, steatosis is exhibited due to an increase in lipid synthesis and impairment in lipid oxidation. Nevertheless, ROS produced in the liver of these patients is neutralized by the increase in antioxidants reported in GSDI patients. This inhibition of ROS prevents the activation of proinflammatory / profibrogenic pathways and thus prevents fibrosis in GSDI. Finally, while glycogen is stored in excessive amounts, the structure of glycogen is intact, thus limiting the negative effects of this event.
On the other hand, GSDIII patients exhibit a strong activation in lipid oxidation, leading to an important production in ROS which are not neutralized. These ROS therefore activate proinflammatory / profibrogenic pathways, as well as hepatic stem cells (HSCs). Furthermore, ROS can induce cellular damage and subsequently lead to fibrosis, cirrhosis and HCC development. Furthermore, abnormal glycogen structure can further activate inflammatory pathways and contribute to this process.

(Herrema., 2007)

accumulation of short-branched glycogen, called limit dextrin. Contrarily to GSDI, G6P levels are decreased, due to reduced glycogenolysis, leading to a decrease in glucose production and associated hypoglycemia. Secondary to abnormalities in glycogen metabolism, lipid metabolism is severely affected. Contrary to GSDI, lipids are not accumulated in GSDIII liver, since G6P levels are very low and lipid oxidation is highly enhanced. This difference between GSDI and GSDIII lipid metabolisms was suggested to be the key player responsible for the different outcomes in these two pathologies (Herrema et al., 2007). Indeed, increased fatty acid oxidation (FAO) in GSDIII leads to an increase in production of ketone body and fatty acid metabolites, as well as reactive oxygen species (ROS). Continuous ROS production could therefore induce profibrogenic and proinflammatory pathways, entailing *de novo* carcinogenesis in GSDIII (*Figure 72*).

Finally, the modified structure of glycogen in GSDIII is not to be neglected, since it was also suggested to be an important factor contributing to carcinogenesis (Demo et al., 2007; Kishnani and Chen, 2007). The importance of this limit dextrin has been confirmed by studying another GSD where glycogen structure is altered – GSDIV. In GSDIV, there is an accumulation of amylopectin (long unbranched polymers of glucose) with poor solubility (Li et al., 2010). That the abnormally structured glycogen causes liver damage is supported by the marked elevation of transaminases in both GSDIII and GSDIV. Concordantly, HCC development has also been reported in GSDIV, accentuating the negative impact of abnormal glycogen, that can lead to fibrosis, cirrhosis and eventually HCC development (de Moor et al., 2000).

The characterizations of hepatic metabolism in different GSDs corroborate that different carcinogenesis processes take place. Indeed, in GSDI, increased ROS production was never reported, in concordance with the absence of fibrosis / cirrhosis and ultimately *de novo* carcinogenesis. Glycogen has a normal structure and therefore its role in GSDI pathology could be less important than in other GSDs. Finally, optimal metabolic control in GSDI patients under dietary therapy can lead to a decrease in glycogen deposits, and thus a decrease in liver injury markers, such as AST / ALT,

while this decrease in not observed in GSDIII patients under metabolic control (Kishnani et al., 2010).

Much can be learned by comparing the complex molecular mechanisms leading to HCC in both GSDI and GSDIII. Interestingly, this comparison could contribute not only to the understanding of tumorigenesis in GSDs, but also to the deciphering of different types of hepatic tumorigenesis in general. This could be achieved in mouse models such as L.G6pc-/- and Agl-/- mice (Pagliarani et al., 2014) (Vidal et al., In revision, *Annex I*). Indeed, Agl-/- mice exhibit all hallmarks of GSDIII, including hepatomegaly (due to glycogen accumulation), intolerance to exercise, muscular alteration and even tumor development (Vidal et al., unpublished data). With this objective, our laboratory has established a collaborative project with Genethon, aiming to link hepatic metabolism and carcinogenesis in L.G6pc-/- mice in comparison to Agl-/- mice and to decipher the underlying mechanisms behind GSDI and GSDIII hepatic carcinogenesis. This should allow us to identify potential therapeutic targets and more specific biochemical markers for HCC, since currently used markers, such as AFP, are not suitable. Furthermore, the development of hepatic tumors will be carefully analyzed in GSDI and GSDIII cohorts of French patients by liver imaging and analysis of biochemical parameters and tumor markers, under the care and supervision of Prof. Labrune.

Down-regulation of HNF1 in GSDI liver and kidneys: A common factor in the development of GSDI hepatic and renal complications?

HNF1 in GSDI livers

HNF1 belongs to the homeobox protein family and is an essential transcription factor for many hepatic genes involved in detoxification, homeostasis and metabolism of glucose, lipid, and amino acids (Shih et al., 2001). There are two isotypes of this protein, which are HNF1A and HNF1B (Harries et al., 2009). These two isoforms are responsible for maturity-onset diabetes of the young (MODY), which is a monogenic form of diabetes mellitus characterized by autosomal dominant inheritance, early age of onset (<25 years) and pancreatic β cell dysfunction (Gardner and Tai, 2012). Indeed,

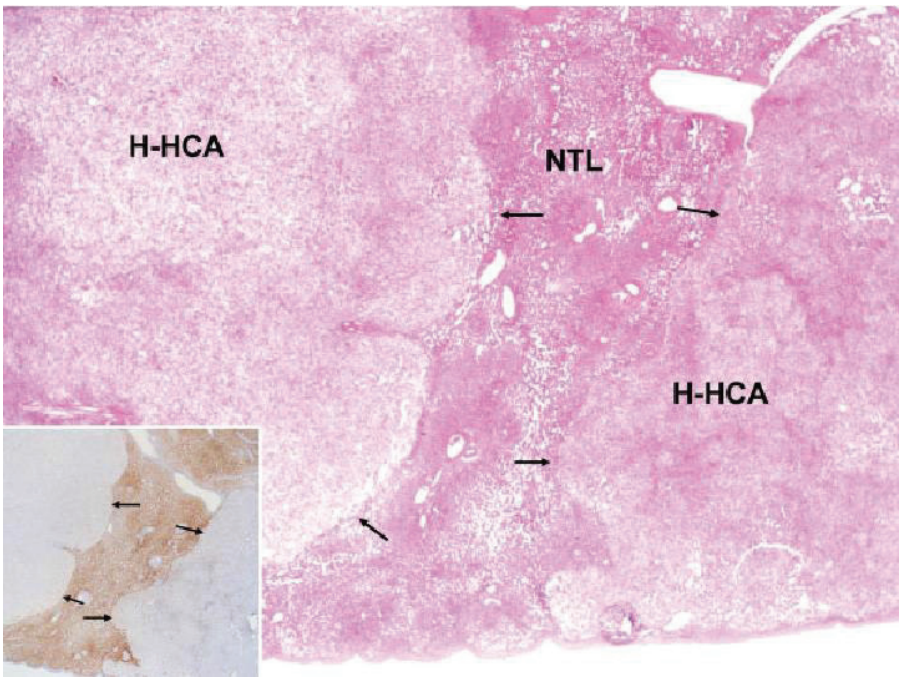

Figure 73: HNF1A-inactivated hepatocellular adenoma (H-HCA)

Two steatotic nodules (limited by arrows) are separated by a thin band of nontumoral liver (NTL) (Hematoxylin & eosin stain, big panel).
This thin band normally expresses liver fatty acid binding protein (FABP1 – target of HNF1A), contrasting with negative H-HCA (small panel).

(Bioulac-Sage et al., 2011)

HNF1A mutations lead to MODY3 and HNF1B to MODY5 (Ellard, 2000). In MODY3, besides metabolic alterations, HNF1A inactivation has been shown to lead to liver adenomatosis (presence of < 10 HCA) (Reznik et al., 2004). HNF1A-mutated HCA (H-HCA) in the general population (*Figure 73*) and in MODY3 exhibit steatosis and present a particular metabolism, characterized by activation of glycolysis and fatty acid synthesis, along with an inactivation of GNG (Calderaro et al., 2013; Nault and Zucman Rossi, 2013). Furthermore, the targets of HNF1A, i.e. FABP1 and UGT2B7, are down-regulated in these tumors (*Figure 73*). These studies led to the classification of HNF1A as a tumor suppressor (Luo et al., 2015; Pelletier et al., 2010).

As observed in H-HCA, steatosis, increased glycolysis and repressed GNG are also features of GSDI HCA. Concordantly, in our study, HNF1A was found to be down-regulated in tumors and L.G6pc-/- livers at the tumoral stage, explaining in part the histological and metabolic similarities between H-HCA and GSDI HCA. Interestingly, another study in GSDI human patients reported HNF1A down-regulation, not only in HCA, but also in the liver samples, in accordance with our observations (Calderaro et al., 2013). It was further shown that this down-regulation of HNF1A in GSDI HCA was not due to a mutation, like in H-HCA in the general population, but rather due to a metabolic repression of HNF1A.

To conclude, further mechanistic studies are required in order to see the extent to which HNF1A down-regulation is responsible for adenoma formation, but also for other metabolic perturbations in GSDI. In the meantime, one could learn a lot by extrapolating the knowledge on HNF1A mutations and their effects on metabolism and tumorigenesis in GSDI.

HNF1 in GSDI kidneys

As mentioned, HNF1B mutations have been associated with MODY5. These patients present renal cysts and renal function decline that precedes diabetes, hence MODY was initially referred to as renal cysts and diabetic syndrome (Faguer et al., 2011; Verhave et al., 2016). It is noteworthy that the predominant site of HNF1B expression is the kidney, while the predominant site of HNF1A expression is the

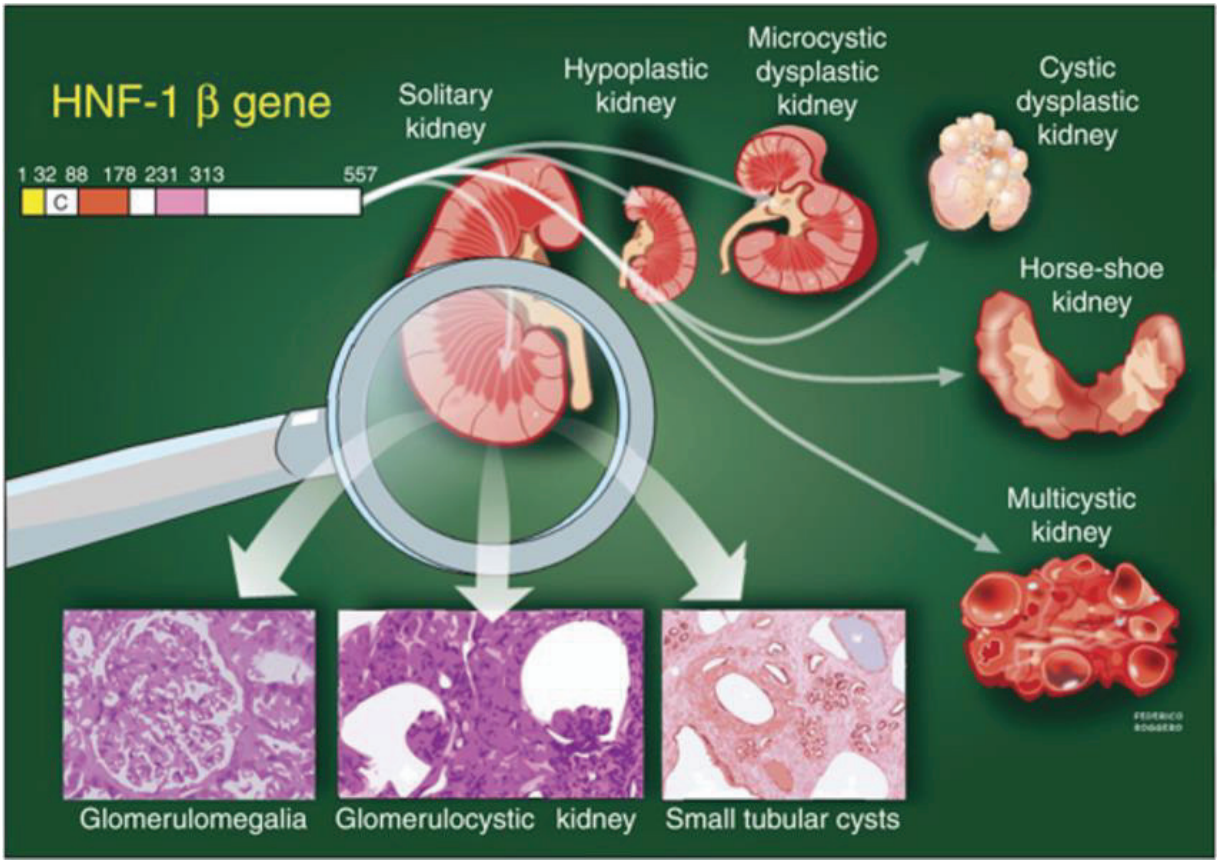

Figure 74: The large spectrum of macroscopic and microscopic renal diseases associated with hepatocyte nuclear factor 1β (HNF-1β) mutations

As most of the identified HNF-1β target gene products colocalize in the primary celium, the crucial organelle that has an important role in controlling the proliferation of tubular cells, it provides the background to explain the large spectrum of different macroscopic and microscopic overt renal diseases, including single kidney, hypoplastic kidney, microcystic hypoplastic kidney, horse-shoe kidney, multicystic kidney, glomerulomegalia, glomerulocystic kidney, or kidney with small tubular cysts, that have been described in patients with alterations in the HNF-1β gene.

(Stratta et al.,2010)

pancreas and liver (Owen et al., 2014). HNF1B is expressed very early in kidney development. Indeed, it has been shown that HNF1B mutations can lead to abnormal nephron development, such as enlarged Bowman's capsule and renal tubular dysgenesis (Massa et al., 2013) (*Figure 74*). Furthermore, HNF1B has been shown to affect genes that are known to be involved in renal cyst formation, such as polycystic kidney disease 2 (PKD2) and polycystic kidney and hepatic disease 1 (PKHD1) (Hiesberger et al., 2005; Igarashi et al., 2005). Therefore, HNF1B plays a central role in renal cyst development in various diseases and is potentially responsible for the similar phenotype in many polycystic kidneys diseases (Faguer et al., 2011).

While the expression of HNF1B has never been assessed in GSDI kidneys in published bibliography, we observed a down-regulation of this gene at the kidney failure and cyst development stage in K.G6pc-/- mice, but not earlier (Gjorgjieva et al., unpublished data). This down-regulation is not surprising, since increased glycolysis and lipogenesis, associated with a decrease in GNG, is observed in GSDI kidneys, due to the excessive amounts of G6P in the tubular cells of the kidneys (Clar et al., 2014; Gjorgjieva et al., 2016a). Thus GSDI kidneys present a highly similar metabolic profile with GSDI livers, with a concomitant down-regulation of HNF1B. Moreover, these data suggest that development of a polycystic kidney disease-like syndrome, characteristic for both MODY and GSDI, could be due to HNF1B down-regulation in both cases.

To conclude, a down-regulation of HNF1A in the liver and HNF1B in the kidneys due to metabolic repression exerted by G6Pase deficiency could be a common underlying cause of hepatic and renal pathology in GSDI.

Cyst development in end-stage kidneys in GSDI: a risk of renal neoplasia?

Renal fibrosis is an important part of CKD progression in GSDI (Gjorgjieva et al., 2016a; Kishnani et al., 2014). In our study we have reported that profibrotic TGF-β1 and subsequent EMT induced by RAS pathway were activated in GSDI kidneys, leading to gradual progression of renal fibrosis (Gjorgjieva et al., 2016a). Renal fibrosis led to the formation of cysts in the kidneys of K.G6pc-/- mice, as observed in GSDI patients, in the later stages of CKD. Cysts seemed to have both tubular and glomerular origin, and

Category I	Simple benign cyst with (1) good through-transmission (i.e., acoustic enhancement), (2) no echoes within the cyst, (3) sharply, marginated smooth wall; requires no surgery.
Category II	Looks benign with some radiologic concerns including septation, minimal calcification, and high density; requires no surgery.
Category IIF	Although calcification in wall of cyst may even be thicker and more nodular than in category II, the septa have minimal enhancement, especially those with calcium; requires no surgery.
Category III	More complicated lesion that cannot confidently be distinguished from malignancy, having more calcification, more prominent septation of a thicker wall than a category II lesion; more likely to be benign than malignant; requires surgical exploration and/or removal.
Category IV	Clearly a malignant lesion with large cystic components, irregular margins; solid vascular elements; requires surgical removal.

Figure 75: Bosniak renal cyst classification system

were observed in a great number and size variety, conferring polycystic kidney disease-like features to GSDI nephropathy.

Cystic kidney diseases can vary in origin and outcome and can have an increased prevalence in renal cancer development (Bonsib, 2009). Indeed, polycystic kidney diseases were associated with a higher incidence of cancer, not only in the kidneys, but also in the liver and colon (Yu et al., 2016). Renal cancer has never been reported in GSDI, yet one can argue if cysts developed in GSDI kidney present pre-neoplastic features and could potentially evolve in renal cell carcinoma. In our study, we have reported one patient with Bosniak II grade cyst. The Bosniak grading system for renal cysts is used to predict the outcome for the patient and is described in *Figure 75*. While it is argued whether Bosniak II cysts present malignant potential, a meta-analysis of 6 studies estimated 15.6% possibility of malignancy for this group (Graumann et al., 2011). Therefore, we can suggest that GSDI patients could be at risk of renal cancer. Furthermore, it has been pointed out that clear cell cysts in acquired cystic diseases are a precursor for renal cell carcinoma, since both present very similar immunological and metabolic features (Hosseini et al., 2014). Thus the morphological, histological, immunological and metabolic aspect of GSDI cysts needs to be determined precisely in order to evaluate the malignant risks associated with this long-term complication.

While GSDI renal metabolism remains in part unknown, G6P levels are increased, leading to glycolysis, lipid synthesis enhancement and lipid oxidation decrease (Clar et al., 2014; Gjorgjieva et al., 2016a), similar to the «Warburg-like» phenomenon observed in the liver. Therefore, we can suggest a pre-neoplastic status not only to GSDI livers, but also to the kidneys. This metabolic reprogramming could thus be responsible for renal cyst development. In accordance with a common mechanism between both tissues, reducing lipid metabolism has the same beneficial effect in the kidney and liver in GSDI.

With the increase in life span in GSDI patients thanks to the dietary therapy, renal complications in older patients are just starting to arise and are observed for the first time. However, cysts were detected only right before the renal failure stage

occurred. Unfortunately, late malignant transformation of cysts could be a possibility in GSDI patients. Therefore, frequent follow up in kidney imaging and renal function should be highly recommended, once a year, as soon as the first symptoms of nephropathy appear.

Treatment strategies for GSDI

While GSDI is a monogenic disease, many metabolic fluxes are altered, resulting in a redirection of G6P toward other pathways, especially glycogen synthesis, glycolysis, *de novo* lipogenesis and nucleotide synthesis. Thus the treatment of GSDI should include increased glucose supply to maintain glycaemia, but it should also avoid glycogen and lipid accumulation in the liver and kidneys. As tumorigenesis can be initiated from any small population of damaged hepatocytes that are actively proliferating, GSDI therapy should target a maximum of hepatocytes in order to prevent disease progression. The same problem should be taken into account for the treatment of CKD.

A strategy aiming to inhibit lipid synthesis in order to prevent deleterious effects of this pathway in GSDI patients might therefore sound like a suitable alternative to prevent both liver and kidney injury. Furthermore, glycolysis and cholesterol synthesis inhibition could also be a solution to GSDI. Indeed, HMG-CoA reductase inhibitor, FAS inhibitors, SCD1 inhibitors have already been used in various pathologies, as lipid lowering strategies in order to decrease lipid injury, but also as anti-cancer strategies, since these pathways are crucial for tumor development and progression (Alkhouri et al., 2009; Smith et al., 2009; Zaytseva et al., 2012). Nevertheless, inhibiting one of the pathways activated in GSDI might not result in a normalization of the parameters, since G6P utilization should be redirected toward the rest of the metabolic fluxes. The successful results obtained in our work by treating GSDIa mice with the lipid-lowering drug fenofibrate relied on the fact that G6P was up-taken by the lipid synthesis pathway and was subsequently metabolized *via* lipid oxidation, avoiding the redirection of G6P towards glycogen and lipid accumulation. Unfortunately, while the lipid-lowering effects of fenofibrate were highly beneficial in both the liver and kidneys of GSDI mice, this strategy did not insure normal glycaemia.

Contrarily to these promising data, the inhibition of glycogen synthesis did not allow the total prevention of hepatic complications in L.G6pc-/- mice. This study was performed in collaboration with Dicerna pharmaceuticals, USA (*Annex II*) who provided an RNA interference vector (RNAi), specifically inhibiting glycogen synthase II (*Gys2*) gene expression in the liver. The delivery of the RNAi in the liver was performed by targeting the asialoglycoprotein receptors thanks to a modified RNA and GalNAc conjugation of a tetraloop hairpin (Thapar et al., 2014). This RNAi efficiently inhibited Gys2 in the liver of L.G6pc-/- mice. Subsequently, this resulted in about 20% decrease in hepatic glycogen and G6P contents that was sufficient to improve liver histology (*Annex II*). Moreover, lipid synthesis and accumulation was also slightly inhibited, due to reduced G6P availability. Unfortunately, this approach did not increase glucose levels in L.G6pc-/- mice, nor it normalized plasmatic cholesterol and TG. The short duration (5 weeks) of the study did not permit the assessment of the effect of Gys2 RNAi on tumor development. Thus the inhibition of glycogen synthesis did not allow us to prevent hepatomegaly in L.G6pc-/- mice. Interestingly, Gys2 inhibition by RNA interference was performed for a longer time to treat Agl-/- mice, which represent a GSDIII mouse model (*Annex II*). Agl-/- mice were injected weekly or monthly for 36 weeks to 12 months with RNAi targeting Gys2. Long-term Gys2 inhibition prevented glycogen accumulation, hepatomegaly, liver injury, fibrosis and nodule development (*Annex II*). However, Gys2 RNAi failed to correct glycaemia in Agl-/- mice, as observed in L.G6pc-/- mice. It is noteworthy that this approach has several advantages compared to viral vectors. Indeed, the development of a gene therapy approach for GSDs is practically limited by transduction efficiency, expression transience, and viral genome size restriction. In contrast to gene therapy, RNAi-mediated inhibition of glycogen synthesis has the advantage of reaching and correcting nearly all of the hepatocytes, thus preventing glycogen accumulation evenly throughout the liver. Indeed, gene therapy essays allowed only mosaic glycogen alleviation. Although Gys2 inhibition had no effect on hypoglycemia, it has the potential to complement a gene therapy approach by correcting liver abnormalities in GSDs and provides therapeutic options to GSD patients with hepatic injury who currently have no therapeutic options. The difference in the success rates obtained in GSDI and GSDIII models could be due to the length of the

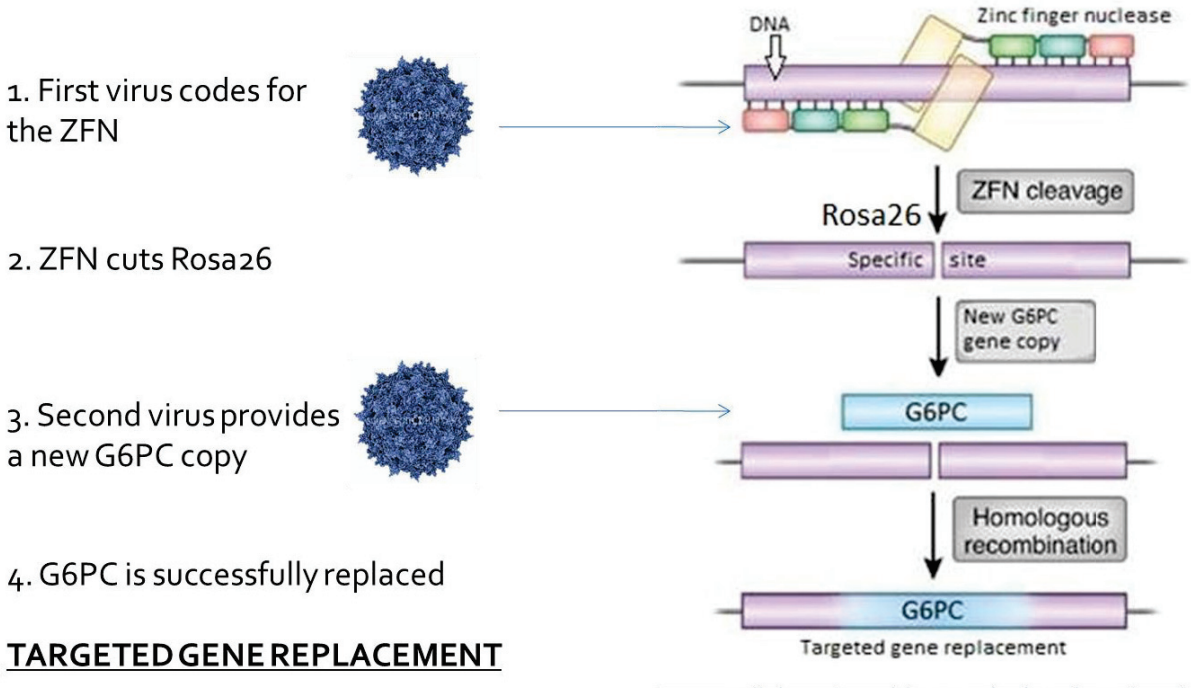

Collaboration with D. Koeberl, Duke University, USA

Figure 76: AAV-ZFN vector gene therapy strategy

AAV-ZFN vectors are used in a dual vector strategy. The first vector containing the zinc finger nuclease (ZFN) is designed to cut DNA in a specific site called Rosa26, which is a safe harbor locus. The specificity of the ZFN to Rosa26 comes from the homology of this nuclease with the Rosa26 locus. Once Rosa26 is cut, the second vector provides a new copy of *G6pc*. The insertion of the new gene is assured by the "sticky ends" added at each extremity of the gene. These so-called sticky ends share perfect homology with the cut Rosa26 locus, facilitating the insertion of the gene and a subsequent homologous recombination, repairing the missing nucleotide bases around the sticky ends and the extremities of the cut DNA.

treatment. Indeed, treating L.G6pc-/- mice for a longer period could result in a prevention of hepatomegaly and liver injury as in Agl-/- mice, but this hypothesis needs to be confirmed. Last, while both GSDI and GSDIII are both characterized by glycogen accumulation and hypoglycemia, they present marked differences in other metabolic pathways, such as lipid metabolism, possibly playing a role in the different outcomes of the RNAi treatment.

Finally, the best curative option for GSDI would be gene therapy, allowing a replacement of the mutated sequence of G6PC or SLC37A4 in the liver and the kidneys. Nevertheless, designing a vector that can transduce a maximum of hepatocytes and renal tubular cells, that does not induce any inflammatory responses nor non-target insertions, and that is not lost overtime, is an extremely delicate task.

Nevertheless, nowadays many advanced gene therapy tools are being developed, opening a new horizon for GSDI gene therapy assays. Indeed, our laboratory, in collaboration with Dr Dwight Koeberl from Duke University, USA, tested an innovative AAV gene therapy strategy, employing ZFN. This approach combines the inoffensive AAV vectors with the ability of ZFN to insert a copy of *G6pc* in harbor loci, allowing a safe integration of the target gene (*Figure 76*). After 12 months of AAV-ZFN injection, L.G6pc-/- mice exhibited normal glycaemia and a normalization of TG, uric acid and BUN levels, due to a two-fold increase in G6Pase activity (unpublished data). Furthermore, hepatic glycogen content was significantly decreased, while hepatic TG had only a tendency to decrease. Nevertheless, this therapy did not change hepatic tumor incidence in L.G6pc-/- mice treated with AAV-ZFN (unpublished data). Interestingly, all of the tumors exhibited an absence of AAV-ZFN or gene insertion, confirming: 1) that these tumors were not a result of an oncogenic insertion of our target gene; 2) the efficiency of the therapeutic vector to protect against tumorigenesis. Finally, an optimization of the vector could allow a more important transduction in the liver, eventually resulting in a larger inhibition of tumor formation, besides normalization of the plasmatic parameters.

At the last International glycogen storage disease conference (IGSD2017) that took place in Groningen, Netherlands, the pediatric endocrinologist Dr. David Weinstein (USA) announced the beginning of the first gene therapy assay in patients with GSDI. This treatment will involve an AAV vector, which was tested in GSDI mouse and dog models. While this announcement is extremely exciting and promising, clinical trials such as these take time to be properly evaluated, validated and optimized. This is why it is crucial to keep deciphering the underlying mechanisms of hepatic and renal GSDI pathologies, in order to get the most out of the gene therapy strategies, or to find other back-up treatment targets.

PUBLICATIONS AND PRESENTATION OF DATA

Publications

- « Progressive development of renal cysts in glycogen storage disease type I »

Human Molecular Genetics, 2016, Vol. 25, No. 17 3784–3797

Monika Gjorgjieva, Margaux Raffin, Adeline Duchampt, Ariane Perry, Anne Stefanutti, Marie Brevet, Antonin Tortereau, Laurence Dubourg, Aurelie Hubert-Buron, Mylene Mabille, Coralie Pelissou, Louis Lassalle, Philippe Labrune, Gilles Mithieux and Fabienne Rajas

- « Mechanisms by Which Metabolic Reprogramming in GSD1 Liver Generates a Favorable Tumorigenic Environment »

Journal of Inborn Errors of Metabolism & Screening 2016, Volume 4: 1–10

Monika Gjorgjieva, Maaike H. Oosterveer, Gilles Mithieux, and Fabienne Rajas

- « Metabolic stress associated with hepatic carcinogenesis in the absence of fibrosis in Glycogen storage disease type Ia »

Submitted to Journal of Hepatology

Monika Gjorgjieva, Julien Calderaro, Laure Monteillet, Marine Silva, Margaux Raffin, Marie Brevet, Caroline Romestaing, Damien Roussel, Jessica Zucman-Rossi, Gilles Mithieux & Fabienne Rajas

- « Lipid burden alleviation – a common target to prevent hepatic and renal complications in Glycogen Storage Disease type Ia »

Submitted to Cell Metabolism

Laure Monteillet, Monika Gjorgjieva, Marine Silva, Vincent Verzieux, Linda Imikirene, Adeline Duchampt, Hervé Guillou, Gilles Mithieux, Fabienne Rajas

Presentations and awards

- **M. Gjorgjieva**, M. Silva, G. Mithieux, F. Rajas - « Metabolic reprogramming favoring hepatic tumorigenesis in Glycogen storage disease Ia »
  BMIC doctoral school PhD days, 21-22 November, 2017, Lyon, France
  Poster presentation
-
- **M. Gjorgjieva**, M. Silva, G. Mithieux, F. Rajas - « Metabolic reprogramming favoring hepatic tumorigenesis in Glycogen storage disease Ia »
  AFEF congress (Association Française pour l'Etude du Foie), 4-7 October 2017 Nice, France
  Oral presentation

- **M. Gjorgjieva**, L. Monteillet, M. Silva, G. Mithieux, F. Rajas - « Effects of Fenofibrate on hepatic complications in glycogen storage disease type Ia in mice »
  International congress for glycogen storage diseases, 13-17 June 2017 Groningen, Netherlands
  Poster presentation

- **M. Gjorgjieva**, M. Silva, G. Mithieux, F. Rajas - « Alteration of cellular defenses during hepatic tumor development in glycogen storage disease type Ia »
  International congress for glycogen storage diseases, 13-17 June 2017 Groningen, Netherlands
  Oral presentation

- **M. Gjorgjieva**, P. Labrune, G. Mithieux, F. Rajas - « Renal cysts in GSD I patients »
  International congress for glycogen storage diseases, 13-17 June 2017 Groningen, Netherlands
  Oral presentation

- **M. Gjorgjieva,** M. Silva, G. Mithieux, F. Rajas - « Hepatic metabolism in glycogen storage disease type 1a »
  G2L2 meeting, 19 May 2017, Lyon, France
  Poster presentation

- **M. Gjorgjieva,** M. Silva, G. Mithieux, F. Rajas - « Alteration of cellular defenses during hepatic tumor development in glycogen storage disease type Ia »
  Early career scientist day at the International agency for research on cancer, 9 May 2017, Lyon, France
  Oral presentation

- **M. Gjorgjieva**, G. Mithieux, F. Rajas - « Alteration of cellular defenses during hepatic tumor development in glycogen storage disease type Ia »
  Metabolism and cancer symposium, 22-23 September 2016, Palavas-les-Flots, France
  Poster presentation

- **M. Gjorgjieva,** A. Stefanutti, M. Raffin, G. Mithieux, F. Rajas - « Autophagy in tumor-free livers and hepatocellular tumors in a glycogen storage disease type 1a mouse model »
  EASL International liver congress, April 2016, Barcelona, Spain
  Poster presentation and e-poster

- **M. Gjorgjieva,** A. Stefanutti, M. Raffin, G. Mithieux, F. Rajas - « Autophagy during hepatic tumor development in a Glycogen storage disease type 1a mouse model »
  Forum Clara Cancéropôle, March 2016, Lyon, France
  Poster presentation

- **M. Gjorgjieva**, J. Clar, G. Mithieux, F. Rajas - « Diet influences the development of hepatocellular adenomas and carcinomas in mice with glycogen storage disease type 1a »
  Oncoriales, July, 2015, Lyon, France
  Poster presentation, award for best poster

- **M. Gjorgjieva**, M. Raffin, A. Stefanutti, G. Mithieux et F. Rajas. - « Autophagy in tumor-free and pretumoral stage livers in a Glycogen storage disease type Ia mouse model »
  Clara Canceropôle Rhône Alpes-Auvergne -7-8 April 2015, Lyon, France
  Poster presentation

- **M. Gjorgjieva**, J. Clar, M. Raffin, A. Duchampt, G. Mithieux et F. Rajas. - « Junk food accelerates pathology development in a nephropathy mouse model »
  Congress of the Francophone society of diabetes (SFD), 24-27 March 2015, Bordeaux, France
  Oral presentation

- **M. Gjorgjieva**, J. Clar, M. Raffin, A. Duchampt, G. Mithieux et F. Rajas - « Effect of diet on the development of nephropathy in a mouse model of glycogen storage disease type 1a »
  Science day SFR, 16/12/2014, Lyon, France
  Poster presentation

- **M. Gjorgjieva**, G. Mithieux et F. Rajas. - « Liver glucose-6 phosphatase deletion reproduces the long-term hepatic pathology development of Glycogen Storage Disease type Ia »
  Pathology meeting, experimental pathology club, 20/11/2014, Paris, France
  Oral presentation

- **M. Gjorgjieva**, J. Clar, M. Raffin, A. Duchampt, G. Mithieux and F. Rajas - « Effect of diet on the development of nephropathy in a mouse model of glycogen storage disease type 1a ».
  G2L2 meeting, 23/05/2014, Grenoble, France
  Award for best oral presentation

Volunteer work

- Organization committee member of the SFR Santé Lyon conference «Metabolism and imaging» scheduled for 5 December 2017, Lyon, France

- Organization committee member of the Francophone Society of diabetes congress (SFD) 21-25 March 2016, Lyon

ANNEX I

Collaboration with Genethon

Rescue of GSDIII phenotype with gene transfer requires liver- and muscle- targeted GDE expression

Patrice Vidal[1,2], Serena Pagliarani[3], Pasqualina Colella[1,4], Helena Costa Verdera[1,2], Louisa Jauze[1,2], Monika Gjorgjieva[8], Francesco Puzzo[1,4], Solenne Marmier[2], Fanny Collaud[1,4], Marcelo Simon Sola[1,4], Severine Charles[1,4], Sabrina Lucchiari[3], Laetitia van Wittenberghe[4], Alban Vignaud[4], Bernard Gjata[4], Pascal Laforet[5,6,7], Edoardo Malfatti[5,6], Gilles Mithieux[8], Fabienne Rajas[8], Giacomo P. Comi[3], Giuseppe Ronzitti[1,4], Federico Mingozzi[1,2,4]

[1]INTEGRARE, Genethon, Inserm, Univ Evry, Université Paris-Saclay, 91002, Evry, France

[2]University Pierre and Marie Curie Paris 6 and INSERM U974, Paris, France

[3]Dino Ferrari Centre, Neuroscience Section, Department of Pathophysiology and Transplantation (DEPT), University of Milan, Neurology Unit, IRCCS Foundation Ca' Granda Ospedale Maggiore Policlinico, Milan, Italy

[4]Genethon, Evry, France

[5]Myology Institute, Neuromuscular pathology reference center, Groupe Hospitalier Universitaire La Pitié-Salpêtrière; Sorbonne Universités UPMC Univ Paris 06, Paris, France

[6]Myology Institute, Neuromuscular Morphology Unit, Groupe Hospitalier Universitaire La Pitié-Salpêtrière; Sorbonne Universités UPMC Univ Paris 06, Paris, France

[7]Paris-Est neuromuscular center, Pitié-Salpêtrière Hospital, APHP, Paris, and Raymond Poincaré Teaching Hospital, Garches, APHP, France

[8]Institut National de la Santé et de la Recherche Médicale, U1213, Lyon, F-69008, France Université Lyon 1, Villeurbanne, F-69622 France

Short title: AAV gene therapy for GSDIII

Corresponding authors:

Federico Mingozzi, PhD

fmingozzi@genethon.fr

Giuseppe Ronzitti, PhD

gronzitti@genethon.fr

Genethon

1 rue de l'Internationale

91000, Evry, France

Abstract (200 max)

Glycogen storage disease type III (GSDIII) is an autosomal recessive disorder caused by a deficiency of glycogen debranching enzyme (GDE), which results in profound liver metabolism impairment and muscle weakness. To date, no cure is available for GSDIII and current treatments are mostly based on diet. Here we describe the development of a mouse model of GSDIII, which faithfully recapitulates the main features of the human condition. We used this model to develop and test novel therapies based on adeno-associated virus (AAV) vector-mediated gene transfer. First, we showed that overexpression of the lysosomal enzyme alpha-acid glucosidase (GAA) with an AAV vector led to a decrease in liver glycogen content but failed to reverse the disease phenotype. Using dual overlapping AAV vectors expressing the GDE transgene in muscle, we showed functional rescue with no impact on glucose metabolism. Liver expression of GDE, conversely, had a direct impact on blood glucose levels. These results provide proof-of-concept of correction of GSDIII with AAV vectors, and indicate that restoration of the enzyme deficiency in muscle and liver is necessary to address both the metabolic and neuromuscular manifestations of the disease.

Introduction

Glycogen storage disease type III (GSDIII) is a rare (incidence of 1 in 100,000 at birth)[1] autosomal recessive disorder caused by mutations in the *AGL* gene encoding for the glycogen debranching enzyme (GDE or amylo-alpha-1,6-glucosidase, EC no. 3.2.1.33, UniProt P35573). GDE is an enzyme with two catalytic sites involved in the conversion of cytosolic glycogen to glucose[2].

The clinical manifestations of GSDIII are characterized by two phases, during childhood, the disease has mainly the features of a metabolic disorder with hepatomegaly and severe fasting hypoglycemia, hyperlipidemia, and hyperketonemia; during adolescence and adulthood, a progressive debilitating myopathy, with a heterogeneous involvement of different muscle groups and exercise intolerance appear, rendering the metabolic impairment less prominent[2]. GSDIII disease burden is important especially in patients that suffer from severe skeletal muscle weakness and exercise intolerance[1, 2]. Histological analysis of muscle biopsies from GSDIII patients confirms the muscle involvement, and shows accumulation of glycogen in large vacuoles that disrupt the myofibrils architecture[3]. Additionally, most of GSDIII patients have a cardiac involvement, although only a small percentage (15%) of them develops cardiomyopathy[2]. Additionally, liver complications such as cirrhosis, development of hepatocellular adenomas (HCA) and hepatocellular carcinomas (HCC) has been described in a significant proportion of GSDIII patients[2].

To date, the only therapeutic approach currently available for GSDIII is symptomatic[2, 4]. During childhood, to avoid recurrent hypoglycemia, patients follow a strict diet regimen with frequent meals rich in complex carbohydrates, typically uncooked cornstarch[5]. High-protein high-fat diet has been proposed for adults GSDIII patients, and a strict ketogenic regimen has been reported to

be efficacious in preventing hypertrophic cardiomyopathy[6, 7]. At present, no therapy has been proposed to address the muscle impairment observed in GSDIII, thus the disease remains an unmet medical need.

The monogenic nature of GSDIII, and the fact that it is caused by a well-defined enzyme deficiency, make the disease a possible target for gene replacement therapies. To this aim, adeno-associated virus (AAV) vectors represent the platform of choice for *in vivo* gene transfer[8]. Data obtained in the context of clinical trials for hemophilia[9], congenital blindness[10], and spinal muscular atrophy[11] demonstrate the safety and therapeutic potential of the AAV vector gene transfer platform. Furthermore, the experience accumulated in large animal models of neuromuscular disorders indicates that systemic administration of AAV vectors results in efficient targeting of muscle[12, 13]. While promising, one of the most important restrictions in the use of AAV vectors is the size of the transgene expression cassette, which is limited to ~5 Kb. Consequently, due to the large size of the GDE cDNA, ~4.6 Kb, the development of AAV vector-based GDE gene transfer strategies is challenging.

Here we describe a new murine model of GSDIII, which faithfully recapitulates the human condition, including body-wide glycogen accumulation, low blood glucose levels, and muscle weakness. Using this model, we tested different gene therapy-based approaches aimed at correcting the disease. Specifically, we showed that overexpression of the lysosomal enzyme alpha-acid glucosidase (GAA) with AAV vectors was not sufficient to fully rescue the GSDIII phenotype *in vivo*. Conversely, using dual overlapping AAV vectors[14-16], for the first time we showed restoration of the GDE enzyme in both liver and muscle thus demonstrating that the expression of the endogenous enzyme in those tissues is required for clearance of cytosolic

glycogen, rescue of muscle strength, and amelioration of blood glucose levels in treated animals. The work presented here provides the framework for the future development of gene therapy approaches to GSDIII.

Results

Development of a murine model of GSDIII which fully recapitulates the human condition

A mouse model of GSDIII ($Agl^{tm1b(EUCOMM)Wtsi}$) was acquired through the International Mouse Phenotyping Consortium (http://www.mousephenotype.org/about-ikmc/eucomm).

Three-month-old GDE knock-out ($Agl^{-/-}$) mice completely lacked GDE expression in liver and skeletal muscle as determined by Western blot (**Figure 1A**) and GDE activity measurement in liver (**Figure 1B**). As expected, the lack of the enzyme was associated with the accumulation of glycogen in liver, heart, different skeletal muscle groups, and brain (**Figure 1C**). Additionally, the block of glycogen degradation in the liver led to a dramatic decrease of glucose-6-phosphate levels in $Agl^{-/-}$ animals (**Figure 1D**).

Detailed histological analysis confirmed the accumulation of glycogen in muscle (**Figure S1**). Interestingly, the accumulation of glycogen was not homogenous in all fibers, as some showed comparable glycogen content to that observed in muscle from wild-type littermates ($Agl^{+/+}$ mice, **Figure S2**). Hematoxylin-eosin (HE) revealed the presence of large vacuoles in muscle fibers that appear to contain periodic acid-Schiff (PAS) –positive material (**Figures 1E,F** and **S1**). The presence of vacuoles filled with glycogen strongly resembles the pattern of glycogen accumulation encountered in muscle biopsies from GSDIII patients[3]. Electron microscopy studies on quadriceps from $Agl^{-/-}$ animals disclosed the presence of large glycogen pools disrupting the myofibrillar structure both in transversal and longitudinal ultrathin sections (**Figure 1G and H**). Higher magnification of transversal section revealed the presence of small areas containing apparently normally structured glycogen granules that misplaced the myofibrils(**Figure 1I**), leading to progressive sarcomeric degeneration.

Perhaps one of the most evident phenotype in young GSDIII patients is the relatively severe and persistent hypoglycemia[1, 4]. Accordingly, 6-month-old $Agl^{-/-}$ mice showed a significant reduction in blood glucose levels (**Figure 2A**) accompanied by a ~three-fold increase in the liver/body weight ratio (**Figure 2B**), consistent with hepatomegaly and similar to what described in GSDIII patients[1, 2]. We then evaluated muscle function in affected animals at 3, 6, and 9 months of age. No differences were observed in total distance traveled and rotarod performance (**Figure 2C,D** and **Table S1**), indicating that glycogen accumulation in muscle and hypoglycemia did not affect general locomotion in $Agl^{-/-}$ mice. Interestingly, when the same mice were tested for muscle strength, we observed a significant ($p=0.006$) ~20% reduction in grip strength and a profound impairment ($p=2.2x10^{-7}$) in the wire-hang test performance (**Figure 2E** and **2F**, respectively). Functional testing repeated in 6- and 9- month-old animals showed similar results (**Table S1**).

These results confirm that the model used in this study recapitulate faithfully the human phenotype and therefore is suitable to test novel therapeutic strategies to treat GSDIII.

High levels of GAA secreted in the bloodstream decreases glycogen accumulation in liver but not in muscle

Previous results obtained *in vitro* suggest that supraphysiological levels of GAA activity can clear glycogen from primary human GSDIII myoblasts[17]. To test whether GAA overexpression has the potential to rescue glycogen accumulation in GSDIII mice, we took advantage of a recently developed AAV vector expressing a secreted form of GAA (AAV-GAA)[18]. Three-month-old GSDIII mice were treated with an AAV-GAA vector at $1x10^{11}$ or $1x10^{12}$ vector genomes (vg)/mouse and followed-up for three months (**Figure 3A**). As expected, the injection of the AAV-GAA vector resulted in a dose-dependent increase of GAA activity in the

bloodstream (**Figure 3B**), and in supraphysiological levels of GAA enzyme activity in all tissues (**Figure 3C**, measured at sacrifice).

Interestingly, the administration of the AAV-GAA vector significantly decreased glycogen accumulation in the liver of $Agl^{-/-}$ mice, both at the $1x10^{11}$ and $1x10^{12}$ vg/mouse dose level ($p = 0.00025$ and $2.7x10^{-6}$ vs. $Agl^{-/-}$ animals, respectively), to levels comparable to those observed in wild-type littermates ($p=0.092$ and 0.639 vs. $Agl^{+/+}$, for the low and high vector dose, respectively, **Figure 3D**). However, this did not lead to a significant improvement in the metabolic phenotype of $Agl^{-/-}$ mice, as the treatment did not improve blood glucose or hepatomegaly (**Figure S3**). Treatment with AAV-GAA had no effect on glycogen accumulation in $Agl^{-/-}$ muscle (**Figure 3D**). Accordingly, grip strength and wire hang performance measured 3 months post gene transfer were not rescued in mice treated with AAV-GAA (**Figure 3E** and **Table S2**). Interestingly, one month after treatment we observed a transient significant reduction in the number of fall per minute in the wire hang test in animal treated with the AAV-GAA vector at the highest dose ($p=0.008$ vs. untreated $Agl^{-/-}$). No improvement in grip strength was observed at any time point (**Table S2**).

Together these results indicate that although high levels of GAA enzyme activity result in a decreased glycogen accumulation in the liver, they fail to rescue glycemia and muscle function in GSDIII mice.

Dual overlapping vectors expressing GDE efficiently rescue glycogen accumulation in muscle of GSDIII mice

Dual overlapping AAV vectors have been used to express genes larger than 5Kb in muscle[13, 14, 19]. We therefore developed a dual AAV vector expressing the GDE transgene in which the 5'

portion (nucleotides 1 to 2688) of the human GDE (hGDE) cDNA was fused with the CMV promoter and second intron of human beta globin (HBB2)[20] (GDE-HEAD, **Figure 4A**). The 3' portion (nucleotides 1693 to 4599) of the hGDE coding sequence was fused with a polyadenylation signal derived from HBB2 (GDE-TAIL, **Figure 4A**). A region of overlap of 996 nucleotides (nucleotides 1693 to 2688 of the GDE cDNA) was used to mediate the homologous recombination of GDE-HEAD and GDE-TAIL vectors. The two overlapping cassettes were pseudotyped[21] into an AAV9 vector and co-injected in $Agl^{-/-}$ mice at a dose of $1x10^{12}$ vg per mouse each (**Figure 4B**). Three months after vector injection, most of the vector genomes were found in liver and heart, whereas quadriceps and triceps had the lowest vector genome copy number (**Figure S4**). However, while Western blot analysis revealed GDE protein expression in heart and skeletal muscles, no protein was detectable in liver (**Figure 4C**). Similarly, hGDE transgene mRNA expression levels, normalized for vector genome copy number, were 50 to 800-fold lower in the liver compared to muscle (**Figure 4D**), suggesting that CMV promoter inactivation in the liver occurred[22]. Accordingly, the absence of expression of the GDE transgene in the liver was associated with lack of correction of the glycemia or hepatomegaly (**Figure S5A,B**).

AAV vector treatment resulted in a significant decrease in glycogen accumulation in several muscle groups but not in the liver (**Figure 4E**). In heart and quadriceps, we observed an inverse correlation (R^2 = 0.9 and 0.97, respectively) between the quantity of GDE protein expressed and the glycogen accumulated in the tissue (**Figure 4 F,G**). Accordingly, the levels of expression of GDE necessary to clear 80% of glycogen could be estimated to be 8% in heart and 2% in quadriceps.

PAS staining confirmed the robust reduction in glycogen accumulation in all muscle groups analyzed, accompanied by a general rescue of the fiber structure as highlighted by HE staining (**Figure 5**). Muscle function was also evaluated by monthly measurement of wire-hang performance and grip strength. In agreement with the biochemical and histological data, the administration of the dual AAV vector expressing GDE significantly rescued wire hang performance to levels undistinguishable to those measured in wild-type animals (p=0.934 and 0.836 vs. $Agl^{+/+}$ at 2 and 3 months post treatment, respectively, **Figure 6A** and **Table S3**). Additionally, a significant increase in the grip strength was observed in $Agl^{-/-}$ mice treated with overlapping vectors three months after the injection (p=0.026 vs. $Agl^{-/-}$, **Figure 6B** and **Table S3**).

These results indicate that CMV-driven GDE transgene expression mediated by overlapping AAV vectors can rescue the muscle phenotype in GSDIII mice. However, the approach has no effect on the liver manifestations of the disease.

Hepatocyte-restricted GDE expression improves glycemia in GSDIII mice

We then tested the dual vector approach by expressing GDE under the transcriptional control of a potent liver-specific promoter[23]. For this experiment, vectors were pseudotyped into AAV8, a capsid that efficiently targets the liver in mice[24]. The injection of $Agl^{-/-}$ mice with $1x10^{12}$ vg/mouse of the combination of the overlapping vectors (GDE-HEAD with the liver-specific promoter and GDE-TAIL), resulted in detectable expression of GDE protein in liver of 5/8 AAV-treated mice, measured by Western blot (**Figure 7A**). Glycogen accumulation in the liver of $Agl^{-/-}$ animals treated with the dual AAV vector was undistinguishable from that measured in wild-type $Agl^{+/+}$ animals (p=0.409, **Figure 7B**). Accordingly, we observed a significant

improvement of the blood glucose in treated $Agl^{-/-}$ mice at all time points tested (p=0.0008 vs. untreated $Agl^{-/-}$, two-way ANOVA time x treatment, **Figure 7C**). Despite the positive impact on glycogen accumulation and glycemia, AAV gene transfer was not able to correct hepatomegaly (**Figure S6**).

These results demonstrate that liver expression of GDE can rescue glycemia and decrease glycogen accumulation but has no effect on hepatomegaly.

Impact of gene transfer on liver metabolism in GSDIII mice

Based on results obtained with gene transfer *in vivo*, we sought to compare the effect of GAA and GDE gene transfer on liver metabolic pathways. To this aim, we analyzed the levels of expression of a panel of genes involved in different pathways of the mouse glucose and glycogen metabolism (**Figure 8A**). The level of expression of 70 genes expressed in the mouse liver was analyzed. When we compared the profile of expression in wild-type $Agl^{+/+}$ animals, untreated $Agl^{-/-}$ mice showed, with some exception, a generalized down-regulation of all the pathways investigated (**Figure 8B**). 43 genes significantly changed in at least one of the three groups analyzed (untreated $Agl^{-/-}$, AAV-GAA, and AAV-GDE overlapping treated $Agl^{-/-}$, $p<0.05$ by ANOVA). Of these 43 genes, only 19 showed an n-fold > ±1.75 (**Table S4**), and 11 genes were changed in untreated $Agl^{-/-}$ mice. 4/11 genes were rescued in animals treated with AAV-GAA vector whereas the treatment with overlapping AAV vectors expressing GDE rescued 8/11 genes (**Table S4**). A general tendency to the normalization of all the genes modified in $Agl^{-/-}$ animals could be observed after treatment with GDE-expressing vectors but not in AAV-GAA treated animals vectors as showed by heat map analysis (**Figure 8C,D**).

These results suggest that GDE expression in the liver mediates a better control of glucose metabolism in the liver.

Discussion

GSDIII is a debilitating neuromuscular and metabolic disease with no curative therapeutic options. This exposes young patients to persistent alterations of glycemia, which become less severe in adulthood when a more pronounced debilitating muscle phenotype appears. The major impact of the disease on the quality of life of patients, and the lack of effective treatments besides dietary management, prompted us to develop new gene therapy approaches to GSDIII.

Here we describe the development and characterization of a mouse model that faithfully recapitulates the disease phenotype in humans, including low blood glucose, hepatomegaly, whole-body accumulation of glycogen, and muscle weakness. With this model, we tested different treatment modalities based on AAV vector gene transfer.

Based on the observation that there is a small percentage of glycogen continuously trafficking from the cytosol to the lysosome[25], we tested whether the overexpression of the lysosomal enzyme GAA could rescue the phenotype of GSDIII. To this aim, we used a highly efficient AAV vector expressing GAA, which was recently demonstrated to mediate whole-body treatment of Pompe disease[18]. Despite achieving supraphysiological levels of GAA activity in most tissues, in GSDIII mice this approach had only a limited and transient effect on muscle performance. A significant reduction of glycogen accumulation was only observed in liver, although no effect on glycemia or hepatomegaly was observed. These results are consistent with data obtained *in vitro* with GSDIII myoblasts treated with recombinant GAA enzyme, in which a partial rescue of glycogen accumulation was observed[17]. Why the effect of GAA on muscle function in GSDIII mice is only transient remains to be assessed. One hypothesis is that, due to the low rate of cytosolic glycogen trafficking to lysosomes in muscle, its pathological accumulation is not fully cleared by GAA overexpression. Based on this, adjuvant therapies

aimed at enhancing autophagy, e.g. by using rapamycin[26], or combination with diet[27-29], may improve the efficacy of this approach in GSDIII. The mechanism(s) underlying the difference in glycogen clearance mediated by GAA in muscle *vs.* liver is also unclear. However, similar observations have been reported after the treatment of GSDIV mice with GAA that resulted in the clearance of liver but not muscle glycogen[30].

Based on the observation that overexpression of GAA alone does not fully correct GSDIII, we sought to address the enzymatic deficiency, hallmark of the disease, by directly restoring the GDE enzyme activity with AAV vectors. The fact that GDE is a large cytosolic protein of 170 kDa with two different enzymatic domains[31], complicates the design of AAV vectors expressing the enzyme and does not allow for the development of gene therapy strategies based on cross-correction[18, 32, 33].

To overcome the limitation of the size of the GDE transgene, we developed a dual AAV vector strategy[13, 14, 19, 34] to express GDE transgene in liver and muscle. CMV promoter-driven GDE transgene expression mediated the complete rescue of muscle function and glycogen accumulation in different muscle groups, including heart[35]. Biochemical parameters correlated with muscle histology and PAS staining, which showed good correction of the disease phenotype. Conversely, due to the silencing of the CMV promoter in liver[22], no liver GDE expression was detected and no correction of glycogen accumulation, hepatomegaly, or glycemia were observed, indicating that targeting muscle alone would not rescue the metabolic impairment hallmark of GSDIII.

To address this limitation and to better explore the role of liver pathology in GSDIII, we designed a dual AAV vector expressing the GDE transgene under the control of a liver-specific

promoter[24]. With this strategy, treated animals showed improved glycemia and clearance of liver glycogen. No effect of gene transfer on hepatomegaly was observed, perhaps indicating that higher expression levels are needed to fully correct the hepatic phenotype in our model.

Gene expression analysis allowed us to compare the impact of GAA *vs.* GDE gene transfer on glucose metabolism in the liver. In untreated knock-out animals *vs.* wild-type controls, the pathways that appeared mostly affected were the regulation of glucose metabolism and the tricarboxylic acid (TCA) cycle. A general normalization of all pathways studied was observed following hepatic GDE gene transfer, while GAA gene transfer mediated the rescue of only a limited subset of genes, further supporting the need for correction of the underlying enzyme defect in GSDIII.

To our knowledge, this is the first proof-of-concept study showing correction of GSDIII *in vivo*. Data presented here also provide insights into the disease and its treatment, in particular on the importance of mobilizing cytosolic glycogen in both liver and muscle to mediate full rescue of the phenotype. Moreover, as metabolic impairment in adults with GSDIII, although less severe than in children, is associated with the development of HCA and HCC[36], the development of effective treatments targeting the liver, in addition to muscle, is highly needed. Thus, future work will be focused on the development of expression cassettes to drive efficient GDE expression in both tissues.

The approach presented here has some limitations associated with the use of dual AAV vectors, specifically i) the low efficiency of reconstitution of the full-length transgene cDNA mediated by the overlapping complementary sequence [15]; and ii) the fact that the homologous recombination

machinery is not equally efficient in all tissues[15]. Alternative strategies could be utilized to enhance the efficiency of homologous recombination to reconstitute the full-length transgene expression cassette. These may include the use of dual hybrid AAV carrying transgene-independent highly recombinogenic DNA sequences[15, 16]. Additionally, small enhancer elements[37] and synthetic promoters[38] combined with AAV serotypes that efficiently target the muscle[39], could increase expression of the GDE transgene.

Finally, data obtained here provide some estimate on the threshold of GDE transgene expression required to obtain therapeutic efficacy. A nearly full rescue of muscle function was observed in GSDIII mice treated with the dual AAV vector expressing the GDE transgene, despite partial restoration of the enzyme expression. This indicates that only a small increment in enzyme activity is sufficient to dramatically improve the muscle phenotype in GSDIII, in line with the concept that the therapeutic threshold, in terms of vector dose, for muscle enzyme deficiencies is lower than that of muscular dystrophies, in which muscle structural proteins are defective[40].

Future efforts will have to focus on improving efficiency of GDE expression in muscle but also in liver, to mediate correction of both the muscle and the metabolic impairment hallmarks of GSDIII. As more information about efficiency of transduction of dual AAV vectors in muscle[14, 16, 19, 41-44] and in other tissues[15, 34] will emerge from preclinical and clinical studies, critical parameters for the successful translation of dual AAV vectors to the clinic will become evident. Specific safety parameters of dual AAV vectors will also have to be carefully defined, such as expression of truncated sequences from the single non-annealed AAV carrying the GDE transgene and transgene immunogenicity.

In conclusion, the work presented here provides the first demonstration of correction of GSDIII in both liver and muscle *in vivo* with dual AAV vectors. Results obtained help defining the levels of GDE protein expression needed to rescue the disease phenotype both at the functional and biochemical level, and lay the fundaments for future translational efforts towards the development of a curative treatment for the disease.

Materials and methods

In vivo studies

The *Agl* knock-out ($Agl^{-/-}$) mice were developed in the frame of the International Mouse Phenotyping Consortium (IMPC). Mice were generated in a pure C57Bl6/J background by replacing exons 6 to 10 of the *Agl* gene with a neomycin expressing cassette. Mice were bred into a mixed BALB/c background for the purpose of this study.

All mouse studies were performed according to the French and European legislation on animal care and experimentation (2010/63/EU) and approved by the local institutional ethical committee (protocol no. 2016-002). AAV vectors were administered intravenously via the tail vein to 3-month-old male $Agl^{-/-}$ mice and wild-type littermates ($Agl^{+/+}$).

Western blot analysis

Mouse tissues were homogeneized in DNAse/RNAse free water and protein concentration determined using the BCA Protein Assay (Thermo Fisher Scientific, Waltham, MA). SDS-PAGE electrophoresis was performed in a 4-15% gradient polyacrylamide gel. After transfer, the membrane was blocked with Odyssey buffer (Li-Cor Biosciences, Lincoln, NE) and incubated with an anti-GDE antibody (Rabbit polyclonal AS09-454, Agrisera), and an anti-actin antibody (Rabbit monoclonal, sc-8432, SantaCruz Biotechnology). The membrane was washed and incubated with the appropriate secondary antibody (Li-Cor Biosciences), and visualized by Odyssey imaging system (Li-Cor Biosciences).

Enzyme activity measurements

GAA activity was measured as previously described[18]. The protein concentration of the samples prior to GAA activity measurement was quantified by BCA (Thermo Fisher Scientific, Waltham, MA). GAA activity was reported as nmol/hour/mg protein when measured in tissue and as nmol/hour/µL when measured in plasma.

GDE activity was measured as previously described[45]. Briefly, 50mg of tissue were homogeneized in 50µL of DNAse/RNAse free water. The lysate was incubated at 37°C with limit dextrin in 4.5 mM EDTA and 0.16 M of phosphate buffer (pH=7). The reaction was then centrifuged. Supernatants were used to measure the glucose produced using a glucose assay kit (Sigma Aldrich, Saint Louis, MO) and by measuring resulting absorbance on an EnSpire alpha plate reader (Perkin-Elmer, Waltham, MA) at 540 nm.

Measurement of glycogen content

Glycogen content was measured indirectly in tissue homogenates as the glucose released after total digestion with *Aspergillus Niger* amyloglucosidase (Sigma Aldrich, Saint Louis, MO). Samples were incubated for 5 min at 95°C and then cooled at 4°C; 25 µl of amyloglucosidase diluted 1:50 in 0.1M potassium acetate pH5.5 were then added to each sample. A control reaction without amyloglucosidase was prepared for each sample. Both sample and control reactions were incubated at 37°C for 90 minutes. The reaction was stopped by incubating samples for 5 min at 95°C. The glucose released was determined as described above.

Histology and electron microscopy

For muscle histology, heart, diaphragm, triceps brachii, quadriceps femoris, tibialis anterior and posterior, gluteus maximus and psoas were snap-frozen in isopentane previously chilled in liquid

nitrogen. Serial 8 µm cross-sections were cut in a Leica CM3050 S cryostat (Leica Biosystems, Nussloch, Germany). To minimize sampling error, 3 sections of each specimen were obtained and stained with HE and PAS according to standard procedures.

Electron microscopic analysis was performed in quadriceps muscles from wild-type and $Agl^{-/-}$ animals. Specimens were fixed with glutaraldehyde (2.5%, pH 7.4), postfixed with osmium tetroxide (2%), dehydrated, and embedded in resin (EMBed-812; Electron Microscopy Sciences, Hatfield, Pennsylvania). Ultrathin sections were stained with uranyl acetate and lead citrate. The grids were observed using an electron microscope (80 kV; Model CM120; Philips Electronics NV, Eindhoven, The Netherlands) and photographed (Morada Soft Imaging System; Olympus France).

Glycemia measurement

Glycemia was measured using sera collected from mice normally fed. A glucose assay kit (Sigma Aldrich, Saint Louis, MO) was used and the resulting absorbance was acquired on an EnSpire alpha plate reader (Perkin-Elmer, Waltham, MA) at a wavelength of 540 nm.

Muscle function tests

Forelimbs wire-hanging test was performed as already reported[18, 46]. A 4 mm-thick wire was used to record the number of fall over a period of 3 minutes. The average number of falls per minute was reported for each animal.

Grip strength was measured as already reported [18, 46]. Using a grip strength meter, (Columbus instruments, San Diego, CA) three independent measurements of the four limbs strength were recorded at each time point. Max values of the weight-normalized grip strength were reported.

Rotarod testing was performed as already reported[18, 47] using a LE8200 apparatus (Harvard Apparatus, Holliston, MA). An accelerating protocol 4-40 rpm in 5 minutes was used. The test was repeated three times and the best performance of each animal was reported.

Production of AAV vectors

All AAV vectors used in this study were produced using an adenovirus-free transient transfection method[48] and purified as described earlier[49]. Titers of the AAV vector stocks were determined using a quantitative real-time PCR (qPCR) and confirmed by SDS-PAGE followed by SYPRO Ruby protein gel stain and band densitometry.

Vector genome copy number determination

Vector genome copy number was determined using a qPCR assay as previously described[20]. The PCR primers used in the reaction were located in the overlapping region of human GDE transgene, forward primer 5'-GTCTTGATAACTGCCACTCA-3', reverse primer 5'-AAAGTAACATGGGATAAGGT-3', for the vector. For the internal control titin gene, the sequences of the forward and reverse primers were 5'-AAAACGAGCAGTGACGTGAGC-3' and 5'-TTCAGTCATGCTGCTAGCGC-3', respectively**.**

In some experiments, a nested PCR was used to amplify of the overlapping region prior to qPCR. Genomic DNA was extracted from 20mg of tissue on a MagNAPure instrument following the manufacturer instructions (MagNAPure 96 system, Roche, Basel, Switzerland). PCR primers used were localized in the regions flanking the overlapping region of human GDE transgene, forward 5'-GTCTTGATAACTGCCACTCA-3' and reverse 5'-AAAGTAACATGGGATAAGGT-3'. Post-amplification genome copy number was determined

by qPCR using a LightCycler 480 (Roche, Basel, Switzerland) as previously described[20]. Oligonucleotides used for qPCR were located in the overlapping region (see Figure S3A) forward 5'-CTGGAGTTGCCACAAAAGGG-3' and reverse 5'-AGTGAGGACTGAATTGTGTC-3'.

Gene Expression analysis

For GDE transgene expression, total RNA was extracted from cell lysates using Trizol (Thermo Fisher Scientific, Waltham, MA). DNA contaminants were removed using the Free DNA kit (Thermo Fisher Scientific, Waltham, MA). Total RNA was reverse-transcribed using random hexamers and the RevertAid H minus first strand cDNA synthesis kit (Thermo Fisher Scientific, Waltham, MA). qPCR was performed with oligonucleotides specific for the GDE transgene (forward 5'-CTGGAGTTGCCACAAAAGGG-3', reverse 5'-AGTGAGGACTGAATTGTGTC-3') and normalized by the levels of expression of GAPDH (forward 5'-GTTGTCTCCTGCGACTTCA-3', reverse 5'-GGTGGTCCAGGGTTTCTTA-3').

For the gene expression analysis with RT² Profiler PCR Array, a Mouse Glucose Metabolism RT² Profiler PCR Array (Qiagen, Hilden, Germany) was used following the manufacturer's directions. The array included 89 genes, 5 of which were housekeeping genes used for normalization. 14 genes were removed because not expressed in mouse liver. The level of expression of the remaining 70 genes was used for the heat map analysis. Six genes, as indicated by the manufacturer, were assigned to two different functional classes. Genes were sorted based on their role in specific glucose metabolism pathways.

Statistical analysis

All the data showed in the present manuscript are reported as mean ± standard deviation. The StatistiXL software (StatistiXL, Broadway, Australia) was used for statistical analysis. p values <0.05 were considered significant. For all the data sets, data were analyzed by parametric tests, alpha = 0.05, (one-way and two-way ANOVA with Tukey's post-hoc correction). The statistical analysis performed for each data set is indicated in each figure legend.

Acknowledgements

The authors thankfully acknowledge Sarah Wells and International Mouse Phenotyping Consortium (IMPC) for providing the GSDIII mouse model. We also thank Guy Brochier, Mai Thao, Angeline Madelaine, and Clemence Labasse from the Neuromuscular Histopathology Unit of Myology Institute for their skillful technical assistance. We also thank Isabelle Richard for her advice on the dual overlapping vector construction. This work was supported by Genethon and the French Muscular Dystrophy Association (AFM). It was also supported by the European Union's research and innovation program under Grant Agreements No. 667751 (to F.M.) and No. 658712 (to F.M. and G.R.) and the ASTRE laboratories of the Essonne general council grant (to F. M.). The financial support of Italian Telethon is gratefully acknowledged (grant GGP15051 to GPC).

Author's contributions

P.V., S.P., P.C., H.C.V., L.J., M.G., F.P., S.M., F.C., M.S.S., S.C., L.V.W., A.V., B.G., and G.R. contributed to the execution of the experiments and data analysis. P.V., S.P., P.C., S.L., P. L.,

E.M., G.M., F.R., G.P.C., G.R. and F.M. contributed to the interpretation of results and provided critical insights into the significance of the work.

G.R. and F.M. directed the study and wrote the manuscript.

Competing interests

P.V., G.R., and F.M. are inventors in patents describing the treatment of GSDIII disease with dual AAV vectors. All other authors declare no conflict of interest.

References

1. Dagli, A, Sentner, CP, and Weinstein, DA (1993). Glycogen Storage Disease Type III. In: Pagon, RA*, et al.* (eds). *GeneReviews(R)*: Seattle (WA).
2. Sentner, CP, Hoogeveen, IJ, Weinstein, DA, Santer, R, Murphy, E, McKiernan, PJ*, et al.* (2016). Glycogen storage disease type III: diagnosis, genotype, management, clinical course and outcome. *Journal of inherited metabolic disease* **39**: 697-704.
3. Di Mauro S, HA, Tsujino S. (2004). *Metabolic disorders affecting muscle.*, McGraw-Hill, New York, 1535-58pp.
4. Lucchiari, S, Santoro, D, Pagliarani, S, and Comi, GP (2007). Clinical, biochemical and genetic features of glycogen debranching enzyme deficiency. *Acta myologica : myopathies and cardiomyopathies : official journal of the Mediterranean Society of Myology* **26**: 72-74.
5. Borowitz, SM, and Greene, HL (1987). Cornstarch therapy in a patient with type III glycogen storage disease. *Journal of pediatric gastroenterology and nutrition* **6**: 631-634.
6. Valayannopoulos, V, Bajolle, F, Arnoux, JB, Dubois, S, Sannier, N, Baussan, C*, et al.* (2011). Successful treatment of severe cardiomyopathy in glycogen storage disease type III With D,L-3-hydroxybutyrate, ketogenic and high-protein diet. *Pediatric research* **70**: 638-641.
7. Dagli, AI, Zori, RT, McCune, H, Ivsic, T, Maisenbacher, MK, and Weinstein, DA (2009). Reversal of glycogen storage disease type IIIa-related cardiomyopathy with modification of diet. *Journal of inherited metabolic disease* **32 Suppl 1**: S103-106.
8. Mingozzi, F, and High, KA (2011). Therapeutic in vivo gene transfer for genetic disease using AAV: progress and challenges. *Nature reviews Genetics* **12**: 341-355.
9. Nathwani, AC, Reiss, UM, Tuddenham, EG, Rosales, C, Chowdary, P, McIntosh, J*, et al.* (2014). Long-term safety and efficacy of factor IX gene therapy in hemophilia B. *The New England journal of medicine* **371**: 1994-2004.
10. Maguire, AM, Simonelli, F, Pierce, EA, Pugh, EN, Jr., Mingozzi, F, Bennicelli, J*, et al.* (2008). Safety and efficacy of gene transfer for Leber's congenital amaurosis. *The New England journal of medicine* **358**: 2240-2248.
11. J., M (2017). AVXS-101 Phase 1 Gene Therapy Clinical Trial in SMA Type 1: Event Free Survival and Achievement of Developmental Milestones. *American Society of Gene and Cell Therapy 20th conference*, vol. 25. Molecular Therapy: Washington DC. p 137.
12. Mack, DL, Poulard, K, Goddard, MA, Latournerie, V, Snyder, JM, Grange, RW*, et al.* (2017). Systemic AAV8-Mediated Gene Therapy Drives Whole-Body Correction of Myotubular Myopathy in Dogs. *Molecular therapy : the journal of the American Society of Gene Therapy* **25**: 839-854.
13. Yue, Y, Pan, X, Hakim, CH, Kodippili, K, Zhang, K, Shin, JH*, et al.* (2015). Safe and bodywide muscle transduction in young adult Duchenne muscular dystrophy dogs with adeno-associated virus. *Human molecular genetics* **24**: 5880-5890.
14. Pryadkina, M, Lostal, W, Bourg, N, Charton, K, Roudaut, C, Hirsch, ML*, et al.* (2015). A comparison of AAV strategies distinguishes overlapping vectors for efficient systemic delivery of the 6.2 kb Dysferlin coding sequence. *Molecular therapy Methods & clinical development* **2**: 15009.
15. Trapani, I, Colella, P, Sommella, A, Iodice, C, Cesi, G, de Simone, S*, et al.* (2014). Effective delivery of large genes to the retina by dual AAV vectors. *EMBO molecular medicine* **6**: 194-211.
16. Ghosh, A, Yue, Y, and Duan, D (2011). Efficient transgene reconstitution with hybrid dual AAV vectors carrying the minimized bridging sequences. *Human gene therapy* **22**: 77-83.
17. Sun, B, Fredrickson, K, Austin, S, Tolun, AA, Thurberg, BL, Kraus, WE*, et al.* (2013). Alglucosidase alfa enzyme replacement therapy as a therapeutic approach for glycogen storage disease type III. *Molecular genetics and metabolism* **108**: 145-147.

18. Puzzo F., CP, Biferi M. G., D. Bali, N. K. Paulk, P. Vidal, F. Collaud, M. Simon-Sola, S. Charles, R. Hardet, C. Leborgne, A. Meliani, M. Cohen-Tannoudji, S. Astord, B. Gjata, P. Sellier, L. van Wittenberghe, A. Vignaud, F. Boisgerault, M. Barkats, P. Laforet, M. A. Kay, D. D. Koeberl, G. Ronzitti, F. Mingozzi (2017). Whole-body rescue of Pompe disease with AAV liver delivery of engineered secretable GAA transgenes. *Science translational medicine* **In press**.
19. Ghosh, A, Yue, Y, Lai, Y, and Duan, D (2008). A hybrid vector system expands adeno-associated viral vector packaging capacity in a transgene-independent manner. *Molecular therapy : the journal of the American Society of Gene Therapy* **16**: 124-130.
20. Ronzitti, G, Bortolussi, G, van Dijk, R, Collaud, F, Charles, S, Leborgne, C*, et al.* (2016). A translationally optimized AAV-UGT1A1 vector drives safe and long-lasting correction of Crigler-Najjar syndrome. *Molecular therapy Methods & clinical development* **3**: 16049.
21. Rabinowitz, JE, Rolling, F, Li, C, Conrath, H, Xiao, W, Xiao, X*, et al.* (2002). Cross-packaging of a single adeno-associated virus (AAV) type 2 vector genome into multiple AAV serotypes enables transduction with broad specificity. *Journal of virology* **76**: 791-801.
22. Loser, P, Jennings, GS, Strauss, M, and Sandig, V (1998). Reactivation of the previously silenced cytomegalovirus major immediate-early promoter in the mouse liver: involvement of NFkappaB. *Journal of virology* **72**: 180-190.
23. Miao, CH, Ohashi, K, Patijn, GA, Meuse, L, Ye, X, Thompson, AR*, et al.* (2000). Inclusion of the hepatic locus control region, an intron, and untranslated region increases and stabilizes hepatic factor IX gene expression in vivo but not in vitro. *Molecular therapy : the journal of the American Society of Gene Therapy* **1**: 522-532.
24. Gao, GP, Alvira, MR, Wang, L, Calcedo, R, Johnston, J, and Wilson, JM (2002). Novel adeno-associated viruses from rhesus monkeys as vectors for human gene therapy. *Proceedings of the National Academy of Sciences of the United States of America* **99**: 11854-11859.
25. Huijing, F (1975). Glycogen metabolism and glycogen-storage diseases. *Physiological reviews* **55**: 609-658.
26. Yi, H, Brooks, ED, Thurberg, BL, Fyfe, JC, Kishnani, PS, and Sun, B (2014). Correction of glycogen storage disease type III with rapamycin in a canine model. *J Mol Med (Berl)* **92**: 641-650.
27. Mayorandan, S, Meyer, U, Hartmann, H, and Das, AM (2014). Glycogen storage disease type III: modified Atkins diet improves myopathy. *Orphanet journal of rare diseases* **9**: 196.
28. Brambilla, A, Mannarino, S, Pretese, R, Gasperini, S, Galimberti, C, and Parini, R (2014). Improvement of Cardiomyopathy After High-Fat Diet in Two Siblings with Glycogen Storage Disease Type III. *JIMD reports* **17**: 91-95.
29. Derks, TG, and Smit, GP (2015). Dietary management in glycogen storage disease type III: what is the evidence? *Journal of inherited metabolic disease* **38**: 545-550.
30. Yi, H, Zhang, Q, Brooks, ED, Yang, C, Thurberg, BL, Kishnani, PS*, et al.* (2017). Systemic Correction of Murine Glycogen Storage Disease Type IV by an AAV-Mediated Gene Therapy. *Human gene therapy* **28**: 286-294.
31. Zhai, L, Feng, L, Xia, L, Yin, H, and Xiang, S (2016). Crystal structure of glycogen debranching enzyme and insights into its catalysis and disease-causing mutations. *Nature communications* **7**: 11229.
32. Ferla, R, Claudiani, P, Cotugno, G, Saccone, P, De Leonibus, E, and Auricchio, A (2014). Similar therapeutic efficacy between a single administration of gene therapy and multiple administrations of recombinant enzyme in a mouse model of lysosomal storage disease. *Human gene therapy* **25**: 609-618.
33. Ruzo, A, Garcia, M, Ribera, A, Villacampa, P, Haurigot, V, Marco, S*, et al.* (2012). Liver production of sulfamidase reverses peripheral and ameliorates CNS pathology in mucopolysaccharidosis IIIA mice. *Molecular therapy : the journal of the American Society of Gene Therapy* **20**: 254-266.

34. Trapani, I, Toriello, E, de Simone, S, Colella, P, Iodice, C, Polishchuk, EV*, et al.* (2015). Improved dual AAV vectors with reduced expression of truncated proteins are safe and effective in the retina of a mouse model of Stargardt disease. *Human molecular genetics* **24**: 6811-6825.
35. Austin, SL, Proia, AD, Spencer-Manzon, MJ, Butany, J, Wechsler, SB, and Kishnani, PS (2012). Cardiac Pathology in Glycogen Storage Disease Type III. *JIMD reports* **6**: 65-72.
36. Demo, E, Frush, D, Gottfried, M, Koepke, J, Boney, A, Bali, D*, et al.* (2007). Glycogen storage disease type III-hepatocellular carcinoma a long-term complication? *Journal of hepatology* **46**: 492-498.
37. Chuah, MK, Petrus, I, De Bleser, P, Le Guiner, C, Gernoux, G, Adjali, O*, et al.* (2014). Liver-specific transcriptional modules identified by genome-wide in silico analysis enable efficient gene therapy in mice and non-human primates. *Molecular therapy : the journal of the American Society of Gene Therapy* **22**: 1605-1613.
38. Liu, YL, Mingozzi, F, Rodriguez-Colon, SM, Joseph, S, Dobrzynski, E, Suzuki, T*, et al.* (2004). Therapeutic levels of factor IX expression using a muscle-specific promoter and adeno-associated virus serotype 1 vector. *Human gene therapy* **15**: 783-792.
39. Duan, D (2016). Systemic delivery of adeno-associated viral vectors. *Current opinion in virology* **21**: 16-25.
40. Le Guiner, C, Montus, M, Servais, L, Cherel, Y, Francois, V, Thibaud, JL*, et al.* (2014). Forelimb treatment in a large cohort of dystrophic dogs supports delivery of a recombinant AAV for exon skipping in Duchenne patients. *Molecular therapy : the journal of the American Society of Gene Therapy* **22**: 1923-1935.
41. Sondergaard, PC, Griffin, DA, Pozsgai, ER, Johnson, RW, Grose, WE, Heller, KN*, et al.* (2015). AAV.Dysferlin Overlap Vectors Restore Function in Dysferlinopathy Animal Models. *Annals of clinical and translational neurology* **2**: 256-270.
42. Koo, T, Popplewell, L, Athanasopoulos, T, and Dickson, G (2014). Triple trans-splicing adeno-associated virus vectors capable of transferring the coding sequence for full-length dystrophin protein into dystrophic mice. *Human gene therapy* **25**: 98-108.
43. Lostal, W, Bartoli, M, Bourg, N, Roudaut, C, Bentaib, A, Miyake, K*, et al.* (2010). Efficient recovery of dysferlin deficiency by dual adeno-associated vector-mediated gene transfer. *Human molecular genetics* **19**: 1897-1907.
44. https://clinicaltrials.gov/ct2/show/NCT02710500.
45. Hers, HG, Verhue, W, and Van hoof, F (1967). The determination of amylo-1,6-glucosidase. *European journal of biochemistry* **2**: 257-264.
46. Zhang, P, Sun, B, Osada, T, Rodriguiz, R, Yang, XY, Luo, X*, et al.* (2012). Immunodominant liver-specific expression suppresses transgene-directed immune responses in murine pompe disease. *Human gene therapy* **23**: 460-472.
47. Sun, B, Zhang, H, Franco, LM, Young, SP, Schneider, A, Bird, A*, et al.* (2005). Efficacy of an adeno-associated virus 8-pseudotyped vector in glycogen storage disease type II. *Molecular therapy : the journal of the American Society of Gene Therapy* **11**: 57-65.
48. Matsushita, T, Elliger, S, Elliger, C, Podsakoff, G, Villarreal, L, Kurtzman, GJ*, et al.* (1998). Adeno-associated virus vectors can be efficiently produced without helper virus. *Gene therapy* **5**: 938-945.
49. Ayuso, E, Mingozzi, F, Montane, J, Leon, X, Anguela, XM, Haurigot, V*, et al.* (2010). High AAV vector purity results in serotype- and tissue-independent enhancement of transduction efficiency. *Gene therapy* **17**: 503-510.

FIGURE 1

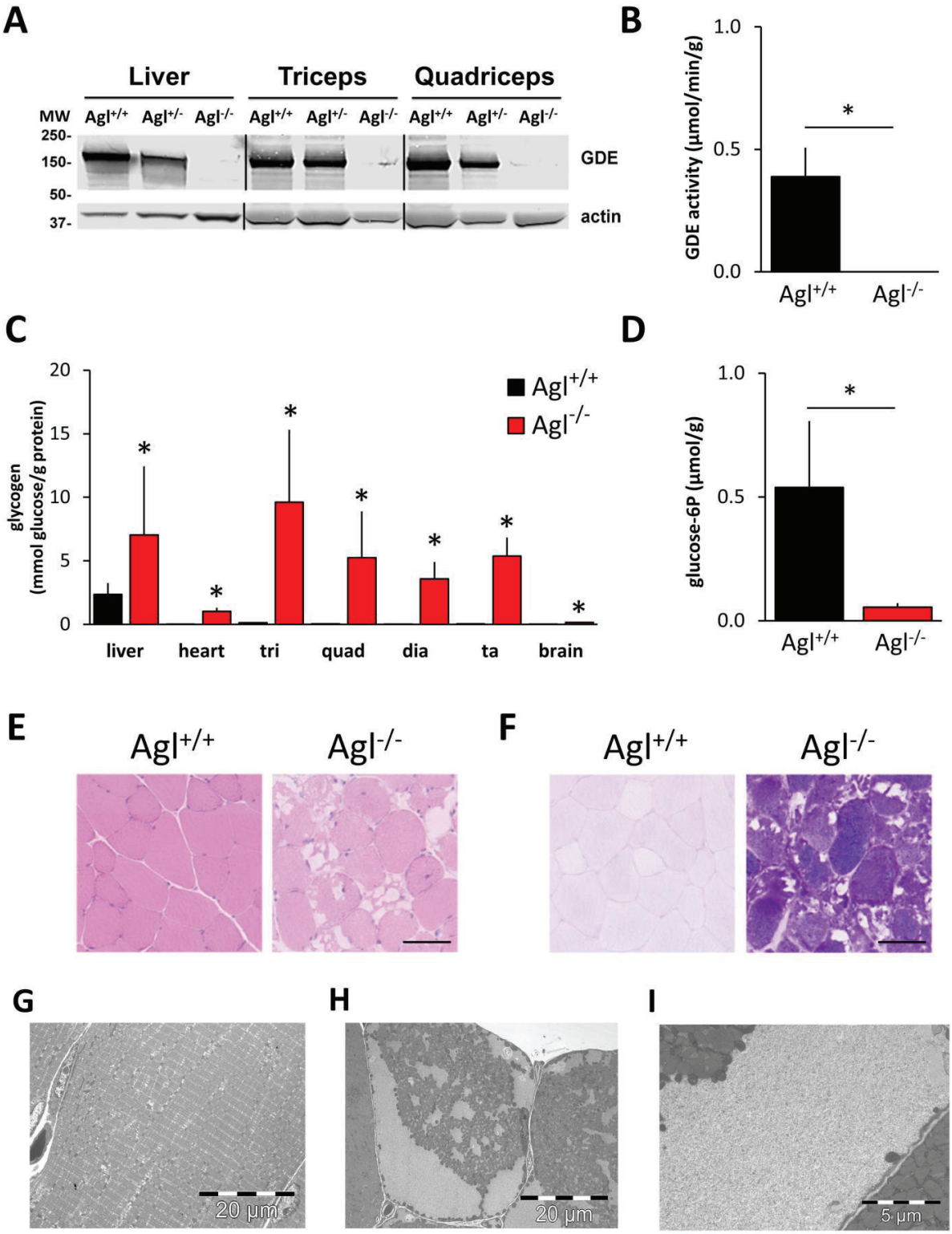
A
Liver
Triceps
Quadriceps
MW
Agl+/+
Agl+/-
Agl-/-
250-
150-
50-
37-
GDE
actin
B
GDE activity (µmol/min/g)
1.0
0.5
0.0
*
Agl+/+
Agl-/-
C
glycogen (mmol glucose/g protein)
20
15
10
5
0
Agl+/+
Agl-/-
liver
heart
tri
quad
dia
ta
brain
D
glucose-6P (µmol/g)
1.0
0.5
0.0
E
Agl+/+
Agl-/-
F
Agl+/+
Agl-/-
G
20 µm
H
20 µm
I
5 µm

Figure 1. Biochemical and histological characterization of $Agl^{-/-}$ mice. Analysis was performed in 3-month old male knock-out ($Agl^{-/-}$), wild-type ($Agl^{+/+}$) or heterozygous ($Agl^{+/-}$) littermates. **(A)** Western blot analysis performed in liver, triceps, and quadriceps. An anti-actin antibody was used as loading control. The positions of molecular weight (MW) markers are indicated on the left. **(B)** GDE activity measured in liver **(C)** Glycogen content in liver, heart, triceps and quadriceps, diaphragm, tibialis anterior, and brain reported as mmol of glucose released by complete enzymatic glycogen digestion per g of protein. **(D)** glucose-6-phosphate measured in liver. All data are shown as mean ± standard deviation. Statistical analyses were performed by ANOVA (*=$p<0.05$ vs $Agl^{+/+}$ animals, n=5). **(E)** Representative images of hematoxylin and eosin and **(F)** periodic acid-Schiff staining of mouse quadriceps. Scale bars = 50µm. **(G,I)** Electron microscopy microphotographs showing respectively the longitudinal **(G)** and the transversal structures **(H)** of quadriceps muscle fibers of a 3 month-old $Agl^{-/-}$ mouse. **(I)** Higher magnification showing a large vacuole constituted of normally structured glycogen granules.

FIGURE 2

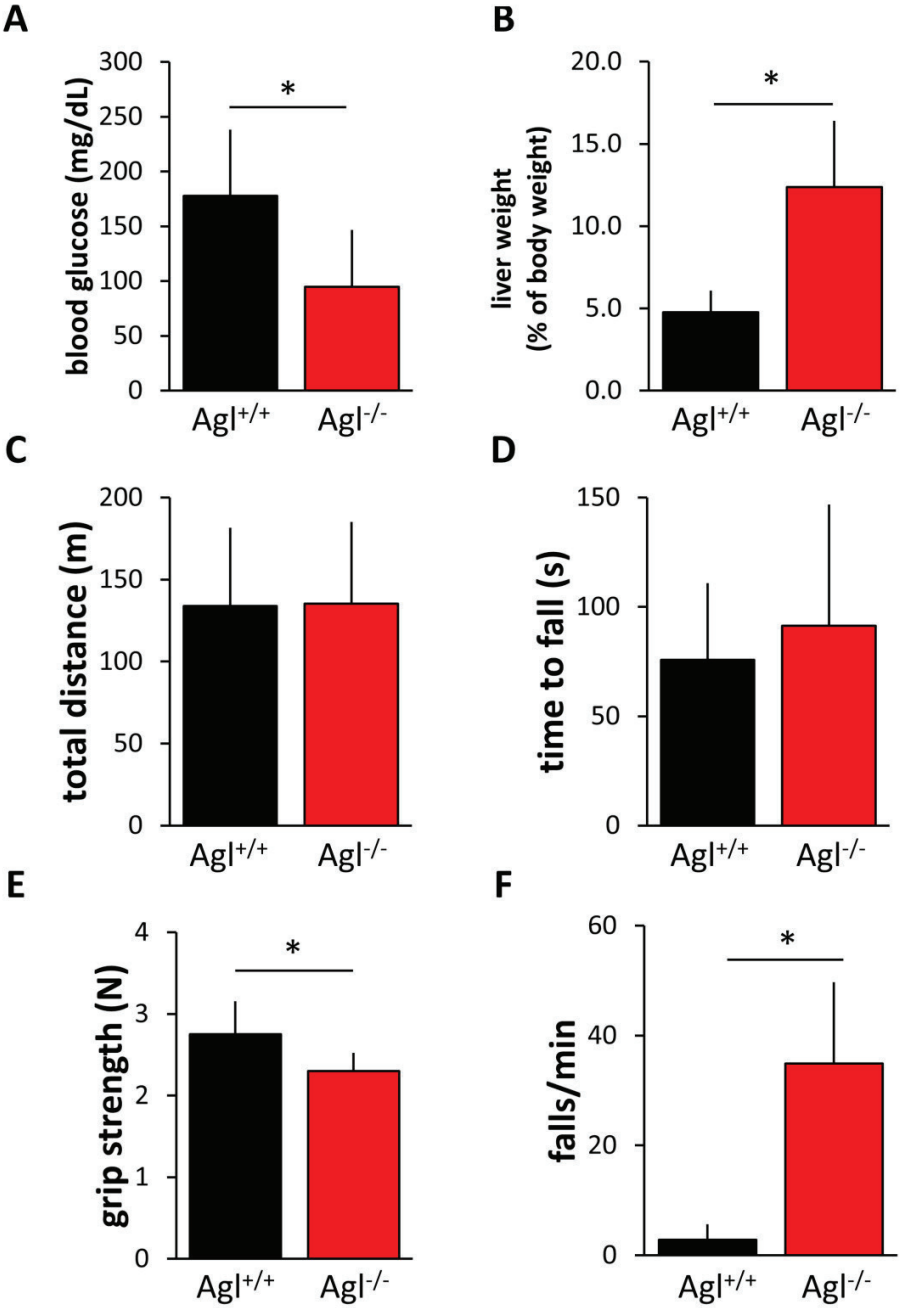

Figure 2. Phenotypic characterization of $Agl^{-/-}$ mice. **(A)** Glycemia measured in 6 month-old male $Agl^{-/-}$ mice and wild-type littermates. Statistical analysis was performed by ANOVA (*= $p<0.05$, n= 23 $Agl^{+/+}$, 52 $Agl^{-/-}$). **(B)** Liver weight expressed as % of body weight measured in 6 month-old $Agl^{-/-}$ mice and wild-type littermates. Statistical analysis was performed by ANOVA (*= $p<0.05$, n= 14 $Agl^{+/+}$, 16 $Agl^{-/-}$). **(C-F)** Functional characterization of the muscle strength in 3-month-old $Agl^{-/-}$ male mice and wild-type ($Agl^{+/+}$) littermates. **(C)** Total distance traveled in 90 minutes **(D)** Time spent on rotarod. **(E)** Grip strength expressed as the average of three independent measurements. **(F)** Wire hang test shown as number of falls/minute. Statistical analyses were performed by ANOVA (*=$p<0.05$ vs $Agl^{+/+}$ animals, n=13 $Agl^{+/+}$, n=9 $Agl^{-/-}$). All data are shown as mean ± standard deviation.

FIGURE 3

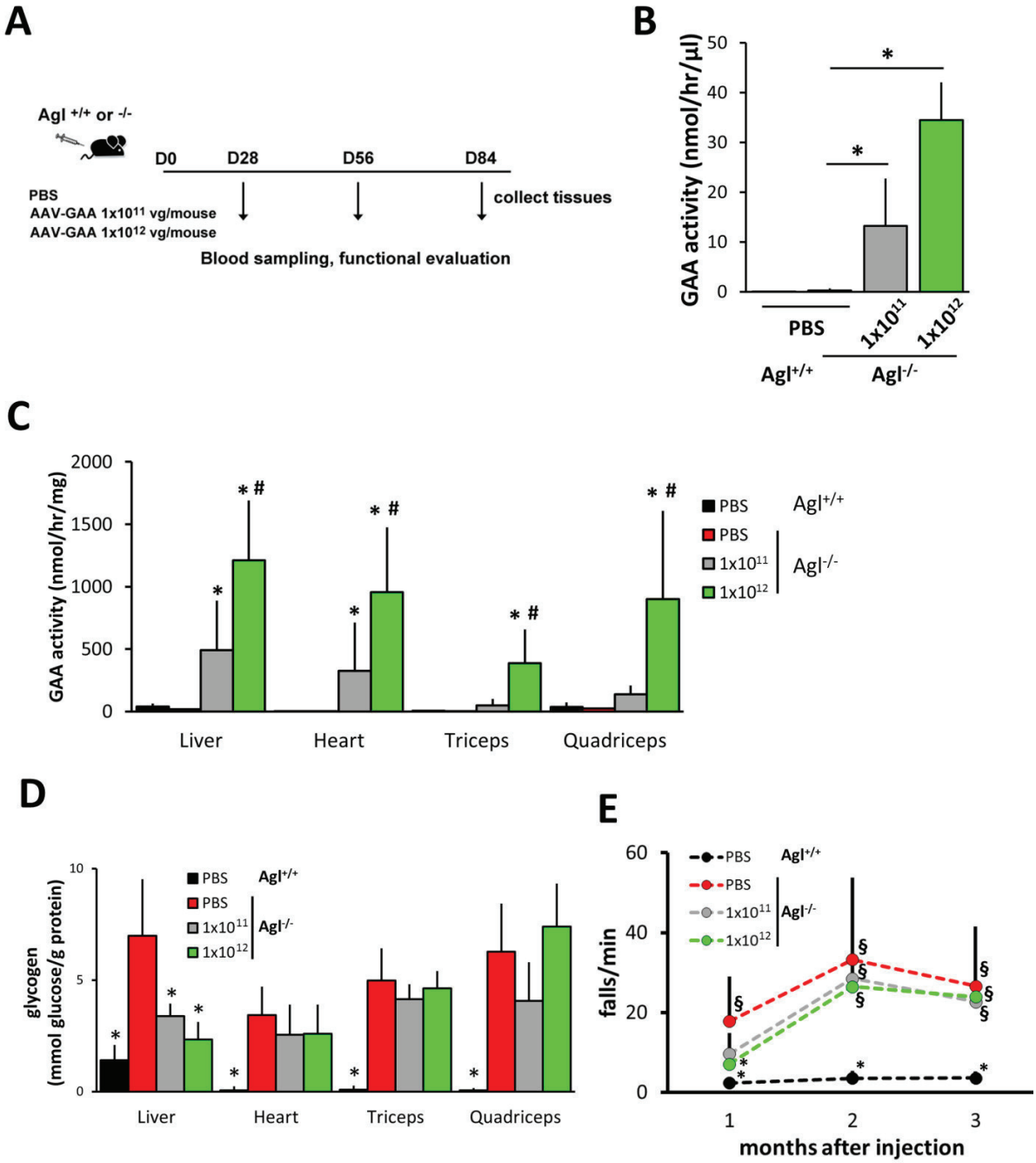

Figure 3. AAV-mediated GAA overexpression rescues glycogen accumulation in the liver of $Agl^{-/-}$ mice. **(A)** 3-month-old $Agl^{-/-}$ mice were injected intravenously with PBS or with $1x10^{11}$ or $1x10^{12}$ vg/mouse of a vector expressing secretable GAA. Wild-type littermates ($Agl^{+/+}$) injected with PBS served as controls. Injected mice were bled and functionally tested at day 28, 56, and 84 and sacrificed 3 months after injection. **(B)** GAA activity measured in serum 3 months post-injection. **(C)** GAA activity measured at sacrifice in liver, heart, triceps, and quadriceps. **(D)** Glycogen content in liver, heart, triceps, and quadriceps measured at sacrifice and reported as mmol of glucose released by complete enzymatic

digestion per g of protein. **(E)** Wire hang test performed 1, 2, and 3 months post-injection. Statistical analyses were performed by ANOVA (*=p<0.05 vs. PBS injected $Agl^{-/-}$, #= p<0.05 vs $1x10^{11}$ AAV-GAA injected mice, §= p<0.05 vs PBS injected $Agl^{+/+}$, n=7-11 mice/group). All data are shown as mean ± standard deviation.

FIGURE 4

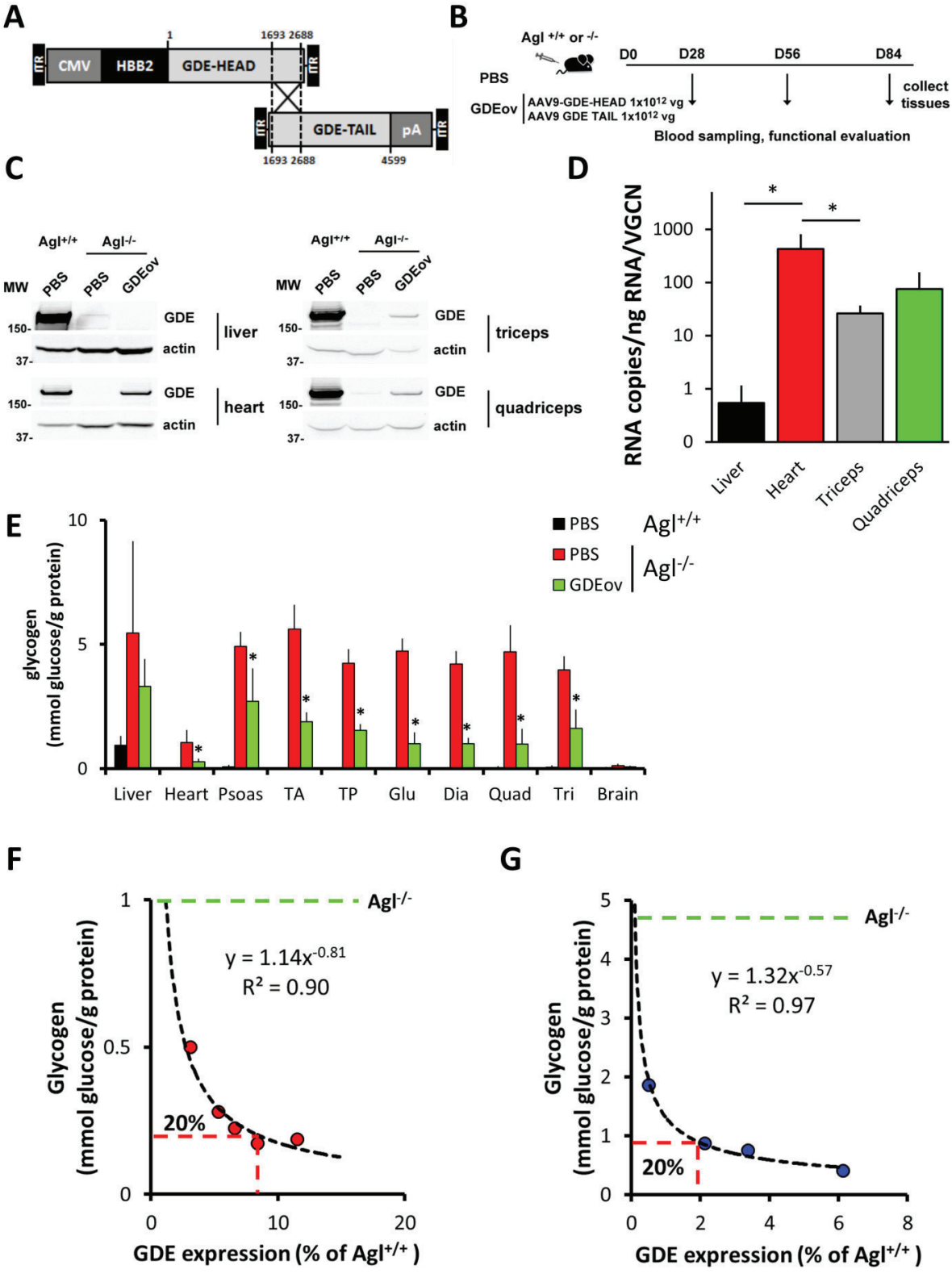
A
ITR
CMV
HBB2
GDE-HEAD
1
1693 2688
ITR
ITR
GDE-TAIL
pA
ITR
1693 2688
4599
B
Agl +/+ or -/-
PBS
GDEov
AAV9-GDE-HEAD 1x10^12 vg
AAV9 GDE TAIL 1x10^12 vg
D0
D28
D56
D84
collect tissues
Blood sampling, functional evaluation
C
Agl+/+
Agl-/-
MW
PBS
PBS
GDEov
150-
37-
GDE
actin
liver
heart
triceps
quadriceps
D
RNA copies/ng RNA/VGCN
1000
100
10
1
0
Liver
Heart
Triceps
Quadriceps
E
glycogen (mmol glucose/g protein)
10
5
0
PBS
PBS
GDEov
Agl+/+
Agl-/-
Liver
Heart
Psoas
TA
TP
Glu
Dia
Quad
Tri
Brain
F
Glycogen (mmol glucose/g protein)
1
0.5
0
Agl-/-
y = 1.14x-0.81
R² = 0.90
20%
0
10
20
GDE expression (% of Agl+/+)
G
Glycogen (mmol glucose/g protein)
5
4
3
2
1
0
Agl-/-
y = 1.32x-0.57
R² = 0.97
20%
0
2
4
6
8
GDE expression (% of Agl+/+)

Figure 4. Gene transfer with a dual AAV vector expressing GDE rescues glycogen accumulation in muscle of GSDIII mice. **(A)** Schematic representation of the AAV9-GDE-HEAD and AAV9-GDE-TAIL vectors. CMV, cytomegalovirus enhancer/promoter; HBB2, human beta-2 globulin; pA, HBB2 polyadenylation signal; ITR, inverted terminal repeats. **(B)** 3-month-old $Agl^{-/-}$ mice were injected intravenously with PBS or with $2x10^{12}$ vg/mouse of the combination of AAV9-GDE-HEAD and AAV9-GDE-TAIL in a 1:1 ratio (GDEov). As control, wild-type littermates ($Agl^{+/+}$) were injected intravenously with PBS. Injected mice were bled and functionally tested at day 28, 56, and 84 and sacrificed 3 months after the injection. **(C)** Western blot analysis for GDE in liver, heart, triceps, and quadriceps. An anti-actin antibody was used as loading control. MW, molecular weight marker. **(D)** hGDE mRNA expression normalized per vector genome copy number in liver, heart, triceps, and quadriceps. **(E)** Glycogen content measured 3 months post-injection and reported as mmol of glucose released by complete enzymatic digestion per g of protein. Statistical analyses were performed by ANOVA (*=$p<0.05$ vs. PBS injected $Agl^{-/-}$). (**F,G**) correlation between GDE protein levels expressed as the percentage of GDE in $Agl^{+/+}$ animals and glycogen accumulation in (**F**) heart and (**G**) quadriceps of $Agl^{-/-}$ treated with dual AAV vectors. The power regression formula and the regression coefficient (R^2) is depicted. The green line indicates glycogen levels in untreated $Agl^{-/-}$ animals, the red line indicates the level of GDE protein expression necessary to obtain the clearance of 80% of glycogen (or 20% of residual glycogen). All data are shown as mean ± standard deviation.

FIGURE 5

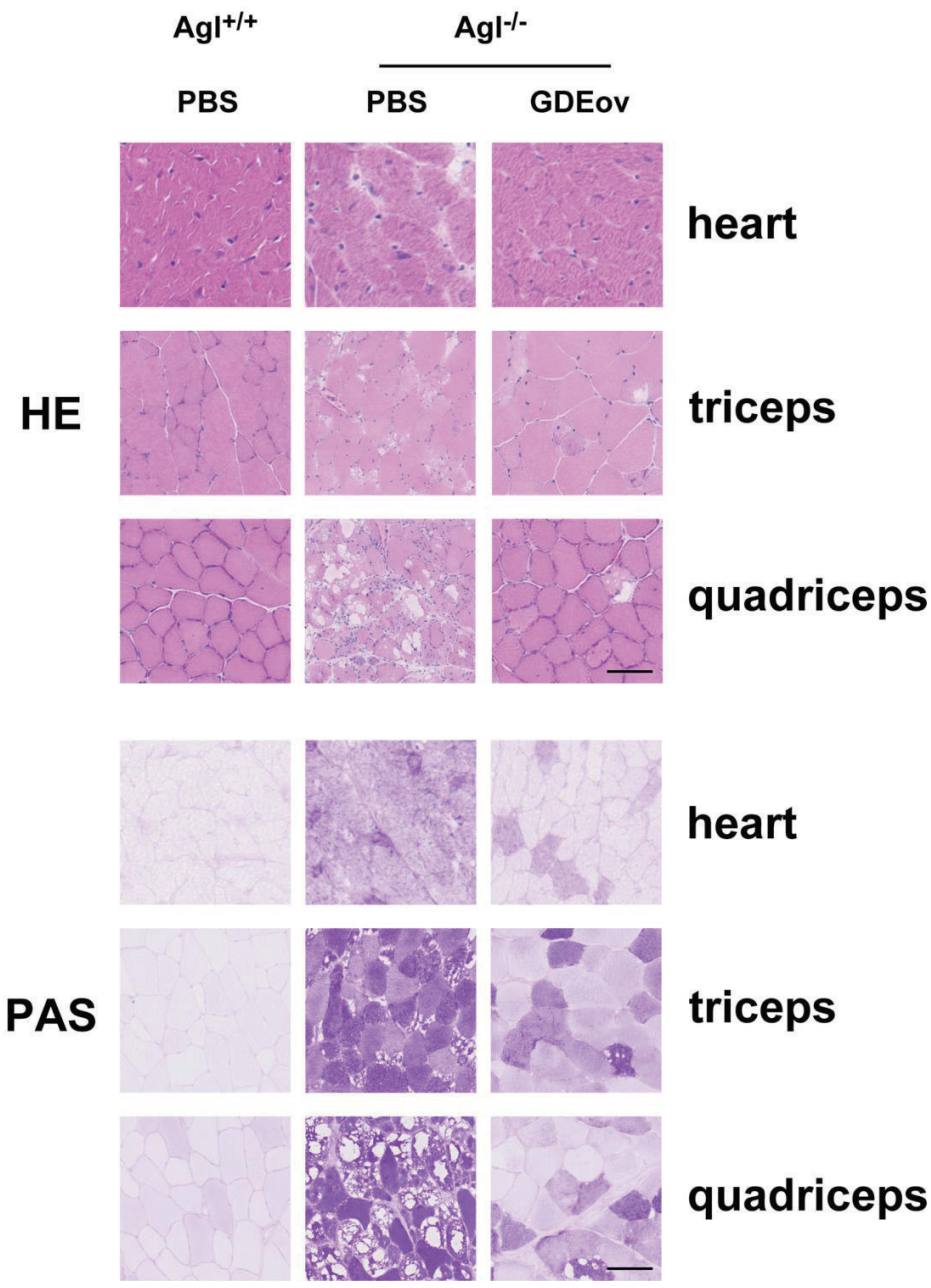

Figure 5 Histological analysis confirms dual AAV vector-mediated rescue of glycogen accumulation in muscle of $Agl^{-/-}$ mice. Hematoxylin-eosin staining (HE, upper panels) and periodic acid Schiff (PAS lower panels) staining performed in heart, triceps, and quadriceps of 6-month-old mice treated as described in figure 4. Scale bars = 50µm.

FIGURE 6

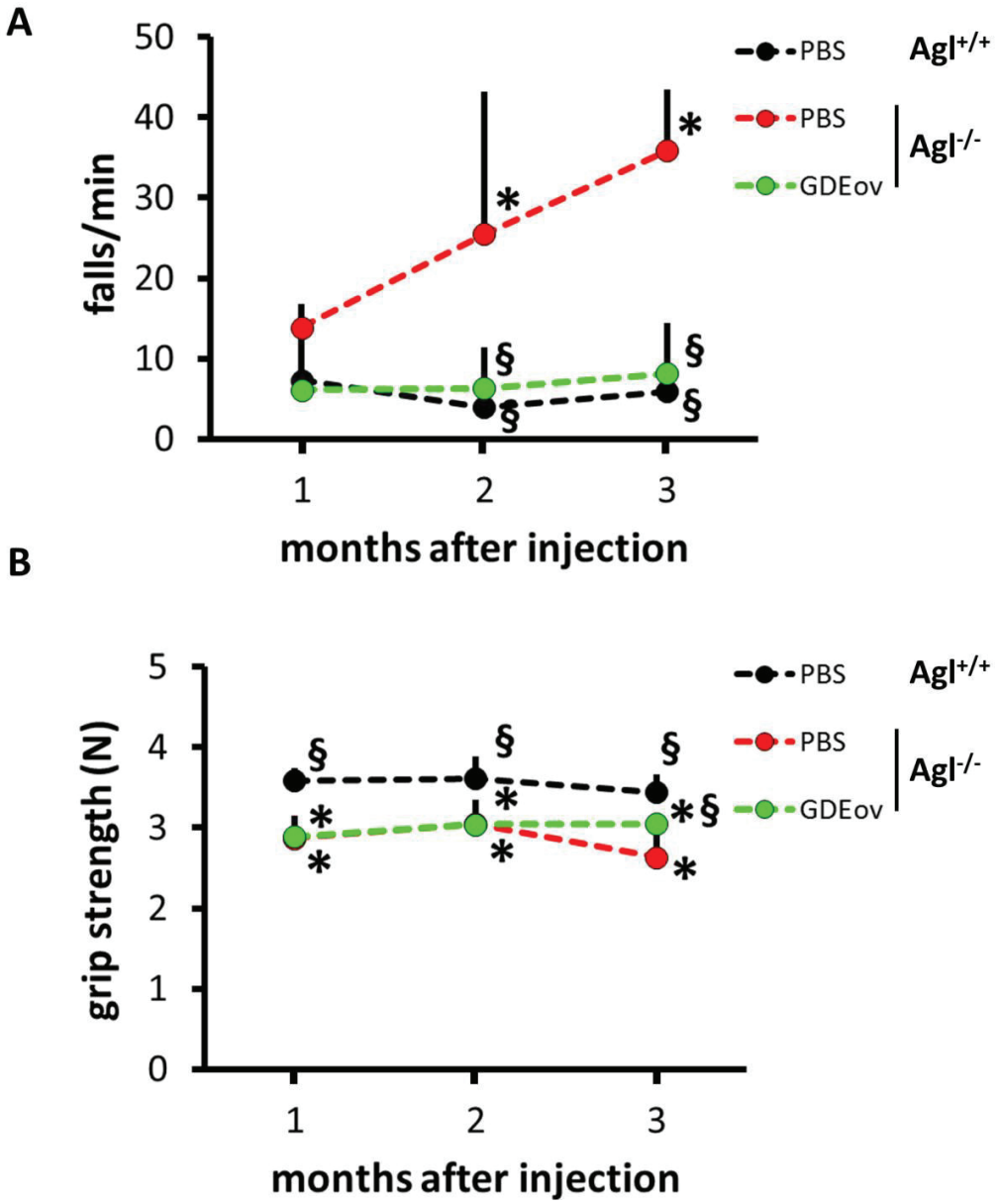

Figure 6. Dual AAV9 vector expressing GDE rescues muscle function in GSDIII mice. Assessment of muscle strength in wild-type and $Agl^{-/-}$ mice treated as described in figure 4. Functional testing was performed 1, 2, and 3 months post treatment. **(A)** Wire hang test shown as number of falls/minute. **(B)** Grip test expressed as the average of three independent measurements. Statistical analyses were performed by ANOVA (*=$p<0.05$, n=5). All data are shown as mean ± standard deviation.

FIGURE 7

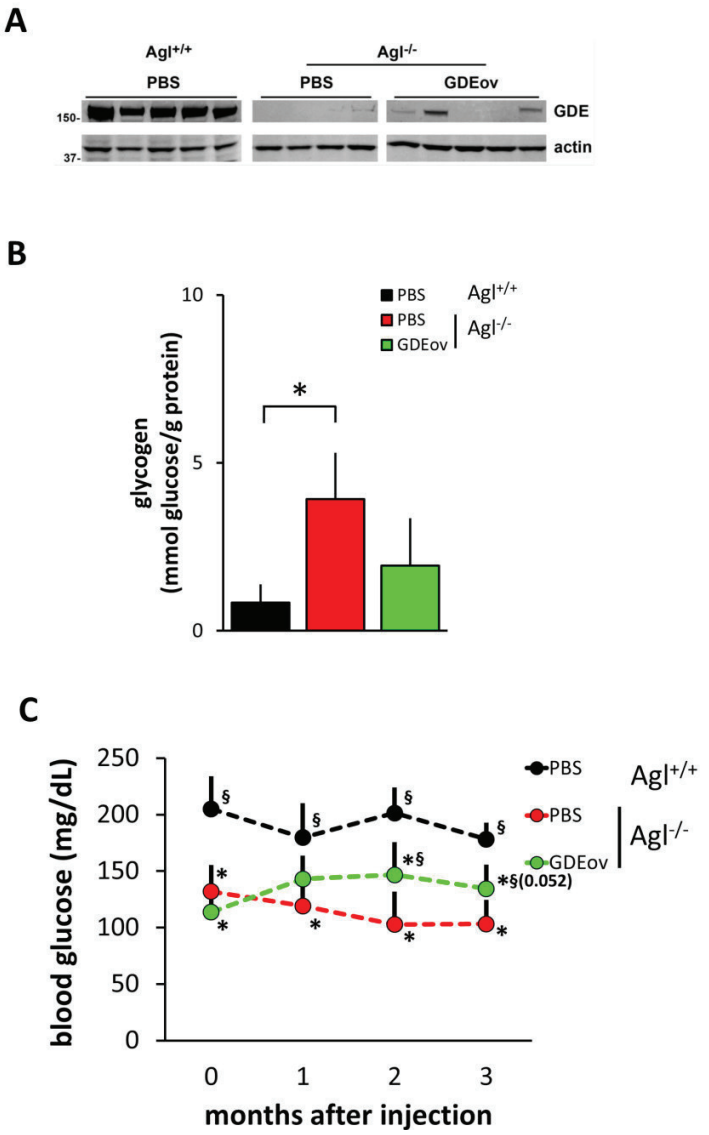

Figure 7. Liver-specific expression of GDE with a dual AAV vector rescues glycemia in GSDIII mice. 3-month-old $Agl^{-/-}$ mice were intravenously injected with PBS or with $2x10^{12}$ vg/mouse of AAV8-hAAT-GDE-HEAD and AAV8-GDE-TAIL (GDEov) vectors at a 1:1 ratio. Wild-type littermates ($Agl^{+/+}$) were used as controls. **(A)** Western blot analysis in liver. An anti-actin antibody was used as loading control. The positions of a molecular weight marker running in parallel with samples are indicated on the left. **(B)** Glycogen content measured in liver 3 months post-injection and reported as mmol of glucose released by complete enzymatic digestion per g of protein. Statistical analyses were performed by ANOVA (*=p<0.05 vs. PBS injected $Agl^{+/+}$). **(C)** Glycemia measured before and 1, 2 and 3 months post-injection. Statistical analyses were performed by two-way ANOVA time x treatment (*=p<0.05 vs PBS injected $Agl^{+/+}$, §=p<0.05 vs. PBS injected $Agl^{-/-}$; $Agl^{+/+}$ n=9, $Agl^{-/-}$ n=4, $Agl^{-/-}$ treated with GDEov n=8 mice/group). All data are shown as mean ± standard deviation.

FIGURE 8

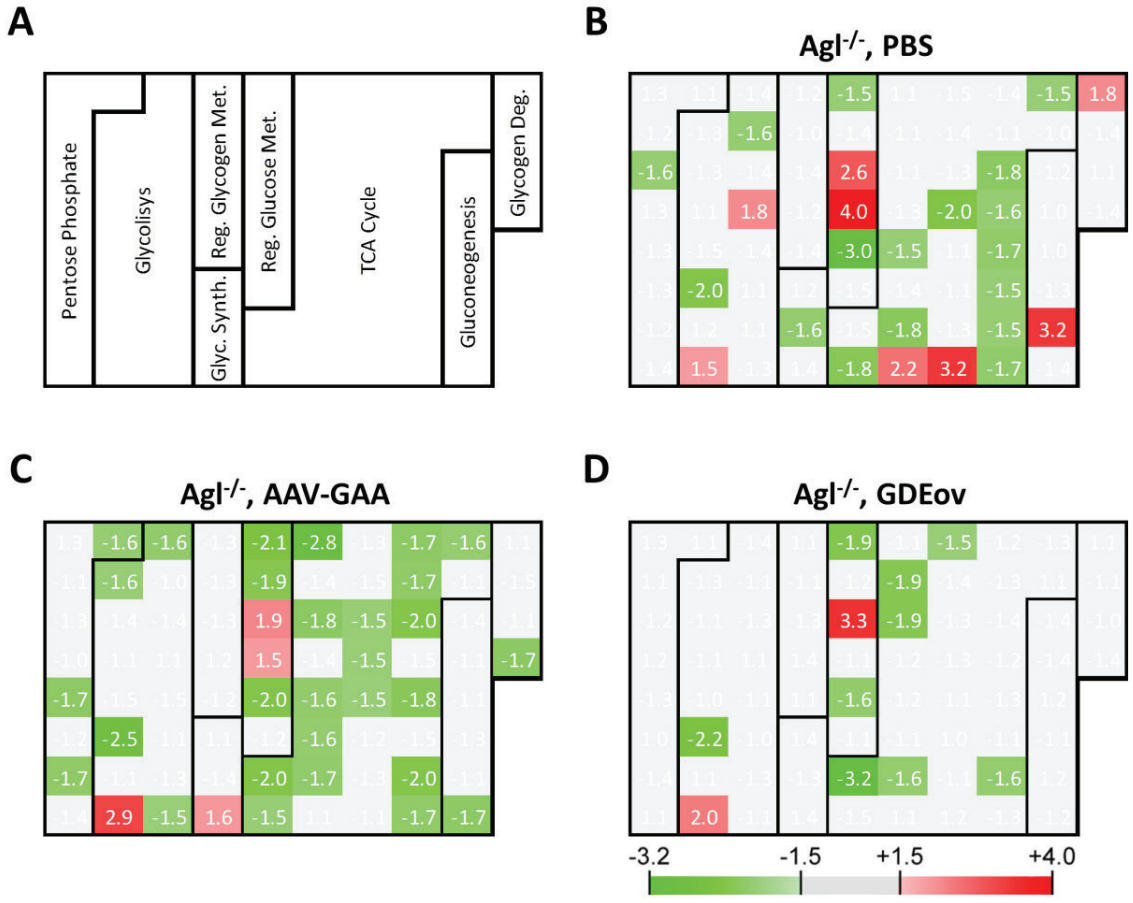

Figure 8. Heat map analysis of the expression profile of genes involved in the mouse glucose metabolism. RNAs were extracted from livers of 6 month-old $Agl^{-/-}$ mice injected intravenously at three months of age with PBS, $1x10^{12}$ vg/mouse of a vector expressing engineered GAA (AAV-GAA), or $2x10^{12}$ vg/mouse of overlapping AAV vectors expressing GDE in the liver (GDEov). Wild-type littermates injected intravenously with PBS were used as controls. **(A)** Functional role of the genes analyzed. The scheme indicates the regions of the heat map corresponding to groups of genes involved in specific pathways, namely, pentose phosphate, glycolysis, glycogen synthesis (Glyc. Synth.), regulation of the glycogen metabolism (Reg. Glycogen Met.), regulation of glucose metabolism (Reg. Glucose Met.), citric acid cycle (TCA cycle), gluconeogenesis and glycogen degradation (Glycogen Deg.). **(B,C,D)** Heat maps indicating the levels of expression of the genes in $Agl^{-/-}$ mice injected with PBS **(B)**, AAV-GAA **(C),** or GDEov **(D)** and normalized to levels measured in $Agl^{+/+}$. Colors scale for fold-change in expression is indicated at the bottom of the graphs.

Supplementary materials

Table S1. Functional characterization of the GSDIII mouse model.

			Month		
	genotype	sex	3	6	9
total distance[a] (m/90min)	$Agl^{+/+}$	M	134 ± 48	86 ± 39	79 ± 40
		F	149 ± 61	102 ± 40	87 ± 43
	$Agl^{-/-}$	M	135 ± 50	84 ± 33	92 ± 33
		F	127 ± 37	77 ± 43	62 ± 36
time to fall[b] (s)	$Agl^{+/+}$	M	76 ± 35	68 ± 26	67 ± 23
		F	70 ± 21	74 ± 34	78 ± 31
	$Agl^{-/-}$	M	91 ± 55	84 ± 49	93 ± 63
		F	84 ± 32	76 ± 29	77 ± 30
grip strength[c] (N)	$Agl^{+/+}$	M	2.75 ± 0.40	2.94 ± 0.33	3.18 ± 0.29
		F	2.58 ± 0.35	2.92 ± 0.33	3.14 ± 0.39
	$Agl^{-/-}$	M	2.30 ± 0.22*	2.23 ± 0.42*	2.41 ± 0.33*
		F	2.09 ± 0.37*	2.00 ± 0.45*	2.07 ± 0.41*
Wire hang[d] (falls/min)	$Agl^{+/+}$	M	2.80 ± 2.83	6.07 ± 3.24	6.35 ± 6.33
		F	2.38 ± 1.61	6.03 ± 3.65	4.00 ± 2.62
	$Agl^{-/-}$	M	34.88 ± 14.82*	40.25 ± 11.95*	22.84 ± 6.99*
		F	21.39 ± 8.80*	30.22 ± 15.99*	22.25 ± 11.22*

[a] total distance traveled over 90 minutes. [b] time to fall from a 4-40 rpm accelerating rod. [c] average grip strength. [d] number of falls per minute measured in a 3-minute interval. Statistical analyses were performed by one-way ANOVA (*, $p<0.05$ vs. $Agl^{+/+}$ mice of the same sex). All data are shown as mean ± standard deviation.

Table S2. Liver-specific GAA expression transiently improves wire-hang performance of $Agl^{-/-}$ mice.

			time post-injection (months)			
	genotype	treatment	0	1	2	3
time to fall (s)	$Agl^{+/+}$	PBS	65 ± 25	84 ± 34	83 ± 28	64 ± 30
	$Agl^{-/-}$	PBS	65 ± 34	65 ± 23	73 ± 36	62 ± 27
	$Agl^{-/-}$	1.E+11	60 ± 19	72 ± 24	71 ± 27	74 ± 19
	$Agl^{-/-}$	1.E+12	62 ± 17	54 ± 13	70 ± 18	61 ± 27
grip strength (N)	$Agl^{+/+}$	PBS	3.55 ± 0.47†	3.52 ± 0.33†	3.51 ± 0.35†	3.46 ± 0.29†
	$Agl^{-/-}$	PBS	2.64 ± 0.35*	2.63 ± 0.34*	2.57 ± 0.29*	2.44 ± 0.23*
	$Agl^{-/-}$	1.E+11	2.91 ± 0.16*	2.68 ± 0.32*	2.57 ± 0.27*	2.59 ± 0.35*
	$Agl^{-/-}$	1.E+12	2.71 ± 0.20*	2.65 ± 0.32*	2.50 ± 0.31*	2.45 ± 0.26*
wire hang (falls/min)	$Agl^{+/+}$	PBS	3.25 ± 2.16†	2.37 ± 1.36†	3.53 ± 1.86†	3.58 ± 1.64†
	$Agl^{-/-}$	PBS	22.30 ± 13.99*	17.85 ± 11.15*	33.29 ± 20.53*	26.64 ± 14.88*
	$Agl^{-/-}$	1.E+11	14.5 ± 5.23*	9.64 ± 3.82†	28.54 ± 11.99*	22.70 ± 10.27*
	$Agl^{-/-}$	1.E+12	15.5 ± 5.53*	7.11 ± 2.20†	26.50 ± 10.78*	23.95 ± 10.75*

[a] time to fall from a 4-40 rpm accelerating rod. [b] average grip strength. [c] number of falls per minute measured in a 3-minute interval. Statistical analyses were performed by one-way ANOVA (*, $p<0.05$ vs. $Agl^{+/+}$; †, $p<0.05$ vs. $Agl^{-/-}$). All data are shown as mean ± standard deviation.

Table S3. Dual AAV vector treatment rescues the muscle impairment in GSDIII mouse model.

			time post-injection (months)			
	genotype	treatment	0	1	2	3
time to fall[a] (s)	$Agl^{+/+}$	PBS	74 ± 24	42 ± 19	29 ± 17	64 ± 24
	$Agl^{-/-}$		62 ± 27	48 ± 20	37 ± 23	65 ± 21
		GDEov	70 ± 35	49 ± 22	45 ± 27	91 ± 46
grip strength[b] (N)	$Agl^{+/+}$	PBS	3.18 ± 0.30†	3.59 ± 0.15†	3.61 ± 0.28†	3.44 ± 0.23†
	$Agl^{-/-}$		2.72 ± 0.22*	2.87 ± 0.26*	3.05 ± 0.29*	2.63 ± 0.28*
		GDEov	3.01 ± 0.18	2.89 ± 0.25*	3.04 ± 0.20*	3.05 ± 0.09*†
Wirehang[c] (falls/min)	$Agl^{+/+}$	PBS	7.76 ± 6.10†	7.28 ± 6.97	3.94 ± 2.03†	5.89 ± 4.02†
	$Agl^{-/-}$		21.39 ± 6.74*	13.87 ± 2.97	25.51 ± 17.76*	35.89 ± 7.59*
		GDEov	18.56 ± 4.82*	6.10 ± 3.21	6.33 ± 5.07†	8.12 ± 6.29†

[a] time to fall from a 4-40 rpm accelerating rod. [b] average grip strength. [c] number of falls per minute measured in a 3-minute interval. Statistical analyses were performed by one-way ANOVA (*, $p<0.05$ vs. $Agl^{+/+}$; †, $p<0.05$ vs. untreated $Agl^{-/-}$). All data are shown as mean ± standard deviation.

Table S4. Gene expression of 19 glucose metabolism-related genes in the liver of $Agl^{-/-}$ mice treated with PBS, AAV-GAA and GDEov vector and compared to the levels observed in $Agl^{+/+}$ animals.

GROUP	GENE ID	GENE NAME	[g]Agl-/-	[h]$Agl^{-/-}$, AAV-GAA	[i]$Agl^{-/-}$, AAV-GDEov
1[a]	ACO1	Aconitase 1	↓	↓	↓
	GCK	Glucokinase	↓	↓	↓
	SDHD	Succinate dehydrogenase complex, subunit D, integral membrane protein	↓	↓	↓
2[b]	IDH2	Isocitrate dehydrogenase 2 (NADP+), mitochondrial	↑	-	-
	PCK2	Phosphoenolpyruvate carboxykinase 2 (mitochondrial)	↑	-	-
	PDP2	Pyruvate dehyrogenase phosphatase catalytic subunit 2	↓	-	-
	PGM1	Phosphoglucomutase 1	↑	-	-
3[c]	IDH1	Isocitrate dehydrogenase 1 (NADP+), soluble	↓	↓	-
	MDH1	Malate dehydrogenase 1, NAD (soluble)	↓	↓	-
	PDHB	Pyruvate dehydrogenase (lipoamide) beta	↓	↓	-
	SDHB	Succinate dehydrogenase complex, subunit B, iron sulfur (Ip)	↓	↓	-
4[d]	DLAT	Dihydrolipoamide S-acetyltransferase (E2 component of pyruvate dehydrogenase complex)	-	↓	↓
	PDK1	Pyruvate dehydrogenase kinase, isoenzyme 1	-	↓	↓
5[e]	CS	Citrate synthase	-	-	↓
	PDK3	Pyruvate dehydrogenase kinase, isoenzyme 3	-	-	↑
6[f]	HK3	Hexokinase 3	-	↓	-
	PDK2	Pyruvate dehydrogenase kinase, isoenzyme 2	-	↓	-
	PYGL	Liver glycogen phosphorylase	-	↓	-
	RBKS	Ribokinase	-	↓	-

[a]not rescued. [b]rescued by both AAV treatments. [c]rescued by GDEov treatment only. [d]modified by both AAV treatments. [e]modified by GDEov treatment. [f]modified by AAV-GAA treatment. [g,h,I] changes in the level of expression (n-fold > ±1.75) in untreated $Agl^{-/-}$ mice, $Agl^{-/-}$ mice treated with $1x10^{12}$ vg/mouse of AAV-GAA, or $Agl^{-/-}$ mice treated with $2x10^{12}$ of GDEov (-, no change; ↑, significant increase ($p<0.05$ by ANOVA); ↓, significant decrease ($p<0.05$ by ANOVA)). All data are shown as mean ± standard deviation.

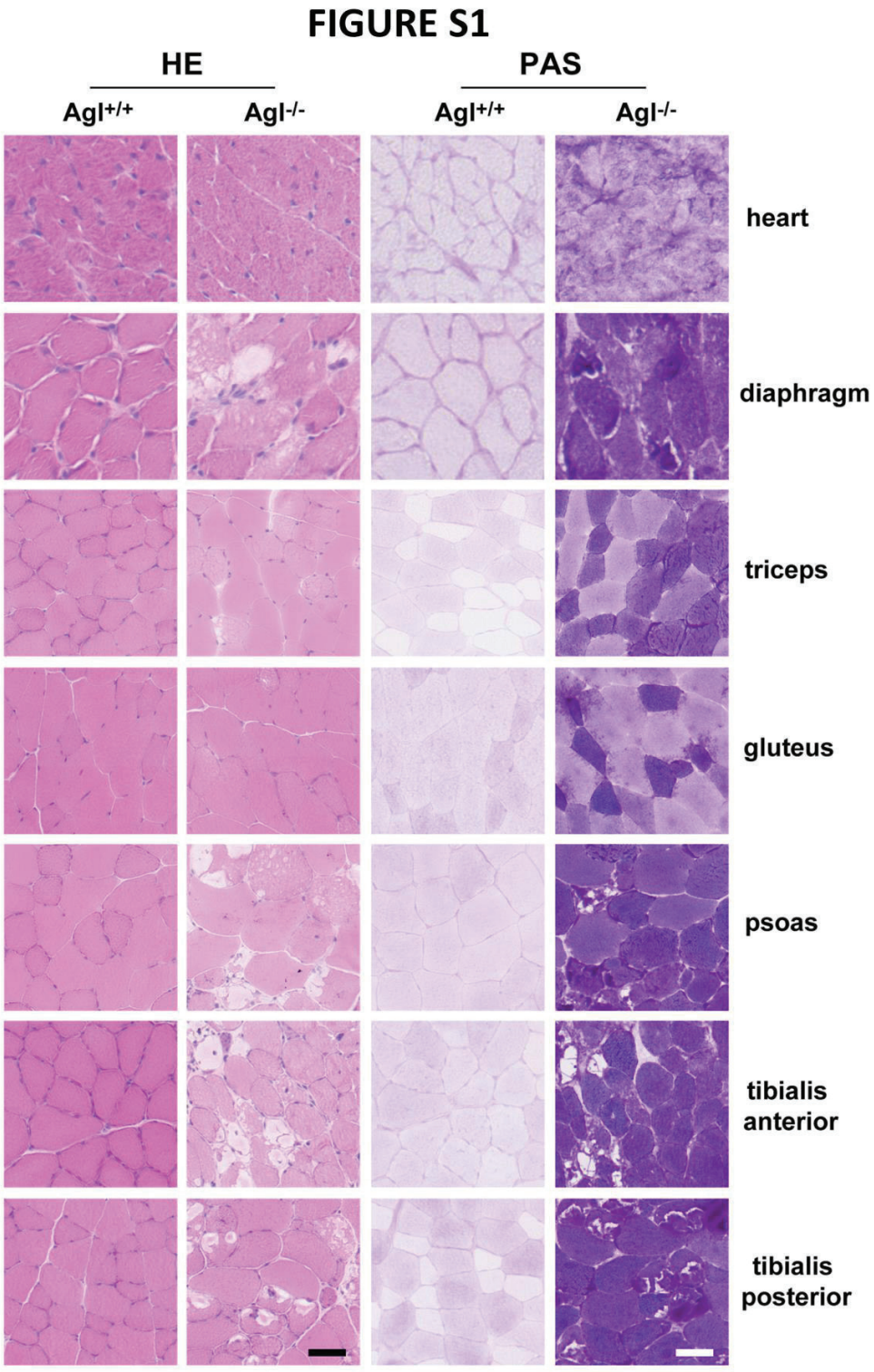

Figure S1 Histological characterization of glycogen accumulation in muscle of $Agl^{-/-}$ mice. Different muscles obtained from 3-month-old $Agl^{-/-}$ mice and wild type littermates ($Agl^{+/+}$) were analyzed by hematoxylin-eosin (HE) and periodic acid-Schiff (PAS) staining. Scale bars = 50µm.

FIGURE S2

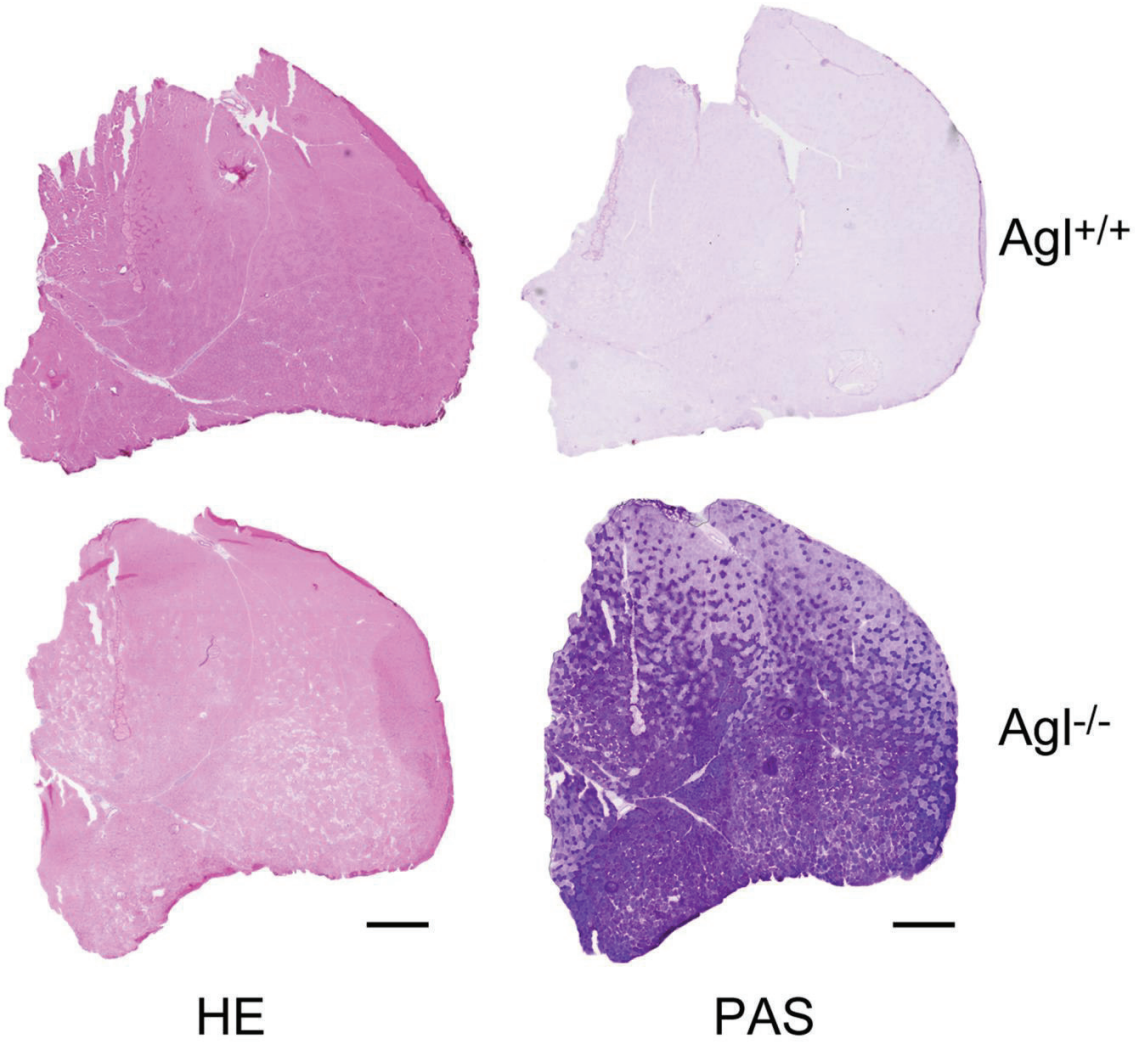

Figure S2. Uneven accumulation of glycogen in quadriceps. Hematoxylin-eosin staining (HE, left panels) and periodic acid-Schiff (PAS right panels) staining performed in quadriceps of 3-month-old $Agl^{-/-}$ mice and wild-type littermates ($Agl^{+/+}$). Scale bars = 500 μm.

FIGURE S3

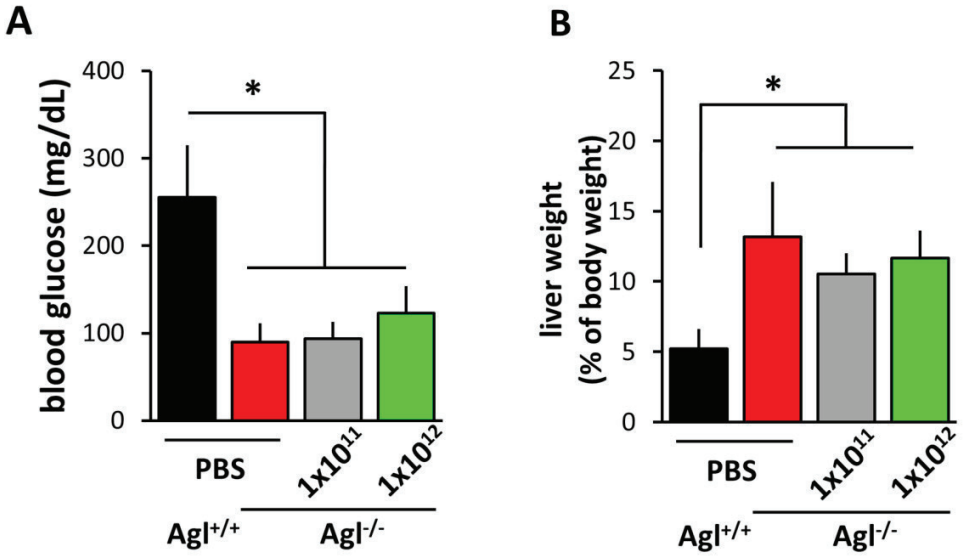

Figure S3. Effect of AAV-GAA gene transfer on the liver of $Agl^{-/-}$ mice **(A)** Glycemia measured 3 months post-injection in mice injected as described in figure 3. **(B)** Liver weight expressed as % of body weight. Statistical analysis was performed by ANOVA (*= $p<0.05$, n= 8). All data are shown as mean ± standard deviation.

FIGURE S4

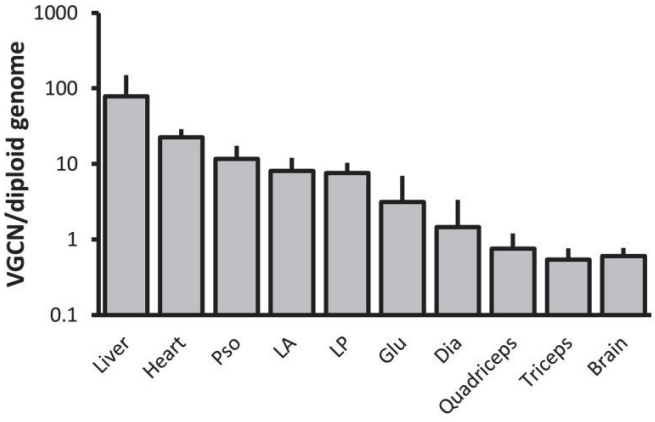

Figure S4. GDEov biodistribution measured by qPCR with oligonucleotides specific for the recombination region. All data are shown as mean ± standard deviation.

FIGURE S5

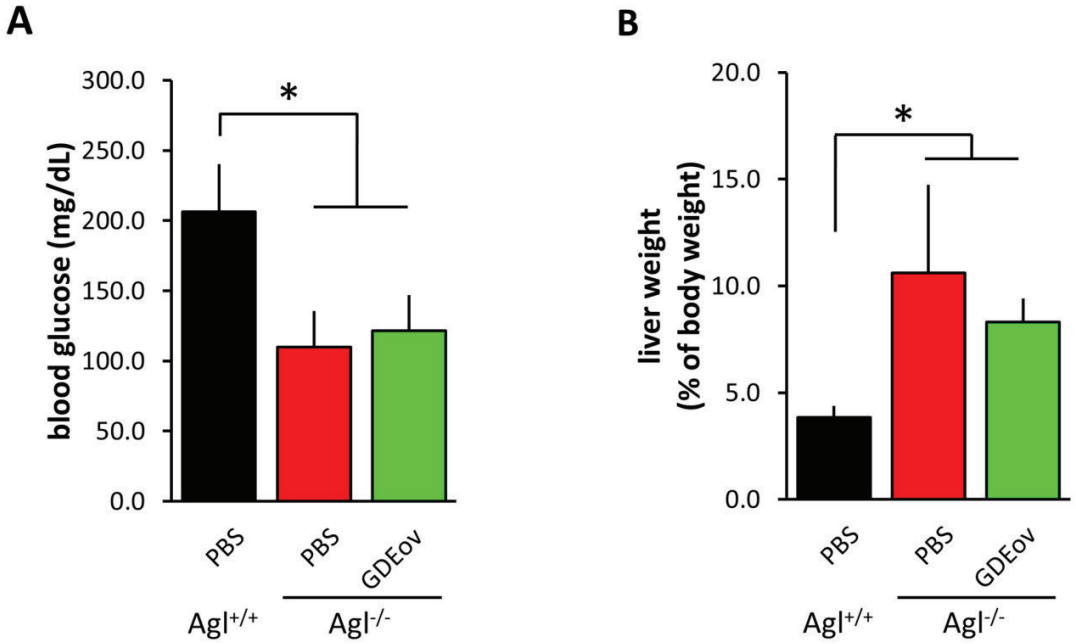

Figure S5. Effect of CMV GDEov gene transfer on the liver of Agl-/- mice **(A)** Glycemia measured 3 months in mice treated as described in figure 4. **(B)** Liver weight expressed as % of body weight. Statistical analysis was performed by ANOVA (*= $p<0.05$, n= 5). All data are shown as mean ± standard deviation.

FIGURE S6

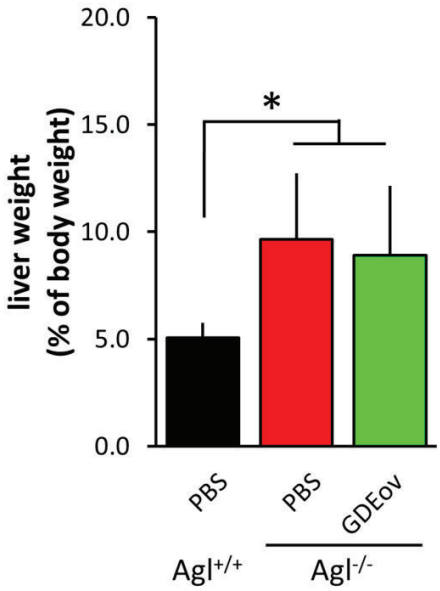

Figure S6. Liver-specific GDEov does not correct hepatomegaly. Liver weight expressed as % of body weight measured in mice treated as described in figure 7. Statistical analysis was performed by ANOVA (*= $p<0.05$, n= 5). All data are shown as mean ± standard deviation.

ANNEX II

Collaboration with DICERNA

HEPATOLOGY

Inhibition of Glycogen Synthase II with RNA Interference Prevents Liver Injury in Mouse Models of Glycogen Storage Disease Type Ia and III

Journal:	*Hepatology*
Manuscript ID	Draft
Wiley - Manuscript type:	Original
Date Submitted by the Author:	n/a

Complete List of Authors:	Pursell, Natalie; Dicerna Pharmaceuticals, Gierut, Jessica; Dicerna Pharmaceuticals Inc. Apponi, Luciano; Dicerna Pharmaceuticals Inc. Zhou, Wei; Dicerna Pharmaceuticals Inc. Dills, Michael; Dicerna Pharmaceuticals Inc. Diwanji, Rohan; Dicerna Pharmaceuticals Inc. Gjorgjieva, Monika ; Institut national de la santé et de la recherche médicale Saxena, Utsav; Dicerna Pharmaceuticals Inc. Yang, Jr-Shiuan; Dicerna Pharmaceuticals Inc. Shah, Anee; Dicerna Pharmaceuticals Inc. Venkat, Nandini; Dicerna Pharmaceuticals Inc. Storr, Rachel; Dicerna Pharmaceuticals Inc. Kim, Boyoung ; Dicerna Pharmaceuticals Inc. Wang, Weimin; Dicerna Pharmaceuticals Inc. Abrams, Marc; Dicerna Pharmaceuticals Inc Raffin, Margaux; Institut national de la santé et de la recherche médicale Mithieux, Gilles; Institut national de la santé et de la recherche médicale Rajas, Fabienne; Institut national de la santé et de la recherche médicale Dudek, Henryk; Dicerna Pharmaceuticals Inc Brown, Bob; Dicerna Pharmaceuticals Inc Lai, Chengjung; Dicerna Pharmaceuticals Inc.
Keywords:	hepatomegaly, steatosis, fibrosis, cirrhosis, neoplasia

SCHOLARONE™
Manuscripts

Inhibition of Glycogen Synthase II with RNA Interference Prevents Liver Injury in Mouse Models of Glycogen Storage Disease Type Ia and III

Natalie Pursell[1], Jessica Gierut[1], Luciano Apponi[1], Wei Zhou[1], Michael Dills[1], Rohan Diwanji[1], Monika Gjorgjieva[2], Utsav Saxena[1], Jr-Shiuan Yang[1], Anee Shah[1], Nandini Venkat[1], Rachel Storr[1], Boyoung Kim[1], Weimin Wang[1], Marc Abrams[1], Margaux Raffin[2], Gilles Mithieux[2], Fabienne Rajas[2], Henryk Dudek[1], Bob D. Brown[1] and Chengjung Lai[1]

[1]Dicerna Pharmaceuticals, Cambridge, MA 02140

[2]Institut national de la santé et de la recherche médicale U1213, Université Lyon 1, Lyon, France

Keywords: hepatomegaly, steatosis, fibrosis, cirrhosis, neoplasia

For Peer Review

Correspondence should be addressed to B.D.B. (bbrown@dicerna.com) and C.L. (clai@dicerna.com)

Dicerna Pharmaceuticals, 87 Cambridgepark Drive, Cambridge, MA 02140, USA

Conflict of Interest

N. P., J. G., L. A., W.Z., R.D., M.D., U.S., J.Y., N.V., R.S., B.K., J.S., N.N., W.W., M.A., H.D., B. D. B. and C. L. are or were employees of Dicerna Pharmaceuticals, which is developing DsiRNAs as therapeutics. M.G., M.R., G. M. and F. R. have received research grant support from Dicerna Pharmaceuticals.

Abbreviations:

GSDs, glycogen storage diseases
GSD III, glycogen storage disease Type III
GYS2, glycogen synthase II
GYG2, glycogenin 2
GBE, glycogen branching enzyme
GLGP, glycogen phosphorylase
GDE, glycogen debranching enzyme
G6P, glucose-6-phosphate
G6Pase, glucose 6-phosphatase
GSD Ia , glycogen storage disease type Ia
GNG, gluconeogenesis
HCA, hepatocellular adenoma
HCC, hepatocellular carcinoma
RNAi, RNA interference
GalNAc, N-Acetylgalactosamine

For Peer Review

H&E, hematoxylin and eosin

PAS, Periodic acid-Schiff

IHC, immunohistochemistry

ALT, alanine transaminase

AST, aspartate transaminase

ALP, alkaline phosphatase

G6pc, gene encodes catalytic subunit of glucose 6-phosphatase.

L-*G6pc*$^{-/-}$, liver-specific deletion of *G6pc*

AAV, adeno-associated virus

IACUC, institutional animal care and use committees

ESCs, embryonic stem cells

CYP3A4, cytochrome P450 3A4

μm, micrometer

mm, millimeter

cm, centimeter

For Peer Review

Abstract

Glycogen storage diseases (GSDs) of the liver are characterized by glycogen accumulation and liver damage. GSD type III (GSD III) is caused by a deficiency of glycogen debranching enzyme activity, resulting in an accumulation of abnormally structured glycogen in the liver, muscles, and heart. Hepatic accumulation of abnormally structured glycogen results in hepatomegaly and could lead to the development of fibrosis, cirrhosis, and hepatocellular adenoma or carcinoma. In this study, we demonstrate that inhibition of glycogen synthesis using an RNA interference approach to silence hepatic glycogen synthase II (*Gys2*) expression prevents glycogen accumulation, hepatomegaly, fibrosis and nodule development in a mouse model of GSD III. Additionally, we show that silencing *Gys2* expression reduces hepatic steatosis in a mouse model of GSD type Ia, where a deficiency of glucose-6-phosphatase impairs the final step of glycogenolysis resulting in a corresponding diversion of excess glucose-6-phosphate to lipid synthesis. *Conclusion*: Our results support therapeutic silencing of *GYS2* expression as a potential approach for improving liver abnormalities and long term injury that are associated with multiple types of GSDs including types I, III, IV, VI and IX.

For Peer Review

Introduction

The hepatic glycogen storage diseases (GSDs) are inherited disorders of glycogen metabolism which present clinically with hepatomegaly, liver injury, failure to thrive, and/or fasting hypoglycemia (1). These GSDs, including types 0, I, III, IV, VI and IX, are caused by deficiencies in enzymes or transporters involved in glycogen synthesis or breakdown (2-7). In a healthy individual, excess postprandial glucose is converted via a multi-enzyme process into UDP-glucose from which an initial glycogen polymer is formed on the glycogenin 2 (GYG2) dimer scaffold via α-1,4 glycosidic linkages using its autoglycosylation activity (Supporting Fig. S1) (8, 9). Glycogen synthase 2 (GYS2) continues to catalyze the addition of UDP-glucose onto existing glucose molecules to increase the length of linear glucose polymer chain. Subsequently, glycogen branching enzyme (GBE) is able to attach a new branch point with α-1, 6 glycosidic linkage that serves as a new initial point for another cycle of linear glucose chain elongation. Working together, GYS2 and GBE build a complicated tree-like structured glycogen molecule with a GYG2 dimer in the center. During periods of fasting, glycogen phosphorylase (GLGP) starts to release glucose-1-phosphate from glycogen until a branching point is encountered. Glycogen debranching enzyme (GDE) activity then is required for transferring and liberating glucose molecules near the branching point before GLGP is able to further process glycogen and release glucose. Glucose-1-phosphate released from glycogen is then converted into glucose-6-phosphate (G6P), and subsequently to glucose by glucose 6-phosphatase (G6Pase) in the final step of glycogenolysis to maintain glucose homeostasis in times of fasting (10).

For Peer Review

GSD type Ia (GSD Ia) is caused by a deficiency of G6Pase and is characterized by the most severe hypoglycemia among all types of GSDs due to redundant role of G6Pase in converting G6P to glucose in the final step of both gluconeogenesis (GNG) and glycogenolysis pathways (11-14). G6Pase is primarily expressed in the liver, kidneys, and intestine (15). Systemic G6Pase deficiency leads to the accumulation of G6P and subsequent metabolic complications such as hypertriglyceridemia, hyperlactacidemia, and hyperuricaemia (16). The accumulation of glycogen and lipid in the liver leads to hepatomegaly and may contribute to the development of hepatocellular adenoma (HCA) or carcinoma (HCC) in some patients (17-20).

The majority of the remaining hepatic GSDs, including types 0, III, VI, and IX, are associated with a milder, fasting, ketotic hypoglycemia due to an active GNG pathway in these patients capable of partially maintaining blood glucose homeostasis and compensating for the defective glycogenolysis pathway (21). The increased activity of the GNG pathway from lipid and protein sources in these patients results in increased ketone body levels. Incidences of GSD III are the highest among all ketotic GSDs (22). GSD III is caused by the deficiency of GDE and is characterized by hepatomegaly and hyperlipidemia with some patients developing liver damage such as elevated circulating liver enzymes, fibrosis, cirrhosis, HCA or HCC (22-24). GSD IV patients have euglycemia but the absence of GBE results in the accumulation of poorly branched glycogen that is associated with failure to thrive, hepatosplenomegaly, and progressive liver cirrhosis leading to death in early childhood (5).

For Peer Review

Patients with hepatic GSDs are not able to efficiently utilize their stored glycogen to generate glucose during periods of fasting. Moreover, accumulated glycogen may either directly or indirectly lead to the development of liver abnormalities in GSD patients. We hypothesized that by preventing glycogen synthesis through the specific inhibition of hepatic GYS2, we could reduce hepatomegaly and liver injury in GSD patients. In this study, we investigated the effect of RNA interference (RNAi) mediated GYS2 enzyme reduction in GSD Ia and GSD III mouse models. We observed that *Gys2* reduction prevented glycogen accumulation, hepatomegaly, liver toxicity and hepatic nodule in GSD III model mice. Additionally, *Gys2* reduction in a GSD Ia mouse model resulted in decreased glycogen and lipid levels. These results support further exploration of *GYS2* reduction by RNAi as a potential novel therapeutics for the prevention of liver injury in hepatic GSDs.

For Peer Review

Materials and Methods

Animal Experimentation

Selection of Lead *Gys2* siRNAs. GYS2-1 and GYS2-2 siRNAs were identified through a process of large-scale screening of siRNAs for mRNA knockdown activity *in vitro* in HEK293 cells stably expressing mouse *Gys2* (Supporting Fig. S2). RNA strands for siRNA duplexes were synthesized purified at Integrated DNA Technologies (Coralville, IA). The GYS2-1 siRNA had a 36/22-mer duplex RNA structure, with a 36-nucleotide sense strand composed of modified RNA and GalNAc conjugation that was annealed to

a 22-nucleotide modified RNA antisense strand. The GYS2-2 had a 25/27-mer duplex RNA structure with a 25-nucleotide modified sense strand annealed to a 27-nucleotide modified RNA antisense strand. The GYS2-2 siRNA duplex was formulated in lipid nanoparticles. The siRNAs were modified with either 2′-OMe or 2′-F on their sugar moieties.

Generation of GSD Mouse Models and *In Vivo* Testing. All animal experiments complied with the animal protocols approved by Dicerna's Institutional Animal Care and Use Committees (IACUC). Mice were kept in a pathogen-free facility, housed using an Innovive disposable caging system with corn cob bedding (Innovive, Inc., San Diego, CA) with free access to Picolab diet for research animals by Purina (Scott Pharma, Marlborough, MA) and water unless otherwise noted. All experiments were done during the 12-hour light cycle. CD-1 mice (Charles River Laboratories, Wilmington, MA) were used for *in vivo* screening of *Gys2* siRNA activity. C57BL/6 mice (Harlan Laboratories, Indianapolis, IN) were used for testing the efficacy of the lead GYS2-1 and GYS2-2 siRNA .

Agl$^{-/-}$ mice were produced from embryonic stem cells (ESCs) with a knockout of the *Agl* gene which were purchased from the European Conditional Mouse Mutagenesis Program (EUCOMM, Germany). ESCs injections and the generation of heterozygous *Agl*$^{+/-}$ mice were performed by geneOway (Lyon, France). Heterozygous *Agl*$^{+/-}$ mice were bred to homozygous for all studies. Wild-type and heterozygous littermates were used as controls.

For Peer Review

L-*G6pc*$^{-/-}$ mice were generated and maintained as described previously (15, 25).

Agl$^{-/-}$ and L-*G6pc*$^{-/-}$ animals were used to evaluate the efficacy of GYS2-1 and GYS2-2 respectively. GalNac-conjugated siRNA (GYS2-1) was injected subcutaneously and LNP-formulated siRNA (GYS2-2) was administered intravenously. Blood samples were collected via tail vein (interim measurement) or cardiac puncture (terminal measurement) and used either as whole blood or processed to serum and plasma. *Agl*$^{-/-}$ mice were subjected to six hours of fasting prior to study termination except where fed-state indicated. L-*G6pc*$^{-/-}$ mice were subjected to six hours of fasting during week four after which blood samples were taken. At study termination, mice were euthanized according to IACUC guidelines and liver tissue samples were collected. Liver samples were stored in RNAlater (ThermoFisher Scientific, Waltham, MA) for RNA preparation, fresh frozen in liquid nitrogen, or fixed in 10% neutral-buffered formalin (VWR International, Radnor, PA).

Analysis of blood chemistry parameters. Interim blood glucose measurements were made on whole blood using a glucometer. Terminal blood collections were processed to serum and plasma for measurement of blood chemistry parameters. Serum chemistry and blood glucose levels were measured by IDEXX BioResearch Laboratories (Grafton, MA). Blood glucose measurements were confirmed using a glucose assay kit (Abcam, Cambridge, MA) according to the manufacturer's instructions. Alanine transaminase (ALT) activity assay kit (Abcam, Cambridge, MA) was used for time-course

For Peer Review

measurement of ALT according to the manufacturer's instructions. For L-*G6pc*$^{-/-}$ mice, plasma glucose, cholesterol, and triglycerides were analyzed as described (15, 25).

RNA Preparation and Real-Time PCR. Tissue samples were homogenized in QIAzol Lysis Reagent using TissueLyser II (Qiagen, Valencia, CA). RNA was then purified using MagMAX Technology according to manufacturer instructions (ThermoFisher Scientific, Waltham, MA). High capacity cDNA reverse transcription kit (ThermoFisher Scientific, Waltham, MA) was used to prepare cDNA. Mouse-specific *Gys2* and *Hprt1* primers (Integrated DNA Technology, Coralville, IA) were used for PCR on a CFX96 or CFX384 Real-Time PCR Detection System (Bio-Rad Laboratories, Inc., Hercules, CA).

Western Blot. Tissue lysates were prepared using TissueLyser II (Qiagen, Valencia, CA) with T-PER Tissue Protein Extraction Reagent and protease inhibitor cocktail (ThermoFisher Scientific, Waltham, MA). Total protein concentration was measured by BCA Protein Assay (ThermoFisher Scientific, Waltham, MA) and equal protein concentrations were resolved by NuPAGE 4-12 % Bis-Tris SDS-PAGE (ThermoFisher Scientific, Waltham, MA). Electrophoresed proteins were transferred to nitrocellulose membranes using the iBlot Dry Blotting System (ThermoFisher Scientific, Waltham, MA) and blocked with Odyssey Blocking Buffer (Li-Cor Biosciences, Lincoln, NE). Membranes were then incubated with rabbit anti-glycogen synthase antibody (Cell Signaling Technology, Danvers, MA) and with mouse anti-glyceraldehyde 3-phosphate dehydrogenase antibody (Abcam, Cambridge, MA). Anti-rabbit IRDye 680 and anti-mouse IRDye 800 secondary antibodies (Li-Cor Biosciences, Lincoln, NE) were used

For Peer Review

for detection and signal intensity was measured using the Odyssey Infrared Imaging System (Li-Cor Biosciences, Lincoln, NE).

Measurement of liver glycogen and glucose-6-phosphate levels. Tissue lysates were prepared in water using TissueLyser II (Qiagen, Valencia, CA). Tissue homogenate was split into two samples of equal volume. The first sample (Glycogen) was incubated at 95 °C for 10 minutes then centrifuged to isolate the supernatant. The supernatant was diluted in water and analyzed by a Glycogen Assay Kit (Abcam, Cambridge, MA). The second sample was immediately centrifuged to isolate the supernatant which was used to measure total protein concentration by BCA Protein Assay (ThermoFisher Scientific, Waltham, MA). Measured glycogen levels were normalized to total protein concentration.

Concentrations of G6P in L-*G6pc*$^{-/-}$ mouse livers were measured as described previously (25).

Histological and Immunohistochemistry Analysis. Tissue were fixed in 10% neutral-buffered formalin overnight and then transferred to 70% ethanol. Embedding in paraffin, preparation of slides, and H&E staining was done at Mass Histology Service (Worcester, MA). PAS (Sigma-Aldrich, St. Louis, MO) and Sirius Red (Abcam, Cambridge, MA) staining were performed according to the manufacturer's instructions. For immunohistochemistry (IHC) experiments, paraffin sections were deparaffinized and rehydrated. Heat-mediated antigen retrieval (citrate buffer, pH 6.0) was performed for

For Peer Review

Ki67 IHC samples. Endogenous peroxidases and alkaline phosphatase were blocked with BLOXALL solution (Vector Laboratories, Burlingame, CA). Rabbit monoclonal anti-Ki67 antibody (1:100 dilution, Abcam, Cambridge, MA), rabbit monoclonal anti-alpha smooth muscle Actin antibody (1:200 dilution, Abcam, Cambridge, MA) and mouse monoclonal anti-CYP3A antibody (1:50 dilution, Santa Cruz Biotechnology, Dallas, TX) were diluted in SignalStain® Antibody Diluent (Cell Signaling Technology, Danvers, MA) and incubated overnight at 4 °C. Binding of the primary antibody was detected using a goat anti-rabbit IgG HRP antibody (Antibodies-online, Atlanta, GA) and SignalStain® DAB Substrate Kit (Cell Signaling Technology, Danvers, MA). Oil Red O Lipid Stain was performed on frozen tissue samples according to the manufacturer's instructions (Abcam, Cambridge, MA) in the presence or absence of hematoxylin. Results were visualized using an Olympus BX51 or a Nikon Eclipse Ti microscope and a Olympus BX61VS slide scanner using Image Pro Premier 9.1, NIS-Elements BR3.2, and Olympus VS-ASW image analysis software respectively.

Assessment of Caspase Activity in Mouse Liver Tissue. Detection of Caspase-3/7 activity in mouse livers was performed essentially as described (26). 100 μg/mL extract was mixed with an equal volume of Caspase-Glo® Reagent (Promega Corporation, Madison, WI) and incubated at room temperature before reading on a SpectraMax M5 Plate Reader (Molecular Devices, Sunnyvale, CA).

For Peer Review

Measurement of Ketone Body Levels. Ketone body levels were measured with Ketone Body Assay kit in terminal serum samples from wild-type and *Agl*$^{-/-}$ mice according to the manufacturer's instructions (Sigma-Aldrich, St. Louis, MO).

Results

Gys2 mRNA Knockdown Inhibits Glycogen Synthesis in Wild-Type Mice

We identified our lead *Gys2* small interfering RNAs (siRNAs) by sequential screening *in vitro* (Supporting Fig. S2). Potent siRNAs were then conjugated with N-Acetylgalactosamine (GalNAc) sugar residues (designated as GYS2-1) or formulated in lipid nanoparticle (designated as GYS2-2) and evaluated for their activity in wild-type mice for specific inhibition of *Gys2* mRNA and GYS2 protein expression in liver (Fig. 1, Supporting Fig. S2). GYS2-1 potently inhibits *Gys2* mRNA (Fig. 1A) and GYS2 protein levels (Fig. 1B, C). Additionally, GYS2-1 and GYS2-2 treatment results in significantly reduced GYS2 protein and glycogen levels in wild-type mice in nearly all hepatocytes (Fig. 1D, E, Supporting Fig. S2G, H), suggesting that both GalNAc and LNP-mediated siRNA delivery mechanisms are able to achieve homogeneous delivery of siRNA to hepatocytes and are suitable for further evaluation of the disease mechanism.

Gys2 mRNA Knockdown Prevents Abnormal Glycogen Accumulation and Hepatomegaly in the *Agl*$^{-/-}$ GSD III mouse model

To evaluate the activity of GYS2-1 as a potential therapeutic to correct liver abnormalities in GSDs, we employed a murine model of GSD III. *Agl*$^{-/-}$ mice have a

For Peer Review

germline mutation in the gene encoding GDE, resulting in accumulation of abnormally structured glycogen that is resistant to efficient breakdown by GLGP (27, 28). These mice develop hepatomegaly with abnormal histomorphology by four weeks of age (Supporting Fig. S3) (27), followed by an elevation of circulating liver enzymes, and progression to periportal fibrosis by approximately eighteen weeks of age (27, 28). *Agl*$^{-/-}$ mice were treated with GYS2-1 weekly from four to thirteen weeks of age or from eight to twenty-six weeks of age. GYS2-1 potently suppressed hepatic *Gys2* mRNA (Fig. 1A) and GYS2 protein (Fig. 1B, C) levels, resulting in a significant reduction of hepatic glycogen levels in the *Agl*$^{-/-}$ mice (Fig. 1D). Blockage of glycogen synthesis with chronic dosing of GYS2-1 reverses the hepatomegaly that is characteristic of *Agl*$^{-/-}$ mice (Fig. 1F, 2). Chronic dosing of GYS2-1 also reverses histomorphological characteristics of *Agl*$^{-/-}$ mice as evidence by hematoxylin and eosin (H&E) and Periodic Acid-Schiff (PAS) staining (Fig. 3A, Supporting Fig. S3A, B) until they are similar to their wild-type littermates.

Interestingly, we observed that *Gys2* mRNA and GYS2 protein levels were downregulated in *Agl*$^{-/-}$ mice in the absence of treatment when compared with their wild-type littermates (Fig. 1A, B, C). This observation suggests there may be physiological feedback in *Agl*$^{-/-}$ mice to mitigate the accumulation of excess glycogen by down-regulation of *Gys2* expression. However, despite this down-regulation of *Gys2* expression, A*gl*$^{-/-}$ mice still exhibit hepatomegaly and histomorphological characteristics of GSD III suggesting that the remaining levels of GYS2 enzyme is sufficient to cause accumulation of glycogen in this GDE-deficient background. Importantly, GYS2-1 was able to further reduce the expression of *Gys2* mRNA and GYS2 protein in *Agl*$^{-/-}$ mice,

For Peer Review

resulting in a reversal of the phenotypic characteristics of GSD III (Fig. 1, 2, 3, Supporting Fig. S3A, B). Analysis of four week old *Agl*$^{-/-}$ mice sacrificed in the absence of treatment indicates that hepatomegaly and abnormal liver morphology occur early in life (Supporting Fig. S3A) (27), suggesting that the GSD III liver phenotype of *Agl*$^{-/-}$ mice is highly reversible with GYS2 inhibition.

Inhibition of GYS2 Protects Against Liver Toxicity and Fibrosis in the *Agl*$^{-/-}$ GSD III Mouse Model

As the life expectancy of patients with GSD III improves with diet control, cases of long-term liver complications continue to be reported (29-31). However, the mechanism remains unclear as to how liver damage in *Agl*-deficient patients leads to long-term complications such as fibrosis, cirrhosis, HCA and HCC. IHC of the livers of untreated *Agl*$^{-/-}$ mice for the cellular proliferation marker Ki67 shows increased clusters of positively-stained cells surrounded by hepatocytes containing large vacuoles (Fig. 3A, B, Supporting Fig. S3B). The increased Ki67-positive cells were detected on hepatocytes and non-hepatocytes, identified based on morphology and by IHC for expression of cell type-specific markers in the PBS treated *Agl*$^{-/-}$ mice (Fig. 3B). One hypothesis is that liver damage induces neighboring cells (hepatocyte or non-hepatocyte) to proliferate, leading to myofibroblast activation in non-hepatocytes and the development of neoplasia in hepatocytes. Livers of *Agl*$^{-/-}$ mice did not have elevated activity of apoptotic caspases 3 and 7 (Supporting Fig. S3C) supporting the hypothesis that slowly progressing liver damage, mediated by a non-apoptotic mechanism, induces cell proliferation in the GSD III mouse model. Notably, in *Agl*$^{-/-}$ mice treated with GYS2-1, cellular proliferation was reduced to the levels of wild-type littermates as evidenced

For Peer Review

by immunohistochemistry for Ki67 (Fig. 3A, Supporting Fig. S3B). We also observed that GYS2-1 treatment completely impeded the development of fibrosis in the livers of *Agl*$^{-/-}$ mice (Fig. 3A, Supporting Fig. S3B). These results suggest that reduction of GYS2 enzyme in the livers of *Agl*$^{-/-}$ mice can prevent hepatocyte damage from excess glycogen accumulation and the resulting development of fibrosis.

When compared to their wild-type littermates, *Agl*$^{-/-}$ mice also display signs of liver damage with elevated levels of circulating alanine aminotransferase (ALT), aspartate transaminase (AST) and alkaline phosphatase (ALP) that were exacerbated by fasting (Fig. 3C, Supporting Fig. S3D) (27, 28). *Gys2* mRNA inhibition with GYS2-1 significantly reduces levels of ALT, AST and ALP in *Agl*$^{-/-}$ mice to near wild-type baseline levels during both fasting and non-fasting conditions (Fig. 3C, Supporting Fig. S3D).

Inhibition of GYS2 Prevents Development of Hepatic Nodules in the *Agl*$^{-/-}$ GSD III Mouse Model

To investigate the long-term effect of inhibiting glycogen synthesis in *Agl*$^{-/-}$ mice, animals were injected with GYS2-1 monthly from 1 to 12 months of age. Repeatedly, inhibition of *Gys2* reduces glycogen synthesis and prevents hepatomegaly, liver toxicity and fibrosis in *Agl*$^{-/-}$ mice (Fig. 4, 5, Supporting Fig. S4A, B, S5, S6). Importantly, small, sporadic nodules ranging from <1 to 3 millimeters (mm) in diameter were noted in the livers of all mice treated with PBS but not in mice treated with GYS2-1. Histopathological analysis of the nodules identified hepatocytes with varying sizes, shapes, and irregular nuclei with a decrease in the number of vacuoles present (Fig. 4, Supporting Figure S6). The largest nodule displays the “pushing border” characteristic indicative of an expanding cell mass that is adjacent to the parenchyma (Supporting Fig.

For Peer Review

S6). Increased cellular proliferation was detected in PBS-treated mice in both the parenchymal and nodule compartments at one year of age as it was in the younger mice (Supporting Fig. S7). In contrast, inhibition of *Gys2* reduces the proliferative index to the levels of wild-type littermates (Supporting Fig. S7). No incidences of the development of hepatocellular carcinoma were observed by histopathology or IHC analysis at one year of age (Supporting Fig. S6, S8). Nonetheless, these results suggest that GYS2-1 treatment effectively prevents long-term liver injury and hyperplasia in the GSD III mouse model. Importantly, normalization of the liver phenotype with a high degree of homogenous morphology throughout the entire liver was achieved with GYS2-1 treatment that was comparable to that of their wild-type littermates (Fig. 4, 5, Supporting Fig. S7, S8), suggesting that a GalNAc-mediated RNAi approach is effective in unbiasedly resolving the underlying disorder of all hepatocytes. This is particularly important for designing therapeutics aimed at preventing hepatic malignancies in livers where widespread and sustained cell proliferation has been observed (Fig. 3, Supporting Fig. S3, S7). Tumorigenesis can theoretically initiate from any small population of damaged hepatocytes that are actively proliferating making the homogenous inhibition of *Gys2* and resulting prevention of hepatocyte damage extremely important for preventing disease progression.

Inhibition of GYS2 Rescues the Liver Phenotype in a GSD Ia Mouse Model with Liver-Specific Deletion of *G6pc*

In addition to GSD III, patients with GSD types I, IV, VI and IX also develop hepatomegaly during the early stages of their disease development (1). In GSD Ia patients, the development of HCA or HCC is well documented (17-19, 32-34) as are

For Peer Review

case reports where liver transplantations were performed on GSD Ia patients as the sole option for the treatment of liver complications (35, 36). GSD Ia is caused by a deficiency of G6Pase and is characterized by the most severe hypoglycemia among all types of GSDs (37). We evaluated the effect of GYS2-2 in a GSD Ia mouse model with liver-specific deletion of *G6pc* gene (L-*G6pc*$^{-/-}$), which encodes catalytic subunit of G6Pase. The L-*G6pc*$^{-/-}$ mice develop liver injury representative of GSD Ia but with less severe hypoglycemia than patients (25). Similar to our observations in *Agl*$^{-/-}$ mice, we demonstrate that GYS2-2 significantly reduced hepatic *Gys2* mRNA expression (Fig. 6A), resulting in a reduction of hepatic glycogen accumulation and a normalization of liver morphology (Fig. 6B, D).

In GSD Ia patients and mice, *G6pc*-deficiency also causes an increase in lipid deposition in the liver, presumably from excess G6P that cannot be converted to glucose and is instead converted into fatty acids (16). We observed a decrease in hepatic G6P accumulation with GYS2-2 treatment (Fig. 6C) corresponding to the observed reduction in hepatic glycogen levels (Fig. 6B) which serves as one of the main source of hepatic G6P production from glycogenolysis. Reduced lipid deposition in the liver was also observed in L-*G6pc*$^{-/-}$ mice treated with GYS2-2 (Fig. 6D), presumably due to reduced availability of hepatic G6P (16). The activity of apoptotic Caspases 3 and 7 was also increased in L-*G6pc*$^{-/-}$ mice compared to wild-type controls (Fig. 7A) suggesting that lipid deposition and damage-induced cellular proliferation in the liver are linked to cell death pathways in the L-*G6pc*$^{-/-}$ GSD Ia mouse model. We thus demonstrate that reduction of hepatic glycogen levels results in the decline of hepatic

For Peer Review

G6P buildup and lipid deposition, thereby preventing liver damage, apoptosis, and cell proliferation in the livers of L-*G6pc*$^{-/-}$ mice treated with GYS2-2 (Fig. 6, 7).

In summary, our results suggest that glycogen accumulation and lipid deposition are able to initiate liver damage cascades resulting in increased cellular proliferation of hepatocytes and non-hepatocytes in both GSD Ia and GSD III mouse models. Suppression of *Gys2* mRNA expression through an RNAi approach reduces glycogen and fatty acid accumulation homogenously and prevents subsequent liver damage of nearly all hepatocytes in mouse models of GSD Ia and GSD III.

Discussion

GSDs are inherited carbohydrate metabolism diseases with underlying problems of improper use and storage of glycogen. Short- and long-term liver complications occur in many types of GSDs for which there are currently no approved pharmacological treatments. We hypothesized that reduction of hepatic glycogen synthesis will reduce liver complications in the absence of any exacerbation of their existing hypoglycemia due to the defective glycogenesis and glycogenolysis pathways in GSD patients. *Gys2* was proposed as a safe target for the elimination of glycogen synthesis due to the fact that patients with impaired GYS2 activity (GSD Type 0) only suffer from mild hypoglycemia (2, 38-40). In this study, we have obtained data in mouse models to support *Gys2* as an effective target for treating liver complications of GSD Ia and GSD III. Reducing *Gys2* expression using an RNAi approach efficiently prevents glycogen accumulation and alleviates hepatomegaly, and subsequently preventing fibrosis and

For Peer Review

nodule formation in GSD III mice. Reduction of glycogen levels through reduction of *Gys2* also reduces lipid accumulation in GSD Ia mice, presumably through the reduction of hepatic G6P production. Together, these results support further exploration of *GYS2* as a target for the treatment of GSD-related liver abnormalities.

Gys2 Knockdown Does Not Exacerbate Hypoglycemia in GSD III or GSD Ia Mice

Both GSD1a and GSD III patients suffer from fasting hypoglycemia. It is critical that any potential therapeutics for treating liver complications do not exacerbate the hypoglycemic phenotype of GSD patients. As expected, given that glycogen is unable to be efficiently utilized as a source of glucose in most GSD patients, we demonstrate that liver-specific *Gys2* inhibition has no effect on glycemia in fasting or fed conditions in GSD III or GSD Ia model mice (Supporting Fig. S10A, B). GSD III patients develop fasting, ketogenic hypoglycemia as a result of fatty acid oxidation during gluconeogenesis as a means to compensate for the deficiency of glycogenolysis (21). Thus, we hypothesized that gluconeogenesis activity would be increased in GSD III mice during fasting in order to maintain blood glucose levels. As hypothesized, we detected an elevation of ketone bodies in *Agl*$^{-/-}$ GSD III mice during fasting (Supporting Fig. S10C). We did not detect any significant difference in the elevation of ketone bodies following treatment of GYS2-1, suggesting *Gys2* inhibition has no effect on gluconeogenesis (Supporting Fig. S10C). This result also suggests that abnormally structured glycogen, and not ketone bodies, causes liver toxicity and subsequent complications in GSD III. Similarly, we also observed that liver-specific *Gys2* reduction had no adverse effect on lipidemia or body weight in *Agl*$^{-/-}$ GSD III or L-*G6pc*$^{-/-}$, GSD Ia

For Peer Review

mice (Supporting Fig. S10D, E, F). These results further support *Gys2 a*s a potentially effective and safe target for treating liver related ailments in GSDs.

Treating Other GSDs with *GYS2* Inhibition, Especially GSD Type IV

In addition to GSD Ia and III, liver complications are also associated with other types of GSDs including types IV, VI and IX (6, 41, 42). Among different types of GSDs, GSD IV patients have most severe, progressive liver cirrhosis and associated problems. Similar to GSD III, GSD type IV (GSD IV) patients suffer from accumulation of abnormally structured glycogen with very long outer branches (known as polyglucosan) due to the deficiency of glycogen-branching enzyme (GBE) (5, 43, 44). Thus, the same therapeutic principle can be applied to GSD IV patients whereby reduction of glycogen production by RNAi of *GYS2* should alleviate liver abnormalities associated with GBE deficiency.

Targeting *GYS1* in Muscle and Heart Tissue for Treatments of GSD III and IV

In addition to liver complications, a high percentage of GSD III and GSD IV patients also eventually develop muscle weakness or heart complications (42, 45, 46). GDE deficiency in muscle and heart tissue results in an accumulation of abnormally structured glycogen. As expected, GYS2-1 treatment does not reduce glycogen accumulation in skeletal muscle due to its liver-specific delivery with GalNAc conjugation (Supporting Fig. S11). Theoretically, glycogen synthase 1 (GYS1), which is predominantly expressed in both muscle and heart tissue where it serves as the main enzyme for glycogen synthesis, can be targeted to improve myopathy and cardiomyopathy in affected patients. An alternative tissue-specific ligand and receptor approach other than the GalNAc-ASGPR system will need to be identified for skeletal

and cardiac muscle-specific delivery. A cholesterol-conjugated siRNA platform for muscle delivery has been reported (47) and is a subject for future investigation for RNAi-mediated inhibition of *Gys1.* Unfortunately, there are no validated methodologies currently for cardiac muscle-specific delivery.

Gene Therapy vs RNAi Therapeutic Approaches

Gene therapy is widely regarded as the curative therapeutic approach for GSD patients. However, initial preclinical results using an adeno-associated virus (AAV) gene delivery approach showed limited correction of glycogen accumulation, hepatomegaly, steatosis, or HCA in GSD Ia mice expressing low levels of transduced G6Pase (48, 49). Development of a gene therapy approach for GSDs is practically limited by transduction efficiency, expression transience, and viral genome size restriction (50). In the case of GSD III, the human *AGL* cDNA is 5 kilobases in length, representing the upper possible limit for gene packaging and delivery in an AAV vector. In addition to viral genome size restrictions, limitations on transduction efficiency and stability of expression may further impact the ability of gene therapy approaches to reduce HCA and HCC by eliminating glycogen accumulation, hepatomegaly and steatosis over the improving and long life-span of GSD patients. In contrast to gene therapy, RNAi-mediated inhibition of glycogen synthesis has advantage to reach and correct nearly all hepatocytes of glycogen accumulation unvaryingly (Supporting Fig. S2G, H, Fig 4, 5) and the subsequent elimination of abnormal cell proliferation thoroughly. Although GYS-2 inhibition has no effect on correcting hypoglycemia, however, it has the potential to complement a gene therapy approach by ameliorating the cellular abnormalities associated with specific

For Peer Review

GSDs and provide therapeutic options to GSD patients with hepatic injury who currently have no therapeutic options.

In summary, our preclinical studies demonstrate that RNAi targeting of *GYS2* is a promising, effective, and safe potential therapeutic for GSD related liver damages.

Acknowledgements

We thank Doug Fambrough, Bart Wise, David Miller, Jennifer Lockridge and Jim Weissman for their review of this manuscript. We thank Geremew Desta for helping with animal care.

For Peer Review

References

1. Wolfsdorf JI, Weinstein DA. Glycogen storage diseases. Rev Endocr Metab Disord 2003;4:95-102.
2. Bachrach BE, Weinstein DA, Orho-Melander M, Burgess A, Wolfsdorf JI. Glycogen synthase deficiency (glycogen storage disease type 0) presenting with hyperglycemia and glucosuria: report of three new mutations. J Pediatr 2002;140:781-783.
3. Bali DS, Chen YT, Austin S, Goldstein JL: Glycogen Storage Disease Type I. In: Pagon RA, Adam MP, Ardinger HH, Wallace SE, Amemiya A, Bean LJH, et al., eds. GeneReviews(R). Seattle (WA), 1993.
4. Dagli A, Sentner CP, Weinstein DA: Glycogen Storage Disease Type III. In: Pagon RA, Adam MP, Ardinger HH, Wallace SE, Amemiya A, Bean LJH, et al., eds. GeneReviews(R). Seattle (WA), 1993.
5. Moses SW, Parvari R. The variable presentations of glycogen storage disease type IV: a review of clinical, enzymatic and molecular studies. Curr Mol Med 2002;2:177-188.
6. Dagli AI, Weinstein DA: Glycogen Storage Disease Type VI. In: Pagon RA, Adam MP, Ardinger HH, Wallace SE, Amemiya A, Bean LJH, et al., eds. GeneReviews(R). Seattle (WA), 1993.
7. Schimke RN, Zakheim RM, Corder RC, Hug G. Glycogen storage disease type IX: benign glycogenosis of liver and hepatic phosphorylase kinase deficiency. J Pediatr 1973;83:1031-1034.
8. Akman HO, Raghavan A, Craigen WJ. Animal models of glycogen storage disorders. Prog Mol Biol Transl Sci 2011;100:369-388.
9. Han HS, Kang G, Kim JS, Choi BH, Koo SH. Regulation of glucose metabolism from a liver-centric perspective. Exp Mol Med 2016;48:e218.
10. Adeva-Andany MM, Gonzalez-Lucan M, Donapetry-Garcia C, Fernandez-Fernandez C, Ameneiros-Rodriguez E. Glycogen metabolism in humans. BBA Clin 2016;5:85-100.
11. Chou JY, Mansfield BC. Mutations in the glucose-6-phosphatase-alpha (G6PC) gene that cause type Ia glycogen storage disease. Hum Mutat 2008;29:921-930.
12. Chou JY, Matern D, Mansfield BC, Chen YT. Type I glycogen storage diseases: disorders of the glucose-6-phosphatase complex. Curr Mol Med 2002;2:121-143.
13. Moses SW. Historical highlights and unsolved problems in glycogen storage disease type 1. Eur J Pediatr 2002;161 Suppl 1:S2-9.
14. Ozen H. Glycogen storage diseases: new perspectives. World J Gastroenterol 2007;13:2541-2553.
15. Mutel E, Gautier-Stein A, Abdul-Wahed A, Amigo-Correig M, Zitoun C, Stefanutti A, Houberdon I, et al. Control of blood glucose in the absence of hepatic glucose production during prolonged fasting in mice: induction of renal and intestinal gluconeogenesis by glucagon. Diabetes 2011;60:3121-3131.
16. Sever S, Weinstein DA, Wolfsdorf JI, Gedik R, Schaefer EJ. Glycogen storage disease type Ia: linkage of glucose, glycogen, lactic acid, triglyceride, and uric acid metabolism. J Clin Lipidol 2012;6:596-600.
17. Franco LM, Krishnamurthy V, Bali D, Weinstein DA, Arn P, Clary B, Boney A, et al. Hepatocellular carcinoma in glycogen storage disease type Ia: a case series. J Inherit Metab Dis 2005;28:153-162.
18. Wang DQ, Fiske LM, Carreras CT, Weinstein DA. Natural history of hepatocellular adenoma formation in glycogen storage disease type I. J Pediatr 2011;159:442-446.
19. Iguchi T, Yamagata M, Sonoda T, Yanagita K, Fukahori T, Tsujita E, Aishima S, et al. Malignant transformation of hepatocellular adenoma with bone marrow metaplasia arising in glycogen storage disease type I: A case report. Mol Clin Oncol 2016;5:599-603.
20. Cassiman D, Libbrecht L, Verslype C, Meersseman W, Troisi R, Zucman-Rossi J, Van Vlierberghe H. An adult male patient with multiple adenomas and a hepatocellular carcinoma: mild glycogen storage disease type Ia. J Hepatol 2010;53:213-217.

For Peer Review

21. Sentner CP, Hoogeveen IJ, Weinstein DA, Santer R, Murphy E, McKiernan PJ, Steuerwald U, et al. Glycogen storage disease type III: diagnosis, genotype, management, clinical course and outcome. J Inherit Metab Dis 2016;39:697-704.
22. Kishnani PS, Austin SL, Arn P, Bali DS, Boney A, Case LE, Chung WK, et al. Glycogen storage disease type III diagnosis and management guidelines. Genet Med 2010;12:446-463.
23. Shen JJ, Chen YT. Molecular characterization of glycogen storage disease type III. Curr Mol Med 2002;2:167-175.
24. Bernier AV, Sentner CP, Correia CE, Theriaque DW, Shuster JJ, Smit GP, Weinstein DA. Hyperlipidemia in glycogen storage disease type III: effect of age and metabolic control. J Inherit Metab Dis 2008;31:729-732.
25. Liu KM, Wu JY, Chen YT. Mouse model of glycogen storage disease type III. Mol Genet Metab 2014;111:467-476.
26. Pagliarani S, Lucchiari S, Ulzi G, Violano R, Ripolone M, Bordoni A, Nizzardo M, et al. Glycogen storage disease type III: A novel Agl knockout mouse model. Biochim Biophys Acta 2014;1842:2318-2328.
27. Haagsma EB, Smit GP, Niezen-Koning KE, Gouw AS, Meerman L, Slooff MJ. Type IIIb glycogen storage disease associated with end-stage cirrhosis and hepatocellular carcinoma. The Liver Transplant Group. Hepatology 1997;25:537-540.
28. Siciliano M, De Candia E, Ballarin S, Vecchio FM, Servidei S, Annese R, Landolfi R, et al. Hepatocellular carcinoma complicating liver cirrhosis in type IIIa glycogen storage disease. J Clin Gastroenterol 2000;31:80-82.
29. Demo E, Frush D, Gottfried M, Koepke J, Boney A, Bali D, Chen YT, et al. Glycogen storage disease type III-hepatocellular carcinoma a long-term complication? J Hepatol 2007;46:492-498.
30. Reddy SK, Kishnani PS, Sullivan JA, Koeberl DD, Desai DM, Skinner MA, Rice HE, et al. Resection of hepatocellular adenoma in patients with glycogen storage disease type Ia. J Hepatol 2007;47:658-663.
31. Kishnani PS, Chuang TP, Bali D, Koeberl D, Austin S, Weinstein DA, Murphy E, et al. Chromosomal and genetic alterations in human hepatocellular adenomas associated with type Ia glycogen storage disease. Hum Mol Genet 2009;18:4781-4790.
32. Beegle RD, Brown LM, Weinstein DA. Regression of hepatocellular adenomas with strict dietary therapy in patients with glycogen storage disease type I. JIMD Rep 2015;18:23-32.
33. Maheshwari A, Rankin R, Segev DL, Thuluvath PJ. Outcomes of liver transplantation for glycogen storage disease: a matched-control study and a review of literature. Clin Transplant 2012;26:432-436.
34. Boers SJ, Visser G, Smit PG, Fuchs SA. Liver transplantation in glycogen storage disease type I. Orphanet J Rare Dis 2014;9:47.
35. Koeberl DD, Kishnani PS, Bali D, Chen YT. Emerging therapies for glycogen storage disease type I. Trends Endocrinol Metab 2009;20:252-258.
36. Mutel E, Abdul-Wahed A, Ramamonjisoa N, Stefanutti A, Houberdon I, Cavassila S, Pilleul F, et al. Targeted deletion of liver glucose-6 phosphatase mimics glycogen storage disease type 1a including development of multiple adenomas. J Hepatol 2011;54:529-537.
37. Soggia AP, Correa-Giannella ML, Fortes MA, Luna AM, Pereira MA. A novel mutation in the glycogen synthase 2 gene in a child with glycogen storage disease type 0. BMC Med Genet 2010;11:3.
38. Nessa A, Kumaran A, Kirk R, Dalton A, Ismail D, Hussain K. Mutational analysis of the GYS2 gene in patients diagnosed with ketotic hypoglycaemia. J Pediatr Endocrinol Metab 2012;25:963-967.
39. Kasapkara CS, Aycan Z, Acoglu E, Senel S, Oguz MM, Ceylaner S. The variable clinical phenotype of three patients with hepatic glycogen synthase deficiency. J Pediatr Endocrinol Metab 2017.
40. Alshak NS, Cocjin J, Podesta L, van de Velde R, Makowka L, Rosenthal P, Geller SA. Hepatocellular adenoma in glycogen storage disease type IV. Arch Pathol Lab Med 1994;118:88-91.

For Peer Review

41. Roscher A, Patel J, Hewson S, Nagy L, Feigenbaum A, Kronick J, Raiman J, et al. The natural history of glycogen storage disease types VI and IX: Long-term outcome from the largest metabolic center in Canada. Mol Genet Metab 2014;113:171-176.
42. Li SC, Chen CM, Goldstein JL, Wu JY, Lemyre E, Burrow TA, Kang PB, et al. Glycogen storage disease type IV: novel mutations and molecular characterization of a heterogeneous disorder. J Inherit Metab Dis 2010;33 Suppl 3:S83-90.
43. Malfatti E, Barnerias C, Hedberg-Oldfors C, Gitiaux C, Benezit A, Oldfors A, Carlier RY, et al. A novel neuromuscular form of glycogen storage disease type IV with arthrogryposis, spinal stiffness and rare polyglucosan bodies in muscle. Neuromuscul Disord 2016;26:681-687.
44. Austin SL, Proia AD, Spencer-Manzon MJ, Butany J, Wechsler SB, Kishnani PS. Cardiac Pathology in Glycogen Storage Disease Type III. JIMD Rep 2012;6:65-72.
45. Mogahed EA, Girgis MY, Sobhy R, Elhabashy H, Abdelaziz OM, El-Karaksy H. Skeletal and cardiac muscle involvement in children with glycogen storage disease type III. Eur J Pediatr 2015;174:1545-1548.
46. Khan T, Weber H, DiMuzio J, Matter A, Dogdas B, Shah T, Thankappan A, et al. Silencing Myostatin Using Cholesterol-conjugated siRNAs Induces Muscle Growth. Mol Ther Nucleic Acids 2016;5:e342.
47. Koeberl DD, Pinto C, Sun B, Li S, Kozink DM, Benjamin DK, Jr., Demaster AK, et al. AAV vector-mediated reversal of hypoglycemia in canine and murine glycogen storage disease type Ia. Mol Ther 2008;16:665-672.
48. Lee YM, Kim GY, Pan CJ, Mansfield BC, Chou JY. Minimal hepatic glucose-6-phosphatase-alpha activity required to sustain survival and prevent hepatocellular adenoma formation in murine glycogen storage disease type Ia. Mol Genet Metab Rep 2015;3:28-32.
49. Sun B, Brooks ED, Koeberl DD. Preclinical Development of New Therapy for Glycogen Storage Diseases. Curr Gene Ther 2015;15:338-347.
50. Liu D, Li C, Chen Y, Burnett C, Liu XY, Downs S, Collins RD, et al. Nuclear import of proinflammatory transcription factors is required for massive liver apoptosis induced by bacterial lipopolysaccharide. J Biol Chem 2004;279:48434-48442.

For Peer Review

Figure Legends

Figure 1. **GYS2-1 treatment reduces *Gys2* mRNA, GYS2 protein expression, and glycogen synthesis in wild-type and GSD III, *Agl*$^{-/-}$ mice.** The lead *Gys2* siRNA conjugate, GYS2-1, was subcutaneously injected into wild-type and *Agl*$^{-/-}$ mice at a 10 mg/kg dose. Wild-type (WT) and *Agl*$^{-/-}$ mice were given 10 weekly doses of GYS2-1 starting at 4 weeks of age and sacrificed at 13 weeks of age after a 6-hour fast. In a second experiment, *Agl*$^{-/-}$ mice were given 18 weekly doses of GYS2-1 starting at 8 weeks of age and sacrificed at 26 weeks of age. Liver samples were collected 24 hours following the final dose. (A) GYS2-1 potently inhibits *Gys2* mRNA expression in both wild-type and *Agl*$^{-/-}$ mice. Compared with wild-type animals, *Agl*$^{-/-}$ mice have lower baseline levels of *Gys2* mRNA expression. (B and C) Western blot analysis shows that GYS2-1 inhibits GYS2 protein expression in both wild-type and *Agl*$^{-/-}$ mice. Compared with wild-type animals, *Agl*$^{-/-}$ mice also has lower GYS2 protein expression levels. (D and E) Measurement of glycogen in prepared liver extracts and in formalin-fixed tissue shows that GYS2-1 treatment reduces the accumulation of glycogen in both wild-type and *Agl*$^{-/-}$ mice. (F) Inhibition of GYS2 synthesis with GYS2-1 treatment effectively prevents hepatomegaly in *Agl*$^{-/-}$ mice.

Figure 2. **GYS2-1 treatment prevents hepatomegaly in GSD III, *Agl*$^{-/-}$ mice.**

GYS2-1, was subcutaneously injected into *Agl*$^{-/-}$ mice weekly at a 10 mg/kg dose starting at 4 or 8 weeks of age and sacrificed at 13 or 26 weeks of age respectively as indicated. Liver samples were collected 24 hours following the final dose. Inhibition of

For Peer Review

GYS2 synthesis with GYS2-1 treatment effectively prevents hepatomegaly in *Agl*$^{-/-}$ mice. Scale bar represents 1 centimeter (cm). WT, wildtype littermate.

Figure 3. **GYS2-1 treatment results in a normalization of liver pathology in a *Agl*$^{-/-}$ GSD III mouse model.** (A) *Agl*$^{-/-}$ mice treated with PBS or GYS2-1 weekly for 18 doses starting at 8 weeks of age. Histological analysis indicates that GYS2-1 is able to prevent the development of abnormal histopathology of *Agl*$^{-/-}$ mice. In GYS2-1 treated animals, H&E or PAS stained liver sections showed a reduction of vacuoles formed from over-accumulation of glycogen molecules. Increased Ki67 positive cells were observed in *Agl*$^{-/-}$ mice and were reduced with GYS2-1 treatment. Sirius red staining and IHC for α-smooth muscle actin (α-SMA) also indicate that GYS2-1 effectively reduces fibrosis of *Agl*$^{-/-}$ mice. Representative images of four individual animals from PBS or GYS2-1 treated groups are shown. Scale bar represents 100 μm. (B) Double staining of Ki67 (dark brown) and CYP3A4 (cytochrome P450 3A4, magenta) or a-SMA (magenta) indicate increased proliferation of both hepatocytes and non-hepatocytes in livers of *Agl*$^{-/-}$ mice. (C) *Agl*$^{-/-}$ mice have elevated liver enzymes that are normalized by treatment with GYS2-1.

Figure 4. **GYS2-1 treatment prevents nodule development in the *Agl*$^{-/-}$ GSD III mouse model.** *Agl*$^{-/-}$ mice were treated with PBS or GYS2-1 monthly for 12 doses starting at one month of age. Liver samples were collected 72 hours following the final dose. (A) Histological analysis indicates that GYS2-1 is able to prevent the development of hepatic nodules in *Agl*$^{-/-}$ mice. Scale bar represents 100 μm. Each liver image shows a representative section from an individual animal. Higher magnification images of

For Peer Review

sections of the nodules are show in (B). Scale bar represents 500 or 100 mm in the upper or lower panel, respectively.

Figure 5. **GYS2-1 treatment prevents fibrosis in the *Agl*$^{-/-}$ GSD III mouse model.** *Agl*$^{-/-}$ mice were treated with PBS or GYS2-1 monthly for 12 doses starting at 1 month of age. Liver samples were collected 72 hours following the final dose and analyzed for collagen deposition using Sirius Red staining. Inhibition of GYS2 levels with GYS2-1 treatment effectively prevents fibrosis in *Agl*$^{-/-}$ mice. Lower panel represents higher magnification of images in upper panel. Representative images of individual animals from PBS or GYS2-1 treated groups are shown. Scale bar represents 1 mm or 200 micrometers (μm) in the upper or lower panel, respectively.

Figure 6. **Inhibition of *Gys2* mRNA expression reduces glycogen accumulation and restores normal liver morphology in a L-*G6pc*$^{-/-}$ GSD Ia mouse model.** L-G6pc$^{-/-}$ mice were dosed intravenously with PBS or GYS2-2 (Gys2 siRNA formulated in lipid nanoparticle) weekly for 5 weeks. Liver samples were collected 48 hours following the final dose. (A) GYS2-2 treatment potently inhibits Gys2 mRNA expression in L-G6pc$^{-/-}$ mice. (B) Measurement of glycogen content in liver extracts indicates that GYS2-2 treatment reduces the accumulation of glycogen in L-G6pc$^{-/-}$ mice. (C) GYS2-2 treatment causes a reduction of liver glucose-6-phosphate levels. (D) Histological analysis indicates that GYS2-2 treatment is able to prevent the development of abnormal histopathology of L-G6pc$^{-/-}$ mice. GYS2-2 treated mice show a reduction in

For Peer Review

vacuoles in H&E-stained liver sections. Reduced fat deposition and a reduction in the number of Ki67 positive cells were observed in L-G6pc$^{-/-}$ mice treated with GYS2-2. Representative images of three individual animals from PBS or GYS2-2 treated groups are shown. Scale bar represents 100 μm.

Figure 7. **Inhibition of *Gys2* mRNA expression reduces liver toxicities in a L-*G6pc*$^{-/-}$ GSD Ia mouse model.**

L-G6pc$^{-/-}$ mice were dosed intravenously with PBS or GYS2-2 (Gys2 siRNA formulated in lipid nanoparticle) weekly for 5 weeks. Liver and blood samples were collected 48 hours following the final dose. (A) Measurement of Caspase-3/7 activity in liver extracts indicates that GYS2-2 treatment reduces apoptosis in L-G6pc$^{-/-}$ mice. (B) GYS2-2 treatment reduces serum markers of liver damage in L-G6pc$^{-/-}$ mice.

For Peer Review

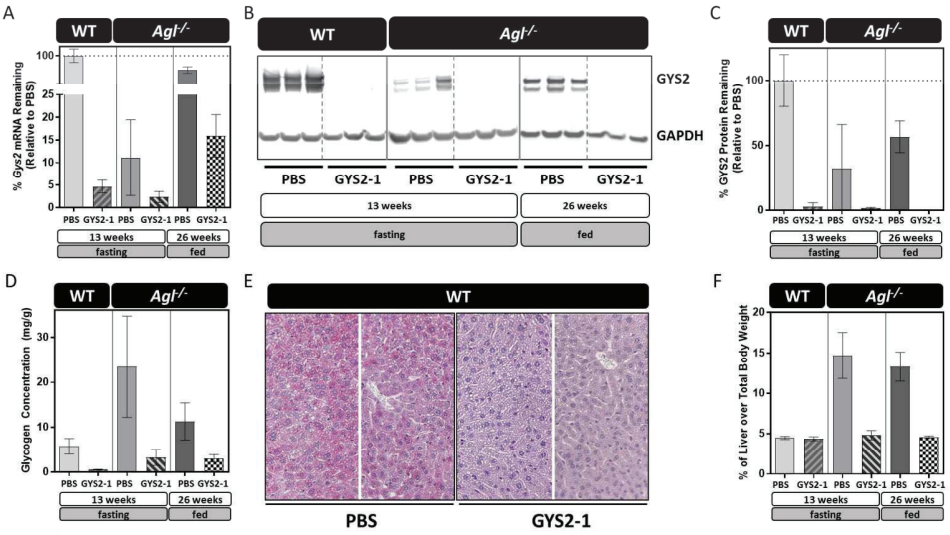

304x171mm (300 x 300 DPI)

er Review



101x30mm (300 x 300 DPI)

For Peer Review

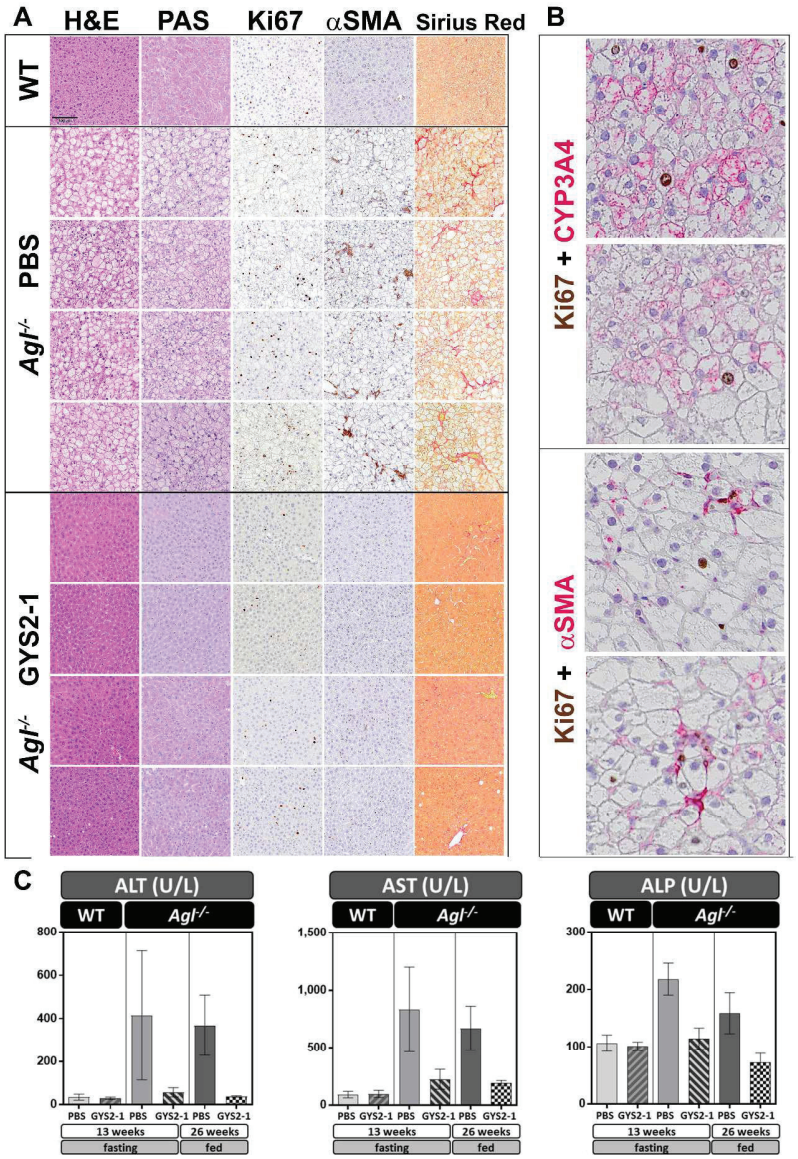

378x555mm (300 x 300 DPI)

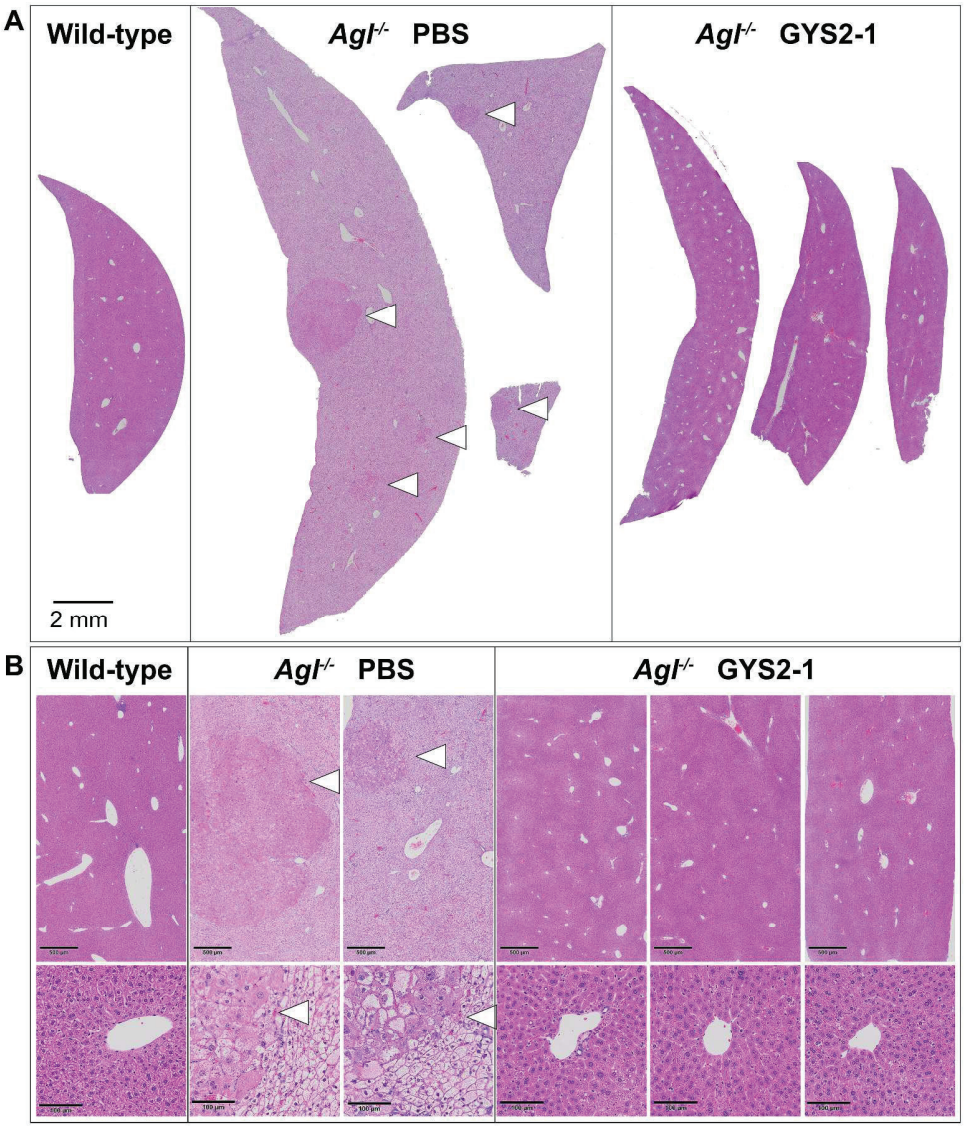

441x514mm (300 x 300 DPI)

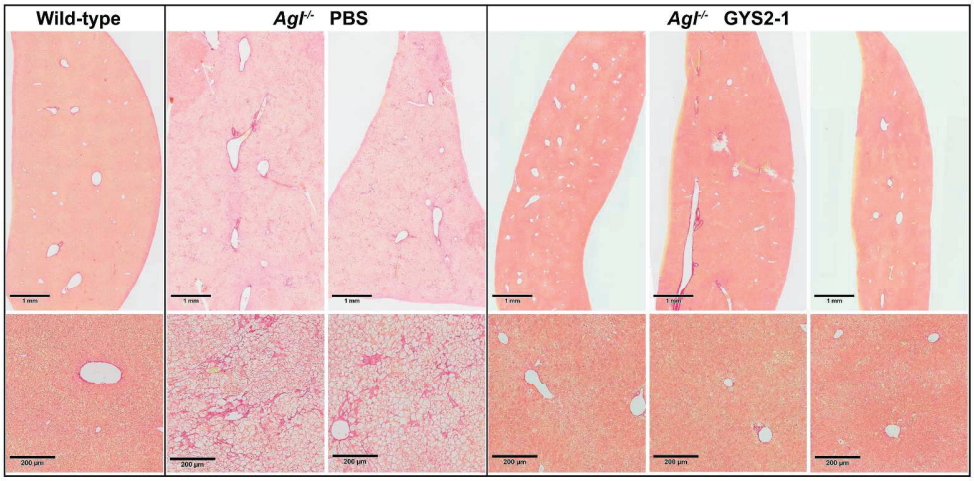

262x129mm (300 x 300 DPI)

eer Review

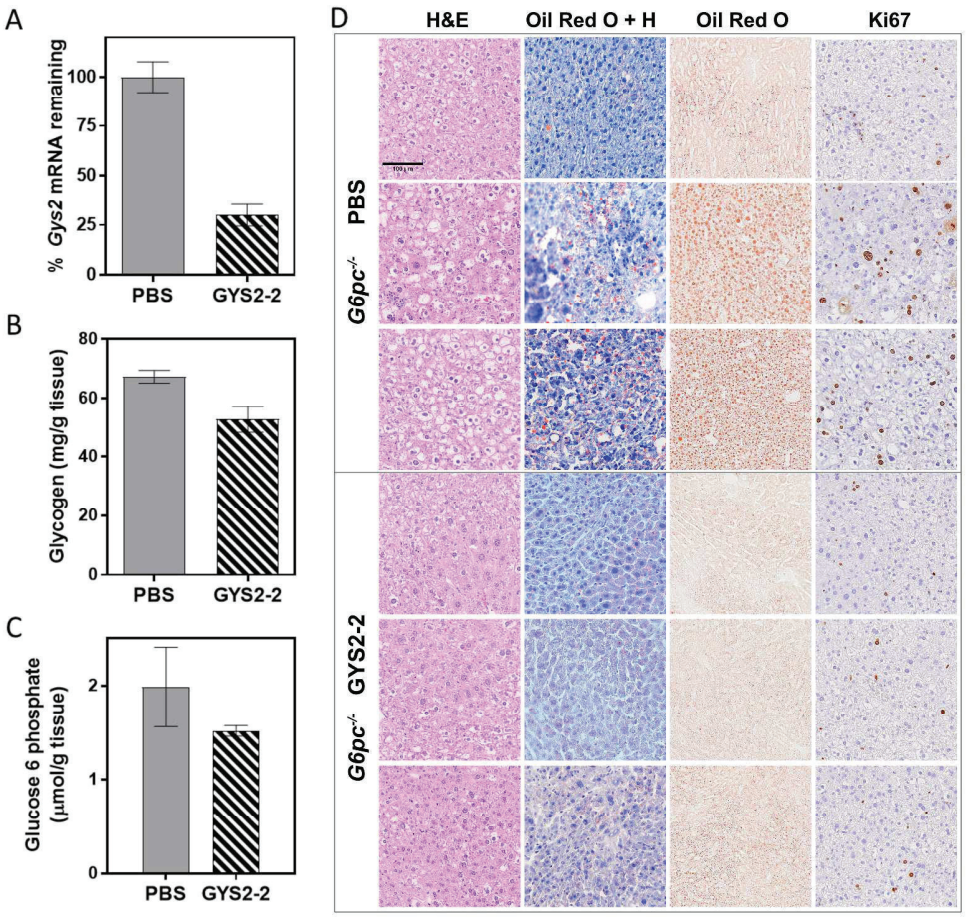

291x276mm (300 x 300 DPI)

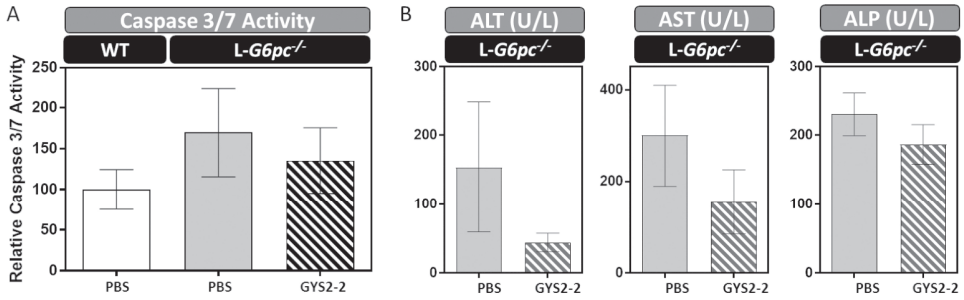

266x83mm (300 x 300 DPI)

For Peer Review

Supporting Information

Inhibition of Glycogen Synthase II with RNA Interference Prevents Liver Injury in Mouse Models of Glycogen Storage Disease Type Ia and III

Natalie Pursell[1], Jessica Gierut[1], Luciano Apponi[1], Wei Zhou[1], Michael Dills[1], Rohan Diwanji[1], Monika Gjorgjieva[2], Utsav Saxena[1], Jr-Shiuan Yang[1], Anee Shah[1], Nandini Venkat[1], Rachel Storr[1], Boyoung Kim[1], Juili Shelke[1], Naim Nazef[1], Weimin Wang[1], Marc Abrams[1], Margaux Raffin[2], Gilles Mithieux[2], Fabienne Rajas[2], Henryk Dudek[1], Bob D. Brown[1] and Chengjung Lai[1]

Supporting Figures S1 to S11

For Peer Review

Supplementary Figure Legends

Supplementary Figure S1. Glycogenesis and Glycogenolysis Pathways.

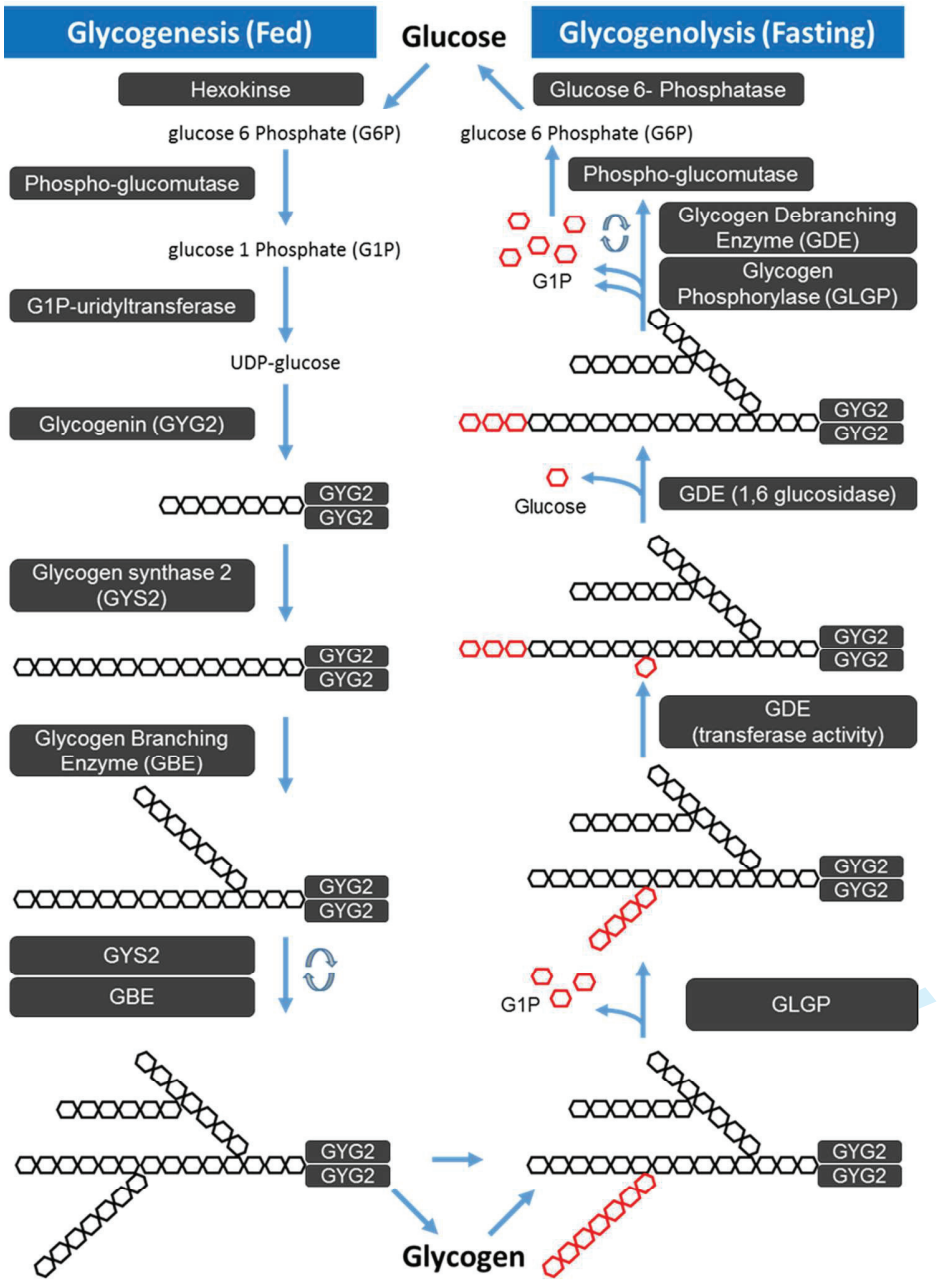

Supplementary Figure S2. Identification of lead *Gys2* siRNAs.

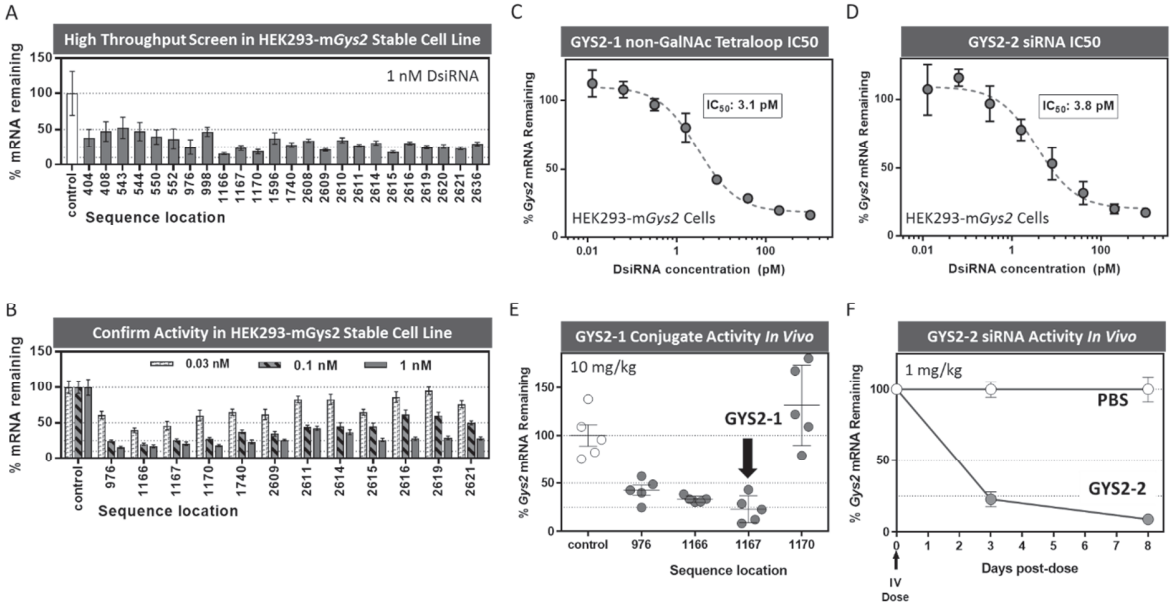

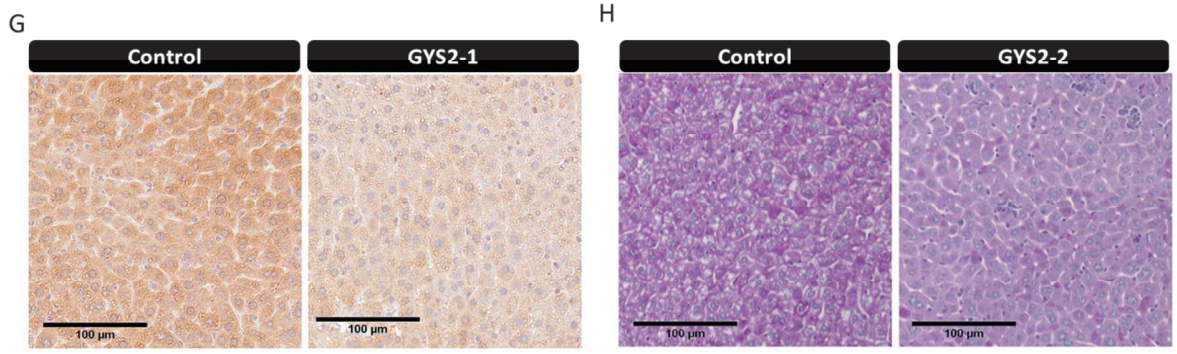

(A) Results from high-throughput screen of *Gys2* siRNA sequences in HEK293 cells stably expressing mouse *Gys2* mRNA (HEK293-mGys2) identifies potent sequences. (B) Activity of best siRNA sequences was confirmed in HEK293-mGys2 with a three-point dose-response. (C) *Gys2*-1167 sequences was converted into a tetraloop conjugate (no GalNAc sugar residues) and its IC50 determined in HEK293-mGys2 cells. (D) *Gys2*-1166 was selected as GYS2-2 and its IC50 measured in HEK293-mGys2 cells. (E) GalNAc sugar residues were added to GYS2-1 and other *Gys2* siRNA

sequences for confirmation of potency *in vivo*. Wild-type mice were given a single, subcutaneous 10 mg/kg dose and sacrificed three days later. RNA was prepared from terminal liver samples and *Gys2* mRNA inhibition measured by RT-PCR. GYS2-1 shows approximately 75% reduction in *Gys2* mRNA. (F) GYS2-2 siRNA was formulated in lipid nanoparticle and intravenously injected into mice at 1 mg/kg. Mice were sacrificed three or eight days post-dose for RNA preparation and *Gys2* mRNA measurement by RT-PCR. (G) The results of immunohistochemistry indicate GYS2-1 reduces GYS protein expression in nearly all hepatocytes. (H) The results of PAS staining indicate GYS2-2 reduces glycogen accumulation in nearly all hepatocytes.

For Peer Review

Supplementary Figure S3. *Gys2* mRNA Knockdown Prevents Abnormal Glycogen Accumulation and Hepatic Abnormalities in the *Agl*$^{-/-}$ GSD III mouse model.

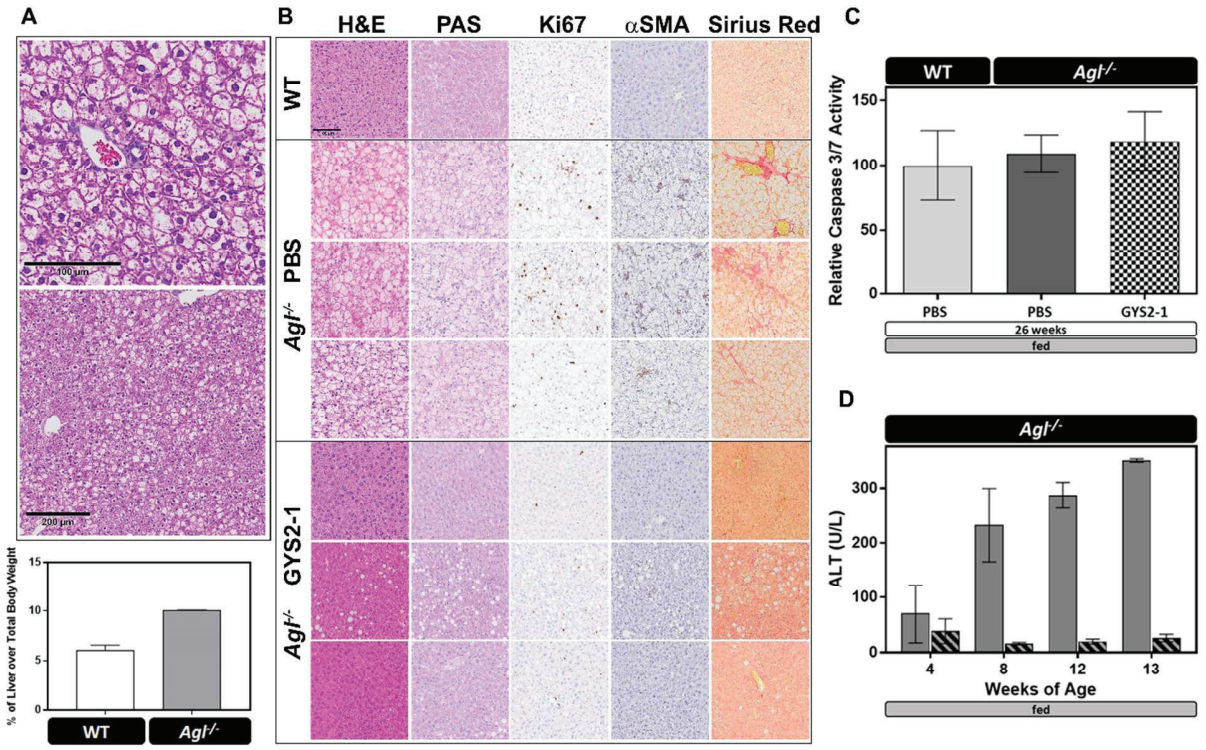

(A) *Agl*$^{-/-}$ mice develop hepatomegaly with abnormal histomorphology by four weeks of age. (B) *Agl*$^{-/-}$ mice treated with PBS or GYS2-1 for 10 doses starting at 4 weeks of age. Histological analysis indicates that GYS2-1 is able to prevent the development of abnormal histopathology of *Agl*$^{-/-}$ mice. In GYS2-1 treated animals, H&E or PAS stained liver sections showed a reduction of vacuoles formed from over-accumulation of glycogen molecules. Increased Ki67 positive cells were observed in *Agl*$^{-/-}$ mice and were reduced with GYS2-1 treatment. Sirius red staining and IHC for α-SMA also indicate that GYS2-1 effectively reduces fibrosis of *Agl*$^{-/-}$ mice. Representative images of three individual animals from PBS or GYS2-2 treated groups are shown. Scale bar represents 100 μm. (C) Measurement of Caspase-3/7 activity in mouse liver extracts does not

show an elevation of the activity of apoptotic Caspases 3 and 7. (D) *Agl*$^{-/-}$ mice show increasing signs of liver damage with increasing age measured by quantification of blood ALT levels which is prevented by GYS2-1 treatment.

For Peer Review

Supplementary Figure S4. GYS2-1 treatment prevents hepatomegaly in GSD III, *Agl*$^{-/-}$ mice.

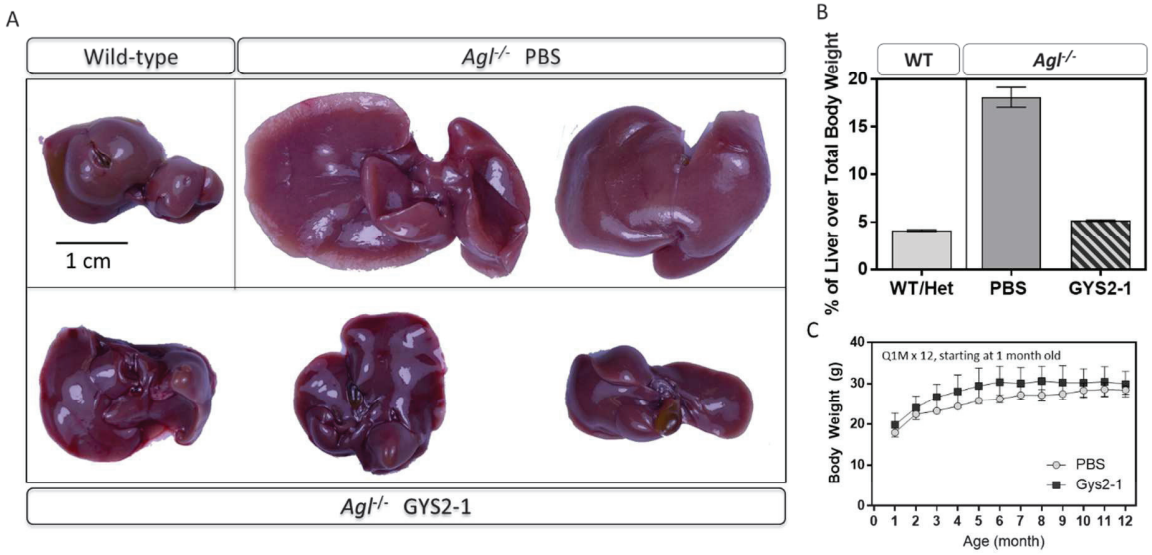

Agl$^{-/-}$ mice were treated with PBS or GYS2-1 monthly for 12 doses starting at 1 month of age. Liver samples were collected 72 hours following the final dose. (A and B) Inhibition of GYS2 synthesis with GYS2-1 treatment effectively prevents hepatomegaly in *Agl*$^{-/-}$ mice. Scale bar represents 1 cm. (C) GYS2-1 treatment has no effects on growth rate of *Agl*$^{-/-}$ mice.

Peer Review

Supplementary Figure S5. GYS2-1 treatment prevents liver toxicity in GSD III, *Agl*$^{-/-}$ mice.

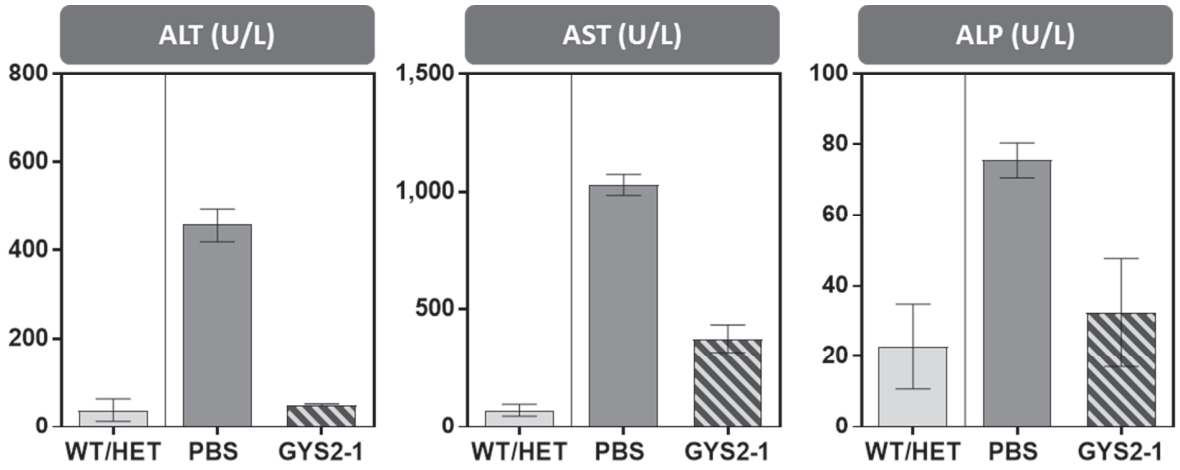

Agl$^{-/-}$ mice were treated with PBS or GYS2-1 monthly for 12 doses starting at 1 month of age. Blood samples were collected 72 hours following the final dose and analyze for circulating transaminases and alkaline phosphatase. Inhibition of GYS2 synthesis with GYS2-1 treatment effectively prevents liver toxicity of *Agl*$^{-/-}$ mice.

For Peer Review

Supplementary Figure S6. Histopathology analysis of growing nodule in *Agl*$^{-/-}$ mice.

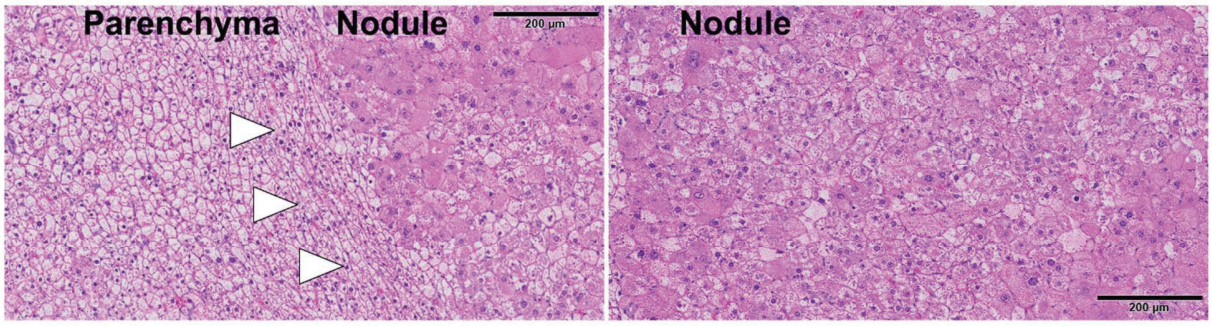

Agl$^{-/-}$ mice were treated with PBS or GYS2-1 monthly for 12 doses starting at 1 month of age. Liver samples were collected 72 hours following the final dose for H&E staining. Junction of parenchyma and nodule were indicated (arrowheads). Scale bar represents 200 μm.

For Peer Review

Supplementary Figure S7. GYS2-1 reduces outspread and sustained abnormal hepatocellular proliferation of *Agl*$^{-/-}$ mice.

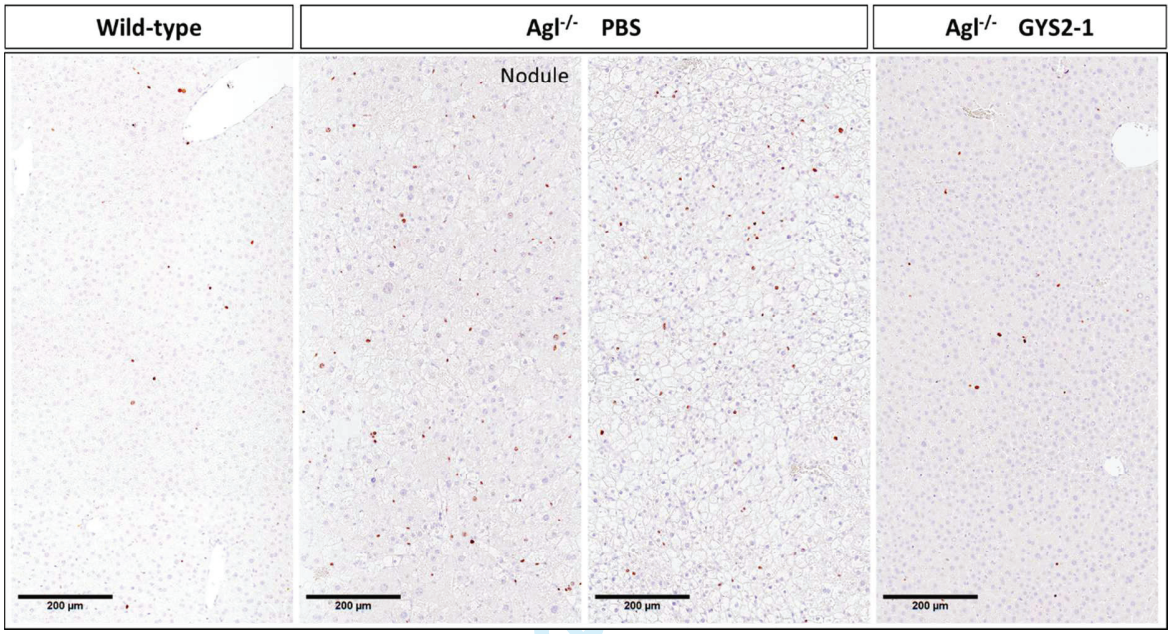

Agl$^{-/-}$ mice were treated with PBS or GYS2-1 monthly for 12 doses starting at 1 month of age. Liver samples were collected 72 hours following the final dose and analyzed for cellular proliferation using IHC for Ki67. Inhibition of GYS2 synthesis with GYS2-1 treatment effectively prevents hepatocellular proliferation in *Agl*$^{-/-}$ mice. Representative images of individual animals are shown. Scale bar represents 200 µm.

For Peer Review

Supplementary Figure S8. No nuclear β-catenin staining were noted of growing nodules in *Agl*$^{-/-}$ mice.

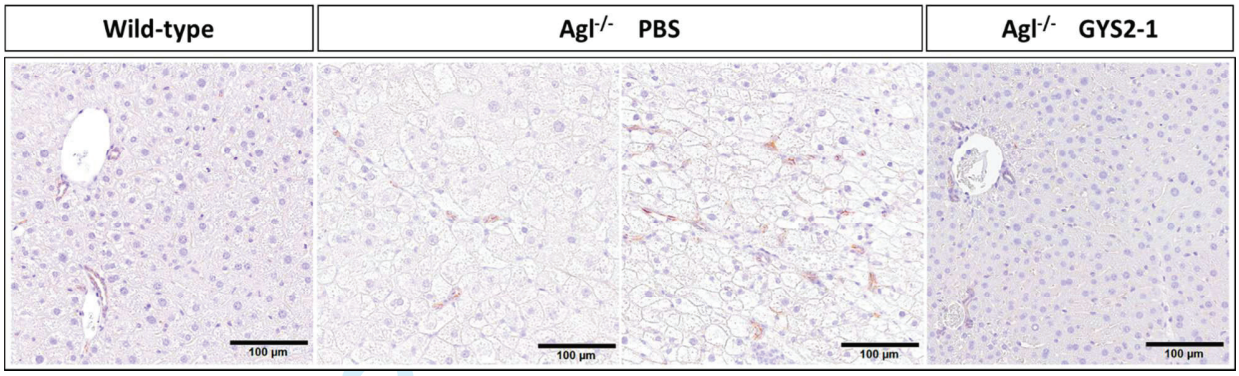

Agl$^{-/-}$ mice were treated with PBS or GYS2-1 monthly for 12 doses starting at 1 month of age. Liver samples were collected 72 hours following the final dose for β-catenin IHC. No nuclear β-catenin staining was noted in the nodules of PBS-treated *Agl*$^{-/-}$ mice.

For Peer Review

Supplementary Figure S9. Correction of liver pathology thoroughly with GYS2-1 treatment in *Agl*$^{-/-}$ mice

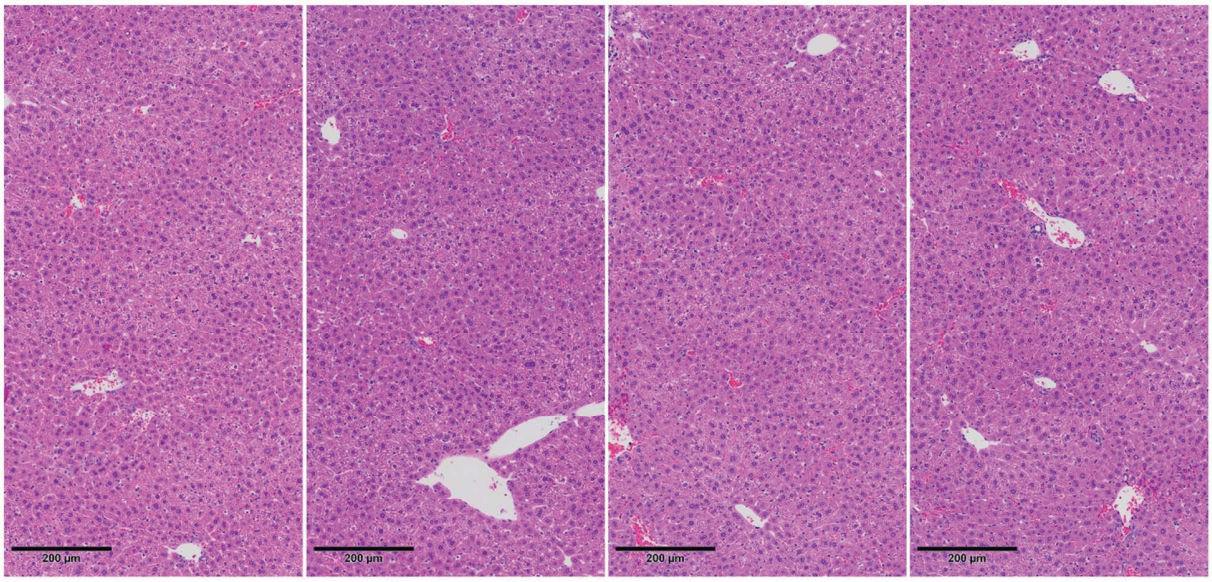

Agl$^{-/-}$ mice were treated with GYS2-1 monthly for 12 doses starting at 1 month of age. Liver samples were collected 72 hours following the final dose for histological analysis. H&E stained sections from four levels throughout the collected tissue sample are shown. The results demonstrate that GYS2-1 treatment fully reverses the liver pathology throughout the entire liver of *Agl*$^{-/-}$ mice until they are indistinguishable from their wildtype littermates.

Peer Review

Supplementary Figure S10. RNAi-mediated reduction of *Gys2* has no adverse effect on glycemia, metaoblism, lipidemia, or body weight in mouse models of GSD Ia and GSD III.

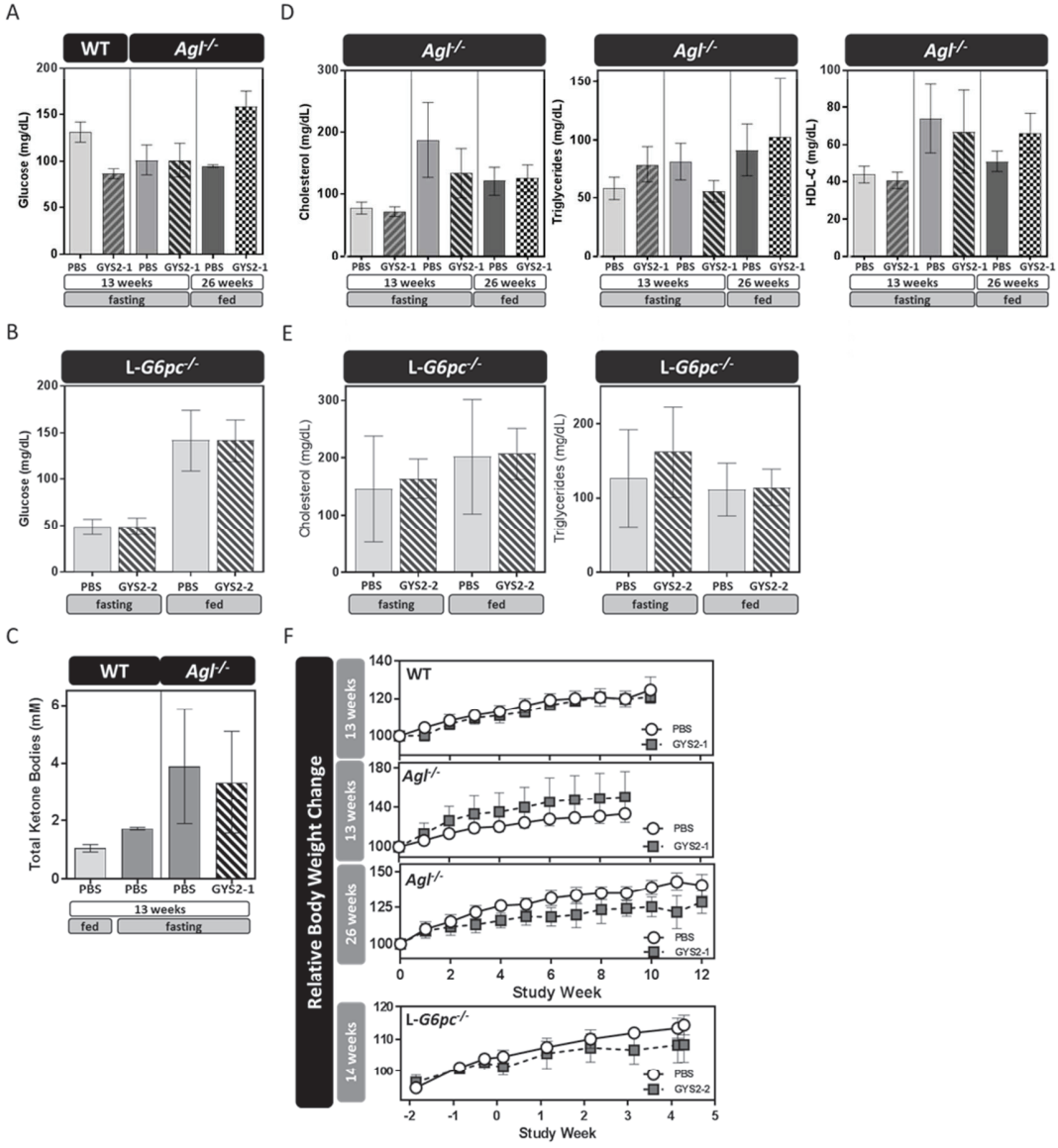

Liver-specific *Gys2* inhibition does not affect in glycemia in mouse models of (A) GSD III or (B) GSD Ia. (C) Increased levels of ketone bodies were measured in blood of *Agl*$^{-/-}$ mice during fasting indicating an increase in gluconeogenesis in the GSD III mouse

model. GYS2-1 treatment had no effect on ketone body levels suggesting *Gys2* inhibition will not affect gluconeogenesis. Reduction of *Gys2* mRNA expression in the liver had no adverse effects on lipidemia in GSD III (D) or GSD Ia (E) mice. (F) GYS2-1 and GYS2-2 treatment did not affect body weight of GSD III or GSD 1a mice, respectively.

For Peer Review

Supplementary Figure S11. GYS2-1 treatment does not reduce glycogen accumulation in skeletal muscle measured by PAS staining of formalin-fixed muscle tissue.

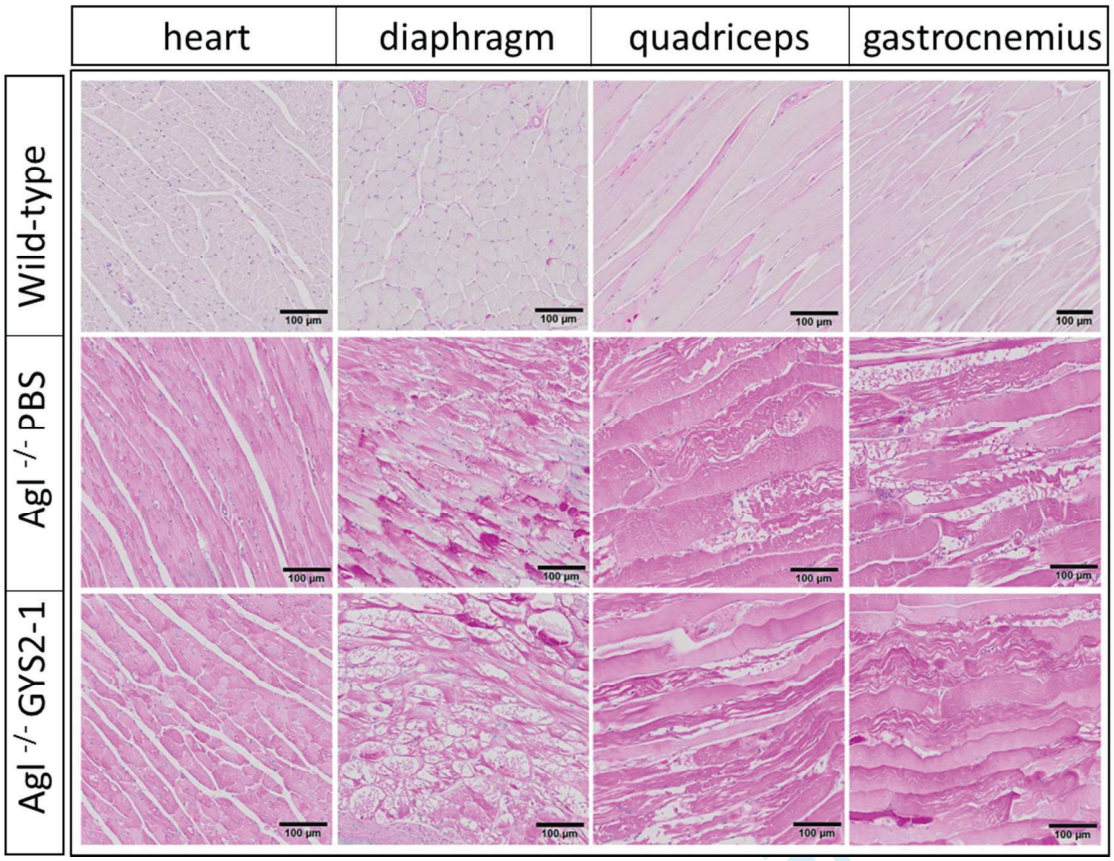

GalNAc-mediated delivery of siRNA conjugates mediated through the ASGPR receptor is liver-specific and GYS2-1 treatment has no effect on cardiac or skeletal muscle.

REFERENCES

Abdul-Wahed, A., Gautier-Stein, A., Casteras, S., Soty, M., Roussel, D., Romestaing, C., Guillou, H., Tourette, J.-A., Pleche, N., Zitoun, C., et al. (2014). A link between hepatic glucose production and peripheral energy metabolism via hepatokines. Mol. Metab. *3*, 531–543.

Abdul-Wahed, A., Guilmeau, S., and Postic, C. (2017). Sweet Sixteenth for ChREBP: Established Roles and Future Goals. Cell Metab. *26*, 324–341.

Adeva-Andany, M.M., González-Lucán, M., Donapetry-García, C., Fernández-Fernández, C., and Ameneiros-Rodríguez, E. (2016). Glycogen metabolism in humans. BBA Clin. *5*, 85–100.

Ahmed, S.S., Li, J., Godwin, J., Gao, G., and Zhong, L. (2013). Gene transfer in the liver using recombinant adeno-associated virus. Curr. Protoc. Microbiol. *Chapter 14*, Unit14D.6.

Aiston, S., Coghlan, M.P., and Agius, L. (2003). Inactivation of phosphorylase is a major component of the mechanism by which insulin stimulates hepatic glycogen synthesis. Eur. J. Biochem. *270*, 2773–2781.

Alkhouri, N., Dixon, L.J., and Feldstein, A.E. (2009). Lipotoxicity in Nonalcoholic Fatty Liver Disease: Not All Lipids Are Created Equal. Expert Rev. Gastroenterol. Hepatol. *3*, 445–451.

Annabi, B., Hiraiwa, H., Mansfield, B.C., Lei, K.J., Ubagai, T., Polymeropoulos, M.H., Moses, S.W., Parvari, R., Hershkovitz, E., Mandel, H., et al. (1998). The gene for glycogen-storage disease type 1b maps to chromosome 11q23. Am. J. Hum. Genet. *62*, 400–405.

Arden, S.D., Zahn, T., Steegers, S., Webb, S., Bergman, B., O'Brien, R.M., and Hutton, J.C. (1999). Molecular cloning of a pancreatic islet-specific glucose-6-phosphatase catalytic subunit-related protein. Diabetes *48*, 531–542.

Baenke, F., Peck, B., Miess, H., and Schulze, A. (2013). Hooked on fat: the role of lipid synthesis in cancer metabolism and tumour development. Dis. Model. Mech. *6*, 1353–1363.

Baffy, G. (2013). Hepatocellular Carcinoma in Non-alcoholic Fatty Liver Disease: Epidemiology, Pathogenesis, and Prevention. J. Clin. Transl. Hepatol. *1*, 131–137.

Baffy, G., Brunt, E.M., and Caldwell, S.H. (2012). Hepatocellular carcinoma in non-alcoholic fatty liver disease: an emerging menace. J. Hepatol. *56*, 1384–1391.

Baker, L., Dahlem, S., Goldfarb, S., Kern, E.F.O., Stanley, C.A., Egler, J., Olshan, J.S., and Heyman, S. (1989). Hyperfiltration and renal disease in glycogen storage disease, type I. Kidney Int. *35*, 1345–1350.

Balfour, J.A., McTavish, D., and Heel, R.C. (1990). Fenofibrate. A review of its pharmacodynamic and pharmacokinetic properties and therapeutic use in dyslipidaemia. Drugs *40*, 260–290.

Bandsma, R.H.J., Prinsen, B.H., de Sain-van der Velden, M., Rake, J.-P., Boer, T., Smit, G.P.A., Reijngoud, D.-J., and Kuipers, F. (2008). Increased de novo Lipogenesis and Delayed Conversion of Large VLDL into Intermediate Density Lipoprotein Particles Contribute to Hyperlipidemia in Glycogen Storage Disease Type 1a. Pediatr. Res. *63*, 702–707.

Bandsma, R.H.J., Smit, G.P.A., and Kuipers, F. (2014). Disturbed lipid metabolism in glycogen storage disease type 1. Eur. J. Pediatr. *161*, S65–S69.

Banka, S., and Newman, W.G. (2013). A clinical and molecular review of ubiquitous glucose-6-phosphatase deficiency caused by G6PC3mutations. Orphanet J. Rare Dis. *8*, 84.

Basseri, S., and Austin, R.C. (2011). Endoplasmic Reticulum Stress and Lipid Metabolism: Mechanisms and Therapeutic Potential. Biochem. Res. Int. *2012*, e841362.

Beegle, R.D., Brown, L.M., and Weinstein, D.A. (2014). Regression of Hepatocellular Adenomas with Strict Dietary Therapy in Patients with Glycogen Storage Disease Type I. JIMD Rep. *18*, 23–32.

Belingheri, M., Ghio, L., Sala, A., Menni, F., Trespidi, L., Ferraresso, M., Berardinelli, L., Rossi, G., Edefonti, A., and Parini, R. (2007). Combined liver-kidney transplantation in glycogen storage disease Ia: a case beyond the guidelines. Liver Transplant. Off. Publ. Am. Assoc. Study Liver Dis. Int. Liver Transplant. Soc. *13*, 762–764.

Bianchi, L. (1993). Glycogen storage disease I and hepatocellular tumours. Eur. J. Pediatr. *152 Suppl 1*, S63-70.

Bioulac-Sage, P., Taouji, S., Possenti, L., and Balabaud, C. (2012). Hepatocellular adenoma subtypes: the impact of overweight and obesity. Liver Int. *32*, 1217–1221.

Boers, S.J., Visser, G., Smit, P.G., and Fuchs, S.A. (2014). Liver transplantation in glycogen storage disease type I. Orphanet J. Rare Dis. *9*, 47.

Bollen, M., Keppens, S., and Stalmans, W. (1998). Specific features of glycogen metabolism in the liver. Biochem. J. *336*, 19–31.

Bonsib, S.M. (2009). Renal Cystic Diseases and Renal Neoplasms: A Mini-Review. Clin. J. Am. Soc. Nephrol. *4*, 1998–2007.

Boztug, K., Appaswamy, G., Ashikov, A., Schäffer, A.A., Salzer, U., Diestelhorst, J., Germeshausen, M., Brandes, G., Lee-Gossler, J., Noyan, F., et al. (2009). A Syndrome with Congenital Neutropenia and Mutations in G6PC3. N. Engl. J. Med. *360*, 32–43.

Brooks, E.D., Little, D., Arumugam, R., Sun, B., Curtis, S., Demaster, A., Maranzano, M., Jackson, M.W., Kishnani, P., Freemark, M.S., et al. (2013). Pathogenesis of growth failure and partial reversal with gene therapy in murine and canine Glycogen Storage Disease type Ia. Mol. Genet. Metab. *109*, 161–170.

Brown, B.D., Cantore, A., Annoni, A., Sergi, L.S., Lombardo, A., Della Valle, P., D'Angelo, A., and Naldini, L. (2007). A microRNA-regulated lentiviral vector mediates stable correction of hemophilia B mice. Blood *110*, 4144–4152.

Bruni, N., Rajas, F., Montano, S., Chevalier-Porst, F., Maire, I., and Mithieux, G. (1999). Enzymatic characterization of four new mutations in the glucose-6 phosphatase (G6PC) gene which cause glycogen storage disease type 1a. Ann. Hum. Genet. *63*, 141–146.

Bunchorntavakul, C., Bahirwani, R., Drazek, D., Soulen, M.C., Siegelman, E.S., Furth, E.E., Olthoff, K., Shaked, A., and Reddy, K.R. (2011). Clinical features and natural history of hepatocellular adenomas: the impact of obesity. Aliment. Pharmacol. Ther. *34*, 664–674.

Calderaro, J., Labrune, P., Morcrette, G., Rebouissou, S., Franco, D., Prévot, S., Quaglia, A., Bedossa, P., Libbrecht, L., Terracciano, L., et al. (2013). Molecular characterization of hepatocellular adenomas developed in patients with glycogen storage disease type I. J. Hepatol. *58*, 350–357.

Calzadilla Bertot, L., and Adams, L.A. (2016). The Natural Course of Non-Alcoholic Fatty Liver Disease. Int. J. Mol. Sci. *1* (5). pii: E7747.

Cha, C., and DeMatteo, R.P. (2005). Molecular mechanisms in hepatocellular carcinoma development. Best Pract. Res. Clin. Gastroenterol. *19*, 25–37.

Chen, Y.T. (1991). Type I glycogen storage disease: kidney involvement, pathogenesis and its treatment. Pediatr. Nephrol. Berl. Ger. *5*, 71–76.

Chen, L.-Y., Shieh, J.-J., Lin, B., Pan, C.-J., Gao, J.-L., Murphy, P.M., Roe, T.F., Moses, S., Ward, J.M., Lee, E.J., et al. (2003). Impaired glucose homeostasis, neutrophil trafficking and function in mice lacking the glucose-6-phosphate transporter. Hum. Mol. Genet. *12*, 2547–2558.

Chen, Y.-T., Scheinman, J.I., Park, H.K., Coleman, R.A., and Roe, C.R. (1990). Amelioration of Proximal Renal Tubular Dysfunction in Type I Glycogen Storage Disease with Dietary Therapy. N. Engl. J. Med. *323*, 590–593.

Chen, Y.T., Bazzarre, C.H., Lee, M.M., Sidbury, J.B., and Coleman, R.A. (1993). Type I glycogen storage disease: nine years of management with cornstarch. Eur. J. Pediatr. *152 Suppl 1*, S56-59.

Chen, Z., Trotman, L.C., Shaffer, D., Lin, H.-K., Dotan, Z.A., Niki, M., Koutcher, J.A., Scher, H.I., Ludwig, T., Gerald, W., et al. (2005). Crucial role of p53-dependent cellular senescence in suppression of Pten-deficient tumorigenesis. Nature *436*, 725–730.

Cho, J.-H., Kim, G.-Y., Pan, C.-J., Anduaga, J., Choi, E.-J., Mansfield, B.C., and Chou, J.Y. (2017). Downregulation of SIRT1 signaling underlies hepatic autophagy impairment in glycogen storage disease type Ia. PLOS Genet. *13*, e1006819.

Chou, J.Y., and Mansfield, B.C. (2008). Mutations in the Glucose-6-Phosphatase-α (G6PC) Gene that Cause Type Ia Glycogen Storage Disease. Hum. Mutat. *29*, 921–930.

Chou, J.Y., Jun, H.S., and Mansfield, B.C. (2010a). Glycogen storage disease type I and G6Pase-β deficiency: etiology and therapy. Nat. Rev. Endocrinol. *6*, 676–688.

Chou, J.Y., Jun, H.S., and Mansfield, B.C. (2010b). Neutropenia in type Ib glycogen storage disease. Curr. Opin. Hematol. *17*, 36–42.

Chou, S.-T., Leng, Q., and Mixson, A.J. (2012). Zinc Finger Nucleases: Tailor-made for Gene Therapy. Drugs Future *37*, 183–196.

Clar, J., Gri, B., Calderaro, J., Birling, M.-C., Hérault, Y., Smit, G.P.A., Mithieux, G., and Rajas, F. (2014). Targeted deletion of kidney glucose-6 phosphatase leads to nephropathy. Kidney Int., 86, 747-756.

Clar, J., Mutel, E., Gri, B., Creneguy, A., Stefanutti, A., Gaillard, S., Ferry, N., Beuf, O., Mithieux, G., Nguyen, T.H., et al. (2015). Hepatic lentiviral gene transfer prevents the long-term onset of hepatic tumours of glycogen storage disease type 1a in mice. Hum. Mol. Genet. *24*, 2287–2296.

Cohen, J.L., Vinik, A., Faller, J., and Fox, I.H. (1985). Hyperuricemia in glycogen storage disease type I. Contributions by hypoglycemia and hyperglucagonemia to increased urate production. J. Clin. Invest. *75*, 251–257.

Cook, W.D., and McCaw, B.J. (2000). Accommodating haploinsufficient tumor suppressor genes in Knudson's model. Oncogene *19*, 3434–3438.

Cooper, M.E. (2004). The role of the renin-angiotensin-aldosterone system in diabetes and its vascular complications. Am. J. Hypertens. *17*, S16–S20.

Cori, G.T., and Cori, C.F. (1952). Glucose-6-Phosphatase of the Liver in Glycogen Storage Disease. J. Biol. Chem. *199*, 661–667.

Cox, M.L., and Meek, D.W. (2010). Phosphorylation of serine 392 in p53 is a common and integral event during p53 induction by diverse stimuli. Cell. Signal. *22*, 564–571.

Cox, D.B.T., Platt, R.J., and Zhang, F. (2015). Therapeutic Genome Editing: Prospects and Challenges. Nat. Med. *21*, 121–131.

Croset, M., Rajas, F., Zitoun, C., Hurot, J.M., Montano, S., and Mithieux, G. (2001). Rat small intestine is an insulin-sensitive gluconeogenic organ. Diabetes *50*, 740–746.

Dall'Armi, C., Devereaux, K.A., and Di Paolo, G. (2013). The role of lipids in the control of autophagy. Curr. Biol. CB *23*, R33-45.

Demaster, A., Luo, X., Curtis, S., Williams, K.D., Landau, D.J., Drake, E.J., Kozink, D.M., Bird, A., Crane, B., Sun, F., et al. (2012). Long-Term Efficacy Following Readministration of an Adeno-Associated Virus Vector in Dogs with Glycogen Storage Disease Type Ia. Hum. Gene Ther. *23*, 407-418.

Demo, E., Frush, D., Gottfried, M., Koepke, J., Boney, A., Bali, D., Chen, Y.T., and Kishnani, P.S. (2007). Glycogen storage disease type III-hepatocellular carcinoma a long-term complication? J. Hepatol. *46*, 492–498.

Dentin, R., Tomas-Cobos, L., Foufelle, F., Leopold, J., Girard, J., Postic, C., and Ferré, P. (2012). Glucose 6-phosphate, rather than xylulose 5-phosphate, is required for the activation of ChREBP in response to glucose in the liver. J. Hepatol. *56*, 199–209.

Derks, T.G.J., and van Rijn, M. (2015). Lipids in hepatic glycogen storage diseases: pathophysiology, monitoring of dietary management and future directions. J. Inherit. Metab. Dis. *38*, 537–543.

De Vadder, F., Kovatcheva-Datchary, P., Goncalves, D., Vinera, J., Zitoun, C., Duchampt, A., Bäckhed, F., and Mithieux, G. (2014). Microbiota-Generated Metabolites Promote Metabolic Benefits via Gut-Brain Neural Circuits. Cell *156*, 84–96.

Doudna, J.A., and Charpentier, E. (2014). The new frontier of genome engineering with CRISPR-Cas9. Science *346*, 1258096.

Eckel, R.H., Grundy, S.M., and Zimmet, P.Z. (2005). The metabolic syndrome. Lancet Lond. Engl. *365*, 1415–1428.

Ellard, S. (2000). Hepatocyte nuclear factor 1 alpha (HNF-1 alpha) mutations in maturity-onset diabetes of the young. Hum. Mutat. *16*, 377–385.

Elpek, G.Ö. (2014). Cellular and molecular mechanisms in the pathogenesis of liver fibrosis: An update. World J. Gastroenterol. WJG *20*, 7260–7276.

El-Serag, H.B., Hampel, H., and Javadi, F. (2006). The association between diabetes and hepatocellular carcinoma: a systematic review of epidemiologic evidence. Clin. Gastroenterol. Hepatol. Off. Clin. Pract. J. Am. Gastroenterol. Assoc. *4*, 369–380.

Emerling, B.M., Weinberg, F., Snyder, C., Burgess, Z., Mutlu, G.M., Viollet, B., Budinger, G.R.S., and Chandel, N.S. (2009). Hypoxic activation of AMPK is dependent on mitochondrial ROS but independent of an increase in AMP/ATP ratio. Free Radic. Biol. Med. *46*, 1386–1391.

Engelholm, L.H., Riaz, A., Serra, D., Dagnæs-Hansen, F., Johansen, J.V., Santoni-Rugiu, E., Hansen, S.H., Niola, F., and Frödin, M. (2017). CRISPR/Cas9 Engineering of Adult Mouse Liver Demonstrates That the Dnajb1–Prkaca Gene Fusion is Sufficient to Induce Tumors Resembling Fibrolamellar Hepatocellular Carcinoma. Gastroenterology. 2017. pii: S0016-5085(17)36148-6..

Faguer, S., Decramer, S., Chassaing, N., Bellanné-Chantelot, C., Calvas, P., Beaufils, S., Bessenay, L., Lengelé, J.-P., Dahan, K., Ronco, P., et al. (2011). Diagnosis, management, and prognosis of HNF1B nephropathy in adulthood. Kidney Int. *80*, 768–776.

Farah, B.L., Landau, D.J., Sinha, R.A., Brooks, E.D., Wu, Y., Fung, S.Y.S., Tanaka, T., Hirayama, M., Bay, B.-H., Koeberl, D.D., et al. (2016). Induction of autophagy improves hepatic lipid metabolism in glucose-6-phosphatase deficiency. J. Hepatol. *64*, 370–379.

Farah, B.L., Sinha, R.A., Wu, Y., Singh, B.K., Lim, A., Hirayama, M., Landau, D.J., Bay, B.H., Koeberl, D.D., and Yen, P.M. (2017). Hepatic mitochondrial dysfunction is a feature of Glycogen Storage Disease Type Ia (GSDIa). Sci. Rep. *7*, 44408.

Faubert, B., Vincent, E.E., Poffenberger, M.C., and Jones, R.G. (2015). The AMP-activated protein kinase (AMPK) and cancer: Many faces of a metabolic regulator. Cancer Lett. *356*, 165–170.

Ferry, N., Pichard, V., Sébastien Bony, D.A., and Nguyen, T.H. (2011). Retroviral vector-mediated gene therapy for metabolic diseases: an update. Curr. Pharm. Des. *17*, 2516–2527.

Field, J.B., Epstein, S., and Egan, T. (1965). Studies in Glycogen Storage Diseases. I. Intestinal Glucose-6-Phosphatase Activity in Patients with Von Gierke's Disease and Their Parents*. J. Clin. Invest. *44*, 1240–1247.

Font-Burgada, J., Sun, B., and Karin, M. (2016). Obesity and Cancer: The Oil that Feeds the Flame. Cell Metab. *23*, 48–62.

Foufelle, F., and Ferré, P. (2002). New perspectives in the regulation of hepatic glycolytic and lipogenic genes by insulin and glucose: a role for the transcription factor sterol regulatory element binding protein-1c. Biochem. J. *366*, 377–391.

Fragiadaki, M., and Mason, R.M. (2011). Epithelial-mesenchymal transition in renal fibrosis – evidence for and against. Int. J. Exp. Pathol. *92*, 143–150.

Franco, L.M., Krishnamurthy, V., Bali, D., Weinstein, D.A., Arn, P., Clary, B., Boney, A., Sullivan, J., Frush, D.P., Chen, Y.-T., et al. (2005). Hepatocellular carcinoma in glycogen storage disease type Ia: a case series. J. Inherit. Metab. Dis. *28*, 153–162.

Froissart, R., Piraud, M., Boudjemline, A.M., Vianey-Saban, C., Petit, F., Hubert-Buron, A., Eberschweiler, P.T., Gajdos, V., and Labrune, P. (2011). Glucose-6-phosphatase deficiency. Orphanet J. Rare Dis. *6*, 27.

Fung, M.K.L., and Chan, G.C.-F. (2017). Drug-induced amino acid deprivation as strategy for cancer therapy. J. Hematol. Oncol.J Hematol Oncol *10*, 144.

Gaj, T., Gersbach, C.A., and Barbas, C.F. (2013). ZFN, TALEN, and CRISPR/Cas-based methods for genome engineering. Trends Biotechnol. *31*, 397–405.

Gardner, D.S., and Tai, E.S. (2012). Clinical features and treatment of maturity onset diabetes of the young (MODY). Diabetes Metab. Syndr. Obes. Targets Ther. *5*, 101–108.

Gautier-Stein, A., Mithieux, G., and Rajas, F. (2005). A Distal Region Involving Hepatocyte Nuclear Factor 4α and CAAT/Enhancer Binding Protein Markedly Potentiates the Protein Kinase A Stimulation of the Glucose-6-Phosphatase Promoter. Mol. Endocrinol. *19*, 163–174.

Geberhiwot, T., Alger, S., McKiernan, P., Packard, C., Caslake, M., Elias, E., and Cramb, R. (2007). Serum lipid and lipoprotein profile of patients with glycogen storage disease types I, III and IX. J. Inherit. Metab. Dis. *30*, 406.

Gerin, I., Veiga-da-Cunha, M., Achouri, Y., Collet, J.F., and Van Schaftingen, E. (1997). Sequence of a putative glucose 6-phosphate translocase, mutated in glycogen storage disease type Ib. FEBS Lett. *419*, 235–238.

Ghosh, A., Shieh, J.-J., Pan, C.-J., Sun, M.-S., and Chou, J.Y. (2002). The Catalytic Center of Glucose-6-phosphatase HIS176 IS THE NUCLEOPHILE FORMING THE PHOSPHOHISTIDINE-ENZYME INTERMEDIATE DURING CATALYSIS. J. Biol. Chem. *277*, 32837–32842.

Ghosh, A., Allamarvdasht, M., Pan, C.-J., Sun, M.-S., Mansfield, B.C., Byrne, B.J., and Chou, J.Y. (2006). Long-term correction of murine glycogen storage disease type Ia by recombinant adeno-associated virus-1-mediated gene transfer. Gene Ther. *13*, 321–329.

Girard, J. (2006). The Inhibitory Effects of Insulin on Hepatic Glucose Production Are Both Direct and Indirect. Diabetes *55*, S65–S69.

Girard, J., Perdereau, D., Foufelle, F., Prip-Buus, C., and Ferré, P. (1994). Regulation of lipogenic enzyme gene expression by nutrients and hormones. FASEB J. Off. Publ. Fed. Am. Soc. Exp. Biol. *8*, 36–42.

Gjorgjieva, M., Clar, J., Raffin, M., Duchampt, A., Stefanutti, A., Mithieux, G., and Rajas, F. (2015). FP045DIET HIGHLY INFLUENCES THE DEVELOPMENT OF NEPHROPATHY IN A MOUSE MODEL OF GLYCOGEN STORAGE DISEASE TYPE Ia. Nephrol. Dial. Transplant. *30*, iii80-iii80.

Gjorgjieva, M., Raffin, M., Duchampt, A., Perry, A., Stefanutti, A., Brevet, M., Tortereau, A., Dubourg, L., Hubert-Buron, A., Mabille, M., et al. (2016a). Progressive development of renal cysts in glycogen storage disease type I. Hum. Mol. Genet. *25*, 3784–3797.

Gjorgjieva, M., Oosterveer, M.H., Mithieux, G., and Rajas, F. (2016b). Mechanisms by Which Metabolic Reprogramming in GSD1 Liver Generates a Favorable Tumorigenic Environment. J. Inborn Errors Metab. Screen. *4*, 2326409816679429.

Graumann, O., Osther, S.S., and Osther, P.J.S. (2011). Characterization of complex renal cysts: a critical evaluation of the Bosniak classification. Scand. J. Urol. Nephrol. *45*, 84–90.

Greene, H.L., Swift, L.L., and Knapp, H.R. (1991). Hyperlipidemia and fatty acid composition in patients treated for type IA glycogen storage disease. J. Pediatr. *119*, 398–403.

Grefhorst, A., Schreurs, M., Oosterveer, M.H., Cortés, V.A., Havinga, R., Herling, A.W., Reijngoud, D.-J., Groen, A.K., and Kuipers, F. (2010). Carbohydrate-response-element-binding protein (ChREBP) and not the liver X receptor α (LXRα) mediates elevated hepatic lipogenic gene expression in a mouse model of glycogen storage disease type 1. Biochem. J. *432*, 249–254.

Grinshpun, A., Condiotti, R., N Waddington, S., Peer, M., Zeig, E., Peretz, S., Simerzin, A., Chou, J., Pann, C.-J., Giladi, H., et al. (2010). Neonatal Gene Therapy of Glycogen Storage Disease Type Ia Using a Feline Immunodeficiency Virus–based Vector. Mol. Ther. *18*, 1592–1598.

Guichard, C., Amaddeo, G., Imbeaud, S., Ladeiro, Y., Pelletier, L., Maad, I.B., Calderaro, J., Bioulac-Sage, P., Letexier, M., Degos, F., et al. (2012). Integrated analysis of somatic mutations and focal copy-number changes identifies key genes and pathways in hepatocellular carcinoma. Nat. Genet. *44*, 694–698.

Gwinn, D.M., Shackelford, D.B., Egan, D.F., Mihaylova, M.M., Mery, A., Vasquez, D.S., Turk, B.E., and Shaw, R.J. (2008). AMPK phosphorylation of raptor mediates a metabolic checkpoint. Mol. Cell *30*, 214–226.

Haagsma, E.B., Smit, G.P., Niezen-Koning, K.E., Gouw, A.S., Meerman, L., and Slooff, M.J. (1997). Type IIIb glycogen storage disease associated with end-stage cirrhosis and hepatocellular carcinoma. Hepatology *25*, 537–540.

Han, J., and Kaufman, R.J. (2016). The role of ER stress in lipid metabolism and lipotoxicity. J. Lipid Res. *57*, 1329–1338.

Harries, L.W., Brown, J.E., and Gloyn, A.L. (2009). Species-Specific Differences in the Expression of the HNF1A, HNF1B and HNF4A Genes. PLOS ONE *4*, e7855.

Hay, N. (2016). Reprogramming glucose metabolism in cancer: can it be exploited for cancer therapy? Nat. Rev. Cancer *16*, 635–649.

Henquin, J.C. (2000). Triggering and amplifying pathways of regulation of insulin secretion by glucose. Diabetes *49*, 1751–1760.

Herbert, K.J., Cook, A.L., and Snow, E.T. (2014). SIRT1 inhibition restores apoptotic sensitivity in p53-mutated human keratinocytes. Toxicol. Appl. Pharmacol. *277*, 288–297.

Herrema, H., Smit, G.P.A., Reijngoud, D.-J., and Kuipers, F. (2007). Does increased fatty acid oxidation enhance development of liver cirrhosis and progression to hepatocellular carcinoma in patients with glycogen storage disease type-III? J. Hepatol. *47*, 298–300.

Hiesberger, T., Shao, X., Gourley, E., Reimann, A., Pontoglio, M., and Igarashi, P. (2005). Role of the hepatocyte nuclear factor-1beta (HNF-1beta) C-terminal domain in Pkhd1 (ARPKD) gene transcription and renal cystogenesis. J. Biol. Chem. *280*, 10578–10586.

Hijmans, B.S., Boss, A., van Dijk, T.H., Soty, M., Wolters, H., Mutel, E., Groen, A.K., Derks, T.G.J., Mithieux, G., Heerschap, A., et al. (2017). Hepatocytes contribute to residual glucose production in a mouse model for glycogen storage disease type Ia. Hepatol. Baltim. Md. (In press)

Horie, Y., Suzuki, A., Kataoka, E., Sasaki, T., Hamada, K., Sasaki, J., Mizuno, K., Hasegawa, G., Kishimoto, H., Iizuka, M., et al. (2004). Hepatocyte-specific Pten deficiency results in steatohepatitis and hepatocellular carcinomas. J. Clin. Invest. *113*, 1774–1783.

Hosseini, M., Antic, T., Paner, G.P., and Chang, A. (2014). Pathologic spectrum of cysts in end-stage kidneys: possible precursors to renal neoplasia. Hum. Pathol. *45*, 1406–1413.

Hutton, J.C., and O'Brien, R.M. (2009). Glucose-6-phosphatase catalytic subunit gene family. J. Biol. Chem. *284*, 29241–29245.

Igarashi, P., Shao, X., McNally, B.T., and Hiesberger, T. (2005). Roles of HNF-1beta in kidney development and congenital cystic diseases. Kidney Int. *68*, 1944–1947.

Inayat, F., Ur Rahman, Z., and Hurairah, A. Hepatocellular Carcinoma in Nonalcoholic Fatty Liver Disease. Cureus *8(8):e754*.

Ingle, P.V., Samsudin, S.Z., Chan, P.Q., Ng, M.K., Heng, L.X., Yap, S.C., Chai, A.S.H., and Wong, A.S.Y. (2016). Development and novel therapeutics in hepatocellular carcinoma: a review. Ther. Clin. Risk Manag. *12*, 445–455.

Inoki, K., Zhu, T., and Guan, K.-L. (2003). TSC2 mediates cellular energy response to control cell growth and survival. Cell *115*, 577–590.

Jansen, M., Ten Klooster, J.P., Offerhaus, G.J., and Clevers, H. (2009). LKB1 and AMPK family signaling: the intimate link between cell polarity and energy metabolism. Physiol. Rev. *89*, 777–798.

Jiang, G., and Zhang, B.B. (2003). Glucagon and regulation of glucose metabolism. Am. J. Physiol. Endocrinol. Metab. *284*, E671-678.

Joung, J.K., and Sander, J.D. (2013). TALENs: a widely applicable technology for targeted genome editing. Nat. Rev. Mol. Cell Biol. *14*, 49–55.

Jun, H.S., Lee, Y.M., Cheung, Y.Y., McDermott, D.H., Murphy, P.M., De Ravin, S.S., Mansfield, B.C., and Chou, J.Y. (2010). Lack of glucose recycling between endoplasmic reticulum and cytoplasm underlies cellular dysfunction in glucose-6-phosphatase-beta-deficient neutrophils in a congenital neutropenia syndrome. Blood *116*, 2783–2792.

Jun, H.S., Cheung, Y.Y., Lee, Y.M., Mansfield, B.C., and Chou, J.Y. (2012). Glucose-6-phosphatase-β, implicated in a congenital neutropenia syndrome, is essential for macrophage energy homeostasis and functionality. Blood *119*, 4047–4055.

Jun, H.S., Weinstein, D.A., Lee, Y.M., Mansfield, B.C., and Chou, J.Y. (2014). Molecular mechanisms of neutrophil dysfunction in glycogen storage disease type Ib. Blood *123*, 2843–2853.

Jung, U.J., and Choi, M.-S. (2014). Obesity and Its Metabolic Complications: The Role of Adipokines and the Relationship between Obesity, Inflammation, Insulin Resistance, Dyslipidemia and Nonalcoholic Fatty Liver Disease. Int. J. Mol. Sci. *15*, 6184–6223.

Kattenhorn, L.M., Tipper, C.H., Stoica, L., Geraghty, D.S., Wright, T.L., Clark, K.R., and Wadsworth, S.C. (2016). Adeno-Associated Virus Gene Therapy for Liver Disease. Hum. Gene Ther. *27*, 947–961.

Kauppinen, A., Suuronen, T., Ojala, J., Kaarniranta, K., and Salminen, A. (2013). Antagonistic crosstalk between NF-κB and SIRT1 in the regulation of inflammation and metabolic disorders. Cell. Signal. *25*, 1939–1948.

Kawaguchi, T., Osatomi, K., Yamashita, H., Kabashima, T., and Uyeda, K. (2002). Mechanism for Fatty Acid "Sparing" Effect on Glucose-induced Transcription REGULATION OF CARBOHYDRATE-RESPONSIVE ELEMENT-BINDING PROTEIN BY AMP-ACTIVATED PROTEIN KINASE. J. Biol. Chem. *277*, 3829–3835.

Kelly, P.M., and Poon, F.W. (2001). Hepatic tumours in glycogen storage disease type 1 (von Gierke's disease). Clin. Radiol. *56*, 505–508.

Kishnani, P.S., and Chen, Y.T. (2007). Important role of abnormal glycogen structure in the development of liver cirrhosis and progression to hepatocellular carcinoma in patients with glycogen storage disease type-III. J. Hepatol. *47*, 300–301.

Kishnani, P.S., Bao, Y., Wu, J.Y., Brix, A.E., Lin, J.L., and Chen, Y.T. (1997). Isolation and nucleotide sequence of canine glucose-6-phosphatase mRNA: identification of mutation in puppies with glycogen storage disease type Ia. Biochem. Mol. Med. *61*, 168–177.

Kishnani, P.S., Faulkner, E., VanCamp, S., Jackson, M., Brown, T., Boney, A., Koeberl, D., and Chen, Y.T. (2001). Canine model and genomic structural organization of glycogen storage disease type Ia (GSD Ia). Vet. Pathol. *38*, 83–91.

Kishnani, P.S., Chuang, T.-P., Bali, D., Koeberl, D., Austin, S., Weinstein, D.A., Murphy, E., Chen, Y.-T., Boyette, K., Liu, C.-H., et al. (2009). Chromosomal and genetic alterations in human hepatocellular adenomas associated with type Ia glycogen storage disease. Hum. Mol. Genet. *18*, 4781–4790.

Kishnani, P.S., Austin, S.L., Arn, P., Bali, D.S., Boney, A., Case, L.E., Chung, W.K., Desai, D.M., El-Gharbawy, A., Haller, R., et al. (2010). Glycogen Storage Disease Type III diagnosis and management guidelines. Genet. Med. *12*, 446–463.

Kishnani, P.S., Austin, S.L., Abdenur, J.E., Arn, P., Bali, D.S., Boney, A., Chung, W.K., Dagli, A.I., Dale, D., Koeberl, D., et al. (2014). Diagnosis and management of glycogen storage disease type I: a practice guideline of the American College of Medical Genetics and Genomics. Genet. Med. Off. J. Am. Coll. Med. Genet. *16*, e1 1530-0366.

Koeberl, D.D., Sun, B.D., Damodaran, T.V., Brown, T., Millington, D.S., Benjamin, D.K., Bird, A., Schneider, A., Hillman, S., Jackson, M., et al. (2006). Early, sustained efficacy of adeno-associated virus vector-mediated gene therapy in glycogen storage disease type Ia. Gene Ther. *13*, 1281–1289.

Koeberl, D.D., Sun, B., Bird, A., Chen, Y.T., Oka, K., and Chan, L. (2007). Efficacy of helper-dependent adenovirus vector-mediated gene therapy in murine glycogen storage disease type Ia. Mol. Ther. J. Am. Soc. Gene Ther. *15*, 1253–1258.

Koeberl, D.D., Pinto, C., Sun, B., Li, S., Kozink, D.M., Benjamin, D.K., Demaster, A.K., Kruse, M.A., Vaughn, V., Hillman, S., et al. (2008). AAV vector-mediated reversal of hypoglycemia in canine and murine glycogen storage disease type Ia. Mol. Ther. J. Am. Soc. Gene Ther. *16*, 665–672.

Koga, H., Kaushik, S., and Cuervo, A.M. (2010). Altered lipid content inhibits autophagic vesicular fusion. FASEB J. *24*, 3052–3065.

Kruiswijk, F., Labuschagne, C.F., and Vousden, K.H. (2015). p53 in survival, death and metabolic health: a lifeguard with a licence to kill. Nat. Rev. Mol. Cell Biol. *16*, 393–405.

Kudo, M. (2001). Hepatocellular adenoma in type Ia glycogen storage disease. J. Gastroenterol. *36*, 65–66.

Kwabi-Addo, B., Giri, D., Schmidt, K., Podsypanina, K., Parsons, R., Greenberg, N., and Ittmann, M. (2001). Haploinsufficiency of the Pten tumor suppressor gene promotes prostate cancer progression. Proc. Natl. Acad. Sci. U. S. A. *98*, 11563–11568.

Kwon, J., Cho, J.-H., Lee, Y.M., Kim, G.-Y., Anduaga, J., and Chou, J. (2016). 165. Liver-Directed Gene Therapy for Murine Glycogen Storage Disease Type IB. Mol. Ther. *24*, S64–S65.

Labrune, P. (2002). Glycogen storage disease type I: indications for liver and/or kidney transplantation. Eur. J. Pediatr. *161*, S53–S55.

Lan, H.Y. (2011). Diverse Roles of TGF-β/Smads in Renal Fibrosis and Inflammation. Int. J. Biol. Sci. *7*, 1056–1067.

Lee, P.J. (2002). Glycogen storage disease type I: pathophysiology of liver adenomas. Eur. J. Pediatr. *161 Suppl 1*, S46-49.

Lee, J.T., and Gu, W. (2013). SIRT1: Regulator of p53 Deacetylation. Genes Cancer *4*, 112–117.

Lee, C.-W., Wong, L.L.-Y., Tse, E.Y.-T., Liu, H.-F., Leong, V.Y.-L., Lee, J.M.-F., Hardie, D.G., Ng, I.O.-L., and Ching, Y.-P. (2012a). AMPK promotes p53 acetylation via phosphorylation and inactivation of SIRT1 in liver cancer cells. Cancer Res. *72*, 4394–4404.

Lee, Y.M., Jun, H.S., Pan, C.-J., Lin, S.R., Wilson, L.H., Mansfield, B.C., and Chou, J.Y. (2012b). Prevention of hepatocellular adenoma and correction of metabolic abnormalities in murine glycogen storage disease type Ia by gene therapy. Hepatology *56*, 1719–1729.

Lee, Y.M., Pan, C.-J., Koeberl, D.D., Mansfield, B.C., and Chou, J.Y. (2013). The upstream enhancer elements of the G6PC promoter are critical for optimal G6PC expression in murine glycogen storage disease type Ia. Mol. Genet. Metab. *110*, 275–280.

Lei, K.J., Shelly, L.L., Pan, C.J., Sidbury, J.B., and Chou, J.Y. (1993). Mutations in the glucose-6-phosphatase gene that cause glycogen storage disease type 1a. Science *262*, 580–583.

Lei, K.J., Pan, C.J., Shelly, L.L., Liu, J.L., and Chou, J.Y. (1994). Identification of mutations in the gene for glucose-6-phosphatase, the enzyme deficient in glycogen storage disease type 1a. J. Clin. Invest. *93*, 1994–1999.

Lei, K.J., Chen, H., Pan, C.J., Ward, J.M., Mosinger, B., Lee, E.J., Westphal, H., Mansfield, B.C., and Chou, J.Y. (1996). Glucose-6-phosphatase dependent substrate transport in the glycogen storage disease type-1a mouse. Nat. Genet. *13*, 203–209.

Leslie, N.R., and Downes, C.P. (2004). PTEN function: how normal cells control it and tumour cells lose it. Biochem. J. *382*, 1–11.

Leslie, N.R., and Foti, M. (2011). Non-genomic loss of PTEN function in cancer: not in my genes. Trends Pharmacol. Sci. *32*, 131–140.

Levy, E., Thibault, L.A., Roy, C.C., Bendayan, M., Lepage, G., and Letarte, J. (1988). Circulating lipids and lipoproteins in glycogen storage disease type I with nocturnal intragastric feeding. J. Lipid Res. *29*, 215–226.

Li, S.-C., Chen, C.-M., Goldstein, J.L., Wu, J.-Y., Lemyre, E., Burrow, T.A., Kang, P.B., Chen, Y.-T., and Bali, D.S. (2010). Glycogen storage disease type IV: novel mutations and molecular characterization of a heterogeneous disorder. J. Inherit. Metab. Dis. *33 Suppl 3*, S83-90.

Liliental, J., Moon, S.Y., Lesche, R., Mamillapalli, R., Li, D., Zheng, Y., Sun, H., and Wu, H. (2000). Genetic deletion of the Pten tumor suppressor gene promotes cell motility by activation of Rac1 and Cdc42 GTPases. Curr. Biol. CB *10*, 401–404.

Limmer, J., Fleig, W.E., Leupold, D., Bittner, R., Ditschuneit, H., and Berger, H.-G. (1988). Hepatocellular carcinoma in type I glycogen storage disease. Hepatology *8*, 531–537.

Lin, Z., and Fang, D. (2013). The Roles of SIRT1 in Cancer. Genes Cancer *4*, 97–104.

Lin, B., Pan, C.J., and Chou, J.Y. (2000). Human variant glucose-6-phosphate transporter is active in microsomal transport. Hum. Genet. *107*, 526–529.

Liu, W., Monahan, K.B., Pfefferle, A.D., Shimamura, T., Sorrentino, J., Chan, K.T., Roadcap, D.W., Ollila, D.W., Thomas, N.E., Castrillon, D.H., et al. (2012). LKB1/STK11 Inactivation Leads to Expansion of a Prometastatic Tumor Subpopulation in Melanoma. Cancer Cell *21*, 751–764.

Lu, H., Fisher, R.P., Bailey, P., and Levine, A.J. (1997). The CDK7-cycH-p36 complex of transcription factor IIH phosphorylates p53, enhancing its sequence-specific DNA binding activity in vitro. Mol. Cell. Biol. *17*, 5923–5934.

Luo, X., Hall, G., Li, S., Bird, A., Lavin, P.J., Winn, M.P., Kemper, A.R., Brown, T.T., and Koeberl, D.D. (2011). Hepatorenal Correction in Murine Glycogen Storage Disease Type I With a Double-stranded Adeno-associated Virus Vector. Mol. Ther. *19*, 1961–1970.

Luo, Z., Zang, M., and Guo, W. (2010). AMPK as a metabolic tumor suppressor: control of metabolism and cell growth. Future Oncol. Lond. Engl. *6*, 457–470.

Luo, Z., Li, Y., Wang, H., Fleming, J., Li, M., Kang, Y., Zhang, R., and Li, D. (2015). Hepatocyte Nuclear Factor 1A (HNF1A) as a Possible Tumor Suppressor in Pancreatic Cancer. PLoS ONE *10*(3):e0121082.

Maheshwari, A., Rankin, R., Segev, D.L., and Thuluvath, P.J. (2012). Outcomes of liver transplantation for glycogen storage disease: a matched-control study and a review of literature. Clin. Transplant. *26*, 432–436.

Malatack, J.J., Finegold, D.N., Iwatsuki, S., Shaw, B.W., Gartner, J.C., Zitelli, B.J., Roe, T., and Starzl, T.E. (1983). LIVER TRANSPLANTATION FOR TYPE I GLYCOGEN STORAGE DISEASE. Lancet *1*, 1073–1075.

Manzia, T.M., Angelico, R., Toti, L., Cillis, A., Ciano, P., Orlando, G., Anselmo, A., Angelico, M., and Tisone, G. (2011). Glycogen storage disease type Ia and VI associated with hepatocellular carcinoma: two case reports. Transplant. Proc. *43*, 1181–1183.

Mao, Y., Yu, F., Wang, J., Guo, C., and Fan, X. (2016). Autophagy: a new target for nonalcoholic fatty liver disease therapy. Hepatic Med. Evid. Res. *8*, 27–37.

Martens, D.H.J., Rake, J.P., Navis, G., Fidler, V., van Dael, C.M.L., and Smit, G.P.A. (2009). Renal Function in Glycogen Storage Disease Type I, Natural Course, and Renopreservative Effects of ACE Inhibition. Clin. J. Am. Soc. Nephrol. CJASN *4*, 1741–1746.

Martin, C.C., Bischof, L.J., Bergman, B., Hornbuckle, L.A., Hilliker, C., Frigeri, C., Wahl, D., Svitek, C.A., Wong, R., Goldman, J.K., et al. (2001). Cloning and characterization of the human and rat islet-specific glucose-6-phosphatase catalytic subunit-related protein (IGRP) genes. J. Biol. Chem. *276*, 25197–25207.

Martin, C.C., Oeser, J.K., Svitek, C.A., Hunter, S.I., Hutton, J.C., and O'Brien, R.M. (2002). Identification and characterization of a human cDNA and gene encoding a ubiquitously expressed glucose-6-phosphatase catalytic subunit-related protein. J. Mol. Endocrinol. *29*, 205–222.

Mason, H.H., and Andersen, D.H. (1955). Glycogen disease of the liver (von Gierke's disease) with hepatomata; case report with metabolic studies. Pediatrics *16*, 785–800.

Massa, F., Garbay, S., Bouvier, R., Sugitani, Y., Noda, T., Gubler, M.-C., Heidet, L., Pontoglio, M., and Fischer, E. (2013). Hepatocyte nuclear factor 1β controls nephron tubular development. Dev. Camb. Engl. *140*, 886–896.

Matern, D., Seydewitz, H., Bali, D., Lang, C., and Chen, Y.-T. (2002). Glycogen storage disease type I: diagnosis and phenotype/genotype correlation. Eur. J. Pediatr. *161*, S10–S19.

McCommis, K.S., and Finck, B.N. (2015). Mitochondrial pyruvate transport: a historical perspective and future research directions. Biochem. J. *466*, 443–454.

Melis, D., Parenti, G., Gatti, R., Casa, R.D., Parini, R., Riva, E., Burlina, A.B., Vici, C.D., Di Rocco, M., Furlan, F., et al. (2005). Efficacy of ACE-inhibitor therapy on renal disease in glycogen storage disease type 1: a multicentre retrospective study. Clin. Endocrinol. (Oxf.) *63*, 19–25.

Menendez, J.A., and Lupu, R. (2007). Fatty acid synthase and the lipogenic phenotype in cancer pathogenesis. Nat. Rev. Cancer *7*, 763–777.

Meng, X.-M., Tang, P.M.-K., Li, J., and Lan, H.Y. (2015). TGF-β/Smad signaling in renal fibrosis. Front. Physiol. *6*:82.

Merle, U., Enckea, J., Tuma, S., Volkmann, M., Naldini, L., and Stremmel, W. (2006). Lentiviral gene transfer ameliorates disease progression in Long-Evans cinnamon rats: An animal model for Wilson disease. Scand. J. Gastroenterol. *41*, 974–982.

Michelotti, G.A., Machado, M.V., and Diehl, A.M. (2013). NAFLD, NASH and liver cancer. Nat. Rev. Gastroenterol. Hepatol. *10*, 656–665.

Minassian, C., Zitoun, C., and Mithieux, G. (1996). Differential time course of liver and kidney glucose-6 phosphatase activity during long-term fasting in rat correlates with differential time course of messenger RNA level. Mol. Cell. Biochem. *155*, 37–41.

Mithieux, G., Ajzannay, A., and Minassian, C. (1995). Identification of membrane-bound phosphoglucomutase and glucose-6 phosphatase by 32P-labeling of rat liver microsomal membrane proteins with 32P-glucose-6 phosphate. J. Biochem. (Tokyo) *117*, 908–914.

Mithieux, G., Bady, I., Gautier, A., Croset, M., Rajas, F., and Zitoun, C. (2004a). Induction of control genes in intestinal gluconeogenesis is sequential during fasting and maximal in diabetes. Am. J. Physiol. - Endocrinol. Metab. *286*, E370–E375.

Mithieux, G., Rajas, F., and Gautier-Stein, A. (2004b). A Novel Role for Glucose 6-Phosphatase in the Small Intestine in the Control of Glucose Homeostasis. J. Biol. Chem. *279*, 44231–44234.

Mithieux, G., Gautier-Stein, A., Rajas, F., and Zitoun, C. (2006). Contribution of intestine and kidney to glucose fluxes in different nutritional states in rat. Comp. Biochem. Physiol. B Biochem. Mol. Biol. *143*, 195–200.

Mithieux, G., Rajas, F., Gautier-Stein, A., and Soty, M. (2017). Adaptation of Hepatic, Renal and Intestinal Gluconeogenesis During Food Deprivation. In Handbook of Famine, Starvation, and Nutrient Deprivation, V. Preedy, and V.B. Patel, eds. (Springer International Publishing), pp. 1–15.

Montagner, A., Polizzi, A., Fouché, E., Ducheix, S., Lippi, Y., Lasserre, F., Barquissau, V., Régnier, M., Lukowicz, C., Benhamed, F., et al. (2016). Liver PPARα is crucial for whole-body fatty acid homeostasis and is protective against NAFLD. Gut gutjnl-2015-310798.

de Moor, R.A., Schweizer, J.J., van Hoek, B., Wasser, M., Vink, R., and Maaswinkel-Mooy, P.D. (2000). Hepatocellular carcinoma in glycogen storage disease type IV. Arch. Dis. Child. *82*, 479–480.

Mundy, H.R., and Lee, P.J. (2002). Glycogenosis type I and diabetes mellitus: a common mechanism for renal dysfunction? Med. Hypotheses *59*, 110–114.

Mundy, H.R., Hindmarsh, P.C., Matthews, D.R., Leonard, J.V., and Lee, P.J. (2003). The regulation of growth in glycogen storage disease type 1. Clin. Endocrinol. (Oxf.) *58*, 332–339.

Murata, S., Yanagisawa, K., Fukunaga, K., Oda, T., Kobayashi, A., Sasaki, R., and Ohkohchi, N. (2010). Fatty acid synthase inhibitor cerulenin suppresses liver metastasis of colon cancer in mice. Cancer Sci. *101*, 1861–1865.

Mutel, E., Abdul-Wahed, A., Ramamonjisoa, N., Stefanutti, A., Houberdon, I., Cavassila, S., Pilleul, F., Beuf, O., Gautier-Stein, A., Penhoat, A., et al. (2011a). Targeted deletion of liver glucose-6 phosphatase mimics glycogen storage disease type 1a including development of multiple adenomas. J. Hepatol. *54*, 529–537.

Mutel, E., Gautier-Stein, A., Abdul-Wahed, A., Amigó-Correig, M., Zitoun, C., Stefanutti, A., Houberdon, I., Tourette, J.-A., Mithieux, G., and Rajas, F. (2011b). Control of Blood Glucose in the Absence of Hepatic Glucose Production During Prolonged Fasting in Mice. Diabetes *60*, 3121–3131.

Narisawa, K., Otomo, H., Igarashi, Y., Arai, N., Otake, M., Tada, K., and Kuzuya, T. (1982). Glycogen storage disease type 1b due to a defect of glucose-6-phosphate translocase. J. Inherit. Metab. Dis. *5*, 227–228.

Nault, J.C., and Zucman Rossi, J. (2013). Molecular Classification of Hepatocellular Adenomas Int J Hepatol. 2013; 2013: 315947.

Nault, J.-C., Couchy, G., Balabaud, C., Morcrette, G., Caruso, S., Blanc, J.-F., Bacq, Y., Calderaro, J., Paradis, V., Ramos, J., et al. (2017). Molecular Classification of Hepatocellular Adenoma Associates With Risk Factors, Bleeding, and Malignant Transformation. Gastroenterology *152*, 880–894.e6.

Newgard, C.B., Brady, M.J., O'Doherty, R.M., and Saltiel, A.R. (2000). Organizing glucose disposal: emerging roles of the glycogen targeting subunits of protein phosphatase-1. Diabetes *49*, 1967–1977.

Oberhaensli, R.D., Rajagopalan, B., Taylor, D.J., Radda, G.K., Collins, J.E., and Leonard, J.V. (1988). Study of liver metabolism in glucose-6-phosphatase deficiency (glycogen storage disease type 1A) by P-31 magnetic resonance spectroscopy. Pediatr. Res. *23*, 375–380.

Okechuku, G.O., Shoemaker, L.R., Dambska, M., Brown, L.M., Mathew, J., and Weinstein, D.A. (2017). Tight metabolic control plus ACE inhibitor therapy improves GSD I nephropathy. J. Inherit. Metab. Dis (2017) 40: 703.

O'Leary, J.G., Lepe, R., and Davis, G.L. (2008). Indications for liver transplantation. Gastroenterology *134*, 1764–1776.

Osada, S., Kanematsu, M., Imai, H., Goshima, S., and Sugiyama, Y. (2008). Hepatic fibrosis influences the growth of hepatocellular carcinoma. Hepatogastroenterology. *55*, 184–187.

Owen, K., Thanabalasingham, G., Kavvoura, F., and Juszczak, A. (2014). MODY due to hepatocyte nuclear factor 1-beta mutations. In Diapedia, (Diapedia.org), https://doi.org/10.14496/dia.41040851259.14.

Özen, H. (2007). Glycogen storage diseases: New perspectives. World J. Gastroenterol. WJG *13*, 2541–2553.

Pagliarani, S., Lucchiari, S., Ulzi, G., Violano, R., Ripolone, M., Bordoni, A., Nizzardo, M., Gatti, S., Corti, S., Moggio, M., et al. (2014). Glycogen storage disease type III: A novel Agl knockout mouse model. Biochim. Biophys. Acta *1842*, 2318–2328.

Panaro, F., Andorno, E., Basile, G., Morelli, N., Bottino, G., Fontana, I., Bertocchi, M., DiDomenico, S., Miggino, M., Saltalamacchia, L., et al. (2004). Simultaneous liver-kidney transplantation for glycogen storage disease type IA (von Gierke's disease). Transplant. Proc. *36*, 1483–1484.

Paradis, V., Zalinski, S., Chelbi, E., Guedj, N., Degos, F., Vilgrain, V., Bedossa, P., and Belghiti, J. (2009). Hepatocellular carcinomas in patients with metabolic syndrome often develop without significant liver fibrosis: a pathological analysis. Hepatol. Baltim. Md *49*, 851–859.

Parker, P., Burr, I., Slonim, A., Ghishan, F.K., and Greene, H. (1981). Regression of hepatic adenomas in type Ia glycogen storage disease with dietary therapy. Gastroenterology *81*, 534–536.

Peeks, F., Steunenberg, T.A.H., Boer, F. de, Rubio-Gozalbo, M.E., Williams, M., Burghard, R., Rajas, F., Oosterveer, M.H., Weinstein, D.A., and Derks, T.G.J. (2017). Clinical and biochemical heterogeneity between patients with glycogen storage disease type IA: the added value of CUSUM for metabolic control. J. Inherit. Metab. Dis. *40*, 695–702.

Pelletier, L., Rebouissou, S., Paris, A., Rathahao-Paris, E., Perdu, E., Bioulac-Sage, P., Imbeaud, S., and Zucman-Rossi, J. (2010). Loss of hepatocyte nuclear factor 1alpha function in human hepatocellular adenomas leads to aberrant activation of signaling pathways involved in tumorigenesis. Hepatol. Baltim. Md *51*, 557–566.

Pellicoro, A., Ramachandran, P., Iredale, J.P., and Fallowfield, J.A. (2014). Liver fibrosis and repair: immune regulation of wound healing in a solid organ. Nat. Rev. Immunol. *14*, 181–194.

Penhoat, A., Mutel, E., Amigo-Correig, M., Pillot, B., Stefanutti, A., Rajas, F., and Mithieux, G. (2011). Protein-induced satiety is abolished in the absence of intestinal gluconeogenesis. Physiol. Behav. *105*, 89–93.

Peyrou, M., Bourgoin, L., and Foti, M. (2010). PTEN in liver diseases and cancer. World J. Gastroenterol. WJG *16*, 4627–4633.

Phang, J.M., Liu, W., Hancock, C.N., and Fischer, J.W. (2015). Proline metabolism and cancer: emerging links to glutamine and collagen. Curr. Opin. Clin. Nutr. Metab. Care *18*, 71–77.

Postic, C., and Girard, J. (2008). Contribution of de novo fatty acid synthesis to hepatic steatosis and insulin resistance: lessons from genetically engineered mice. J. Clin. Invest. *118*, 829–838.

Proud, C.G. (2006). Regulation of protein synthesis by insulin. Biochem. Soc. Trans. *34*, 213–216.

Puc, J., Keniry, M., Li, H.S., Pandita, T.K., Choudhury, A.D., Memeo, L., Mansukhani, M., Murty, V.V.V.S., Gaciong, Z., Meek, S.E.M., et al. (2005). Lack of PTEN sequesters CHK1 and initiates genetic instability. Cancer Cell *7*, 193–204.

Rajas, F., Bruni, N., Montano, S., Zitoun, C., and Mithieux, G. (1999). The glucose-6 phosphatase gene is expressed in human and rat small intestine: regulation of expression in fasted and diabetic rats. Gastroenterology *117*, 132–139.

Rajas, F., Jourdan-Pineau, H., Stefanutti, A., Mrad, E.A., Iynedjian, P.B., and Mithieux, G. (2007). Immunocytochemical localization of glucose 6-phosphatase and cytosolic phosphoenolpyruvate carboxykinase in gluconeogenic tissues reveals unsuspected metabolic zonation. Histochem. Cell Biol. *127*, 555–565.

Rajas, F., Labrune, P., and Mithieux, G. (2013). Glycogen storage disease type 1 and diabetes: learning by comparing and contrasting the two disorders. Diabetes Metab. *39*, 377–387.

Rajas, F., Clar, J., Gautier-Stein, A., and Mithieux, G. (2015). Lessons from new mouse models of glycogen storage disease type 1a in relation to the time course and organ specificity of the disease. J. Inherit. Metab. Dis. *38*, 521–527.

Rake, J.P., Visser, G., Labrune, P., Leonard, J.V., Ullrich, K., and Smit, G.P.A. (2002a). Glycogen storage disease type I: diagnosis, management, clinical course and outcome. Results of the European Study on Glycogen Storage Disease Type I (ESGSD I). Eur. J. Pediatr. *161 Suppl 1*, S20-34.

Rake, J.P., Visser, G., Labrune, P., Leonard, J.V., Ullrich, K., and Smit, G.P.A. (2002b). Guidelines for management of glycogen storage disease type I—European study on glycogen storage disease type I (ESGSD I). Eur. J. Pediatr. *161*, S112–S119.

Reddy, S.K., Austin, S.L., Spencer-Manzon, M., Koeberl, D.D., Clary, B.M., Desai, D.M., Smith, A.D., and Kishnani, P.S. (2009). Liver transplantation for glycogen storage disease type Ia. J. Hepatol. *51*, 483–490.

Reitsma-Bierens, W.C.C., Smit, G.P.A., and Troelstra, J.A. (1992). Renal function and kidney size in glycogen storage disease type I. Pediatr. Nephrol. *6*, 236–238.

Reznik, Y., Dao, T., Coutant, R., Chiche, L., Jeannot, E., Clauin, S., Rousselot, P., Fabre, M., Oberti, F., Fatome, A., et al. (2004). Hepatocyte nuclear factor-1 alpha gene inactivation: cosegregation between liver adenomatosis and diabetes phenotypes in two maturity-onset diabetes of the young (MODY)3 families. J. Clin. Endocrinol. Metab. *89*, 1476–1480.

Ribeiro-Oliveira, A., Jr, Nogueira, A.I., Pereira, R.M., Boas, W.W.V., Dos Santos, R.A.S., and Simões e Silva, A.C. (2008). The renin-angiotensin system and diabetes: an update. Vasc. Health Risk Manag. *4*, 787–803.

Rittelmeyer, I., Rothe, M., Brugman, M.H., Iken, M., Schambach, A., Manns, M.P., Baum, C., Modlich, U., and Ott, M. (2013). Hepatic lentiviral gene transfer is associated with clonal selection, but not with tumor formation in serially transplanted rodents. Hepatol. Baltim. Md *58*, 397–408.

Rivlin, N., Brosh, R., Oren, M., and Rotter, V. (2011). Mutations in the p53 Tumor Suppressor Gene. Genes Cancer *2*, 466–474.

Roach, P.J., Depaoli-Roach, A.A., Hurley, T.D., and Tagliabracci, V.S. (2012). Glycogen and its metabolism: some new developments and old themes. Biochem. J. *441*, 763–787.

Rooks, J.B., Ory, H.W., Ishak, K.G., Strauss, L.T., Greenspan, J.R., Hill, A.P., and Tyler, C.W. (1979). Epidemiology of Hepatocellular Adenoma: The Role of Oral Contraceptive Use. JAMA *242*, 644–648.

Ruderman, N.B., Julia Xu, X., Nelson, L., Cacicedo, J.M., Saha, A.K., Lan, F., and Ido, Y. (2010). AMPK and SIRT1: a long-standing partnership? Am. J. Physiol. - Endocrinol. Metab. *298*, E751–E760.

Sakaguchi, K., Herrera, J.E., Saito, S., Miki, T., Bustin, M., Vassilev, A., Anderson, C.W., and Appella, E. (1998). DNA damage activates p53 through a phosphorylation–acetylation cascade. Genes Dev. *12*, 2831–2841.

Salganik, S.V., Weinstein, D.A., Shupe, T.D., Salganik, M., Pintilie, D.G., and Petersen, B.E. (2009). A detailed characterization of the adult mouse model of glycogen storage disease Ia. Lab. Investig. J. Tech. Methods Pathol. *89*, 1032–1042.

Sanchez-Cespedes, M., Parrella, P., Esteller, M., Nomoto, S., Trink, B., Engles, J.M., Westra, W.H., Herman, J.G., and Sidransky, D. (2002). Inactivation of LKB1/STK11 is a common event in adenocarcinomas of the lung. Cancer Res. *62*, 3659–3662.

Sanchez-Pareja, A., Clément, S., Peyrou, M., Spahr, L., Negro, F., Rubbia-Brandt, L., and Foti, M. (2016). Phosphatase and tensin homolog is a differential diagnostic marker between nonalcoholic and alcoholic fatty liver disease. World J. Gastroenterol. *22*, 3735–3745.

van Schaftingen, E., and Gerin, I. (2002). The glucose-6-phosphatase system. Biochem. J. *362*, 513–532.

Schmitt, F., Remy, S., Dariel, A., Flageul, M., Pichard, V., Boni, S., Usal, C., Myara, A., Laplanche, S., Anegon, I., et al. (2010). Lentiviral vectors that express UGT1A1 in liver and contain miR-142 target sequences normalize hyperbilirubinemia in Gunn rats. Gastroenterology *139*, 999–1007, 1007-2.

Schmitz, G., Hohage, H., and Ullrich, K. (1993). Glucose-6-phosphate: A key compound in glycogenosis I and favism leading to hyper- or hypolipidaemia. Eur. J. Pediatr. *152*, 77–84.

Schuppan, D., and Afdhal, N.H. (2008). Liver Cirrhosis. Lancet *371*, 838–851.

Seki, E., and Schwabe, R.F. (2015). Hepatic Inflammation and Fibrosis: Functional Links and Key Pathways. Hepatol. Baltim. Md *61*, 1066–1079.

Shackelford, D.B., and Shaw, R.J. (2009). The LKB1-AMPK pathway: metabolism and growth control in tumour suppression. Nat. Rev. Cancer *9*, 563–575.

Shelly, L.L., Lei, K.J., Pan, C.J., Sakata, S.F., Ruppert, S., Schutz, G., and Chou, J.Y. (1993). Isolation of the gene for murine glucose-6-phosphatase, the enzyme deficient in glycogen storage disease type 1A. J. Biol. Chem. *268*, 21482–21485.

Shieh, J.-J., Pan, C.-J., Mansfield, B.C., and Chou, J.Y. (2003). A Glucose-6-phosphate Hydrolase, Widely Expressed Outside the Liver, Can Explain Age-dependent Resolution of Hypoglycemia in Glycogen Storage Disease Type Ia. J. Biol. Chem. *278*, 47098–47103.

Shih, D.Q., Bussen, M., Sehayek, E., Ananthanarayanan, M., Shneider, B.L., Suchy, F.J., Shefer, S., Bollileni, J.S., Gonzalez, F.J., Breslow, J.L., et al. (2001). Hepatocyte nuclear factor-1alpha is an essential regulator of bile acid and plasma cholesterol metabolism. Nat. Genet. *27*, 375–382.

Shimazu, T. (1981). Central nervous system regulation of liver and adipose tissue metabolism. Diabetologia *20 Suppl*, 343–356.

Shimazu, T., and Fujimoto, T. (1971). Regulation of glycogen metabolism in liver by the autonomic nervous system. IV. Neural control of glycogen biosynthesis. Biochim. Biophys. Acta *252*, 18–27.

Singh, R., Kaushik, S., Wang, Y., Xiang, Y., Novak, I., Komatsu, M., Tanaka, K., Cuervo, A.M., and Czaja, M.J. (2009). Autophagy regulates lipid metabolism. Nature *458*, 1131–1135.

Slonim, A.E., Lacy, W.W., Terry, A., Greene, H.L., and Burr, I.M. (1979). Nocturnal intragastric therapy in type I glycogen storage disease: effect on hormonal and amino acid metabolism. Metabolism. *28*, 707–715.

Smith, B.W., and Adams, L.A. (2011). Non-alcoholic fatty liver disease. Crit. Rev. Clin. Lab. Sci. *48*, 97–113.

Smith, M.B., Lee, N.J., Haney, E., and Carson, S. (2009). Drug Class Review: HMG-CoA Reductase Inhibitors (Statins) and Fixed-dose Combination Products Containing a Statin: Final Report (Portland (OR): Oregon Health & Science University) /NBK47273/.

Soty, M., Gautier-Stein, A., Rajas, F., and Mithieux, G. (2017). Gut-Brain Glucose Signaling in Energy Homeostasis. Cell Metab. *25*, 1231–1242.

Stambolic, V., MacPherson, D., Sas, D., Lin, Y., Snow, B., Jang, Y., Benchimol, S., and Mak, T.W. (2001). Regulation of PTEN transcription by p53. Mol. Cell *8*, 317–325.

Stoot, J.H., Coelen, R.J., de Jong, M.C., and Dejong, C.H. (2010). Malignant transformation of hepatocellular adenomas into hepatocellular carcinomas: a systematic review including more than 1600 adenoma cases. HPB *12*, 509–522.

Sun, B., Li, S., Yang, L., Damodaran, T., Desai, D., Diehl, A.M., Alzate, O., and Koeberl, D.D. (2009). Activation of glycolysis and apoptosis in glycogen storage disease type Ia. Mol. Genet. Metab. *97*, 267–271.

Sun, M.-S., Pan, C.-J., Shieh, J.-J., Ghosh, A., Chen, L.-Y., Mansfield, B.C., Ward, J.M., Byrne, B.J., and Chou, J.Y. (2002). Sustained hepatic and renal glucose-6-phosphatase expression corrects glycogen storage disease type Ia in mice. Hum. Mol. Genet. *11*, 2155–2164.

Thapar, R., Denmon, A.P., and Nikonowicz, E.P. (2014). Recognition Modes of RNA Tetraloops And Tetraloop-Like Motifs By RNA Binding Proteins. Wiley Interdiscip. Rev. RNA 5(1):49-67*5*.

Themis, M., Waddington, S.N., Schmidt, M., von Kalle, C., Wang, Y., Al-Allaf, F., Gregory, L.G., Nivsarkar, M., Themis, M., Holder, M.V., et al. (2005). Oncogenesis following delivery of a nonprimate lentiviral gene therapy vector to fetal and neonatal mice. Mol. Ther. J. Am. Soc. Gene Ther. *12*, 763–771.

Tong, X., Zhao, F., Mancuso, A., Gruber, J.J., and Thompson, C.B. (2009). The glucose-responsive transcription factor ChREBP contributes to glucose-dependent anabolic synthesis and cell proliferation. Proc. Natl. Acad. Sci. U. S. A. *106*, 21660–21665.

Ullrich, S.J., Sakaguchi, K., Lees-Miller, S.P., Fiscella, M., Mercer, W.E., Anderson, C.W., and Appella, E. (1993). Phosphorylation at Ser-15 and Ser-392 in mutant p53 molecules from human tumors is altered compared to wild-type p53. Proc. Natl. Acad. Sci. U. S. A. *90*, 5954–5958.

Urnov, F.D., Rebar, E.J., Holmes, M.C., Zhang, H.S., and Gregory, P.D. (2010). Genome editing with engineered zinc finger nucleases. Nat. Rev. Genet. *11*, 636–646.

Van Obberghen, E., Baron, V., Delahaye, L., Emanuelli, B., Filippa, N., Giorgetti-Peraldi, S., Lebrun, P., Mothe-Satney, I., Peraldi, P., Rocchi, S., et al. (2001). Surfing the insulin signaling web. Eur. J. Clin. Invest. *31*, 966–977.

Verhave, J.C., Bech, A.P., Wetzels, J.F.M., and Nijenhuis, T. (2016). Hepatocyte Nuclear Factor 1β–Associated Kidney Disease: More than Renal Cysts and Diabetes. J. Am. Soc. Nephrol. JASN *27*, 345–353.

Vijay, A., Elaffandi, A., and Khalaf, H. (2015). Hepatocellular adenoma: An update. World J. Hepatol. *7*, 2603–2609.

Villar-Palasí, C., and Guinovart, J.J. (1997). The role of glucose 6-phosphate in the control of glycogen synthase. FASEB J. Off. Publ. Fed. Am. Soc. Exp. Biol. *11*, 544–558.

Viollet, B., Foretz, M., Guigas, B., Horman, S., Dentin, R., Bertrand, L., Hue, L., and Andreelli, F. (2006). Activation of AMP-activated protein kinase in the liver: a new strategy for the management of metabolic hepatic disorders. J. Physiol. *574*, 41–53.

Visser, G., Rake, J.P., Kokke, F.T.M., Nikkels, P.G.J., Sauer, P.J.J., and Smit, G.P.A. (2002). Intestinal function in glycogen storage disease type I. J. Inherit. Metab. Dis. *25*, 261–267.

Wang, D.Q., Fiske, L.M., Carreras, C.T., and Weinstein, D.A. (2011). NATURAL HISTORY OF HEPATOCELLULAR ADENOMA FORMATION IN GLYCOGEN STORAGE DISEASE TYPE I. J. Pediatr. *159*, 442–446.

Watanabe, S., Horie, Y., and Suzuki, A. (2005). Hepatocyte-specific Pten-deficient mice as a novel model for nonalcoholic steatohepatitis and hepatocellular carcinoma. Hepatol. Res. *33*, 161–166.

Watford, M. (1993). Hepatic glutaminase expression: relationship to kidney-type glutaminase and to the urea cycle. FASEB J. Off. Publ. Fed. Am. Soc. Exp. Biol. *7*, 1468–1474.

Wingo, S.N., Gallardo, T.D., Akbay, E.A., Liang, M.-C., Contreras, C.M., Boren, T., Shimamura, T., Miller, D.S., Sharpless, N.E., Bardeesy, N., et al. (2009). Somatic LKB1 Mutations Promote Cervical Cancer Progression. PLOS ONE *4*, e5137.

Wolfsdorf, J.I., Keller, R.J., Landy, H., and Crigler, J.F. (1990). Glucose therapy for glycogenosis type 1 in infants: comparison of intermittent uncooked cornstarch and continuous overnight glucose feedings. J. Pediatr. *117*, 384–391.

Wu, Z., Asokan, A., and Samulski, R.J. (2006). Adeno-associated virus serotypes: vector toolkit for human gene therapy. Mol. Ther. J. Am. Soc. Gene Ther. *14*, 316–327.

Xu, C., Chakravarty, K., Kong, X., Tuy, T.T., Arinze, I.J., Bone, F., and Massillon, D. (2007). Several transcription factors are recruited to the glucose-6-phosphatase gene promoter in response to palmitate in rat hepatocytes and H4IIE cells. J. Nutr. *137*, 554–559.

Yang, L., Li, P., Fu, S., Calay, E.S., and Hotamisligil, G.S. (2010). Defective Hepatic Autophagy in Obesity Promotes ER Stress and Causes Insulin Resistance. Cell Metab. *11*, 467–478.

Yeung, F., Hoberg, J.E., Ramsey, C.S., Keller, M.D., Jones, D.R., Frye, R.A., and Mayo, M.W. (2004). Modulation of NF-κB-dependent transcription and cell survival by the SIRT1 deacetylase. EMBO J. *23*, 2369–2380.

Yi, C.-X., la Fleur, S.E., Fliers, E., and Kalsbeek, A. (2010). The role of the autonomic nervous liver innervation in the control of energy metabolism. Biochim. Biophys. Acta BBA - Mol. Basis Dis. *1802*, 416–431.

Yiu, W.H., Pan, C.-J., Ruef, R.A., Peng, W.-T., Starost, M.F., Mansfield, B.C., and Chou, J.Y. (2008a). The angiotensin system mediates renal fibrosis in glycogen storage disease type Ia nephropathy. Kidney Int. *73*, 716–723.

Yiu, W.H., Pan, C.-J., Ruef, R.A., Peng, W.-T., Starost, M.F., Mansfield, B.C., and Chou, J.Y. (2008b). Angiotensin mediates renal fibrosis in the nephropathy of glycogen storage disease type Ia. Kidney Int. *73*, 716–723.

Yiu, W.H., Pan, C.-J., Mead, P.A., Starost, M.F., Mansfield, B.C., and Chou, J.Y. (2009). Normoglycemia alone is insufficient to prevent long-term complications of hepatocellular adenoma in glycogen storage disease type Ib mice. J. Hepatol. *51*, 909–917.

Yu, T.-M., Chuang, Y.-W., Yu, M.-C., Chen, C.-H., Yang, C.-K., Huang, S.-T., Lin, C.-L., Shu, K.-H., and Kao, C.-H. (2016). Risk of cancer in patients with polycystic kidney disease: a propensity-score matched analysis of a nationwide, population-based cohort study. Lancet Oncol. *17*, 1419–1425.

Zadra, G., Batista, J.L., and Loda, M. (2015). Dissecting the Dual Role of AMPK in Cancer: From Experimental to Human Studies. Mol. Cancer Res. *13*, 1059–1072.

Zahler, M.H., Irani, A., Malhi, H., Reutens, A.T., Albanese, C., Bouzahzah, B., Joyce, D., Gupta, S., and Pestell, R.G. (2000). The application of a lentiviral vector for gene transfer in fetal human hepatocytes. J. Gene Med. *2*, 186–193.

Zaytseva, Y.Y., Rychahou, P.G., Gulhati, P., Elliott, V.A., Mustain, W.C., O'Connor, K., Morris, A.J., Sunkara, M., Weiss, H.L., Lee, E.Y., et al. (2012). Inhibition of fatty acid synthase attenuates CD44-associated signaling and reduces metastasis in colorectal cancer. Cancer Res. *72*, 1504–1517.

Zhou, G., Myers, R., Li, Y., Chen, Y., Shen, X., Fenyk-Melody, J., Wu, M., Ventre, J., Doebber, T., Fujii, N., et al. (2001). Role of AMP-activated protein kinase in mechanism of metformin action. J. Clin. Invest. *108*, 1167–1174.

Zingone, A., Hiraiwa, H., Pan, C.-J., Lin, B., Chen, H., Ward, J.M., and Chou, J.Y. (2000). Correction of Glycogen Storage Disease Type 1a in a Mouse Model by Gene Therapy. J. Biol. Chem. *275*, 828–832.

Zucman-Rossi, J., Jeannot, E., Nhieu, J.T.V., Scoazec, J.-Y., Guettier, C., Rebouissou, S., Bacq, Y., Leteurtre, E., Paradis, V., Michalak, S., et al. (2006). Genotype-phenotype correlation in hepatocellular adenoma: new classification and relationship with HCC. Hepatol. Baltim. Md *43*, 515–524.

RÉSUMÉ EN FRANÇAIS

La glycogénose de type I (Glycogen storage disease type I - GSDI) est une maladie métabolique rare, résultant de l'absence de production endogène de glucose par l'organisme, ce qui conduit les patients à des hypoglycémies sévères en absence de traitement (Froissart et al., 2011; Kishnani et al., 2014; Rake et al., 2002a, 2002b). Cette maladie génétique est due à un déficit de l'enzyme glucose-6 phosphatase (G6Pase), entrainé par des mutations de la sous-unité catalytique G6PC de la G6Pase pour la GSD de type Ia et des mutations au niveau de la sous-unité de transport G6PT pour la GSD de type Ib. Cette enzyme est exprimée au niveau du foie, des reins et de l'intestin, qui sont les trois organes producteurs de glucose. Au niveau moléculaire, les deux types de GSDI présentent des altérations métaboliques très similaires, entrainant des atteintes hépatiques, rénales et intestinales. En effet, le déficit en G6Pase résulte en une forte accumulation en glucose-6 phosphate, car ce dernier ne peut pas être converti en glucose libre, menant à des perturbations métaboliques importantes. En plus des hypoglycémies, les patients présentent une hypertriglycéridémie, une hypercholestérolémie, une acidose lactique et une hyperuricémie.

Depuis les années 80, ces patients sont soumis à un contrôle nutritionnel très strict, en particulier pendant la nuit, ce qui a permis d'allonger considérablement leur espérance de vie. Ces mesures diététiques basées sur des repas fréquents, incluant une nutrition nocturne, permettent d'éviter les hypoglycémies et l'acidose lactique. La consommation de sucres lents, en particulier de farine de maïs crue (Maïzena®), permet une libération lente de glucose au niveau intestinal, afin de maintenir une glycémie normale pendant un temps de jeûne plus long entre les repas. Malgré ce suivi médical, les patients développent des complications à long terme, telles que des tumeurs hépatiques, une maladie chronique rénale et des hyperlipidémies sévères (Kishnani et al., 2014). Une étude rétrospective européenne a montré que le contrôle métabolique permettait de limiter ces complications, mais les mécanismes moléculaires sous-jacents restent mal connus (Rake et al., 2002). Le nombre limité de patients rend les études très difficiles. Ainsi, pour mieux comprendre les mécanismes impliqués dans

le développement des complications hépatiques et rénales et trouver de nouvelles cibles de traitements pour la GSDI, l'utilisation de modèles animaux est indispensable.

Les modèles murins et canins d'invalidation totale de la G6Pase ne survivent pas après le sevrage en absence d'un apport de glucose quasi-constant. Pour cette raison, notre laboratoire a récemment développé des modèles de souris avec une invalidation du gène codant pour la G6PC de façon tissu-spécifique, dans le foie (souris L.G6pc-/-), les reins (souris K.G6pc-/-) ou l'intestin (souris I.G6pc-/-). Ces souris sont viables et régulent leur glycémie grâce à l'induction de la production de glucose par les autres organes néoglucogéniques. Seules les souris L.G6pc-/- présentent une hypoglycémie lors de jeûnes courts, car elles sont incapables de mobiliser leur glycogène hépatique. Au cours d'un jeûne plus long, la glycémie de ces souris est maintenue grâce à l'induction de la néoglucogenèse rénale et intestinale (Abdul-Wahed et al., 2014; Mutel et al., 2011a).

L'objectif de ce travail était de mieux caractériser le développement des complications hépatiques et rénales à long-terme associées à la GSDI. Effectivement, avec l'introduction de la thérapie nutritionnelle, l'espérance de vie des patients a augmenté, mais ceci a mis en évidence le développement de complications qui étaient jusqu'alors rarement observées. Ainsi, une connaissance plus approfondie des mécanismes moléculaires impliqués dans le développement de tumeurs hépatiques et la néphropathie est cruciale pour une meilleure prise en charge des patients. Grâce au développement de modèles animaux reproduisant ces pathologies associées à la GSDI (sans entrainer la mort précoce de l'animal), nous avons pu caractériser, dans une première partie les **liens entre métabolisme et développement tumoral** chez les souris L.G6pc-/-, puis identifier **les étapes du développement de la maladie rénale liées à l'apparition des kystes** dans une deuxième partie, et finalement, démontrer le **rôle clé de l'accumulation des lipides dans le développement de ces pathologies rénale et hépatique**. Cette dernière étude permet de suggérer que le fénofibrate, un médicament hypolipidémiant, permettrait de prévenir, ou au moins de ralentir l'apparition de ces pathologies chez les patients atteints de GSDI.

Dans **la première partie** de ce travail, les souris L.G6pc-/- ont été utilisées pour déterminer les mécanismes menant à la tumorigenèse hépatique, caractéristique de la GSDI. De façon intéressante, les souris L.G6pc-/- développent l'ensemble des symptômes caractéristiques de la pathologie hépatique retrouvée chez les patients atteints de GSDI, associés à des perturbations métaboliques comme une acidose lactique, une hyperuricémie, une hypertriglycéridémie et une hypercholestérolémie. Rapidement après l'invalidation du gène *G6pc*, les souris développent une hépatomégalie, due à l'accumulation du glycogène, puis une stéatose et, à long terme, des adénomes hépatocellulaires (AHC), pouvant se transformer en carcinomes hépatocellulaires (CHC) (Mutel et al., 2011a) (cf paragraphe V.1 de la partie Literature data). En effet, dans le cas de la GSDI, la carcinogenèse est un processus linéaire, comprenant d'abord la formation des AHC, qui se transforment par la suite en CHC, mais l'apparition de CHC *de novo* n'a jamais été observée. Les souris L.G6pc-/- développent des AHC dès 9 mois après la délétion du gène *G6pc* chez 20% des souris nourries en régime standard, et plus de 90% des souris présentent des AHC multiples après 18 mois. Quelques cas de CHC ont également été détectés à cet âge. Les souris L.G6pc-/- sont ainsi un modèle de tumorigenèse unique qui permet l'étude des mécanismes moléculaires à l'origine du développement et de la transformation tumorale en relation avec les perturbations chroniques du métabolisme lipidique et glucidique. En effet, les liens entre les perturbations métaboliques menant à la stéatose hépatique et au développement des tumeurs sont particulièrement clairs dans cette pathologie. Au cours de ma thèse, j'ai eu l'opportunité de décrire ces liens dans une revue publiée dans «Journal of Inherited Errors of Metabolism and Screening» (JIEMS) (Gjorgjieva et al., 2016b).

Au niveau des foies des souris L.G6pc-/-, les conséquences de la reprogrammation métabolique entrainée par la déficience en G6PC menant à l'accumulation de quantités importantes de glycogène et lipides ont été analysées au cours du processus de tumorigenèse. Ces souris ont été soumises à un régime riche en gras et en sucre (high fat / high sucrose – HF/HS) pendant 9 mois, car il a été démontré précédemment que ce régime accélérait fortement le développement tumoral dans notre modèle animal de GSDIa (Rajas et al., 2015). Le métabolisme et les défenses

cellulaires ont été analysés à deux stades différents, identifiés comme stade pré-tumoral (4 mois de régime) et stade tumoral (9 mois de régime).

En analysant les souris au stade tumoral, nous avons constaté que l'incidence tumorale était fortement augmentée avec le régime hypercalorique, puisque près de 90% des souris présentaient des tumeurs macroscopiques, dont 30% ont été diagnostiqués comme des CHC. De plus, les souris ont développé des CHC en absence de fibrose hépatique, comme observé chez les patients GSDI, ce qui n'est pas le cas général de tumeurs hépatiques. En effet, dans le foie, la carcinogenèse est très souvent précédée par l'installation d'une inflammation chronique associée au développement d'une fibrose hépatique, pouvant évoluer en cirrhose (Cha and DeMatteo, 2005). En analysant les voies menant à la fibrose, comme la transition épithélio-mésenchymateuse (TEM), aucune activation des voies pro-fibrotiques n'a pu être observée, expliquant l'absence de fibrose dans les foies des souris L.G6pc-/- au stade tumoral. En effet, la voie TGF-β1 qui active la TEM n'est pas induite dans les foies et les tumeurs des souris L.G6pc-/-. De plus, l'expression des marqueurs mésenchymateux n'est pas modifiée, comparée aux souris WT, avec un maintien de l'expression des marqueurs épithéliaux, démontrant que ce processus n'a pas été activé. Finalement, les foies et les tumeurs des souris L.G6pc-/- présentent une perte de l'expression de certains gènes suppresseurs de tumeur, comme HNF1α, PTEN et p53, indiquant qu'il y a plusieurs facteurs potentiels pouvant mener à la tumorigenèse.

En lien avec ces modifications, le métabolisme des hépatocytes L.G6pc-/- se caractérise par une forte activation de la glycolyse, due à l'augmentation de glucose-6 phosphate intracellulaire, qui mène à une surproduction de lactate au stade prétumoral et tumoral. D'une façon intéressante, le transport du glucose dans les hépatocytes et sa phosphorylation par la glucokinase sont diminués aux deux stades. Comme dans la plupart des cancers, l'expression de l'isoforme M2 de la pyruvate kinase est augmentée dans les AHC et CHC. En parallèle, l'oxydation mitochondriale du pyruvate est fortement diminuée, avec une diminution de l'expression de MPC1. De plus, la synthèse lipidique (lipogenèse *de novo*) est augmentée (augmentation de *Fasn*, *Acaca*, *Elovl6* et *Scd1*) et l'oxydation lipidique est diminuée drastiquement (inhibition de *Ppara*, *Cpt1*,

Cyp4a10 et *Cyp4a14*). Dans les tumeurs, les voies de la lipogenèse *de novo* et de l'oxydation des lipides semblent diminuées par rapport au stade prétumoral. Finalement, l'implication des deux isoformes Chrebp-α et Chrebp-β semble différente entre le stade prétumoral et tumoral.

Cette reprogrammation métabolique des hépatocytes GSDI, caractérisée par une augmentation de la glycolyse, de la lipogenèse et une diminution de la respiration mitochondriale abouti à un phénotype «Warburg-like», très souvent observé dans les cancers glycolytiques. En effet, cette reprogrammation est très favorable à la formation et la progression des tumeurs, car elle favorise une prolifération rapide. Ainsi, ce phénotype confère aux hépatocytes GSDI un statut pré-néoplasique.

Finalement, l'accumulation de glycogène et de lipides dans le cas de la GSDI entraine une perturbation des voies de défense cellulaire, comme l'autophagie, des réponses contre le stress du réticulum endoplasmique (RE) ou le stress oxydatif. Tous ces processus ont pour but de maintenir l'homéostasie cellulaire et leur dysfonctionnement peut favoriser le développement tumoral. Une forte diminution de l'autophagie et de la réponse contre le stress oxydatif a été observée dans le foie des souris L.G6pc-/- dès le stade prétumoral. De façon concomitante, une activation progressive de certaines voies du stress RE, due à une forte diminution de la protéine chaperonne BiP, indique l'installation d'un stress chronique du RE au cours de la tumorigenèse dans les foies des souris L.G6pc-/-. D'une façon intéressante, l'autophagie était réactivée dans les tumeurs hépatiques, favorisant probablement leur progression par la provision des nutriments recyclés nécessaires pour la prolifération.

Pour conclure, la déficience en G6Pase au niveau du foie mène à une profonde modification du métabolisme et des défenses cellulaires, comparable à une cellule tumorale, expliquant la forte incidence du développement tumoral observée chez la plupart des patients GSDI. En effet, la plupart des patients atteints de GSDI développent des tumeurs hépatiques à l'âge adulte, avec une forte incidence de transformation en CHC (Calderaro et al., 2013; Franco et al., 2005; Kishnani et al., 2014). Les études chez les souris L.G6pc-/- nous ont permis de décrire les modifications métaboliques favorisant la tumorigenèse hépatique et pourront par la

suite nous permettre d'identifier de nouvelles cibles pharmacologiques (comme la PK-M2) et des marqueurs précoces de la transformation tumorale, afin de proposer une meilleure prise en charge des patients atteints de GSDI. Les résultats de ce travail ont été soumis pour publication.

Dans **la deuxième partie**, nous avons caractérisé la progression de la maladie chronique rénale (MCR) dans le modèle de souris invalidées pour la G6PC rénale (souris K.G6pc-/-). Ces souris développent une néphropathie avec l'apparition d'une microalbuminurie dès 6 mois d'invalidation (Clar et al., 2014) (cf paragraphe V.1 de la partie Literature data). De plus, elles présentent une néphromégalie due à une forte accumulation de glycogène et de lipides au niveau du cortex rénal. Cela se traduit aussi par une clarification tubulaire et une perte d'intégrité des podocytes / pédicelles au niveau des glomérules. A ce stade précoce de la néphropathie, l'activation de la voie Rénine-Angiotensine (RAS) mène à une augmentation de l'expression de TGF-β1, facteur pro-fibrotique. Cet axe de signalisation RAS/TGF-β1 est souvent responsable du développement des néphropathies dans le cadre de l'obésité et du diabète de type 2 (Ribeiro-Oliveira et al., 2008). Malgré l'activation de cette signalisation, aucun signe de fibrose n'a pas été observé au stade précoce de la maladie dans les reins K.G6pc-/- .

Après les 6 mois d'invalidation, au cours du temps, nous avons pu observer une perte de la fonction de filtration des reins, accompagnée par un développement de fibrose progressive. La majorité des souris présentaient une insuffisance rénale à 15 mois d'invalidation, caractérisée par une albuminurie et l'accumulation de déchets (urée) dans le sang. L'activation progressive de RAS/TGF-β1 à long-terme a abouti à l'activation de la TEM et au développement d'une fibrose rénale, avec l'apparition de kystes rénaux. Plus précisément, des dépôts de collagène ont été détectés dans l'espace interstitiel au niveau des tubules (fibrose interstitielle), ainsi qu'au niveau des glomérules (glomérulosclérose). De façon intéressante, ces dépôts de collagène ont été désignés comme la cause principale de la formation de kystes rénaux. Effectivement, ces kystes ont une origine glomérulaire et tubulaire. La découverte des kystes rénaux chez la souris a mené à l'analyse d'une cohorte des patients atteints de la GSDI, montrant aussi la présence de kystes chez l'homme. La cohorte de 32 patients

analysée est suivie à Paris, par le Prof Philippe Labrune, et comporte des patients ayant de 1 à 53 ans, dont 27 sont atteints de GSDIa et 5 de GSDIb. Ces patients ont été répartis en 3 groupes ; groupe 1 : patients sans problèmes rénaux détectés, groupe 2 : patients avec les premiers symptômes d'une néphropathie (microalbuminurie et hyperfiltration glomérulaire) et groupe 3 : patients avec une néphropathie avancée. Seuls les patients du groupe 3 présentaient des kystes rénaux. Plus précisément, 7 patients parmi les 32 présentaient des kystes rénaux, représentant 22% de la cohorte, ce qui nous a permis de conclure que l'incidence d'apparition des kystes rénaux est très élevée dans le cas de la GSDI. De plus, 3 parmi les 7 patients ont atteint le stade d'insuffisance rénale, suggérant que les kystes rénaux sont un signe précoce de cette étape de la néphropathie. En conclusion, cette étude souligne la nécessité de suivre de près la fonction rénale chez ces patients, même chez les individus jeunes et a montré que les complications hépatiques ne sont pas les seules complications à long-terme dans le cadre de la GSDI. Cette étude a été publiée dans «Human Molecular Genetics» (Hum. Mol. Gen.) en 2016 (Gjorgjieva et al., 2016a).

Dans **la troisième partie** de ce travail, nous avons étudié le rôle des lipides dans le développement de la pathologie hépatique et rénale. De façon intéressante, la déficience en G6PC se traduit par l'activation des mêmes voies métaboliques dans le foie et les reins, même si l'accumulation des lipides est moins marquée dans les reins. Malgré l'effet néfaste important du glycogène présent en quantité excessive dans le foie et les reins, les lipides semblent avoir un effet propre sur la progression de la pathologie. En effet, il a été suggéré que l'accumulation rénale de lipides peut activer la voie RAS, menant à une activation de la voie pro-fibrotique TGF-β1, comme c'est le cas dans la néphropathie associée au diabète de type 2 (Clar et al., 2014; Cooper, 2004; Ribeiro-Oliveira et al., 2008; Yiu et al., 2008a). Au niveau hépatique, la présence excessive des lipides est connue pour avoir des effets très néfastes, comme observés dans les pathologies regroupées sous le nom de «non-alcoholic fatty liver disease» (NAFLD), (Alkhouri et al., 2009; Jung and Choi, 2014).

Dans cette étude, nous avons montré que les souris L.G6pc-/- et K.G6pc-/- nourries en régime riche en gras et sucre (HF/HS), présentent une forte accélération

des complications hépatiques et rénales, caractérisées par une augmentation des marqueurs de dommage hépatique et une perte plus rapide de la fonction rénale, respectivement. Après 9 mois de régime HF/HS, nous avons montré une accumulation de lipides plus importante dans le foie des souris L.G6pc-/- et dans les reins des souris K.G6pc-/-, bien que le taux de glycogène est resté inchangé dans le foie et était diminué dans les reins. L'accélération des complications à long-terme suite à l'exacerbation de l'accumulation lipidique induite par un régime HF/HS montre clairement un rôle crucial des lipides dans la GSDI, indépendamment des taux de glycogène. De façon intéressante, l'accumulation de lipides est entrainée par une activation de la lipogenèse *de novo,* mais aussi par une forte inhibition de l'oxydation des lipides (Abdul-Wahed et al., 2014; Clar et al., 2014; Mutel et al., 2011a).

Dans le but de limiter l'accumulation des lipides, nous avons traité les souris L.G6pc-/- et K.G6pc-/- avec un agoniste de PPARα, le fénofibrate, permettant d'activer l'oxydation lipidique. Ce traitement est couramment utilisé comme hypolipidémiant chez les patients obèses. Le fénofibrate a été administré de façon chronique pendant 3 mois. Le début du traitement a été réalisé à un stade de développement précoce des pathologies rénale et hépatique, c'est à dire 6 mois après l'invalidation du gène *G6pc*. Après 3 mois de traitement, le fénofibrate a complètement reversé la stéatose hépatique chez les souris L.G6pc-/-, en augmentant l'oxydation lipidique par l'activation de PPARα et ses gènes cibles (*Cpt1*, *Acadl*, *Fabp1*, *Cyp4a10*, *Acox1*). De plus, la synthèse lipidique a également été augmentée, illustrée par l'augmentation de l'expression des gènes de la lipogenèse *de novo* (*Fasn*, *Acaca*, *Scd1*, *Elovl6*), indiquant un turn-over des lipides très important. De façon intéressante, le taux de glycogène a été normalisé par ce traitement, car le fénofibrate a permis le détournement du glucose-6 phosphate de la voie de la synthèse de glycogène vers le turn-over lipidique. La diminution des lipides a donc mené à une normalisation des marqueurs de dysfonctionnement hépatique, comme les transaminases (AST et ALT), ainsi qu'à une histologie hépatique normale. Finalement, ce traitement a permis l'augmentation de l'expression des gènes suppresseurs de tumeur comme PTEN et AMPK, qui étaient réprimés chez les souris non-traitées, suggérant un possible effet bénéfique dans la prévention du développement tumoral (non étudié ici).

L'augmentation de turnover lipidique menant à la normalisation du taux de glycogène et de lipides a été également observée dans les reins des souris K.G6pc-/- traitées au fénofibrate. Ceci a mené à une normalisation des marqueurs d'atteinte rénale comme l'albuminurie et la lipocaline-2. L'effet le plus marquant de la diminution des lipides rénaux a été la prévention quasi-totale de la fibrose rénale, mettant en évidence le rôle crucial des lipides dans la néphropathie de la GSDI.

Ainsi, le fénofibrate a permis une réorientation du métabolisme des cellules G6pc-/- en détournant l'utilisation du glucose-6 phosphate de la synthèse du glycogène vers la synthèse lipidique. Ceci a conduit à la normalisation du taux de glycogène dans les deux organes. Malgré une augmentation de la synthèse des lipides, le fénofibrate a permis la normalisation du taux de lipides, en activant la dégradation lipidique. Ainsi le fénofibrate permet de restaurer un phénotype quasi-normal dans les cellules atteintes de GSDI, malgré l'impossibilité de produire du glucose. Un traitement au fénofibrate des patients atteints de GSDI pourrait donc avoir l'avantage de prévenir à la fois l'hypertriglycéridémie et les complications rénales et hépatiques. En revanche, ce traitement ne permettra pas d'éviter les hypoglycémies. Cette étude a été soumise pour publication.

En conclusion, grâce à une meilleure connaissance des pathologies hépatiques et rénales au niveau moléculaire, nous pourrons mieux maîtriser le développement des tumeurs hépatiques et de l'insuffisance rénale par l'application de traitements pharmacologiques adaptés. Parallèlement, j'ai pu aussi participer à l'évaluation de nouvelles thérapies, comme la thérapie génique ciblée (gene editing), qui semblent très prometteuses et permettraient d'améliorer sensiblement la qualité de vie des patients GSDI, dès le plus jeune âge.